PROMOTING SUSTAINABILITY IN THE ENERGY SECTOR IN NEPAL-WITH A FOCUS ON BIODIESEL FUEL

by

ARJUN BAHADUR KC (CHHETRI)

Submitted in partial fulfilment of the requirements
for the degree of Doctor of Philosophy

at

Dalhousie University
Halifax, Nova Scotia
August 2012

DALHOUSIE UNIVERSITY

DEPARTMENT OF CIVIL AND RESOURCE ENGINEERING

The undersigned hereby certify that they have read and recommend to the Faculty of Graduate Studies for acceptance a thesis entitled "PROMOTING SUSTAINABILITY IN THE ENERGY SECTOR IN NEPAL-WITH A FOCUS ON BIODIESEL FUEL" by ARJUN BAHADUR KC (CHHETRI) in partial fulfillment of the requirements for the degree of Doctor of Philosophy.

Dated: AUGUST 27, 2012

External Examiner: _____

Research Supervisor: _____

Examining Committee: _____

_____

_____

Departmental Representative: _____

DALHOUSIE UNIVERSITY

DATE: AUGUST 27, 2012

AUTHOR: ARJUN BAHADUR KC (CHHETRI)

TITLE: PROMOTING SUSTAINABILITY IN THE ENERGY SECTOR IN NEPAL-WITH A FOCUS ON BIODIESEL FUEL

DEPARTMENT OR SCHOOL: DEPARTMENT OF CIVIL AND RESOURCE ENGINEERING

DEGREE: Ph.D. CONVOCATION: MAY YEAR: 2013

_____

Signature of Author

DEDICATION

I dedicate this work to my loving family.

TABLE OF CONTENTS

LIST OF TABLES

LIST OF FIGURES

ABSTRACT

This study analyzes the sustainability of various energy sources including micro hydro power and biodiesel in the context of Nepal. The main focus is on the development of biodiesel fuels from non-edible oil resources including waste cooking oil, jatropha and soapnut oil feedstocks grown on the marginal lands of Nepal.

Biodiesel fuel samples were prepared by acid and/or base catalyst transesterification. Both single stage and dual stage transesterification processes were employed depending on the free fatty acid content of the oil feedstock. The oil to biodiesel conversion rate and total yield were monitored. The quality of the biodiesel fuels including viscosity etc was confirmed by an external laboratory and all fuels met the ASTM fuel quality requirements.

Canola, jatropha and soapnut biodiesel fuels were tested to determine some atomization properties - density, surface tension and viscosity - at elevated temperatures and pressures. The density of three biodiesel fuels and diesel were determined up to 523 K and 7 MPa using a capacitance type densitometer. The results showed a linear relationship with temperature and pressure over the measured range. The experimental data were well within the range of canola and other biodiesel fuels found in the literature. Kay's mixing rule was used to predict the density of some biodiesel blends and the results were found to be in agreement with less than 5% error with the measured data.

The surface tension was measured using a pendant drop apparatus for all three biodiesel and diesel fuels for temperatures and pressures up to 473K and 7 MPa. Results showed a linear relationship with temperature as well as with pressure. Temperature has a higher effect on surface tension than pressure.

The viscosity of all three biodiesel and diesel fuels were measured using a torsional vibration viscometer up to 523 K and 7 MPa. Results showed that the viscosity-temperature relationship of all three biodiesel fuels tested followed a modified Andrade equation which was also applicable when temperature and pressure were both applied simultaneously. The measured and regressed kinematic and dynamic viscosities obtained were comparable with values in the literature.

LIST OF ABBREVIATIONS AND SYMBOLS USED

ABBREVIATIONS

ADB	Asian Development Bank
AEPC	Alternative Energy Promotion Centre
ANOVA	Analysis of Variance
AOCS	American Oil Chemists Society
ASTM	American Society of Testing Materials
ATF	Air Turbine Fuel
BEES	Battelle Environmental Evaluation System
BMRC	Mass Rail Corporation Ltd.
BN	Basic needs
BSP	Biogas Support Program
CADEC	Community Awareness Development Centre
CBOs	Community based organizations
CCD	Charged Coupled Device
CDM	Clean Development Mechanism
CDM-PDD	Clean Development Mechanism Project Design Document
CER	Certified Emission Reduction
CFPP	Cold Filter Plug Point
CMS	Central Bureau of Statistics
CSD	Commission on Sustainable Development
CSt	Centistoke
DI	Direct Injection
DME	Dimethyl ether
DSA	Drop Shape Analysis
DSD	Division for Sustainable Development
EeI	Energy Indicator
EIA	Energy Information Administration
EIU	Environmental Impact Unit

ELRTS	Elevated Light Rail Transit System
EMP	Environment Management Plan
EN	European Standard
EN14214	European Standard for Biodiesel fuel
ESAP	Energy Sector Assistant Program
FA	Fatty Acid
FAME	Fatty Acid Methyl Ester
FAO	Food and Agricultural Organization
FFA	Free Fatty Acid
FID	Flame ionization detection
GC	Gas Chromatography
GDP	Gross Domestic Product
GHG	Greenhouse Gases
GJ	Giga Joule
GON	Government of Nepal
GWh	Gigawatt hour
GWP	Global warming potential
HAN	Hotel Association of Nepal
ID	Internal Diameter
IDI	Indirect Injection (IDI)
ISO	International Standard Organization
ITDG	Intermediate Technology Development Group
IUCN	International Union for Conservation of Nature
K	Degree Kelvin
KOH	Potassium Hydroxide
kPa	Kilo Pascal
kW	Kilowatt
KWh	Kilowatt hour
LCC	Life cycle cost
LDC	Least Developed Countries
LIHD	Low-Input High-Diversity

LPG	Liquified Petroleum Gas
MCT	Main Central Thrust
MDG	Millenium Development Goals
MFT	Main Frontal Thrust
MHFG	Micro Hydro Functional Group
MHP	Micro hydro power
MJ	Mega Joule
MoA	Ministry of Agriculture
MoCS	Ministry of Commerce and Supplies
MoE	Ministry of Environment `
MFSC	Ministry of Forest and Soil Conservation
MOF	Ministry of Finance
MoLR	Ministry of Land Reform
MPa	Mega Pascal
MT	Metric Tonnes
MW	Megawatt
NaOH	Sodium Hydroxide
NE	Net energy
NEA	Nepal Electricity Authority
NER	Net energy ratio
NGO	Non-governmental organizations
NOC	Nepal Oil Corporation
NPC	National Planning Commission
NPR	Nepalese Rupees
NRDP	Non-renewable resource depletion potential
Oh	Ohnesorge number
PEPP	Petroleum Exploration Promotion Project
PIU	Parameter Impact Unit
PPA	Power Purchase Agreement
ppm	Parts Per Million
PV	Photovoltaic

RC	Recycle Ratio
Re	Reynolds number
REBAN	Restaurants and Bar Association of Nepal
RECAST	Research Centre for Applied Science and Technology
REDP	Rural Energy Development Program
RI	Renewability indicator
RPS	Renewable portfolio standard
SD	Sustainable development
SEWRA	Solar and Wind Energy Resource Assessment
SHS	Solar Home System
SMD	Sauter Mean Diameter
SNV	Netherlands Development Organization Nepal
SSP	Solar Energy Support Program
TAN	Total acid number
UN	United Nations
UNCTAD	United Nations Conference on Trade and Development
UNDP	United Nations Development Program
US	United States
VDC	Village Development Committee
WB	World Bank
WCED	World Commission on Environment Development
WCO	Waste Cooking Oil
We	Weber number
WECS	Water and Energy Commission Secretariat

SYMBOLS

English

A	Macro state of the anthroposphere
A	Wetted area of the capacitor plate in equation A.10

C	Capacitance in equation A.10
Ce	Economic capital
Ci	Cost at the ith stage of the life cycle in equation 3.1
Cs	Social capital
Cn	Environmental capital (natural capital)
Comm, NI	Community needs and interest in equation 3.13
d	Depth of submergence of the capacitor plate
dM	Rate of depreciation of man-made capital
dN	Rate of depreciation of natural capital in equation 3.27
Δd	Change in depth of capacitor submergence
E	Environment
Ec	Cohesion energy
EM_{GWPi}	Emission of ith green house gas per kilometre in equation 3.2
EQ_{ij}	Environmental Quality of i^{th} parameter and j^{th} factor in equation 3.19
f*	Resonant frequency in equation 6.2
Δf	Bandwidth in equation 6.2
Fo	Evolution equation in the ecosphere
g	Acceleration due to gravity
$G_{i,j}$	Interaction parameter (Pa.s)
ΔG	Activation energy
HNI	Human needs and interests or social needs
h	Plank's constant
Jo	Intensity J of the γ rays passing through a material
K	The system constant in equation A.8
K	System stiffness
K_o	Initial dielectric constant
ΔK	Change in dielectric constant due to change in temperature, pressure and fuel type
mCi	Size of source in millicuries

mi	Amount of non-renewable fuel consumed
ms	True mass of the sinker
ms*	Apparent mass of the sinker
M	Transducer mass
N	Natural Earth System (macro state of ecosphere)
N	Avogadro number
NI	Individual needs and interest in equation 3.13
P	Pressure
Pc	Critical pressure
[P]	Temperature-independent parameter called parachour of pure components
QL	Quality of life in equation 3.14
r	Radius of sphere in equation A.17
R	Ideal gas constant
RC_i	Recycle ratio of a non-renewable resource
S	Sustainable development
S	Total savings for a country
S	Surface area in equation 6.2
SD	Social development
SG	Specific gravity
Soc, NI	Society needs and interests in equation 3.13
Sp, NI	Species needs in equation 3.13
t	Distance between the plates in equation A.10
T	Temperature
Tb	Mean boiling point (K) in equation 2.21
T_{br}	Reduced temperature at normal boiling point
T_c	Critical temperature
TR	Reference temperature
T_{rs}	Reduced temperature at saturation
V	Molar volume in equation 2.1
V	Velocity of the falling ball

V_i^o	Molar volume of the pure liquid
Vm	Molar volume of the mixture in 2.16
Vs	Specific volume
VsR	Experimental volume
Vs (T, p)	Temperature- and pressure-dependent volume of the sinker
$\overline{w}$	Scarcity factor of non-renewable resource
$Y_{i,j}$	Mole fraction in equation 2.1.10
Y	Gross national product
Z	Sustainability index
ZRA	Rackett constant

Greek

μ	Dynamic viscosity
$\mu_{i,j}$	Viscosity of individual components (Pa.s) in equation 2.10
μ_m	Mean viscosity of mixture (Pa.s) in equation 2.10
η	Kinematic viscosity
ρ_b	Density of test liquid at normal boiling point
ρ_f	Density of the fluid being tested,
ρ^R	Experimental density value in kg/m^3
ρs	Density of the falling ball,
σl	Surface tension of liquid
τ	Shear stress
$\emptyset_i$	GWP coefficient of ith green house gas in equation 3.2

ACKNOWLEDGEMENTS

First of all, I would like to take this opportunity to express my utmost gratitude and profound respect to my supervisor Prof. Dr. K. Chris Watts for his excellent advice, enthusiastic guidance and continuous encouragement throughout this thesis. I have been amazingly fortunate to have a supervisor like him; without his superb guidance and creative suggestions, this thesis could not have been completed. I highly appreciate Dr. Watts for his continuous support and pushing me to rethink and rewrite so as to produce the best work possible. The financial support provided by him through the Natural Science and Engineering Research Council (NSERC) is highly also appreciated.

I am also very grateful to Dr. Lei Liu for his useful suggestions and encouragements during the entire thesis work. His suggestions have always led to the positive contribution to this thesis. Similarly, I would like to express my sincere thanks to Dr. Martin Tango for his continuous support and encouragement for this thesis work. Dr. Tango has his guidance throughout the course work as well as in research. My special thanks also go to Dr. Cecil Allen who always gave practical and valuable suggestions regarding experimental processes and thesis organization.

I also highly appreciate the cooperation provided by Dr. Suzanne Budge during lab testing. I also thank Hazel Walling and Ann Timmins for their great support for the lab work.

I highly appreciate and thank Ray Dube, Dean Grijm, John Pyke, Jan Kujel, Brian Lieken all of whom supported during the lab works.

Thanks to M. S. Zaman who helped me in many ways throughout the study period. Support from Dr. Fida Hasan, Bishnu Acharya, Alok Dhungana and Ramesh Thapa is also highly appreciated. I would like to thank Dharmendra Parekh and Rabindra Nath Sukla for their cooperation.

I also thank Krishna KC, Kiran Neupane and Nirmal Neupane for collecting data from Nepal and arranging for some test materials. I appreciate Bishnu Adhikari for his continuous support and encouragement. I also extend my appreciation to Prof. Dr. Govind Pokharel for his encouragement and support. Thanks to Bob Hawkesworth, coordinator of the Municipal Climate Change Action Centre, who always encouraged me for my work as well as for this research.

Most important of all, my special thanks go to my mother Hari Maya KC who constantly encouraged me to focus on my thesis. Last but not least, this thesis would not have been possible without the continuous support and love from my wife Sanju, my sons Animesh and Sanjit, and all my family members. None of this would have been possible without their love and care. I dedicate this thesis to my wife and kids, and my family in Nepal for their unconditional love and support.

.

CHAPTER 1 INTRODUCTION

1.1 BACKGROUND

Prof. Richard E. Smalley, a Nobel Laureate in Chemistry, in 1996 ranked "energy" as the number one issue among the ten most critical issues people will have to confront in the 21st Century. In 2008, approximately 85% of the global energy supply (approximately 15 Terawatts) came from fossil fuels (EIA, 2010A). The global total carbon dioxide equivalent emissions for the same year was approximately 30 billion tonnes and is expected to increase to over 42 billion tonnes by 2035 (EIA, 2010 B). The world population is expected to reach approximately 10 billion by 2050 and will need approximately 60 terawatts of energy based on the current rate of increasing energy demand (Smalley, 2005). As the demand for energy is increasing, there is an ever increasing gap between the supply and demand of fossil fuels due to the increase in population , changes in lifestyles, rapid industrialization and urbanization. It is also evident that the current global energy system is not sustainable because of the climate change impacts of greenhouse gas emissions and over reliance on declining reserves of fossil fuels (Amezaga et al., 2010). Hence, looking for sustainable energy resources has been one of the most common development agenda today.

Approximately 26% of the world's total energy is consumed in the transportation sector alone (Ou et al., 2010). Liquid fuels are dominant sources of energy for transportation accounting over 50% of world liquid fuel consumption. EIA (2010A) projected that from 2007 to 2035, growth in transportation energy use accounts for 87% of the total increase in world liquid fuels consumption. It is also anticipated that the share of liquid fuels in the transportation sector will rise by 61% from 2007 to 2035 (EIA, 2010A). Due to the declining reserves of petroleum fuels, their alternatives are being sought seriously. Biodiesel and bioethanol are the liquid biofuels that can supplement or replace the petroleum based liquid fuels because of their similar properties.

Energy is considered to play a central role in sustainable development and reducing poverty. It is a key driver for various aspects of development including social, economic, environment, access to water, agriculture, education and health among others, hence energy cannot be seen in isolation from any development initiatives as set out by Millenium Development Goals (MDGs) in 2000. The MDGs aim to eradicate extreme poverty and hunger, ensure environmental sustainability of development initiatives, promote a global partnership in development and resource management among others. Even though none of the MDGs with respect to energy have been specified, they cannot be achieved without significant improvement in the quality as well as quantity of energy services in developing countries. As reported by UNCTAD (2009), least developed countries (LDCs) which are characterized by low income, weak human resource capacity, and high economic vulnerability suffer severe distress due to the rise of food and energy prices. Access to modern energy services, utilization of natural resources in an unsustainable way including deforestation and land use, and energy security are the major three problems LDCs including Nepal are facing today.

Nepal is a landlocked and least developed country in South Asia with no proven reserves of fossil fuel resources. The primary energy supply mostly comes from traditional biomass sources such as fuel wood, agricultural residues and animal wastes. The Energy Synopsis report prepared by Water and Energy Commission Secretariat (WECS) Nepal in 2010 indicated that approximately 87% of the total primary energy was derived from traditional biomass, 12% by commercial sources (petroleum and electricity) and less than 1% from the alternative resources during the year 2008-2009. This was equivalent to the annual consumption of 401 million gigajoules (GJ). Moreover, Nepal spends over 50% if its earnings from its commodity export to import petroleum products which provided only approximately 11% of total energy consumed in the country (MOF, 2007). Even through, Nepal has a significant amount of foreign debt for oil import, the country still faces shortage of petroleum products all the year around because of its inability to import sufficient quantity of petroleum products given the rising price of imported petroleum. Besides that the importation of petroleum products at high prices to meet the increasing local demand has proved to be a great burden to the Nepalese economy.

Nepal's transport sector is the second largest energy consumer only after the domestic sector. The energy consumption in this sector is rising continuously at a rate of 8.9% annually and uses approximately 9 % of the total energy consumed in Nepal (WECS, 2010). Over 63.2% of the total petroleum consumption occurs in the transportation sector followed by approximately 16.6% in residential sector, 10.5% in agriculture sector, 8.2% in commercial sector and slightly over 1.4% in industrial sector. It was also found that High Speed Diesel took the highest share with 67% of all energy used in the transportation sector followed by approximately 20% Motor Spirit (gasoline), 12% Air Turbine Fuel (ATF) and 1% Liquefied Petroleum Gas (LPG) fuel.

Low CO_2 emitting and sustainably produced liquid biofuels play an important role to reduce demand for petroleum fuels especially in transport sector. Biofuels are considered to offer greater energy security, better vehicle performance, reduced emissions of greenhouse gases and particulates and at the same time support local development. Large quantities of ethanol mainly produced from sugar cane, corn and cassava are used as a substitute for gasoline and biodiesel produced from crops such as, soybean, palm oil, canola, sunflower coconuts, jatropha oil etc are being increasingly used as a diesel substitute. Global production of biofuels is growing and it seems will continue to do so steadily. Bioethanol production tripled and reached to 62 billion litres mainly in the United States and Brazil between 2000 and 2007 and biodiesel production expanded even more rapidly from less than 1 billion to almost 11 billion litres annually (FAO, 2008).

On the other hand, enormous demand for biofuels has created a fear of more land being converted to agricultural use. Meeting such an increasing demand for biofuels without jeopardising global food supplies, natural ecosystems such as forests is a significant challenge. However, Cai et al. (2011) in a recent study showed that producing second generation of biofuel feedstocks on abandoned and degraded cropland, low-input high-diversity (LIHD) mixtures of native perennials as energy crops on the grassland with marginal productivity may fulfill 26-55% of the current global liquid consumption without affecting the use of productive land for conventional crops and current pasture

land. This would even be more evident with the development of new generation of biofuel production technologies such as dimethyl ether (DME) production using the Fischer-Tropsch process and solid catalyst for biodiesel processing and cellulosic ethanol process for bioethanol production.

A great deal of efforts has been made to find the sustainable alternatives energy resources. Plant oil and animal fats in the form of methyl and ethyl esters offers such alternatives. These are renewable resources and even the least developed countries can produce in their waste lands, reducing their dependency in imported fossil fuel. Plant oils and animal fats are converted to methyl or ethyl esters (biodiesel) by removing glycerol molecules via a chemical process called transesterification resulting in a low viscosity fuel and other properties comparable with petroleum diesel. Biodiesel can be used either as a direct substitute or as an additive to petroleum diesel fuel in compression ignition engines. One of the most promising features of biodiesel fuel is that it can be used in the existing design of diesel engines with very little or no modifications. This thesis focuses on promoting sustainable energy development with a special focus on biodiesel fuels from non-edible oil feedstocks including jatropha, soapnut and waste cooking oils as a sustainable energy alternative to conventional diesel in the Nepalese context. In addition to the biodiesel fuels, other sustainable energy resources such as micro hydro power are also discussed for their potential. A detailed review of sustainability analysis has been presented from the literature. Strong sustainability indicators have been correlated as the components for the sustainability evaluation of micro hydro projects, biodiesel fuels and other renewable resources quantitatively and qualitatively wherever possible.

The full potential of biodiesel fuels can be assessed by testing the engine performance and fuel combustion as well as atomization characterisation tests of the biodiesel fuels. The engine test is a standard test and requires operating the diesel engine. Several studies have been carried out and results have been reported (Peterson et al., 1987; Peterson et al., 1992; Goodrum et al., 1996 and Peterson and Reece, 1996). Allen (1998) designed an engine test facility and carried out the tests to determine the atomization properties of pure biodiesel fuel as a function of magnitude and spread of droplet sizes. The present

study is limited to assessing the potential of some newer oil for biodiesel feedstocks, and promoting these renewable alternatives as a sustainable fuel for diesel supplement or replacement. This study also focused on fuel characterization and atomization properties determination of canola, jatropha, soapnut and waste cooking oils. Some strategic and policy considerations for the promotion of biodiesel as an alternative fuel for Nepal are also charted.

1.2 RATIONALE

The major rationale of this study is to assess the technical feasibility of biodiesel production in order to lessen the dependence on petroleum fuel to increase the energy security of Nepal. The consumption of diesel in diesel engines also produces a significant amount of greenhouse gases (GHGs), particulate matters and other harmful pollutants affecting people's health and the environment. Blending even a small percentage of biodiesel with diesel will significantly reduce the total GHGs emissions and emission of pollutants. Economic development, energy security and GHGs reductions are the major drivers for the development for biodiesel fuels in Nepal.

An evaluation for sustainability of energy sources based on the universally accepted criteria of sustainable development has been carried out. While the global sustainability of biodiesel development is affected by various factors, sustainability analysis based on local criteria was used in order to see its long-term potential in the context of Nepal.

Availability of feedstocks and their evaluation in terms of sustainability is not enough for any feedstocks to be considered as a source for biodiesel production. The biodiesel fuel must fulfill the criteria for fuel properties as well as atomization characterization for efficient combustion. This study focused on assessing the potential biodiesel feedstocks for their fuel and the atomization properties such as density, surface tension and viscosity. These properties change with the amount of diesel fuel the biodiesel fuel is blended with. Micro hydro power and biodiesel fuel were evaluated for their

sustainability. As there is no concrete policy for biodiesel development in Nepal yet, this study also provides useful information for policy makers, investors and related stakeholder to pursue the development of biodiesel fuels in Nepal.

1.3 THESIS OBJECTIVES

a. Feasibility study of jatropha as a potential feedstock for biodiesel production; and model the scenarios for jatropha production potential in waste lands for biodiesel production in Nepal.

b. Identification and characterization of biodiesel derived from soapnut oil as a potential new oil feedstock in Nepal.

c. Sustainability analysis of alternative energy sources focusing on biodiesel fuels in Nepalese perspectives.

d. Verification of fuel properties of canola, jatropha and soapnut biodiesel according to the relevant ASTM standard.

e. Characterization of biodiesel fuels from canola, jatropha and soapnut oil for atomization properties such as density, surface tension and viscosity at elevated temperatures and pressures.

f. Characterization of blended fuels of diesel with biodiesel fuels from canola, jatropha and soapnut oil for atomization properties such as density, surface tension and viscosity at elevated temperatures and pressures.

g. Study the potential of waste cooking oil biodiesel production in Kathmandu, the capital City of Nepal.

h. Policy and strategy recommendation for biodiesel development and promotion in Nepal.

1.4 ORGANIZATION OF THESIS

This thesis is organized in nine chapters. Figure 1.1 presents the outline of the thesis pictorially. This chapter (Chapter 1) introduces the overall thesis highlighting the thesis objectives and offers rationale for pursuing this research. This chapter also outlines how this thesis has been organized. Chapter 2 presents the overview of currently used and potential energy sources in Nepal. As this thesis also contains testing and characterization of different biodiesel feedstocks, a summary of review of experimental methods and theoretical prediction models is also presented in this chapter. Chapter 2 also summarizes the past and current petroleum energy demands in Nepal. Details of experimental methods and prediction models are provided in Appendix A. Chapter 3 discusses the theory of sustainability related to natural resource use and sustainable energy development. This chapter also includes the review of several sustainability models used to evaluate the sustainability of resources. Using the universally accepted sustainability criteria, micro hydro projects and biodiesel fuels are evaluated. This chapter discusses the strategy and policy recommendation for biodiesel development and promotion in Nepal. The potential feedstocks for biodiesel production in Nepal is discussed in Chapter 4. Chapter 5 briefly discusses the operating principles of diesel engines, fuel characterization tests according to ASTM Standards and atomization characteristics of biodiesel products at various temperatures and pressures. Chapter 6 explains how the test samples were collected and prepared for the transesterification process, and fatty acid profile determination of the feedstock oils. This Chapter also discusses the experimental procedure for atomization properties tests at high temperatures and pressures that includes density, surface tension and viscosity determination.

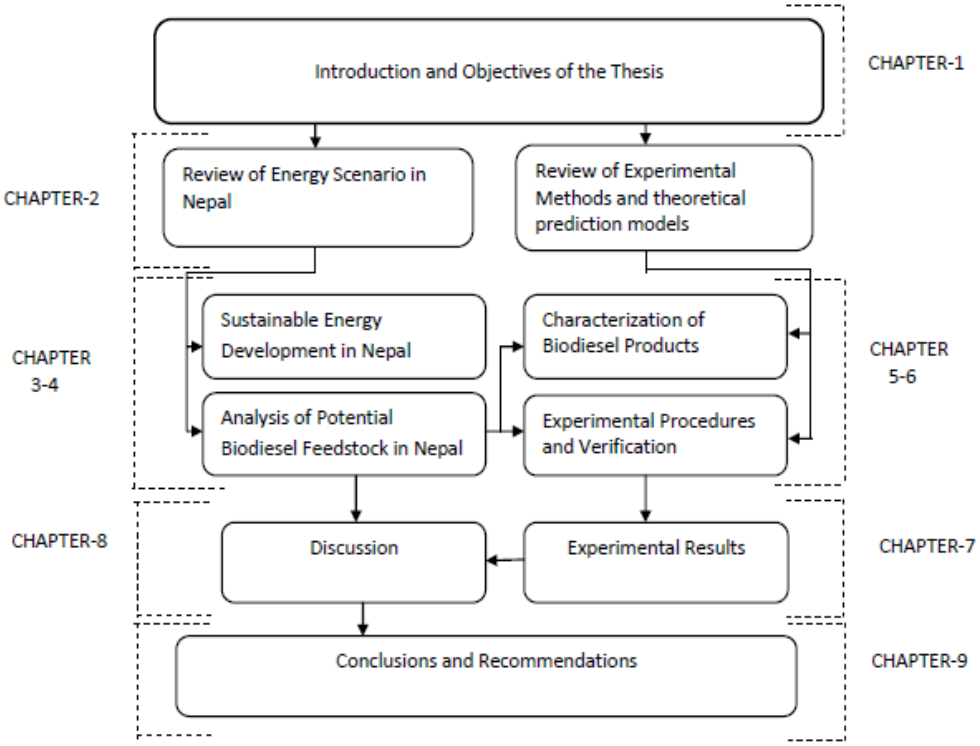

Figure 1.1 Organization of the thesis

Chapter 7 presents the experimental results and contains three parts: the first part (Section 7.1) contains the results of the field survey carried out to assess the potential of biodiesel production from waste cooking oil from different vendors within the Ring Road of Kathmandu City. The second part (Section 7.2) contains the details of biodiesel transesterification process for canola, soapnut, jatropha, and waste cooking oil, results of biodiesel fuel characterization tests, Iatroscan test to determine conversion efficiency of transesterification process, and the fatty acid profile for biodiesel feedstocks used in this research. The third part (Sections 7.3, 7.4 and 7.5) contains the results of density tests from high temperature-pressure densitometer, surface tension test results from a Krauss surface tension meter and viscosity test results obtained from rolling ball and torsional oscillating viscometers. Chapter 8 provides the overall discussion of the experimental results and compares the results with contemporary studies whenever feasible. Chapter 9 presents the conclusions drawn from this research and recommendations made for the potential research in the future.

1.5 CONTRIBUTION TO THE NEW KNOWLEDGE

a. This study has shown experimentally that soapnut, jatropha and waste cooking oil could be the potential oil feedstock for biodiesel production in Nepal. Soapnut oil was investigated for the first time for the possible biodiesel source.

b. Sustainability analysis of biodiesel fuels in Nepalese perspectives has been carried out and shown that biodiesel fuels are sustainable against all set criteria including economic, environmental and social, at least locally. Further discussion on food security and institutional component of sustainability has also been introduced.

c. A complete set of tests for the atomization properties (density, viscosity and surface tension) of biodiesel fuels from soapnut, canola and jatropha at elevated temperatures and pressures has been carried out as pure biodiesel and as blends with petro diesel.

d. Nepal still lacks a biodiesel development and promotion policy. This study has recommended some policy and strategy for biodiesel development in Nepal.

CHAPTER 2 LITERATURE REVIEW

2.1 ENERGY SCENARIO IN NEPAL

2.1.1 A Review of Energy Resources and Consumption in Nepal

Located between latitudes 26°22'N to 30°27'N and longitudes 80°04'E to 88°12'E, Nepal is a landlocked country bordered by China and India in South Asia (Figure 2.1). Nepal has a total of 147,181 km^2 of territory. Nepal is characterized by its diverse topography, geology and climate, (Upreti and Shakya, 2010). Nepal is predominantly a mountainous country with huge geographical and climatic variations within a very short span of its width of 130-255 km. The country's elevation varies from 64 m above the sea level to the peak of the world's highest mountain, the Mt. Everest, which is 8848 m. Nepal has numerous river systems that flow from high altitude mountains in the north to the plain in the south. It is one of the countries with most hydropower resources in the world (Ale and Shrestha, 2008), though very little has been harnessed to date.

The population of Nepal was reported to be 26.6 million with an average population growth rate of 1.4 % in 2011 (CBS, 2011). Nepal's GDP per capita was US $ 551 in 2010 and the GDP growth rate was 3.5% (MOF, 2010).

Figure 2.1 Map of Nepal www.sanog.org/sanog4/images/nepal_map.gif (accessed on July 10, 2010)

Energy is considered to be one of the vital inputs to socio-economic development of any country. Due to the insufficient supply of energy for industrial and transportation requirements, Nepal's economic development is severely hampered. Despite the availability of huge energy resources such as hydropower, the average per capita energy consumption in Nepal is approximately 15 GJ, one of the lowest in the world (Shrestha et al. 2003). According to WECS (2006) report, the share of overall consumption is dominated by the traditional fuel (86.8%) followed by commercial (12.66%), petroleum products (9.02%), coal (2.01%) and electricity (1.63%) and renewable 0.54% as presented in Figure 2.2). The same report also revealed that only approximately 33% of the Nepalese population currently has access to electricity from the national grid (in urban and semi-urban areas) and about 7% from non-grid (micro-hydropower and solar). Of the total traditional fuel sources used, over 74% energy is supplied by fuel wood, 7% by animal dung and 5% by residues by agricultural residues. Figure 2.3 shows the sectoral energy consumption in Nepal.

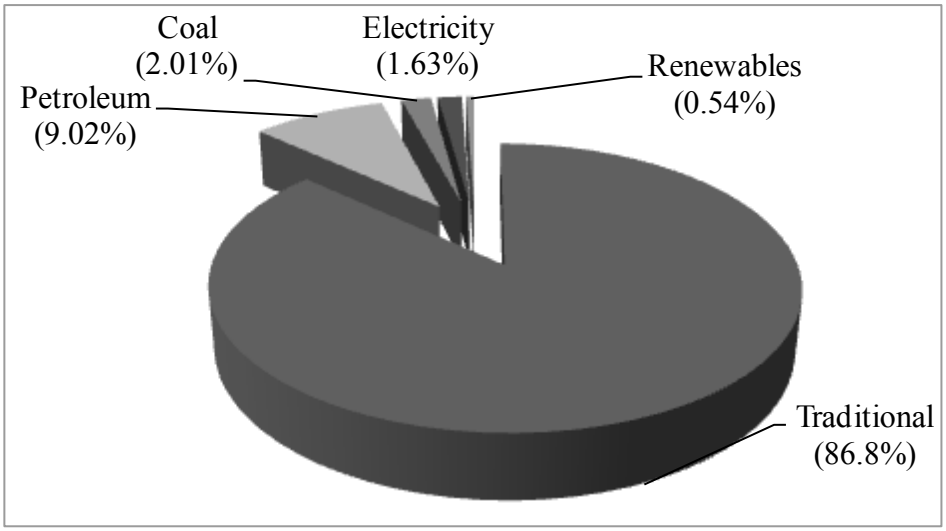

Figure 2.2 Energy consumption by fuel types (WECS, 2006)

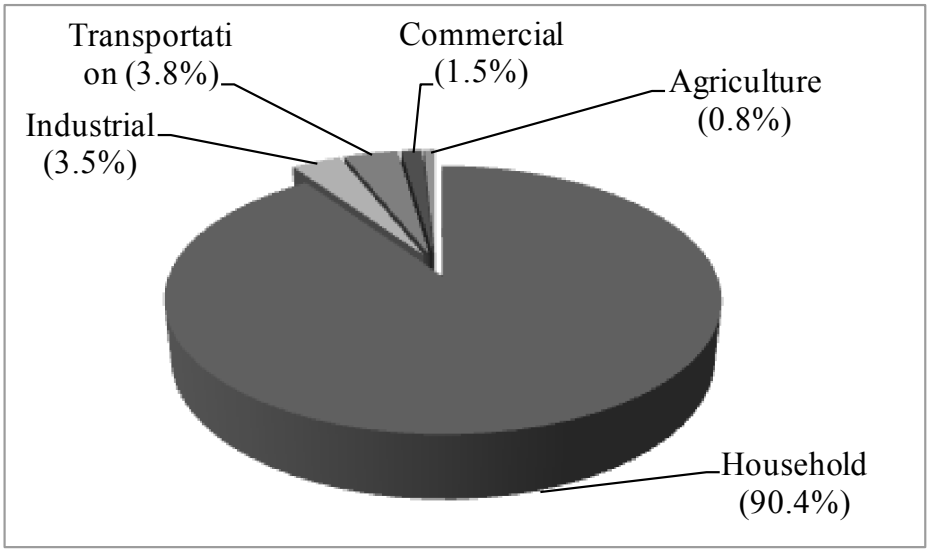

Figure 2.3 Sectoral energy consumption in Nepal (WECS, 2006)

Nepal spent about 40% of its total commodity export earnings to import fossil fuels in 2002-2003 and 51% in 2004-2005 which provided little over 11% of total energy consumed in the country (MOF, 2007). The trend is increasing significantly in recent years. In 2004-2005, the total commodity export earning was NPR 59 billion (Figure 2.1.4).

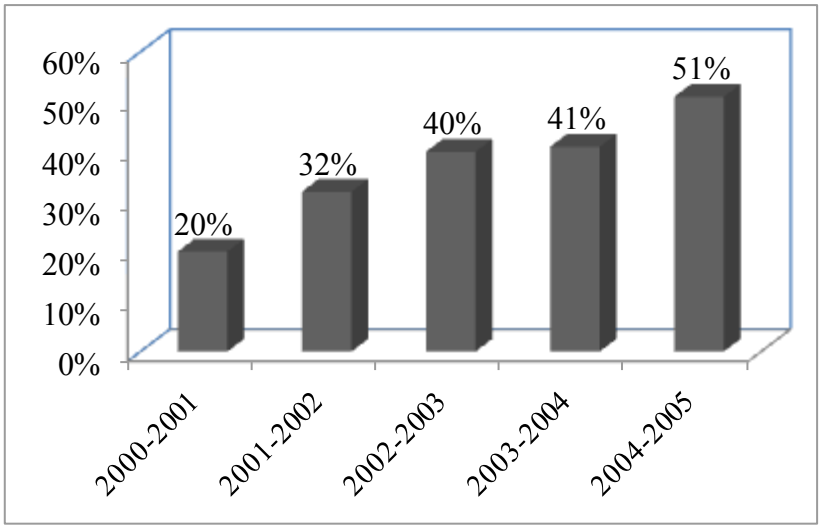

Figure 2.4 Import of petroleum products against commodity export in Nepal (MOF, 2007)

2.1.2 Fossil Fuels and Imports

With an increase in population and rapid urbanization, the consumption of petroleum products is found to increase significantly. It is reported that the demand of petroleum products is sharply growing in Nepal at a rate of 12% each year, which is one of the highest in South Asia (NOC, 2007). Nepal currently imports 100% of its needed petroleum products including diesel, petrol, kerosene, aviation oil, furnace oil and cooking gas from India (Ale and Shrestha, 2008). Nepal purchases crude oil in Kuwait, transports it to Kolkata India for processing and refining, and then transports it to Nepal via road, a total of approximately 1200 km.

There is some scientific evidence that Nepal has some petroleum resources. In order to see the feasibility of petroleum exploration in Nepal, the Petroleum Exploration Promotion Project (PEPP) was initiated by the Department of Mines and Geology in 1982. The major objective of this project was to promote feasibility of petroleum exploration and development activities in Nepal. Several investigations have indicated the presence of a buried blind thrust fold at the base of the Siwalik at the front part of the Main Frontal Thrust (MFT) mainly in the Dhangadi -Nepaljung basin (Nakarmi et al.,

2002). It is believed that the Paleocene rocks are also geologically favourable to act as a good reservoir and source rocks for occurrence of petroleum products in Nepal. However, it has not yet been confirmed by drilling in such sites to prove the most awaited discovery of petroleum in Nepal.

The Water and Energy Commission Secretariat (WECS, 1996) reported that a total reserve of 300 million m^3 of methane associated with ground water distributed over an area of 26 km^2 in Kathmandu Valley is the only natural gas reserve identified so far in Nepal. This report also indicated that the quality of natural gas found in the Kathmandu Valley is viable for domestic as well as industrial applications. However, more qualitative tests are required to reconfirm this conclusion. The reserve will last for 30 years supplying natural gas for 21,000 families at 70% recoverable basis.

Coal consumption is currently met through imports from India. The annual import of coal is about 250,000 tons per year (Nakarmi et al., 2002). The Department of Mines and Geology indicated that there are a few coal resources, especially lignite occurrences in Nepal. Current estimates showed that annual coal production could be about 20,000 tons per year at present (Nakarmi et al., 2002). Raza (2005) reported that the total coal reserve in Nepal was estimated to be 5 million tones. A detailed scientific drilling and exploration is required to investigate the potential of petroleum products.

Figure 2.5 shows the total petroleum import from 1993-1994 to 2008-2009 in Nepal (NOC, 2009). The trend showed that the import of petroleum products sharply increased from 1993-1994 to 2000-2001. After 2000-2001, the import of petroleum products slightly decreased until 2007-2008 due to the political conflict in the country. In 2008-2009, the import of petroleum products increased sharply again as the political conflict was settled.

In 1993-1994, the diesel consumption was 195.47 million litres. In the year 2008-2009, this amount increased by 61.35% and the total diesel consumption was 489.22 million litres in the year 2008-2009 (Figure 2.5). This diesel is used not only for transportation

fuel but also for irrigation pumps, generator sets and other applications. Bhattarai (2009) reported that there was a huge scarcity of diesel in 2007-2008 and the total diesel supply was just over 48% of the total demand. Nepal imported the equivalent of approximately 13 billion rupees in 2007-2008 for diesel fuel.

The import of liquefied petroleum gas (LPG) also increased from 9,308 million tonnes in 1993-1994 to 116 million tonnes in 2008-2009. However, the import of kerosene did not increase, unlike diesel and gasoline and LPG in 2008-2009 because of the people's migration to the urban and sub-urban areas where they have access to electricity and liquefied petroleum gas (LPG).

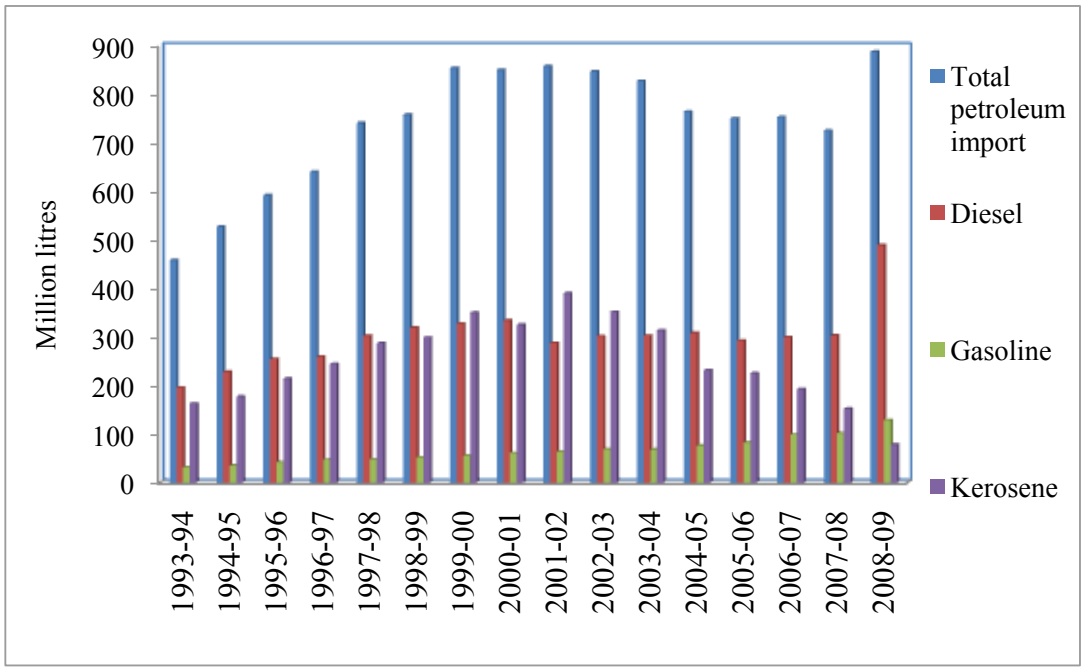

Figure 2.5 Import of different types of fossil fuel in Nepal (NOC, 2009)

2.1.3 Hydropower

There are over 6,000 rivers and rivulets, 80 glaciers, 17 alpine lakes, 40 other lakes, 11 hot springs, all flowing to the Indian territory towards the south (Oli, 2001). However,

the mountainous topography also makes it difficult to build a comprehensive national electrical grid. The theoretical hydropower potential of Nepal with an annual average water runoff of 225 billion m^3 from over 6000 rivers, is estimated to be approximately 83,000MW while technically and economically feasible hydro potential is estimated to be around 43,000MW (Zahnd and Kimber, 2009). Only approximately 1% of the total hydropower resources have been exploited so far (Ale and Bade Shrestha, 2008).

There are three river basin systems and some southern rivers with varying hydropower potentials. Karmacharya (2004) presented the estimated potential and technically feasible hydropower from three river basins and some southern rivers as shown in Table 2.1.1. Some experts have argued that a holistic basin wise development concept is necessary in order to facilitate the equitable socio-economic development of the country.

Table 2.1 Hydropower potential in Nepal (Karmacharya, 2004)

No	**River basin/region**	**Potential (MW)**	**Technically and economically feasible (MW)**
1	Sapta Koshi (East & Central)	22350	11400
2	Sapta Gandaki (Western)	20650	5725
3	Karnali and Mahakali (Far western)	36180	26482
4	Southern Rivers	4100	1125
	Total	83280	44724

Figure 2.6 shows the projection of power requirement based on the current electricity demand until 2024-2025. According to the Nepal Electricity Authority (NEA, 2007), electricity demand is growing by approximately 10% annually. The NEA forecast indicated that the power demand will be approximately 13099 GWh, by 2025 which is equivalent to about 2900 MW. Based on Table 2.1, over 40,000 MW of production is economically feasible. However, the current power production in Nepal is only approximately 700 MW from the beginning of 2007-2008 and has not increased until

recently. This slow pace of development of hydropower is hindering the industrial and commercial sector development in Nepal as there is a huge shortfall of power supply.

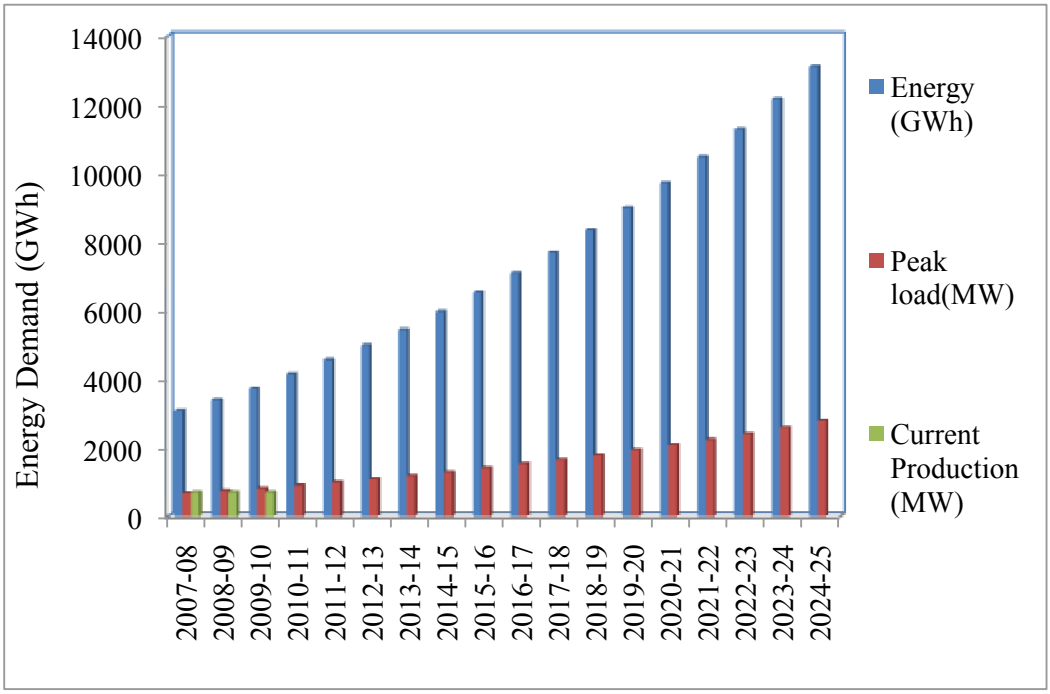

Figure 2.6 Load forecast for 2007-08 and 2024-25 (NEA, 2007)

Several reasons have been cited for the slow pace of hydropower development in Nepal. Despite such huge power potential, policy inconsistencies, planning deficiencies, anomalies in licensing practices, constraints for power purchase agreements for private sectors power development, environmental and financial constraints, security issues and social problems have been seen as major hurdles for hydropower development in Nepal. Hence, in order to expedite the development of hydropower, consistent hydropower policies, integrated planning for road and power transmission infrastructure development, clear licensing and owning policies are essential. Power Purchase Agreements (PPAs) are seen as taking too long which discourages the private sector and also increases the investment costs for the projects. Proper compensation for land for hydro development and rehabilitation policies are required to avoid social problems at the project sites. Development of hydropower projects will not only boost the Nepalese economy but can

also earn large revenue by exporting power to India. India's energy need is sharply increasing to meet the double digit economic growth.

2.1.4 Micro Hydro Power

The majority of Nepalese rural communities are isolated and scattered. Supplying electricity through the national grid in such areas is geographically challenging and a very costly endeavor. Recognizing the tremendous prospect for the development of hydropower, the Government of Nepal has postulated rural electrification on a larger scale to alleviate rural poverty (NPC, 2003). The development of micro-hydro power (MHP) is one of the strategies of the Government of Nepal.

Micro hydro provides electricity in remote areas of Nepal which otherwise may take several years to be connected to the national grid. The energy systems, which generate power from 1 kW -100 kW are termed as micro hydro systems in Nepal. As of 2003, there are 2065 micro-hydro systems in operation with an installed capacity of more than 1.4 MW in various parts of the country. Among them, approximately 1500 kW are peltric systems (1-5 kW capacity), 5500 kW are non peltric micro- hydro systems and 7000 kW are of mechanical type (CADEC, 2003). Table 2.2 shows the status of the micro-hydro power installation.

Table 2.2 Installation of MHP in Nepal to 2003 (CADEC, 2003)

Year of Installation	**Non-peltric (kW)**	**Peltric unit (kW)**	**Mechanical (kW)**	**Total (kW)**
Till Dec 1998	2867.2	857.9	7052.2	10777.3
1999	386.5	226.4	14.3	627.2
2000	719.5	213.5		933
2001	891	81.2	10	982.2
2002	434.3	100.4		534.7
2003	231.1	25		256.1
Total	5529.6	1504.4	7076.5	14110.5

Nepal has enough technical capability to develop micro hydro equipment and accessories. Various types of turbines such as propeller, cross flow, Pelton wheels, multipurpose power units, peltric sets (Pelton wheel and induction motor as a generator assembled together) and traditional improved Ghattas (traditional water wheels with improved efficiency) needed for the MHPs are already developed and manufactured in Nepal. More than 15 companies are engaged in such endeavours. Some local and rural people are also being trained by different agencies to operate and manage micro hydro systems.
MHPs are expected to play a key role in the rural development in Nepal creating local economic opportunities. Even though financing the renewable energy projects is always a great concern, MHPs in Nepal are easily financed by local entrepreneurs and business communities and there is a favourable environment to get support from local banks. There are already a significant number of micro hydro systems financially supported by local communities and local banks as well as local entrepreneurs.

In terms of policy, a state owned public sector called Nepal Electricity Authority, which is responsible for electrification in the country, has no plans to construct new hydro power plants in the MHP range in hilly and mountain areas thus leaving the only option of locally managed MHPs for the electrification of these areas (Banskota and Sharma, 1997; Banskota and Sharma, 1997a). Currently, the Alternative Energy Promotion Centre (AEPC) under the Ministry of Environment is responsible for promoting renewable energy technologies including micro hydro projects in the country. Similarly, Energy Sector Assistance Program (ESAP) and Rural Energy Development Program (REDP) of United Nations Development Projects (UNDP) are also actively disseminating micro hydro technology in the country in association with AEPC.

2.1.5 Biofuels

2.1.5.1 Biomass

Traditional energy sources such as biomass have remained an important primary energy source for over 80% of the population in rural Nepal. Of the total traditional energy resources as showed in the Economic Survey of Nepal (MOF, 2009), fuel wood, livestock

residue and agricultural residue account for 89.2%, 6.6% and 4.2% respectively (Figure 2.7). Over 15 million metric tonnes (MT) of air dried fuel wood were consumed in private households in 1999 while the annual sustainable fuel wood production from accessible forests was only 7 million tonnes (Zahnd et al., 2006). Each household in rural areas consumes between 20-40 kg of fuel wood burning in open fires on a daily basis for cooking, lighting and space heating. Burning fuel wood not only creates an imbalance in natural resources but also has several impacts on the inhabitants due to the indoor pollution.

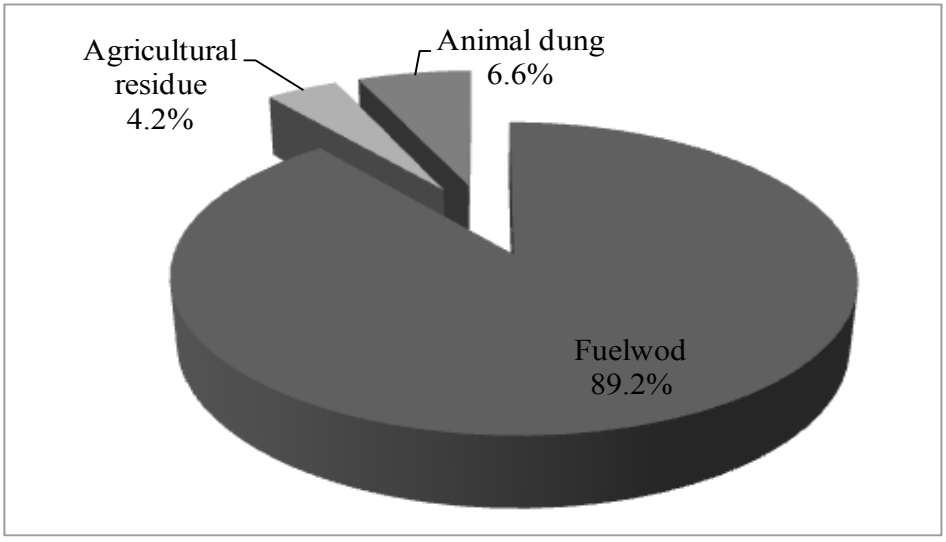

Figure 2.7 Share of traditional biomass energy resources in Nepal (MOF, 2009)

Zahnd et al. (2006) reported that the fuel wood consumption along with agri-residue and animal dung is ever increasing. Figure 2.8 is the summary of biomass used since 1990 till 2002. This shows that biomass fuel has a large contribution in the Nepalese economy. The challenge remains to maintain the sustainable use of biomass by searching into alternate energy sources to reduce the pressure on forest resources and to save the environment.

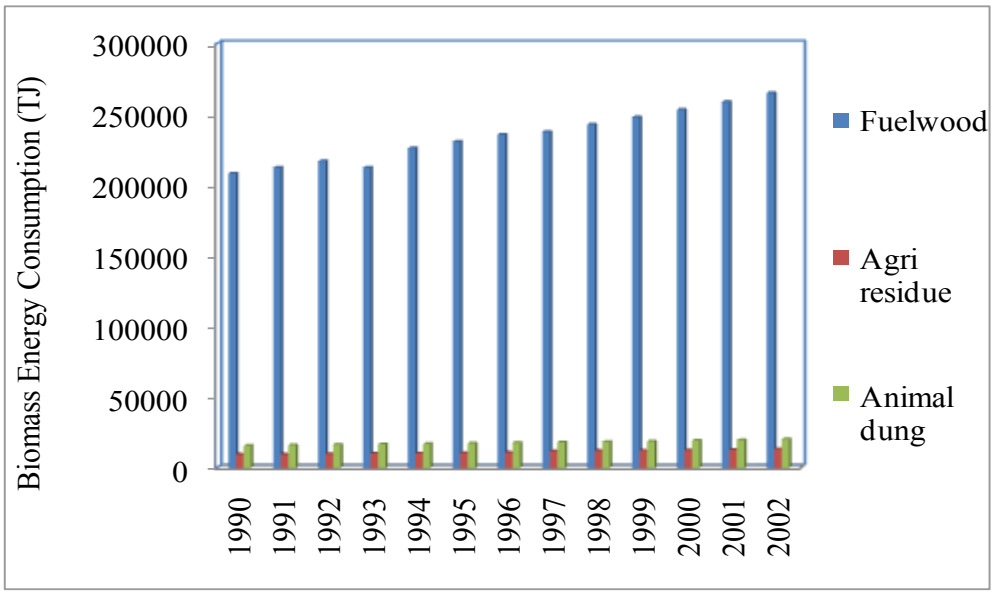

Figure 2.8 Nepal's biomass energy consumption pattern (Zahnd et al., 2006)

Except for the domestic combustion of biomass, there are some brick kilns and cement industries that use the woody biomass combustion. Industrial gasification of biomass has recently come into the limelight but is limited to the pilot and demonstration stage to date.

2.1.6 Biogas

Biogas is a renewable fuel produced by anaerobic digestion of organic materials such as animal dung, sewage, energy crops and other biomass materials. Biogas, which is produced from animal dung has been a major source of energy in rural and semi-urban areas of Nepal. Even though the biogas technology was started from 1970s in Nepal, the biogas installation went up quickly after 1992. Figure 2.9 shows the growth trend of biodiesel in Nepal from 1992 to 2009.

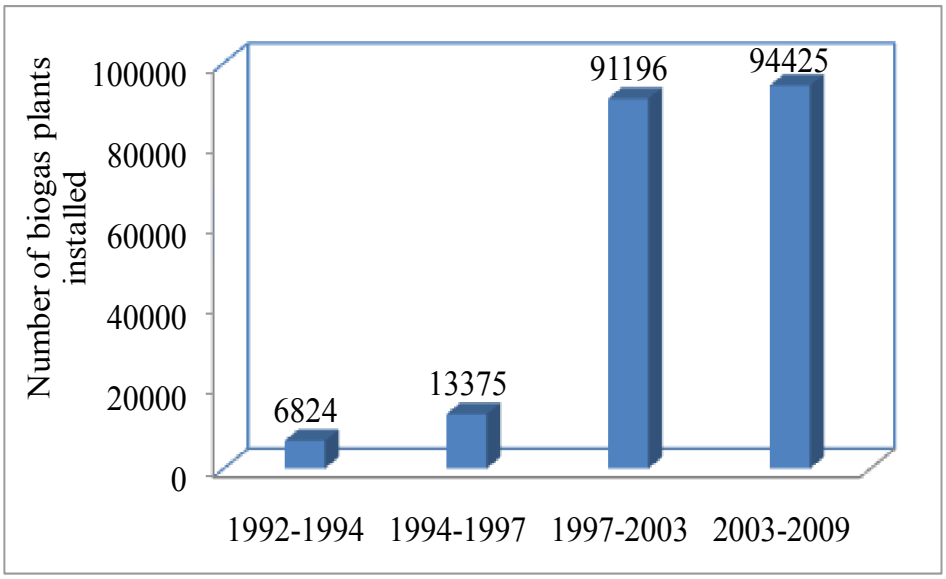

Figure 2.9 Biogas plant installations in Nepal from 1992 to 2009.

Table 2.3 shows the total biogas plants installation potential for Nepal. Of the total potential of 1.023 million biogas plants, approximately 0.504 million plans are feasible. The potential was estimated based on the total households with cattle and buffaloes as of 2001. BSP-Nepal is an ISO 9001-2000 certified in recognition of its strong quality and subsidy administration system. According to BSP (2009), there are 205,820 family sized biogas plants (4, 6 and 10 m3) installed in various parts of the country.

Table 2.3 Total biogas installation potential in Nepal (BSP, 2009)

Technical potential of biogas plants	1.023 million
Market potential	0.504 million
Total installed until 2009	205,820

BSP offers financial as well as technical support for the families willing to install biogas plant in Nepal. The Government of Nepal through over 200 micro finance institutions offers micro-loans to the families willing to install biogas plants at a household level. The biogas sector also generates over 11,000 jobs in the country (AEPC, 2008). The Biogas development program is being developed as a first Clean Development Mechanism CDM

project in Nepal. The CDM has become the alternate source of financing biogas projects in longer terms. Currently, Nepal receives half million dollars annually as a CDM fund for biogas development. Thus, CDM generates substantial revenue which can be used to offset foreign aid and sustain the household energy technology offering global environmental benefits (Pandey, 2006). Hence biogas plays an important role in the Nepalese energy sector.

2.1.7 Liquid Biofuels

Liquid biofuels are the renewable energy sources derived from biological origin. Biodiesel, bioethanol, biomethanol, pyrolysis oils are liquid biofuels. These biofuels are produced from biomass using chemical extraction or processing. Liquid biofuels are required to derive from non-food biomass materials. So far, no liquid biofuels have been produced commercially in Nepal.

With huge geographical diversity (76 m from sea level to the highest peak in the world at a short width of less than 300 km), Nepal is rich in biodiversity, particularly renewable biomass resources. It has numerous varieties of fruit bearing plants and vegetables with different types of edible and non-edible oils. Liquid biofuels are one of the clean fuels that can be used for cooking, lighting, running vehicles and generation of power to run stationary engines. Currently gasoline and diesel are used for transportation and stationery engine and fuel oil is used for thermal generation. The production of liquid biofuel in Nepal can substitute or replace at least some part of fossil fuel import in the country.

2.1.8 Biodiesel

As discussed in Section 2.1.2, Nepal imports all petroleum products to meet its requirement for transportation as well as for stationary engines. Biodiesel is a feasible alternative to supplement or replace petrodiesel. Nepalese forests are reported to have

vast quantity of oil bearing plants and nuts which can be utilized to produce biodiesel as an alternative fuel.

Various community based organizations and private companies have recently started jatropha faming in the country. Alternative Energy Promotion Centre (AEPC) Nepal is responsible for the promotion of all alternative energy in Nepal. AEPC has signed agreements with 11 organizations to produce jatropha seedlings to produce feedstock for biodiesel. AEPC (2009) recently signed contracts with four organizations to carry out pilot tests for biodiesel production from jatropha as a feedstock.

Chapter 4 discusses the availability of potential biodiesel feedstocks in Nepal as well as some policy issues and recommendations for jatropha promotion in Nepal.

2.1.9 Bioethanol

Production of bioethanol is also very important in Nepal as the transportation industries face a severe shortage of gasoline all the year-round. Figure 2.10 shows a glimpse of gasoline shortage as the motorcyclist lined up to get a few litres of gasoline. Nepal imported 31.47 million litres of gasoline in 1993-1994 which increased to 101.62 million litres in 2007-2008 (Figure 2.1.10) (NOC, 2009). In 2008-2009, the total gasoline import was 128.37 million litres. Hence, there is a huge opportunity for bioethanol production to supplement gasoline in Nepal. Bioethanol can be produced by hydrolysis or fermentation of forestry and agricultural residue, starchy foods such as corn stalks, cereal crops, sugar cane, sugar beet, switchgrass, sweet sorghum and molasses. Molasses from sugar mills could be the greatest potential source of bioethanol in Nepal.

Figure 2.10 Motorcyclists in queue to get gasoline in Kathmandu, Nepal on March 3, 2008 (http://johnlambert.files.wordpress.com/2008/03/gasshortage.jpg)

Silveira and Khatiwada (2010) studied the potential for ethanol production and fuel substitution in Nepal. This study was based on the established sugarcane production reported in the literatures. The study showed that 18.045 million litres ethanol can be annually produced in Nepal at present without compromising the food production such as sugarcane and sugar. This can reduce as much as 14% of gasoline import and annual savings of US$ 10 million if 20% ethanol mix to gasoline (E20) is introduced. This will have a positive impact in reducing a significant amount of greenhouse gases from the transportation sector. This will help to create more jobs and improve the industrial base in the country. The Government of Nepal in November 2007 has directed a blend of 10% ethanol in gasoline. However, there is no real production of ethanol in the country to date. Hence, bioethanol can play a significant role in the Nepalese transportation sector.

2.1.10 Other Biomass

Solid biomass can be converted to liquid fuels such as biomethanol. Converting waste biomass such as agricultural and forest residues, municipal waste into biomethanol can also supplement gasoline for transportation purposes offering environmental and economic benefits. However, no research has been done to date to produce biomethanol for transportation fuel.

2.1.11 Solar Energy

Nepal lies in the ideal 30° North "solar belt" with approximately 300 sunny days a year. Solar irradiation measured in three different geographical locations in Nepal over the course of two years (2004 – 2005) showed the intensity of 1,950 – 2,100 kWh/year (with an average of 5.342 – 6.027 kWh/m^2 per day). The extreme values were 3.5 kWh/m^2 per day on a rainy overcast monsoon day in July in Kathmandu (1300 m altitude), and 9.9 kWh/m^2 per day on a sunny late autumn day in November, in Simikot in Humla (at 3,000 m altitude). Solar photovoltaic (PV) modules installed at an angle of 30° south (considered as the "Nepal standard") can intercept 4.8 – 6.0 kWh/m^2 solar energy on a daily average in most places in Nepal (Zahnd et al., 2006).

Solar energy has been very popular in rural areas. There are mainly three types of solar-related technologies adopted in Nepal, namely: photovoltaic (PV) technology-related technology for lighting, communication towers and water pumping; active thermal solar collectors for drying herbs and fruits (solar dryers); and domestic solar water heating technologies. The Energy Sector Assistance Program (ESAP) of Alternative Energy Promotion Center (AEPC) is supporting Solar Energy Support Program (SSP) which is funded by Denmark, Norway and the Government of Nepal. SSP had installed 87,245 solar home systems (SHS) by the end of 2007 (AEPC, 2008). SSP has also planned to install approximately 150,000 SHS by the month of March 2012 as the demand continues to grow.

ESAP started providing subsidies from 1997 for the installation of SHS between 10 W to 75 W for lighting, but the sizes of 30-50 W are more popular (Pokharel, 2007). SHS provide lighting loads for an average of four hours a day in rural areas. In addition to the electricity generation, solar technologies are used for drying agricultural and herbal products. Most of the dryers used in Nepal are of the box type (with an average of 1.5 m^2 irradiation area), but the tunnel and cabinet type dryers are also found in the market (Pokharel, 2007). Over 1000 of such dryers are operational in various parts of the country.

Domestic solar water heating systems are the most popular and simple technologies used in Nepal from the mid 1970s. These systems are available in the ranges from 100 -600 litres in capacity. Over 50,000-80,000 such systems are reported to have been installed in households and hotels in urban areas of Nepal (Zahnd et al., 2006).

2.1.12 Wind Energy

Due to its high mountain terrain, Nepal has very good wind energy potential in the mountains. Even though there were previous attempts to harness wind as a source of mechanical and electrical power generation, no significant achievement has been made so far. Nepal Electricity Authority (NEA) established a pilot project of 30 kW in Kagbeni, Mustang, in 1989 as a rural electrification project, but the project failed due to the collapse of the tower. The development of wind energy in high mountain terrains avoids the extension of costly grid electricity to those areas. Wind energy can generate a large sum of revenue from the Clean Development Mechanism (CDM) funding.

A study carried out by SEWRA (2006) reported that the potential area available for wind power development in the country is above 6000 sq. km. The average wind power density within this area exceeds 300 watt/m^2. It was also estimated that more than 3,000 MW of electricity could be generated at the rate of 5 MW per sq km. The study also showed that the high and middle mountain areas of the country have the most generating potential for wind power. The annual average energy potential is found to be an average of 3.38 MWh/m^2 at different geographic locations. SEWRA (2006) also reported that resource grid generated at 50 m height over Kagbeni of Mustang region showed very high (as high as 46.76 m/s) wind speed, and 238 kW/m^2 power density. In Nepal, it is estimated that the commercially viable wind power generation potential is approximately 500 MW (SEWRA, 2006)). Dahal et al., (2004) reported that Kali Gandaki valley of the western district of Mustang is one of the famous river valleys for wind which generally flows toward upstream (south to north). The wind data also reveals that the variation of wind speed generally ranges from 0 m/s to 23 m/s. Rajbhandari, (1998) reported that there is a

potential of generating over 200 MW of electrical power within 12 km valley of Kagbeni area alone.

2.1.13 Geothermal/Hydrothermal Energy

The Ninth Plan (1996-2001) of government recognized the role of geothermal energy in Nepal. In 2001, government of Nepal began to update the profile of geothermal locations which are popular and easily accessible. There are reports that there are 30 prominent geothermal locations confined to three distinct tectonic areas in Nepal which are feasible to use as energy sources (Ranjit, 2005a). These springs are located in the higher Himalayas and north of the Main Central Thrust (MCT), situated between the lower and higher Himalayas. The other set of geothermal reserves are located close to the MCT and the last set of reserves is located in the Main Boundary Fault of the country which was developed as a result of the collision of the Indian Plate with the Eurasian Plate.

The maximum surface temperatures recorded in some of the thermal springs are in the range of 347 K in the Sribagar area in Nepal. This is followed by 344 K in Bhurung Tatopani at Myagdi district and temperatures above 313 K were recorded for six other springs (Ranjit, 2005b).

The chemical composition of geothermal water in Nepal was reported by Ranjit (2005a). The reports indicated that the pH of geothermal water ranged from 7-9. The chemical constituents found in geothermal water were Na, K, Mg, Cl, SO_4, HCO_3, SiO_2, and B. The chemicals indicated that geothermal water in Nepal has extensive interaction with rocks even at low temperatures. The reports of chemical analyses of geothermal water including isotopic composition showed that a large geothermal reservoir exists in the western Nepal. Hence, there also exists a good opportunity to exploit this energy resource for various direct heating uses in this region because of the favorable terrain. Further studies are needed to assess the electricity generation potential in Nepal.

2.2 REVIEW OF EXPERIMENTAL METHODS AND THEORETICAL PREDICTION MODELS

This section contains a description of fuel atomization properties such as density, viscosity and surface tension and the existing models for their prediction. A review of experimental methods for these properties is presented in Appendix A.

2.2.1 Density

The density of a material is defined as the mass of a given volume of material under specific conditions. The material becomes denser if the amount of material per unit volume increases. Specific gravity, which is different than density is the ratio of density of given volume of sample material to the density of the same volume of water. The density of fluids is affected by temperature and pressure. However, the variation due to temperature and pressure is much higher in gases than in liquids. Despite the simplicity in its definition, the accurate measurement of density of fluids is complex.

Density is one of the important properties of biodiesel fuels. Different techniques are available to predict and measure the density of biodiesel fuels. However, it is of great interest to measure the density of biodiesel fuels at elevated temperatures and pressures because the fuel atomization in the engine environment occurs at high temperature and pressure. There are various types of density measuring techniques available which can be used at different temperatures and pressures for various types of fluid.

2.2.2 Prediction Models for Density

The molar volume V for a fluid can be expressed as a function of temperature and pressure P (Hong-Yi and Guojie, 1995).

$$V=f(T,P) \tag{2.1}$$

The modified Rackett equation expresses the relationship between the specific volume of liquid and the temperature. The equation used to estimate the specific volume (Vs) with reference to the temperature can be expressed as below.

$$Vs=V_{sR}\ Z_{RA}^{\varphi} \qquad (2.2)$$

where V_{sR} is the experimental volume, Vs is the volume at the reference temperature T_R, $\varphi = \left(1 - T_{rs}\right)^{2/7}$ - $(1\text{-}T_r - R)^{\frac{2}{7}}$ and Z_{RA} is the unique Rackett constant for each compound which can be determined if at least two experimental densities are known as shown in equations 2.3 and 2.4.

$$V_{sR=}\ Z_{RA}\ \frac{RT_C}{P_c} \qquad (2.3)$$

T_c and P_c, T_{rs} are critical temperature and pressure and reduced temperature at saturation. The Rackett constant Z_{RA} can be found using the relationship given by:

$$Z_{RA} = \left(\frac{V_S P_c}{RT_c}\right)^{\frac{1}{1+(1-T_{rS})^{\frac{2}{7}}}} \qquad (2.4)$$

The Rackett equation modified by the Spencer and Danner (1972) can also be used to estimate the temperature dependent density of pure components of any liquid using the following relationships:

$$\rho = \frac{\rho^R}{Z_{RA}^{\varphi}} \qquad (2.5)$$

where ρ^R is the experimental density value in kg/m^3 at the reference temperature T_R, Tc is the critical temperature.

The density temperature correlation differs from liquid to liquid and different temperature ranges. This equation can be used to predict the density at higher temperatures and

atmospheric pressure. This equation was used by Yuan et al. (2003) to calculate the density of biodiesel. However, this equation cannot be used to predict the density of liquid at higher pressures.

2.2.3 Theory of Viscosity

Viscosity is defined as the measure of internal resistance of the fluid to flow. The viscosity of liquids can be described by suspending two horizontal parallel plates in a liquid separated by a very small distance, y_0 (Figure 2.11). If the upper plate is maintained to be stationary and the lower plate is set to move, the layers of the liquid right next to the lower plate will also start to move. The movement of the bottom layer of fluid will result in the movement of layers above it. The velocity of a fluid layer in contact with the stationary plate will be zero at steady state conditions, while the absolute velocity of the fluid layer with moving layers will be v_o. It is considered that for Newtonian fluids the velocity profile in the intermediate fluids layers changes linearly with distance y from the stationary plate.

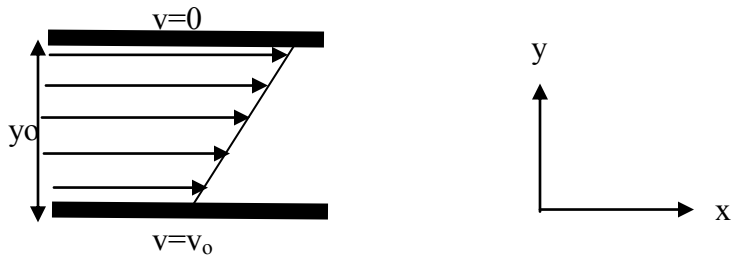

Figure 2.11 Relative movement of fluids particles in the presence of shear stresses

The velocity can thus be expressed by the following relationship:

$$v = v_o \frac{y}{yo} \tag{2.6}$$

A shear stress acts opposite to the direction of motion to maintain the upper plate stationary by the surface area of the plate. This shear stress is proportional to the velocity of the lower plate and inversely proportional to the distance of the two plates and can be

expressed by the relationship as presented in equation (2.7). This is also known as Newton's Law of viscosity.

$$\tau_{y,x} = -\mu \frac{dv_x}{dy} \quad (2.7)$$

where ɽ is the shear stress, the subscript 'y' denotes the area over which the shear stress acts, the subscript x is the direction in which the shear stress acts. The minus sign indicates that shear stress is applied from the region of higher velocity to a lower velocity.

Dividing and multiplying the right side with density of the liquid, the equation can be expressed as in (2.8).

$$\tau_{y,x} = -\frac{\mu}{\rho} \frac{\rho dv_x}{dy} \quad (2.8)$$

By definition, the dynamic viscosity divided by density is called kinematic viscosity ($\eta = \frac{\mu}{\rho}$). Hence the equation 2.9 is reduced to the following.

$$\tau_{y,x} = -\nu \frac{\rho dv_x}{dy} \quad (2.9)$$

The kinematic viscosity is defined as the quantity obtained by dividing the dynamic viscosity by the density of the fluid at the same temperature and pressure. It is referred to as the momentum diffusivity of the fluids. Viscosity is the major factor resisting motion in a laminar flow. However, when the flow regime is increased to the turbulent region, pressure differences resulting from eddy currents offer more resistance to motion than viscosity (Kandill, 2005).

2.2.4 Models for Predicting Viscosities of Liquids

There are various methods available for predicting viscosity of fluids including biodiesel fuels. One of the widely used models for predicting viscosity of binary mixtures was given by Grunberg and Nissan (1949). The equation can be expressed as:

$$\ln \mu_m = \sum y_i \, l_n \mu_i + \Sigma_{i+j} \Sigma \, y_i \, y_j \, Gij \tag{2.10}$$

where μ_m is the mean viscosity of mixture (Pa.s), $\mu_{i,j}$ is the viscosity of individual components (Pa.s), $y_{i,j}$ is the mole fraction and Gi,j is the interaction parameter (Pa.s). This was reported to be one of the most suitable equations to estimate the viscosity of liquid mixtures. This method was developed to estimate the viscosity of binary mixtures. It was reported that good results were obtained for some associated fluids with errors less than 5-10% (Allen, 1998). This method is applicable in cases where the viscosity of individual components is known. Allen (1998) derived a simple correlation function for biodiesel viscosity prediction from the Grunberg and Nissan (1949) equation by omitting the interaction parameter, and is presented in equation 2.11. This equation can be used for predicting the viscosity of mixtures

$$\mu_m = e^{(\Sigma x_i \, ln\mu)} \tag{2.11}$$

where η_m is the viscosity of the mixture (Pa.s), $\eta_i$is the viscosity of component i, (Pa.s) and $x_i$is the mass fraction of the component i.

Camunas et al. (2001) developed a model for predicting viscosity of liquids at high temperature and high pressure as shown in Equation 2.12.

$$\mu\,(p,T) = \mu_o(T)\, e^{\left(D\, ln\left[\frac{E\,(T)+p}{E(T)+p_o}\right]\right)} \tag{2.12}$$

where D and E are temperature dependent constants, pressure (p_o)= 0.1 MPa, μ(T) is the temperature dependent viscosity at a reference pressure and can be obtained using the

following relationship $\eta\ (T) = A(T)\ e^{\left(\frac{B}{T-C}\right)}$.The constants A, B and C were found experimentally for each pressure. Thus the temperature and pressure dependent viscosity equation can be expressed as equation (2.13).

$$\mu\ (p,T) = Ae^{\left[\frac{B}{T-C}\right]}e^{\left(D\ ln\left[\frac{E\ (T)+p}{E(T)+0.1}\right]\right)} \tag{2.13}$$

Eyring and co-workers developed the following semi-empirical expression for liquid viscosity (Macias-Salinas et al., 2009).

$$\mu = \left(\frac{\delta}{\alpha}\right)^2 \frac{Nh}{V}\ e\exp\left(\frac{\Delta G}{RT}\right) \tag{2.14}$$

where N is Avogadro number, h is Plank's constant and R is ideal gas constant, V is the liquid molar volume, T is the temperature, δ and α are length parameters that represent the distance between molecules, ($\frac{\delta}{\alpha}$ is taken as 1 with no loss of accuracy), and ΔG is the activation energy needed to start the movement of the liquid. The value of ΔG is determined empirically. For liquid mixtures, the viscosity expression based on Eyring theory can be expressed as below.

$$\mu_m = \frac{(\mu V)_{ID}}{V_m}\exp\left(\frac{\Delta G*}{RT}\right) \tag{2.15}$$

$$(\mu V)_{ID}=\exp[\textstyle\sum_{i=1}^{c} x_i\ ln\left(\mu_i^o \mu V_i^o\right)] \tag{2.16}$$

where, V_m is the molar volume of the mixture, V_i^o is the molar volume of the pure liquid, $\mu_i^o$is the viscosity of pure liquid, ΔG* is the excess activation free energy of flow and $(\mu V)_{ID}$ is the kinematic viscosity of an ideal solution.

There are various other models developed to calculate the viscosity of biodiesel and its blends at high temperature. Tat and Van Gerpen (1999) developed an equation by modifying the Andrade equation which was also used by Tate et al, (2005) and Joshi and Pegg (2007) in order to predict the viscosity of pure biodiesel and its blends.

$$\ln(\eta)=A+\frac{B}{T}+\frac{C}{T^2} \quad (2.17)$$

where μ is kinematic viscosity, T is absolute temperature, A, B and C are the constants specific to the fluids.

2.2.5 Surface Tension

The surface tension is an important property of any liquid. The cohesive forces between liquid molecules is defined as surface tension. The liquid molecules form a thin film making it more difficult to move the liquid from the surface than to move it when submerged. The polar liquid molecules in the bulk liquid arrange themselves so that the cohesive forces between the molecules are shared by the neighboring molecules which lead to zero net force. However, in the surface, the molecules lack an equalizing force leading it to a non-zero net force. This force per unit length along the liquid surface is known as surface tension. It is known that distilled water at 293.15 K has a surface tension of 72.8 mN/m. The tension force between the two immiscible liquids, such as water and oil is called interfacial tension. Gibbs defined surface energy as the difference between actual energy of the system and sum of the energy of its components if there was no interface between them. The interface as defined by Gibbs is a mathematical surface with no thickness.

Surface energy is the energy needed to create a surface. The energy per unit interfacial area needed for the separation of two liquid molecules is also termed as cohesion energy (E_c). The cohesion energy is considered to be twice the surface tension of the liquid σ_l.

$$\sigma_l=\frac{E_c}{2} \quad (2.18)$$

2.2.6 Prediction Models for Surface Tension

The surface tension of any liquid mixture is not a simple function of the surface tension of the pure components because in a mixture the pure components of the surface are not necessarily the same as the bulk (Reid et al., 1987). The study also indicated that the surface tension of a mixture calculated using the sum of the mole fraction average is usually less than the measured surface tension.

Allen et al. (1999), Tate (2005) and Joshi (2007) used the Macleod-Sudgen method to determine the surface tension of methyl esters. The following was the correlation used:

$$\sigma = ([p] \times \rho_b)^4 \left[\frac{1 - T_r}{1 - T_{br}} \right]^{4n} \tag{2.19}$$

Here, ρ_b is the density of test liquid at normal boiling point, T_r is the reduced temperature (T_r=T/T_c) and T_{br} is the reduced temperature at normal boiling point.

For pure non-aqueous compounds the Sugden equation presented by Meissner and Michaels (1949), was reported to offer good correlation with experimental data while predicting the surface tension of pure components. The Sugden expression is presented below:

$$\sigma = \left(\frac{[P]}{M} \times \rho \right)^4 \tag{2.20}$$

where σ is the surface tension of the pure component (mN/m), M is the molecular weight (g/mole), $[p]$ is a-temperature-independent parameter called "parachour" of pure components, ρ is the density of the liquid in (g/ml).

Ejim et al., (2007) used the following model to estimate the surface tension.

$$\sigma = \frac{673.7 \times SG \times \left(1 - \frac{T}{T_c}\right)^{1.232}}{(1.8 \times T_b)^{1/3}} \qquad (2.21)$$

where σ is surface tension, (mN/m), T_b is the mean boiling point (K), T is the temperature at which σ is determined, SG is the specific gravity, T_c is the critical temperature (K). Here, it is necessary to find the critical temperature T_c, to determine the surface tension. T_c can be found from the following equation:

$$\mathrm{Tc} = 9.5233 \times \left[\exp\left(-9.314 \times 10^{-4} T_b - 0.544442 SG + 6.4791 \times 10^{-4} T_b SG\right)\right] T_b^{0.81067} \times SG^{0.53691} \qquad (2.22)$$

2.3 SUMMARY OF CHAPTER 2

A literature review of the overall energy scenario in Nepal has been presented in Section 2.1. All energy sources and their potentials to be exploited have been discussed. Section 2.2 contains a description on fuel atomization properties such as density, viscosity and surface tension. This section also provided description on existing models for predicting these properties. A review of experimental methods for these properties has been also reviewed and is presented in Appendix A.

In the next Chapter, various theory of sustainability has been discussed and sustainability of micro hydro and biodiesel fuels has been evaluated using strong sustainability criteria.

CHAPTER 3 EVALUATING SUSTAINABILITY OF ENERGY DEVELOPMENT IN NEPAL

This chapter presents a review of the theory of sustainability and various models for evaluating the sustainability of energy resources and fuels. The advantages and drawbacks of these models have also been discussed. Sustainability of micro hydro projects and biodiesel fuel in the Nepalese context has been evaluated using the strong sustainability criteria.

3.1 THEORY OF SUSTAINABILITY

The issue of sustainable development emerged from numerous environmental movements. This issue in terms of technological development was raised more directly by the International Union for Conservation of Nature (IUCN) in Ottawa conference in 1986 and by Brundtland Commission report "Our Common Future" in 1987. The Earth Summit held in Rio De Jeneiro Brazil in 1992 was the leading international forum to bring sustainable development agenda into the global development.

Sustainability issues are more prevalent today because of the adverse impacts of human activities on the environment. The United Nations Division for Sustainable Development (DSD, 2012) states the economic, environmental and social components should be integrated in order to achieve sustainable development at all levels of development activities. DSD is a UN agency that promotes sustainable development globally through technical assistance and capacity building. The World Commission on Environment Development (WCED, 1987) defines sustainability "as the development endeavor that meets the needs of the present generation without compromising the future generations needs". However, neither is there a limit of the need of the present generation nor can the need of the future generations be predicted in advance. Even though the definition of sustainability remains highly contentious, there is no disagreement of the need to make all development endeavors environmentally sustainable and socially acceptable.

Sustainability analysis offers a guideline for future development so that the natural resources are used in such a way that they have little or no negative impacts on the environment. However, most of the 'development stakeholders' today use sustainability to make their plans, programs, and policies more saleable rather than concentrating on operational and practical aspects. The projects implemented at a community or regional level could have an impact at the global level depending on its scale. The social equity, the quality of the output from a project and the environmental impacts at the local level are the key factors affecting sustainability at the project level. The impact of system boundary, the time horizon, and with system quality for which the projects serve or might have impacts on the environment are the key three factors that define the sustainability of any system, including energy. However, it is extremely difficult to define such factors at the operational level. It is essential that the decision making to promote sustainable development and its implementation at the operational level should represent the interest of all the stakeholders.

Sustainable development is directly linked to global development objectives. Moreover, the holistic approach of sustainable development has always been linked to energy development and energy development has always been the centre point of sustainability issue because these projects have several impacts on the environment. The alleviation of poverty, sustainability and stakeholders' participation are projected as global objectives of sustainable development (Lele, 1991). The rampant use of natural resources with improper policies creates severe socio-environmental problems. The lack of resources for large populations in the least developed countries forces them to use vulnerable natural resources for their survival. This has been an issue even in developed countries as development activities have exerted tremendous pressure in depleting natural resources such as fossil fuels. It is widely accepted that there has been irreversible damage to the natural environment that has caused climate change, ozone layer depletion, land degradation and biodiversity loss (Goodland, 1992; Costanza et al 1997; Goodland 1999). The technological development and the economic growth that mankind has advanced, the extraction of energy from fossil resources, and production of large volume of wastes have raised serious concerns

about global sustainability. In order to maintain the global sustainability, any system that supplies energy must be clean and renewable.

Despite its widespread acceptance as a nominal goal for policy makers, sustainability is still a very complex issue and is interpreted differently. The ecological economists argue that the natural capital has a key role to play in resource flow for economic life support services on which the human beings depend (Prugh et al., 2000). Daly and Cobb (1989) expressed the opinion that the natural capital stock should always be kept intact to maintain the sustainability from the flow of resources, as a minimum condition for sustainability. Daly (1994) defined natural capital as the stock that results in the flow of natural resource. The economy is considered to be an open subsystem of the global ecosystem. In order to pursue any economic development activity maintaining the natural capital and ecological sustainability requires that the rate of harvest of renewable resources must not exceed its regeneration rate (Prugh et al., 1999). Similarly, any wastes generated because of the economic activity should not exceed the Earth's assimilative capacity. Another most significant activity to achieve a true sustainability is that the earnings from the depleted natural resources including coal, oil etc should be offset by developing the renewable resources on which future generation can depend.

There are many different criteria developed and used to evaluate sustainability in general as well as different energy sources in particular (Pezzey and Toman, 2002; Segnestam, 2002; Omer, 2008; Lozano, 2008; Winrock International, 2010). Most authors include the environmental, social and economic attributes when evaluating sustainability of any development activity. Some researchers also include technological sustainability as part of sustainability because of the efficiency component of the technology used to harness the natural resources.
Munasinghe (1992) illustrated the concept of sustainability in a sustainable development triangle as shown in the Figure 3.1. The triangle has economic, social and environmental elements of sustainability with the interrelationship of each element to the other. Economic sustainability assumes the exploitation of a maximum benefit

while maintaining the stock of natural capital intact. The maximum benefit is related to the economic efficiency that ensures optimum production and consumption of resources. The maximum sustainable consumption obtained from the natural resource is the amount that can be consumed without impoverishing themselves (Hicks, 1946). The economic sustainability must ensure that the key economic services are delivered effectively even during economic recessions. The environmental sustainability according to Munasinghe (1992) focuses on the long-term viability and health of living organisms. This applies both to the natural as well as artificially managed ecosystems such as agriculture systems. Over exploitation of natural resources causes resource degradation, loss of biodiversity and pollution which are undesirable to human beings and pose a threat on health and resilience. Environmental sustainability requires that an ecological system should maintain a safe level of biodiversity for an infinite time horizon and any by-products of consumption should not exceed the assimilative capacity of the earth.

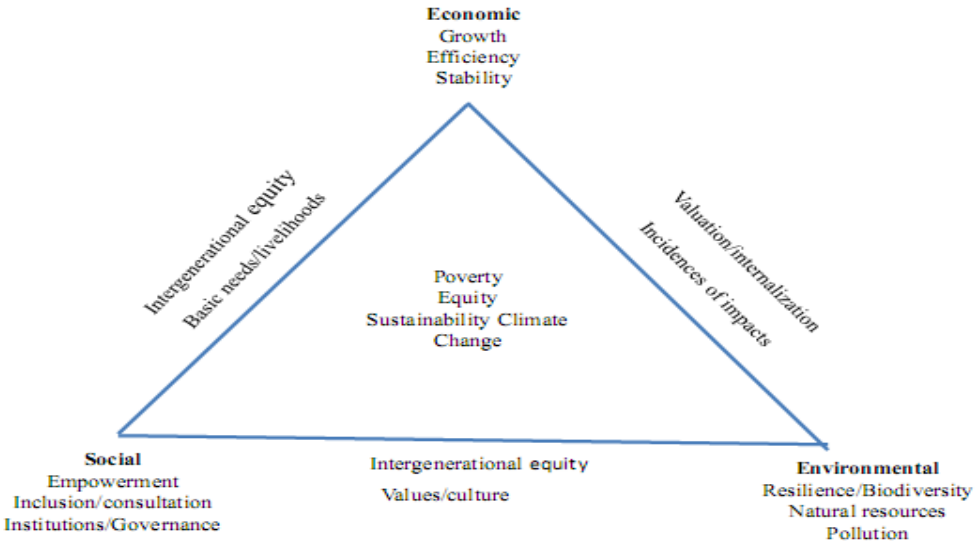

Figure 3.1 Sustainable development triangle – key elements and interconnections (Redrawn from Munasinghe, 1992)

Similar to that of environmental sustainability, social sustainability is related to reducing vulnerability and maintaining the health of social, cultural and institutional systems. The development projects should address the socio-economic need of the individual as well as the overall society maintaining the social capital intact through

shared learning, enhanced education and social values. It is common that the economic analysis of the projects is more focused on the rate of return than the long-term negative impacts that may ruin the socio-cultural diversity locally as well as globally. For any projects to be socially sustainable, participation of local people in the project, maintaining the ecological and economical capitals, maintaining the socio-cultural diversity is extremely essential. Goldemburg (1996) argued that energy has a strong linkage with economic well-being, human livelihood and the environment. The issue of sustainability in energy development emerged due to the fact that major energy resources come from non-renewable fossil resources. Moreover the rampant use of these resources is making the globe insecure for all living beings because of enormous environmental problems caused by their energy source extraction and utilization (Hohmeyer, 1996). The sustainability of energy sources has brought the discussion into the development and operationalization phase of any development activities. Theoretically, the operationalization phase has two views expressed as weak and strong sustainability. Sustainability requires non-decreasing consumption of environmental goods and services to maintain the total capital stock of the society (Common and Perrings, 1992).

The United Nations (1999) extended the framework for sustainable development through the Commission on Sustainable Development (CSD) and outlined four primary dimensions, namely: social, economic, environmental, and institutional. Kunen and Chalmers (2010) developed a framework and criteria for the sustainable development of biofuels. Khatiwada (2010) carried out a detailed sustainability analysis for bioethanol production in Nepal using these four indicators of sustainability. Based on the review of these studies, a summary of sustainability criteria and their components to evaluate sustainability of biodiesel fuel is presented in Table 3.1 below, in which a fifth dimension, food security, has been added.

Table 3.1 Sustainability criteria for evaluating the biofuels (Summarized from Kunen and Chalmers (2010) and Khatiwada, 2010)

Environmental	Fossil fuel substitution
	Renewability
	Life cycle energy balances
	Life cycle GHG balances
	CO_2 emissions from fuel substitution in automobiles
	Local air pollution
	Water and wastewater management
	Land-use change (direct and indirect)
	Land and soil pollution
	Utilization of natural resources
	Protecting forests (avoiding deforestation)
Economic	Investment (cost benefit analysis)
	Dollar savings on oil import, improved trade balances
	Availability of resources
	Agricultural and industrial growth, diversification
	Economic instruments: subsidies/tax exemptions
	Carbon trading under CDM program
	Energy security
Social	Employment generation, and wages
	Rural and local development
	Workers' facility and safety
	Poverty reduction
	Equality, equity and cultural
Institutional	Stakeholders
	Technical
	Political
Food Security	Local and national food security, food vs fuel use

3.2 METHODS FOR EVALUATING SUSTAINABILITY

3.2.1 Life Cycle Method for Fuel Sustainability

Various methods have been developed to evaluate sustainability of fuels as well as other development activities. Zhou et al. (2007) developed a life cycle method to evaluate the sustainability of fuels including conventional gasoline, conventional diesel oil, compressed natural gas, mixture of 85% natural gas derived methanol and 15% gasoline by volume (M85), mixture of 85% corn ethanol and 15% gasoline by volume (E85), and pure ethanol (E100) derived from cassava. Zhou et al. (2007) used economic, environmental, energy and renewability indicators to evaluate sustainability of the fuels which is summarized below. The life cycle analysis was used to evaluate different indicators.

Economy Indicator (EcI) was evaluated using the life cycle cost (LCC) per kilometer of the fuels to the consumers. The fuel with the lowest life cycle cost to the consumers was considered to be more sustainable than others. The LCC is represented by the following equation, where C_i is the cost at the i_{th} stage of the life cycle to the consumers (Zhou et al. (2007).

$$LCC = \sum_i C_i \tag{3.1}$$

Environment Indicator (EnI) was evaluated using the total carbon dioxide (CO_2) emissions and their corresponding global warming potential (GWP) of the fuels evaluated. The analysis was also based on the assumption that the CO_2 produced from biofuel burning is considered biogenic and will not contribute to global warming. The fuel with the lowest GWP per kilometer among the fuels was considered more sustainable than others. The life cycle analysis reported that the life cycle CO_2 emission from cassava-based ethanol and gasoline were 191 g CO_2/km and 490 g CO_2/km respectively Zhou et al. (2007). The CO_2 emissions from the ethanol during the operational stage is considered to be biogenic. The EnI is represented by the

following equation, where $\emptyset_i$ is GWP coefficient of i_{th} green house gas and EM_{GWPi} is the emission of i_{th} green house gas per kilometre (Zhou et al. (2007).

$$\text{GWP} = \sum_{\emptyset_i} \times EM_{GWPi} \quad (3.2)$$

Energy Indicator (EeI) is evaluated as the ratio of net energy (NE) yield minus energy consumed during the life cycle of its production to the gross energy (GE) produced by the fuel during its combustion Zhou et al. (2007). It is expressed in terms of MJ/MJ. E represents the total energy consumed during its production life cycle.

$$NE = \frac{GE-E}{GE} \quad (3.3)$$

Renewability Indicator (RI) relates whether the natural resources are being exploited in a renewable mode or not. If the natural resources are extracted at a rate higher than it can be replenished, it is non-renewable or vice versa. Renewability is measured in terms of non-renewable resource depletion potential (NRDP) and is expressed by the following relationship Zhou et al. (2007):

$$\text{NRDP} = \sum_{i=1}^{n} \overline{w}\ m_i\ (1\text{-}RC_i) \quad (3.4)$$

where $\overline{w}$ is the scarcity factor of non-renewable resource, RC_i is the recycle ratio of a non-renewable resource and m_i is the amount of non-renewable fuel consumed and $m_i = \frac{100}{RE_i}$ where RE_i is the remaining amount of one kind of non-renewable resource before it becomes extinct. NRDP takes into account the amount of fossil fuel used and its scarcity relative to other fossil fuels (Zhou et al. (2007).

This is a simple model combining the economic, environmental and renewability indicators. In order to use this model practically, the life cycle emission of the fuels per km to the consumer is required. Also, the life cycle emission is required to estimate the emissions from conventional petroleum fuel and the alternative fuel such

as biodiesel fuel being evaluated. This model does not consider the social indicator to evaluate the sustainability. The model also requires evaluating renewability in terms of the non-renewable resource depletion potential. The details of the data required by this model were not available and this model was not used in this study.

3.2.2 Earth System Model

The Earth System Model for evaluating sustainable development globally was proposed by Schellnhuber (1998;1999;2001) and Claussen et al.(1999). This theory assumes a coupled dynamic relationship between humans and the environment (Phillips, 2010). The Earth System Analysis also depicts the relationship between the ecosphere and the anthroposphere. The Natural Earth system, which is also known as the ecosphere includes both the biotic as well as the abiotic world including socio-economic and cultural activities of human beings (Phillips, 2010). The ecosphere consists of the atmosphere, the geosphere or lithosphere, the hydrosphere, and the biosphere while the anthroposphere is part of the environment made or modified for use in human activities and human habitants. The Natural Earth Systems N is represented by the vector $\dot{N}$ as a function of time *t* (Schellnhuber, 1998;1999). The vector $\dot{A}$ represents the anthroposhere as a function of time. The Natural Earth System Model and the global climate impact model for the historical past is represented by equation 3.5.

$$\dot{N}(t) = \frac{d}{dt}N(t) = F_o\,(N, t); \quad \dot{A}(t) = \frac{d}{dt}A(t) = G_o\,(N,A) \tag{3.5}$$

where F_o represents as the evolution equation in the ecosphere and F_o and G_o are the functions , N is the macro state of ecosphere, A is the macro state of the anthroposphere. Equation 3.5 shows that the ecosphere (N) is independent of any influence from the anthroposphere (A) over time.

Schellnhuber (1998) argued that the impact of human interventions in the environment of the past cannot be compared to that of today as the impacts are greater today than in the past in terms of scale as well as geographical spread. Hence, using the same approach as for the past, a coupled dynamic relation between the ecosphere and anthroposphere for the present day can be expressed by equation 3.6 (Schellnhuber, 1998).

$$\dot{N}(t) = \frac{d}{dt}N(t) = F_1\,(N,A;\,t); \quad \dot{A}(t) = \frac{d}{dt}A(t) = G_1\,(N,A) \tag{3.6}$$

In equation 3.6, the N and A are strongly related as human actions and directly influence the environment. Schellnhuber (1998;1999;2001) expressed the Earth System at a most basic level as presented below.

$$E = (N,\ H) \tag{3.7}$$

where N=(a,b,c...), and H= (A, S) and a, atmosphere; b, biosphere; c, cryosphere, etc and H consists of the anthroposphere (A) which is described as the total sum of all lives, actions and products of humanity and 'S' is the Global Subject. The change in the dynamic relationship between the anthroposphere and the ecosphere can be expressed with a new factor M (t), which is the management strategy selected to direct sustainable development and is expressed by Schellnhuber (1998;1999;2001) as below.

$$\dot{N} = F_2\,(N, A; t; M(t)); \quad \dot{A} = G_2\,(N,A;M(t)) \tag{3.8}$$

Schellnhuber (1998;1999;2001) defined sustainable development at any specific point in time as expressed by the following equation.

$$S(t) = E(t) - H_{NI}(t) \tag{3.9}$$

where S is sustainable development, E is the environment, H_{NI} represents human needs and interests or social needs, t is the time.

This equation tells that the sustainable development is affected by nature and amount of impact on the environment (Phillips, 2010). The more humans consume from the environment to meet their needs (H_{NI}), the lower the level of sustainable development (S). If the value of H_{NI} is higher than E, the development becomes unsustainable. In other words, if H_{NI} has less impact on E, the level and nature of sustainable development is better. Hence, maintaining E at the highest level at any point in time, the higher level of sustainability can be achieved (Phillip, 2010).

The environment E is composed of Atmosphere (Atmo), Biosphere (Bio), Hydrosphere (Hydro), and Lithosphere (Litho) and is presented as below.

$$E(t) = (Atmo + Bio + Hydro + Litho) \quad (3.10)$$

This equation suggests that E can be obtained from the sum of determined or attributed values of the sub-spheres for a specified point in time either using real-time data or prediction models. The operation of any system including E has clear limits for safe operation before failure (Phillips, 2010). The sub-spheres of E can compensate for a certain period of time before reaching the critical level or overload. Thus, E has distinct operational boundary parameters within the context of limit available in spatial-temporal boundaries which can be represented as follows.

$$E(t) = (E_0 \leq E \leq E_{max}) \quad (3.11)$$

where E is dependent on space and time taken for evolution, adaptation, mitigation and repair of the system(s) related to sub-spheres.

The human needs and interest (H_{NI}) continue to increase as each generation of humans desire to have more than past generation. H_{NI} is dependent upon E for humans to

survive. If H_{NI} continue to increase at the increasing detriment to E, there is a limit for H_{NI} based on the resources and services such as oil and gas, clean air, biomass and so. If E degrades in such a way that it cannot readjust and return to its original position, E would be considered unsustainable (Phillips, 2010). At any specified point in time, there is a limit of H_{NI} that can be obtained from determined or attributed value of E which can be represented by the equation below (Schellnhuber, 1998;1999;2001).

$$H_{NI}(t) = [H_{NI0} \leq H_{NI} \leq H_{NImax}] \quad (3.12)$$

The values of H_{NI} at any time 't' can be obtained from the relationship of individual (I) needs and interest (NI), community needs and interest (comm, NI), society needs and interests (soc, NI), species needs (sp, NI). The relationship is shown below.

$$H_{NI}(t) = [I(NI), Comm(NI), Soc(NI), Sp(NI)] \quad (3.13)$$

The needs and interests in any time NI (t) can be found as follows:

$$NI(t) = [QL, Ec, So, BN[\quad (3.14)$$

$$BN(t) = [Sh, F, En, Rep] \quad (3.15)$$

In equations 3.14 and 3.15, QL is the quality of life, Ec is economic, So is social, BN is basic needs, Sh is shelter, F is food and water En is energy, Rep is the reproduction of species. The equations 3.13-3.15 characterize the nature and component of E to maintain H_{NI}. The NI starts at the individual level and the hierarchy moves to community, social and species level as defined in equation 3.13. At each level of hierarchy, there will be different requirements of NI (Schellnhuber, 1998;1999;2001). Even through each stage of hierarchy requires minimum basic needs (BN), each generation seeks improvement in their condition from the previous generation. Fulfilling BN ensures the minimum necessary conditions for human survival. Once the

basic need for individuals is met, the NI is targeted towards achieving the NI for society as represented by equation 3.13 (Schellnhuber,1998; 1999;2001).

Human needs and interest (H_{NI}) at any time are dependent on social development (SD), the technology development (T) and knowledge (K) with an infinite boundary as expressed by the following equation:

$$HNI\ (t) = f\ (SD,T,\ K)\ \rightarrow\infty \tag{3.16}$$

To achieve sustainable development (S) in any time, the value of E must be greater than H_{NI} and can be presented by the following equation as proposed by Schellnhuber, (1998;1999;2001).

$$E\ (t) > HNI\ (t) \leftrightarrow\ \ S\ (t) > 0 \tag{3.17}$$

If the value of E is less than or equal to H_{NI}, sustainable development would not occur as there should be a continuous source of E for H_{NI} (Figure 3.2). This can be presented by the equation below:

$$E\ (t) \leq H_{NI}\ (t) \leftrightarrow S\ (t) \leq 0 \tag{3.18}$$

Schellnhuber (1998) defined historical past as a preindustrial age, before the Industrial Revolution (IR) as shown in Figure 3.2. The assumption is that humans started affecting the processes on the environment since the beginning of the Industrial Revolution.

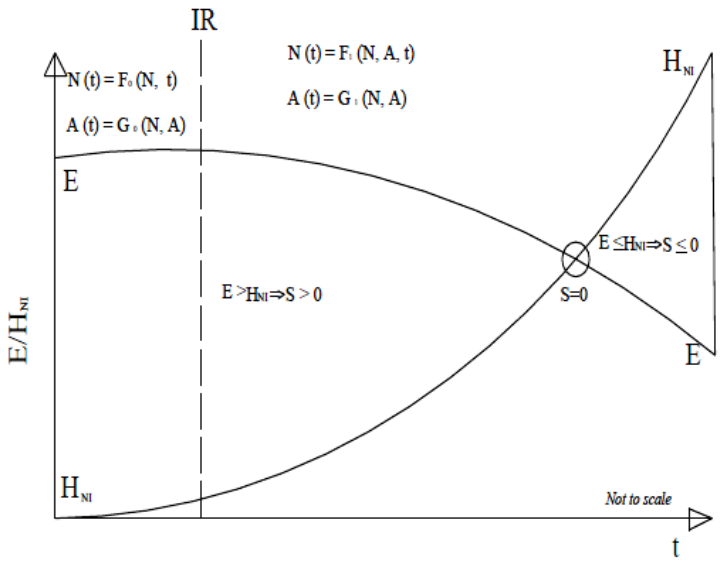

Figure 3.2 Relationship between environment (E) and human needs and interests (HNI) (Philip 2010)

Sustainable development indicator S can be obtained by calculating the values of E and H_{NI} using the equation 3.9 at any time in the range of $0 \leq x \leq 1$. This indicates that the value of E should be kept as high as possible. The less the impact of H_{NI} has on E, the more sustainable the development or resource level is. From the equation 3.18, sustainable development is considered to occur even at E= 0.001 considering the accuracy at three decimal places (Philip, 2010).

3.2.3 Evaluating sustainable development using the Earth System Model

To evaluate the sustainability using the theory described in the Earth System Model, Philip (2010) presented a case study carried out by Bangalore Mass Rail Corporation Ltd (BMRC, 2005) in India for the development of an Elevated Light Rail Transit System (ELRTS) in North-South and East-West corridors. The impacts and benefits of the existing transportation system (the baseline) and the proposed ELRTS (the project) were evaluated using the tool called Battelle Environmental Evaluation System (BEES), USA considering with and without an Environment Management Plan (EMP) for both the scenarios (Dee et al., 1973). This process took into account 40 parameters

of the three components including physical, socio-economic and biological components. A Parameter Impact Unit (PIU) was assigned for each parameter based on the expert's opinion and field study. The Environmental Impact Unit (EIU) for each scenario was estimated using equation 3.19.

$$EIU = \sum_{i=n}^{n=1} EQ_{ijPIU_i} \quad (3.19)$$

EIU = Environmental Impact Unit

PIU = Parameter Importance Unit of i^{th} parameter

EQ_{ij} = Environmental Quality of ith parameter and j^{th} factor.

The Environment (E) component consists of physical (P) and biological component (B) and socio-economic (SE) in terms of air quality, terrestrial ecosystem, water and land as shown in Table 3.2 as a result of the BEES model.

Table 3.2 Results from BEES for the Bangalore Metro Railway System (BMRC, 2005)

Environment aspect and components	Parameter Impact Unit (PIU)	Project EIU	
		Without project-North South (NS)	With project and EMP North-South (NS)
Physical			
Air quality	395	202	275
Water table/quality	130	122	122
Land	40	39	38
Total	565	363	435
Biological			
Terrestrial ecosystem	150	139	149
Aquatic ecosystem	15	12	14
Total	165	151	163
Socio-economic	270	51	228
Total	1000	565	826

The sustainable development parameter S was estimated using $S = E\text{-}H_{NI}$. The value of E was calculated between $0 \leq E \leq 1$. The total EIU values for physical and biological components for North-South corridor without Environmental Management Plan (EMP) were 363 and 151 respectively. Similarly, the value of SE for existing system was 51. In an ideal situation, the maximum values of P, B and SE were apportioned as 565, 165 and 270 respectively.

$$E = \frac{\sum P + \sum B}{\sum Pmax + \sum Bmax} = \frac{363+151}{565+165} = 0.704 \quad \text{and } H_{NI} = \frac{SEmax - \sum SE}{SEmax} = \frac{270-51}{270} = 0.811$$

This shows that $S \leq H_{NI} \leftrightarrow S \leq 0$ which means that the North-South Railway system currently is not sustainable in terms of air quality, ecosystem function and socio-economic impact as E is less than H_{NI}. The North-South Railway system was analyzed using the same BEES model with Environment Management Plan. The values of P, B and SE with EMP were increased to 435, 163 and 228 respectively with increment of +72, +12 and +177 respectively compared to the values without EMP.

$$E = \frac{\sum P + \sum B}{\sum Pmax + \sum Bmax} = \frac{435+163}{565+165} = 0.819 \quad \text{and } H_{NI} = \frac{SEmax - \sum SE}{SEmax} = \frac{270-228}{270} = 0.155$$

From these calculations, $S=E\text{-}H_{NI}= 0.819\text{-}0.155= 0.669$. Therefore, $E > H_{NI} \leftrightarrow S > 0$ as expressed in equation 3.17. Similar analysis for East-West Railway system with and without the project with EMP was performed and found that the project with EMP was found sustainable with the value of E being higher than H_{NI}.

The Earth System Model is still a work in progress model. The model has addressed the human-environment relationship and human's impact upon the natural environment to fulfil their needs. The level of sustainable development has been quantified and presented through an Environmental Impact Assessment (EIA) based case study. This model also offers an opportunity to see how humans interact with the environment over time. However, the use of this model requires a complete full cycle project analysis with all the project parameters that interact with human and

environment and is not easy to quantify. The data of this level were not available in case of Nepal regarding different energy technology evaluation. Hence, this method was not used.

3.2.4 The Talos Method of Measuring Sustainable Development

Talos (2003) (Brabant Centre for Sustainability Issues) defined sustainability as an enhancement to quantity and quality of natural capital (ecological), social capital (people's well being) and economic capital for a development activity. The Centre also argues that improvement of one capital cannot take place at the cost of others. The development activity carried out at any time should be sustainable over time and for the future through the generations. The development activity should be sustainable locally as well as globally. Talos has followed the sustainability guiding principles as social solidarity, economic efficiency and ecological resilience (Rotmans et al., 2001).

The social solidarity represents guaranteeing of the democratic rights, legal stability, and cultural diversity. It is the social equity and a quality of life that a member is entitled in a society. The quality of life is measured in terms of various conditions with respect to healthcare, housing and education that determine the well being in a society. The economic efficiency assumes that the available production means are used as efficiently as possible without compromising the future utilization of resources. To meet the criteria for a sustainable development, the level of income of individuals should be sufficient to meet the necessary needs of individual and society. The ecological resilience implies the preservation of natural resources for human life as well as protecting the natural diversity. This requires maintaining a balance between the use of natural resources by humans and the regenerative capacity of the nature (Talos, 2003).

The sustainable development is monitored in terms of capital stocks of each component: social capital stocks, economic capital stocks and ecological capital stocks

as shown in Figure 3.3 visualises the range and development of three indicators in the main triangle as a smaller triangle inside. The actual condition of each capital is shown by the inside triangles while the outside triangle indicates the ideal situation of each capital based on science and expert's judgement.

In Talos, the contributions of each capital in different circumstances were evaluated using certain scoring criteria to evaluate the contribution of any activity to the respective capital stocks (Talos, 2003). The evaluation can be done either quantitatively or qualitatively by giving a numeric score depending on the availability of the data. Talos allocated 1-100 score from unacceptable to optimal condition for sustainability. For example, Talos evaluated social sustainability in terms of employment and resident labour force (social stock). Whether a region imports or exports labour can be expressed as a ratio between employment and labour force. The labour market is considered to be in balance when the demand and supply of labour stock are equal, corresponding to a maximum value of 100. The conditions for social sustainability were expressed by Talos as follows.

Socially acceptable value is $100 < x \leq 105$ or $95 \leq x < 100$.
Social limit value is $105 < x \leq$ and/or $90 x < 95$.
Socially unacceptable value is $x > 110$ or $x < 90$.

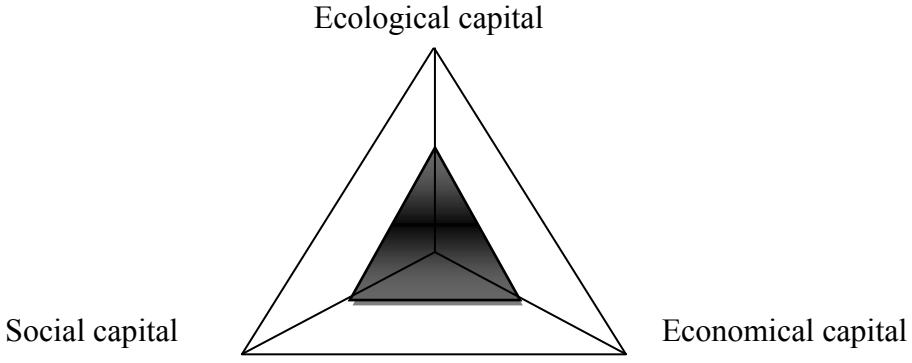

Figure 3.3 Sustainability indicators as defined by Talos (2003)

Similar scores can also be used to evaluate the economic as well as environmental stocks. The same principle can be applied to evaluate the sustainability of energy

projects if relevant data are available that help to determine the capital stocks for all three indicators. This evaluation method is consistent with the fundamental definition of sustainable development as defined by WCED (1987) and Benton (1999).

It is believed that the Talos method makes the interaction and communication between scientific disciplines and different arenas in the society. This is a simple method where the concept and results of evaluation can be visualized pictorially. However, the connection between the three forms of capitals has not been explained. This method has also been blamed for being too subjective for choosing requirements, indicators and stocks. This method was not applied to evaluate the sustainability of micro hydro and biodiesel fuels as the data level was not available to suit this model.

3.2.5 Social Well-Being Measurement Model

Dasgupta and Maler (1998) discussed a model economy where various capital stocks such as labour, goods, manufactured capital and natural resources are required in order to produce goods and services to maintain the society. These components are part of an economy which is a continuous function and is expressed as $t \geq 0$. Dasgupta and Maler (1998) considered a non-deteriorating durable product (manufactured capital) with its stock at t as $K_t \geq 0$. Any consumable product can be produced with its own stock (K), the stock of labour (L_t) and any intermediate product (X) are inputs to generate economic goods (capital). The accumulation of physical capital is expressed by the following equation.

$$\frac{dK_t}{dt} = F(K_t, L_t, X_t) - C_t - E_t. \quad (3.20)$$

where Ct (≥ 0) is the aggregate consumption and E_t (≥ 0) is the expenditure on increasing the natural resource base.

In the analysis of resource management, Dasgupta (1982) argued that resources are positive, and a degrader of resources or pollution is negative. The size of aggregate stock of natural resources can be represented by $S_t \geq 0$ at any time t. S_t is also a natural rate of regeneration of the resource base $M(S_t)$ where M (S) is a differentiable function. If the resources are considered to be minerals, S_t would be the known reserves at any time t and M(S)= 0 for all S. In addition of the resource base, the stock of knowledge at any time t is denoted by Z_t and can be expressed by the following relationship.

$$Z_t = \int_{\infty}^{t} E_t \, dt \tag{3.21}$$

$$\frac{dZ_t}{dt} = E_t \tag{3.22}$$

where E_t is the expenditure during extraction of natural resources such as exploration, clean up etc. If the resource base is assumed to be augmented at the rate N (E_t, Z_t, S_t) where N is also a continuously differentiable function and is non-decreasing in E and Z. The resource base dynamics can be presented by the following expression:

$$\frac{dS_t}{dt} = M(S_t) - R_t + N(E_t, Z_t, S_t) \tag{3.23}$$

As defined by WCED (1987), sustainable development should be achieved in such a way that it does not leave its footprint for future generation. Pezzey (1992) discussed a number of scenarios for the interpretation of sustainable development and one of them is presented below.

Any economic activity is sustainable if $\frac{dU_t}{dt} \geq 0$ (3.24)

where U is a utilitarian function which should be reduced in the short-term in order to accumulate assets. The accumulation maintains the flow of U at a higher level in the future. This theory permits some sacrifices at the initial stage to make sure that the

future generations do not need to experience the compromise for their well being (Pezzy, 1992).

This model is focused only on the social well-being of the society and does not include complete evaluation of all the three forms of capitals. This method was not employed in this research.

3.2.6 Weak Sustainability Model

Pearce et al. (1990) stated that the well being of humans depends upon the availability of capital that creates goods and services. The capital includes both man-made and natural capitals including skills and knowledge. Daly (1999) argued that weak sustainability requires the sum of man-made and natural capitals be maintained intact as they substitute each other. Weak sustainability assumes that all natural resources can be converted to manufactured or man-made capital (Bell and Morse, 1999). Weak sustainability equates to the economic sustainability but ignores the environmental and socio-economic aspect of the development endeavour (Bell and Morse (1999) as shown in equation 3.24 below.

Capital stock environment/ecology (*energy resources are part of this*)= C_n
Capital stock economy= C_e
Capital stock society = C_s

$$C_n+C_e =K \tag{3.25}$$

where C_n is the natural capital and C_e is the manufactured capital (economic) at any time $t>0$ and K is constant. By the definition of weak sustainability, C_n and C_e are substitutable; hence, it can be said that $2C_e=K$, which still fulfils the condition of weak sustainability. C_n is the natural capital and some portion of it are renewable which regenerates and substitutes itself (Pokharel, 2006). However, if part of C_n is changed

into man-made capital C_e, then there is no renewing process to replace the depleted natural resource (Ayres et al., 2001). For example, the CO_2 emitted from fossil fuel combustion cannot be recycled back to nature and natural capital becomes a part of irreversibility (Pearce et al, 1994) and forms the basis for weak sustainability. Based on the above mentioned facts, the weak sustainability at any time horizon 't' can be interpreted as the change in natural and economic capital in a system as presented in equation 3.25. In equation 3.25, the social input component is non-existent as defined in weak sustainability proposition.

$$\frac{dCn_t}{dt} \geq 0, \frac{dCe_t}{dt} \geq 0 \tag{3.26}$$

Roberts (2004) presented a conceptual diagram showing the differences in the conversion of natural and human capital for weak sustainability case (Figure 3.4). From the figure, as time moves to the right, it is clear that the natural capital decreases continuously while the human capital goes on increasing as a part of the natural capital is converted to human capital with time during any development endeavors, which is the definition of weak sustainability.

Weak sustainability can also be explained based on gross national product. Pearce and Atkinson (1995) suggested the following relationship to explain a weak sustainability and proposed that an economy is weakly sustainable if the sustainability index $Z > 0$ as follows.

$$Z = \frac{S}{Y} - \frac{dM}{Y} - \frac{dN}{Y} \tag{3.27}$$

$$Z > 0 \text{ if and only if } \frac{S}{Y} > \frac{dM}{Y} + \frac{dN}{Y}$$

where Z is a sustainability index, Y is the gross national product, S is total savings for a country, dM is the rate of depreciation of man-made capital and dN is the rate of depreciation of natural capital. It means that weak sustainability is achieved if an

economy saves more than the combined depreciation of natural and manufacturers' capital.

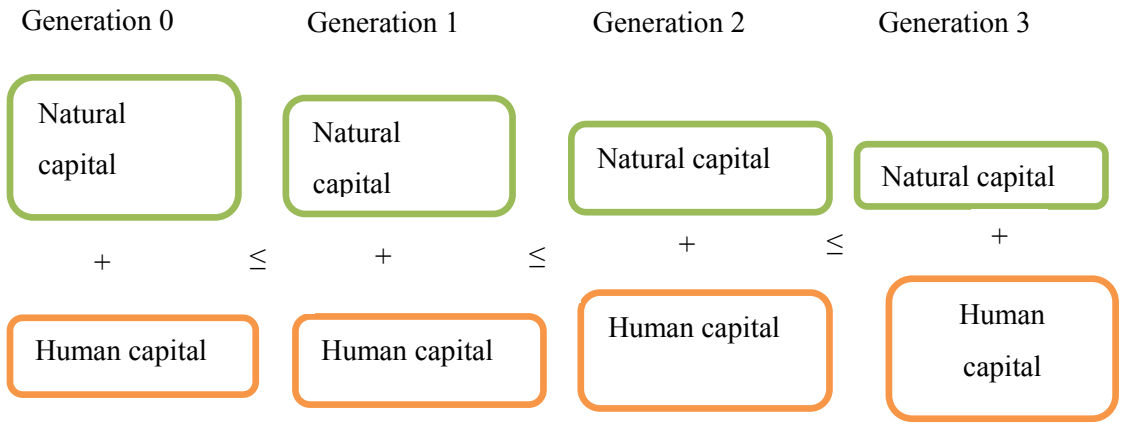

Figure 3.4 Conversion of natural capital to human capital in weak sustainability concepts (Roberts, 2004)

The weak sustainability is based on the theory that the savings earned from the exploitation of natural resources are invested in manufactured or human capital as a substitutable resource for natural capital. As an example of weak sustainability, Gowdy and McDaniel (1999) reported a practical case study of a small Pacific Island nation of Nauru that has an extreme implication in their natural resources. Nauru had one of the world's richest phosphate mining found around 1900. After mining for nearly 100 years, most of the land now is completely devastated and has become biologically impoverished. People can hardly grow anything on that land now. During that period, people of Nauru had a very high per capita income from phosphate mining, but later all the money they earned selling their natural capital has been spent. People are facing a bleak future as their economic development followed weak sustainability. Once transferred into the manufactured capital, there is no way to return the manufactured capital back to natural capital (Ayres et al.,1998). The oil reserves exploited for economic benefit and some of the earned money utilized to build any type of productive capital, i.e. production of cars or wind energy farms is an example of weak sustainability. Weak sustainability does not account for the long-term future.

In weak sustainability model, the man-made capital and natural capital in aggregate are kept in intact over time and they complement each other. This model does not take into account the social capital into account. This method was not used to evaluate the sustainability of energy resources in this work.

3.2.7 Strong Sustainability

Due to the excessive exploitation of natural resources, there are several environmental problems such as global warming, ozone layer depletion, ground water contamination. The Earth has a limited carrying capacity and the excessive use of natural resources could cross the limit of its carrying capacity. The issue of strong sustainability is not limited to economic and energy systems but also to the biodiversity considering the economic system as a subsystem of the whole ecological world (Pokharel, 2006). Strong sustainability reflects the throughput to the economic process such as energy, water, air, etc. affects the ecological biodiversity and all wastes of the economic processes are sunk into the natural ecosystem. Energy from our ecological system is used as an input to the economic processes and emissions of such energy are also given back to ecology. Economic processes or developments are an intermediate means (Daly, 1977) whereas, energy is the prime mover in this process. Daly (1999) reported that the future generations also have the ownership claims to as much natural capital as the present generation. As defined by WCED (1987), sustainability is the form of development that meets the needs of the present generation keeping the natural resources intact for future generations to meet their needs. In a practical sense, sustainability refers to environmental (C_n), economical (C_e), and social components (C_s) that need to be addressed for the long-term sustainability of this planet. Based on the strong sustainability criteria, sustainable development (SD_t) at any time is the function of the three capitals:

$SD_t = f(C_n + C_e + C_s)$ for an infinite time horizon (3.28)

According to above-mentioned definition, the strong sustainability is presented in the form of three capital stocks by the following equation:

$C_n + C_e + C_s \geq$ constant for any time 't',

provided that $\frac{dCn_t}{dt} \geq 0, \frac{dCe_t}{dt}$ $\frac{dCs_t}{dt} \geq 0$ (3.29)

From the definition of strong sustainability C_n and C_e are not substitutable, they are rather complementary stocks. The assumption is that none of the capital stocks may decrease over a longer period. This is supported by the concept developed by Roberts (2004) which showed the differences in the conversion of natural and human capital for the strong sustainability case (Figure 3.5). The human capital/manufactured capital goes on increasing with the increase in human needs but the natural capital should be kept intact.

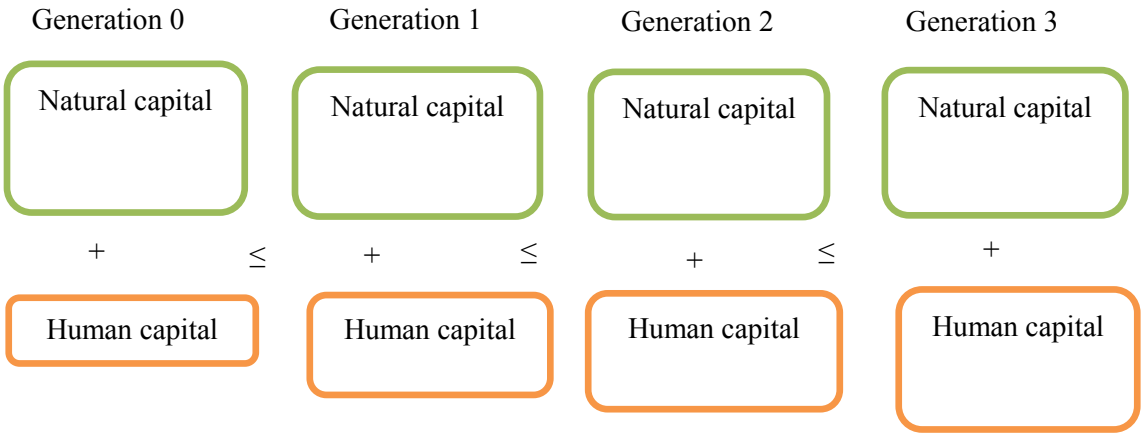

Figure 3.5 Conversion of natural capital to human capital in strong sustainability concepts (Roberts, 2004)

Daly (1999) mentioned that non-renewable natural resources (natural capital) can be consumed only when functional and physical replacement is accomplished without damaging or crossing the carrying capacity of the Earth, for example, consuming fossil

fuels without damaging biodiversity and installing new functional wind energy farms by earned capital to generate the equal amount of energy in the future. Goodland (1992), Costanza et al. (1997) put forward that the "critical natural resources (which cannot be replaced by other capital resources)" (Pearce et al., 1990) be conserved, waste produced due to human activities be within the assimilative capacity of the ecosystem, and future generation's ownership on natural resources must be ascertained. Costanza et al. (1997), Daly (1991) further mentioned that the scale, carrying capacity and equity are the key concerns of any activities that allocate the scarce resources. Prugh et al. (1999) argued that in order to achieve sustainability in energy development, the rate of harvest of renewable resources (such as forest, fish etc.) should not exceed the rate of generation, the waste generated from the economic activities should not exceed the Earth's carrying capacity and the depletion of non-renewable resources (such as coal, oil, natural gas etc) should be offset by investing in the development of renewable substitution for them such as (wind, solar etc).

This method is the most comprehensive method to evaluate the sustainability. This method takes into account all the universally accepted indicators of sustainability. In this method, the natural capital should in no way be negatively impacted due to the resource consumption. This method was used to evaluate the sustainability of micro hydro projects and biodiesel fuel in Nepal.

3.3 EVALUATING SUSTAINABILITY OF SOME ENERGY SOURCES IN NEPAL USING SUSTAINABILITY INDICATORS

Nepal faces a severe scarcity of commercial transport fuels at all times. Hence in the Nepalese context, the evaluation of sustainability requires considering the hard currency Nepal spends to import and subsidize the petroleum products and long hauls required to transport fuels from Kolkata to Nepal. The air pollution including greenhouse gas emissions (CO_2, CH_4, N_2O) and criteria air contaminants (NO_x, SO_x, CO, VOCs etc.) caused by the transport and use of imported petroleum products, the

energy security of Nepal, food security and water pollution caused by the processing of fuel such as biodiesel fuels are also required to take into account while analyzing sustainability of fuels in Nepal. Furthermore, employment generation from the alternate energy sources are being promoted, their economic impact in local and regional should also be evaluated. The empowering of local institutions such as cooperatives, research institutions, private and non-governmental organizations and local communities in terms of knowledge and capacity are also key factors contributing to the sustainable development of alternative energy sources in Nepal. Based on the indicators listed in Table 3.1 and using the evaluation methods based on strong sustainability theory, the following projects are evaluated for their sustainability in the Nepalese context.

3.3.1 Evaluation of Sustainability of Micro Hydro Projects (MHP)

A case study of a community based decentralized micro hydro project is presented and evaluated for sustainability using the criteria as described in 3.2.6 for the strong sustainability case. Two micro hydro projects, one in Thangpaldhap village (Handi Khola II-26 kW) and the other in Thangpalkot village (Handi Khola III-20 kW) in Sindhupalchowk district in Nepal are evaluated for natural capital (environmental capital) (Cn), economic capital (Ce) and social capital (Cs). The physical interpretation is such that any intervention due to the utilization of natural resources should not cause net negative impacts in the environment, economics and society. The change of natural capital (dCn_t/dt), economic capital (dCe_t/dt) and social capital (dCs_t/dt) with time should not be negative in the long-term as presented in equation 3.28. Figure 3.6 below depicts a model with input capitals and output capitals for a typical micro hydro system.

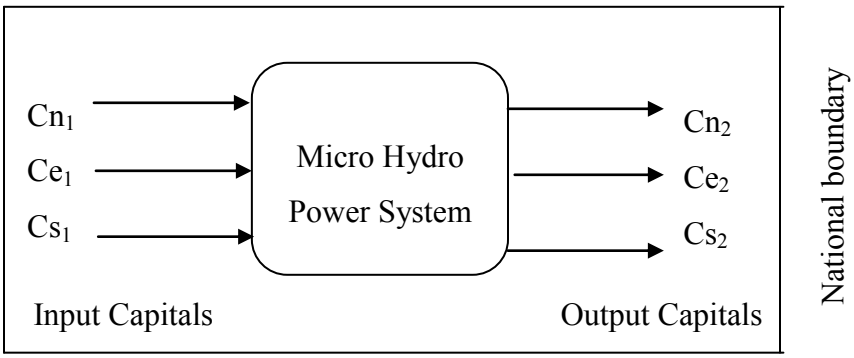

Figure 3.6 Input and output capitals to an energy system within a defined boundary

3.3.1.1 Environmental Condition, dCnt/dt ≥ 0, (from Figure 3.6, Cn_2 - Cn_1 ≥ 0)

This condition, in case of decentralised micro hydro projects, indicates that the change in environmental capital must be greater than or equal to zero after the system is installed, operated and used. Existing irrigation canals and the diversion system were used with little improvement. In both of these projects, the natural capitals as input to the system are water and surrounding environment. From the existing literature, there are no irreversible impacts on these resources as well as no depletion of such natural capital (Pokharel et al., 2007; Broek and Lemmes, 1997). No additional adverse impacts were reported on the flora and fauna in the local ecosystem due to the development of the micro hydro projects (Pokharel, 2006).

In the context of hilly and rural regions of Nepal, the output from the MHP is electricity and/or mechanical energy. Electricity is used for lighting purposes which replaces kerosene used for domestic lighting using kerosene wick lamps. A typical kerosene lamp is approximately 25% efficient and consumes an average of 0.041 litres/hour and 1 litre of kerosene is approximately equivalent to 9.7 kWh (Plas and De Graaff, 1988; Broek and Lemmes, 1997). The kerosene lamp is assumed to operate for 6 hours per day for a year and is replaced by a 25 watt incandescent bulb operating for the same period. However, each household who used to have one kerosene wick lamp

now uses three 25 watt incandescent bulbs. The mechanical energy is utilized for agro-processing instead of human labour. Table 3.3 summarises the emissions from the kerosene wick lamp and electricity generation from a micro hydro project. The emission from hydro power production for non-reservoir schemes is approximately 15 gCO_2e/kWh (Gagnon and Van de Vate, 1997). Moreover, CDM-PDD (2011) reported that the emission factor for kerosene from kerosene wick lamp is 0.0719 tonnes/GJ. The heating value of kerosene is 37 MJ/litres (Ashton and Cassidy, 2007).

Table 3.3 Electricity and kerosene in rural lighting from environmental perspectives

Lighting source	**Before MHP (one kerosene wick lamp)**	**After MHP (one 25-watt incandescent bulb)**	**Remarks**
	Kerosene	Electricity	Majority of cases
Type of Lamp	Kerosene Wick	Incandescent lamps	Majority of users
Annual consumption (@6 hours/day for 365 days)	89 litre (equal to 863 kWh)	54.75 kWh	1 litre kerosene = 9.7 kWh, 89litres = 400 watt, 1 kerosene wick lamp consumes 0.041 litres/hour
Nominal output of luminous flux	40 Lumen (lm)	210 Lumen (lm)	Kerosene wick lamp 25% efficient
GHG emissions/year (CO_2e)	236.77 x 10^{-3} tonnes from one wick- lamp use	0.821 x 10^{-3} tonnes from three 25-watt incandescent bulb	Emission factor for kerosene wick lamp is 0.0719 tonne/GJ and hydro power is 15 gCO_2e/kWh
Local air pollution	Not estimated	No	Various studies & reports, mentioned that MHP has minor & insignificant impacts (Banskota and Sharma, 1997; Broek and Lemmes, 1997; World Bank, 1996)
Water pollution	Not known	Very minor	
Local ecological impact	Not estimated	Minor	

The CO_2e emission for a typical from kerosene wick lamp is estimated to be 236.77 x 10^{-3} tonnes annually whereas the emission from the electricity from micro hydro project is $0.81x10^{-3}$ tonnes annually. As stated in 3.3.1.1:

$Cn_2 - Cn_1 = 0.81 \times 10^{-3} - 236.77 \times 10^{-3} = -235.96 \times 10^{-3}$ tonnes.

The CO_2e emission from kerosene burning is significantly higher than the emission from the life cycle of the project and hence, the environmental condition for constant or increased natural capital is well satisfied ($Cn_2 - Cn_1 \geq 0$). Moreover, the reduction in the use of kerosene will help improve indoor air quality leading to reduced respiratory diseases. In other words, environmental capital could be considered increased after installation, operation and use of MHP.

3.3.1.2 Economic Condition, $dCet/dt \geq 0$, (from Figure 3.6, $Ce_2 - Ce_1 \geq 0$)

Table 3.4 below shows the investment cost, revenue generated and regular maintenance cost including regular salary for operators (Pokharel et al., 2003). Based on these financial parameters, the payback periods estimated were 16 years for Handikhola –II and 26 years for Handikhola-III respectively. In Nepal, micro hydro projects were subsidized at 50% of their total cost. The payback period after the subsidy is also presented in Table 3.4. UNEP (2006) reported that a micro hydro turbine can last up to 30 years and the civil structure with regular maintenance can last up to 100 years. Considering the life span of micro hydro projects to be 30 years, both projects are financially feasible from community investment perspectives. The data indicate that communities can repay their investment and make some financial gains directly from the revenue generated from electricity generation within the project life time. Moreover, there will be some salvage value of equipment after the life of the project as an additional income from the project. As these projects were subsidized from the fund provided by United Nations Development Program (UNDP), the payback for the community is reduced by half. However, several studies including that

of Intermediate Technology Development Group (ITDG) by Khennas and Barnett (2000) have reported that financial recovery from the MHP system is possible even without subsidies.

All the micro hydro components including turbines, generators, penstock pipes and other parts are manufactured locally in Nepal. The development of micro hydro will help to generate employment within the country. It will also add the tax revenue to the government impacting positively to the natural economy.

Table 3.4 MHP schemes of Thampalkot VDC in Sindhupalchowk District in Nepal

MHP Project	Capacity (kW)	Investment (Rs.)	Revenue (Rs./yr)	Maintenance cost (Rs./yr)	Simple payback (yr)	Project cost after subsidy @50% (Rs.)	Payback after subsidy (years)	Benefit HH
Handi khola MH II	26	2167164	224400	91200	16	1083582	8	271
Handi khola MH III	20	2109212	168000	86400	26	1054606	13	215
Total	49							486

In addition of the investment income generated by micro hydro projects, a large increase in employment was also generated during construction and afterwards. Table 3.5 below shows the unskilled, skilled employment generated by both the projects. These projects also generated permanent employment for the operation and maintenance of micro hydro projects in the communities. Introduction of MHP also offered several end use opportunities including commercial and industrial activities. Because of the availability of electricity two saw mills, one agro-processing mill, three poultry farms, an electronics repair centre, a photo studio and a battery charging

station were established creating a total of eight jobs in the end use sector in these two communities.

In these project areas, people were previously using kerosene wick lamp for each household on an average. After the installation of micro hydro projects, people use three bulbs per household on average. The luminaries available from the incandescent bulbs were better than that of kerosene wick lamps. Another important economic gain is avoidance of flow of money from the village to import the fossil fuels and dry cells. The total economic capital (ie. economic benefits) is explicitly more than before. So the condition of constant or increased economic capital is satisfied ($Ce_2 - Ce_1 \geq 0$). Hence, MHPs are found to be economically sustainable.

Table 3.5 Employment opportunity generated by Handikhola II and III VDC (Pokharel et al., 2003)

Projects	Unskilled labor during implementation number	Skilled labor during implementation in number	Direct employed in O&M, round the year	Employment in end-use sector, round the year
Handikhola -II	32520	370	3	4
Handikhola -III	23650	285	2	4

3.3.1.3 Social Condition, $dCs_t/dt \geq 0$, (from Figure 3.6, $Cs_2-Cs_1 \geq 0$)

Handdikhola II and III project beneficiary communities invested their social capital to build the project in terms of time, labour and other capitals to build the micro hydro project. The project installed in both communities offered several social benefits.

- Better lighting of houses,
- Diminished likelihood of fire at homes from kerosene.

- Access to audio-visual means (radio and television), which may play a role in developing the informational and educational level of the rural population.
- Lighting of schools and home, which can improve the education of the children and enhance adult education program.
- Permanent and reliable energy supply in health centers to preserve medicines which will have a positive impact on the health system of the community.
- Lighting of roads and trails around the villages to enhance public security.
- Agro processing like grinding, hulling etc, which would reduce the drudgery of people, especially women and children.
- Better livelihood through new opportunities to earn wages and salary locally.
- Enhanced empowerment process due to decentralized systems.
- Saving of money from reduced kerosene imports.

Table 3.6 Benefits and impacts of MHP life cycle

MHP life cycle	Positive Impacts	Negative impacts
Manufacturing and production of components	Employment Profit, salary Infrastructure Government revenue	Water Pollution Air Pollution Health Hazard Import of inputs
Transportation	Employment	GHG emission, Drudgery
Installation	Employment Skill Enhancement	Human health risk (Accidental)
Operation & Maintenance	Employment Skill Enhancement Replacement of imported fossil fuels	Human health (accidental)
Dismantling, Recycling, reuse	Employment Resource saving	Pollution Human health (accidental)

In these project villages, before the installation of the micro hydro projects, the food processing activities were done manually. These processes are time consuming, repetitive, arduous and mostly done by women and sometimes with the help of children. The primary processing of agricultural products such as rice husking, wheat, corn and millet grinding, food preparation in inefficient open fire stoves are some of the examples of drudgery. In addition to these activities, women had to spend several hours in collecting firewood from the nearby forests and carry a heavy load of firewood. Table 3.7 below shows the qualitative measurement of drudgery for women before and after the installation of micro hydro projects. The drudgery is categorized from very severe with a score of 5 to very mild with a score of 1 as shown in Table 3.7. Before the installation of micro hydro projects, the drudgery level for women in the project areas was assumed to be at its highest level (very severe). Due to the installation of the agro-processing mills, the time and energy spent in manual rice husking, millet, corn and wheat grinding were avoided, and the drudgery level is considered to be reduced to 3, a moderate level.

Table 3.7 Intensity of drudgery in the project areas before and after the installation of micro hydro project

Score	**Intensity of drudgery (before MHP project)**	**Intensity of drudgery (After MHP project)**
5	Very severe	
4	Severe	
3	Moderate	Moderate
2	Mild	Mild
1	Very mild	Very mild

All of the above-mentioned social capitals are hard to quantify in terms of money but they are strongly implicit benefits to the local communities. So the condition of constant or increased social capital ($Cs_2 - Cs_1 \geq 0$) is well fulfilled by MHP system.

3.3.1.4 Institutional Sustainability of Micro Hydro Projects

Institutional sustainability is a very important aspect of sustainability for community based and decentralized micro hydro projects. Both the micro hydro projects cited in this study are operated and managed by local communities. Local communities are organized in the form of community based organizations (CBOs) representing each cluster of households in the project area. A Micro Hydro Functional Group (MHFG) is formed representing each CBOs. These organizations are registered as a non-profit organization in the district administration office. The Micro Hydro Functional Group identifies and selects candidates suitable to be an operator and manager and sends them for training. Thus, these micro hydro projects are operated and managed by the trained persons from among the community members. This strategy helps to enhance the capacity of the local people and to take ownership of the project. The electricity tariff is also determined by the community members representing CBOs and MHFG. A maintenance fund is also set up for regular maintenance and operation of the micro hydro projects. In summary, there are fully functional community based organizations for the operation and maintenance of the projects. These micro hydro projects have achieved institutional sustainability.

3.3.2 Evaluation of Sustainability of Biodiesel Fuels

Similar to that of micro hydro projects, the sustainability of biodiesel fuels is evaluated for environmental, economic, social and institutional indicators as described in 3.2.6. The evaluation criteria from Table 3.1 were used to assess the sustainability of biodiesel fuel. As it is difficult to quantitatively evaluate all the components of sustainability from Table 3.1, many of them are discussed from the sustainability point of view qualitatively only.

Biodiesel processing requires a large amount of chemicals such as methanol. As Nepal does not have fossil fuel production, the processing will still be largely dependent on

the import of fossil fuels. One of the ways to avoid this problem is to produce methanol (used in the transesterification of biofuels) from distillation of waste biomass such as wood. In this way, biodiesel can be produced more independently.

3.3.2.1 Environmental Sustainability

As defined in Table 3.1, net energy balance to produce biodiesel and the greenhouse gas (GHG) emissions from its life cycle chain are the major components of the environmental indicators of biodiesel sustainability. In order for biodiesel fuel to have net positive impact from the life cycle emissions, biodiesel emissions should be less than those of diesel.

3.3.2.2 GHG Emissions Reduction

$(S\&T)^2$ Consultants Inc (2010) carried out a complete life cycle analysis for canola biodiesel for Canola Council of Canada. Figure 3.7 shows the system boundary and various stages of life cycle for canola biodiesel analysis.

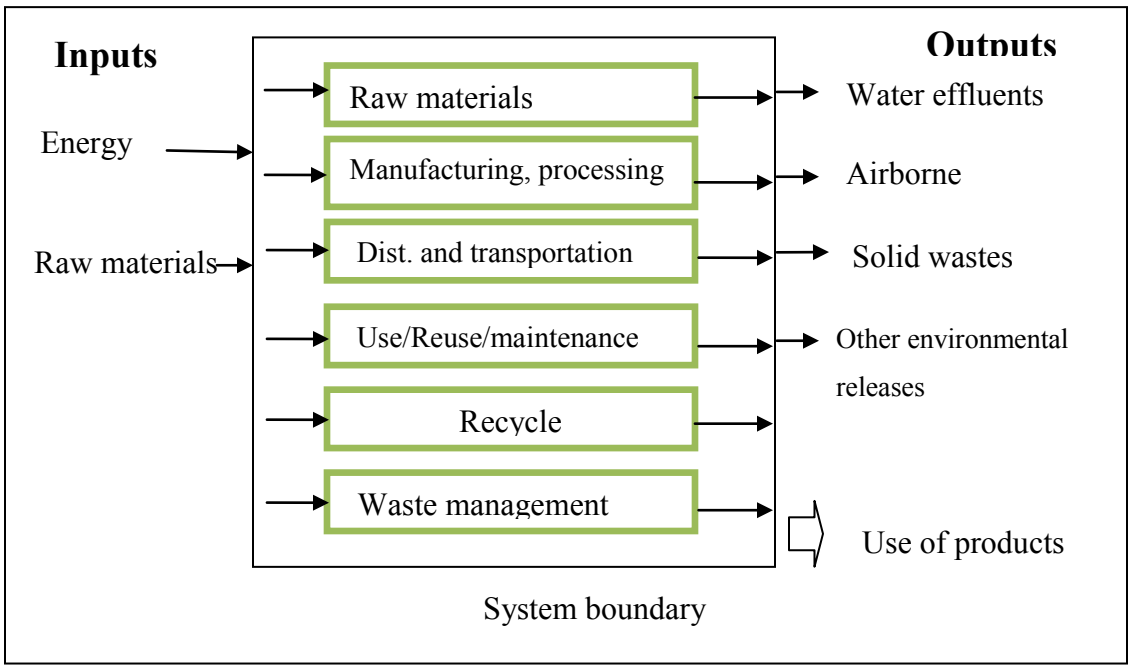

Figure 3.7 System boundary, input and output for canola biodiesel ($(S\&T)^2$ consultants inc., 2010)

The life cycle emission analysis of petro-diesel and canola biodiesel B100 was carried out by $(S\&T)^2$ Consultants Inc. in 2010 for Canola Council of Canada. The life cycle analysis included the CO_2e emissions from the vehicle operation, materials in vehicle, assembly and transport, fuel dispensing, fuel storage and distribution, fuel production, feedstock transport, land use change, cultivation, fertilizer manufacturing, gas leakage and flares, emissions displaced by co-products, and carbon in end use from CO_2e in air. The analysis showed that the canola biodiesel B100 has 90.1 % lower emission than regular petro-diesel. The petro-diesel was found to have 1428.7 g CO_2e/km while the canola biodiesel was found to have 141.2 gCO_2e/km. The use of canola biodiesel reduced 1287.2 gCO_2e/km travelled. The total GHG reduction was reported to be 2.97 kgCO_2/litres of biodiesel.

$$\text{Avoided GHG emissions (\%)} = \frac{GHG\ emissions\ from\ diesel - GHG\ emissions\ from\ biodiesel}{GHG\ emissions\ from\ diesel} \times 100 = \frac{(1428.7-141.2)}{1428.7} \times 100 = 90.1\%$$

Similarly, Whitaker and Heath (2009) carried out a full life cycle analysis of petro-diesel and jatropha biodiesel in the transport sector in India. The study showed that there was 62% reduction in GHG emissions from the life cycle of jatropha biodiesel B100. Sheehan et al. (1998) also reported that the use of soybean biodiesel reduces net CO_2 emissions by 78.45% compared to petro-diesel. The same study reported that, for 20% mix of soybean biodiesel (B20) with petro-diesel, the CO_2 emissions in urban buses is reduced by 15.66%. Coronado et al. (2009) estimated the CO_2 emission reduction from Brazilian transport sector using the 78.45% reduction in CO_2 emissions for replacing petro-diesel with 100% biodiesel (B100). Janaun and Ellis (2010) analysed and reported that the biodiesel has a clear advantage in GHG emission reduction over petro-diesel. The GHG emissions will further reduce for biodiesel fuel production in Nepal as more human energy will be in use for feedstock growing and harvesting because of the limitation of transportation infrastructure and geographical set up. Moreover, the GHG emissions from fossil fuel input for each unit of petro-diesel in Nepal may be higher than the values used in this analysis because Nepal has

to transport the crude oil from Kuwait to Kolkata City of India, refine there and transport diesel from Kolkata to Nepal.

In addition to the GHG emissions, biodiesel also reduces the emission of other pollutants including carbon monoxide, particulate matters, and other unburned hydrocarbons significantly because of the presence of oxygen in its molecular structure, improving the overall air quality. From all the studies including life cycle analysis, it is clear that biodiesel contributes to net environmental benefit over petro-diesel and fulfills the condition of environmental sustainability as defined in equation 3.30:

$$dCn_t/dt \geq 0 \qquad (3.30)$$

3.3.2.3 Energy Balances

Energy balance is used to compare the useful energy produced by the system to the net energy consumed during the life cycle, which is also referred as net energy ratio (NER) (Pradhan et al., 2005). The amount of fossil fuel input to produce biodiesel is reported in various studies. Sheehan et al. (1998) reported that for every unit of fossil energy consumed, biodiesel yields 3.2 units of energy from its life cycle. $(S\&T)^2$ Consultants Inc. (2010) in the life cycle analysis of canola biodiesel reported that NER (joules consumed/joules delivered) were 4.35 and 3.93 for petro-diesel and biodiesel respectively. This shows that the fossil fuel contribution to produce biodiesel is lower compared to the fossil fuel input to produce the same unit of energy from petro-diesel. Fore et al. (2011) reported that the NER of canola biodiesel 1.78 and that of soybean biodiesel was 2.05. Various system inputs affect the NER as there are different fertilizer requirements for different biodiesel feedstock. The study further reported that the soybean requires less fertilizer than canola production, hence has the higher NER. Similarly, Wang et al. (2011) studied the life cycle assessment of the economic, environment and energy performance of jatropha biodiesel in China and reported that the NER of 1.47 including co-products utilization, and farm energy input. A life cycle

assessment carried out for jatropha biodiesel as a transportation fuel in rural India reported an NER of 1.85.

Pleanjai and Gheewala (2009) carried out a life cycle energy analysis of biodiesel production from palm oil in Thailand and reported that the NER of palm oil biodiesel even without co-product utilization was 2.42 and with co-product were 3.58. This indicates a significant improvement in the net energy ratio. In case of Nepal, the NER for jatropha and other biodiesel fuels would be very similar to that of Indian case studies. The NER may slightly increase as there will be more human energy input in the life cycle chain because of the geographical and economical situation. The fossil fuel energy input will also decrease as there will be less petro-diesel to be imported from India.

In addition to the life cycle GHG emissions and positive net energy ratio, biodiesel is considered to be less toxic to the environment. Biodiesel is also easily biodegradable. Hence, in terms of GHG emissions, net energy balance and other environmental benefits, the use of biodiesel fuels satisfies the environmental condition of strong sustainability.

3.3.2.4 Economic Sustainability

Biodiesel offers several positive benefits. One of the most important benefits of biodiesel promotion is that it can reduce the dependence of oil imported from foreign countries. Nepalese economy can reduce its dependence on unstable, fluctuating and volatile oil markets. Moreover, reduction in the import of oil can save a large sum of hard earned dollars. The other benefit of biodiesel is that the overall energy efficiency of biodiesel is higher than diesel itself. The US Department of Energy reported that the 3.24 units of energy can be produced per unit of energy used in the production of soybean biodiesel (US Department of Energy, 2006). The potential of less energy intensive biodiesel production is possible in Nepal as human energy is used for cultivation, harvesting and transportation.

The other important aspect of biodiesel production in Nepal is that a significant amount of capital remains within the country. As Nepal is largely agricultural based economy, the capital remaining in the country can encourage local entrepreneurs and industries and add jobs in the local market enhancing the local economy. Goldemberg (2003) reported that biofuel creates one of the highest numbers of jobs from its life cycle. In addition to the transportation fuels, biodiesel can be used for pumping water for irrigation, water and wastewater treatment, all of which will have a positive impact in the local as well as the national economy.

Biodiesel production costs largely depend on feedstock cost, conversion efficiencies, processing capacity and energy prices, among others. The feedstock cost on the other hand, depends on availability and market competitiveness. The co-product utilization such as meal and glycerin utilization from residue also plays an important role in determining the price of biodiesel. Biodiesel production is in its conceptual and pilot phase in Nepal. Adhikari and Wegstein (2011) recently carried out a financial analysis of biodiesel production from jatropha oilseeds in Nepal. The cost components considered were crude oil production and transport cost, labor cost, energy required during transesterification, methanol and catalyst cost, interest in loan repayment for a 1000 litre/day capacity biodiesel processing plant. The analysis showed that the biodiesel production cost was $0.89/litre for the first year, $1.03/litre in the fifth year and $1.24 /litre in the tenth year. The biodiesel price is similar to that of the commercial diesel available in the market. The economic sustainability of biodiesel can easily be justified based on the very high cost of diesel, yet, a very scarce resource in Nepal.

3.3.2.5 Social Sustainability

The social sustainability has very closely connected to the economic, environmental, safety sustainability and food security. Biodiesel produces less air pollution than diesel and the people will have improved health conditions locally and regionally. Biodiesel is considered to be less toxic to the environment. Biodiesel has a higher flash point

than diesel and is safer to handle, store and transport. As biodiesel is produced locally, there is a higher energy security compared to that of imported diesel. Locally produced biodiesel also provides economic opportunities for the local and regional population. On the other hand, biodiesel policies if not carefully implemented, may compete with food (see sections 3.3.2.5). With all the positive attributes, biodiesel can fulfill the condition for social sustainability.

3.3.2.6 Institutional Sustainability

Institutional framework comprises of a set of fundamental social, political and policy rules that establish the basis for program implementation. Nepal has a very good example of achieving institutional sustainability in the micro hydro sector, where government, international non-governmental organizations, local governments, community based organizations and village level governments work collaboratively. As biodiesel is relatively a new and emerging field, its promotion and development should include activities such as awareness generation, research and development, incentives formulation, institutional linkages among others. Biodiesel sustainability is strongly linked with sustainable supply of feedstocks, which is supplied from commercial farming or cooperative farmers which has a direct link with agriculture, farmers' associations, forest users group etc. In order to connect small farmers to the biodiesel industry, a carefully designed institutional arrangement is required between the feedstock producers and biodiesel refining companies.

Technical and financial support, tax exemption to small farmers and entrepreneurs are some of the important elements of the sustainability arrangement for biodiesel promotion at the early stages. Biodiesel development requires people with skill in refining, processing, transportation and handling and waste management. Academic and training institutions should be at the forefront at the early phase of the development as technical capacity building is an integral part of any new technology development including biodiesel. The Alternative Energy Promotion Centre (AEPC) under the Ministry of Environment (MoE) is taking the lead in other renewable energy

development initiatives including ethanol. The AEPC has started some study and support program for feedstock growing farmer. Considering the urgency of the fuel supply, AEPC should accelerate the biodiesel promotion by coordinating donor agencies, international non-governmental organizations and local government. In summary, institutional sustainability for biodiesel promotion can be achieved with effective utilization of the current knowledge of the institutions in other renewable energy sector and providing financial and technical capacity at a different level.

3.3.2.7 Food Security

Currently, more than 95% of the world biodiesel has been produced from edible oils (Gui et.al, 2008). With more uncertainty and increase in the price of fossil fuel, this rate is increasing, especially in the developing world where food is scarce. Some recent studies expressed serious concerns over the use of edible oil for biodiesel production and suggested that biodiesel should be produced from the non-edible, non-food grade plant and vegetable oils to avoid the competition with food (Chhetri, et al. 2008; Balat, 2011). Nepal is a net importer of food and diverting the agricultural land into biofuel production will have serious impacts on the food balance. In terms of food vs. fuel debate, food security can be achieved in two ways. The farmland should not be diverted away from food to produce biodiesel feedstock and the food crops should not be used for fuel purposes. Food security can be achieved by assigning the wasteland and non-cultivated agricultural land for energy crops. The use of wastelands for energy crops will replenish wasteland and prevent landslides as well. The other way to achieve food security is to use non-edible oil feedstocks such as jatropha, soapnut, algae biodiesel production. Seed cakes from jatropha oil can be used as fertilizer to replace the chemical fertilizer to produce energy crops reducing the environmental impacts from its life cycle chain (Gubitz et al., 1999). Recent interest in biodiesel production from non-edible feedstocks such as jatropha curcas and microalgae is a positive step towards producing sustainable biodiesel feedstocks without competing with edible oil and conventional agricultural lands. In Nepal, due to urban migration and for various other reasons, a significant amount of non-cultivated

agricultural land is available which is suitable for jatropha and other feedstock production. The only way to produce sustainable biodiesel production without competing with food is to utilize the non-cultivated agricultural land and wasteland to produce biodiesel fuels.

3.3.3 Other Energy Sources

There are other energy sources which are being promoted as sustainable energy sources such as biogas, solar thermal, solar photovoltaic and wind energy resources. Biogas has been one of the most successful programs in rural Nepal where over 250,000 households have installed family size biogas plants digesting organic matters and producing methane for cooking gas. Solar thermal has been another success story in the country where over 300 sunny days are available in a year. Solar photovoltaic and wind energy are also gaining ground in isolated remote areas where there is no possibility of grid extension. Even though the small scale wind and solar photovoltaic are becoming very attractive because of the government subsidies, they are very expensive means of power generation. Moreover, the solar photovoltaic and wind turbine components are all imported from outside and the investment money goes out of the country with not much impact in the industrial development locally. However, they are clean sources of energy with a positive impact in the society and fall under the weak sustainability category.

3.4 SUMMARY AND CONCLUSION OF CHAPTER 3

In this Chapter, existing theories on sustainable development and sustainability of natural resources are reviewed and summarized. The indicators for weak and strong sustainability have been discussed. Micro hydro projects and biodiesel fuels are evaluated for their sustainability using the strong sustainability indicators. The discussion indicates that the renewable energy sources including micro hydro and biofuels are considered to be sustainable in the Nepalese context.

The next Chapter discusses on the potential feedstock availability for biodiesel production in Nepal.

CHAPTER 4 POTENTIAL OF BIODIESEL FEEDSTOCKS IN NEPAL

4.1 BACKGROUND

Nepal is endowed with huge natural resources over its entire area of about 14.1 million hectares. The country's topography is constituted with Mountains, Hills and Terai (plains). Nepalese forests are reported to have a vast quantity of oil bearing plants and nuts. Over 286 oil bearing plants are found in Nepal and out of them 92 species produce seeds with oil content exceeding 30% (Singh, 1980). In some cases, it has been reported that the oil content reaches as high as 80% (Shrestha et al 2003, Boswell 1998). Pine oil (pinus roxburghii) is one of such oil bearing plants with estimated 3 million tonnes of oil annually (Kumar et al., 2006). Biodiesel can also be produced from dhaka (*Aregmone mexicana*), nageswhor (*Mesua ferrea*), jatropha (*Jatropha curcas*), soapnut oil (*Sapindus mukurossi*), mahua oil (*Madhuca Indica*), seabuckthorn oil (*Hippophae rhamnoides L.*), caster oil, hempseed oil, rapeseed oil, soybean oil, waste cooking oil and animal fat available in Nepal.

Rapeseed and soybean oils are edible oils and are not considered as a biodiesel source in Nepal. However, these resources have not been exploited commercially. Sal (*Shorea robusta*) is also a highly seed producing plant with high oil content. The total Sal seed oil production estimated for the period 1984-1986 was 0.43 million litres (Vantomme et al., 2002; Jackson, 1994). As the major forest of Nepal is comprised of a large quantity of Sal trees, the actual harvesting of Sal seed and oil could increase by several fold. However, there is no information available on the type and quality of oil from Sal seed. Hence, this was not included in this work.

Johnston and Holloway (2007) estimated that Nepal has the potential of producing 49.04 million litres of biodiesel from animal fats and lipids. They estimated that Nepal's biodiesel could be worth up to US$17910000. This research indicated that there is a

significant potential for biodiesel production from lipids and fats in Nepal. Due to the large volume of diesel use, there is a significant opportunity for diesel replacement by biodiesel in Nepal. The annual diesel consumption in Nepal has been discussed in Chapter 2.

4.2 JATROPHA OIL

Jatropha curcas L. is a plant that belongs to *Euphorbiaceae* family which produces a significant amount of oil from its seeds. Jatropha is a non-edible oil-producing plant found in arid, semi-arid and tropical regions globally. It is a drought resistant perennial plant that can grow in marginal lands living over 50 years (Boswell, 2003). (Pramanik, 2003) reported that jatropha seed contains approximately 30 to 50% of oil by weight of the seed and from 45 to 60% of oil by weight of the kernel itself. In addition to the oil production, the jatropha tree has several beneficial properties including its use in the production of natural pesticides etc. (Chhetri et al., 2007). It is a rapidly growing tree and is easily propagated.

Figure 4.1 shows jatropha planted in Nepal (locally called 'Sajiwan') as a living fence to protect crops. Jatropha grows below 1400 meters of elevation requiring a minimum rainfall of 250 mm, with an optimum rainfall between 900-1200 mm (Bosswell, 2003). Jatropha is considered to be one of the most promising potential feedstocks to produce biodiesel in Europe, Africa and Asian including Nepal.

Figure 4.1 Jatropha planted as a living fence, its fruit and seed from Nepal (The

Jatropha can be grown all over Nepal in tropical and sub-tropical climatic areas of 70 out of 75 districts of Nepal. Jatropha can be propagated either by seed or by stem cutting (Bhattarai, 2009). Jatropha produces non-edible oil (Chalatlon et al., 2011) and can be grown in degraded land. Jatropha has several advantages over other biodiesel feedstocks.

- Low cost seeds,
- High oil content
- Increased safety due to higher flash point compared to diesel Smaller gestation period
- Grows both in good and degraded soil
- Grows in low and high rainfall areas
- Seeds can be harvested in the non-rainy season
- Multi plant use including biodiesel, soap, organic fertilizer and mosquito repellent.

Of the total of 14.1 million hectares (ha), 21 % of the land is agricultural land in Nepal (Parajuli, 2009). Joshi et al. (2008) reported that 13% of the total land area is pasture, 8% is non agricultural land, 40% is forest and 18% others. Hence, the total cultivated and non-cultivated agricultural lands are 2.96 and 1.13 million ha respectively. Similarly, the pasture land area is 1.83 million ha, forest area is 5.64 million ha and others 2.54 million ha respectively (Figure 4.2).

In addition, approximately 2.38 million hectares of land is in buffer zones of various national parks and wild life reserves, of which 0.39 million hectares is climatically suitable for jatropha production. The ecological distribution of the country indicates that approximately 21 % of the mountains, 51% of the hills and 28 % of the terai have uncultivated land (Parajuli, 2009). This study showed that about 30% (4.23 million hectares) of the total land of Nepal is considered favorable for jatropha cultivation.

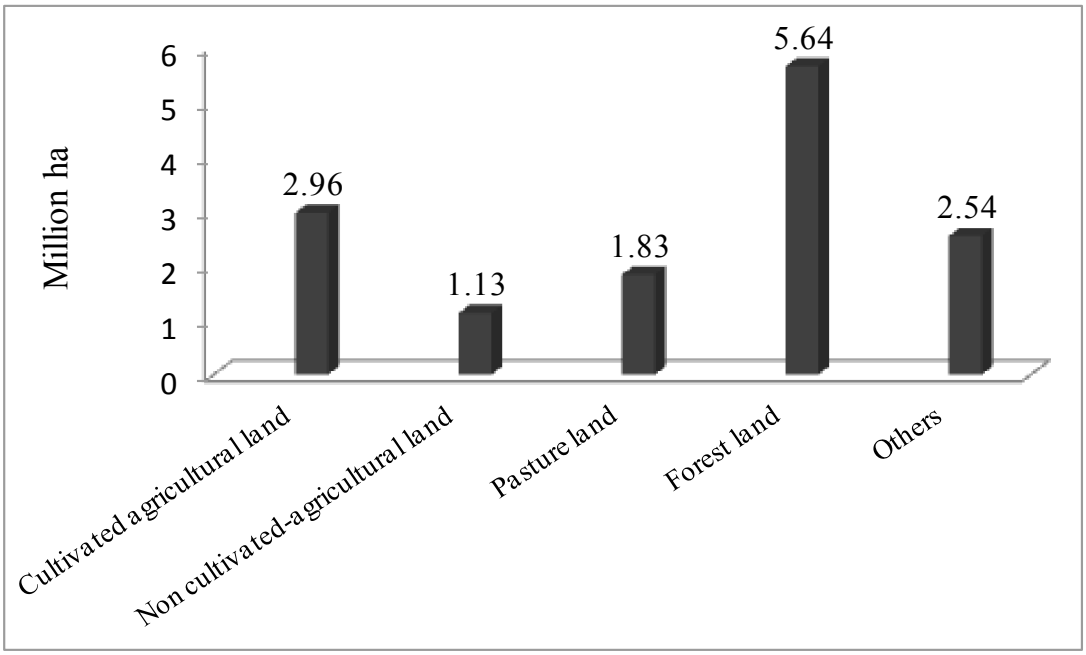

Figure 4.2 Land use pattern in Nepal (Joshi et al., 2008)

Bhattarai (2009) reported that jatropha needs 2m x 2m area for each plant and 2500 plants can be grown per hectare of land. Boswell (1998) estimated that the jatropha oil yield in Madagascar was 2400 litres/ha/year and Nicaragua 1630 litres/ha/year. Biswas et al. (2010) estimated that 1750 kg of oil can be produced per ha of land in India. Pokharel and Sharma (2008) estimated that approximately 1000 litres of jatropha oil per hectares of land per year can be produced in Nepal's climatic condition based on average seed yields and 30% oil content in seed. For the purpose of estimating the potential of jatropha, 1000 litres/ha/year has been used in this work.

Several theoretically potential scenarios for the production of jatropha biodiesel are examined based on the total land available where jatropha cultivation is climatically feasible (Figure 4.3). Here, Scenario-1 is the total jatropha biodiesel production potential based on 100% of climatically favorable land in Nepal (4.23 million ha), which has a potential of producing 4230 million litres of biodiesel. Similarly, Scenario-2, Scenario-3 and Scenario-4 show the potential of biodiesel production considering jatropha production in 50%, 20% and 5% of the total climatically favorable land. If jatropha is produced in 20% of the total land climatically favorable for its cultivation, 846 million litres of biodiesel can be produced, which is 175 % more than the total diesel consumption for the year 2008-2009 in Nepal (489 million litres).

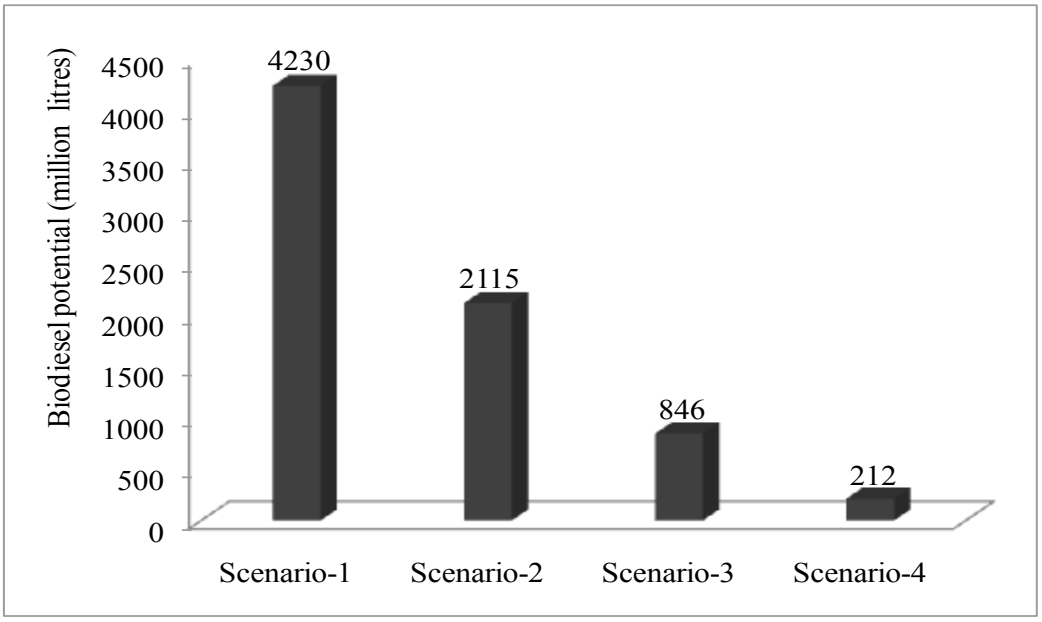

Figure 4.3 Theoretical potential for jatropha biodiesel production based on total land climatically favorable for jatropha production (million litres per year)

Other scenarios were examined for jatropha production for available non-cultivated agricultural and buffer zone areas (Figure 4.4). The total non-cultivated agricultural land in Nepal is estimated to be approximately 1.13 million ha, and the buffer zone suitable for jatropha production is estimated to be 0.39 million ha (Parajuli, 2009). In Scenario-5, it was assumed that 100 % of the non-cultivated agricultural land and 100% of the buffer

area can be used for jatropha production. A total of 1516 million litres of jatropha biodiesel can be produced in this Scenario annually. Scenario-6 assumes 50% of non-cultivated agricultural land and 50% of buffer zone area be used for jatropha production with a potential biodiesel production of 758 million litres annually. Scenario-7 represents 20% of non-cultivated agricultural land and 20% buffer area which is climatically suitable for jatropha production which is equivalent to 0.30 million ha that can potentially produce 303 million litres of jatropha biodiesel. This amount can replace approximately 62% of the total diesel consumed in Nepal in 2008-2009. Scenario-8 assumes that if only 5% of the total non-cultivated agricultural and 5% of the buffer zone area used for jatropha production, it has the potential of producing 76 million litres of jatropha biodiesel. This is approximately 16 % of the total diesel consumed in Nepal in 2008-2009. This means that even if only 5% of the non-cultivated agricultural land and 5% of buffer zone areas are used for jatropha cultivation, approximately 16 % of the total diesel import can be avoided. If 20% blend of jatropha biodiesel is used, it is sufficient to blend with 78 % (381 million litres) of total diesel consumed in Nepal in 2008-2009. Hence, jatropha biodiesel could potentially change the total diesel import scenario in Nepal.

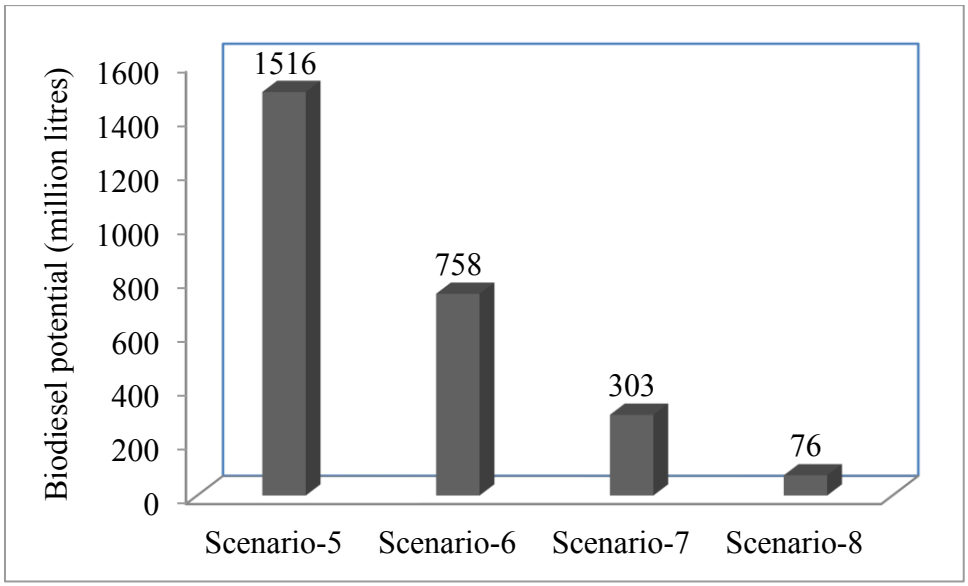

Figure 4.4 Potential for jatropha biodiesel production based on total non-cultivated agriculture land and Buffer Zone areas for jatropha biodiesel production (million litres per year)

4.2.1 Carbon Sequestration from Jatropha Plantation

Plantation of jatropha sequesters a significant amount of carbon dioxide. Hooda and Rawat (2006) estimated that jatropha plantations can sequester 8-10 tonnes of carbon dioxide per hectare annually. Here, 8 tonnes per ha of carbon sequestration has been considered for estimation. Assuming such a project is developed as the Clean Development Mechanism (CDM) project in Nepal, its value for various scenarios has also been presented in the Table 4.1. The value of carbon was assumed to be $7 per tonnes based on the CDM transaction for the biogas programs in Nepal.

Table 4.1 Carbon dioxide sequestration under different scenario of jatropha plantation (Author's estimation)

Scenario	Type of land	Total potential area (million ha)	Annual carbon sequestration (million tonnes CO_{2e})	Potential CDM grant (million dollars)
Scenario-1	100% of climatically favorable land	4.23	33.84	236.88
Scenario-2	50% of climatically favorable land	2.12	16.92	118.44
Scenario-3	20% of climatically favorable land	0.85	6.77	47.38
Scenario-4	5% of climatically favorable land	0.21	1.69	11.84
Scenario-5	100% of non-cultivated land and 100% of buffer area	1.52	12.13	84.90
Scenario-6	50% of non-cultivated area and 50% of buffer area	0.76	6.06	42.45
Scenario-7	20% of non-cultivated area and 20% of buffer area	0.30	2.43	16.98
Scenario-8	5% of non-cultivated area and 5% of buffer area	0.08	0.61	4.48

Similarly, replacement of diesel by biodiesel can help reduce two-thirds of the total emissions. Table 4.1 shows the total CO_2e offset generated by the replacement of diesel by biodiesel. Hence, developing jatropha plantations and biodiesel production can help reduce the environmental impact as well as earn money from the global carbon market.

4.2.2 Initiatives for Jatropha Development in Nepal

A recent annual budget of Government of Nepal has made a special provision to help community organizations and cooperatives to plant jatropha as feedstock for biodiesel production (GON, 2008). As a result, many community based organizations and private entrepreneurs have started to plant jatropha aiming at producing biodiesel. The Alternative Energy Promotion Centre (AEPC), Nepal, has signed agreements with 11

organizations to produce jatropha seedlings to produce feedstock for biodiesel. In addition to this, dozens of other private and community organizations have started planting jatropha in different parts of the countries. In 2009, AEPC signed contracts with four organizations to carry out pilot tests for biodiesel production from jatropha as a biodiesel feedstock. Two of these organizations have recently completed installation of transesterification plants which can process biodiesel up to 1000 litres/day. Netherlands Development Organization Nepal (SNV) has also been involved in carrying out supply chain analysis of jatropha production in some parts of Nepal. Another international non-governmental organization (Winrock International) is carrying out a pilot project initiative for operating irrigation pumps from biodiesel. However, there are neither appropriate incentives for the communities, entrepreneurs and small businesses to pursue this initiative nor any supporting policies to promote biodiesel development despite a huge demand for biodiesel in the country.

4.3 SOAPNUT OIL

Soapnut (Sapindus mukurossi), a tropical and subtropical tree with potential to produce oil for biodiesel feedstock. Soapnut is reported to be widely grown in forests areas in Nepal in the elevation range of 300-2000m (Olsen, 1997). It is reported that Sapindus mukorossi species of soapnut grows in altitudes from 200 to 1500 m in regions with precipitation between 1500 to 2000 mm/year (Haryana-online.com, 2007). Soapnut is a non-edible oil being considered for a feedstock for biodiesel production. For this study, the soapnut seeds were collected from the elevation of 1300 m where the average annual rainfall is 1500 mm /year (Chhetri et al., 2008). Soapnut grows in deep loamy and leached soils preventing potential soil erosion. The wood from the soapnut tree can also be used for various applications including building construction and agricultural implements. Thus, integration of soapnut plantation in community forests would help to produce more seeds as a potential source for the biodiesel feedstock.

4.3.1 Soapnut Plant Description

Figure 4.5 (Haryana-online.com, 2007) and 4.6 are the soapnut tree showing fruit, seed, seed shell and the kernel. Soapnut is found in tropical and sub-tropical climate areas in various parts of the world (Chhetri et al., 2008). S. mukorossi and S. trifoliatus are the main two varieties of soapnut species widely found in South Asia including Nepal. Ucciani et al. (1994) reported that the oil content in S. trifoliatus seed kernels was on average 51.8% of seed weight. The same report also claimed that S. mukorossi has also a similar oil content. As the soapnut oil is considered non-edible, this can have a significant potential for biodiesel production.

Figure 4.5 Soapnut tree

Figure 4.6 Soapnut fruit, seed, seed shell and kernel

Soapnut has been traditionally used to make soap, surfactant and medicinal treatments. Soapnut fruit shells have been in use as natural laundry detergents from ancient times Mandava (1994) reported that saponin from soapnut shells can be used for the treatment of varierties of soil contaminants. Some other studies also indicated that soapnut has a great potential to be used as a natural surfactant for washing the soil contaminants with organic compounds (Roy et al., 1997; Kommalapati, 1998). Windholz (1983) reported that the use of saponin has no external toxic effects on human skin and eyes. Thus, the use of soapnut seed oil as a biodiesel source becomes a "waste-to-energy" model (Chhetri et al., 2008). Thus, planting soapnut trees in community forestry and in barren lands provides a sink for carbon sequestration as well as feedstock for biodiesel production (Chhetri et al., 2008).

Nepal has a long history of soapnut export especially to its southern neighbor, India, and to some other countries. Nepal exported 32 non-timber forest products of the total value of 8.1 million US dollar in the year 1997/1998 (Olsen, 1997). The same report claimed that the total export of soapnut from Nepal to India was up to 52% of the total non-timber forest (Olsen, 1997). It showed that there is a potential of soapnut oil availability as biodiesel feedstock. The multiple uses of the tree including for laundry detergent, medicinal applications help enhance the life cycle economics of the feedstock as a source for biodiesel production.

Even though there is no study on the total potential production of soapnut oil in the country, Eastern Region Forest Training Centre, Biratnagar carried out a detailed study on soapnut production in Baitadi (Acharya, 2009). Baitadi is a district in far western Nepal (Figure 4.7).

Baitadi district has approximately 1,520,000 hectares of land. It is a hilly district with a suitable climate for soapnut production. Figure 4.8 shows the production of soapnut seed between 1998/1999 to 2008/2009. The maximum production was recorded in the year 2006-2007 with a total production of 578,150 kg based on the export data from the district forest office (Figure 4.8).

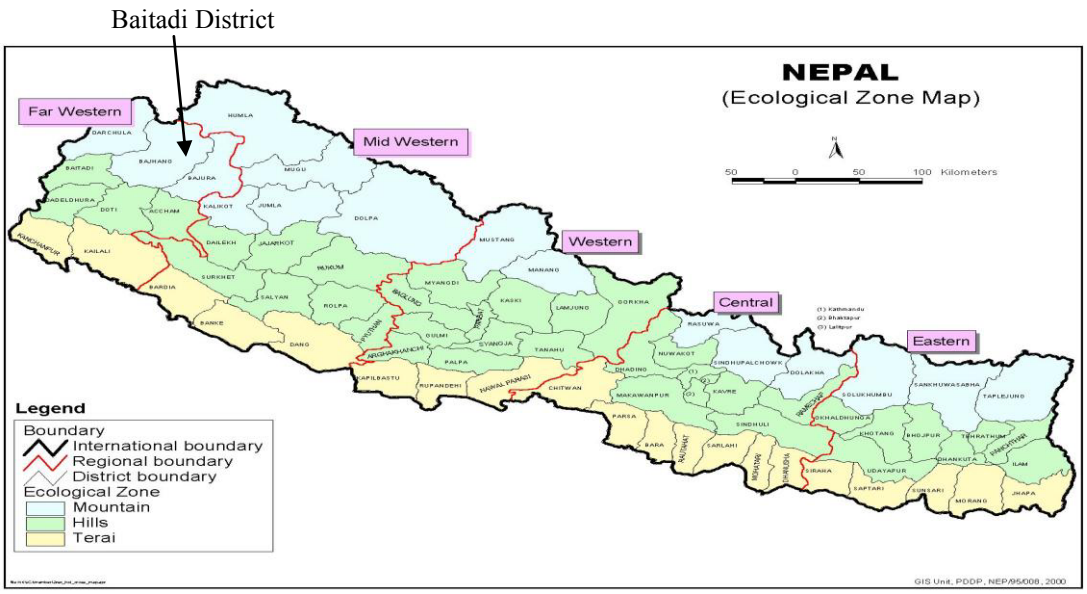

Figure 4.7 Map of Baitadi District in Western Nepal (www.un.org.np/reports/maps/npcgis/ NatBio00002.jpg)

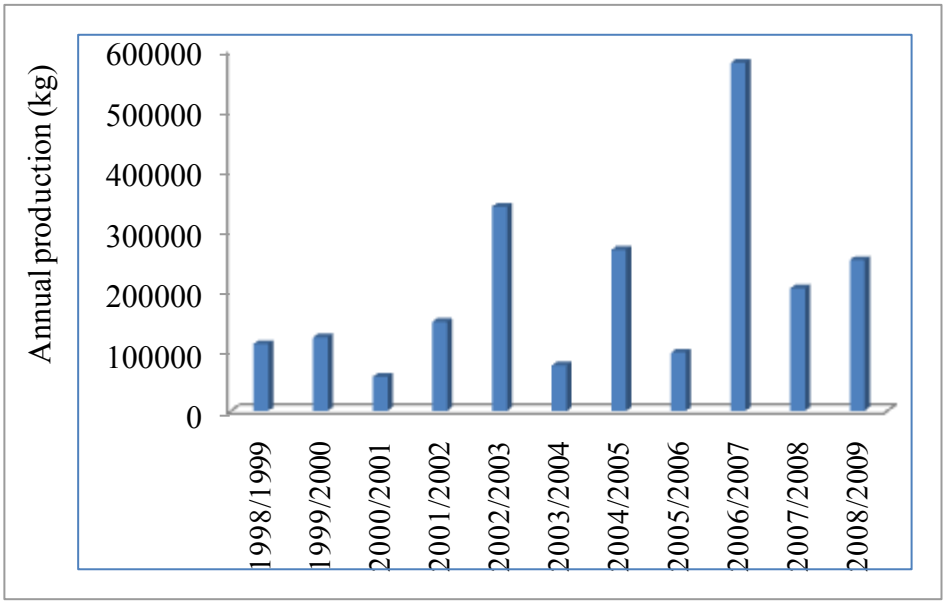

Figure 4.8 Soapnut export from Baitadi district in different years (Acharya, 2009)

Most of the produce was sold to India. The farmers and entrepreneurs are attracted to produce soapnut because of its monetary value in the market. Acharya (2009) reported

that the price of soapnut seed was NPR 20/kg in 2005-2006 and increased to NPR 50/kg in 2008-2009 with a total sale of NPR 10,150,000 only in Baitadi district (1US$=NPR 89 as of 2012). This production came from personal land of some entrepreneurs and some from plantations in the community forestry. Iqbal (1991) reported that each tree can produce between 50 to 100 kg of fruit per year.

Soapnut can be produced in a climate area similar to that of jatropha. As reported in Section 4.2, approximately 30% of the total land which is equivalent to 4.23 million hectares is suitable for soapnut production as well. However, it depends on the national policy to promote jatropha or soapnut or both.

4.4 WASTE COOKING OIL

A significant amount of waste cooking oil is generated throughout the world, including in the developed countries. As estimated by Energy Information Administration (EIA), approximately 100 million gallons of waste cooking oil is produced annually in the USA with an average per capita waste cooking oil production of 3.18 kg (Radich, 2006). For this study, per capita waste cooking oil production in Canada is assumed to be 3.18 kg per year, similar to that of US. Statistic Canada (2006) estimated the total population of Canada to be 33 millions. Based on that assumption, the total waste cooking oil generation in Canada is approximately 135,000 tons/year. Similarly, Kulkarni and Dalai (2006) reported that EU produced approximately 700,000-1,000,000 tonnes/yr of waste cooking oil. As reported by Carter et al. (2005), The UK produces over 200,000 tonnes of waste cooking oil annually. Dumping waste cooking oils illegally into rivers and landfills causes environmental problems (Yang et al., 2007). Biodiesel production from the waste cooking oil offers significant environmental benefits.

In addition to the road transportation fuels, biofuel ic claimed to be a sustainable alternative to aviation fuel (Kivits et al., 2010). A recent report revealed that the Dutch Airline KLM will begin using biofuel derived from waste cooking oil in more than 200

flights between Paris and Amsterdam (The Associated Press, 2011). The report further clarified that the airline needs minimal modification to the current jet engines to use biofuels (Kivits et al., 2010). The test flights were carried out successfully using 50-50 mix of biofuel with regular jet fuels. Similar tests were carried out in 2009 by Air New Zealand using 50/50 jatropha /Jet-A blend. Some commercial airlines also tested successfully with 25/25/50 % algae/jatropha/Jet-A blend, and no differences in performance were reported (Kivits et al., 2010). The major aim of the biofuel flights is to cut the greenhouse gas emissions from KLM's carbon emissions to reduce the impact on biodiversity and food supply. Currently, approximately 3% of the total emission in Europe is attributed to air travel. As per the European Union Directive (2008/101/EC), aircraft operators are to have a mandatory reduction of 3% in their historical aviation emissions effective from January 1, 2012 to December 31 2012. Similarly, they are to have a mandatory emission reduction from their historical emissions by 5% after 2012. The Calgary based West Jet Airlines has partnered with KLM and Air France and the new initiative may also have an impact in Canadian aviation industry in terms of the biofuel use in their commercial flights. Similarly, Virgin Atlantic and Virgin America have also planned to have biofuels to represent 10% of their fuel mix by 2020.

Different types of vegetables oils are commonly used for cooking and preparation of foods in restaurants, fast foods, hotels, bakeries and sweets shops. The oil serves as a heat-transfer medium and becomes an important ingredient of the cooked fried foods. The frying is commonly used repeatedly at high temperatures and various chemical processes such as fission, hydrolysis, polymerization and oxidation occur during frying (Al-Kahtani, 1991). After repeated use, the accumulation of decomposition products deteriorates the quality of fried food. The quality deterioration necessitates the replacement of frying oil with new oil and the discarded used oil can be used for various other purposes, one of them is as a biodiesel feedstock.

There is no data available on the per capita oil consumption in Nepal. Ramesh and Murughan (2008) reported that the per capita annual oil consumption in India, Pakistan and USA are 11.2, 16.1 and 48 kg/person/yr respectively, while the world average per

capita oil consumption is 17.8 kg/person/yr. China's per capita annual oil consumption was reported to be 17 kg/person/yr in 2008. As reported by Radich (2006), the average per capita waste cooking oil production in USA is 3.18 kg annually. Based on this data, the waste cooking oil production can be estimated to be 8.5% of the total oil used.

It was reported that there are over 100 star-rated and non-rated hotels in Kathmandu. There are 64 star-rated hotels registered with Hotel Association of Nepal (HAN) in Katmandu (HAN, 2008). Moreover, there are 47 non-star rated hotels registered with HAN. Restaurants and Bar Association of Nepal (REBAN) has slightly over 100 members affiliated with it. However, over 400 restaurants could be operating without proper registration in Kathmandu (Neupane, 2010).

The population of Kathmandu Metropoliton City was 670000 in 2006 and was projected to be 1,011,105 by 2011 (Pant and Dongol, 2009). However, due to the political insurgency in the last 15 years, many people have migrated to Kathmandu from across the country and the real population is believed to be much higher than reported by Pant and Dongol (2009). Considering the current population of Kathmandu has reached approximately 1 million and the average per capital annual oil consumption of Kathmandu is similar to that of India, which is 11.2 kg/person, the total oil consumption will be approximately 11 million kg. If approximately 8.5% of the oil is assumed to be generated as waste cooking oil, then the total potential of waste cooking oil generation in Kathmandu is approximately 0.88 million kg, which is equivalent to approximately 1.01 million litres annually, assuming the density of waste cooking oil was 900kg/m^3.

A field survey was conducted in Kathmandu in order to assess the feasibility of waste cooking oil for biodiesel production. The survey data has been analyzed and presented in Section 7.1.

4.5 ANIMAL FAT

Nepal consists of a large livestock population that includes cattle, water buffalo, sheep, goats and poultry. Pariyar (2006) reported that livestock population consisted of 6.96 million cattle (including yaks and hybrids), 3.95 million water buffalo, 0.82 million sheep, and 6.98 million goats in 2003-2004. Maltsoglou and Taniguchi (2004) indicated that three out of four households in Nepal own livestock. Livestock production is very well integrated into agricultural crop production systems. Nepal imports live animals from India to fulfill the high demand of meat in Kathmandu and other parts of the country. Nepal also exports a small number of live animals to China, India, Bangladesh from the bordering areas (MOAC, 2008).

Joshi et al. (2003) reported that buffaloes contribute approximately 64% of the total meat consumed in Nepal following by goat meat (20%), pork (7%), poultry (6%) and mutton (2%) respectively. However, meat production and processing industries are not developed systematically and there are no designated slaughterhouses for meat production. There is no provision of animal fat collection as all the slaughtering activity is very scattered. Hence, there is no availability of animal fat to produce biodiesel on a commercial scale at this time. However, once awareness increases in the use of waste fat for biodiesel production, this resource could be available in the future for such purposes.

4.6 RESIN AND TURPENTINE

Production of resin and turpentine is one of the major forest sector bio-product industries in Nepal. Karthikeyan and Mahalakshmi (2007) carried out an experimental study for the feasibility of turpentine obtained from the resin of pine trees to use as a dual fuel mixed with diesel in direct injection engines. The study reported that all other performance and emission parameters except volumetric efficiency, were found to be better than those of diesel for 75% load. Approximately 40–45% smoke reduction was obtained with a dual fuel mode. The NOx emission was similar to that of diesel at 75% load. The study proved

that approximately 75% diesel replacement is feasible using turpentine with little engine modification. Based on the data available in fiscal year 2006/07, 12 industries in Nepal produced about 13.60 million litres of resin and turpentine. Pokharel and Sharma (2008) reported that the Nepalese forest sector has a total potential of approximately 27.21 million litres of these oils which could be used as dual fuel mixed fuel with diesel in Nepal. This preliminary information indicates that such resources could be used as a feedstock for the biodiesel production biodiesel in Nepal.

4.7 OTHER RESOURCES

In addition to the abovementioned oil sources, there are a number of other oil bearing plants potential for biodiesel production including dhaka (aregmone mexicana), nageswhor (mesua ferrea), mahua oil (madhuca indica), seabuckthorn oil (Hippophae rhamnoides L.), caster oil, hempseed oil etc. Studies have yet to be done in order to determine the oil content, oil characteristics and feasibility of these oils for biodiesel production.

Sal seed oil is another potential feedstock for biodiesel production in Nepal (Panhwar, 2005). It is a tree found in the tropical and sub-tropical climate area of Nepal. The sal forest is found to be distributed over 1 million hectares of forest in Nepal (GON, 1989). It extends from a few metres to 1500 m above mean sea level. As the major forest of Nepal, sal seed could produce a significant amount of oil. Panhwar (2005) carried out tests to determine the fatty acid profile of sal seed oil as presented in Table 4.2. Jackson (1994) reported that Nepalese sal forest has a potential to produce over 430,000 litres of sal seed oil. As the fatty acid properties are similar to that of other plant oils, this could also be a potential source for biodiesel production. However, no research has been carried out to date to study the feasibility of this resource in Nepal.

Table 4.2 Fatty acid composition (%) in sal seed (Panhwar, 2005)

Palmitic (C16:0)	Stearic (C18:0)	Oleic (C18:1)	Linoleic (C18:2)	Arachidic (C20:0)
4.5	44.2	42.2	2.8	6.3

4.8 POLICY RECOMMENDATIONS FOR BIODIESEL PROMOTION IN NEPAL

4.8.1 Regulatory Requirement for Blending

Different countries in the world have regulatory provisions requiring a certain percent renewable fuel content in fossil fuel use. Based on the Canadian Environmental Protection Act, 1999, Canada requires at least 5% renewable fuel content on gasoline use by September 2010 (Canada Gazette, 2010). This provision also requires 2% renewable fuel content in diesel and heating distillate oil by 2010. Nepal's neighbor, India, has a very ambitious biodiesel blend requirement of 20% blend primarily by jatropha biodiesel beginning with 2011-2012. Based on the Europeon Commission directive 2009/20/EC, it is mandatory that there should be 7% blend of fatty acid methyl ester in diesel fuel. Even though there is 10% blend in ethanol required from a regulatory perspective in Nepal, there are no fuel blend requirements for biodiesel yet. Establishing a blend requirement for biodiesel will be an effective policy to encourage jatropha cultivation and biodiesel production. This will save large amounts of money being spent on fuel imports, create economic opportunities for small business, entrepreneurs and community based organizations such as cooperatives and reduce air pollution and potentially earn revenue from the Clean Development Mechanism (CDM) of Kyoto Protocol generating carbon offsets. However, for developing countries like Nepal, the policy should be clearly directed that no land used for food production can be used to produce biodiesel fuel to avoid food vs fuel conflicts. However, at present, edible food and oils are more expensive than diesel so the market itself will not allow using food for fuel in Nepal.

4.8.2 Research and Development

Research programs for assessment of appropriate plant varieties for high yield, identification of lands, collection of seeds and transportation to the processing plants, oil extraction technologies, transestification and production of biodiesel, transport of biodiesel to the depot for necessary blending and distribution of blended diesel to the retail stores are fundamental to the success of biodiesel development programs (Bishwas et al., 2010). All these aspects should be studied carefully to enable biodiesel to have a competitive price with diesel. The initial phase will be on experimentation, demonstration and communication of the biodiesel opportunities until the biodiesel production initiative gains momentum. The next phase will be the involvement of private entrepreneurs throughout the country. Leading universities and research institutions should be involved to identify appropriate cultivation methods, planting procedures, planting densities, manure practices and propagation by cutting or seedlings. Setting up some demonstration plants in different parts of the country to understand the yield, effectiveness of the cultivation technique in different locations and potential economic benefits is essential. Research should focus on both improvements of the generic varieties as well as diffusion of the best cultivation techniques at a commercial level so as to have a high yield of jatropha.

4.8.3 Quality Control

Production of a standard quality biodiesel is very important. The biodiesel produced from any feedstock should meet certain quality standards for the clean and safe operation of the engines. The European biodiesel standard EN 14214 describes the requirements and test method for fatty acid methyl ester, which is the most common type of biodiesel. The US has adopted the ASTM D6751 standard for biodiesel. D6751 is also used in many other countries around the world including Canada, Brazil, Malaysia, Greece, Singapore and the Philippines (ASTM, 2009). These standards specify the viscosity, pour point, flash point, glycerine content, cetane number, catalyst content and other qualities. Nepal also should adopt either ASTM D6751 or EN14214 to maintain the quality of biodiesel

produced from the various feedstocks for the sustainable and clean operation of biodiesel in the engines.

The quality of biodiesel is not only important from the point of fulfilling the regulatory requirement, but it is also important to tackle the extreme climates. Nepal having some sub-alpine, alpine and trans-himalayan ecological zones, sufficient measures should be taken to use biodiesel effectively. The cold climate could have a serious impact on biodiesel fuel during engine start-up and storage. Table 4.3 below shows the temperature extremes in different ecological zones in Nepal.

Table 4.3 Temperature extremes in Nepal (min/avg/max by Ecologocal Zones (K) (Nayaju and Lilleso, 2000)

Ecological Zones	Days> 303 K Min-Max	Max Temp (k) Min-Max	Days < 273 K Min-Max	Min Temp (K) Min-Max
Lower Tropical	199-246	314-319	Less than 1/10	273-268
Upper tropical	62-215	308-318	Less than 1/10	271-280
Sub-Tropical	0-173	302-313	0-53	264-277
Temperate	0-47	296-315	0-132	259-273
Sub-Alpine	None	293-299	145-229	255-260
Alpine	-	-	-	-
Trans-Himalayan	None	-	195	247

The cloud point of biodiesel, which is one of the most important characteristics of biodiesel varies generally between 258 to 288 K. The cloud point of canola, soapnut and jatropha biodiesel used in this study were 272, 278 and 275 K. The biodiesel needs to be stored at slightly higher than the cloud point temperature. From Table 4.3, it is clear that there are minimum temperatures in the winter which might result in biodiesel solidification, plug the biodiesel fuel filter, and jell the fuel itself. The sub-alpine, temperate and alpine zones have approximately 0-53, 0-132 and 145 – 229 days with less than 273 K annually and issues related to cloud point, cold filter plugging and pour point during storage and engine operation needs to be given attention. Even though the current

road network is not extended to those areas, with the rapid development of infrastructure, further road networks are anticipated in the future. Insulated storage tanks or addition of some additives should be considered. The lower tropical, upper tropical and sub-tropical zones will generally have no issues with biodiesel use. Currently the road network is limited in these zones only.

4.8.4 Awareness

Farmer and entrepreneurs should be sensitized to the biodiesel initiatives in the country during the first phase of implementation. AEPC, the ministry of forestry and other relevant institutions can organize various information dissemination programs in public forums and other communication media. Educating students in schools and colleges would also have a great impact in awareness generation. Radio and TV will also be effective means of communication for awareness generation. Human resource development packages to train people for cultivation, harvesting, oil extraction and maintenance of processing centre should be developed. Capacity building for small cultivators, farmers, and options to access the micro financing opportunities and subsidies should be well communicated to generate the interest of entrepreneurs and small businesses to pursue the jatropha program.

4.8.5 Institutional Framework and Private Sectors

Alternative energy development is the responsibility of AEPC under the Ministry of Environment, science and technology (MoEST). The land use planning is also a key aspect of the potential jatropha initiatives in Nepal as various types of non-cultivated land needs to be utilized for its production. This is looked after by the Ministry of Land Reform (MoLR). The cultivation practices and necessary supplies of subsidies to farmers including fertilizer importation for all agricultural and non-agricultural production falls under the jurisdiction of the Ministry of Agriculture (MoA). Nursery development and plant development initiatives could be contributed by experts from Ministry of Forest and

Soil Conservation (MFSC). The diesel transport, storage, blending and retailing is the responsibility of Ministry of Commerce and Supplies (MoCS) and the same facilities needs to be utilized for biodiesel storage, transport and blending. Hence a well coordinated effort to be coordinated by the national institution like National Planning Commission (NPC) which can bring all these ministries together including some international organization for technology transfer is very important in effective implementation of the jatropha development program in Nepal. Currently there is no mechanism of such a framework and coordination. Involving the private sector through public-private partnership model based on Nepal's successful approach could bring a sustainable impact in the sector in the long run.

4.8.6 Carbon Credit Linkage

Pokharel (2007) estimated that the total greenhouse gas emissions (GHGs) from the Nepalese energy sector were 3.8 million tCO_2e in 2003 and 39% of the total GHGs emission was contributed by diesel alone. At the same time, Nepal has also generated income selling the carbon credits from the biogas sector. The Community Development Carbon Fund of World Bank is buying carbon credit from Nepalese Clean Development Mechanism (CDM) projects (biogas) at \$7/t CO_2e from biogas up to one million tonnes annually (WB, 2009). Dhakal and Raut (2010) did an analysis of the various CDM projects and concluded that bio-energy utilization could also be one of the potential projects for CDM grants. In jatropha cultivation and biodiesel production, carbon credits can be achieved in two ways. First, carbon credits can be received for the plantation of jatropha plants which takes carbon dioxide from the atmosphere and works as a carbon sink. Secondly, carbon credits can be received from certified reduction of CO_2e emission due to replacement of diesel by biodiesel. Hence, jatropha cultivation and biodiesel production initiatives could benefit if developed as CDM or other carbon off-setting projects in Nepal.

4.8.7 Financial Incentives

Nepal has several financial incentives to promote renewable energy technologies. AEPC (2009) policy document illustrates that each household in the Terai region installing a biogas plant will receive NPR 9000 subsidy for installation. Similarly, each household installing biogas in hilly and remote areas will receive NPR 12,000 and NPR 15,000 respectively. A subsidy is also available for micro hydropower (MHP) generation. A subsidy of NPR 12,000 is available for each household to install MHP of 5 kW capacities not exceeding NPR 97,000 per kW of generation. Similarly, for MHPs between 5 kW and 500 kW, NPR 15,000 per household will be provided not exceeding NPR 125,000 per kW generated. There are also transportation subsidies for micro hydro equipments to transport to the installation sites. Subsidies are also available for solar photovoltaic electricity generation at a household level. Such subsidy ranges from NPR 5000 in accessible areas to NPR 7000 in remote areas for capacities between 10-18 watt capacities. Over 18 watt capacity, the subsidy for each installation is NPR 6000 in accessible areas and NPR 10,000 in remote areas. There are subsidies for solar cookers, dryers and water pumping for irrigation and drinking water projects. Subsidies are also available petroleum products being used in the country.

As other renewable energy sources, promotion of biodiesel would also need financial incentives in the form of subsidies, grants and loans. Community based organizations, micro enterprises, and private businesses should be provided with financial incentives for jatropha cultivation, technology for oil extraction and biodiesel processing so that biodiesel production can take momentum quickly. The incentives could also include skill of human resource development through training. Since biodiesel feedstocks could be grown in areas with less access to transportation, incentives should be offered for their transport to the processing stations as well as transferring processed biodiesel into the retailers. Moreover, the successful development of jatropha biodiesel industry would also require appropriate pricing policies for jatropha seeds and biodiesel. Suitable tax exemptions at the beginning of the development phase can also play a great role for cultivators and other stakeholders.

4.9 SUMMARY OF CHAPTER 4

In this Chapter, major potential feedstocks for biodiesel production in Nepal have been discussed. Jatropha has been studied and discussed as one of the major feedstock sources for biodiesel production in Nepal based on the suitability of climatic and soil conditions. Various scenarios have been developed to estimate the potential of jatropha biodiesel production and possible diesel replacement. The benefit of jatropha from carbon sequestration perspective has also been discussed. The potential of greenhouse gas (GHG) emission reduction by switching from diesel to biodiesel or biodiesel blends and sale of the carbon into the international market has been discussed. In addition to jatropha, the potential of other non-edible oil resources such as soapnut, resin and turpentine, waste cooking oil has also been described. Some policy recommendations have been made in order to promote biodiesel as a sustainable alternative fuel.

The next chapter discusses the fuel and atomization characterization of biodiesel products.

CHAPTER 5 DIESEL ENGINES AND CHARACTERIZATION OF BIODIESEL PRODUCTS

5.1 DIESEL ENGINES TYPES AND OPERATING PRINCIPLES

Diesel engines are the internal combustion engines widely used in the transportation as well as in industrial sectors today. An internal combustion engine operates by burning its fuel inside the engine. Combustion fuel creates high temperature and pressures gas which is allowed to expand that moves a piston, turbine blades or rotor doing useful work. Internal combustion engines are engines which typically can run only on a single fuel type. Diesel engines are of two types namely Direct Injection (DI) diesel engines and Indirect Injection (IDI) diesel engines (Challen and Baranescu, 1999). The fuel in the direct injection diesel engines is injected into the combustion chamber under high pressure through a nozzle with single or multiple orifices of small sizes, directing the fuel into the piston. Similarly, in the case of indirect injection diesel engines, the fuel is injected in an auxiliary chamber adjacent to the combustion chamber and burning gases exit the chamber with a very high velocity giving a greater ability for mixing of fuel and air.

Diesel engine cars, trucks and generators can be two or four stroke internal combustion engines. Only the four stroke engine is discussed for purposes of this thesis. The four strokes of the engine cycle constitute intake, compression, power and exhaust cycle. The piston moves down drawing the fresh air into the cylinder during the intake stroke (downward). In the compression stroke (upward), the air is compressed and the fuel is injected. Combustion starts in the third stroke and continues as long as the fuel is injected. As the fuel burns, expansion of gases takes place increasing temperature and pressure which drives the piston downward. The cylinder compression pressure is in the range of 2-4 MPa and the corresponding temperature is nearly 40^{o}C initially at the beginning of the ignition (Joshi, 2007). At the later stage, the combustion occurs at a rate governed by diffusion and continues until all the fuel is used. The peak pressure is in the range of 5-8 MPa. The fuel combustion continues. In the exhaust or the last stroke, the

exhaust valve is opened and the upward stroke of the piston drives the combustion products (exhaust) out of the cylinder.

5.2 FUEL CHARACTERIZATION OF BIODIESEL PRODUCTS

Biodiesel is a diesel engine fuel comprised of mono-alkyl esters of long chain fatty acids derived by transesterification of plant or vegetable oils and animal fats, designated as B100, that meets the requirements of ASTM D 6751 (US) or EN 14214(EU). Biodiesel fuel meeting such requirements have similar properties to that of conventional diesel fuel.

ASTM is recognized in the United States and Canada by most government entities. The European specification EN14214 is very similar to the ASTM D6751, and is in fact slightly more stringent in a few areas since EN 14214 was developed for B100 use whereas ASTM D 6751 that was developed for the use of B20 or lower blends. ASTM D6751 is thus the minimum standard that is acceptable as B100 biodiesel blend. ASTM D6751 needs to meet the standards set for cold filter plug point (CFPP), pour point, oxidative stability, sulfur content, water and sediment content, flash point, kinematic viscosity at 400C, cetane number, carbon residue, acid number, glycerin and other residuals in the final product.

Biodiesel must meet each of the properties listed in ASTM 6751 to eliminate or minimize the problems due to biodiesel fuel use. EN14214 includes the majority of parameters specified in the US biodiesel standard ASTM D6751. The respective limits for these parameters in these two standards are the same or very similar. Yet the standards differ slightly in their intended use and test methods. Moreover, the European biodiesel standard includes the allowable alcohol level (should be less than 0.20% by mass) in the end product. This property is not included in ASTM 6741 standard. However, ASTM requires the alcohol test if the flash point of the test fuel does not meet the required standard. It is reported that the biodiesel may still contain 2-3% methanol after the separation. The residual alcohol level in biodiesel is recommended to be low. Van

Gerpen et al., (2004) reported that even with 1% methanol content in the biodiesel can lower its flashpoint from 170^{o}C to less than 40^{o}C. ASTM has a flashpoint specification of 130^{o}C that limits the amount of alcohol to a very low level (less than 0.1%). Due to the reduced flashpoint limits, ASTM standard is comparable with the EN14214. Moreover, the EN14214 for alcohol is intended basically for methanol. The fuel characterization tests of biodiesel from different feedstocks are discussed in Chapter 7.

5.3 ATOMIZATION PROPERTIES OF BIODIESEL FUELS

Fuel atomization is a very important characteristic of liquid fuels which enhances the proper mixing and complete combustion in direct injection engines increasing the engine efficiency thus reducing pollutant emissions. Atomization is the process in which the liquid jets are broken into small droplets by a fuel atomizer. The physical properties of liquid fuel that affect the atomization in a diesel engine are density, viscosity and surface tension (Lefebvre, 1989). Allen (1998), Tat and Van Gerpen (1999), Yuan et al. (2003), Knothe (2004), Joshi (2007) reported that density, viscosity and surface tension are the most important atomization properties of liquid fuels in direct injection engines. Other properties that affect fuel atomization are latent heat of vaporization, thermal conductivity, boiling point, specific heat capacity, heat of combustion, jet diameter, relative velocity between jet and surrounding. The use of high viscous fuel delays atomization by suppressing the instability required for the fuel jet to break up in a direct injection engine. The higher density fuel severely affects atomization. The use of fuel with higher surface tension opposes the droplet formation from the liquid jet (Lefebvre, 1989). In order to function properly, a diesel engine requires a balanced value of atomization properties including density, viscosity and surface tension.

The Sauter Mean Diameter (SMD) is considered as an indicator of the quality of atomization in diesel engines. Allen (1998) and Allen et al. (1999; 1999a) studied the atomization properties of biodiesel fuel from their fatty acid compositions at 40^{o}C for different oil feedstocks. Allen (1998) concluded that the viscosity of biodiesel from

typical oils may vary as much as by 100% affecting the atomization characteristics of biodiesel fuels. According to Lee et al. (2005), the SMD in a biodiesel spray is higher than that of conventional diesel because the higher surface tension and viscosity of the biodiesel influence the spray characteristics.

Ejim et al. (2007) did a comparison of atomization properties of seven different biodiesel fuels with 17 binary and tertiary mixtures with diesel at 80^{o}C using a direct injector and found that the change in viscosity causes 90% change in SMD and density causes 2% change in SMD values. Hiroyasu et al. (1989) reported that the SMD increases with an increase in kinematic viscosity and surface tension. However, the SMD decreases with an increase in ambient and injection pressures (Arai et al., 1984 and Hiroyasu, 1991). Hence, viscosity plays a major role in SMD and atomization. Allen (1998) reported that the SMD of biofuel is approximately 5-40% higher than that of diesel fuel predicted with 5-6% accuracy using their viscosity and surface tension values.

The spray characteristics are highly dependent on the type and fuel characteristics. The breaking regime of the fuel jet is determined by various non-dimensional numbers such as Weber number (We), Reynolds number (Re) and Ohnesorge number (Oh) (Beale and Reitz, 1999). All these three numbers are affected mostly by the fuel atomization properties such as density, viscosity and surface tension (Recart et al., 2002; Lee and Park, 2002). For example, the Ohnesorge number is given by the relationship from dynamic viscosity (μ) of the fuel, liquid density (ρ), surface tension (σ) and drop diameter (d) as follows.

$$Oh = \frac{\mu}{(\rho.d.\sigma)^{0.5}} \qquad (5.1)$$

Arai et al.(1984) reported that fuel atomization does not occur at the nozzle exit of the injector but the liquid jet breaks up at a certain distance from the nozzle exit, which is also called jet break up length. As shown in Figure 5.1, spray tip, jet breakup length, spray angle and drop size distribution are the most important parameters of fuel spray.

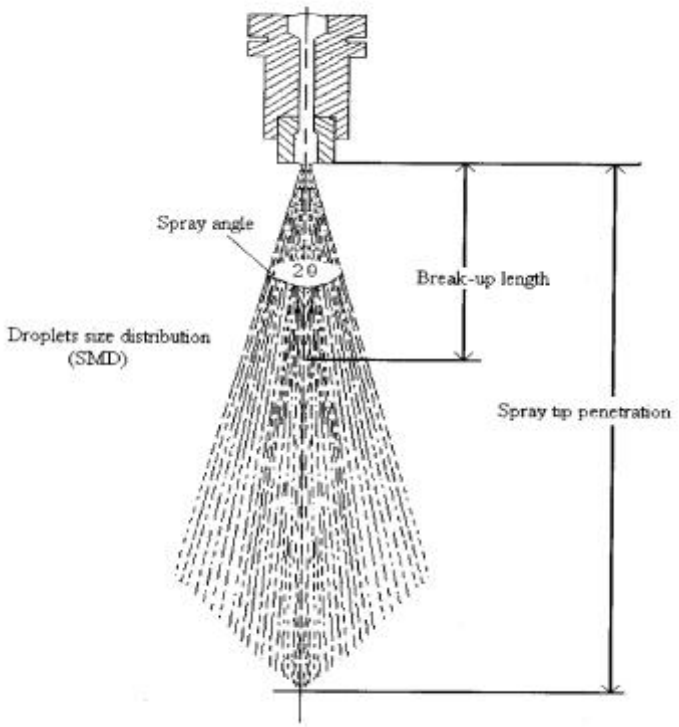

Figure 5.1 Fuel spray parameters (Arai et al., 1984)

The jet breakup length is the unbroken portion of the injected fuel jet which is affected by injection velocity and ambient pressure. The spray tip penetration is influenced by injection temperature and pressure. According to Arai et al.(1984), the spray tip penetration increases with pressure at which it is injected but decreases with an increase in ambient pressure. Kim et al. (2002) reported that the spray tip penetration decreases with an increase in ambient temperature. The spray angle is also affected by injection pressure and velocity. Hiroyasu (1991) reported that the spray angle increases with an increase in injection pressure and velocity. The spray angle reaches a maximum value and then slightly decreases to a constant value corresponding to a complete spray.

5.4 SUMMARY OF CHAPTER 5

In summary, atomization is affected by density, surface tension and viscosity of the fuels used. These properties are affected by temperatures and pressures. As noted in Section

5.1, high pressures and temperatures occur during the compression stroke. In order to characterize the atomization properties of various biodiesel feedstocks, the density, viscosity and surface tension are studied at high temperature and pressure and presented in Chapter 7.

CHAPTER 6 EXPERIMENTAL PROCEDURES AND VERIFICATION SAMPLE COLLECTION

Plant oils and fats constitute different types of fatty acids. Fatty acids are the major indicators of whether an oil or fat feedstock has a potential to be a biodiesel source. Moreover, the nature of the fatty acids present in the oil or the fat can in turn affect the characteristics of the biodiesel fuel. In this work, samples of neat (unprocessed) jatropha and soapnut oil were tested to determine their corresponding fatty acid content in order to assess the potential feedstock available for biodiesel production in Nepal.

6.1 CANOLA OIL AND BIODIESEL SAMPLE COLLECTION

Canola oil was purchased from Atlantic Superstore in Halifax was used for transesterification in lab to produce canola biodiesel. This biodiesel produced was used for the fuel characterization. A commercial methyl ester biodiesel produced by Milligan Biotech (Saskatchewan, Canada) was used as a biodiesel sample for testing density, surface tension and viscosity at elevated temperatures and pressures.

6.1.1 Jatropha and Soapnut Sample Collection

6.1.1.1 Samples for Fatty Acid Profile Determination

Jatropha (*Jatropha curcas*) seeds collected from the seed selling centre in Samakhusi Kathmandu were cold pressed in "Sundhara Oil Expeller" at the Research Centre for Applied Science and Technology (RECAST) laboratory in Tribhuwan University, Nepal. From 1000 grams of jatropha seed, approximately 278 grams of oil (27.8%) was recovered. Because only the cold press method was used for oil extraction, the oil content

recorded here is lower than reported in the literature (Chhetri et al., 2008a). Some oil might have been lost in the expeller. Solvent extraction could enhance oil recovery.

Soapnut seeds (*S. mukorossi*) were collected from the seed selling centre at Koteshwor, Kathmandu, Nepal. Both of these seed selling centres collect seeds from several districts of central and eastern Nepal. The kernels were separated from the shells for oil extraction. The kernels were then cold pressed and approximately 1.5 grams of oil was recovered from 5 grams of kernels for duplicate samples (30% oil content) (Chhetri et al., 2008a).

In order to produce biodiesel from jatropha by the transesterification process, five litres of neat jatropha oil sample and two litres of jatropha biodiesel were purchased from Aaditya Aromedic & Bio Energies Pvt. Ltd., Tarsadi, Gujarat State of India. However, the particular jatropha biodiesel sample purchased did not pass any of the ASTM standards during tests by an independent laboratory. Hence, neat jatropha oil was transesterified by the author into biodiesel for further tests.

Similarly, five litres of soapnut oil sample were purchased from Satya International in western Nepal. This company collects soapnut seed from over 30 districts and uses the cold press method to extract the oil. Thus, this was considered a well representative sample of soapnut oil from Nepal. Samples were used to determine the fatty acid profile of jatropha and soapnut oil using gas chromatography (GC) using the procedure described in 6.1.2.3.

6.1.2 Collection of Waste Cooking Oil Sample

6.1.2.1 Waste Cooking Oil Sample from Local Halifax Restaurant

In this experiment, waste cooking oil was collected from a local Indian restaurant (Taj Mahal Restaurant) in Halifax, which serves fast food as well as continental foods. The objective of collecting the waste cooking oil from Taj Mahal Restaurant was to simulate the waste cooking oil produced in Nepal. The spices used, food types used for frying and cooking temperatures and food exposure time are similar to those used by the restaurants/hotels in Nepal. It is reported that the production of waste cooking oil is a function of the frying temperature and length of use as well as the material used for frying (Chhetri et al., 2008b).

The oil used for cooking was pure canola oil. The waste oil sample was taken from the fryer which was used for frying potatoes and other vegetable-based food items. Four litres of oil samples were collected from a collecting drum in which the waste cooking oil was dumped once every two days for approximately 2-3 weeks period. The oil sample is assumed to be representative as it is collected from the oil stored for 2-3 weeks from several batches of waste oil. The temperature observed during frying was in the range of 403.15-448.15 K. This temperature is comparable with the temperature (408.15-453.15 K) for preparing French fries reported by Rywotycki (2002). The temperature was recorded by a REED ST-883 high temperature infrared thermometer that measures temperatures in the range of 223.15 to 973.15 K. The temperature range was recorded at three different times in a day. However, due to the significant temperature fluctuation in boiling oil, the maximum temperature was difficult to determine. The variation could be up to approximately 5-10%. Depending on the quantity of food used for frying, the oil was discarded sometimes at the end of each day and sometimes once in two or three days (Chhetri et al., 2008b). The water from the oil was driven off by heating it to 104 ^{o}C for 15 minutes. Before starting the acid catalyst esterification, the oil was filtered with 150 micro filter cloth.

6.1.2.2 Cooking Oil Supply in Nepal

No literature was found about the potential of using cooking oil as a feedstock for biodiesel production in Nepal. An open ended questionnaire was developed to conduct a feasibility survey of waste cooking oil potential in Nepal. The survey was focused in Kathmandu city, the capital of Nepal, surrounded by a ring road as shown in the map (Figure 6.1). The red color is the densely populated area within the ring road and a survey was carried out randomly in all these areas to make it more representative. The survey was conducted between July 2009 and February 2010 in Kathmandu valley.

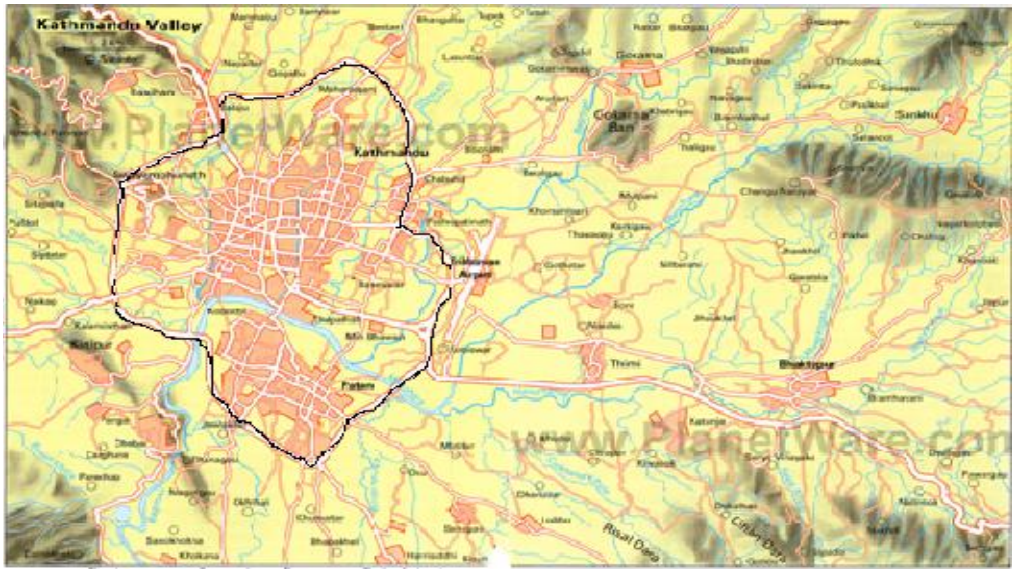

Figure 6.1 Map of Kathmandu City (http://airglobe.com.np/india/trekdmin/pictures/1259653619.jpg)

6.1.2.3 Determination of Fatty Acid Methyl Ester (FAME) Profile

For both jatropha and soapnut oils, acid catalyzed transesterification with H_2SO_4 in methanol (0.5 N) was used to produce fatty acid methyl ester (Budge et al., 2006). FAME were characterized using gas chromatography (GC) with flame ionization detection (FID) using a 50% cyanopropyl polysiloxane phase (Agilent Technologies, DB-23; 30 m x 0.25 mm ID). Helium was used as the carrier gas and the gas line was equipped with an

oxygen scrubber. The following temperature program was employed: 426.15K for 2 min, hold at 447.15 K for 0.2 min after ramping at 275.45 K min-1 and hold at 493.15 K for 3 min after ramping at 275.65 K min-1. FAME were reported as weight percent of total FA. Each FA was described using the shorthand nomenclature of A:Bn-X, where A represents the number of carbon atoms, B the number of double bonds and X the position of the double bond closest to the terminal methyl group. The lipid class composition was determined using thin-layer chromatography with FID on the IATROSCAN TH-10 Analyzer MKIII. Each biodiesel sample was dissolved in chloroform and applied to a chromarod. The chromarods were then developed in a tank containing a 48:48:4:1 hexane:petroleum ether:diethyl ether:formic acid solvent system for 25 minutes. After developing they were oven dried and then scanned until just after the phospholipid peak, lipids were identified by comparison of retention times to that of pure standards. Data were analyzed with Peak Simple Chromatography software and area percent for differential response of lipids was used to calculated lipid content as weight percent of total (Chhetri at al., 2008a). This gave the fatty acid profile of the biodiesel sample.

6.1.2.4 Determination of Free Fatty Acids in Oil Samples

A.O.C.S. official method (Ca 5a-40) was used to determine the free fatty acid content in the soapnut oil. Ethyl alcohol (95%) was mixed with the oil samples for this procedure. Sodium hydroxide solution (0.25N) was prepared for the titration. The alcohol was first neutralized with 0.25 N alkali solutions in 1% phenolphthalein indicator. Considering the fatty acid content range lies between 1-30%, 7.05 grams of oil samples were mixed with 75 ml of 95% ethyl alcohol. The titration was carried out with 0.25 N alkali solution prepared using sodium hydroxide. The titration was carried out until the color of indicator persisted for over 30 seconds. The free fatty acid content was then expressed as the free fatty acids as:

$$\text{Oleic acid},\% = (\text{mL of alkali} \times N \times 28.2)/(\text{Weight of sample}) \quad (6.1)$$

The canola oil used for this experiment was found to have 0.78% free fatty acid. A single stage transesterification using sodium hydroxide was used to produce biodiesel. The waste cooking oil sample had 6.5% free fatty acid content. The free fatty acid content of jatropha and soapnut oil was 14.5% and 17.5% respectively. Any oil with higher than 1 % free fatty acid cannot be transesterified with base catalyst process due to excessive soap formation. Hence, a two stage transesterification was used. Ma and Hanna (1999), Freedman et al. (1984) and Tiwari et al.(2007) recommended that the free fatty acid content should be less than 1% for base catalyst transesterification. However, Ramadhas et al. (2005) recommended ≤ 2% free fatty acid, Canakci and Van Gerpen (1999) recommended <3% and Zhang et al. (2003) recommended <0.5% free fatty acid content for efficient base catalyst transesterification process. In this work, acid catalyst esterification process was used to lower the free fatty acid below 1% for waste cooking oil, soapnut and jatropha oils.

ACS grade, 98% concentration 36 M sulfuric acid was used for the acid catalyst process. The oil sample and methanol were heated to 323.15 K±275.15K and mixed together. Sulfuric acid was added and a magnetic stirrer was used to properly mix the reactants. The concentrations of sulfuric acid used were 1%, 1.5%, 2%, 2.5% and 3% (v/v). The reaction was continued for an hour and samples were taken to test the free fatty acid concentration. It was found that the 3% sulfuric acid concentration reduced the free fatty acid below 1% in an hour which made it feasible for base catalyst transesterification for both jatropha and soapnut oils. A further experiment was carried out using 3% H_2SO_4 concentration to demonstrate a stable product for the free fatty acid concentration. The product was then heated to 383.15 K to remove the water and was then used for the base catalyst transesterification process.

6.2 BIODIESEL TRANSESTERIFICATION

One of the most common ways of producing biodiesel is by transesterification of triglycerides present in vegetable oils and animal fats. Transesterification is a chemical

reaction that involves vegetable oil and an alcohol yielding fatty acid alkyl esters (i.e., biodiesel) and glycerol in the presence of a catalyst. The triglycerides are the main component of vegetable oil consisting three long chain fatty acids esterified to a glycerol backbone. After the reaction of triglycerides with alcohol, the three fatty acid chains are released from the glycerol and combine with alcohol forming fatty acid alkyl esters, which are commonly known as fatty acid methyl ester or FAME. Methanol is the most commonly used alcohol used in transesterification process. However, ethanol is also used depending on the availability and objectives. Methanol has a cost advantage over ethanol, however ethanol can be produced from fermentation which, after drying, could help to make the process free of fossil fuels for process reaction. Figure 6.2 shows a schematic of transesterification process using methanol.

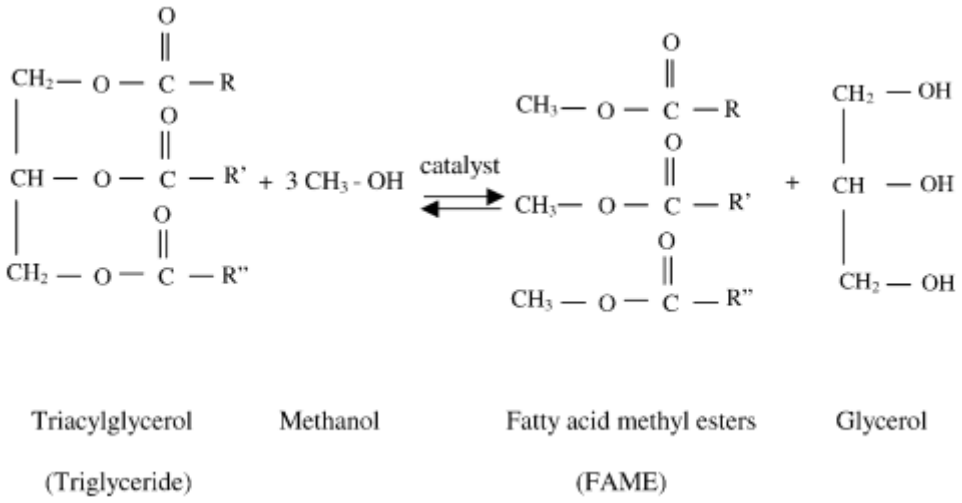

Figure 6.2 A schematic representation of the transesterification of triglycerides (vegetable oil) with methanol to produce fatty acid methyl esters (biodiesel) (Zhang et al., 2003)

In this work, all transesterification reactions were carried out in glass batch reactors. Sodium hydroxide (S320-500) pellets from Fisher Scientific were used as the catalyst for the transesterification process. The amount of sodium hydroxide required was determined by titration with the 99% isopropyl alcohol for each batch and oil to be used for biodiesel (methyl/ethyl ester) production. Technical grade 98% methyl alcohol was used as the catalyst for both the acid catalyst esterification and base catalyst transesterification

methods. 100% technical grade ethyl alcohol was used to produce biodiesel ethyl ester from waste cooking oil and canola oil. All experiments were carried out under a fume hood for safety reasons.

First an acid catalyst esterification was performed using sulfuric acid. When the free fatty acid content was reduced to less than 1%, then the base catalyst transesterification was carried out to produce biodiesel. The base catalyst transesterification experiment was carried out for 30 minutes at 333.15 ±275.15 K using a magnetic stirrer.

6.2.1 Blend Preparation

Different blends were prepared in order to study the atomization characteristics of the biodiesel samples. For canola, jatropha and soapnut biodiesel, B100, B80, B50, B20 were prepared on a volume basis. The atomization property test was also carried out for pure diesel (B0). B100 is 100% biodiesel, B80 is 80% biodiesel and 20% diesel mix and B0 is 100% diesel.

6.2.2 Sample Storage

Leung et al. (2006) reported that biodiesel oxidation increases when it is stored at higher temperatures and air exposure. In order to avoid the degradation, the space above all biodiesel samples was filled with nitrogen and the containers were made air tight. The samples were then stored in a refrigerator at 278.15 K. Dark glass bottles were used to avoid exposure to sunlight causing photochemical reactions.

6.3 DENSITY MEASUREMENT

In this research, a capacitance type densitometer was used to measure the variation of liquid level by measuring the frequency at elevated temperatures and pressures. The philosophy of density determination using capacitance is that the submergence depth of

the capacitors in the test fluid causes the dielectric constant of the capacitor to change due to a change in frequency.

6.3.1 Description of Experiment Using Capacitance Type Densitometer

Joshi (2007) described this particular densitometer in detail. A summary is given here. A capacitance type densitometer that can operate up to 573.15 K and 7 MPa was used to measure the density of biodiesel and its blends. The high pressure reservoir was constructed using SS TP 304 L with an inner diameter of 48.90 mm and outer diameter of 60.33 mm with accuracy of 0.25 mm and working length (depth) of 152.4 mm with a total height of 215.9 mm. Figure 6.3 and 6.4 show a schematic diagram and a digital image of the densitometer respectively. The lid of the densitometer was made using SSTP 304L with 10 TPI (threads per inch). Two capacitor plates were placed with 70 mm in length. The capacitor plates were attached to the lid of the densitometer in which a stirrer and an external motor was attached so as to obtain proper mixing to obtain a uniform temperature in the container. A 4-bladed impeller with a 5 mm diameter shaft was used. The shaft was attached to the lid of the cylinder which is capable of withstanding high temperatures and pressures. In order to avoid the damage of the stirrer O-rings and the retainer rings at high temperature, a refrigerated bath (Lauda-Brinkman Model RMS-6) with an ethylene glycol/water mixture (70:30) was circulated through the cooling sleeve of the packing gland assembly. The test liquid temperature was measured by using a K type thermocouple (SCASS-125G-4-SHX, Omega) inserted into the side of the reservoir. Since the liquid was stirred continuously, one thermocouple gave the temperature of the whole container of oil. In order to avoid evaporation, oxidation and combustion at high temperatures, the experiment was carried out under a nitrogen environment.

The variation in capacitance was measured using a Hex Schmitt-Trigger Inverter (MC74HC14AN), 5 – volt power supply, and a Fluke 1900 A Multi-Counter. The wire from the capacitor plates to the circuit was connected through the lid using a Swagelok fitting in order to avoid leakage at elevated pressures.

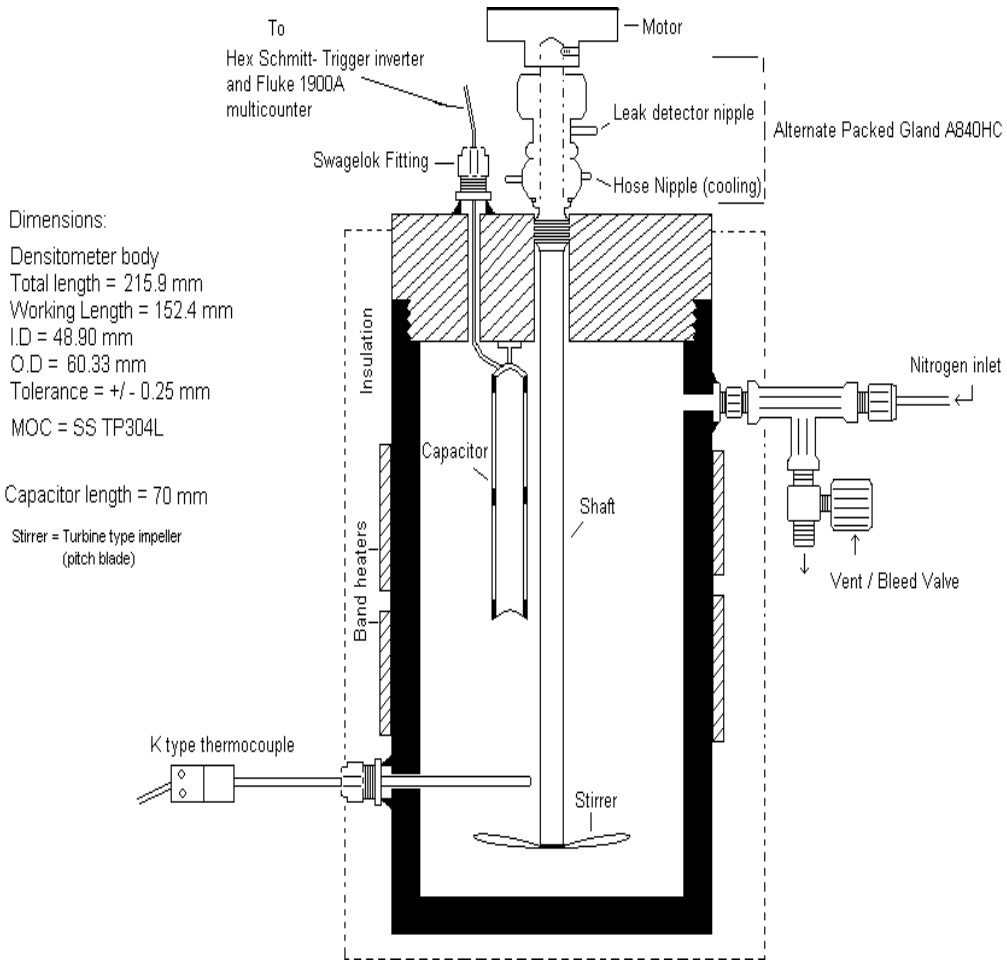

Figure 6.3 Schematic of capacitance type densitometer (Joshi, 2007)

The capacitor plates were held together at spacing of 0.85 mm through a set of screws and specially machined Teflon spacer rings (Figure 6.5). The Teflon spacer rings were used to avoid contacting of the holding screws with the capacitor plates.

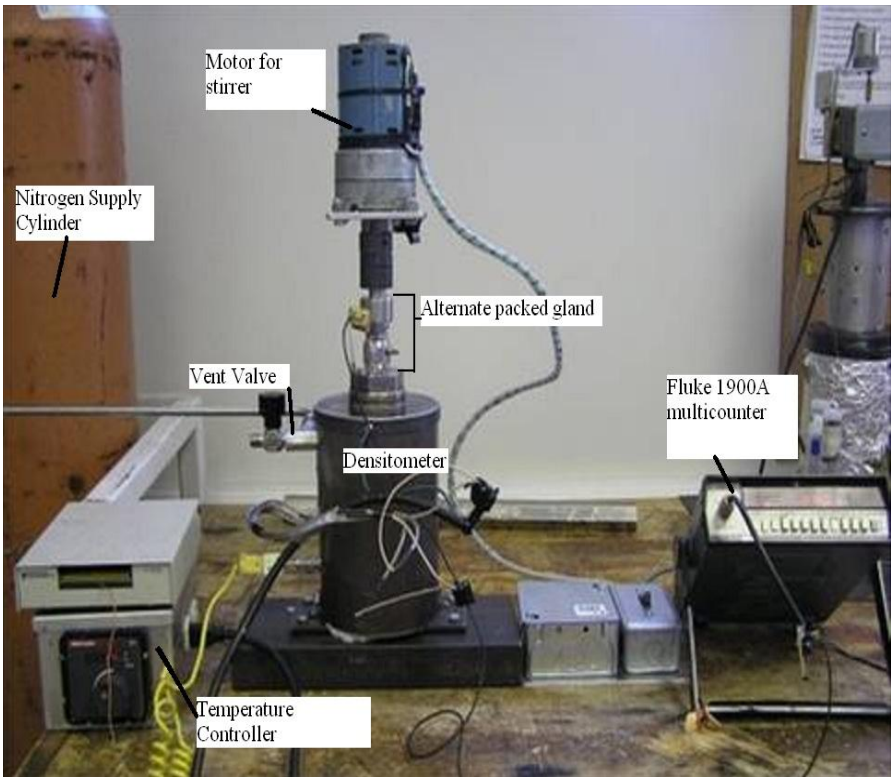

Figure 6.4 Capacitance type densitometer

Nitrogen gas was used to pressurize the test fluid through the inlet port of the top side of the reservoir. A pressure gauge attached on the nitrogen cylinder was used to directly read pressure of the test liquid. The reservoir was heated with a band heater with 600 watts of 63.5 mm inner diameter (MBH 2520600A/120m Omega) and 50.8 mm width and another band heater of 450 watts of 63.5 mm inner diameter (MBH2515450A/120, Omega) and 38.1 mm width. Glass wool was used to insulate the reservoir in order to avoid heat loss. The pressure was released using a vent valve (SS-14DPM4) purchased from Atlantic Valve and Fitting Co.).

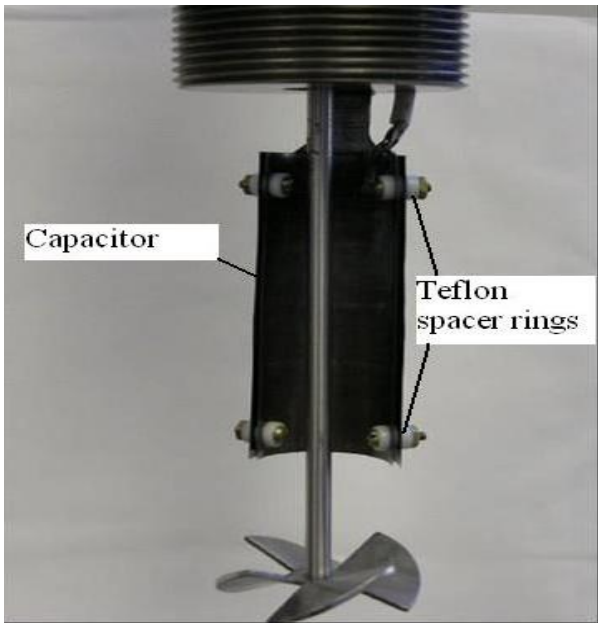

Figure 6.5 Capacitor plate and mixer

Before each new test, the reservoir and the capacitor were cleaned with toluene followed by acetone and dried with air. A base frequency of 58.5±0.1 kHz was recorded in the air at the beginning of each test at room temperature to ensure repeatability and cleanliness. The system was fully assembled after the test fuel was filled in the reservoir. Nitrogen gas was supplied to prevent the oxidation of oil during heating even when the test was carried out at room temperature. Nitrogen was also used to pressurize the reservoir when measuring the density of biodiesel and diesel fuels at elevated pressures. The heating of the reservoir was controlled by using the X4 type PCM-1 controller unit. The frequency was recorded at specific temperatures between 293.15 K and 523.15 K and gauge pressures from 0.10 MPa to 7 MPa. The stirrer was used to achieve the uniform mixing. Three tests were carried out for each sample for a specific temperature and pressure and the results obtained were averaged. Each experiment took about 2.5 hours to complete.

6.3.2 Calibration for Effect of Capacitor Submergence

Capacitance is dependent on both the depth of submergence of the capacitor and the dielectric constant of each fuel blend. In order to vary the depth of submergence, two spacing discs with a 15 mm thickness and 7.5 mm thickness were used alone and in

combination. The test fuel in the reservoir was kept constant but only the depth of submergence was varied using those spacing discs.

The frequency change due to the change in submergence depth was recorded for each sample blend. The reservoir level of the densitometer was kept constant and the submergence depth was varied so that the change in volume of test fuel due to elevated temperature and/or pressure could be investigated. The submergence depth was found to be inversely proportional to the frequency output for all samples tested.

6.4 VISCOSITY MEASUREMENT

Viscosity was initially measured by a rolling ball viscometer, and later by a torsional oscillation resonance viscometer

6.4.1 Description of Rolling Ball Viscometer.

A rolling ball viscometer was designed and constructed by Joshi (2007) in order to measure the viscosity of biodiesel and its blends at temperatures up to 573.15 K and pressures from atmospheric to 6.9 MPa.

As shown in Figure 6.6, the rolling ball viscometer consists mainly of a tube and a sphere. Quartz was selected for both the tube and the ball material, in order to avoid the errors due to thermal expansion at high temperatures. The quartz ball has a very low linear thermal expansion coefficient (5.4 x 10-7 K-1). Figure 6.7 shows the locally constructed rolling ball viscometer used for the experiment.

The length of the tube is 241 mm, diameter of the spherical ball was 3 mm and the inner diameter of the tube was 3.125 mm. The diameter ratio (d/D) of the sphere to the tube was 0.96. The tube was placed in an outer cylindrical shell of 24 mm inner diameter, 10 mm thickness with two end caps. Teflon cross holders were used to hold the tube in its

position. They also served the purpose of aligning the sensor system with the tube. A metal cap with a hole and 'O' rings were used to hold the ball within the tube. The two light sensing assemblies were placed 19 cm apart to calculate the travel time required for the ball through the fluid at known tilt angles (10^o, 20^o, 30^o, 40^o, 45^o and 60^o). The density of the rolling ball was 2203 kg/m^3 and the diameter of the quartz ball was 0.003m.

The light sensing assembly is one of the most important parts of the system. It consisted of stainless steel light guides with a special glass window of 5 mm diameter assembled in the light guides. The light guide was held perpendicular to the tube with the help of the two Teflon cross holders. Teflon packing rings were placed on either side of glass window so that it could withstand the pressures preventing the test fluid flowing out of the assemblies. A laser transmitter (wave length 630-680 nm, class II laser) was attached to the light guide on the outer side through a Teflon holder to prevent heating of the laser transmitter due to heat conduction from the test fluid through the light guide. Two light detecting photodiodes were attached to detect the frequency of the light.

A thermocouple sensor was used to measure the temperature of the fluid. A K-type thermocouple (Class 125G-4SGX, Omega) was assembled to measure the temperature of the test fluid. Heating of the fluid inside the cylindrical tube was controlled by an on/off temperature controller unit. A PCI-MIO-16E-4 National Instrument data acquisition system was used for the acquisition of temperature signals. The temperature was set 288.15-293.15 K lower than the desired temperature in order to avoid a temperature overshoot.

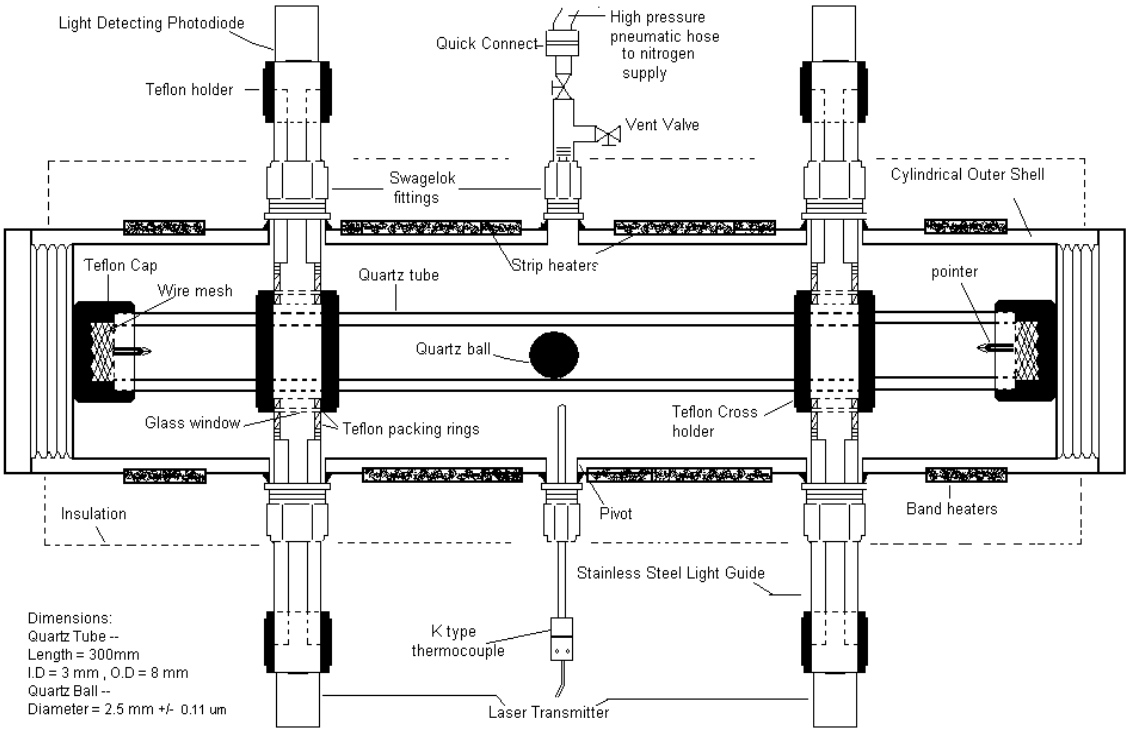

Figure 6.6 Schematic of rolling ball viscometer (Joshi, 2007)

Figure 6.7 Rolling ball viscometer

As the system was designed for high temperature and high pressure viscosity measurement, a vent valve and supply valve for nitrogen gas were installed through a Swagelok fitting in the centre of the assembly. Nitrogen gas was used to pressurize the

assembly in the case of pressured viscosity measurements. The complete assembly was placed on a metal stand through a pivot. The tilt angle was changed using a mechanical lock and was initially measured by a protractor attached on the pivot calibrated for the corresponding tilt angles. Later on, mechanical stops were used to ensure consistent tilt angles. A high pressure but flexible pneumatic hose was used to supply nitrogen from the nitrogen cylinder. The flexible hose was used to prevent the hindrance while tilting the assembly for different angles. The supply valve and flexible hose was connected by a quick connect assembly. The major advantage of this quick connect assembly was to allow the free movement of the assembly from the supply valve and to maintain the tilt angle through the experimental procedure.

Before testing a fluid, the quartz ball was cleaned using hydrochloric acid to remove any sticky dirt. The viscometer assembly was cleaned with toluene followed by acetone and dried by air after each set of experiments.

The test fluid was poured very slowly into the cylindrical tube to avoid the formation of the bubbles inside the tube, since bubble formation resulted in erroneous readings and sometimes prevented the ball from moving from one place to another. When bubbles were suspected, a small vibration on the cylindrical assembly caused the bubble to rise and be removed.

To start the experiment, the test fluid was filled from one of the sides of the outer cylinder, while keeping the other end closed. The entire system was filled with test fluid. The test fluid was filled in such a way that some overflow was allowed while tightening the end caps so that no gas was in the cylinder and no bubbles were formed. The assembly was pressurized by nitrogen. To heat the system, two 250 W band heaters on the end of the outer shell and four 125 W strip heaters were used in the middle portion of the outer shell. The heat was conducted from the outer shell to the test fluid. The temperature was controlled using 4X type PCM-1 with RCV SMT 232 controller from Omega Engineering Inc.

The laser was turned on after the required temperature and pressure were achieved. The frequency output was recorded by the light detector photodiodes. A Labview 7.1 program was used to monitor the frequency of both the sensors as well as the ball. The frequency variation in the two sensors was noted while the ball passed through the sensors and the time was measured between the two signals. The time interval was used to calculate the velocity of the ball which was required to calculate the viscosity of the liquid.

6.4.1.1 Calibration of the Rolling Ball Viscometer

The rolling ball viscometer was calibrated using water as a liquid medium. The rolling time of the quartz ball was measured at different tilt angles of 10, 20, 30, 40, 45 and 60 degrees. The data were collected by tilting both from left to the right and from right to the left. The average data were collected by taking the rolling time taken by the ball for 5 times each from left to the right and from right to the left. The calibration constant (K) was obtained from the time taken by the ball to roll between the sensors placed at 19 cm apart of the fluid vessel.

6.4.1.2 Problems in Viscosity Measurement by Rolling Ball Viscometer

Measuring the viscosity at high temperatures and pressures posed a great challenge. When the temperature was raised, there was an expansion of the liquid as well as the material from which viscometer was built, the glass tube in which the ball travels and the glass window through which the laser light passed. The sealant used for holding the glass window reacted with hot oil allowing the oil to leak into the other side of the tube. Once the oil leaked, the signal was weak as the laser beam had to pass a high depth of liquid. This made it difficult to detect the correct signal at which the ball passed the laser. Due to this reason, experiments at temperatures higher than 373.15 K were not carried out using rolling ball viscometer.

6.4.2 Torsional Oscillation Resonance Viscometer

A torsional oscillation resonance viscometer was subsequently used to measure the viscosity of biodiesel blends at high temperatures and pressures. The torsional oscillation viscometer is a surface loading device that is used to measure the viscosity at the interface between the liquid and the solid surface. A constant amplitude was maintained at all times during the measurements. The viscosity of the fluid is determined from the power required to achieve the constant amplitude.

Figure 6.8 is the ViscoScope sensor with model number VA 300L-yy that can measure low viscosity ranging from 0.1-2500 mPa.s (density g/cm^3 for absolute viscosity) (Marimex, 2010). This viscometer can measure the viscosity up to 723.15 K and 6500 Psi. Figure 6.9 is the VD250 transmitter for data recording. The accuracy of this viscometer ±2% or 1 digit maximum.

Figure 6.8 ViscoScope Sensor VA300L-yy

Figure 6.9 VS D250 with display in DIN rail housing

Figures 6.10 and 6.11 illustrate the operating principle of the torsional oscillation resonance viscometer. This viscometer is based on the torsionally resonating sensor bulb. When connected to the power, the drive coils excite the cross bar into a resonant vibration and the drive shaft twists back and forth due to resonance. The drive shaft is welded to the sensor. The resonant vibration results in a micron size motion of the sensor surface. The compliant sheath which acts as the spring for resonance is welded to the sensor and provides the integrity for the sensor. The drive mechanism is hermetically sealed in order to allow resonance vibration. The sensor has no moving parts and hence the vibration is barely felt.

The measurement principle is that the torsional viscometer determines the extent to which the rotational motion of an inertial element driven by a torsion wire is damped by immersion in the fluid. Hafer and Laesecke (2003) developed an equation to measure the viscosity by torsional viscometer as below.

$$\mu \text{ x } \rho = - \left(\frac{m}{s}\right)^2 (\pi f *) \left(\frac{\Delta f}{f^*} - \frac{\Delta f_o}{f_o^*}\right)^2 \qquad (6.2)$$

where μ is the dynamic viscosity of the fluid, ρ is the density, m is the mass, S is the surface area, f* is the resonant frequency and Δf is the bandwidth. The subscript zero represents the equivalent quantities in vacuum conditions.

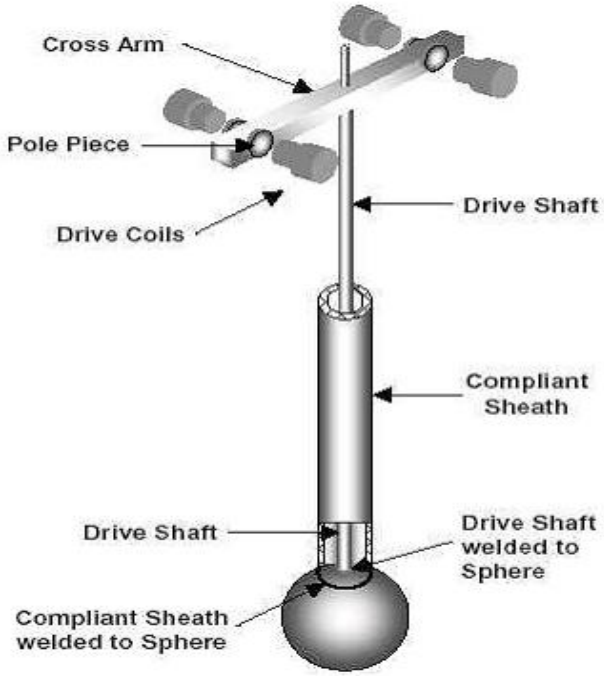

Figure 6.10 Operating principle of torsional oscillation resonance viscometer

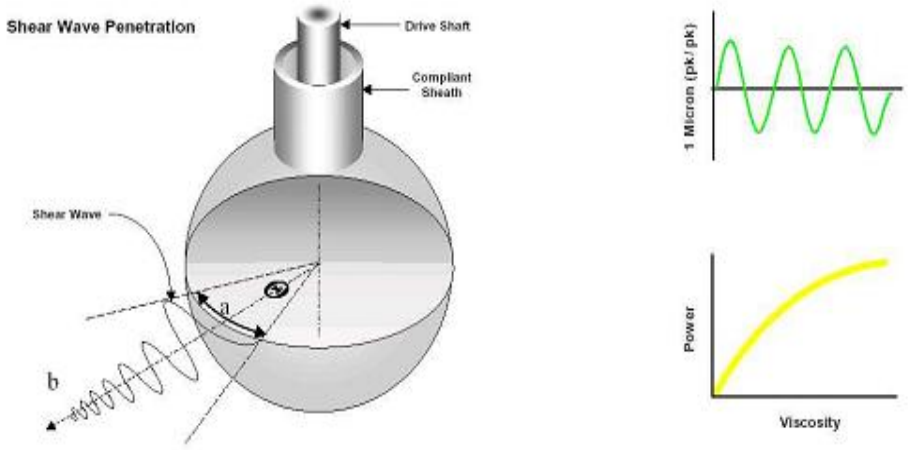

Figure 6.11 Torsionally generated sinusoidal wave in torsionally oscillating viscometer (Marimex, 2010)

Torsional viscometers do not measure absolute viscosity but measure the viscosity multiplied by the density of the test fluid. The ViscoScope process viscometer is also a continuous viscometer and can measure the viscosity of liquid in-line.

6.5 SURFACE TENSION MEASUREMENT

6.5.1 Apparatus

High pressure pendent drop (PD-E 1700) and drop shape analysis (DSA 100 V1.9) was used to measure the dynamic and equilibrium surface tension of different biodiesel blends at various temperatures and pressures. The PD-E-1700 was built by EUROTECHNICA and the DSA V1.9 was built by KUSS (Germany) as shown in Figure 6.12 and 6.13.

Figure 6.12 High-pressure pendent drop (PD-E 1700) and drop shape analysis (DSA100 V1.9)

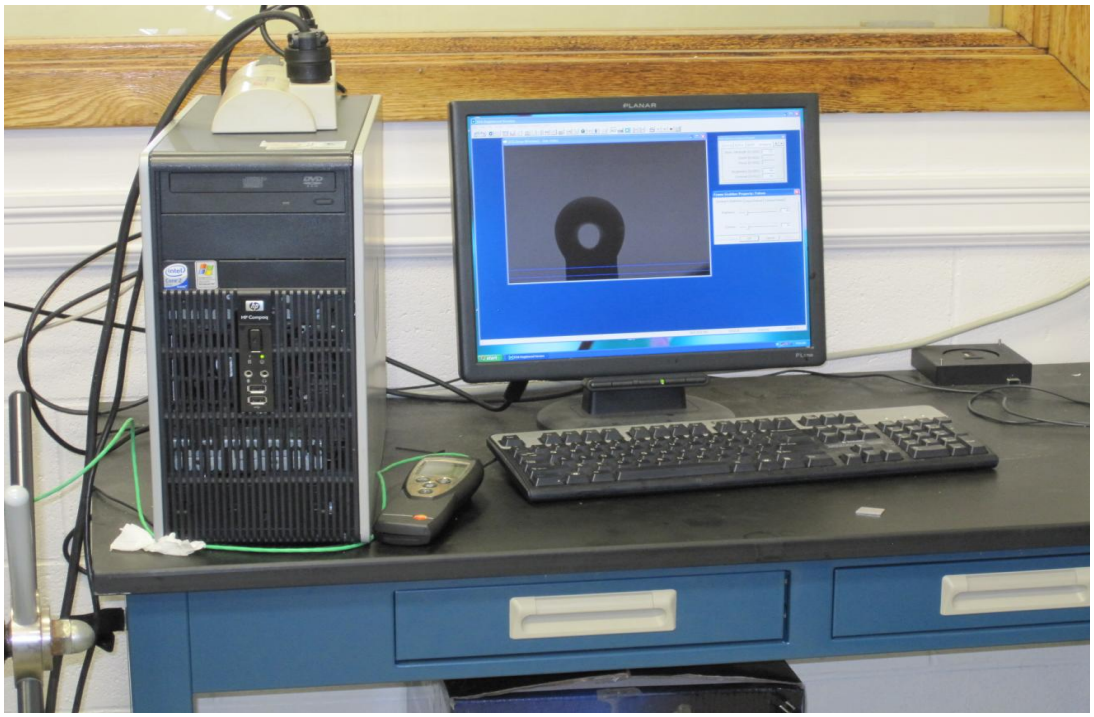

Figure 6.13 Pendent drop shape analysis acquiring pendent drop (DSA100 V1.9)

A schematic diagram of the high-pressure pendant drop apparatus is shown in Figure 6.14. The major component of this system is a high-pressure cell with windows in two sides. The maximum operating pressure and temperature of this cell is 69 MPa and 473.15 K respectively. The drop shape analysis DSA100 V1.9 consists of high-resolution CCD camera with a light source. The high-pressure cell is located between the CCD camera and light source. The pendant drop shape analysis method determines the surface tension of various liquids and is considered one of the most accurate techniques for a large range of temperatures and pressures (Yang et al., 2005). In this method, a pendant oil drop is formed on the tip of the stainless-steel needle installed at the top of the pressure cell in an air or nitrogen. With a digital image acquisition system from DSA100 V1.9, a digital image is acquired. The software requires the density of the test liquid (biodiesel) and density of the gas (either air or nitrogen) surrounding the test liquid. The surface tension of the pendant oil drop surrounded by either air or nitrogen is determined by using Young-Laplace equation of capillarity by finding the best numerically calculated surface profile to fit the physically observed drop profile.

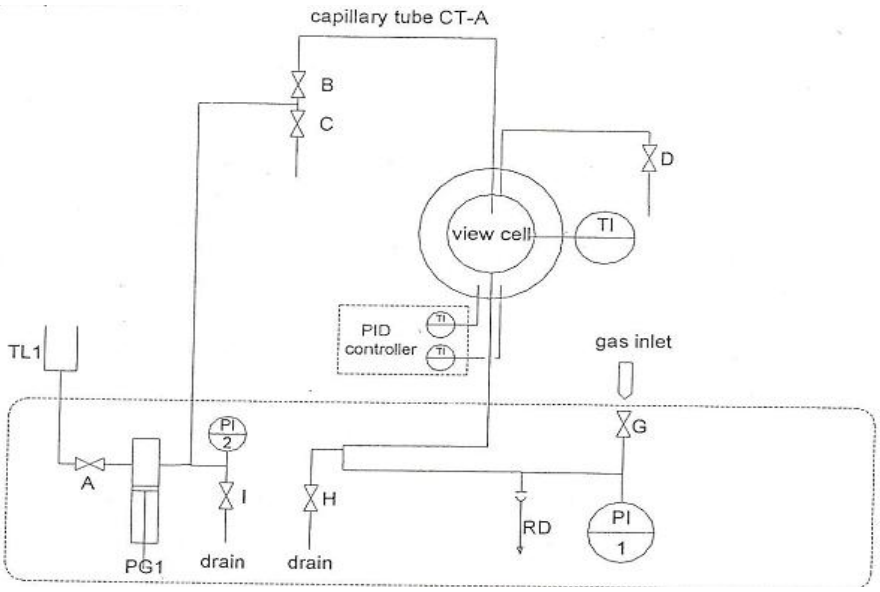

Figure 6.14 A schematic diagram of the high-pressure pendent drop (PD-E 1700) surface tension system (Drop Shape Analysis Manual, 2006)

6.5.2 Accuracy and Reproducibility of the Measurement

The correct optical alignment, cleanliness and functionality of the system were confirmed by determining the surface tension of distilled water as 72.8±1.3% mN/m. This confirmation test was carried out after each test for different blends. The instrument was cleaned with isopropyl alcohol (99% concentration) followed by acetone and dried with nitrogen gas after completing the test of each blend of biodiesel fuel in order to avoid contamination from the subsequent test samples.

Setting the temperature at a particular point was a difficult task. The control was manual and was ±274.65 K from the set point and the average temperature was taken. As density was one of the inputs to the analyzer, any errors in density could also affect the accuracy of the surface tension results. For each pendant drop created during the test, the surface tension reading was measured five times and an average was taken. Three pendant drops were created and corresponding measurements were taken to ensure the satisfactory repeatability at each specified temperature and pressure test.

6.5.3 Measurement Procedure

When the surface tension of water was found to be 72.8±1.3% mN/m, the test was conducted for different blends of biodiesel for pure canola biodiesel, jatropha biodiesel blends, soapnut biodiesel and pure diesel. The surface tension was measured from room temperature up to 473.15K which was the maximum allowable temperature for the equipment. In the case of pure diesel, the test was carried out for the temperature up to 448.15K because the boiling point of diesel starts at approximately 453.15K and evaporation takes place after this temperature. The maximum allowable pressure for this equipment is 69 MPa. However, the test was carried out from atmospheric pressure to 7 MPa. At the beginning of the test, the surface tension was measured using air as the reference gas. At higher temperatures and pressures, nitrogen was used as the reference gas. At elevated temperatures and pressures, it usually took 15-20 minutes to reach a stable value of temperature (± 0.5 K) inside the pressure cell.

A pendant drop was created by turning the screw piston pump clockwise until the sample was forced to reach toward the pressure view cell and finally to the capillary tube. (Figure 6.15) The digital images were then focused, acquired sequentially, captured and stored in the computer. The drop shape analysis DSA100 V1.9 determined the surface tension of each pendant drop formed for each experiment. The other data recorded were radius of curvature at the apex point and the volume as well as surface area of the pendant drop. The input data required for the software was the density of the liquid sample and the gas phase and the temperature in K.

In this work, the readings were recorded for pressures 0.10, 1.83, 3.50, 5.30, 7.00 MPa and temperatures 293, 323, 373, 423, and 473 K respectively. In case of diesel, the temperature readings were recorded for 293, 323, 373, 423, and 448 K for all five pressures.

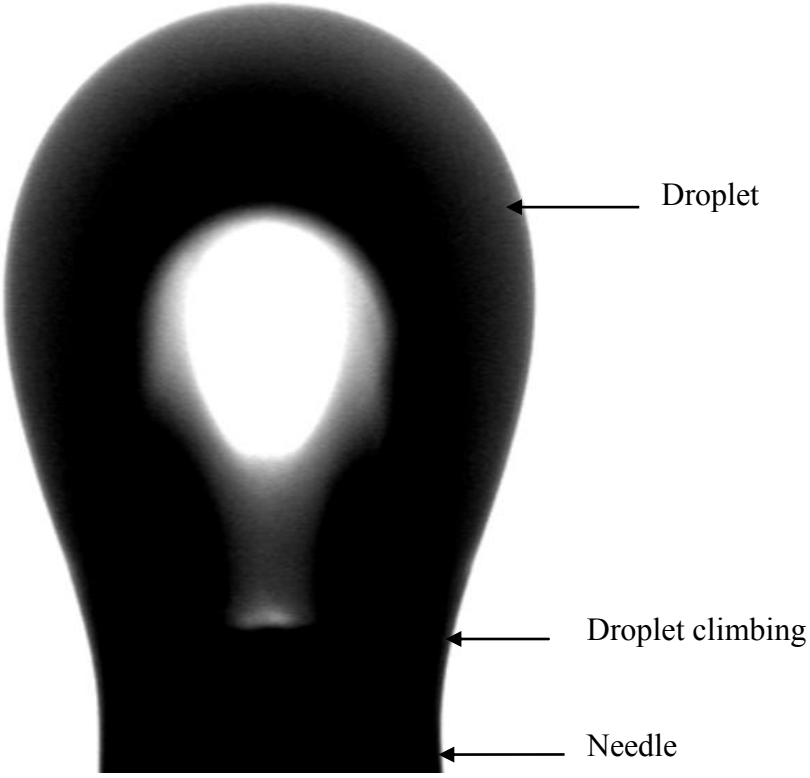

Figure 6.15 Droplet on the needle

CHAPTER 7 EXPERIMENTAL RESULTS

7.1 WASTE COOKING OIL SURVEY RESULTS

A survey was carried out to provide the basic information about waste cooking oil resources for planning and decision making on the potential feedstock availability for biodiesel production in Nepal. All the field surveys were conducted by an in-person visit and the data were analyzed. The survey sample questionnaire is presented in Appendix B. The survey captured the very basic facets of waste cooking oil information within the Ring Road of Kathmandu Valley. This area is the most densely populated area in Kathmandu Valley and all business centres, government operations and tourism activities occur here. Data were collected from the proprietors, owners, the managers or the front desk persons. The survey was conducted between June 2009 and February 2010. The objectives of this survey was to gather information on the average volume of oil consumed in a week, the duration of oil replacement, types of oil used and the end use of waste cooking oil. Technical information such as maximum temperature of frying was not available in most of the surveys.

7.1.1 Waste Cooking Oil Production by Restaurants Type

The estimate of waste cooking oil resources within the Ring Road of Kathmandu Valley of Nepal was compiled according to restaurant type, type of oil used and end use of waste cooking oil. Information was obtained from a total of 57 restaurants, hotels and other waste cooking oil generating vendors were contacted. Table 7.1 shows the type of business, total number of business surveyed and the minimum and maximum annual waste cooking oil generation from various types of businesses.

Table 7.1 Maximum and minimum annual waste cooking oil generation by business type

Business type	Number of business	Minimum annual generation (l/year)	Maximum annual generation (l/year)
Hotels	14	8332	12528
Lodges and guest houses	7	3387	6973
Restaurants (unspecialized)	23	12700	19843
Fast food restaurants	12	8372	11338
Bakery and sweets	1	525	1050
Total	57	33,316	51,732

According to the official website of the Hotel Association of Kathmandu, Nepal, there are 6 five-star hotels, 9 four-star hotels, 8 three-star hotels, 42 two-star hotels and 46 non-rated hotels in Kathmandu. It was assumed that there are approximately equal numbers of non-rated hotels running in the areas without affiliation to the Hotel Association of Nepal (HAN). Similarly, there are slightly over 100 restaurants and bars registered to Restaurants and Bar Association of Nepal (REBAN) in Kathmandu. A similar number of restaurants and bars are considered to be operated without registration. The survey represents approximately 15% of the total numbers of hotels and restaurants within the ring road of Kathmandu. The total waste cooking oil production could reach to a maximum of 350,000 litres/year based on the 15% of the samples surveyed. The survey focused on three-star, two-star and non-rated hotels and registered and non registered restaurants and bars in Kathmandu. The four and five-star hotels were reluctant to provide information for the survey.

Figure 7.2 shows the share of various types of businesses generating waste cooking oil within Ring Road of Kathmandu Valley. The restaurants (unspecialized) were found to be the highest contributor (40%) for waste cooking oil generation followed by hotels (22%), fast food restaurants (21%), lodges and guest houses (12%) and bakery and sweets (2%). The minimum annual waste cooking oil generation from the 57 businesses

surveyed was approximately 33,000 litres and maximum waste cooking oil generation was approximately 51,700 litres.

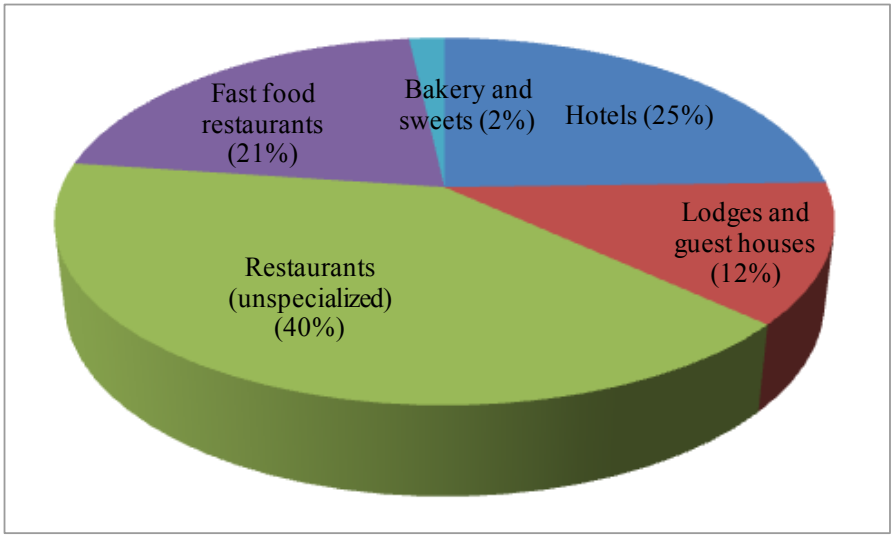

Figure 7.1 Share of waste cooking oil generation by business types

7.1.2 Oil Used in Various Businesses by Oil Type

The survey results showed that over 79% of the businesses were using soybean oil for their cooking or frying (Figure 7.3). Soybeans are produced and processed in the southern part of Nepal. The survey also showed that vegetable oils such as mixes of soybean/no name vegetable oil brand were least preferred (5%). Similarly, approximately 9% and 7% of waste cooking oil was generated from soybean/mustard mix and mustard oil use respectively.

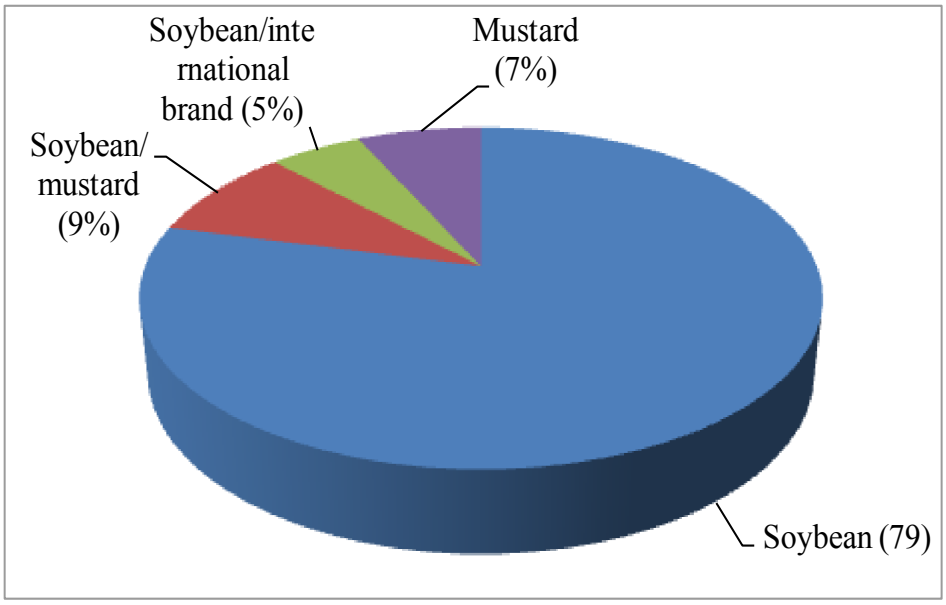

Figure 7.2 Oil use by oil type

7.1.3 Existing Use of Waste Cooking Oil

It was found that all of the businesses surveyed operate all the year around. Some of the waste cooking oil being generated is being used for some other purposes such as soap making, animal feed preparation and some were thrown in the drain. Figure 7.4 shows the current status of the waste cooking oil use in the survey area. It shows that oil produced from approximately 53% of the businesses was used for soap making. The waste oil produced from approximately 14% of the businesses was used for animal feed preparation and some portion of this quantity was thrown in the drain. The survey also indicated that the oil generated from 7% of the businesses was used both for soap making as well as animal feed preparation. Oil generated from approximately 4% businesses was used solely for animal feed preparation.

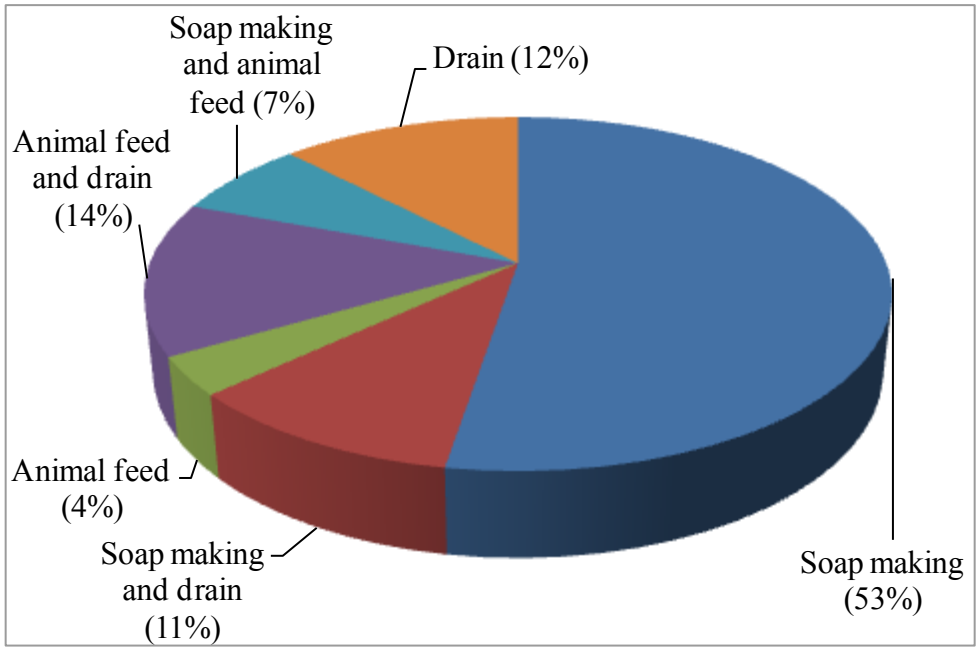

Figure 7.3 Existing use of waste cooking oil

7.1.4 Quality of Waste Cooking Oil

Only quantitative data were collected. However, the quality of waste cooking oil is also very important in order to determine how easily the feedstock could be converted to biodiesel fuel. The contaminants that could be in the waste cooking oil include food debris, bone, cleaning agents, chemicals, dissolved spices and water. It may not be possible to filter out some of these wastes. The lower quality of oils can cause difficulty in the transesterification process, lower the yield and increase the processing cost.

7.1.5 Interpretation of Results

A number of trends can be drawn from this survey. The unspecialized restaurants were by far the most oil generating businesses willing to provide used cooking oil among those surveyed followed by hotels, fast food restaurants, lodges and guest houses and bakery and sweet shops respectively. The survey appears to have a least representation

from sweets shops and the bigger franchise hotels. As the oil being generated is used for soap making and animal feed, the respondents were not sure of its benefit for sale to use in biodiesel production.. Since a significant part of waste cooking oil was diverted for animal feed production, determining its quality would be very important. This survey also showed that there was no use of animal fats in cooking and frying industries within the Ring Road of Kathmandu Valley currently. No data on animal fat production was available in the literature.

The business owners were not aware of feasibility of using waste cooking oil for biodiesel production. This is because biodiesel has gain attention only recently. There has not been much awareness among the common population about biodiesel and its potential uses as diesel replacement. Section 4.8.4 discussed the potential strategies to increase awareness for biodiesel as an alternative energy resource in the country.

7.2 BIODIESEL FUEL PRODUCTION AND CHARACTERIZATION

7.2.1 Canola Oil Biodiesel

Even though biodiesel can be produced from a variety of feedstocks, canola oil is the source with the most potential for biodiesel in Canada. According to a survey by Natural Resource Canada (2007), the total diesel consumption for on road vehicles in Canada in 2005 was approximately 10 billion litres. In 2005/2006, Canada produced 9.66 million tons of canola and exported 4.9 million tons. In 2006, it was reported that Canada had a surplus of more than a million tonne of canola oil after consumption and export to other countries which could be used to produce biodiesel to meet near to mid-term demand of biodiesel feedstock (Buth, 2007). It was also argued that canola is not considered a subsistence food source such as corn or wheat and no new land needs to be converted into canola farms for this purpose. Hence, Canada can easily meet its portfolio standard of 2% blend in the total diesel consumption using canola oil along with other available feedstocks.

Biodiesel samples were prepared in the laboratory from canola oil, waste cooking oil, jatropha oil and soapnut oil. These samples were used to test for the ASTM fuel characterization. Biodiesel from jatropha oil and soapnut oil were used to carry out the test to determine density, surface tension and viscosity at elevated temperatures and pressures. For canola oil biodiesel, commercial biodiesel produced from Milligan Biotech was used to carry out the tests for density, surface tension and viscosity.

In this work, biodiesel (ethyl ester) was prepared from canola oil bought from the Atlantic Superstore in Halifax, Canada. The viscosity of canola oil was determined at room temperatures using a falling ball viscometer. It was found that the average viscosity of the canola oil sample used in this test was 69 mm^2/sec at 294 K. The density of canola oil measured at 294 K was 900 kg/m^3. Density was measured by measuring the weight of oil to the volume of the same weight of liquid. From titration, the total amount of catalyst required per litre of canola oil for transesterification was determined to be 8 grams of NaOH. 280 ml technical grade 99.99% ethanol was used per litre of canola oil. First the ethanol and catalysts mixture and oil were heated separately to 323 K. Then both were poured into the reactor vessel in which the reaction was to be carried out. Transesterification was carried out using a heating plate and a magnetic stirrer. The reaction temperature was 333±2 K. The observed average reaction time to complete the transesterification was 20 minutes. This was determined by analyzing samples taken at 5, 10, 15, 20 and 25 minutes. After heating to 333 K for 20 minutes, the mixture was left for about 24 hours to settle the glycerin phase from the biodiesel phase by gravity (Figure 7.5). Most of the excess alcohol and catalysts were contained in the glycerin phase. The ethyl ester biodiesel samples were collected and stored in a refrigerator at 278 K for further analysis in a gas chromatograph (GC).

The samples collected for the Iatroscan analysis were not neutralized and might have further reacted for some time as the sample was warmer than room temperature and contained some catalyst in it.

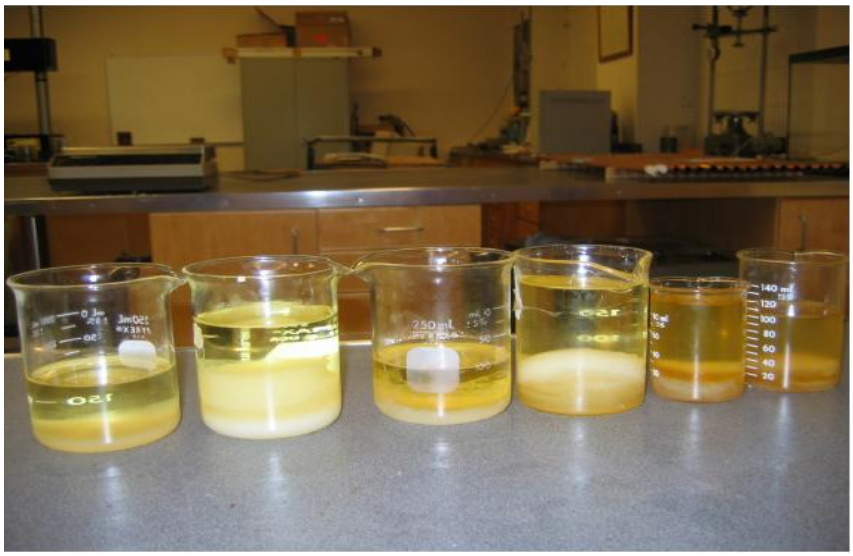

Figure 7.4 Canola biodiesel and glycerin separated in two distinct phases

7.2.1.1 Fatty Acid Content Analysis for Canola Biodiesel

Fatty acid contents are the major indicators of the properties of biodiesel. From gas chromatography analysis, it was found that the biodiesel (ethyl ester) derived from canola oil contained 60.28% oleic acid followed by 20.02% linoleic acid, 8.73% linolenic acid, 4.77% palmitic acid, 1.97% stearic acid, 1.28% ecosenoic acid and rest the others. Table 7.2 shows the summary of fatty acid contents in canola oil biodiesel. Biodiesel from canola oil contained the highest amount of oleic acid among other fatty acids in the product. More than 60% of the fatty acids were found to be mono-unsaturated (C18:1). Poly-unsaturated fatty acids were found to be approximately 28% (C18:2, C18:3). Only approximately 7% fatty acids were saturated. Palmitic acid and stearic acid were the major saturated fatty acids found in the canola oil biodiesel. Approximately 2% of the products were unidentified. The amount and type of fatty acid content in the biodiesel are the major factors that determine the viscosity and surface tension of biodiesel. The qualitative and quantitative analysis of fatty acid content is comparable with the study reported by Lang et al. (2001) for canola oil.

Table 7.2 Fatty acid composition of esters prepared from canola oil

Type of fatty Acids	Carbon Chain	This work (canola)	Canola biodiesel (Lang et al., 2001)
Myristic	C14:0	0.242	0
Palmitic	C16:0	4.77	4.4
Palmitoleic	C16:1	0.363	0
Stearic	C18:0	1.978	2.3
Oleic	C18:1	60.284	69.4
Linoleic	C18:2	20.029	18.0
Linolenic	C18:3	8.731	5.9
Arachidic	C20:0	0.582	0
Ecosenoic	C20:1	1.283	0
Lignoceric acid	C24:0	0.117	0
Others		1.621	0

7.2.1.2 Conversion Efficiency of Canola Biodiesel

The concentration of the catalyst is a very important factor that determines the conversion efficiency. During the transesterification of canola oil, samples were taken every 5 minutes until 25 minutes when it was considered that the reaction was complete. The ester conversion was obtained from the Iatroscan analysis of those selected samples (Figure 7.5). The average overall conversion achieved in this work was 92.4%. Issariyakul (2008) reported the ethyl ester conversion of canola oil to 96.5%. The variation in ester yield could be due to several reasons including the different reaction conditions, presence of some water in the alcohol even after drying that may lead to the formation of some soap.

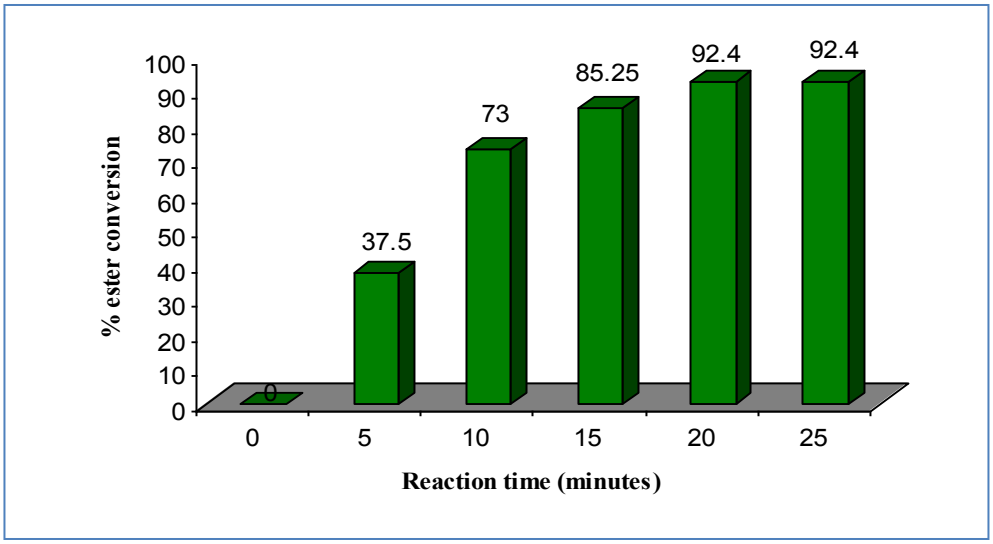

Figure 7.5 Canola oil ethyl ester conversion with time analyzed from Iatroscan

7.2.1.3 Fuel Characterization for Canola Biodiesel

To ensure a quality and independent determination of the properties, the biodiesel fuel characterization tests were carried out in Bently Tribology Services in, Minden, Nevada, USA. The canola biodiesel sample produced from transesterification in the laboratory was tested according to ASTM Biodiesel Fuel Quality Assurance Standard Test. Table 7.3 shows the summary of test methods used, the standard limit as recommended by ASTM and the test results for this work.

Table 7.3 Fuel properties of canola oil biodiesel

Test name	Test Method	Results (This work)	Standard Limit
Free Glycerin (mass %)	ASTM D6584	0.038	Max 0.020
Monoglycerides (mass%)	ASTM D6584	0.350	NA
Diglycerides (mass %)	ASTM D6584	0.353	NA
Triglycerides (mass%)	ASTM D6584	0.445	NA
Total Glycerin (mass%)	ASTM D6584	1.186	0.024
Flash Point, Closed cup (K)	ASTM D93	449	Min 403
Phosphorous (ppm)	ASTM D 4951	5	Max 10
Calcium+Magnesium (ppm)	EN 14538	1	Max 1
Sodium+potassium (ppm)	EN 14538	117	Max 5
Water+Sediment (vol%)	ASTM D 2709	0	Max 0.05
Sulfur by UV (ppm)	ASTM D 5453	1	Max 15
TAN (mgKOH/g)	ASTM D 664	0.30	Max 0.80
Viscosity @ 313 K (cSt)	ASTM D 445	5.36	1.9-6.0
Sim.Dis., 90% recovery(K)	ASTM D 2887	639	Max 633
*Cetane Index	ASTM D 976	61	Min 47
Cloud Point (K)	ASTM D 2500	272	NA
Pour Point (K)	ASTM D 97	250	NA

* *This may not be correct for biodiesel fuel since the correlation nomograph is defined for diesel fuel.*

7.2.1.4 Free and Total Glycerin, Mono-, Di-and Triglyceride Content for Canola Biodiesel

The free and total glycerin contents were found to be 0.038 and 1.186 % exceeding the ASTM limit of 0.020 and 0.24 % respectively. Similarly, the mono-, di- and triglyceride content were found to be 0.350, 0.353 and 0.445 respectively. ASTM does not have a standard for mono-, di- and triglyceride content in the final biodiesel products. However, the European Standard (EN) specifies that the mono-, di- and triglycerides in the final biodiesel product should not exceed 0.8, 0.20 and 0.20% (mass %) respectively. Here, the diglyceride and triglyceride from canola biodiesel exceeded the EN requirements. The

results could have been triggered due to insufficient washing and time allowed for gravity settling, among others.

7.2.1.5 Total Acid Number for Canola Biodiesel

The ASTM standard for acid value (acid number) for pure biodiesel is 0.8 mgKOH/g. The acid value is the total amount of potassium hydroxide necessary to neutralize the free acids in the biodiesel sample. The test result for the total acid number for canola oil ethyl ester was found to be 0.30 mg KOH/g.

7.2.1.6 Cloud Point and Pour Point for Canola Biodiesel

The cloud and pour point are also important properties of biodiesel fuel. Cloud point is the temperature at which a cloud of wax crystals first appear in the oil when it is cooled. The pour point is the lowest temperature at which the oil sample can still be moved. These properties are related to the use of biodiesel in the cold temperature. The cloud point of ethyl ester produced from canola oil was found to be 272 K. The pour point of canola oil ethyl ester was found to 250 K.

7.2.1.7 Cetane Number/Cetane Index for Canola Biodiesel

The cetane number is the indicator of the ignition property of the biodiesel fuel. The higher the cetane number, the more efficient the ignition is. Because of the higher oxygen content, biodiesel has a higher cetane number compared to petroleum diesel. As the cetane number can only be found by testing directly in an actual engine, the calculated cetane index is considered an indicator of ignition quality when such direct testing in engine is not feasible. The cetane index of canola oil biodielsel from this experiment was found to be 61.

7.2.1.8 Water and Sediment for Canola Biodiesel

The test results showed that there was neither water nor sediment content in the sample. A rotary evaporator was used to drive off the water and any remaining alcohol. A complete removal of water and unreacted alcohol was determined when the constant weight was achieved during the rotary evaporation of canola biodiesel sample. The ASTM standard for water and sediment is 0.05% by volume of the sample.

7.2.1.9 Sodium and Potassium for Canola Biodiesel

ASTM has no standard set for sodium and potassium separately while the European standard (EN) has set maximum allowable limit of 5 ppm. The sodium and potassium content of the canola biodiesel from this work was found to be 117 ppm. The pH of the sample biodiesel sample was found to be 9.5 which was the indicator of catalyst remaining in the sample.

7.2.2 Soapnut Oil Biodiesel

7.2.2.1 Analysis of Soapnut Oil

The soapnut oil sample was analyzed for its moisture content, free fatty acid content, energy content, viscosity and total acid number in Isotek lab, Oklahama, USA. The soapnut oil was found to have a viscosity of 220 mm^2/s and an energy content of 37.68 MJ/kg. The moisture content of the oil was found to be 0.16%. Table 7.4 shows the summary of analysis of soapnut oil.

Table 7.4 Result of analysis of soapnut oil

Analysis	Result	Method
Moisture content	0.16 %	AOCS Ca 2c-25
Free fatty acid	17.5 %	AOCS Ca 5a- 40
Energy Content	37.68 MJ/kg	ASTM D240
Viscosity @40^{o}C (313 K)	220 mm^{2}/s	ASTM D445
Total acid number	34.8	

7.2.2.2 Biodiesel Production from Soapnut Oil

The oil was first treated with sulfuric acid to reduce the free fatty acids and was then taken to the second stage of transesterification i.e. base catalyst transesterification. For each batch of reaction, titration was carried out and the required amount of catalyst was determined. The amount of base catalyst needed ranged from 6 gm/l to 10 gm/l of oil. The variation was due to the difference in free fatty acid content which remained from the acid catalyst transesterification process.

Figure 7.6 shows the sample of soapnut oil. The oil is very viscous and dark colored. Figure 7.7 shows the glass reactor mounted on a heater and magnetic stirrer. Sodium hydroxide was dissolved in methanol to form sodium methoxide to use as the catalyst. The oil and methoxide were heated to 323 K. The methoxide solution was mixed with the oil and stirred. The temperature of the reaction was maintained at 333±2 K. The stirrer ran at 400 rpm. The time was recorded and samples were taken every 10 minutes to determine the conversion profile to biodiesel methyl esters.

Figure 7.6 Soapnut oil sample

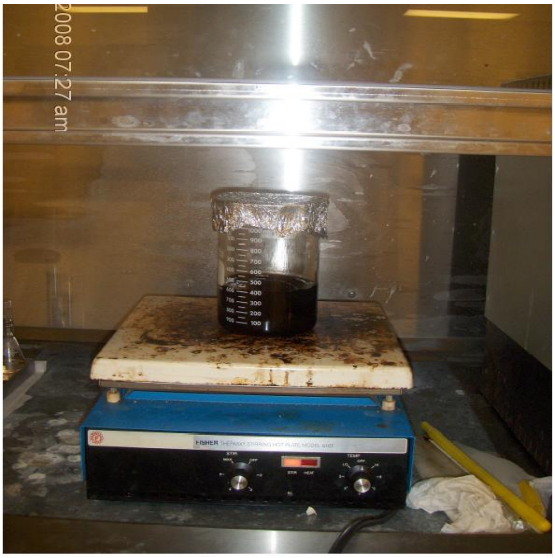

Figure 7.7 Batch transesterification process

The reaction was allowed to continue for about an hour. After completion of the reaction, the glycerol settled down as shown in Figure 7.8. In order to properly separate the methyl ester and glycerol, the final product was transferred to a separating funnel as shown in Figure 7.9.

Figure 7.8 Biodiesel and glycerin layer

Figure 7.9 Biodiesel and glycerin separation

7.2.2.3 Glycerin Removal from Soapnut Biodiesel

Upon completion of the transesterification reaction, the product was allowed to cool down to room temperature to separate the glycerin and biodiesel layers. The phase separation

between glycerin and biodiesel occurred quickly and a distinct layer could be seen within 10 minutes of settling. However, the ester layer was not clear indicating that the separation was incomplete. Hence, the product was left for further settling for 12 hours (Figure 7.9).

Removal of glycerin is an important task during biodiesel production as ASTM specifies that the free glycerin and total glycerin content in the final product should be less than 0.020 % and 0.24 % by mass respectively. In order to help settle the free glycerin down, commercial glycerin was added from the top of the flask (Figure 7.10 and 7.11). The biodiesel samples tested for glycerin content after the separation met the specified ASTM standards for free and glycerin content.

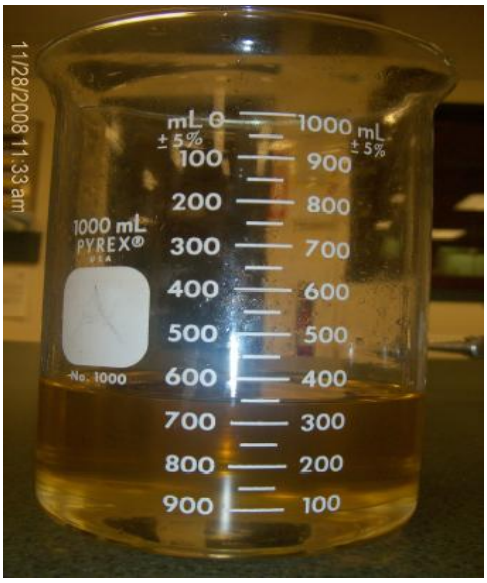

Figure 7.10 Commercial glycerin addition

Figure 7.11 Commercial glycerin removal

7.2.2.4 Washing of Soapnut Biodiesel

The biodiesel produced had a pH of 9.75. The glycerol portion was drained and the remaining part was washed with warm distilled water creating a fine mist using a nozzle spray. During mist washing, the vessel was filled with about half full of unwashed biodiesel and a fine mist of water was sprayed from the top in such a way that the surface of the biodiesel layer was not broken so as to avoid the soapnut formation. The only way to avoid forming emulsion of soap was to spray the water as gently as possible. Since the biodiesel has a lower specific gravity, water settled down to the bottom and the biodiesel remained on the top. The washing continued until clear wash water was observed as in Figure 7.12. Usually 4-6 washes were enough to complete the washing. When washing was complete, the sample pH was measured to be 7.20. In some of the batches, the biodiesel was found to have a pH between 8.5-9.0. In this case, a few drops of acetic acid were used to neutralize any base catalyst remained in the biodiesel. The biodiesel results in a lighter color than the oil feedstock due to the removal of glycerin and the soap.

Figure 7.12 Soapnut biodiesel washing with warm distilled water

7.2.2.5 Drying of Soapnut Biodiesel

Due to the use of water for washing, it is possible that biodiesel might contain higher amount of water than specified in ASTM standard. A vacuum pump was used to extract any water left with biodiesel sample (Figure 7.13). The vacuum pump was used while the sample was gently heated. The fuel quality test carried out after the drying showed there was no water left in the sample. Figure 7.14 shows the final biodiesel product.

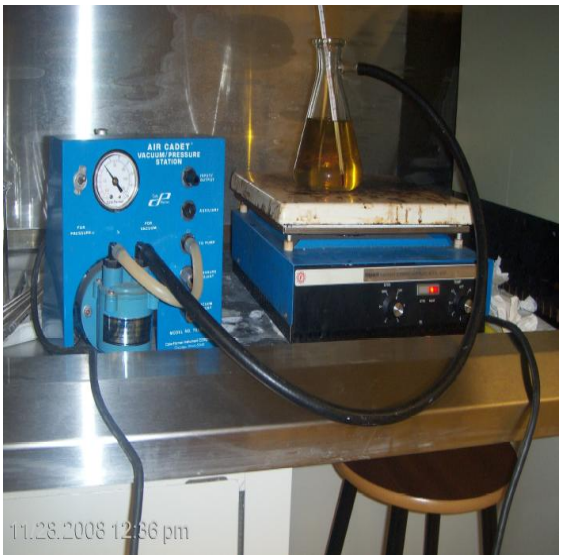

Figure 7.13 Removal of water by vacuum pump

Figure 7.14 Final soapnut product biodiesel

7.2.2.6 Fatty Acid Analysis of Soapnut Biodiesel

The biodiesel produced from the transesterification of soapnut oil was analyzed to determine the fatty acid (FA) composition. The FA content of rapeseed, soybean and sunflower oil were cited from the literature as a reference comparison. It was found that

oleic acid (18:1) was the major constituent in soapnut biodiesel with 52.64 % by weight. Similarly, 23.85% eicosenic acid (20:1) was present in the second highest amount among the fatty acids following by 7.02% arachidic acid (20:1), 4.73% linoleic acid (18:2), 4.67% palmitic acid (16:0), 1.94% alpha or gamma-linolenic acid (18:3), 1.45% stearic acid (22:0), 1.09% erucic acid (22:1) and others. Soapnut biodiesel was found to contain approximately 15% of saturated fatty acids, 77% monounsaturated fatty acids, and rest polyunsaturated fatty acids, totaling approximately 85% unsaturated fatty acids. As the soapnut oil contains a very high amount of monounsaturated fatty acids, it is in a liquid state at normal temperature and pressure, despite its higher viscosity. The chromatogram from a GC analysis to determine the fatty acid content in soapnut oil biodiesel is presented in Figure C.1 (Appendix C).

7.2.2.7 Fuel Characterization of Soapnut Biodiesel

The fuel characterization test of soapnut biodiesel was carried out using ASTM test procedures for fuel quality standard at Bently Tribology Services, Inc, Minden, NV, USA. Table 7.2.4 is the summary of test results of soapnut biodiesel prepared in the lab.

Table 7.5 Fuel characterization for biodiesel fuel from soapnut oil

Test name	Test method	Limit	Results
Free Glycerine (%mass)	ASTM D6584	Max 0.020	0.004
Monoglycerides (mass %)	ASTM D6584	N/A	0.052
Diglycerides (mass %)	ASTM D6584	N/A	0.044
Triglycerides (mass %)	ASTM D6584	N/A	0.087
Total Glycerin (mass %)	ASTM D6584	Max 0.240	0.187
Flash Point, Closed Cup (K)	ASTM D 93	Min 430	381
Methanol Content (wt %)	EN 14110	Max 0.20	0.024
Phosphorous (ppm)	ASTM D4951	Max 10	0
Water & Sediment (vol %)	ASTM D2709	Max 0.050	0
Sulfur, by UV (ppm)	ASTM D5453	Max 15	7
TAN (mg KOH/g)	ASTM D664	Max 0.50	0.18
Viscosity @ 313 K(mm^2/s)	ASTM D445	1.9 - 6.0	5.04
Cloud Point (K)	ASTM D2500	N/A	278
*Cetane Index	ASTM D976	N/A	64
API Gravity @ 288.6 K(°API)	ASTM D1298	N/A	31.5
Cloud Point (K)	ASTM D2500	N/A	284

* This may not be correct for biodiesel fuel since the correlation nomograph is defined for diesel fuel.

7.2.2.7.1 Total and Free Glycerin, Mono-, Di- and Triglycerides Content of Soapnut Biodiesel

The free glycerin, and total glycerin content were found to be 0.004 and 0.187% respectively. The ASTM allowable limit for free and total glycerin are 0.020 and 0.240 % respectively. ASTM does not have any standards for mono-, di- and triglycerides content in the final biodiesel product. However, the European Standard for biodiesel (EN14214) recommends that the mono-, di- and triglyceride content should not exceed 0.8, 0.2 and 0.2 % by mass respectively. The test results fall within the specification of European standard for soapnut biodiesel in this work.

7.2.2.7.2 Total Acid Number (Acid Value) of Soapnut Biodiesel

The total acid number (TAN) value is the total amount of potassium hydroxide necessary to neutralize the free fatty acids in the biodiesel sample. The ASTM standard for total acid number (TAN) for pure biodiesel is 0.8 mgKOH/g. The acid value for soapnut biodiesel was found to be 0.18. Fuel with a high acid number can cause degradation of rubber parts in older engines which has rubberized parts in it. The acid value can further be improved by controlling the transesterification, cleaning and drying.

7.2.2.7.3 Cloud Point of Soapnut Biodiesel

The cloud point of soapnut biodiesel was measured to be 284 K. Sarin et al. (2009) reported the cloud point of palm, jatropha and pongamia biodiesel were 289, 277 and 272 K respectively. The cloud point of soapnut biodiesel was found lower compared to cloud point of palm oil but higher than jatropha and pongamia oils.

7.2.2.7.4 Cetane Number (CN)/Cetane Index (CI) of Soapnut Biodiesel

The cetane index of soapnut oil biodiesel calculated using ASTM D976 was found to be 64. There is no cetane index value recommended by ASTM but the cetane number should not be less than 47 based on ASTM D613. The Nomograph for calculating the cetane index is presented in Figure C.2 in Appendix C.

7.2.2.7.5 Water and Sediments of Soapnut Biodiesel

There was no water and sediment content in the biodiesel sample. A vacuum pump in combination with heating was used to drive off the water and any remaining alcohol. The ASTM D2709 standard limit for water and sediment is 0.05%.

7.2.2.7.6 Viscosity of Soapnut Biodiesel

The viscosity of the soapnut biodiesel was found to be 5.04 mm^2/s at 313 K. ASTM D445 recommends that the viscosity at 313 K should be between 1.9-6.0 mm^2/s. The soapnut viscosity was found within the allowable limit recommended by ASTM.

7.2.2.7.7 Phosphorus of Soapnut biodiesel

ASTM D4951 requires that the phosphorus content of the biodiesel fuel should not exceed 10 ppm. The phosphorus content of the soapnut biodiesel produced in this work was not detectable.

7.2.2.7.8 Flash Point and Methanol Content of Soapnut Biodiesel

The flash point is the temperature at which the fuel ignites when exposed to a spark. The flash point of soapnut biodiesel was found to be381 K. The ASTM D93 recommends that the flash point should be higher than 403 K. The test method also suggests that if the flash

point of the biodiesel is between 366 K to 402 K, then the methanol content must be tested. This was done and it was found that the methanol content was 0.020 % which was within the ASTM recommended limit below 0.20% by weight.

7.2.2.8 Fatty Acid Conversion Analysis of Soapnut Biodiesel

During acid catalyst transesterification, all the free fatty acids were converted into biodiesel. Some fatty acids were also converted to biodiesel. There was approximately 41% of fatty acids (and free fatty acids) converted to biodiesel at the beginning before the start of base catalyst process. The Iatroscan was used to determine the free fatty acid content and oil to methyl ester conversion for soapnut biodiesel samples taken during the base catalyst transesterification. Samples were taken at 0, 10, 20, 30, 40 and 60 minutes respectively. Each sample was spotted in three chromarods to obtain triplicate data. The results are shown in Figure 7.15-7.18 which clearly showed that the reaction was complete and all oil was converted to biodiesel after 20 minutes of reaction. The methyl ester seen at the beginning is the result of the acid catalyst transesterification. After 10 minutes of reaction, the conversion to biodiesel was found to be approximately 58%. The conversion after 20 minutes of reaction was approximately 98%.

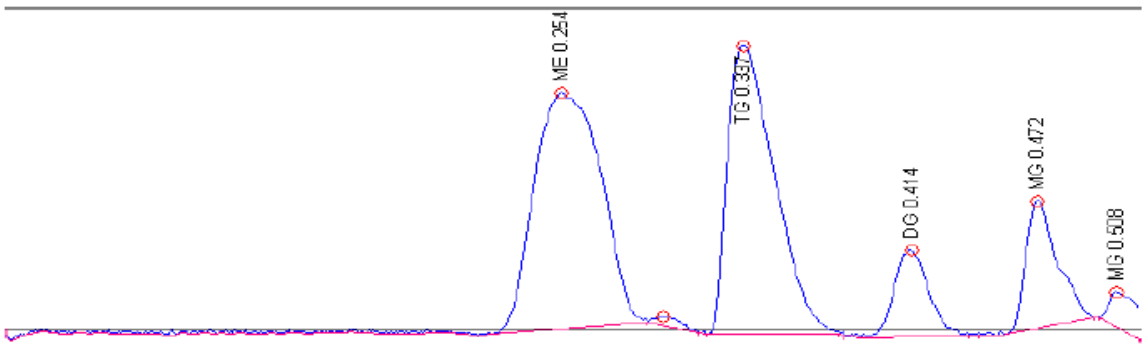

Figure 7.15 Iatroscan result for soapnut biodiesel at the beginning of base catalyst transesterification

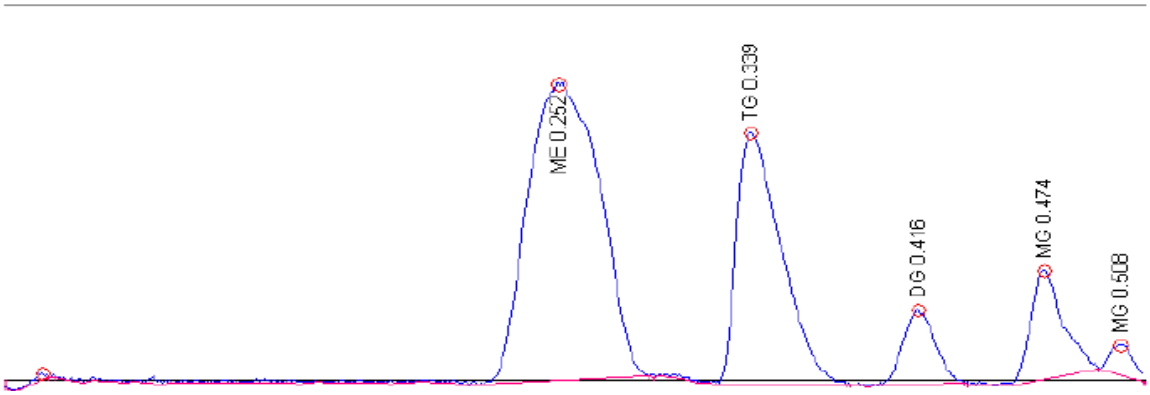

Figure 7.16 Iatroscan result for soapnut biodiesel after 10 minutes of the base catalyst transesterification

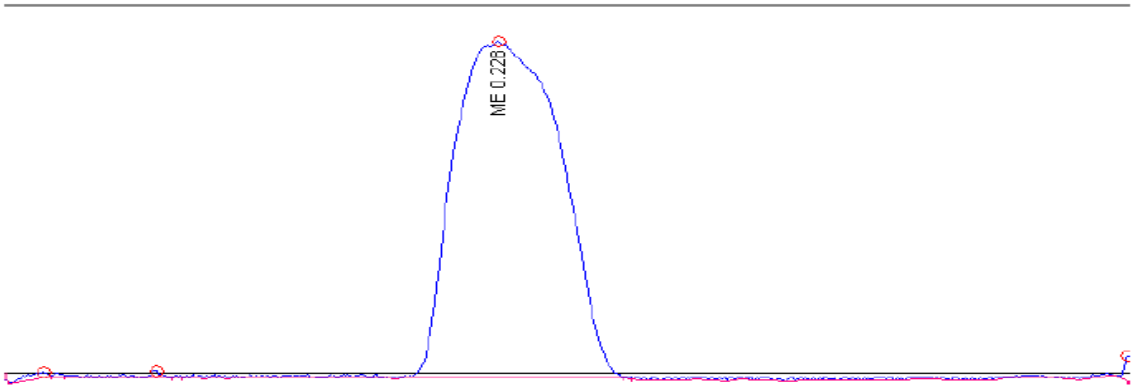

Figure 7.17 Iatroscan result for soapnut biodiesel after 20 minutes of the base catalyst transesterification

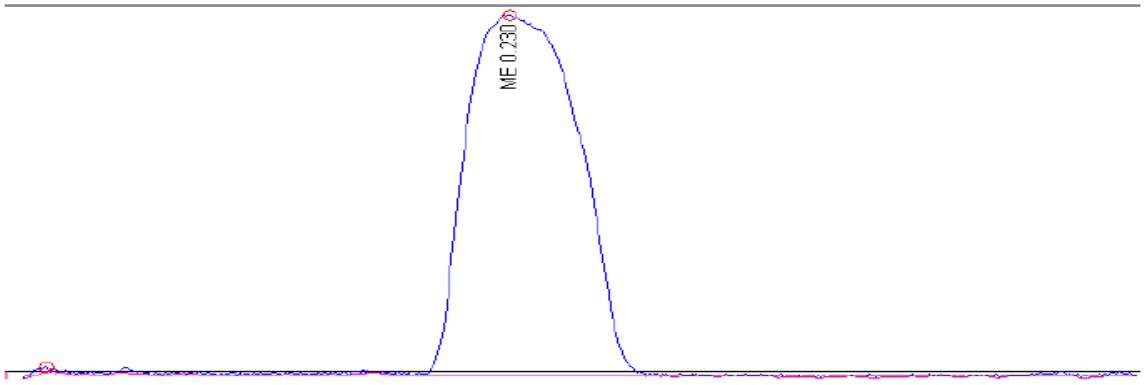

Figure 7.18 Iatroscan result for soapnut biodiesel after 30 minutes of the base

7.2.3 Jatropha Oil Biodiesel

7.2.3.1 Analysis of Jatropha Oil

The fatty acid analysis of jatropha oil was carried out in the Marine Oil Lab in Food Science Department of Dalhousie University. It was found that the sample contained 47.79% oleic acid, 32.27% linoleic acid, 13.37% palmitic acid, 5.43% stearic acid and 1.93% others (Tale 7.6). Palmitic and stearic acid were the major saturated fatty acids found in jatropha oil. The total unsaturated fatty acid content in jatropha oil was found to be approximately 80%. The overall fatty acid content of jatropha oil was comparable with the results reported by Gubitz et al. (1999). The gas chromatic analysis of jatropha biodiesel is presented in Figure C.3 in Appendix C.

Table 7.6 Iatroscan result for soapnut biodiesel after 30 minutes of the base

Fatty acid content	Structure	Amount (%) (this work)	% as reported by Gubiz et al (1999)
Lauric acid	12:0	0.31	
Palmitic acid	16:0	13.38	14.1-15.3
Palmitoleic acid	16:1	0.88	0-1.3
Stearic acid	18:0	5.44	3.7-9.8
Oleic acid	18:1	45.79	34.3-45.8
Linoleic acid	18:2	32.27	29.0-44.2
Others		1.93	
Total		100	

7.2.3.2

7.2.3.3 Production of Jatropha Biodiesel

Similar to that of soapnut oil, jatropha oil was also converted to biodiesel by a two-stage transesterification process because of its high free fatty acid content. The amount of catalyst needed was determined by titration with 99% isopropyl alcohol mixed with jatropha oil sample in 1% phenolphthalein solution and 0.1% sodium hydroxide solution. The amount of catalyst was found to be between 6 mg/l to 10 mg/l depending on the fatty

acid content remaining from the acid treatment. Sodium hydroxide was used as the catalyst for the base catalyst transesterification reaction.

All the production, cleaning and washing were similar to that of soapnut biodiesel. Figure 7.19 shows the jatropha oil which is a dark brown thick liquid and jatropha biodiesel which is a clear yellow colored biodiesel. The biodiesel washing and drying were carried out in a similar way as described in the case of soapnut oil biodiesel.

Figure 7.19 Jatropha oil and jatropha biodiesel

7.2.3.4 Iatroscan Analysis of Jatropha Biodiesel Conversion

The free fatty acid content and oil to biodiesel (methyl ester) conversion of jatropha oil was analysed using Iatroscan. The biodiesel samples were taken during the base catalyst transesterification reaction to determine the conversion rate with respect to time. Samples were taken at 0, 10, 20, 30 and 60 minutes respectively. Each sample was spotted in three chromatods to obtain triplicate data. At the beginning, there was about 19% of fatty acids (and free fatty acids) converted to biodiesel (Figure 7.20). After 10 minutes of the base catalyst reaction, approximately 55% conversion was found (Figure 7.21). The conversion

after 20 minutes of reaction was approximately 99% (Figure 7.22). After 20 minutes, there was no significant difference in conversion (Figure 7.23).

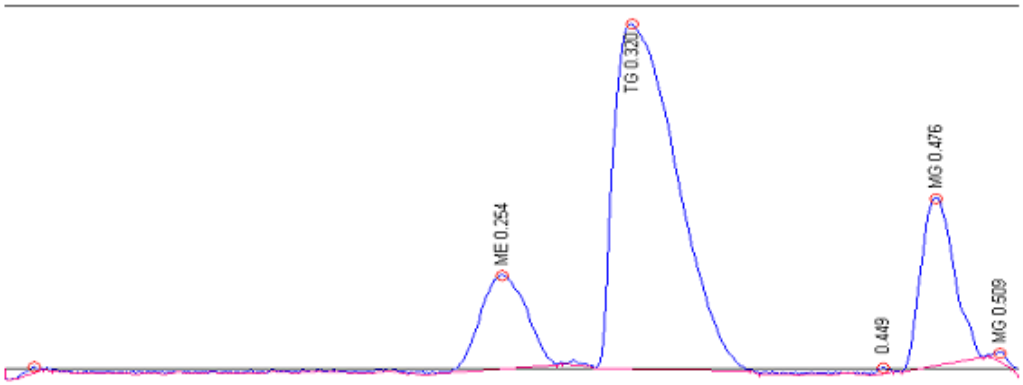

Figure 7.20 Iatroscan result for jatropha biodiesel at the beginning of the base

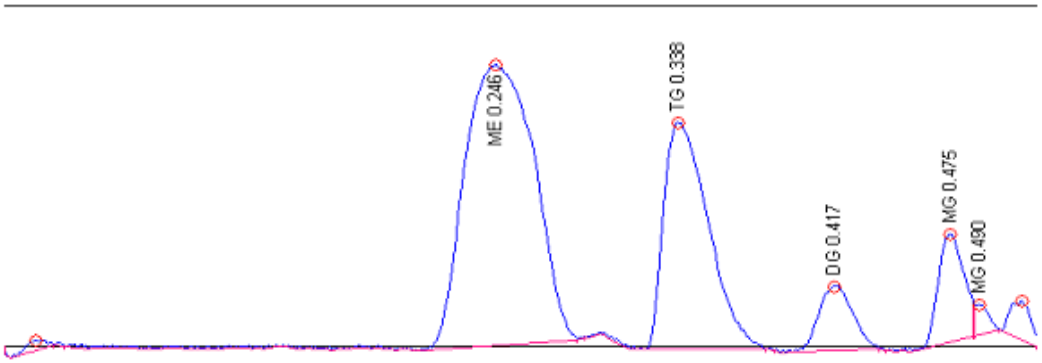

Figure 7.21 Iatroscan result for jatropha biodiesel after 10 minutes of the base catalyst transesterification

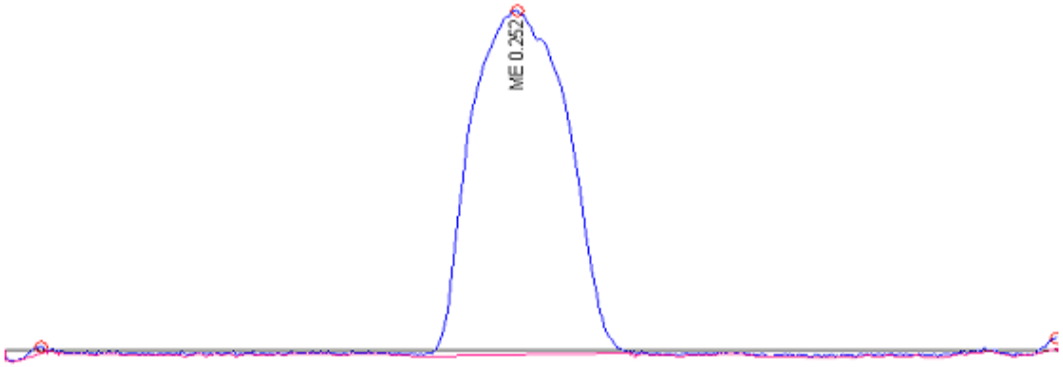

Figure 7.22 Iatroscan result for jatropha biodiesel after 20 minutes of the base catalyst transesterification

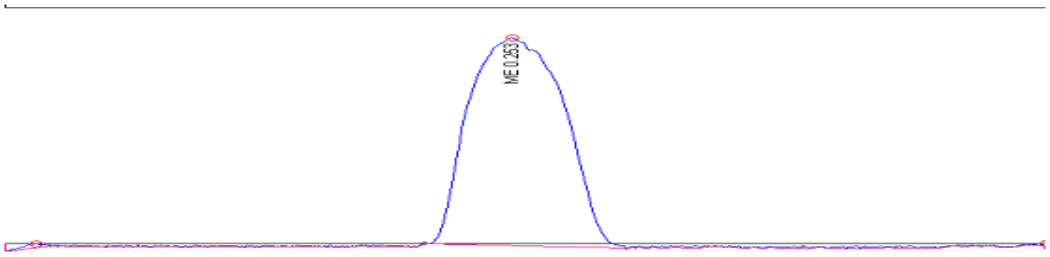

Figure 7.23 Iatroscan result for jatropha biodiesel after 30 minutes of the base catalyst transesterification

7.2.3.5 Fuel Characterization of Jatropha Biodiesel

The biodiesel fuel characterization test was carried out in Bently Tribology Services in, Minden, Nevada, USA. Table 7.7 shows the summary of test results for fuel characterization of jatropha biodiesel. Jatropha biodiesel produced in this work met all of the specifications required by ASTM D6751. The viscosity of jatropha biodiesel was 4.20 mm^2/s at 313 K whereas the ASTM D445 specified value is between 1.9-6.0 mm2/s. Similarly the total acid number for jatropha biodiesel was found to be 0.15 mgKOH/g against 0.8 mgKOH/g set by ASTM. The free and total glycerin, mono, di and triglycerides were also within the specified limit.

Table 7.7 Fuel characterization for biodiesel fuel from jatropha oil

Test name	Test method	ASTM Limit	Results
Free Glycerine (%mass)	ASTM D6584	Max 0.020	0.006
Monoglycerides (mass %)	ASTM D6584	N/A	0.074
Diglycerides (mass %)	ASTM D6584	N/A	0.019
Triglycerides (mass %)	ASTM D6584	N/A	0.005
Total Glycerin (mass %)	ASTM D6584	Max 0.240	0.104
Flash Point, Closed Cup (K)	ASTM D 93	Min 403	433
Methanol Content (wt %)	EN 14110	Max 0.20	0.024
Phosphorous (ppm)	ASTM D4951	Max 10	2
Water & Sediment (vol %)	ASTM D2709	Max 0.050	0
Sulfur, by UV (ppm)	ASTM D5453	Max 15	6
TAN (mg KOH/g)	ASTM D664	Max 0.50	0.15
Viscosity @ 313 K(mm^2/s)	ASTM D445	1.9 - 6.0	4.20
Cloud Point (K)	ASTM D2500	N/A	275
Sim. Dist., 50% Recovery (K)	ASTM D2887	N/A	634
*Cetane Index	ASTM D976	N/A	58

* This may not be correct for biodiesel fuel since the correlation nomograph is valid for diesel fuel.

7.2.4 Waste Cooking Oil Biodiesel

7.2.4.1 Biodiesel Production from Waste Cooking Oil

Waste cooking oil contains a high free fatty acid which required the use two stage process. In the first stage, H_2SO_4 with methanol was used to reduce the free fatty acid to less than 1%. Biodiesel ethyl ester from waste cooking oil was produced using sodium hydroxide as catalyst using transesterification process. Figure 7.24 shows the waste cooking oil and biodiesel ethyl ester with glycerin layer at the bottom. The glycerin from biodiesel layer was separated by gravity method. The separated biodiesel was washed using a separating funnel and applying a fine mist with warm water from the top.

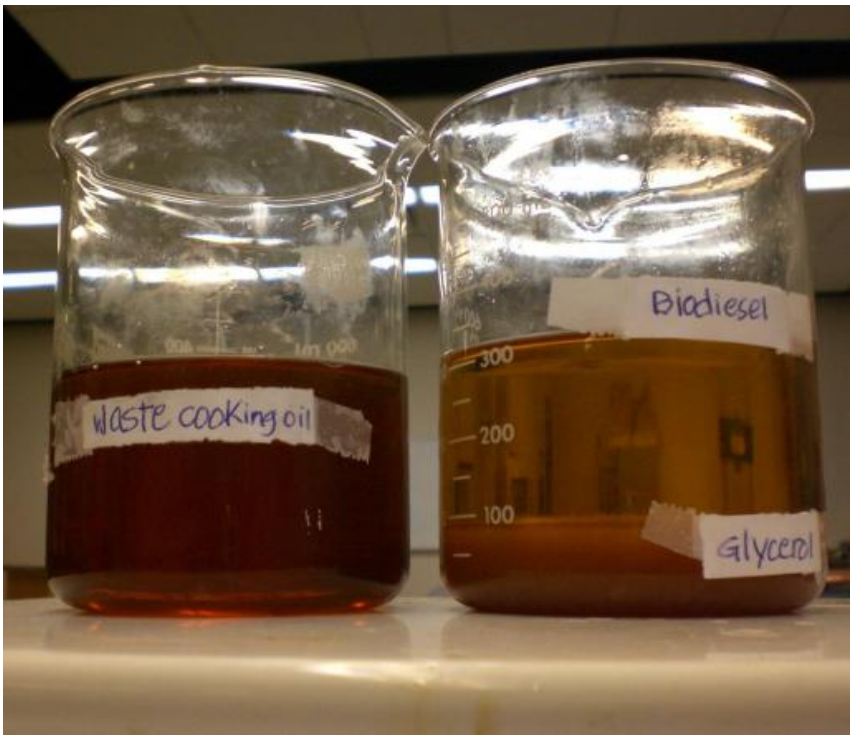

Figure 7.24 Biodiesel and glycerol layer from waste cooking oil

7.2.4.2 Conversion Efficiency and Effect of Catalysts Content on Waste Cooking Oil

The conversion of waste cooking oil to biodiesel was monitored by testing samples taken every 5 minutes for 25 minutes. The biodiesel conversion efficiency was obtained from the Iatroscan analysis. Duplicate samples were taken and the average result was plotted. The average overall conversion achieved was 94.5%. After 20 minutes, further conversion was not significant (Figure 7.25).

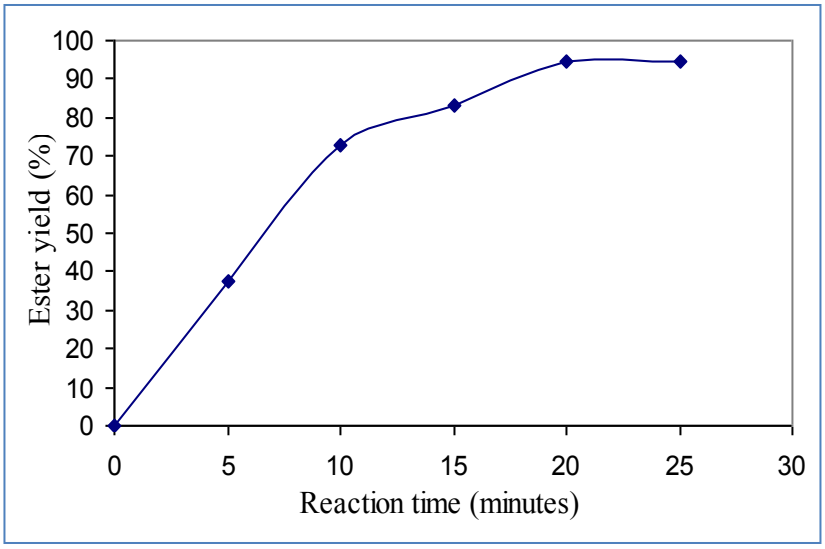

Figure 7.25 Trend of ester conversion with time

The amount of catalyst had an impact in the conversion of esters during the transesterification process. The titration indicated that the optimum amount of catalyst for the particular waste cooking oil was 8 grams per 100 ml oil. The reaction was carried out using 4, 6, 8, 10 and 12 grams per 100 ml of oil. With 4 grams per 100 ml, no reaction was observed as there was no separated layer of ester and glycerin. With the concentration of 6, 8 and 10 grams per 100 ml, approximately 50%, 94% and 40% conversion was obtained respectively (Figure 7.26).

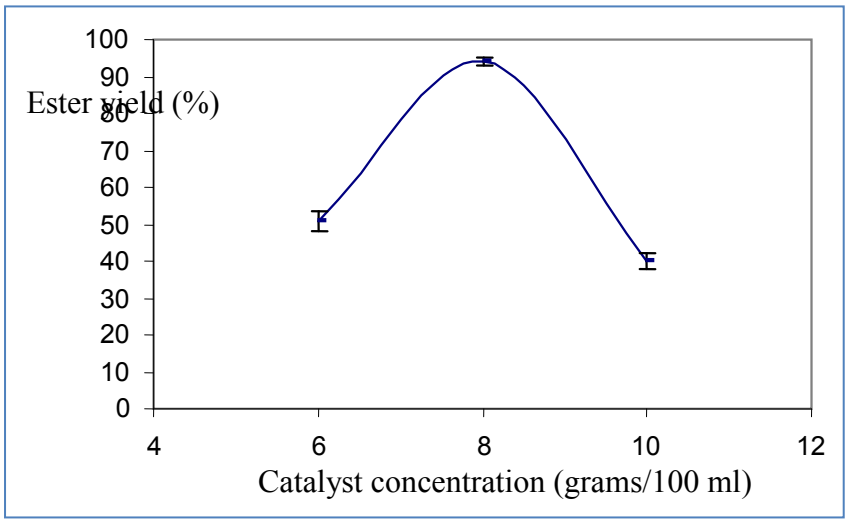

Figure 7.26 Conversion efficiency under different catalyst concentrations

It was observed that the production of ester yield decreased with the increase in sodium hydroxide. With 12 gram per 100 ml of catalyst, complete soap formation was observed. This is because the higher amount of catalyst caused soap formation (Attanatho et al., 2004). The rise in soap formation makes the biodiesel dissolve into the glycerol layer. Triplicate samples were used and the maximum standard deviation from the mean was found to be approximately 4%.

7.2.4.3 Fatty Acid Content Analysis of Waste Cooking Oil

Fatty acid contents are the major indicators of the properties of biodiesel. From gas chromatography analysis, it was found that the biodiesel derived from waste cooking oil used in this study contains oleic acid (59.7%) followed by linoleic acid (19.31%), linolenic acid (6.82%), palmitic acid (5.18%), stearic acid (2.1%), ecosenoic acid (1.21%) and rest the others. Table 7.8 shows the summary of fatty acid content in the waste cooking oil. Biodiesel from the waste cooking oil sample contained the highest amount of oleic acid among other fatty acids in the product.

Table 7.8 Fatty acid composition of biodiesel from waste cooking oil

Type of fatty acids	**Carbon Chain**	**Waste cooking oil (this work)**	**Waste cooking oil (Issariyakul et al., 2007)**
Myristic	C14:0	0.11	0.41
Palmitic	C16:0	5.18	8.22
Palmitoleic	C16:1	0.52	0.89
Stearic	C18:0	2.1	5.61
Oleic	C18:1	59.7	48.83
Linoleic	C18:2	19.31	10.94
Linolenic	C18:3	6.82	2.68
Arachidic	C20:0	0.61	0.56
Eicosenoic	C20:1	1.21	0.97
Lignoceric acid	C24:0	0.08	
Others		4.36	20.89

7.2.4.4 Viscosity and Density of Oil and Biodiesel from Waste Cooking Oil

The density of the sample of waste cooking oil measured at 294 K was 920 kg/m^3. The viscosity of the waste cooking oil was measured by using a falling ball viscometer. Falling ball viscometer was borrowed from Petroleum Laboratory of Civil and Resources Engineering, Dalhousie University. Triplicate samples were used for the experiment. It was observed that the average viscosity of unprocessed waste cooking oil was 70 mm^2/sec at 294 K. The ASTM standard for biodiesel viscosity is 1.9-6.0 mm^2/sec at 313 K.

7.2.4.5 Fuel Characterization of Biodiesel from Waste Cooking Oil

Table 7.9 shows the summary of test method used, the standard limit as recommended by ASTM and the fuel characteristic test results for the waste cooking oil biodiesel.

Table 7.9 Fuel Properties of biodiesel from waste cooking oil (WCO)

Test name	Test Method	Standard Limit	Result	European EN14214
Free Glycerin (mass %)	ASTM D6584	Max 0.020	0.022	
Monoglycerides (mass %)	ASTM D658	NA	0.293	0.8
Diglycerides (mass %)	ASTM D6584	NA	0.19	0.2
Triglycerides (mass%)	ASTM D6584	NA	0.061	0.2
Total Glycerin (mass%)	ASTM D6584	0.24	0.566	
Flash Point, Closed cup (^oC)	ASTM D93	Min 130	164	
Phosphorous (ppm)	ASTM D 4951	Max 10	2	
Sodium+potassium (ppm)	EN 14538	Max 5	66	
Calcium+Magnesium (ppm)	EN 14538	Max 1	1	
Water+Sediment (vol%)	ASTM D 2709	Max 0.05	0	
Sulfur by UV (ppm)	ASTM D 5453	Max 15	2	
TAN (mgKOH/g)	ASTM D 664	Max 0.80	0.29	
Viscosity @ 40^oC mm^2/sec	ASTM D 445	1.9-6.0	5.03	
*Cetane Index	ASTM D 976	Min 47	61	
Cloud Point (^oC)	ASTM D 2500	NA	-1	
Pour Point (^oC)	ASTM D 97	NA	-16	
Density @15^oC g/cm^3	-	NA	0.87	0.86-0.90

* This may not be correct for biodiesel fuel since the correlation nomograph is defined for diesel fuel.

7.2.4.6 Monoglyceride, Diglyceride and Triglyceride Content of Biodiesel from Waste Cooking Oil

Even though ASTM does not specify any standard values, the European biodiesel standard (EN14214) recommends that the triglyceride, diglyceride and monoglyceride content should not exceed 0.8, 0.2 and 0.2 % respectively. The experimental results were found within the limits of the European Standard.

7.2.4.7 Total Acid Number of Biodiesel from Waste Cooking Oil

The test result for the total acid number for waste cooking oil ethyl ester was found to be 0.29. ASTM standard for acid value (acid number) for pure biodiesel is 0.8 mgKOH/g. This can further be improved by controlling the transesterification process, cleaning and drying.

7.2.4.8 Cloud Point and Pour Point of Biodiesel from Waste Cooking Oil

The pour point of the waste cooking oil biodiesel was found to be 257 K. The cloud point of ethyl ester produced from waste cooking oil was found to be 272 K.

7.2.4.9 Cetane Index of Biodiesel from Waste Cooking Oil

Because of the higher oxygen content, biodiesel has a higher cetane index compared to petroleum diesel. The cetane index of waste cooking oil from the experiment was found to be 61. ASTM D976 recommends the minimum cetane index to be 47.

7.2.4.10 Water and Sediment Content of Biodiesel from Waste Cooking Oil

There was no water and sediment content found in the biodiesel sample. A rotary evaporator was used to drive off the water and any remaining alcohol. The complete removal of water and unreacted alcohol was determined when the constant weight was achieved during the rotary evaporation. The ASTM standard for water and sediment is 0.05% by volume of the sample.

7.2.4.11 Total and Free Glycerin, Sodium and Potassium of Biodiesel from Waste Cooking Oil

The total and free glycerin values for waste cooking oil biodiesel were found to be 0.022 and 0.566 % respectively, slightly exceeding the ASTM specified value. ASTM requires that the free and total glycerin for biodiesel should not exceed 0.020 and 0.024% respectively.

The sodium and potassium content of the waste cooking biodiesel was found to be 66 ppm. The ASTM allowable limit for sodium and potassium content is 5 ppm. There could be several reasons for exceeding this impurity. The pH of the sample was found to be 9.6 which is the indicator of sodium hydroxide catalyst remained in the final product. The number of washes needs to be continued until the pH of the biodiesel is close to 7.

7.3 DENSITY MEASUREMENT OF DIESEL AND BIODIESEL BLENDS

7.3.1 Calibration for Capacitor Submergence Depth

Figures 7.27-7.28 are the calibration results due to submergence of the capacitor for biodiesel blends for canola oil biodiesel and soapnut oil biodiesel. The value of K_o (dielectric constant) is taken as the slope of this line which is found to be negatively linear. The frequency was measured by varying the submergence depth of capacitance for petroleum diesel, canola, soapnut and jatropha biodiesel. The frequency data were linearly regressed with depth of submergence of capacitor using MINITAB. R^2 values from the regression for diesel and various blends of biodiesel are presented in Table 7.10 below. R^2 values were found to vary from 0.993 to 1.000.

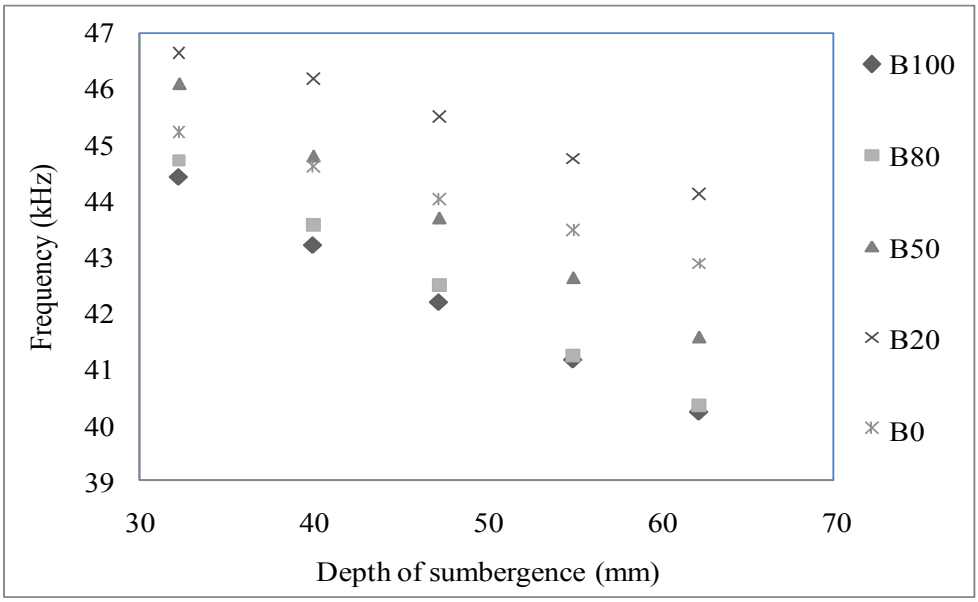

Figure 7.27 Effect of depth and frequency output measured for various blends

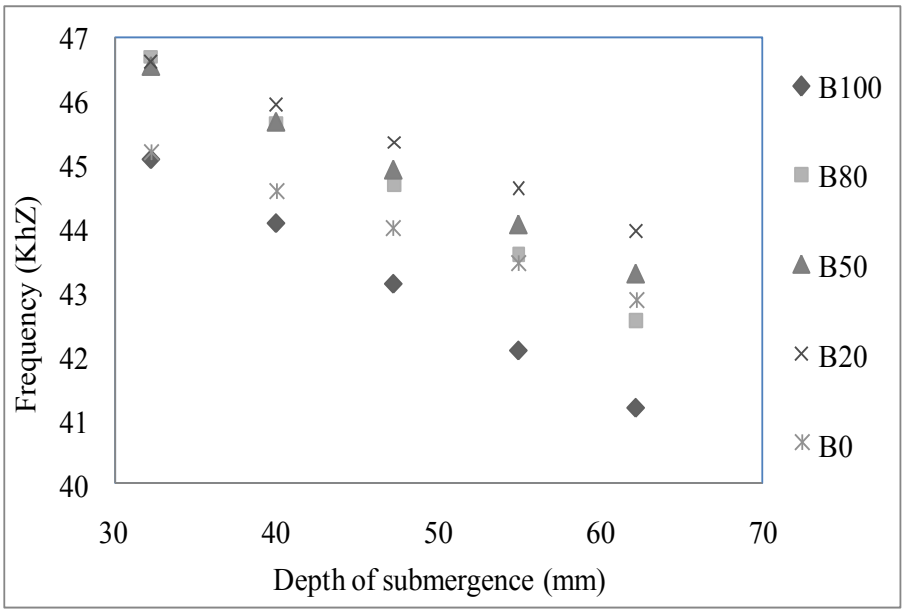

Figure 7.28 Effect of depth and frequency output for various blends of soapnut oil

Table 7.10 R^2-values for biodiesel blends and diesel

R^2 value					
Blend	B100	B80	B50	B20	B0
Canola biodiesel	0.998	0.998	0.999	0.993	
Jatropha biodiesel	0.999	1.000	0.985	0.999	
Soapnut biodiesel	1.00	1.000	1.000	0.999	
Diesel					1.000

7.3.2 Temperature Effect on the Dielectric Constant

To measure the effect of temperature on the dielectric constant, the capacitor plates were totally submerged in diesel and biodiesel sample blends and the capacitance was measured at various temperatures. Thus, the resulting frequency gave the variation in K, the dielectric constant. For full submergence, the frequency was found to increase as the temperature increased. When pressure was applied to a temperature, the frequency increased but the total increment was smaller compared to the temperature alone results. Frequencies were measured from room temperature to 523 K for all the blends of test fuels. The pressure was varied from atmospheric pressure to 7.00 MPa. It was observed that frequency increased linearly with temperature as well as with combination of temperature and pressure (Appendix D.1-D.4).

A regression analysis of frequency output was performed with respect to temperatures and pressures. The regression model obtained is represented below.

$$F = a \times T - b \times P + c \tag{7.1}$$

where F is frequency in kHz, T is the absolute temperature in K, P is the absolute pressure in kPa and a, b and c are fuel dependent constants (Table 7.11). The R^2 values in all cases are higher than 0.90 which indicates a good correlation. Figure 7.29 shows the error bars on the calibration constant for frequency as a function of temperature for canola B20 at atmospheric pressure in the full submergence test. In the Figure, each data point is represented by the average of three observations.

Table 7.11 Calibration constants for frequency as a function of temperature and pressure

Constant	B100	B80	B50	B20	B0
a	0.016	0.017	0.015	0.006	0.006
b	0.179	0.181	0.063	0.055	0.044
c	37.631	37.625	39.004	41.765	41.784
R^2	0.935	0.949	0.975	0.900	0.972

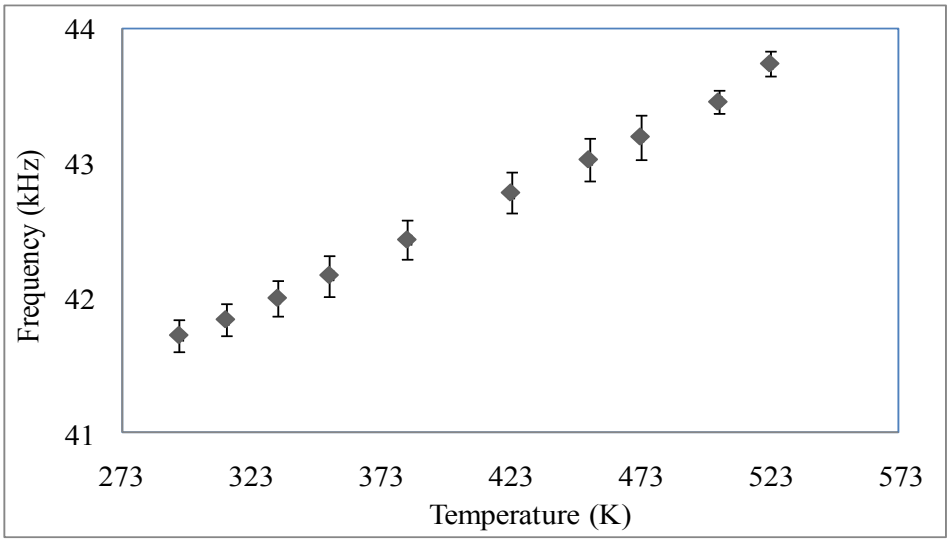

Figure 7.29 Example of error bars on calibration constant for canola B20 at atmospheric pressure in full submergence

7.3.3 Effect of Pressure on the Dielectric Constant

The effect of pressure on the dielectric constant was also studied. When the pressure was applied in the liquid reservoir, the reservoir level slightly decreased due to pressure. As the frequency is inversely proportional to the depth of submergence of the capacitor, the frequency should increase if the pressure has no effect on dielectric constant. However, the measurements showed that the frequency is decreased as the pressure is increased. This could be due to the fact that dielectric constant is affected by pressure. Hence, the effect of pressure on dielectric constant was also taken into consideration while calculating the density of the liquid as given by the equation 7.2 as below:

$$d=do + \Delta f_p/\Delta f_d \quad (7.2)$$

where Δfp is change of frequency due to pressure, Δfd is change of frequency due to depth of submergence, do is the depth of submergence at room temperature and atmospheric pressure and d is the net depth of submergence.

7.3.4 Density Measurement

The change in the depth (Δd) of the test diesel and biodiesel for different temperatures and pressures was determined using the equations A.12 and A.13 in Appendix A. The total depth of the test diesel and biodiesel in the reservoir was calculated by adding the calculated Δd to the initial depth of the biodiesel. The volume of the test diesel and biodiesel was then used to determine the density of the test diesel and biodiesel for each temperature and pressure.

7.3.4.1 Density of Diesel Fuel

Figure 7.30 below shows the plot of densities of diesel as a function of temperature for five pressures. The densities were found to decrease nearly linearly with temperature for all five pressures. It was found that there was a small change in the density of diesel at room temperature for all five pressures. The density of diesel reduced from 851 kg/m^3 at 296 K to 682 kg/m^3 at 523 K. Similarly, the density varied from 873 kg/m^3 at 296 K to 703 kg/m^3 at 7.00 MPa. Reduction in the densities was found to be more significant when the temperature was increased to 523 K.

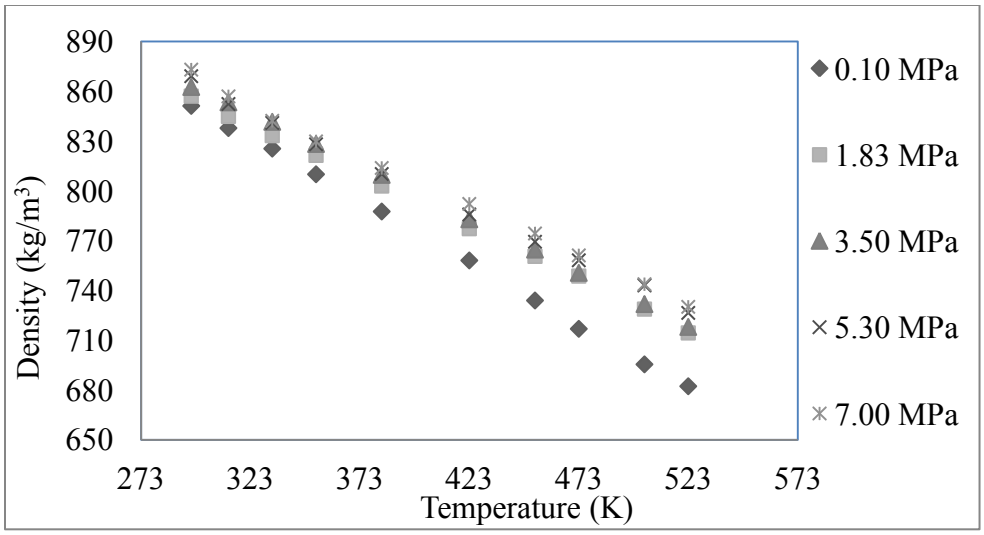

Figure 7.30 Densities of diesel (B0) as a function of temperature for five pressures

The estimated diesel data were regressed with temperature and pressure using MINITAB and the following regression equation was obtained.

$$\text{Density } (\rho) = 1036 - 0.643\ T + 0.00423\ P \qquad (7.3)$$

where T is absolute temperature in K, P is absolute pressure in kPa and ρ is the density in kg/m^3.

The R^2 value was found to be 0.984 indicating a good correlation with the model parameters. The p-value in ANOVA table was 0.000 (<0.05). The regression data for diesel are presented in Table D.1 in Appendix D. The measured and regressed density and absolute and % error are also presented in Table D.2 and D.3.

7.3.4.2 Density of Canola Biodiesel and Its Blends

Densities of canola biodiesel and its blend with diesel were measured for five pressures at different temperatures as presented in Figure 7.31. Theoretically, density decreases when the temperature of liquid increases, inversely, the density increases when the pressure in the liquid increases. In this work, the densities were found to decrease nearly linearly with increase in temperatures. The densities in the other hand increased as the pressure was

increased as shown in Figure 7.32. As the pressure was applied together with temperature, the net effect resulted in the decrease in density. The density trend in Figure 7.31 below is due to the combined effect of temperatures and pressures. The temperature had a higher effect in density than the pressure.

The densities of canola B100 decreased from 885 kg/m^3 at room temperature to 721 kg/m^3 at 523 K at atmospheric pressures. When the pressure was increased to 1.83 MPa at room temperature, the density increased to 886 kg/m^3 from 885 kg/m^3 and then decreased to 741 kg/m^3 at 523 K. Similarly, the density increased to 898 kg/m^3 at room temperature with 7.00 MPa and then decreased to 765 kg/m^3 at 523 K.

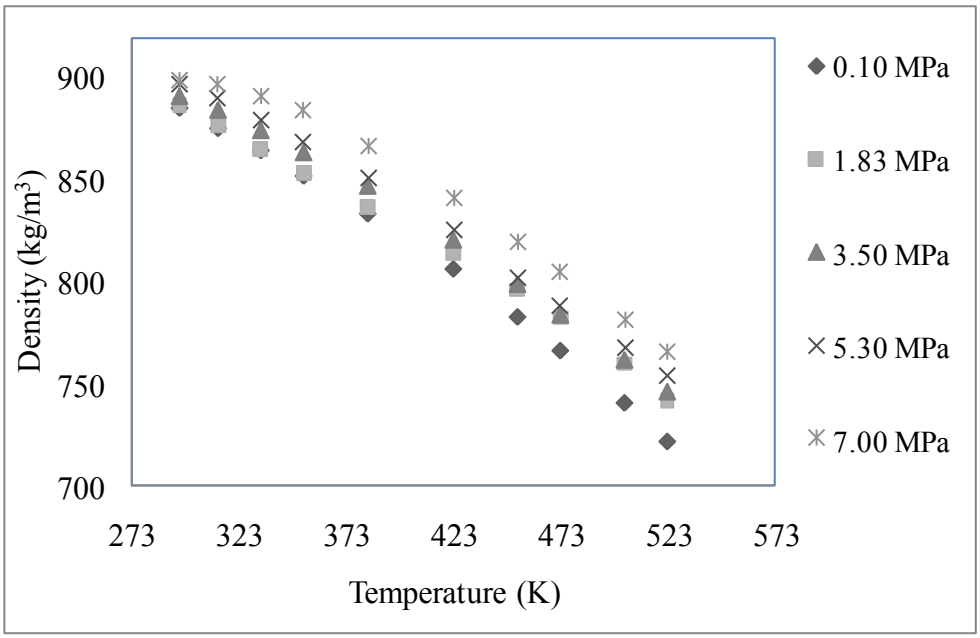

Figure 7.31 Densities of canola biodiesel (B100) as a function of temperature for five pressures

The densities for each temperature for canola B100 obtained from experiment were also plotted as a function of pressure. Figure 7.32 shows nearly a linear relationship between the densities and increasing pressure. When the temperature was kept constant and pressures were increased, the slope of the line obtained was positive but the effect of pressure on density was smaller compared to that of the effect of temperature.

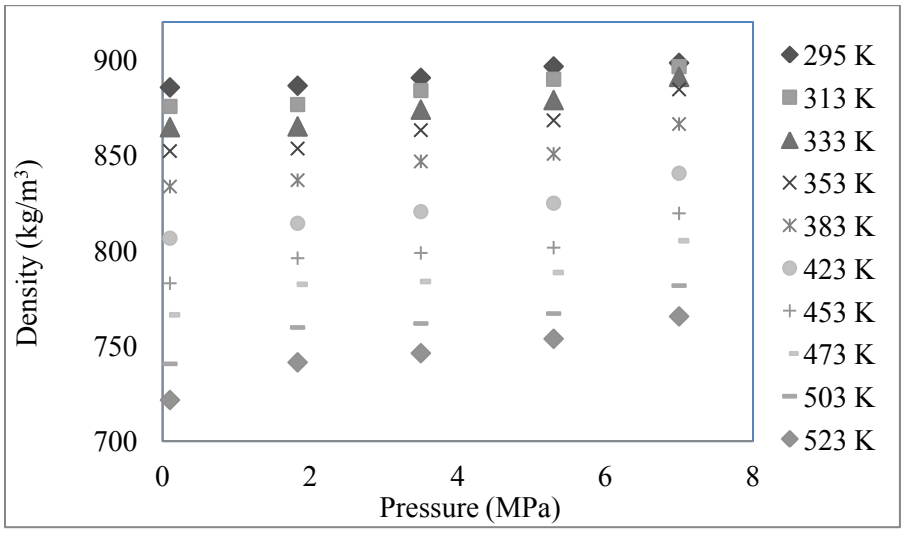

Figure 7.32 Measured densities of canola biodiesel (B100) as a function of pressure for temperatures between room temperatures and 523 K

The density data were regressed with temperatures and pressures for canola biodiesel B100 and the following model equation was obtained. The R^2 value is found to be 0.986 which indicates a good correlation of the model parameters.

$$\text{Density } (\rho) = 1076 + 0.00421\ P - 0.650\ T \tag{7.4}$$

A generalized regression equation for all biodiesel blends and diesel for five pressures and the temperatures between room temperature and 523 K was obtained and presented below in equation 7.5.

$$\text{Density } (\rho) = C - M \times T + N \times P \tag{7.5}$$

where C is the constant, M is temperature coefficient, T is the temperature in K, N is pressure coefficient and P is the pressure in kPa.

Figure 7.33 represents the plot of regressed densities of canola biodiesel B100 for five pressures between the temperatures 295 and 523 K using equation 7.5. Table D.4 in the Appendix D shows the regression data for canola biodiesel B100. Tables D.5 and D.6 in

Appendix D show the measured and regressed densities and absolute and % error for canola biodiesel B100 for five pressures between 295 to 523 K.

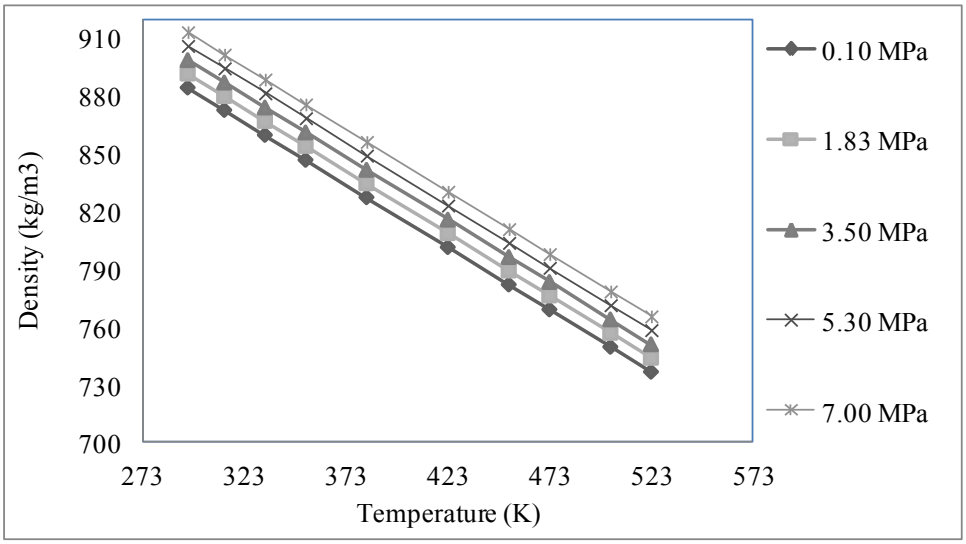

Figure 7.33 Regressed densities of canola biodiesel (B100) as a function of temperature for five pressures using equation 7.5

Table 7.12 shows the regression constants, R^2 values and p-values for all canola biodiesel blends for five pressures and temperatures between 295 to 523 K. All blends of canola biodiesel were found to have high R^2 values indicating a good correlation between the model parameters.

Table 7.12 Density of canola biodiesel B100 from regression of the experimental data

Blend	**Constant (C)**	**M**	**N**	**R^2**	**ANOVA (p-value)**
B100	1076	-0.650	0.00421	0.986	0.000
B80	1087	-0.680	0.00361	0.985	0.000
B50	1044	-0.787	0.00940	0.984	0.000
B20	1007	-0.555	0.00789	0.962	0.000

The measured density data showed some non-linear trend in some cases. Hence, non-linear regression was also carried out to see if the densities follow non-linear relationship using XLSTAT. Table 7.13 shows the summary of non-linear regression data carried out for all canola biodiesel blends. The R^2 values of both linear analysis (Table 7.12) and non-linear analysis (7.13) are also very similar.

Table 7.13 Summary of regression data for canola biodiesel blends

Blends	Non-linear regression model	R^2
B100	863.96+0.55 T+0.009 P -0.002 T^2-0.000002 P^2	0.995
B80	1074.25- 0.96 T+0.007 P +0.0016 T^2-0.000001 P^2	0.991
B50	1027.32- 0.69 T+0.005 P+0.008 T^2+0.0000003 P^2	0.990
B20	939.92-0.07 T+0.017 P-0.001 T^2-0.000004 P^2	0.997

Figure 7.34 shows the plot of regressed densities of canola biodiesel B100 using non-linear regression. The R^2 value for canola biodiesel B100 was 0.995. The R^2 value of the linear fit for the data in Figure 7.34 was found to be 0.992.

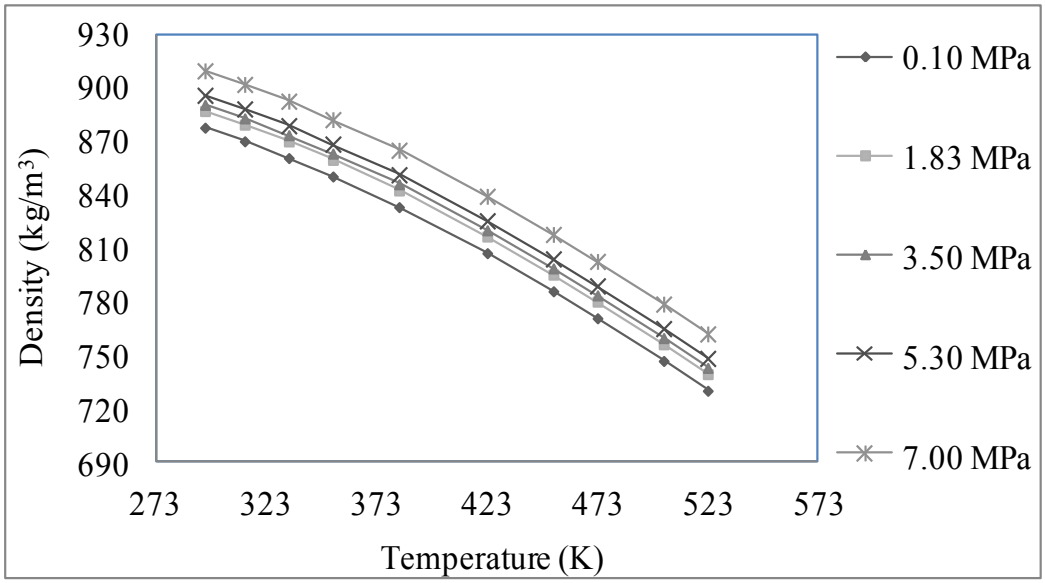

Figure 7.34 Densities of canola biodiesel (B100) as a function of temperature for five pressures obtained from non-linear regression

Figure 7.35 shows the measured densities for canola biodiesel blend B80 as a function of temperature for five pressures. Densities of canola B80 also varies linearly with temperature for all pressures. The R^2 value from the regression for B80 was found to be 0.991 indicating a good correlation of the measured data with the regression model. However, the graph plot is seen slightly curved downwards. The density of canola B80 decreased from 882 kg/m^3 at room temperature to 704 kg/m^3 at 523 K at atmospheric

pressure. Similarly, the density decreased from 905kg/m^3 at room temperature to 754 kg/m^3 at 7.00MPa.

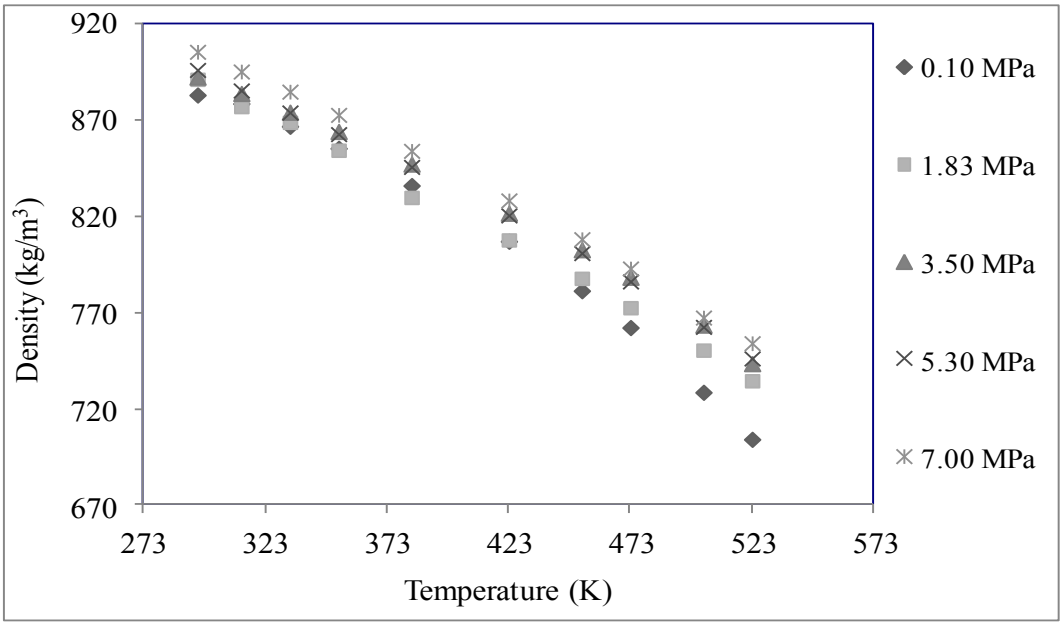

Figure 7.35 Densities of canola biodiesel (B80) as a function of temperature for five pressures

Figure 7.36 shows the plot of densities of canola biodiesel B80 obtained from linear regression. The R^2 value was found to be 0.991. Similar trend was found for canola biodiesel B50 and B20.

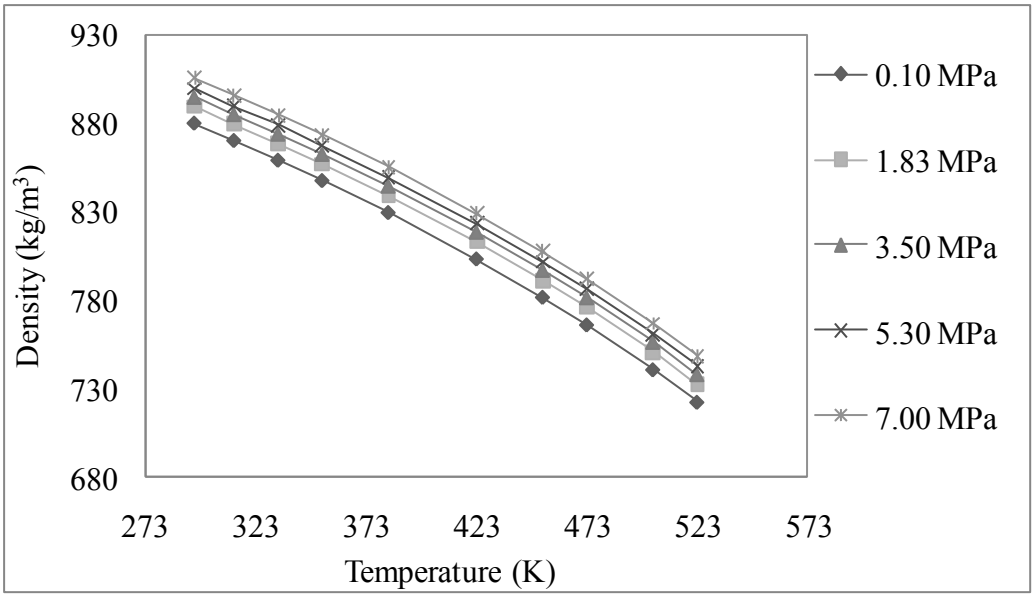

Figure 7.36 Densities of canola biodiesel (B80) as a function of temperature for five pressures obtained from non-linear regression

Figure 7.37 shows the regressed densities of canola oil biodiesel B80 as a function of temperature for five pressures between 293 to 523 K using model equation 7.5. The R^2 value is 0.985. Table D.7 in Appendix D represents the summary of regression data for canola biodiesel B80. Tables D.8 and D.9 represents the summary of measured and regressed densities, absolute and % error for canola biodiesel B80.

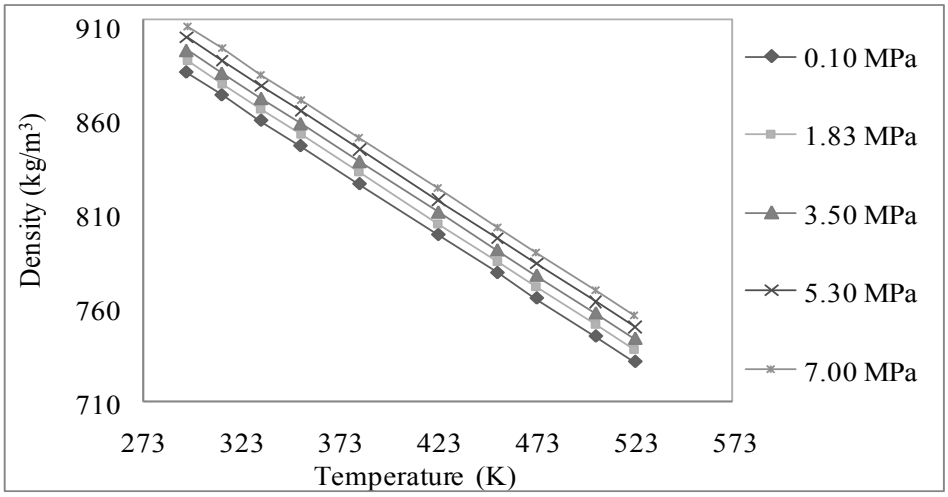

Figure 7.37 Regressed density of canola biodiesel (B80) as a function of temperature for five pressures

Figure 7.38 represents the measured densities of canola B50 as a function of temperature for five pressures. The measured density of canola B50 decreased from 875 kg/m^3 at room temperature to 716 kg/m^3 at 523 K at atmospheric pressure. Similarly, the density decreased from 900 kg/m^3 at room temperature to 779 kg/m^3 at 7.00 MPa. The measured and regressed densities of canola biodiesel B50 for 0.10, 3.50 and 7.00 MPa for temperatures between 295 to 523 K are shown in Figure 7.39. Table D.10 in Appendix D shows the summary of regression data for canola biodiesel B50. The R^2 value of 0.984 indicates a high correlation of the data for the regression model equation 7.5. Tables D.11 and D.12 represent the measured and regressed densities, absolute and % error of canola biodiesel B50 for five pressures between 295 and 523 K.

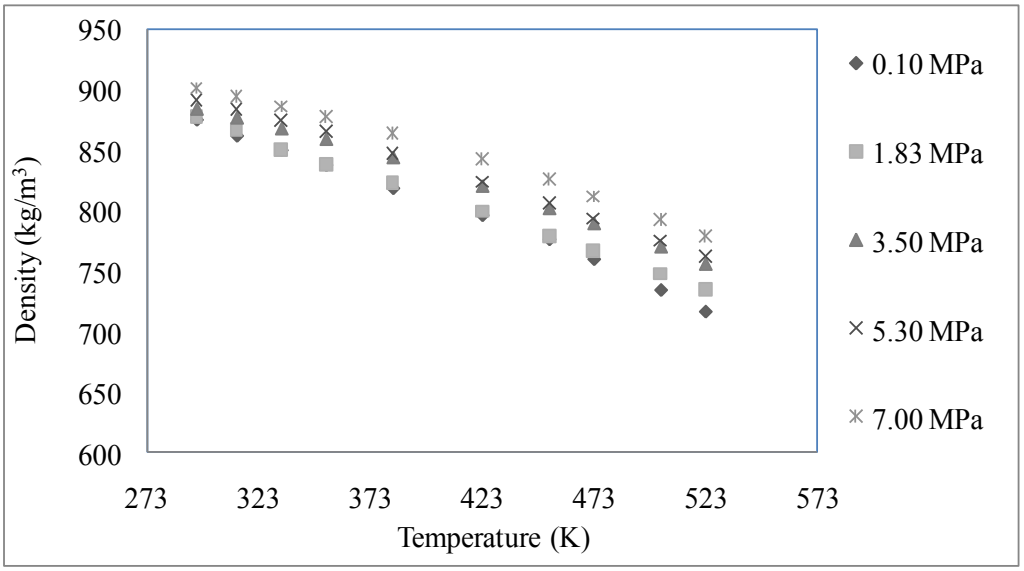

Figure 7.38 Density of canola biodiesel (B50) as a function of temperature for five pressures (MPa)

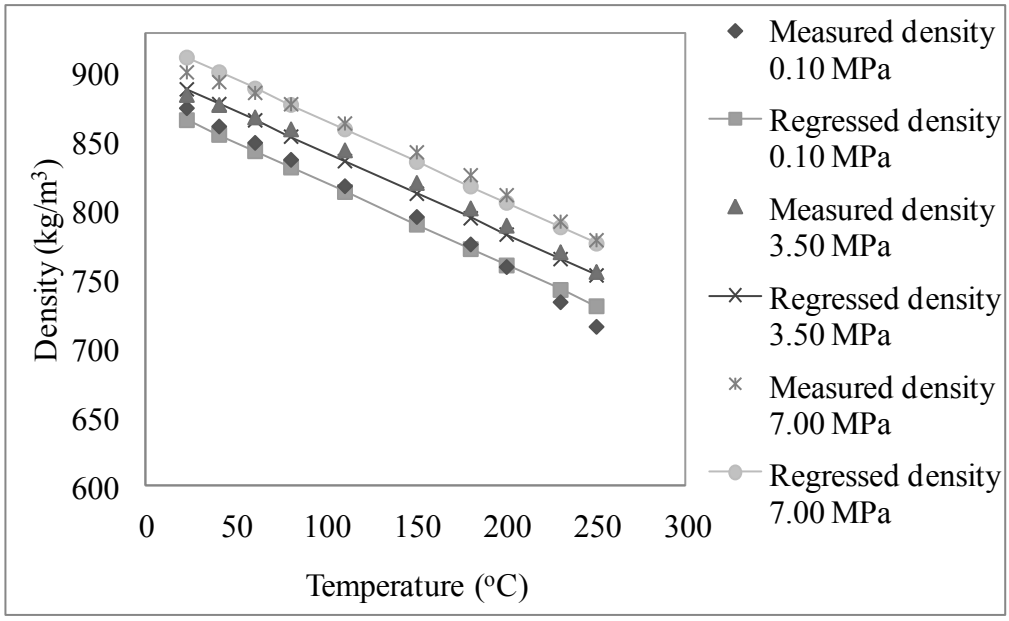

Figure 7.39 Measured and regressed density of canola B50 for 0 .10, 3.50 MPa and 7.00 MPa

The measured densities of canola B50 were also plotted as a function of pressure for the temperature range between 293 and 523 K and are shown in Figure 7.40. The results showed that the pressure had higher impacts in density at higher temperatures than at lower temperatures.

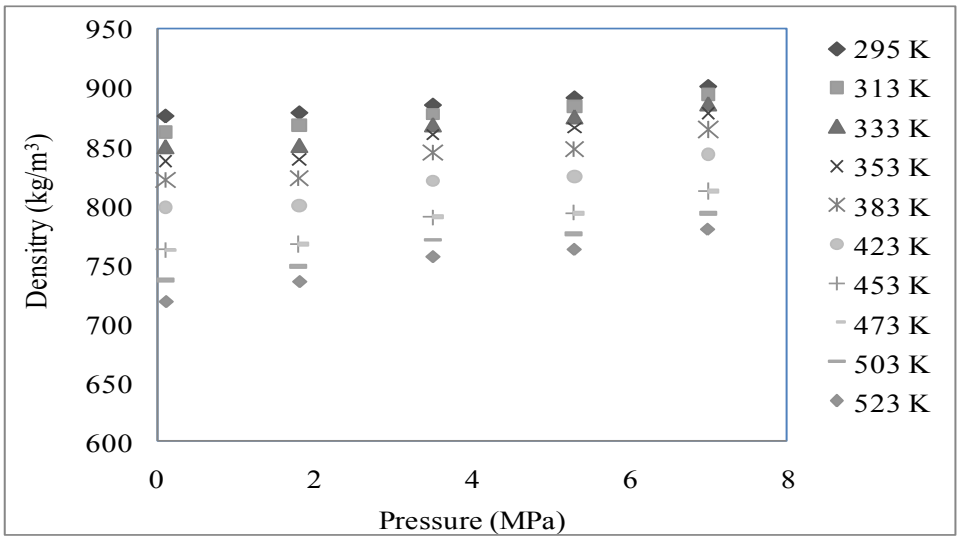

Figure 7.40 Density of canola biodiesel (B50) as a function of pressure for different temperatures

As in other blends, the densities of canola biodiesel B20 was measured for five pressures between the temperatures 293 to 523 K. The density of canola biodiesel B20 decreased from 863kg/m^3 at room temperature to 694kg/m^3 at 523 K at atmospheric pressure. Similarly, the density decreased from 886kg/m^3 at room temperature to 789kg/m^3 at 523 K for 7.00 MPa.

The measured densities are shown in Figure 7.41. The densities decreased nearly linearly with increase in temperature and pressure which is indicated by R^2 value of 0.962. It was found that there is a small change in the densities of canola biodiesel B20 at room temperature for all pressures. Reduction in the density was found more significant when the temperature was increased at higher pressures. The density in Figure 7.41 is due to the combined effect of temperatures and pressures for canola B20.

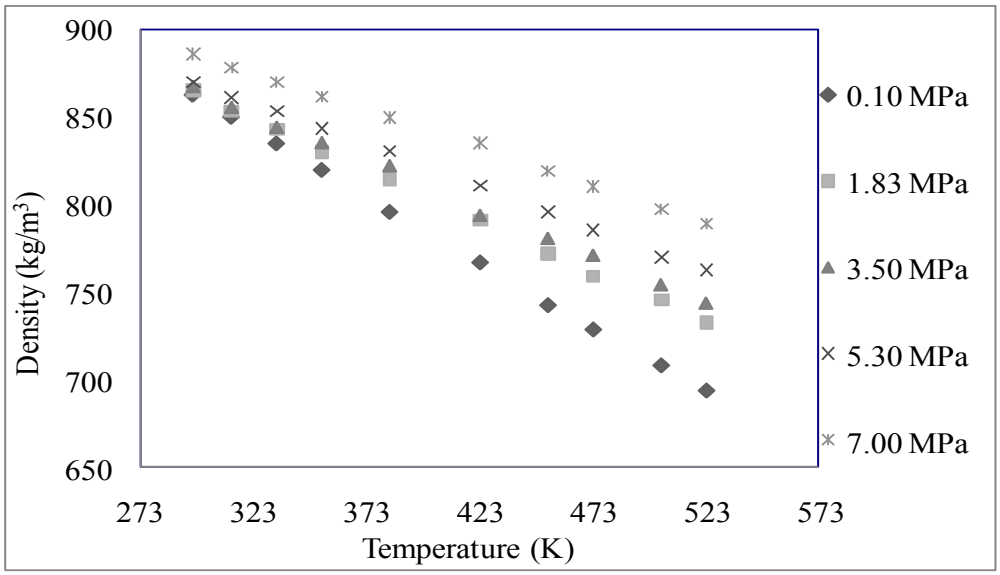

Figure 7.41 Density of canola biodiesel (B20) as a function of temperature for five pressures (MPa)

Figure 7.42 represents the regressed density for canola biodiesel B20 at five pressures. Similar to that of other canola biodiesel blends, the temperature is found to have higher effect in density compared to that of pressure. Table D.13 in Appendix D shows the regression data for canola biodiesel B20 for five pressures and temperatures between room temperature and 523 K. Table D.14 and D.15 represent the summary of measured and regressed densities, absolute and % error for canola biodiesel B20.

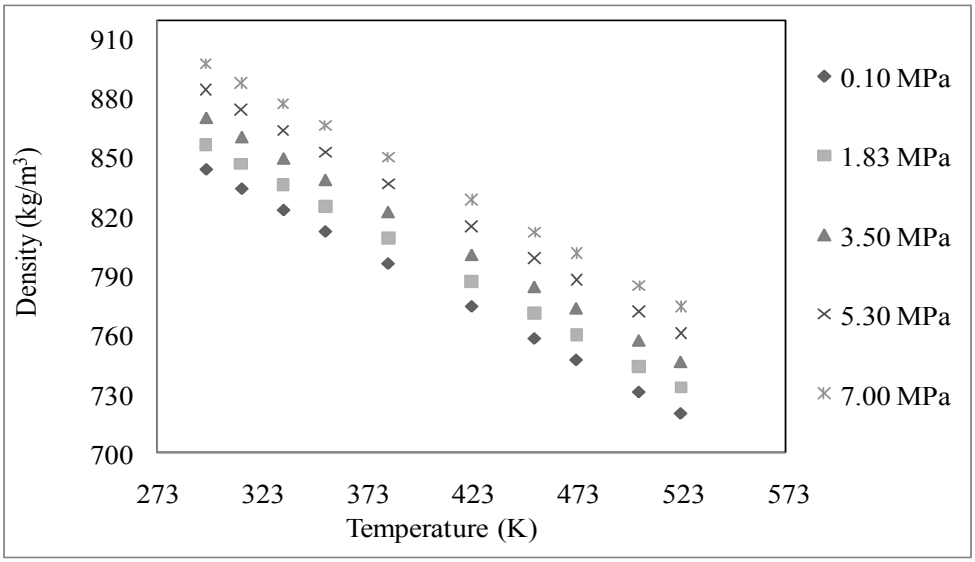

Figure 7.42 Regressed density of canola B20 for five pressures and at different temperatures

7.3.4.3 Density of Jatropha Biodiesel and Its Blends

The measured densities of jatropha biodiesel B100 at temperatures from 295 to 523 K for five pressures is presented in Figure 7.43. Similar to that of canola biodiesel, the densities of jatropha B100 decreased nearly linearly with increase in temperatures and pressures. The densities showed smaller change in room temperature for all pressures compared to the higher temperatures. The measured density data were regressed for five pressures and temperatures between room temperature and 523 K. Table D.16 in Appendix D is the summary of regression data for jatropha biodiesel B100. The R^2 value from regression was found to be 0.971 and p value from ANOVA was found to be 0.000 (<0.05). Table D.17 and D.18 represents the summary of measured and regressed density of jatropha biodiesel B100 for five pressures. Tables D.17 and D.18 also contain absolute error and % error for all measured data. Table 7.14 shows the regression constants for measured densities of jatropha biodiesel and its blends for five pressures and temperatures between room temperature and 523 K.

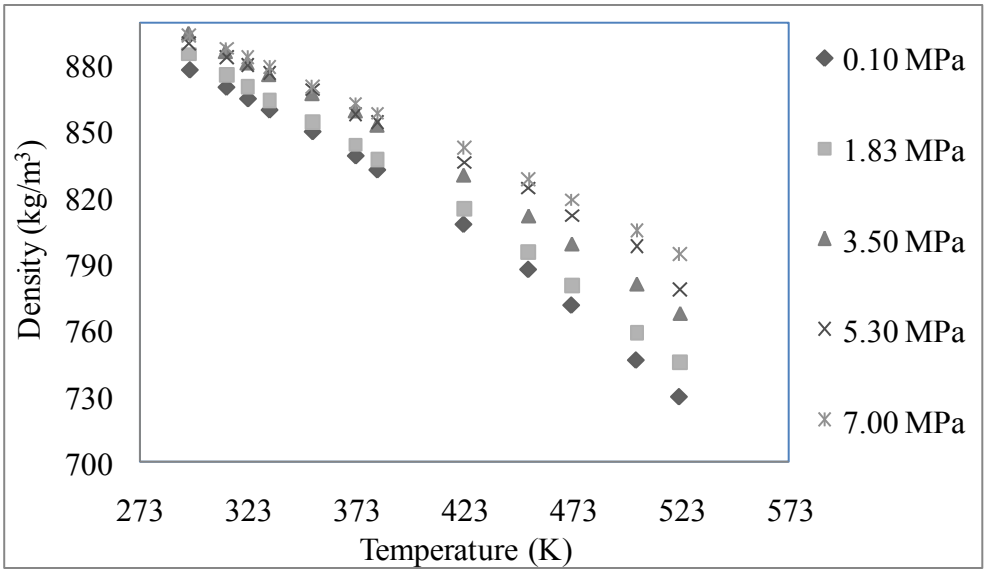

Figure 7.43 Densities of jatropha biodiesel B100 as a function of temperature for five pressures

Table 7.14 Regression constants for jatropha biodiesel blends using equation 7.5

Biodiesel Blend	Temperature coefficient (M)	Pressure coefficient (N)	Constant (C)	R^2	p-value (ANOVA)
B100	-0.547	0.00488	1037	0.971	0.000
B80	-0.510	0.00462	1019	0.987	0.000
B50	-0.589	0.00527	1039	0.969	0.000
B20	-0.506	0.00489	1003	0.958	0.000

Figure 7.44 represents the measured densities of jatropha biodiesel B80 for temperatures from 295 to 523 K for five pressures. The densities of jatropha B80 decreased nearly linearly with increase in temperatures and pressures. Similar to that of jatropha biodiesel B100, a small change in the density was observed for jatropha biodiesel B80 at room temperature compared to at higher temperatures.

The measured densities were regressed for five pressures and temperatures between room temperature and 523 K. Table D.19 in Appendix D is the summary of regression data for jatropha biodiesel B80. The R^2 value from regression was found to be 0.969 and p value from ANOVA was found to be 0.000 (<0.05). Table D.20 and D.21 represents the summary of measured and regressed densities of jatropha biodiesel B100 for five

pressures. Table D.20 and D.21 also shows measured and regressed densities as well as absolute and % error for all measured data with respect to the regressed data.

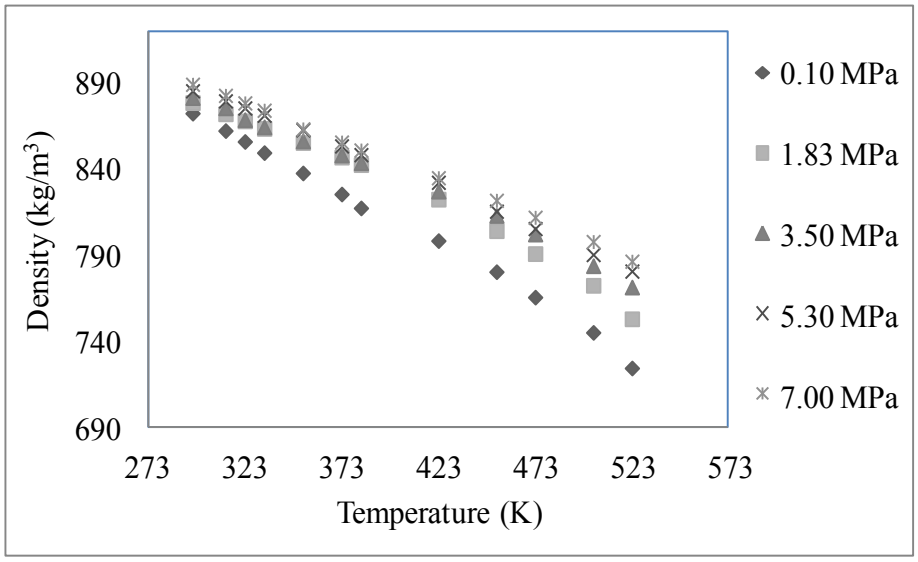

Figure 7.44 Densities of jatropha biodiesel (B80) as a function of temperature at five pressures

Figure 7.45 shows the measured densities of jatropha biodiesel B50 for temperatures from 295 to 523 K for five pressures. The density decreased nearly linearly with increase in temperatures and pressures. A small change in density was observed at room temperature compared to that of higher temperatures where the change in densities was more significant. The measured densities were regressed for five pressures and temperatures between room temperature and 523 K. Table D.22 in Appendix D represents the summary of regression data for jatropha biodiesel B50. The R^2 value from regression was found to be 0.989 and p value from ANOVA was found to be 0.000 (<0.05). Table D.23 and D.24 represent the summary of measured and regressed densities and absolute and % error of jatropha biodiesel B50 for five pressures.

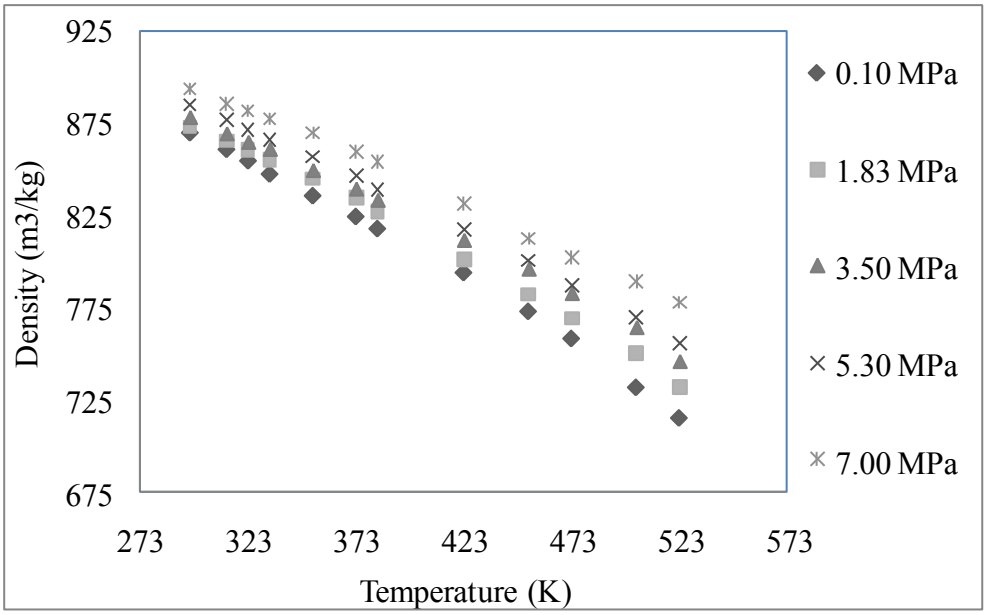

Figure 7.45 Densities of jatropha biodiesel (B50) as a function of temperature at five pressures

Figure 7.46 shows the measured densities of jatropha biodiesel B20 for temperatures between room temperature to 523 K for five pressures. As in other biodiesel blends, the density decreased nearly linearly with increase in temperatures and pressures. The measured densities were regressed for five pressures and temperatures between room temperature and 523 K. Table D.25 in Appendix D is the summary of regression data for jatropha biodiesel B20. The R^2 value from regression was found to be 0.958 and p value from ANOVA was found to be 0.000 (<0.05). Table D.26 and D.27 represent the summary of measured and regressed densities and absolute and % error of jatropha biodiesel B20 for five pressures. It is observed that at higher temperatures, the pressure has a higher impact on density than at lower temperatures.

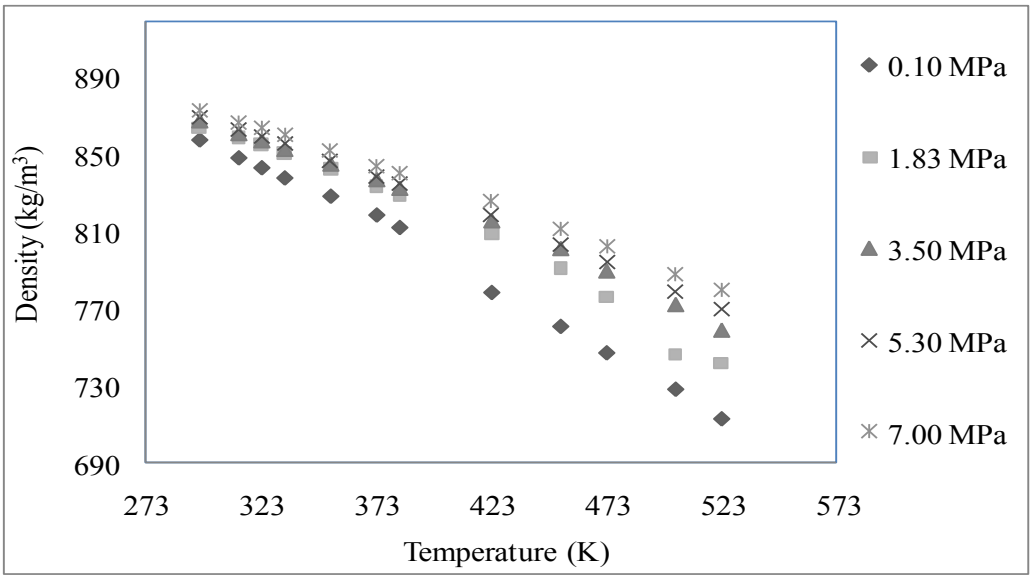

Figure 7.46 Densities of jatropha biodiesel (B20) as a function of temperature at five pressures

Some of the measured densities also showed non-linear trend in some cases, Hence, non-linear regression analysis was performed using XLSTAT. Table 7.15 shows the regression equations obtained from non-linear regression. The equations showed that the coefficients for the square terms were quite small. Figure 7.47 is the plot from non-linear regression analysis of jatropha biodiesel B100. All other blends also showed similar trends. The R^2 values from linear and non-linear analysis did not differ much.

Table 7.15 Summary of regression data for jatropha biodiesel blends

Blends	**Non-linear regression model**	**R^2**
B100	1017.62-0.66 T+0.004 P+0.0009 T^2+0.0000007 P^2	0.977
B80	1145.95-1.72 T+0.016 P+0.004 T^2-0.000003 P^2	0.983
B50	980.49-0.35 T+0.0085 P-0.000072 T^2 -0.000001 P^2	0.992
B20	859.69+0.29 T+0.016 P-0.001 T^2-0.000003 P^2	0.973

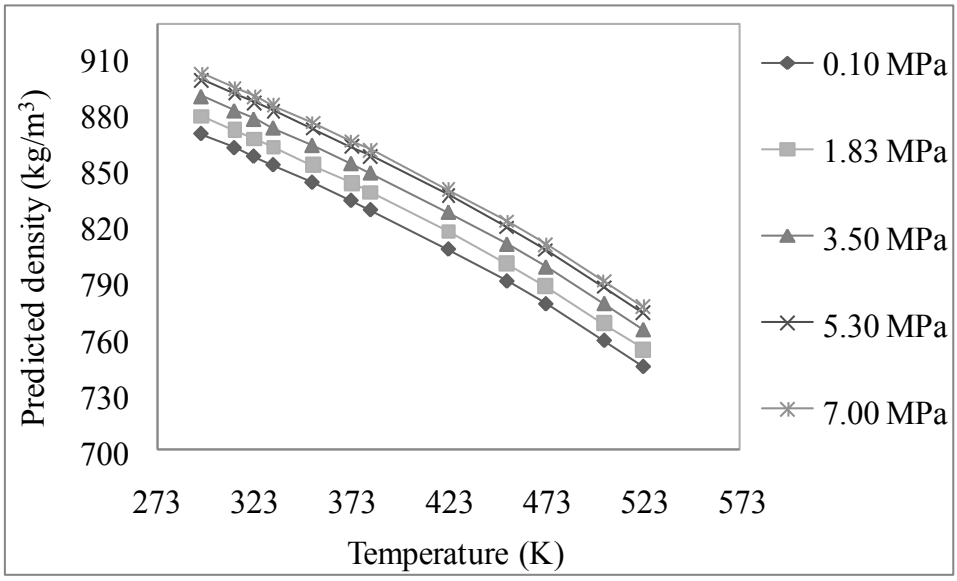

Figure 7.47 Densities of jatropha biodiesel (B100) as a function of temperature at five pressures obtained from non-linear regression

7.3.4.4 Density of Soapnut Biodiesel and Its Blends

Densities of soapnut biodiesel and its blends were also measured for five pressures and temperatures between room temperatures and 523 K. The measured densities for five pressures and temperatures between room temperatures and 523 K are presented in Figure 7.48. The results showed that the densities decreased nearly linearly with increase in temperatures for all pressures. Figure 7.49 is the plot of regressed densities of soapnut biodiesel B100 using the equation 7.5. The measured densities were also plotted as a function of pressures between 295 and 523 K (Figure 7.50). It was found that the densities increased nearly linearly as pressure increased. However, the pressure has more impact on densities at higher temperatures than at lower temperatures.

The measured densities were regressed for five pressures and temperatures between room temperature and 523 K. Table D.28 in Appendix D is the summary of regression data for soapnut biodiesel B100. The R^2 value from regression was found to be 0.987 and p value from ANOVA was found to be 0.000 (<0.05). Three of the observations were found to have large standardized residuals. Tables D.29 and D.30 represent the summary of

measured and regressed densities and absolute and % error for soapnut biodiesel B100 for five pressures.

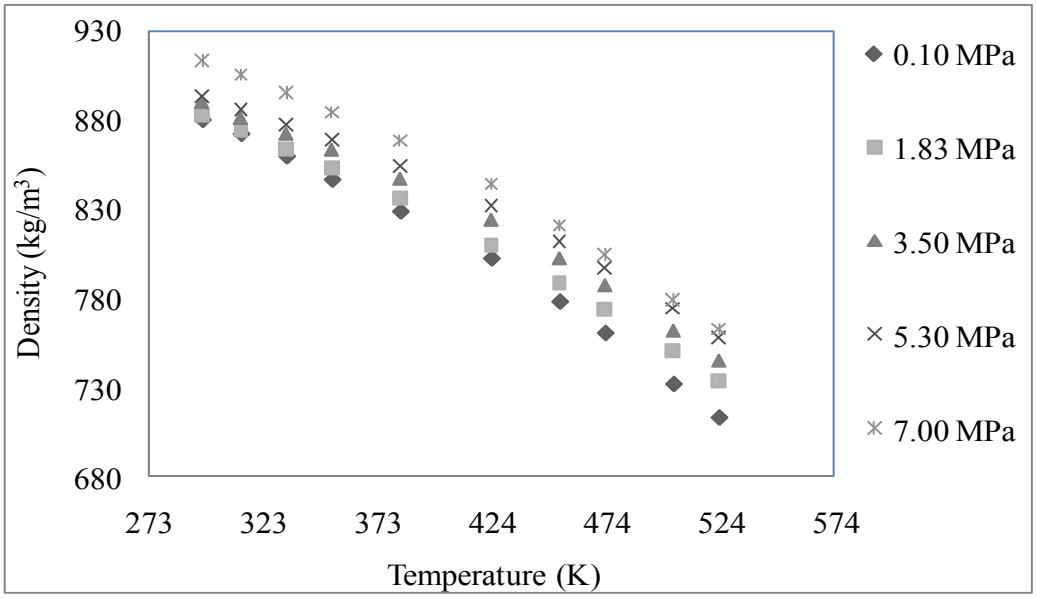

Figure 7.48 Densities of soapnut biodiesel (B100) as a function of temperature at five pressures

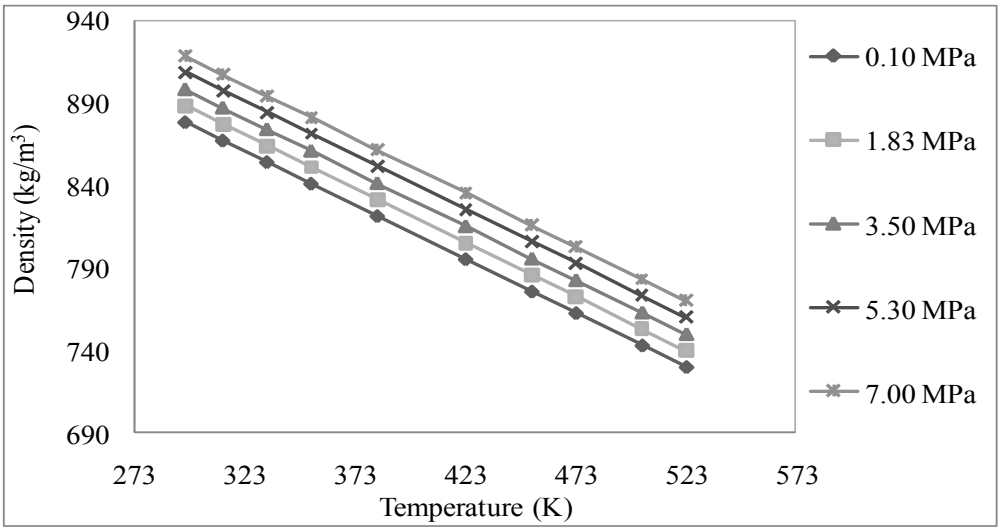

Figure 7.49 Regressed densities of soapnut biodiesel (B100) as a function of temperature for five pressures using equation 7.5

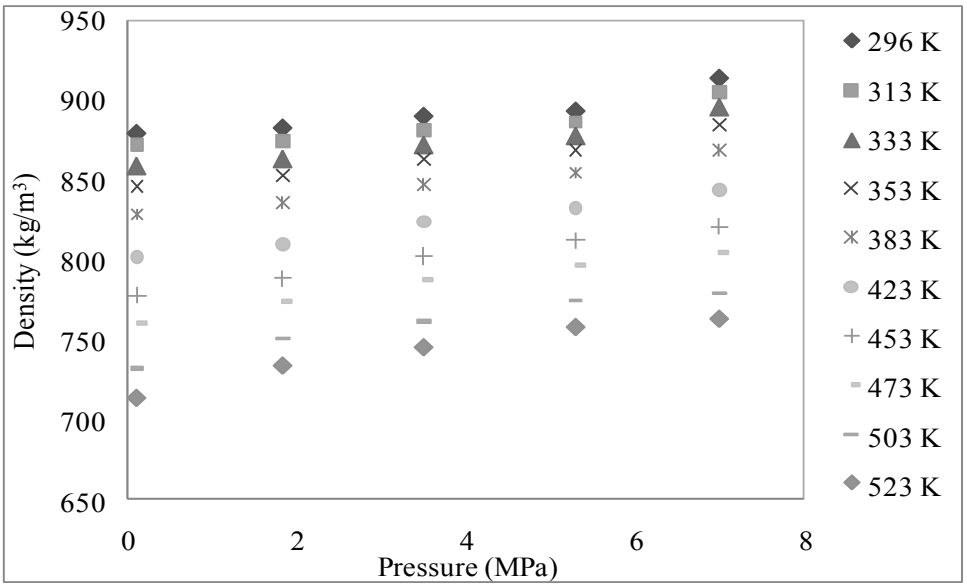

Figure 7.50 Densities of soapnut biodiesel (B100) as a function of pressure at different temperatures

Figure 7.51 represents the measured densities of soapnut biodiesel B80 for temperatures between 295 to 523 K for five pressures. The densities of soapnut biodiesel B80 decreased nearly linearly with increase in temperatures for each pressure.

The measured densities of soapnut biodiesel B80 were regressed for five pressures and temperatures between 295 and 523 K. The R^2 value from regression was found to be 0.987 and p value from ANOVA was found to be 0.000 (<0.05). Table D.31 in Appendix D is the summary of regression data for soapnut biodiesel B80. Tables D.32 and D.33 represent the summary of measured and regressed densities and absolute and % error for soapnut biodiesel B80 for five pressures. These tables also contain the absolute and relative errors for each temperature and pressure between 295 and 523 K.

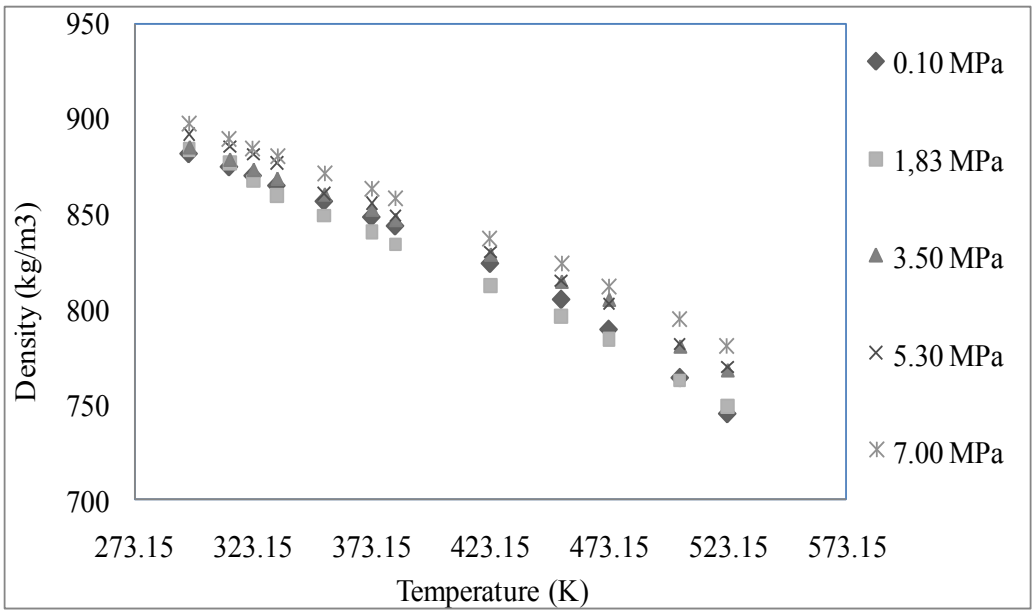

Figure 7.51 Densities of soapnut biodiesel (B80) as a function of temperature at five pressures

Figure 7.52 shows the measured densities of soapnut biodiesel B50 for temperatures between 296 to 523 K for five pressures. The densities of soapnut biodiesel B50 decreased nearly linearly with increase in temperatures for each pressure.

The measured densities of soapnut biodiesel B50 were regressed for five pressures and temperatures between room temperature and 523 K. The R^2 value from regression was found to be 0.963 and p- value from ANOVA was found to be 0.000 (<0.05). One of the observations was found to have large standardized residual. Table D.34 in Appendix D show the summary of regression data for soapnut biodiesel B50. Tables D.35 and D.36 represent the summary of measured and regressed densities and absolute and % error for soapnut biodiesel B50 for five pressures. These tables also contain the absolute error and total error (%) for each temperature and pressure between 295 and 523 K.

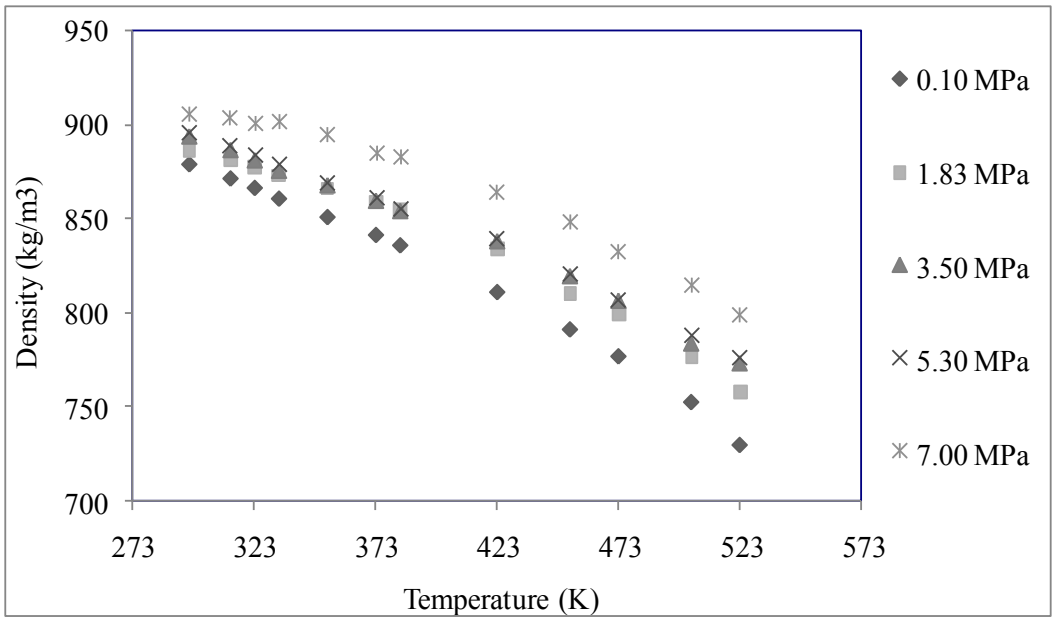

Figure 7.52 Densities of soapnut biodiesel (B50) as a function of temperature at five pressures

Figure 7.53 shows the measured densities of soapnut biodiesel B20 for temperatures between 296 to 523 K for five pressures. The density of soapnut biodiesel B20 decreased nearly linearly with increase in temperatures for each pressure.

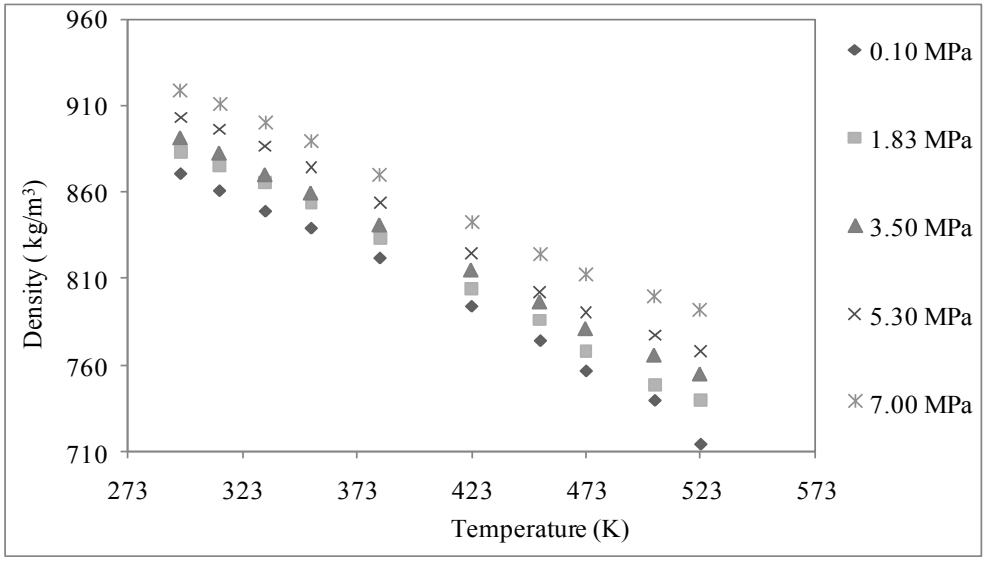

Figure 7.53 Densities of soapnut biodiesel (B20) as a function of temperature at five pressures

The measured densities of soapnut biodiesel B20 were regressed for five pressures and temperatures 296 and 523 K. The R^2 value from regression was found to be 0.993 and p value from ANOVA was found to be 0.000 (<0.05). Figure 7.54 represents the plot of regressed densities of soapnut biodiesel B20 using equation 7.5. Table D.37 in Appendix D shows the summary of regression data for soapnut biodiesel B20. Tables D.38 and D.39 represent the summary of measured and regressed densities and absolute and % error for soapnut biodiesel B20 for five pressures. These tables also contain the absolute and relative errors.

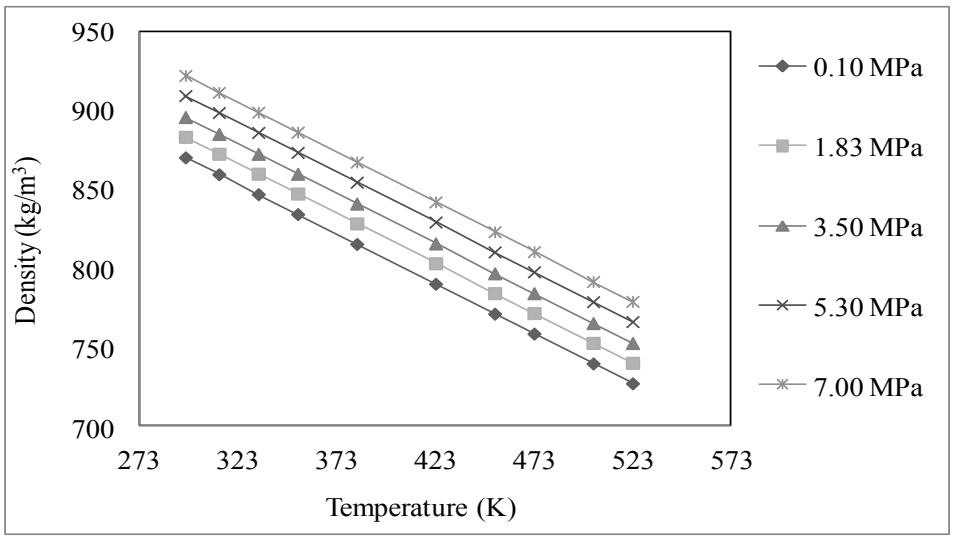

Figure 7.54 Regressed densities of soapnut biodiesel (B20) as a function of temperature at five pressures using equation 7.5

Table 7.16 is the summary of regression constants, the R^2 values and p-values from ANOVA for soapnut biodiesel B100 and its blends for five pressures between room temperature and 523 K. The temperature has a higher effect on density that the pressure.

Table 7.16 Regression constants for soapnut biodiesel and its blends

Biodiesel Blend	Temperature coefficient (M)	Pressure coefficient (N)	Constant (C)	R^2	p-value (ANOVA)
B100	-0.653	0.00580	1071	0.987	0.000
B80	-0.541	0.00310	1040	0.982	0.000
B50	-0.543	0.00661	1035	0.963	0.000
B20	-0.631	0.00752	1056	0.993	0.000

Because of the fact that some density data showed slightly non-linear trend, non linear regression was performed on the density data. Table 7.17 shows the regression equations and R^2 from the non-linear analysis. Figure 7.54 is the plot of regressed densities obtained from non-linear regression analysis. The R^2 values obtained from linear and non-linear analysis were not much different.

Table 7.17 Summary of regression data for soapnut biodiesel blends

Blends	Non-linear regression model	R^2
B100	$990.23-0.47\ T+0.007P+0.001\ T^2-0.000001\ P^2$	0.995
B80	$1267.30-2.57\ T+0.004P+0.006\ T^2+0.000000\ P^2$	0.993
B50	$992.78-0.72\ T+0.030\ P+0.001\ T^2-0.000007\ P^2$	0.991
B20	$662.95+2.31\ T+0.010\ P-0.007\ T^2+0.000002\ P^2$	0.996

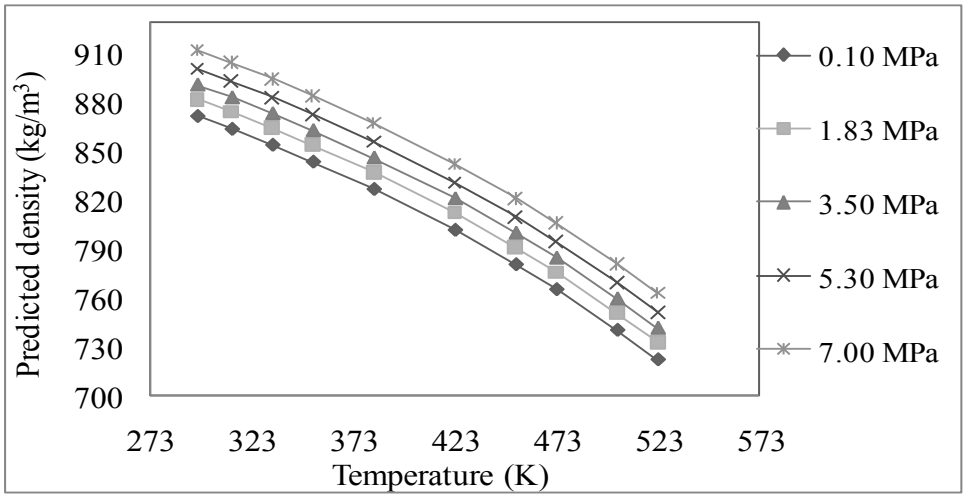

Figure 7.55 Regressed densities of soapnut biodiesel (B20) as a function of temperature at five pressures using equation 7.5

7.4 SURFACE TENSION MEASUREMENT OF DIESEL AND BIODIESEL FUELS

Surface tensions of canola biodiesel B100 have been measured from room temperature up to 473 K for five pressures. Similarly, surface tensions of jatropha and soapnut oil biodiesel blends B100, B80, B50, B20 and diesel (B0) were measured for five pressures and five temperatures. The details of surface tension measured for canola biodiesel B100, jatropha and soapnut biodiesel and their blends including diesel and model prediction results are presented below.

7.4.1 Diesel Fuel

The surface tension of pure diesel (B0) was measured and plotted as a function of temperature for five pressures and as a function of pressure for five temperatures (Figures 7.56-7.57). The results showed that surface tension decreased linearly both for temperature and pressure variations. At atmospheric pressure, the surface tension of diesel decreased from 25.84 mN/m at 293 K to 15.84 mN/m at 448 K. The surface tension decreased from 19.67 mN/m at 293 K to 13.73mN/m at 448 K at 7.00 MPa.

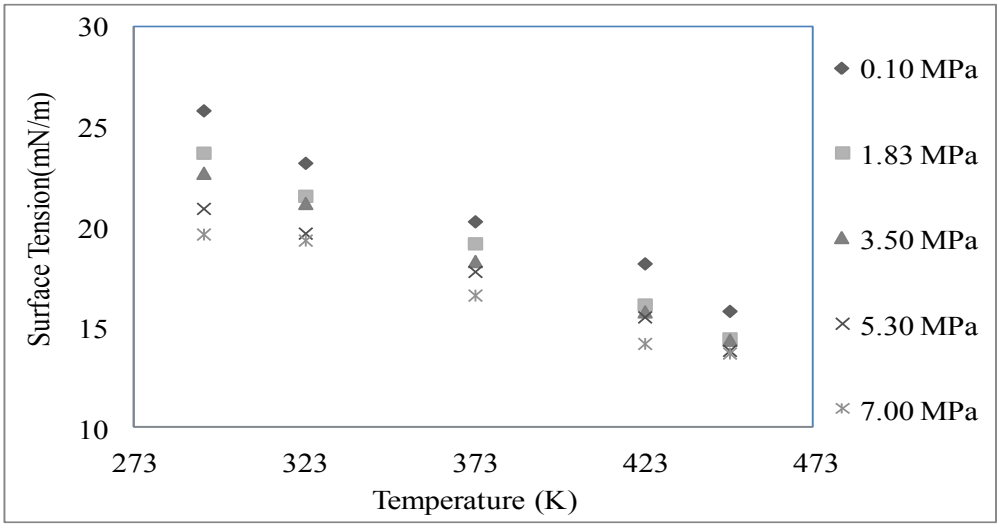

Figure 7.56 Surface tensions of diesel (B0) as a function of temperature for five pressures

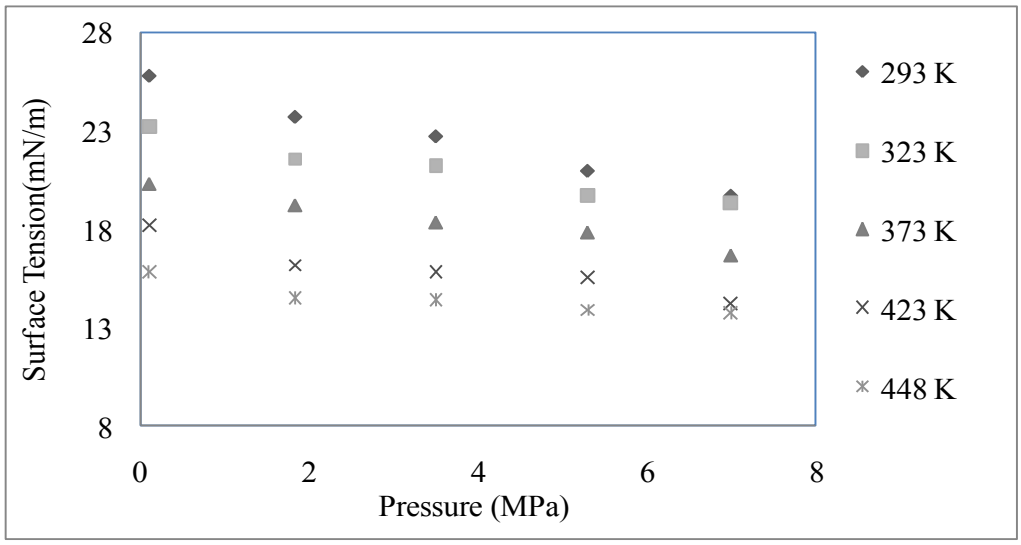

Figure 7.57 Surface tension of diesel (B0) as a function of pressure for five temperatures

A linear regression for surface tension on pressure and temperature was performed and the regression equation is presented below (equation 7.6). The R^2 value was found to be 0.965. The p-value of analysis of variance (ANOVA) was found to be zero (<0.05) indicating the significance of the relationship as shown in Table E.1 (Appendix E). The probability plot for the regressed values and the residuals are presented in Figures E.1 and E.2 respectively in Appendix E.

$$\text{Surface Tension } (\sigma) = 39.7 - 0.0519\ T - 0.000545\ P \qquad (7.6)$$

where T is the absolute temperature in K and P is the absolute pressure in kPa

The measured and regressed surface tension values and absolute and % errors for diesel fuel is presented in Table E.2 in Appendix E.

The maximum temperature at which the surface tension was measured for pure diesel was at 448 K. Above this temperature, the pendant drop could not be retained as some components of diesel would have started evaporating before reaching this temperature. The boiling temperature of diesel starts at 422 K (Kim et al., 2009) and diesel has a low flash

point which starts at 339 K (Li et al., 2010). Figure 7.58 is the plot of surface tension of diesel with time measured for 10 minutes at 448 K and 7.00 MPa. The surface tension shows a decreasing trend as this is close to the boiling point of diesel

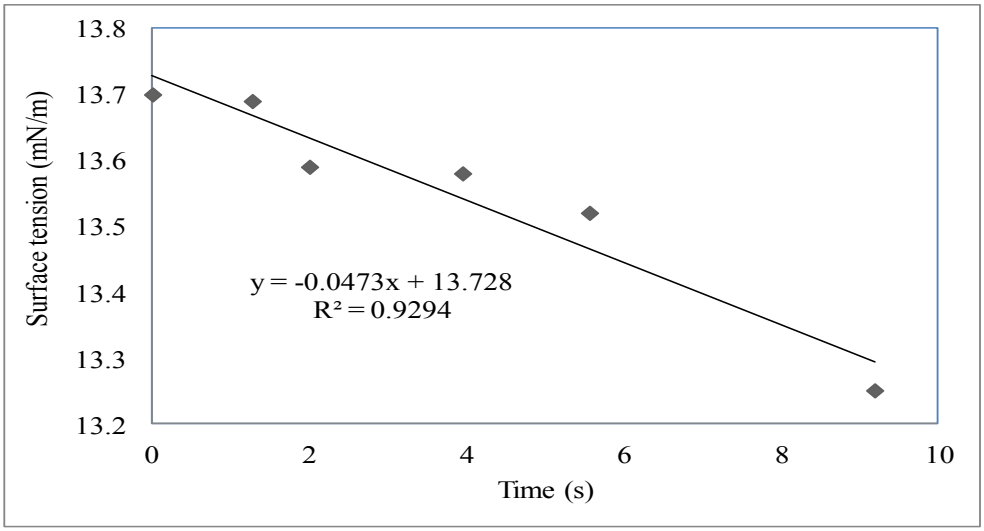

Figure 7.58 Surface tension of diesel measured at 448 K and 7.00 MPa with time

7.4.2 Canola Biodiesel

Figure 7.59 shows surface tension measured at five temperatures and five pressures for canola biodiesel B100. Each point is the average value of three measured surface tension values. Each value was the average of the five readings of the surface tension from a pendent drop created during the tests. It was observed that the surface tension of canola B100 decreases linearly at an average rate of 0.063 mN/m/ K.

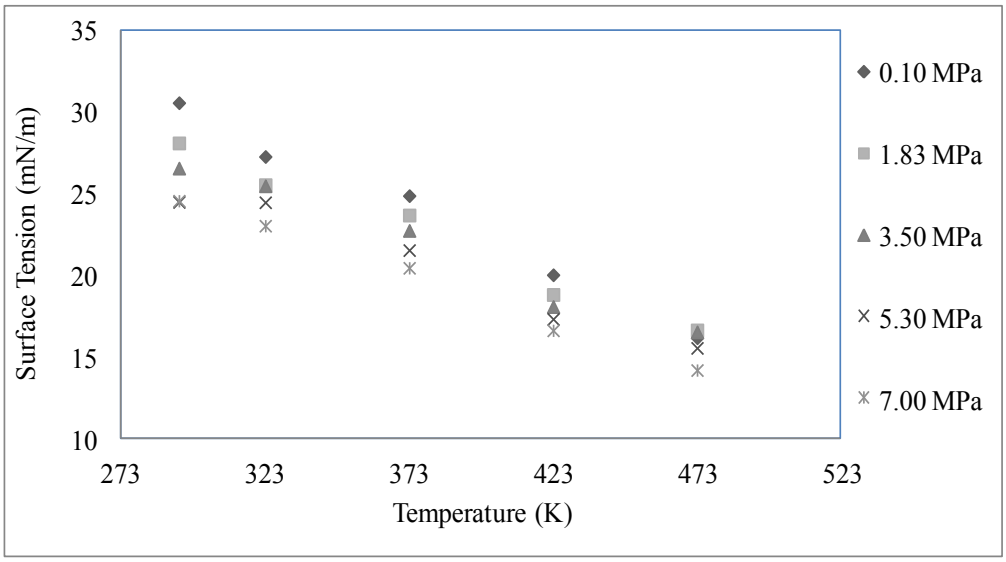

Figure 7.59 Surface tension of canola B100 as a function of temperature for five pressures

A regression on the experimental data was carried out with temperature and pressure. The following regression equation was obtained (equation 7.7). The R^2 value was found to be 0.980 with a P-value of 0.00 (<0.05) in ANOVA table using MINITAB. Table E3 in Appendix E shows the regression model to predict the surface tension of canola biodiesel B100 as a function of temperature and pressure. The probability plot regressed and residual values of surface tension resulted in p>0.05 and are shown in Figures E.3 and E.4 in Appendix E. The regression of measured surface tension data is presented in the following equation.

Surface tension (σ) = 47.7 - 0.0638 T - 0.000549 P (7.7)

where T is the absolute temperature in K and P is the absolute pressure in kPa.

The temperature and pressure dependent surface tension model can be generalized as the equation 7.8 below.

Surface tension (σ) = C-A*T-B*P (7.8)

Figure 7.60 is the plot of regressed surface tension values obtained using equation 7.8 for canola biodiesel B100. The surface tension is highest at lowest temperature and pressure and decreases linearly as temperature and pressure increases.

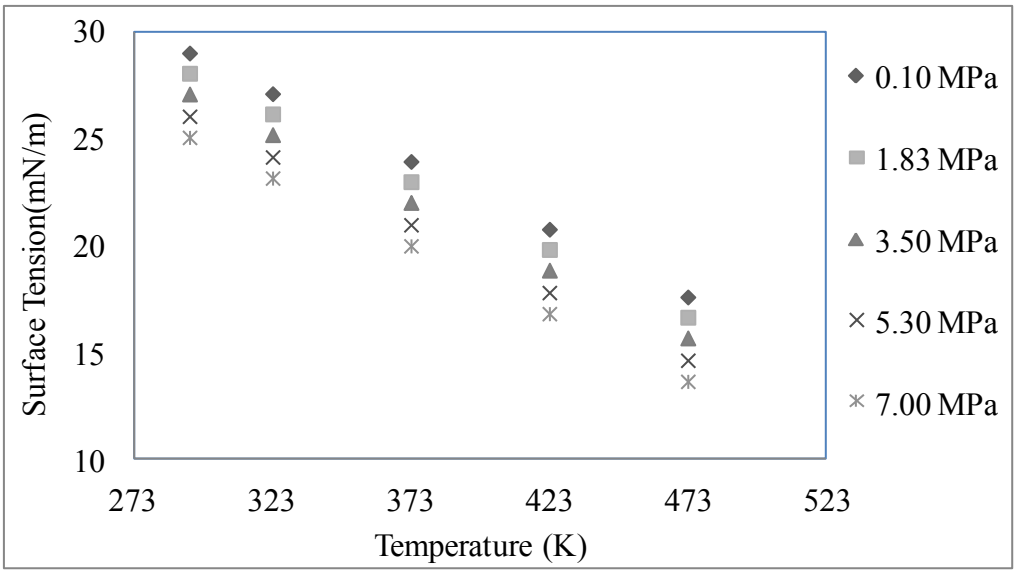

Figure 7.60 Values of regressed surface tension for canola B100 for five temperatures and five pressures using the regression equation 7.8

The measured and regressed surface tension values of canola biodiesel B100 for five pressures and five temperatures are presented in Table E.4 in Appendix E. The absolute and % errors are also presented in the same Table.

7.4.3 Jatropha Biodiesel and Its Blends

The surface tension of jatropha biodiesel blends B100, B80, B50 and B20 were measured and plotted for five pressures and five temperatures.

As shown in Figure 7.61, the surface tension of jatropha biodiesel B100 was found to decrease from 30.10 mN/m at 293 K to 17.82 mN/m at 473 K for atmospheric pressure. Similar trends were observed for pressures 1.83 MPa, 3.50 MPa and 5.30 MPa. However

for 7.00 MPa, the surface tension slightly increased from 20.65 mN/m at 293 K to 21.04 mN/m at 323 K and then decreased to 15.23 mN/m at 473 K. The model equation obtained from regression (equation 7.8) of jatropha biodiesel surface tension data indicated that both the temperature and pressure coefficients are negative and should follow a decreasing trend. There were two observations with large standardized residuals (Table E.5 in Appendix E). One of the probable reasons for such result could be due to the difficulty in temperature stabilization during observation as it was manual temperature control. No literatures were found in support of this trend.

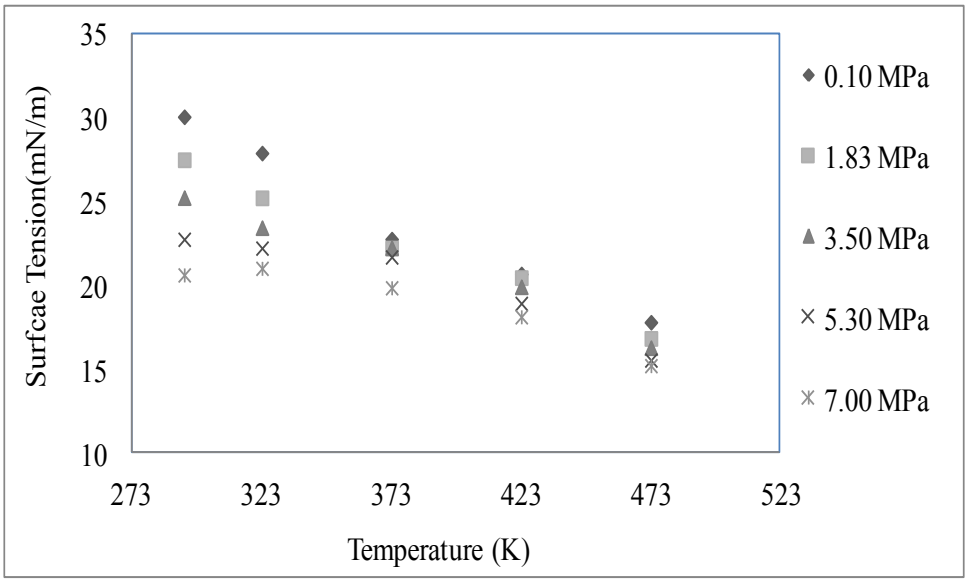

Figure 7.61 Surface tension of jatropha B100 as a function of temperature for five pressures

Figure 7.62 shows surface tension of jatropha biodiesel B100 as a function of pressure for five temperatures. This also shows a linear relationship. At 293 K, the surface tension of canola B100 decreased from 30.10 mN/m at 0.10 MPa to 20.65 mN/m at 7.00 MPa. For 373 K, the surface tension decreased from 22.79 mN/m at 0.10 MPa to 19.88 mN/m at 7.00 mPa. Similarly, for 473 K, the surface tension decreased from 17.82 mN/m at 0.10 MPa to 15.23 mN/m at 7.00 MPa.

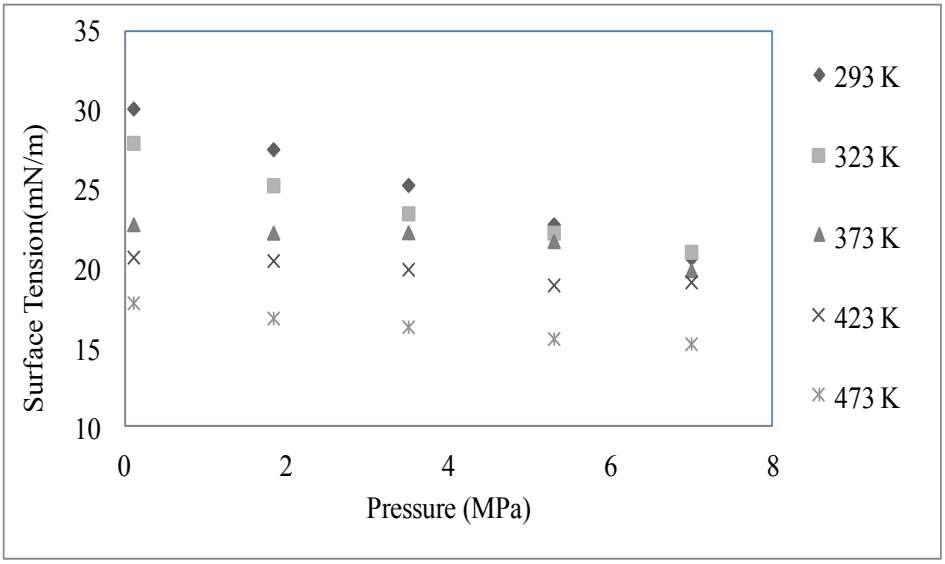

Figure 7.62 Surface tension of jatropha B100 as a function of pressures for five temperatures

Figure 7.63 represents the surface tension values for jatropha biodiesel and its blend including diesel. It was found that the surface tension values decreased linearly as the temperature increases. At atmospheric pressure, the surface tension of jatropha B100 decreased from 30.10 mN/m at 293 K to 17.82 mN/m at 473 K. For jatropha B80, the surface tension decreased from 28.95 mN/m at 293K to 17.41 mN/m at 473 K. Similarly the surface tension for jatropha B50 and B20 decreased from 26.45 mN/m and 28.57 mN/m at 293 K to 16.23 mN/m and 16.31 mN/m at 473 K respectively. The diesel surface tension decreased from 25.84 mN/m at 293 K to 15.84 mN/m at 473 K.

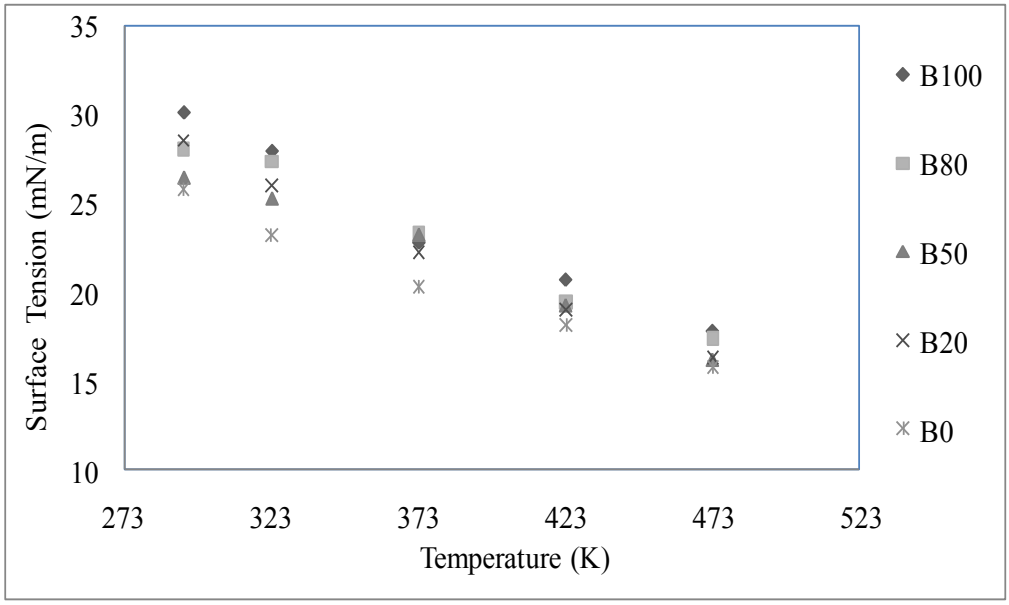

Figure 7.63 Surface tension of jatropha biodiesel B100 and its blends and diesel at atmospheric pressure

Table 7.18 shows the regression coefficients for jatropha B100 and its blends for temperatures between 293 K to 473 K at atmospheric pressure and was compared with pure diesel. The average surface tension decreased by 0.06 mN/m/K for all blends.

Table 7.18 Regression coefficients of jatropha biodiesel and its blends with respect to diesel at atmospheric pressure

Fuel Type	Slope (mN/m/K)	Intercept (mN/m)	R^2
B100	-0.06	49.70	0.976
B80	-0.06	48.67	0.983
B50	-0.06	48.16	0.993
B20	-0.05	43.92	0.983
B0	-0.05	40.99	0.985

Jatropha B100 and its blends were also plotted as a function of temperature at 3.50 MPa (Figure 7.64). The surface tension decreased from 25.27 mN/m at 293 K to 16.30 mN/m at 473 K for jatropha B100. For jatropha B80, B50 and B20, the surface tension values decreased from 25.67 mN/m, 22.45 mN/m and 23.63 mN/m at 293 K to 16.25 mN/m, 15.06 mN/m and 14.84 mN/m respectively at 473 K.

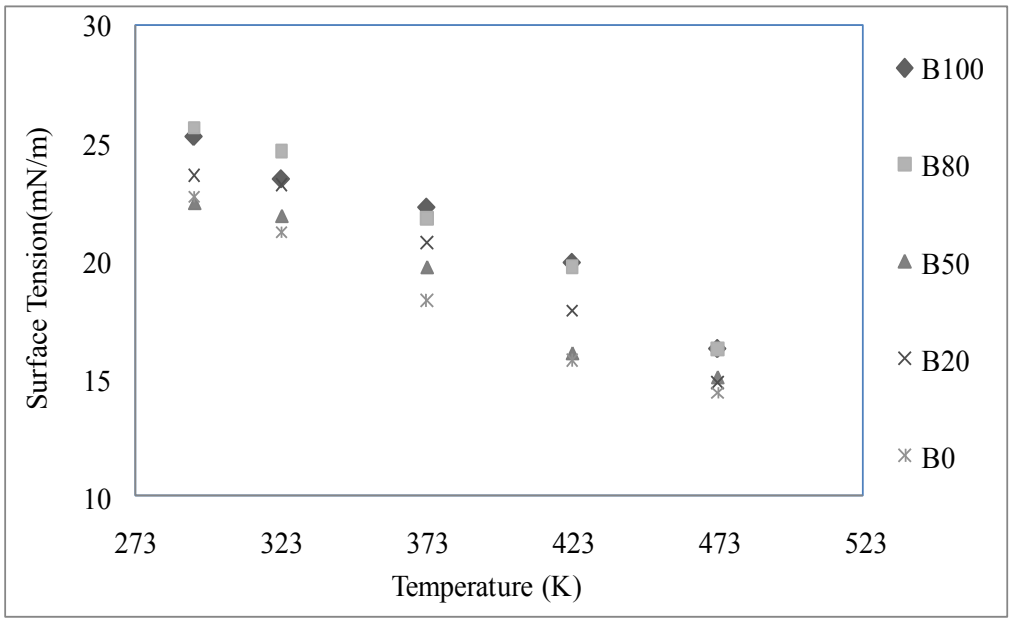

Figure 7.64 Surface tension of jatropha biodiesel and its blends and diesel at 3.50 MPa

It was observed that the surface tension decreased linearly with temperature by 0.04 mN/m/K for all blends at 3.50 MPa. The regression coefficients for all blends expressed as a function of temperature is presented in Table 7.19.

Table 7.19 Regression coefficients of jatropha biodiesel and its blends with diesel at 3.4 MPa

Fuel Type	Slope (mN/m/K)	Intercept (mN/m)	R^2
B100	-0.04	39.09	0.968
B80	-0.05	41.21	0.989
B50	-0.04	36.07	0.967
B20	-0.05	39.12	0.979
B0	-0.04	36.52	0.986

The surface tension of jatropha biodiesel and its blends including diesel were plotted as a function of temperature at 7.00 MPa (Figure 7.65). The surface tension for all blends B100, B80, B50, B20 and B0 is found to decrease linearly from 293 K to 473 K at this pressure at an average rate of 0.03 mN/m /K. The R^2 values are summarized in Table 7.20. The R^2 values show a high correlation for the observed data sets.

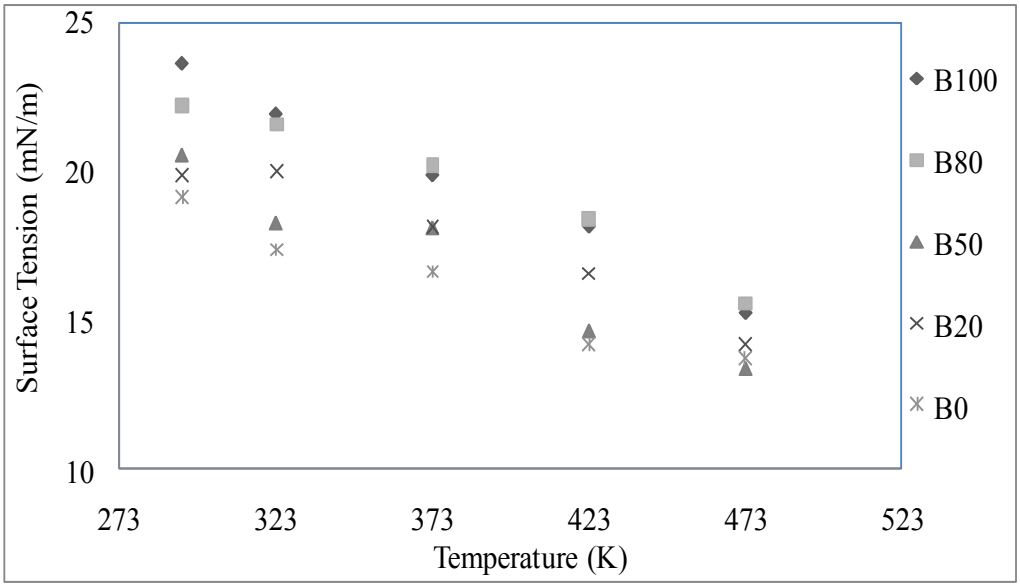

Figure 7.65 Surface tension of jatropha biodiesel and its blends and diesel at 7.00 MPa

Table 7.20 Regression coefficients of jatropha biodiesel and its blends with respect to diesel at 7.00 MPa

Fuel Type	Slope (mN/m/K)	Intercept (mN/m)	R^2
B100	-0.04	36.65	0.992
B80	-0.03	33.20	0.967
B50	-0.03	31.52	0.941
B20	-0.03	30.04	0.959
B0	-0.03	27.49	0.951

Surface tension of jatropha biodiesel blends were measured with time at different pressures and temperatures. Figure 7.66 shows the surface tension variation of jatropha biodiesel B100 at 373 K and 423 K at 7.00 MPa. It shows that surface tension remains almost constant with time. This observation was made for the same pendant drop for about 10 minutes.

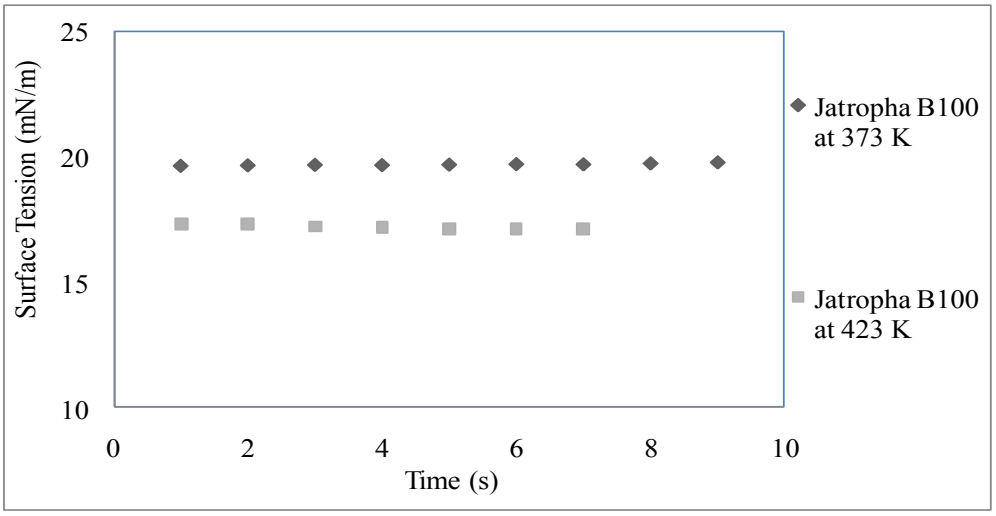

Figure 7.66 Surface tension of jatropha biodiesel B100 at 7.00 MPa with time for two temperatures

A linear regression was performed in order to determine the relationship between surface tension, temperature and pressure for jatropha biodiesel and its blends. Table 7.21 is the summary of the regression data including the R^2 value. The R^2 value indicated that there is a linear relation between surface tension and temperature and pressure for all blends including diesel. The experimental data followed the regression equation 7.8 with the regressions constants presented in Table 7.21.

Table 7.21 Regression coefficients of jatropha biodiesel and its blends with diesel for five temperature and five pressures

Fuel Type	C	A	B	R^2
B100	41.90	-0.048	-0.000671	0.904
B80	43.20	-0.053	-0.000420	0.959
B50	37.40	-0.041	-0.000820	0.911
B20	41.1	-0.049	-0.000685	0.916
B0	37.8	-0.046	-0.000545	0.971

The regression data for surface tension of jatropha biodiesel B100 for five temperatures and five pressures is presented in Table E.5 in Appendix E. The summary of measured and regressed surface tension values and absolute and % errors for jatropha biodiesel B100 is presented in Table E.6. The probability plot of regressed values and residuals for

jatropha biodiesel B100 are presented in Figures E.5 and E.6. Table E.7 represents the regression data for surface tension of jatropha biodiesel B80 for five temperatures and five pressures. Figure E.7 shows the probability plot of regressed values of surface tension of jatropha biodiesel B80 for five temperatures and five pressures. Similarly, Figure E.8 shows the probability plot of residual values of surface tension of jatropha biodiesel B80. Table E.8 is the summary of measured and regressed surface tensions and absolute and % errors of jatropha biodiesel B80 for five temperatures and five pressures.

Table E.9 in Appendix E represents the regression data for surface tension of jatropha biodiesel B50 for five temperatures and five pressures. Figures E.9 and E.10 are the probability plot of regressed and residual values of surface tension of jatropha oil biodiesel B50. Table E.10 shows the measured and regressed surface tensions and absolute and % errors of jatropha biodiesel B50 for five temperatures and five pressures.

Table E.11 in Appendix E shows the regression data for the surface tension of jatropha biodiesel B20 for five temperatures and five pressures. Figures E.11 and E.12 are the probability plot of regressed and residual values of surface tension of jatropha oil biodiesel B20. Table E.12 is the summary of measured and regressed surface tensions and absolute and % errors of jatropha biodiesel B20 for five temperatures and five pressures.

From the regression data it is found that the constants for temperature are larger than for pressure. Hence, it can be concluded that temperature has a greater effect than pressure on the surface tension of all jatropha blends and of diesel.

7.4.4 Soapnut Biodiesel and Its Blends

Surface tension of soapnut biodiesel and its blends showed a very similar trend as seen in the case of biodiesel from canola and jatropha biodiesel blends. The measured values of surface tension were the average values from at least three readings. For each pressure, the surface tension was found to decrease linearly with temperature. Figure 7.67 shows the

surface tension of soapnut biodiesel for five pressures and five temperatures. For soapnut biodiesel B100, the surface tension decreased from 29.50 mN/m at 293 K to 16.95 mN/m at 473 K at atmospheric pressure. A similar trend was observed for 1.83 MPa, 3.50 MPa and 5.30 MPa. At 7.00 MPa, the surface tension of soapnut B100 decreased from 22.78 mN/m at 293 K to 14.84 mN/m at 473 K. However, there was a slight increase of surface tension value at temperatures 373 and 423 K. However, the surface tension value of canola B100 at 323 K at 7.00 MPa appears to be an outlier as shown in the Figure 7.67. The R^2 values from regression for soapnut biodiesel B100 at 7.00 MPa was found to be 0.851. However, the R^2 value using the regression equation 7.8 for all pressures and temperatures was found to be 0.929. Hence, the regression model still holds good correlation with the measured values.

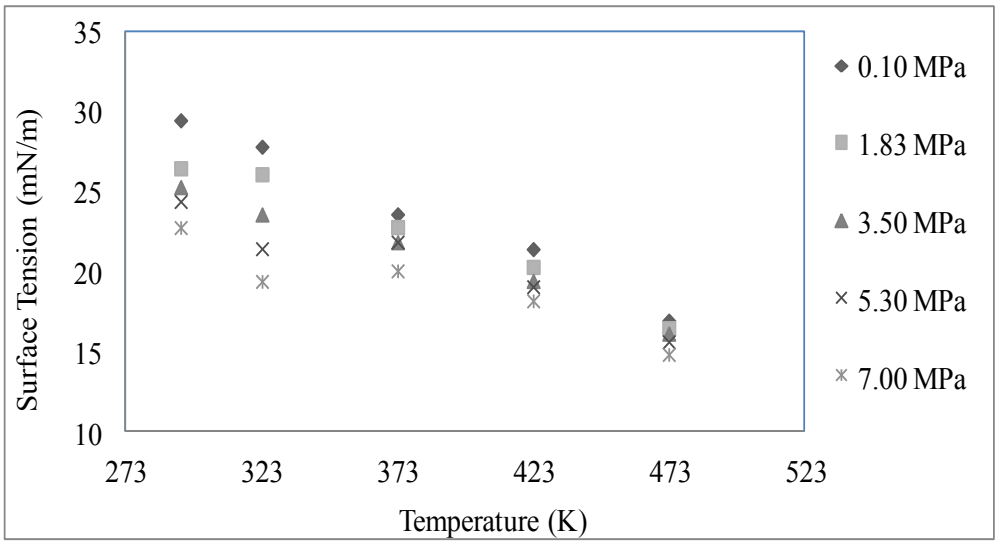

Figure 7.67 Surface tension of soapnut biodiesel (B100) as a function of temperature for five pressures

Figure 7.68 represents the surface tension of soapnut biodiesel B100 as a function of pressure. The surface tension decreased linearly with pressure for each temperature. At 293 K, the surface tension decreased from 28.18 mN/m at 0.10 MPa to 21.27 mN/m at 7.00 MPa. For 473 K, the surface tension decreased from 14.31 mN/m at 0.10 MPa to 13.64 mN/m at 7.00 MPa. However, the slope of the line was found to be higher due to

temperature than the pressure which indicates that temperature has higher impact on surface tension compared to pressure.

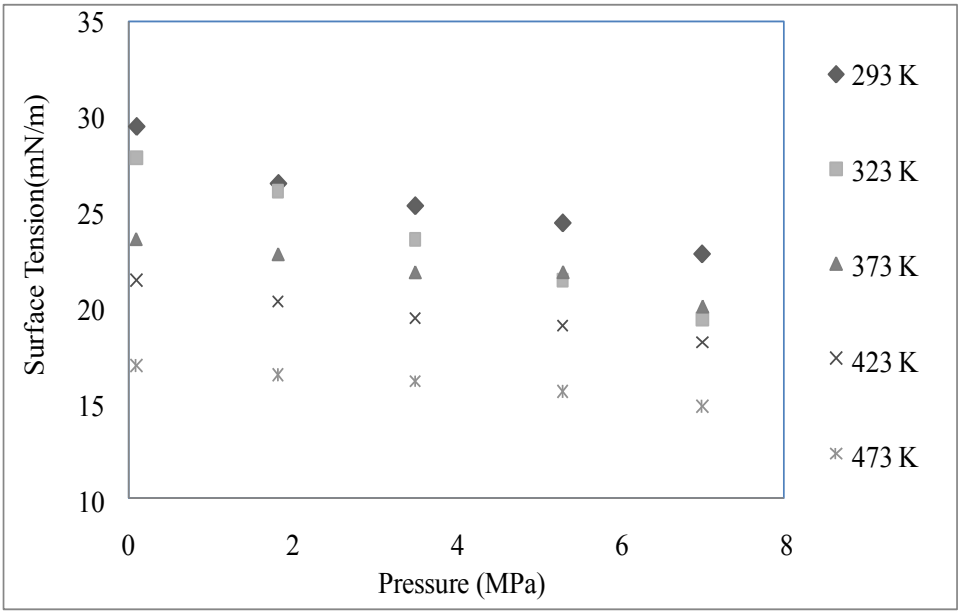

Figure 7.68 Surface tension of soapnut biodiesel B100 as a function of pressure for five temperatures

Figure 7.69 represents the surface tension of soapnut biodiesel and its blends and diesel. The surface tension for soapnut biodiesel B100 decreased from 29.50 mN/m at 293 K to 16.95 mN/m at 473 K at atmospheric pressure. For diesel, the surface tension decreased from 25.84 mN/m at 293 K to 15.84 mN/m at 448 K at atmospheric pressure. Surface tension for all blends linearly decreased with temperature by an average rate of 0.06 mN/m/K. Table 7.22 represents the values of regression coefficients for biodiesel blends and diesel in atmospheric pressure. All R^2 values are higher than 0.95 indicating a high correlation of the experimental data sets recorded.

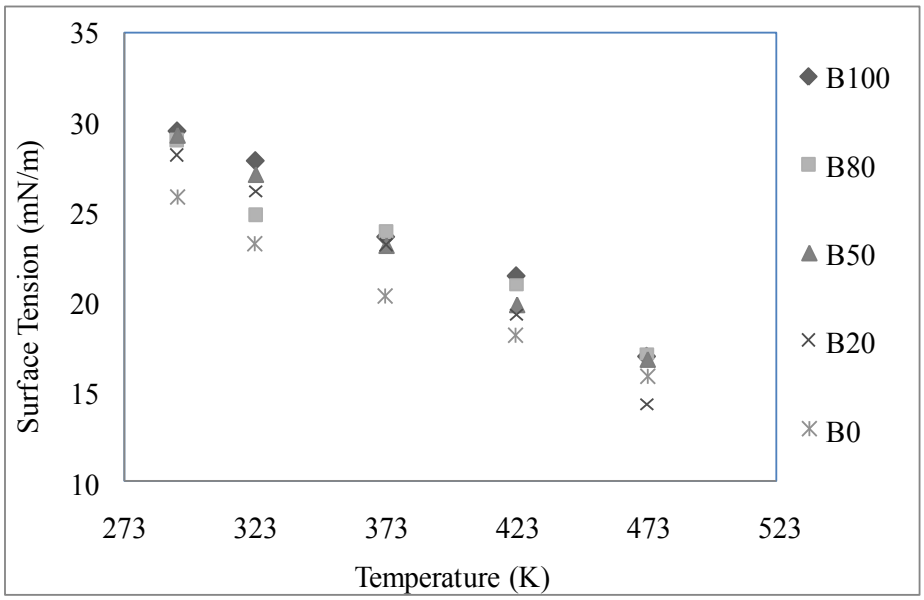

Figure 7.69 Surface tension of soapnut biodiesel and its blends with diesel at atmospheric pressure

Table 7.22 Regression coefficients of soapnut biodiesel and its blends and diesel at atmospheric pressure

Fuel Type	Slope (mN/m/K)	Intercept (mN/m)	R^2
B100	-0.06	49.74	0.990
B80	-0.06	45.67	0.953
B50	-0.06	49.50	0.997
B20	-0.07	50.73	0.988
B0	-0.05	40.99	0.984

Surface tension of soapnut biodiesel and its blends with diesel were plotted for 3.50 MPa at various temperatures (Figure 7.70). The surface tension of soapnut biodiesel B100 decreased from 25.32 mN/m at 293 K to 16.14 mN/m at 473 K. For soapnut biodiesel B80, the surface tension decreased from 24.43 mN/m at 293 K to 16.87 mN/m at 473 K. For B50, the surface tension decreased from 25.89 mN/m at 293 K to 16.45 mN/m at 473 K and for B20, the surface tension decreased from 24.14 mN/m at 293 K to 14.38 mN/m at 473 K. For diesel, the surface tension decreased from 22.73 mN/m at 293 K to 14.40 mN/m at 448 K.

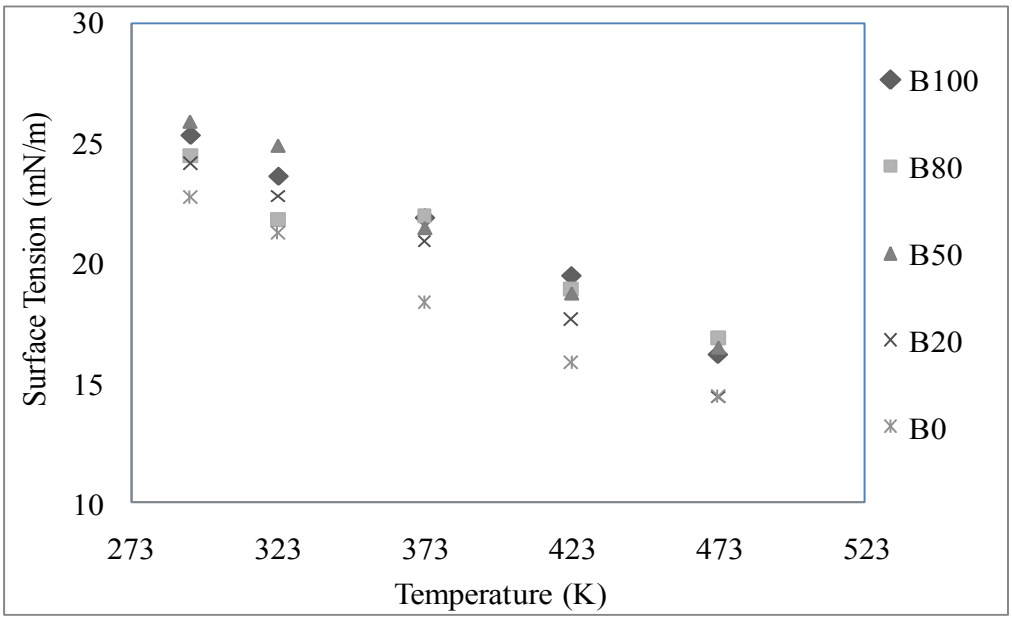

Figure 7.70 Surface tension of soapnut biodiesel and its blends and diesel at 3.50 MPa

Table 7.23 shows the regression coefficient of soapnut biodiesel and its blends and diesel at 3.4 MPa. The surface tension decreased at an average rate of 0.044 mN/m/K for soapnut biodiesel blends and diesel. The R^2values indicates a high correlation of the set of experimental data.

Table 7.23 Regression coefficients of soapnut biodiesel and its blends with diesel at 3.4 MPa

Fuel Type	Slope (mN/m/K)	Intercept (mN/m)	R^2
B100	-0.04	39.76	0.988
B80	-0.04	35.40	0.927
B50	-0.05	42.06	0.993
B20	-0.05	40.29	0.986
B0	-0.04	36.52	0.986

The surface tension results were expressed as a function of temperature for all blends of soapnut biodiesel and diesel at 7.00 MPa (Figure 7.71). It was found that the surface tension decreased linearly as the temperature was raised from 293 K to 473 K. The surface tension decreased from 22.78 mN/m at 293 K to 14.84 mN/m at 473 K for B100, from 22.33 mN/m to 15.45 mN/m for B80, from 24.70 mN/m at 293 K to 14.89 mN/m at 473 K for B50 and from 19.67 mN/m at 293 K to 13.64 mN/m at 473 K for B20.

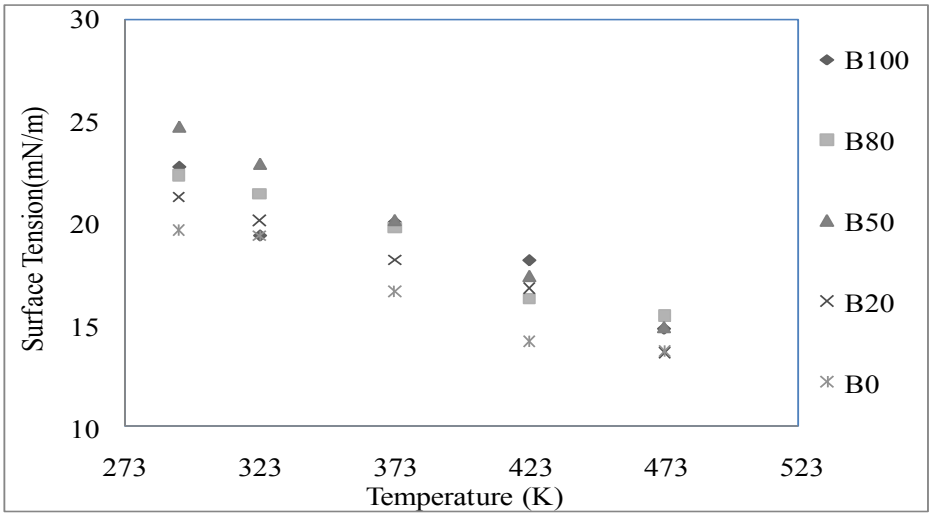

Figure 7.71 Surface tension of soapnut biodiesel and its blends and diesel at 7.00 MPa

Table 7.24 shows the regression coefficients of the soapnut biodiesel and its blends with respect to diesel. It was found that the surface tension decreased linearly at an average value of 0.04 mN/m/K. The R^2 value indicates a high correlation for the experimental data observed.

Table 7.24 Regression coefficients of soapnut biodiesel and its blends with respect to diesel at 7.00 MPa

Fuel Type	Slope mN/m/K	Intercept (mN/m)	R^2
B100	-0.04	32.87	0.851
B80	-0.04	34.61	0.966
B50	-0.05	40.54	0.999
B20	-0.04	33.29	0.980
B0	-0.03	30.74	0.952

A linear regression was performed to determine the relationship between surface tension and temperature and pressure for all blends for biodiesel and diesel. This regression model follows the same equation as presented in 7.5. Table 7.25 is the summary of regression data including R^2 and the constants A, B and C. The constants for temperatures are higher

than for pressures implying that the temperature has a higher effect on surface tension than pressure for all blends of soapnut biodiesel and diesel.

Table 7.25 Regression coefficients of soapnut biodiesel and its blends including diesel at elevated temperatures and pressures

Fuel Type	C	A	B	R^2
B100	43.00	-0.0508	-0.000670	0.929
B80	39.1	-0.0426	-0.000650	0.886
B50	43.8	-0.0609	-0.000476	0.989
B20	43.3	-0.0570	-0.000627	0.949
B0	37.8	-0.046	-0.000545	0.971

The surface tension values were measured retaining the pendant drop for longer duration to observe if the time has any significant effect in it. Figure 7.72 represents the surface tension of soapnut biodiesel blends B50 and B80 with time at 7.00 MPa. The surface tension was found to be unchanged with time for soapnut biodiesel B50 and B80.

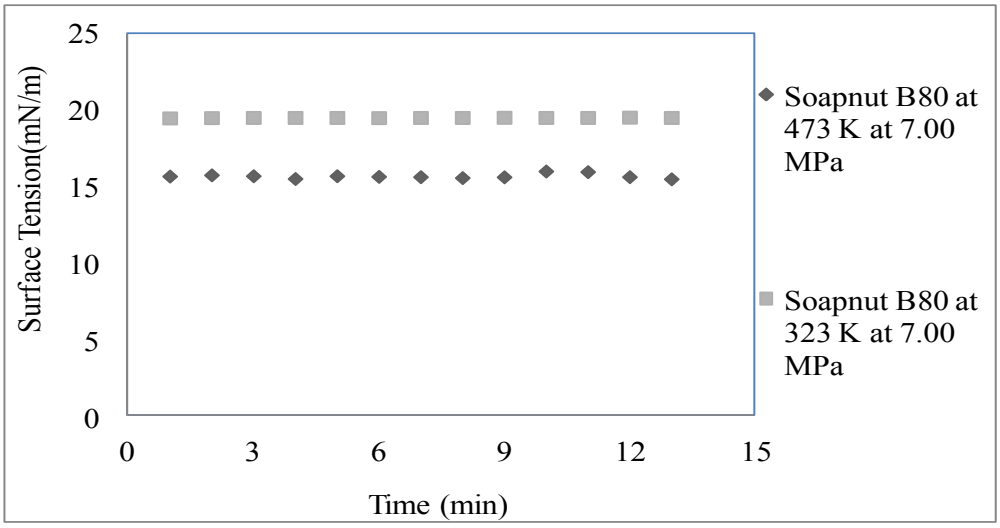

Figure 7.72 Surface tension of soapnut biodiesel B80 for two temperatures with time at 7.00 MPa

Tables E.13, E.14, E.15 and E.16 in Appendix E show the regression data of surface tension for soapnut biodiesel B100, B80, B50 and B20 for five temperatures and five

pressures respectively. Figures E.13, E.14, E.15 and E.16 in Appendix E show the probability plot of regressed surface tension values using equation 7.5 for soapnut biodiesel B100, B80, B50 and B20 respectively. Similarly, Figures E.17, E.18, E.19 and E.20 show the probability plot of residuals for surface tension for soapnut biodiesel B100, B80, B50 and B20 respectively. The p-value of probability plot for all blends are higher than 0.05 indicating a good correlation of the measured data and the regression equation. Tables E.17, E.18, E.19 and E.20 show the summary of measured and regressed surface tensions and absolute and % errors for soapnut biodiesel B100, B80, B50 and B20 for five temperatures and five pressures respectively.

7.4.5 Error Analysis of Surface Tension

Based on the average surface tension of measured values and the regressed values, the absolute errors as well as % error were estimated for diesel, canola, jatropha, and soapnut biodiesel. Table E.2 in Appendix E shows the absolute and % error for diesel for five temperatures and five pressures.

The errors for all temperatures and pressures for canola B100 are presented in Table E.4 in the Appendix E. The largest error of 1.56 mN/m was found for the first reading at 293 K at atmospheric pressure. This point also appears to be an outlier in a scatter plot.

Similarly, the absolute and % errors for jatropha biodiesel for five temperatures and pressures are presented in Tables E.6, E.8, E.10 and E.12 in Appendix E. Similarly the errors for soapnut biodiesel for five temperarures and pressures are presented in Tables E.17-E.20 in Appendix E. Some of the errors might have occurred due to the difficulty in controlling the temperature during the measurements. Some errors might have occurred due to the calibration of the instruments. As mentioned in Section 6.5.2, the calibration was done to ±1.3%. Some of the errors might have occurred due to some impurities in the samples despite careful handling. The random errors were minimized by taking the average

of five readings for each pendant drop. The data recorded was taken as the average of three pendant drops. As density was one of the inputs for surface tension measurement, any error which occurred during the density measurements might also have had an impact in overall surface tension results.

7.5 VISCOSITY MEASUREMENT

7.5.1 Viscosity Measurement from Rolling Ball Viscometer

The rolling ball viscometer was calibrated using water as a fluid medium in order to determine the instrument constant. The calibration procedure using distilled water for the rolling ball viscometer is discussed in Chapter 6. The constants were determined for different tilt angles. Table 7.26 shows the tilt angles, average rolling time for the quartz ball, velocity at which the ball travelled during the test at different tilt angles and the instrument constant for the rolling ball viscometer used in this work.

Table 7.26 Calibration constants for rolling ball viscometer

Tilt angle (θ)	Average rolling time (t)	Velocity (m/s)	Calibration constant (K) (Nm^2/ kg)
60	4.025	0.0472	3.6944E-08
45	4.710	0.0403	3.0009E-08
40	5.096	0.0372	2.6999E-08
30	6.091	0.0311	2.1887E-08
20	8.200	0.0231	1.6257E-08
10	13.394	0.0141	9.9231E-09

Using the instrument constants determined from the calibration, the viscosity of canola oil biodiesel B100 was measured from 295 K to 523 K at atmospheric pressure. The viscosity for canola biodiesel was measured for tilt angles 60, 45 and 40 degrees. Figure 7.73 shows the results of dynamic viscosities for canola biodiesel B100 at atmospheric pressure and temperatures from room temperature to 523 K for the tilt angle of 60 degrees and from room temperature to 473 K for tilt angles of 45 and 40 degrees. The results showed that the viscosity values were very close (4.2 %) for all the three tilt angles. The kinematic

viscosities were calculated using the measured density values. Figure 7.74 shows the kinematic viscosities for canola biodiesel B100. Table 7.26 shows the dynamic and kinematic viscosities of canola biodiesel B100 for temperatures between 295 K and 523 K.

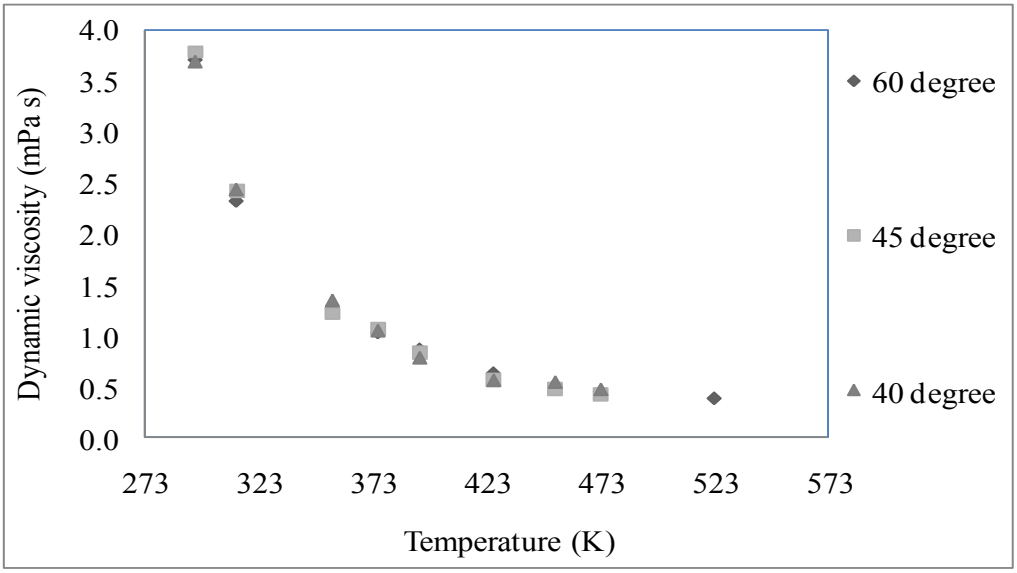

Figure 7.73 Dynamic viscosity of canola B100 at three tilt angles using rolling ball viscometer

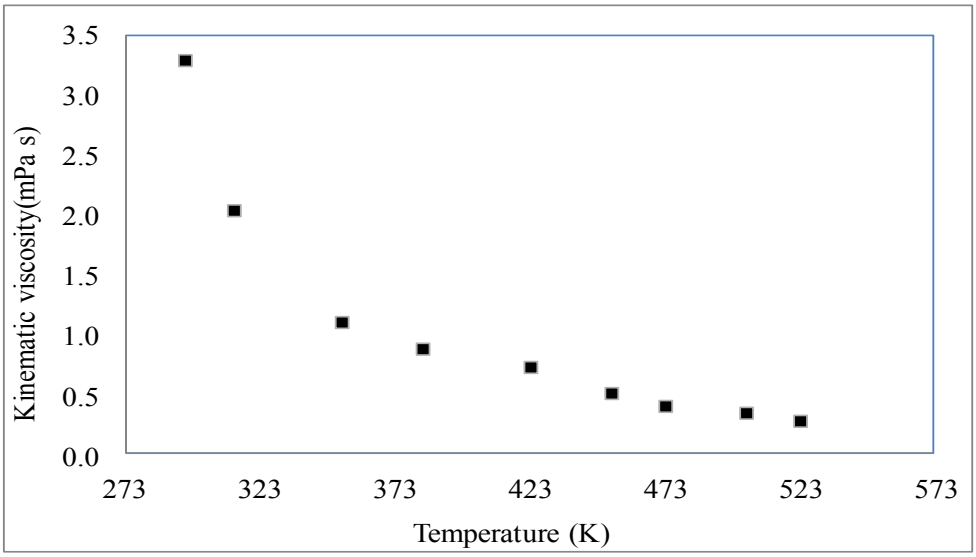

Figure 7.74 Kinematic viscosity of canola biodiesel B100 at tilt angle 60 degree using rolling ball viscometer

Table 7.27 Dynamic and kinematic viscosity of canola biodiesel B100 measured using rolling ball viscometer

Temperature (K)	Dynamic viscosity (mPa-s)	Kinematic viscosity (mm^2/s)
295	3.72	4.20
313	2.33	2.66
355	1.28	1.48
375	1.04	1.22
394	0.87	1.03
426	0.63	0.79
453	0.52	0.66
473	0.45	0.59
523	0.39	0.54

However, there were number of technical difficulties while measuring the viscosity from this particular rolling ball viscometer. The oil repeatedly leaked into the light sensors at high temperatures and pressures. The light source also burnt few times due to excessive heating of the equipment. Because of these reasons, it was not possible to acquire more data and the experiment with this instrument was not continued. A new viscometer called ViscoScope viscometer which works in the principle of torsional oscillation was purchased and used to measure the viscosities of diesel and biodiesel samples at different temperatures and pressures. It was found that the viscosity values obtained from rolling ball viscometer were significantly lower than the viscosities obtained from the ViscoScope equipment. For example, the viscosity of canola B100 at 313 K obtained from rolling ball viscometer was 2.66 mm^2/s while the viscosity obtained from ViscoScope viscometer was 4.90 mm^2/s, which is a difference of approximately 46%. Kinematic viscosity data for other temperatures were also found to be in the same range.

7.5.2 Viscosity Measurement from ViscoScope Viscometer

The ViscoScope viscometer was used to measure the viscosity of diesel and biodiesel fuels. The output of the viscometer was the dynamic viscosity times the density (mPa-s × kg/m^3) of the test fuel. Dynamic viscosity of the test fuel was obtained by dividing the measured value by the density of the fluid at same temperature and pressure. The

kinematic viscosity was obtained by dividing the measured value by density twice. The tests were carried out from room temperature and the temperature was raised in the steps of 10 K up to 523 K. The pressures ranged from atmospheric to 7.00 MPa absolute.

7.5.2.1 Kinematic Viscosity of Water

As a check on the functioning of the instrument, the kinematic viscosity of distilled water was measured from room temperature to 363 K at atmospheric pressure. Figure 7.75 shows the kinematic viscosities of distilled water from three tests. The values were compared with the standard viscosities of water from literature. The results showed that the kinematic viscosity values differed by a maximum of 7.34 % from the standard values. Similar results were obtained when the tests were carried out from 363 K down to room temperature.

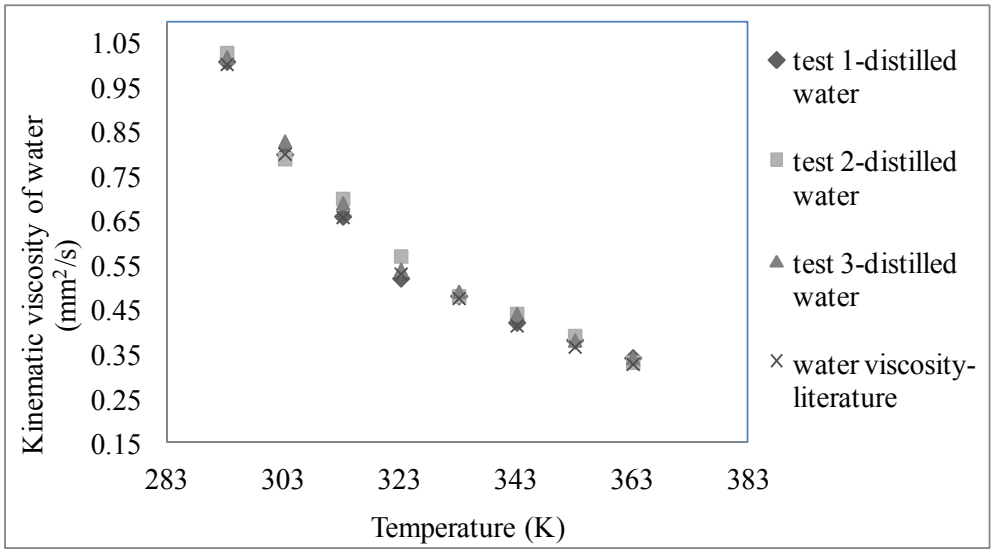

Figure 7.75 Measured kinematic viscosities of distilled water at atmospheric pressure

7.5.2.2 Viscosity of Diesel Fuel

Figure 7.76 shows the kinematic viscosities of diesel (B0) fuel for five pressures at different temperatures. Between the ranges from room temperature to 523 K, the viscosity

of diesel was found to increase as the temperature decreased. The viscosities of diesel were also found to increase as the pressure increased from atmospheric to 7.00 MPa. At atmospheric pressure the viscosity of diesel decreased from 3.05 mm^2/s at room temperature to 0.43 mm^2/s at 523 K. At 1.83 MPa, the viscosity of diesel decreased from 3.13 mm^2/s at room temperature to 0.36 mm^2/s at 523 K. A similar trend was obtained for the kinematic viscosities of diesel at other pressures and temperatures.

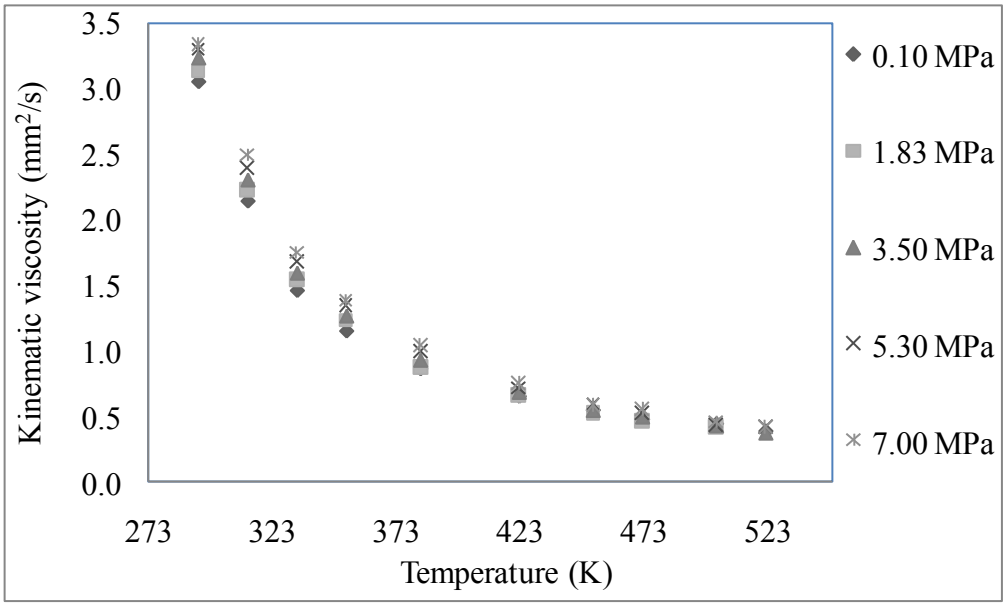

Figure 7.76 Measured kinematic viscosities of diesel (B0) for five pressures at different temperatures

Tat and Van Gerpen (1999) developed an equation by modifying the Andrade equation (equation 7.9) to predict the viscosity of diesel and biodiesel fuels. The same relationship was also employed by Tate et al. (2005) and Joshi and Pegg (2007) in order to predict the viscosities of pure biodiesel and its blends.

$$\ln(\eta) = A + \frac{B}{T} + \frac{C}{T^2} \qquad (7.9)$$

where μ is kinematic viscosity, T is absolute temperature, A, B and C are the constants specific to the fluids.

The measured kinematic viscosity data of diesel were regressed using equation 7.9. Equation 7.9 is considered to be a second order polynomial equation and the values of constants A, B and C were found using MINITAB. The regression results showed that the measured data follow the model equation 7.9. Table 7.28 shows the summary of regression coefficients A, B, C and R^2 values for five pressures and different temperatures for diesel fuel. The R^2 value for atmospheric pressure was found to be 0.998 and rests of the other pressures were found to be 0.999 indicating a good fit with the experimental data. This correlation is valid for up to 523 K based on the experimental data. Table E.1 and E.2 in the Appendix E shows the summary of measured kinematic and dynamic viscosities of the diesel fuel for five pressures. The table also shows the absolute and % errors for diesel fuel from regression. The maximum error of 4.05% occured at 333 K at atmospheric pressure. Table E.3 shows the regression data with R^2 value of 0.998 and p value of ANOVA was 0.000(<0.05). Figure E.1 shows the probability plot of regressed kinematic viscosities of diesel fuel with p value of 43.8 % (>0.05).

Table 7.28 Regression constants of kinematic viscosities of diesel fuel for five pressures at different temperatures

Pressures (MPa)	A	B	C	R^2
0.10	-1.5	-305	313899	0.998
1.83	-2.35	302	211214	0.999
3.50	-2.38	379	194494	0.999
5.30	-2.41	463	174399	0.999
7.00	-2.76	757	119676	0.999

7.5.2.3 Viscosity of Canola Biodiesel and Its Blends

The viscosity of a biodiesel fuel is dependent on temperature. As temperature increases, the average speed of the molecules in the liquid increases, the average intermolecular forces between the molecules decrease thus decreasing the viscosity of the liquid (Zhu and Granick, 2001). The measurement also indicated that all the biodiesel blends showed similar qualitative behavior at all temperatures and pressures measured in this work.

Figure 7.77 shows the dynamic viscosity times the density (mPa-s×kg/m^3) of canola oil biodiesel (B100), its blends (B80, B50 and B20) and diesel (B0) at atmospheric pressure. In order to get the kinematic viscosity, the measured data were divided twice by the measured density at respective pressures and temperatures and is presented in Figure 7.78. The kinematic viscosities of the biodiesel blends varied for different blends of biodiesel. The diesel, obviously, was found to have the lowest viscosity at all temperatures compared to all blends of canola biodiesel. The kinematic viscosity of canola biodiesel decreased from B100 to B20 at all temperatures. However, the changes in kinematic viscosity were more significant at lower temperatures than at higher temperatures. Table 7.29 is the summary of regression coefficients for kinematic viscosities of canola biodiesel and its blends including diesel. The high R^2 value indicated a good correlation of the measured data with the model equation 7.9.

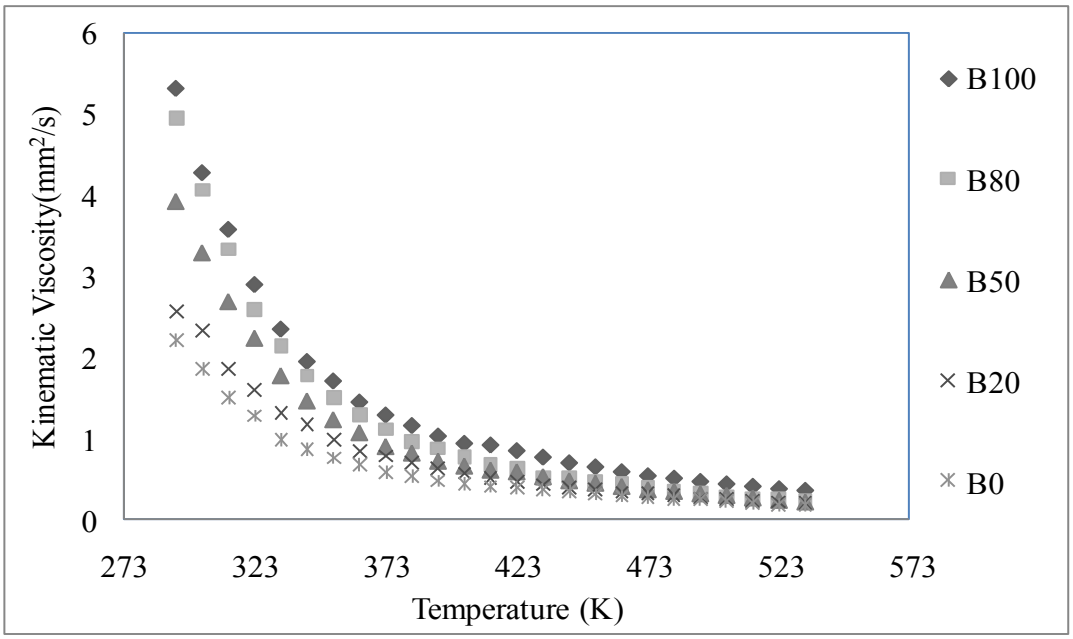

Figure 7.77 Measured dynamic viscosity times the density of canola biodiesel, its blends and diesel for atmospheric pressure at different temperatures (mPa-s×kg/m^3)

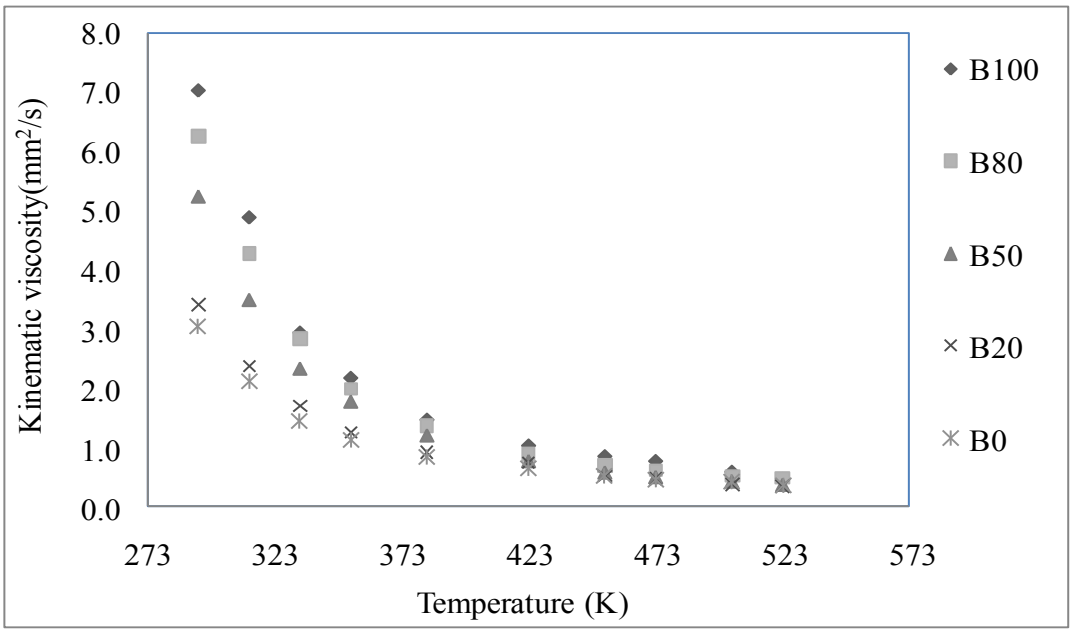

Figure 7.78 Kinematic viscosity of canola biodiesel, its blends and diesel for atmospheric pressure at different temperatures (mm^2/s)

Table 7.29 Regression coefficients of canola biodiesel and its blends at atmospheric pressure

Canola biodiesel blends/diesel	A	B	C	R^2
B100	-2.31	409	246800	0.999
B80	-2.10	135	301833	0.999
B50	-3.22	884	160956	0.997
B20	-3.56	1224	47311	0.999
B0	-1.5	-305	313899	0.998

Figure 7.79 shows the kinematic viscosity of canola B100 at atmospheric pressure from room temperature to 523 K. Figure 7.80 is the regressed kinematic viscosity of canola B100 at atmospheric pressure for the same temperature range. The measured values were found to have a good fit with the regressed values from the model as the R^2 value as found to be 0.995.

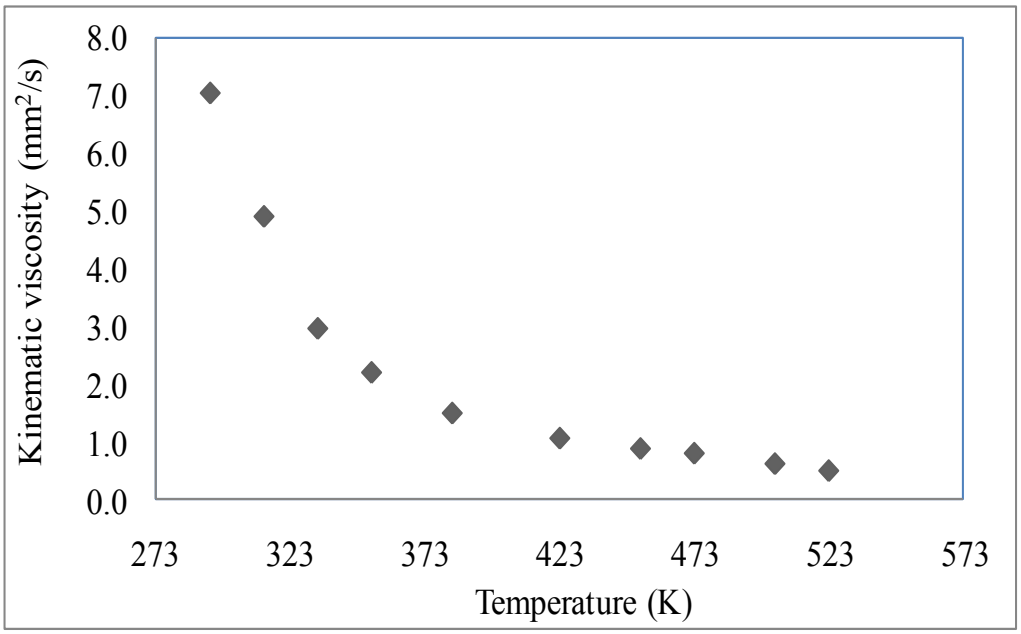

Figure 7.79 Kinematic viscosities of canola biodiesel B100 for atmospheric pressure at different temperatures (mm^2/s)

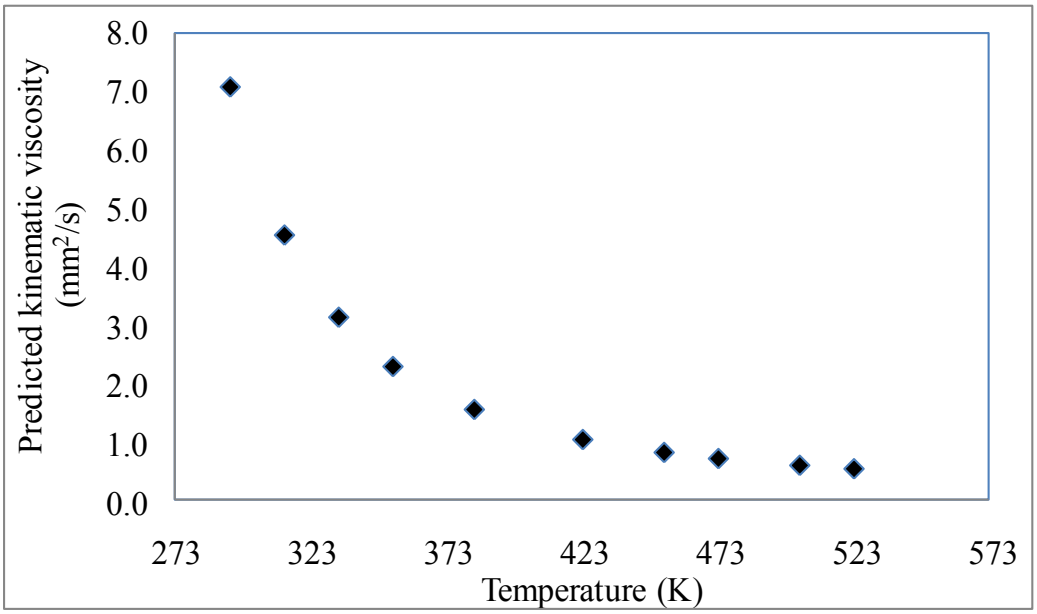

Figure 7.80 Regressed kinematic viscosities of canola B100 for atmospheric pressure at different temperatures (mm^2/s)

Figure 7.81 shows the kinematic viscosities of canola biodiesel B100 for five pressures at different temperatures. The kinematic viscosities decreased with increase in temperature

but increased as the pressure increased from atmospheric to 7.00 MPa. The kinematic viscosity data were regressed with temperatures for five pressures using equation 7.9. Table 7.30 shows the values of regression constants A, B and C and R^2 for canola biodiesel B100 for five pressures. Table E.4-E.8 in the Appendix E shows the regression data for canola biodiesel B100 for five pressures for different temperatures. Tables E.9 and E.10 show the measured and regressed kinematic viscosities and dynamic viscosities of canola B100 for five pressures from room temperature to 523 K. The absolute and % errors for canola biodiesel B100 are also presented in Tables E.9 and E.10. Figure E.2 in the Appendix E shows the probability plot of regressed kinematic viscosities of canola biodiesel B100 at atmospheric pressure and different temperatures.

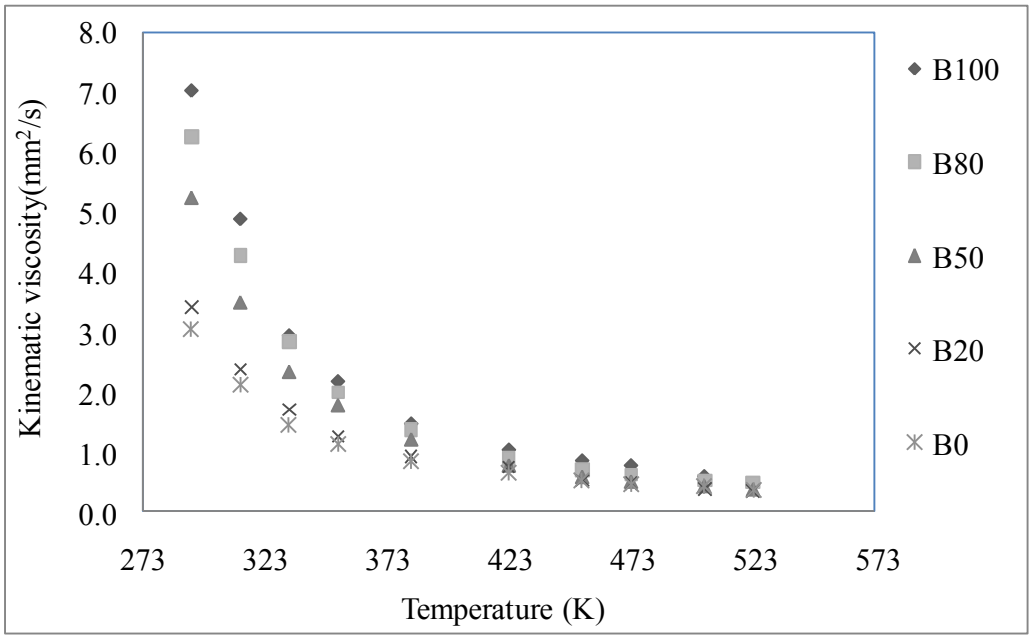

Figure 7.81 Measured kinematic viscosities of canola biodiesel B100 for five pressures at different temperatures (mm2/s)

Table 7.30 Regression coefficients for canola biodiesel B100 for five pressures at different temperatures using equation 7.9

Absolute Pressure (MPa)	A	B	C	R^2
0.10	-2.31	409	246800	0.995
1.83	-2.32	450	236660	0.997
3.50	-2.26	454	231432	0.996
5.30	-2.25	490	220519	0.996
7.00	-2.35	562	209140	0.995

Figure 7.82 is the plot of measured kinematic viscosities of canola biodiesel B80 for five pressures at temperatures between room temperature and 523 K. The kinematic viscosities decreased with increase in temperature but increased as the pressure increased from atmospheric to 7.00 MPa. Table 7.31 is the summary of regression constants and R^2 values for viscosities of canola biodiesel B80. Tables E.11-E.15 in Appendix E presents the summary of regression data for canola B80 for five pressures from room temperature to 523 K. The measured and regressed kinematic viscosities of canola biodiesel B80 for five pressures are tabulated in Table E.16 and E.17 in Appendix E. These tables also include dynamic viscosities and absolute and % errors for canola biodiesel B80.

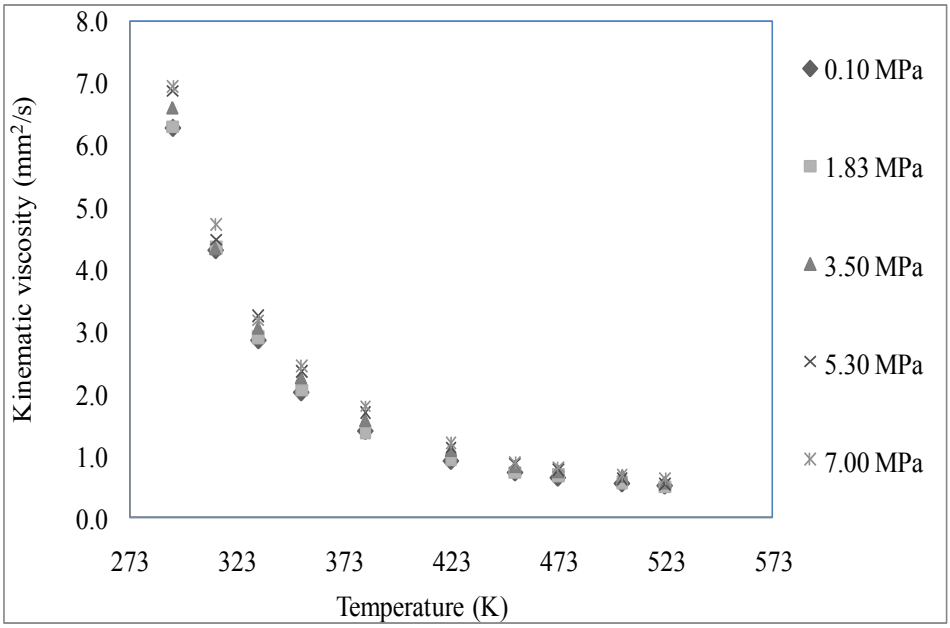

Figure 7.82 Measured kinematic viscosities for canola biodiesel B80 for five pressures at different temperatures (mm^2/s)

Table 7.31 Regression constants for canola biodiesel B80 for five pressures at different temperatures

Pressures (MPa)	A	B	C	R^2
0.10	-2.10	135	301833	0.999
1.83	-2.22	263	275037	0.999
3.50	-2.20	395	235108	0.998
5.30	-3.31	1242	84292	1.000
7.00	-2.48	696	175387	0.998

Figure 7.83 is the plot of measured kinematic viscosities of canola biodiesel B50 for five pressures at different temperatures. The kinematic viscosities decreased with increase in temperature but increased as the pressure increased from atmospheric to 7.00 MPa. Table E.18 in Appendix E shows the regression data for canola biodiesel B50 for atmospheric pressure and different temperatures. Table 7.32 shows the values for regression constants A, B, C and R^2. Tables E.19 and E.20 show the summary of measured and regressed kinematic viscosities of canola B50 for five pressures at different temperatures. The dynamic viscosities, absolute and % errors for canola biodiesel B50 for all the measurements are also presented in Tables E.19 and E.20.

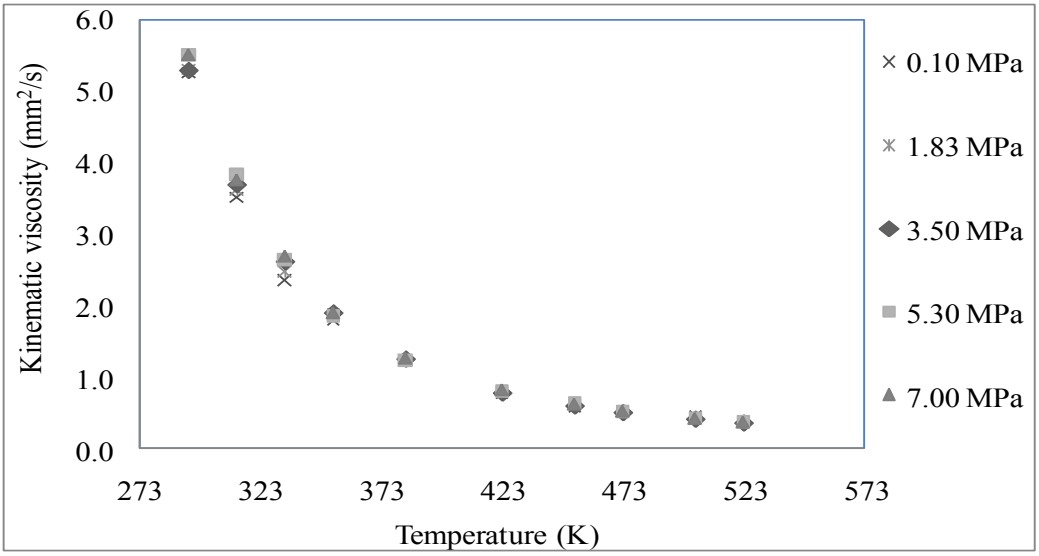

Figure 7.83 Measured kinematic viscosities for canola biodiesel B50 for five pressures at different temperatures (mm^2/s)

Table 7.32 Regression constants for canola biodiesel B50 for five pressures at different temperatures

Pressures (MPa)	A	B	C	R2
0.10	-3.22	884	160956	1.000
1.83	-3.64	1198	106741	1.000
3.50	-4.32	1688	21771	1.000
5.30	-3.76	1265	61147	1.000
7.00	-4.13	1564	44353	1.000

Figure 7.84 is the plot of measured kinematic viscosities of canola biodiesel B20 for five pressures for different temperatures. The kinematic viscosities decreased as the temperature increased from room temperature to 523 K as the pressure increased from atmospheric to 7.00 MPa. Table 7.33 shows the values of regression constant A, B, C and R^2 for canola biodiesel B20. The high R^2 values indicate a good correlation with the model equation. Table E.21 shows the regression data for canola biodiesel B20 for atmospheric pressure for different temperatures. Tables E.22 and E.23 in the Appendix E show the summary of measured kinematic viscosities of canola biodiesel B20 for five pressures at different temperatures. The absolute and % errors for viscosities of canola B20 is also presented.

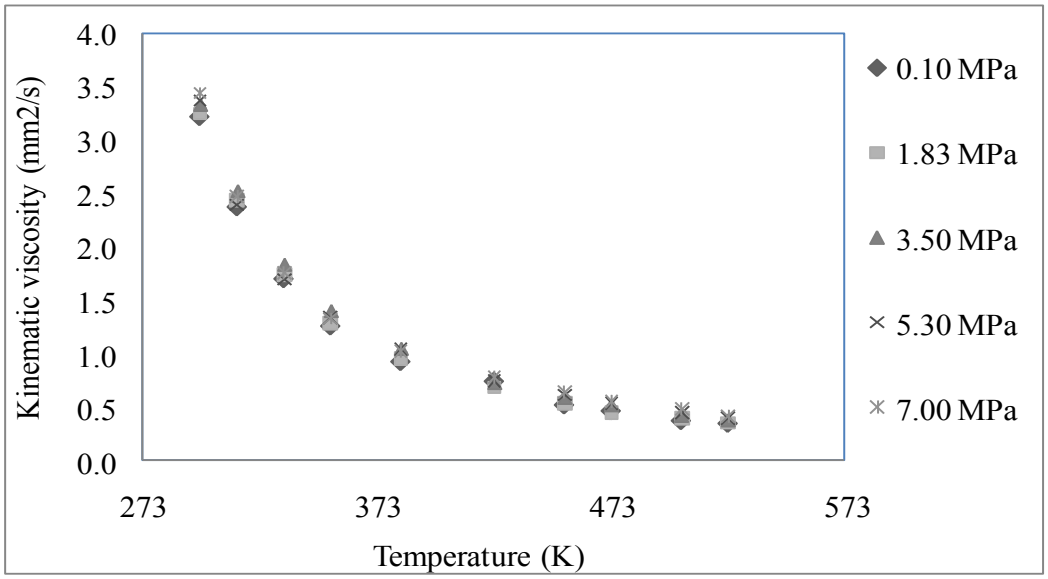

Figure 7.84 Measured kinematic viscosities for canola biodiesel B20 for five pressures at different temperatures (mm^2/s)

Table 7.33 Regression constants of kinematic viscosities for canola biodiesel B20 for five pressures at different temperatures

Pressures (MPa)	A	B	C	R2
0.10	-3.56	1224	47311	0.997
1.83	-3.41	1098	74618	0.999
3.50	-3.64	1374	14338	0.999
5.30	-2.81	792	112357	0.998
7.00	-2.28	430	175474	0.996

7.5.2.4 Viscosity of Jatropha Biodiesel and Its Blends

Figure 7.85 shows the product of dynamic viscosities and the density (mPa-s × kg/m^3) of jatropha oil biodiesel, its blends and diesel measured at atmospheric pressure. The product of dynamic viscosity and density of jatropha biodiesel blends increased as the biodiesel blend ratio increased from B0 to B100. The diesel (B0) was found to have the lowest value for all temperatures compared to that of all blends of jatropha biodiesel.

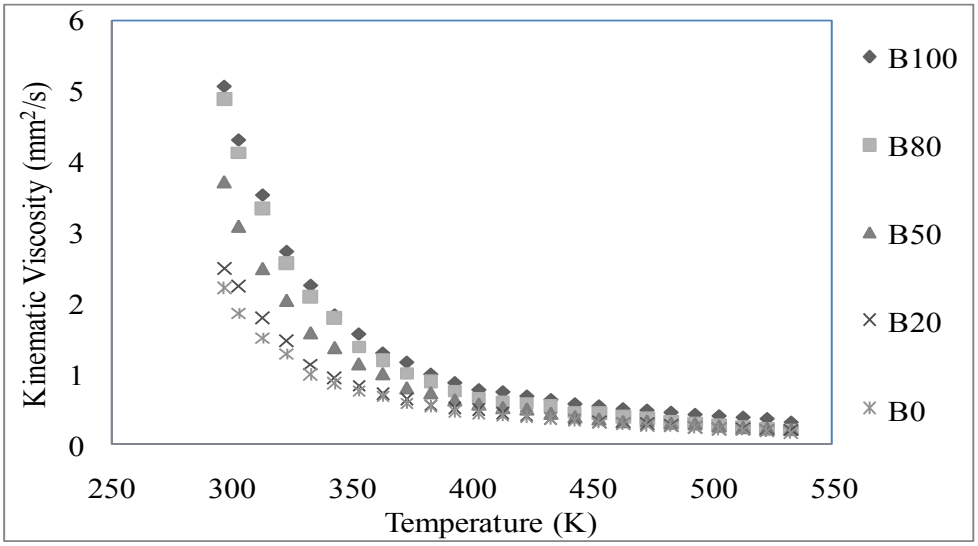

Figure 7.85 Dynamic viscosity times the density of jatropha biodiesel, its blends and diesel at atmospheric pressure for different temperatures (mPa-s x kg/m^3)

Figure 7.86 shows the kinematic viscosities of jatropha biodiesel and its blends including diesel for atmospheric pressure at different temperatures. The kinematic viscosities show similar quality behavior to that of canola biodiesel and its blends. The change in the viscosity among the blends was found significant at lower temperatures while the change was found smaller at higher temperatures. Table 7.34 shows the regression constants A, B, C and R^2 for jatropha biodiesel, its blends and diesel at atmospheric pressure (0.10 MPa) for different temperatures.

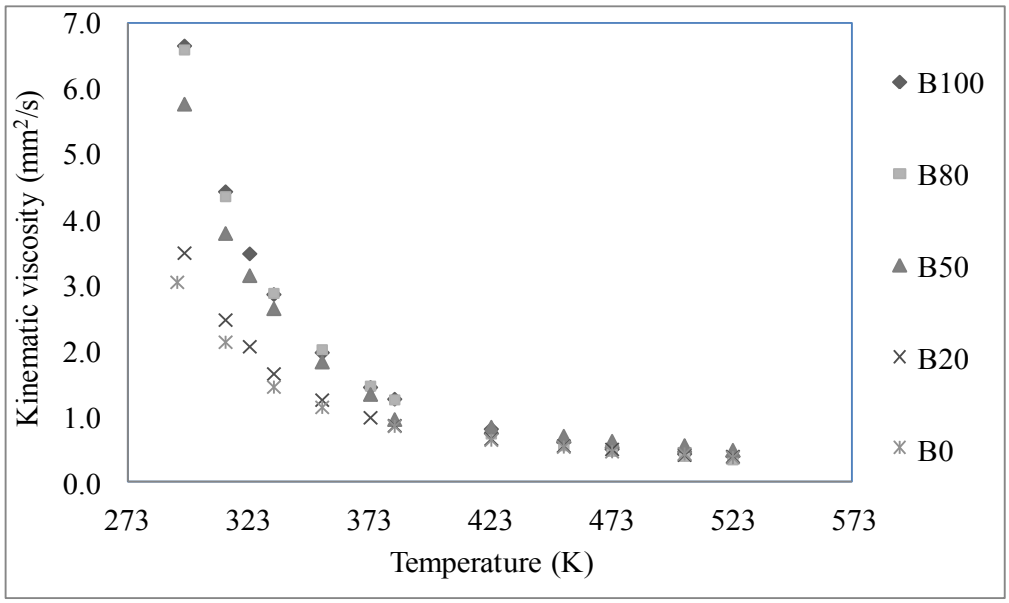

Figure 7.86 Kinematic viscosities of jatropha biodiesel, its blends and diesel at atmospheric pressure for different temperatures (mm^2/s)

Table 7.34 Regression constant of kinematic viscosities for jatropha biodiesel B100 for five pressures at different temperatures obtained from regression using equation 7.9

Jatropha biodiesel blends	A	B	C	R^2
B100	-2.67	300	311982	1.000
B80	-3.44	774	240809	1.000
B50	-0.35	-1225	550624	0.999
B20	-1.00	-767	425701	0.999
B0	-1.50	-305	313899	0.998

Figure 7.87 shows the measured kinematic viscosities of jatropha biodiesel B100 for five pressures between room temperature to 523 K. The kinematic viscosities decreased as the temperature increased from room temperature to 523 K. The kinematic viscosity increased as the pressure increased from atmospheric to 7.00 MPa. The measured kinematic viscosity data were regressed with temperatures for five pressures using equation 7.9. Table 7.35 shows the values of regression constants A, B and C and R^2 for kinematic viscosities of jatropha biodiesel B100. Table E.24 shows the regression data for jatropha biodiesel B100 for atmospheric pressure. Figure E.3 is the probability plot for jatropha biodiesel B100 at

atmospheric pressure. Table E.25 and E.26 in the Appendix E represent the summary of measured kinematic viscosities of jatropha biodiesel blends for five pressures at different temperatures. These tables also show the dynamic viscosities as well as absolute and % errors from regressed values for jatropha biodiesel B100 for five pressures and different temperatures.

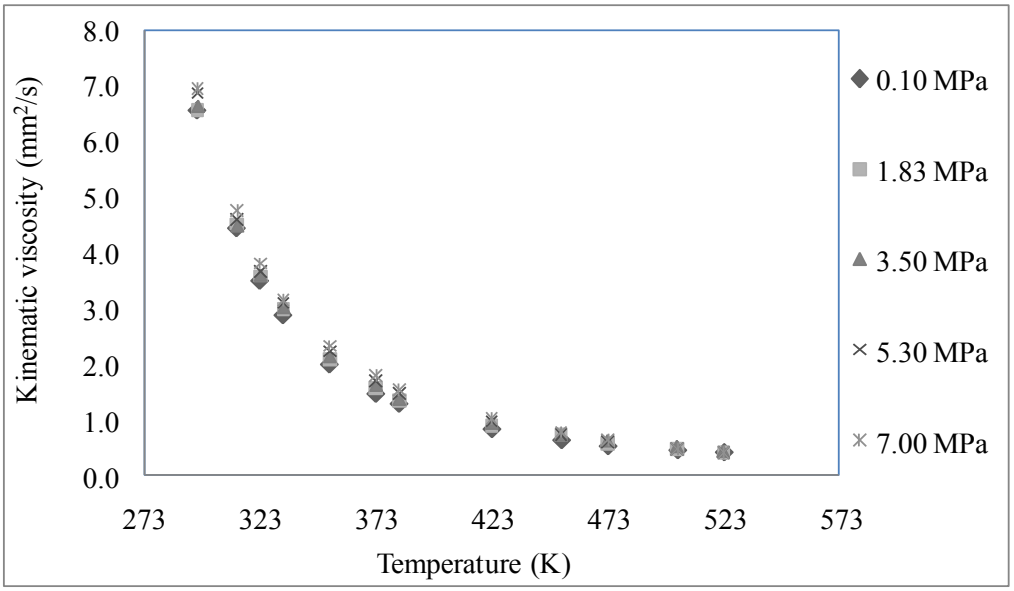

Figure 7.87 Kinematic viscosities of jatropha biodiesel B100 for five pressures at different temperatures (mm^2/s)

Table 7.35 Regression constants A, B, C and R^2 for kinematic viscosities of jatropha biodiesel B100 for five pressures at different temperatures

Pressures (MPa)	A	B	C	R2
0.10	-2.67	300	311982	1.000
1.83	-2.97	666	229034	0.999
3.50	-2.79	575	240281	1.000
5.30	-3.79	1324	106544	0.999
7.00	-4.22	1691	36552	0.999

Figure 7.88 shows the measured kinematic viscosities of jatropha biodiesel B80 for five pressures at different temperatures. The measured viscosity data were regressed with temperatures for five pressures using equation 7.9. The kinematic viscosities increased

with the increase in the pressure and decreased with increase in temperature. Table 7.36 shows the values of regression constants A, B and C and R^2. Tables E.27 and E.28 show the summary of measured kinematic viscosities for jatropha biodiesel B80 for five pressures at different temperatures. The dynamic viscosities at respective temperatures and pressures are also presented in the same tables. Absolute and % errors from regressed values are also presented.

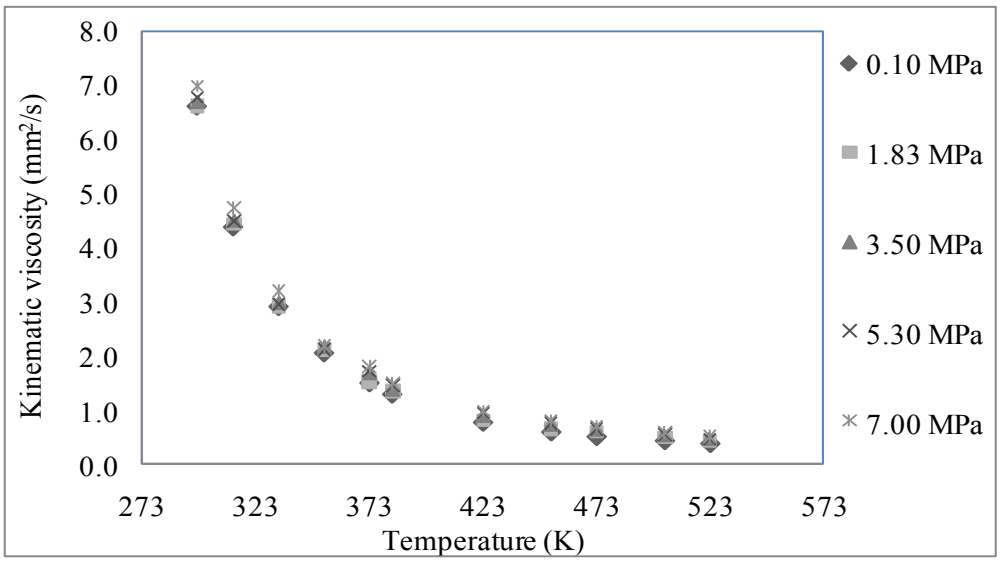

Figure 7.88 Kinematic viscosities for jatropha biodiesel B80 for five pressures at different temperature (mm^2/s)

Table 7.36 Regression constants A, B, C and R^2 for kinematic viscosities of jatropha biodiesel B80 for five pressures at different temperatures

Pressures (MPa)	A	B	C	R^2
0.10	-3.44	774	240809	1.000
1.83	-2.40	149	334564	0.999
3.50	-2.37	224	310636	0.999
5.30	-2.48	366	276804	0.999
7.00	-2.15	170	309857	0.999

Figure 7.89 shows the measured kinematic viscosities of jatropha biodiesel B50 for five pressures at different temperatures. The kinematic viscosities increased as the pressure

increased from atmospheric to 7.00 MPa. The measured viscosity data were regressed with temperatures for five pressures using equation 7.9. Table 7.37 shows the values of regression constants A, B and C and R^2 for jatropha biodiesel B50. Tables E.29 and E.30 represents the summary of kinematic and dynamic viscosities for jatropha biodiesel blends for five pressures at different temperatures. These tables also include absolute and % errors for jatropha biodiesel B50.

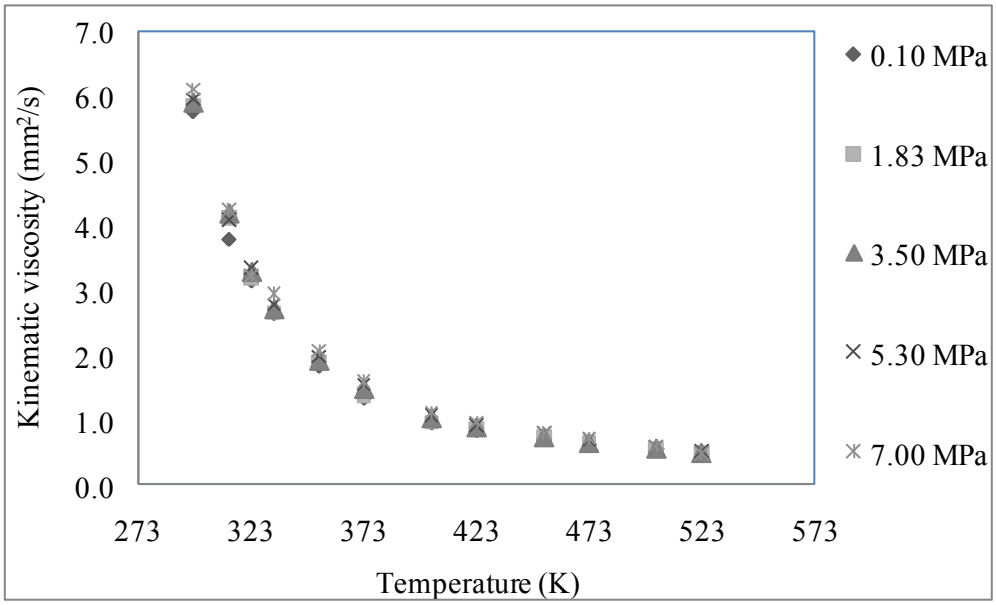

Figure 7.89 Measured kinematic viscosities of jatropha biodiesel B50 for five pressures at different temperature (mm^2/s)

Table 7.37 Regression constants A, B, C and R^2 for kinematic viscosities of jatropha biodiesel B50 for five pressures at different temperatures

Pressures (MPa)	A	B	C	R^2
0.10	-0.350	-1225	550624	0.999
1.83	-0.466	-1119	531708	0.998
3.50	-0.993	-698	453693	0.999
5.30	-1.21	-464	402306	0.999
7.00	-1.27	-72	330450	0.998

Figure 7.90 shows the measured kinematic viscosities of jatropha biodiesel B20 for five pressures at different temperatures. The kinematic viscosities increased as the pressure increased from atmospheric to 7.00 MPa. The measured data were regressed with temperatures for five pressures using equation 7.9. Table 7.28 shows the values of regression constants A, B and C and R^2 for jatropha biodiesel B20. The R^2 values indicate a very good fit of the measured data with the model equation. Tables E.31 and E.32 in the Appendix E show the summary of kinematic and dynamic viscosities for jatropha biodiesel blends for five pressures at different temperatures. These tables also show the absolute and % errors for the viscosities of jatropha B20.

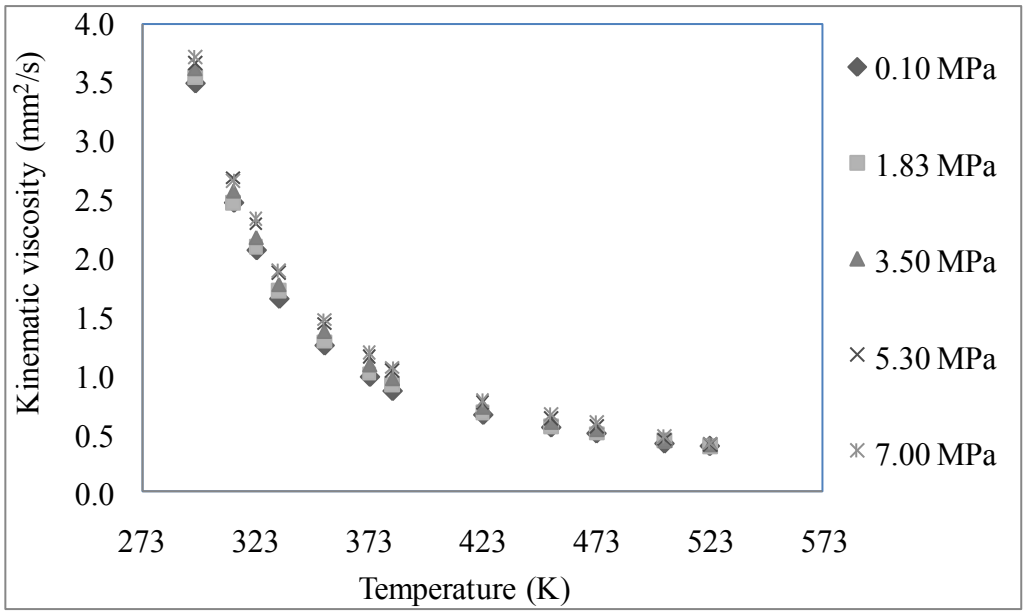

Figure 7.90 Measured kinematic viscosities for jatropha biodiesel B20 for five pressures at different temperature (mm^2/s)

Table 7.38 Regression constants A, B, C and R^2 for kinematic viscosities of jatropha biodiesel B20 for five pressures at different temperatures

Pressures (MPa)	A	B	C	R^2
0.10	-1.00	-767	425701	0.992
1.83	-2.40	73	265876	0.998
3.50	-2.46	452	192239	0.999
5.30	-3.05	940	100186	0.999
7.00	-3.50	989	85511	0.998

7.5.2.5 Viscosity of Soapnut Biodiesel and Its Blends

Figure 7.91 shows the product of dynamic viscosity and density (mPa-s × kg/m^3) of soapnut oil biodiesel, its blends and diesel at atmospheric pressure. The value of the product increased as the blend ratio increased.

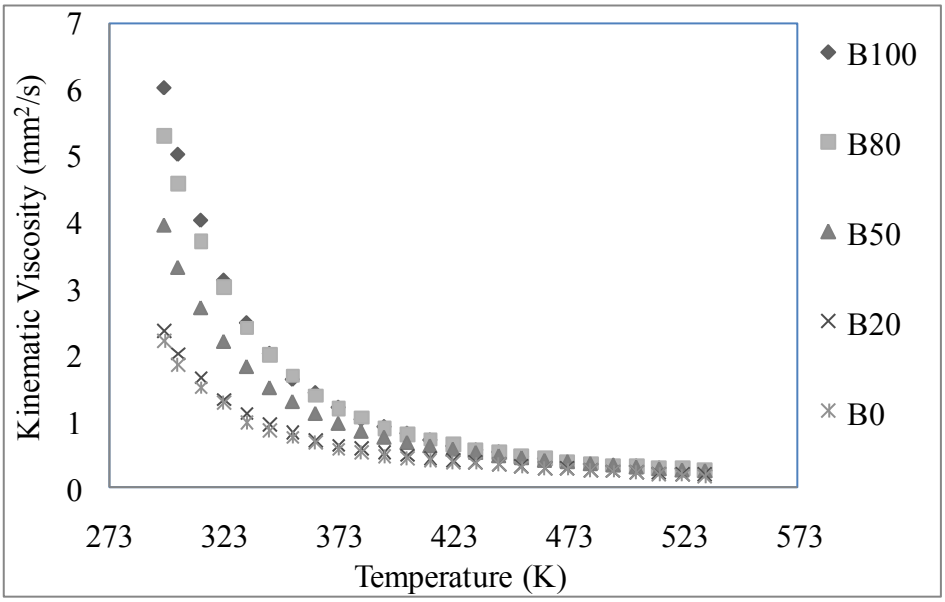

Figure 7.91 Dynamic viscosity times the density of of soapnut biodiesel and its blends for atmospheric pressure at different temperatures (mPa-s x kg/m^3).

Figure 7.92 represents the kinematic viscosities of soapnut biodiesel blends and diesel for atmospheric pressure for different temperatures. The kinematic viscosities were found to increase from B0 to B100 among the blends at all temperatures. However, the change in kinematic viscosities among the blends was found significant at lower temperatures while the change was found smaller at higher temperatures. Table 7.39 shows the regression constants of soapnut biodiesel blends and diesel for atmospheric (0.10 MPa) pressure at different temperatures using the equation 7.9.

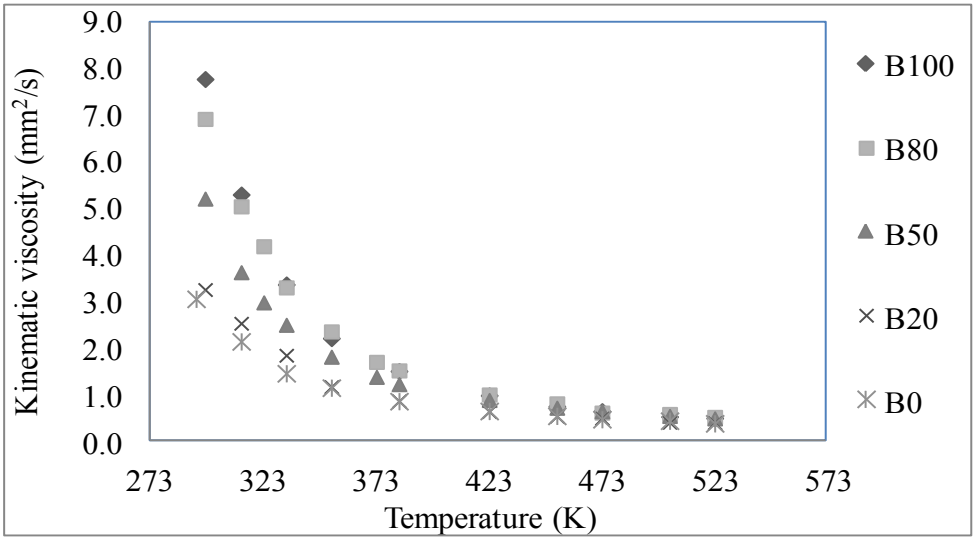

Figure 7.92 Kinematic viscosity of soapnut biodiesel and its blends for atmospheric pressure at different temperatures (mm^2/s)

Table 7.39 Regression constants A, B, C and R^2 for kinematic viscosities of soapnut biodiesel blends at atmospheric pressure

Jatropha biodiesel blends	A	B	C	R^2
B100	-1.76	-244	409392	0.999
B80	-2.13	142	320515	0.998
B50	-1.30	-424	386472	1.000
B20	-1.15	-628	386682	0.999
B0	-1.50	-305	313899	0.998

Figure 7.93 shows the measured kinematic viscosities of soapnut biodiesel B100 for five pressures at different temperatures. The kinematic viscosities decreased with increase in temperature and increased as the pressure increased from atmospheric to 7.00 MPa. The measured kinematic viscosity data using equation 7.9. Table 7.40 shows the regression constants A, B and C and R^2 for soapnut biodiesel B100. The high R^2 value indicates a high correlation of the measured data with the model equation. Tables E.33 and E.34 in Appendix E show the summary of kinematic and dynamic viscosities for soapnut biodiesel B100 for five pressures at different temperatures. The tables also include the absolute and % errors of viscosities of soapnut biodiesel B100.

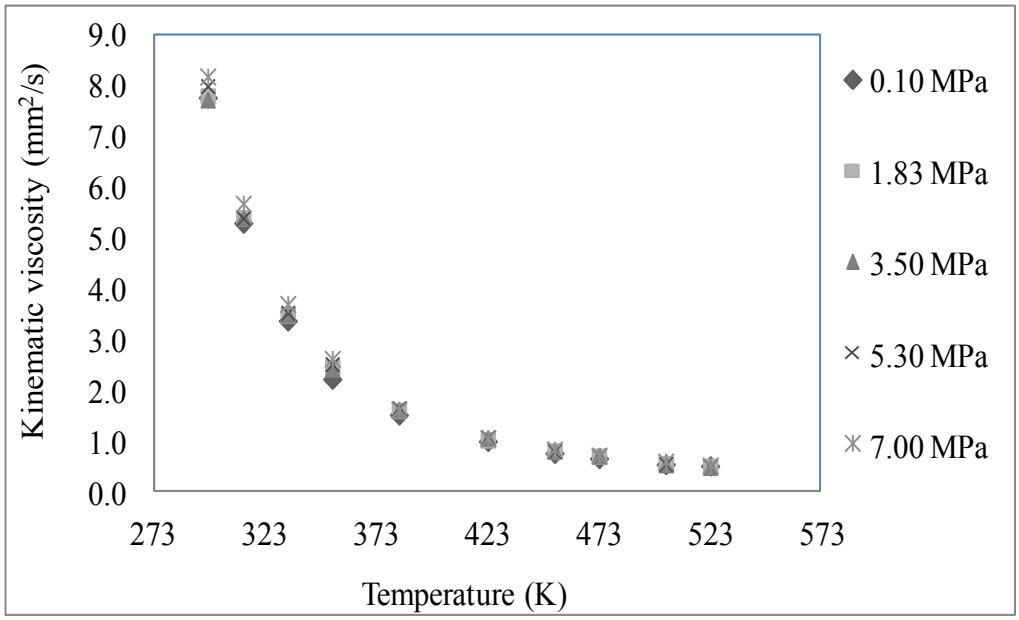

Figure 7.93 Measured kinematic viscosities of soapnut biodiesel B100 for five pressures at different temperatures (mm^2/s)

Table 7.40 Regression coefficients for soapnut biodiesel B100 for five pressures at different temperatures using equation 7.9

Pressures (MPa)	A	B	C	R^2
0.10	-1.76	-244	409392	0.999
1.83	-2.60	456	276338	1.000
3.50	-3.04	792	212905	0.999
5.30	-2.80	620	245672	1.000
7.00	-2.41	727	302802	1.000

Figure 7.94 shows the measured kinematic viscosities of soapnut biodiesel B80 for five pressures at different temperatures. The kinematic viscosities increased as the pressure increased from atmospheric to 7.00 MPa. The kinematic viscosity data were regressed with temperatures and the values of regression constants A, B and C and R^2 are summarized in Table 7.41. Tables E.35 and E.36 present the summary of measured kinematic viscosities, dynamic viscosities and absolute and % errors for five pressures at different temperatures for soapnut biodiesel B80.

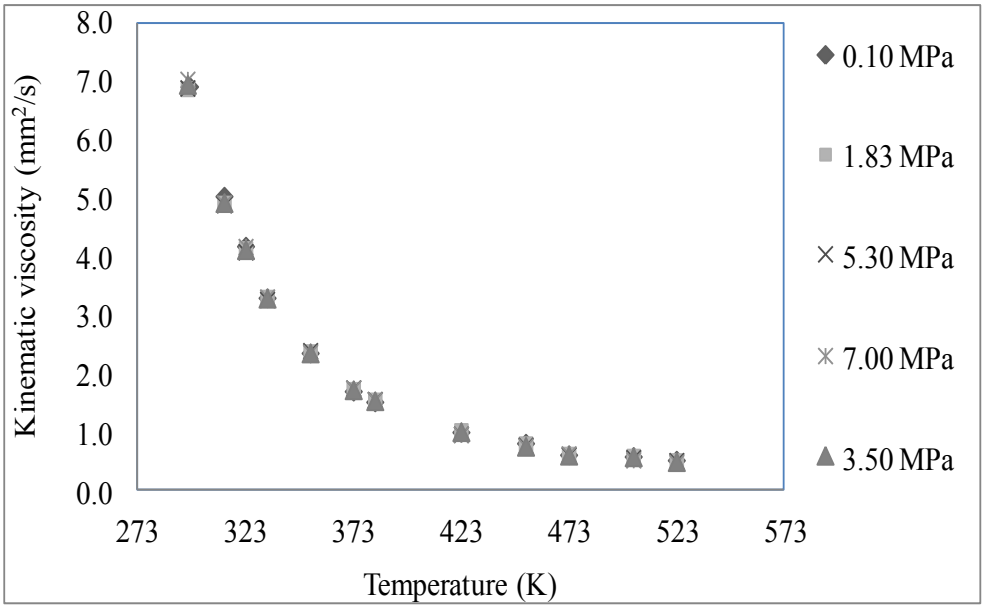

Figure 7.94 Measured kinematic viscosities for soapnut biodiesel B80 for five pressures at different temperature (mm^2/s)

Table 7.41 Regression coefficients for soapnut biodiesel B80 for five pressures at different temperatures for using equation 7.9

Pressures (MPa)	A	B	C	R^2
0.10	-2.13	142	320515	0.998
1.83	-2.45	411	267419	0.998
3.50	-2.50	409	273367	0.998
5.30	-2.54	444	265684	0.999
7.00	-2.89	672	229824	1.000

Figure 7.95 shows the measured kinematic viscosities of soapnut biodiesel B50 for five pressures at different temperatures. The kinematic viscosities increased as the pressure increased from atmospheric to 7.00 MPa while the viscosities decreased as the temperature increased. The measured kinematic viscosity data were regressed with temperatures using equation 7.9. Table 7.42 shows the values of regression constants A, B and C and R^2. The R^2 values show a good correlation of the measured data with the model equation. Tables E.37 and E.38 in Appendix E show the summary of measured kinematic viscosities,

dynamic viscosities and absolute and % errors of soapnut biodiesel B50 for five pressures at different temperatures.

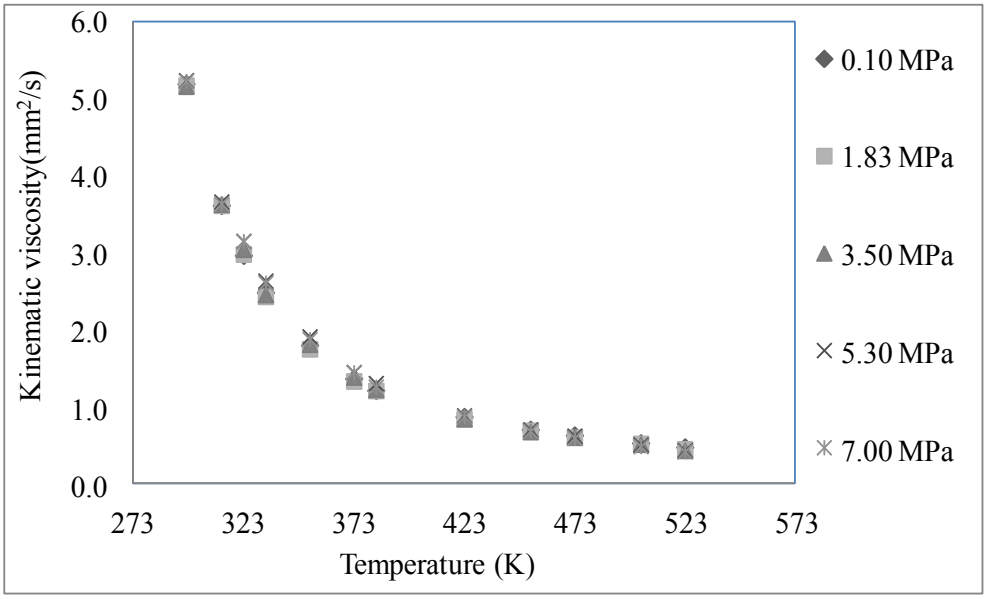

Figure 7.95 Measured kinematic viscosities of soapnut biodiesel B50 for five pressures at different temperature (mm^2/s)

Table 7.42 Regression coefficients of soapnut biodiesel B50 for five pressures atdifferent temperatures

Pressures (MPa)	A	B	C	R^2
0.10	-1.30	-424	386472	1.000
1.83	-1.38	-406	387806	0.999
3.50	-1.96	32	308709	0.999
5.30	-2.68	612	200514	0.999
7.00	-2.79	660	196123	0.999

Figure 7.95 shows the measured kinematic viscosities of soapnut biodiesel B20 for five pressures at different temperatures. It is observed that the kinematic viscosities increased as the pressure increased from atmospheric to 7.00 MPa. The measured kinematic viscosity data were regressed with temperatures. Table 7.44 shows the values of regression constants A, B and C and R^2 for soapnut biodiesel B20. The R^2 value shows a high correlation. Tables E.39 and E.40 in Appendix E show the summary of measured kinematic viscosities, dynamic viscosities and absolute error for soapnut biodiesel B20 for five pressures at different temperatures. The maximum absolute error was found to be 0.04

mm^2/s for soapnut biodiesel B20 for five pressures and temperatures between room temperature and 523 K.

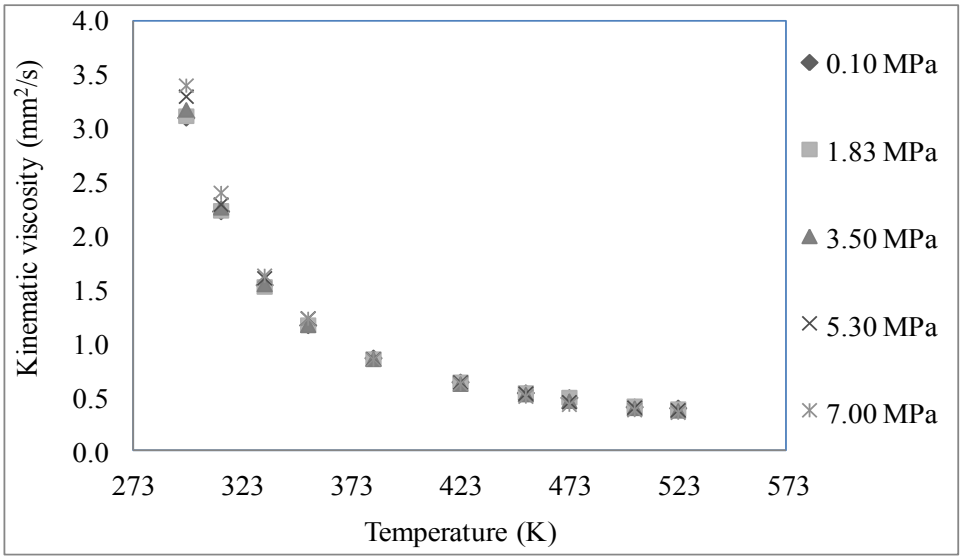

Figure 7.96 Measured kinematic viscosities of soapnut biodiesel B20 for five pressures at different temperature (mm^2/s)

Table 7.43 Regression coefficients of soapnut biodiesel B20 for five pressures at different temperatures

Pressures (MPa)	A	B	C	R^2
0.10	-1.15	-628	386682	0.999
1.83	-1.10	-670	394800	0.999
3.50	-1.34	-540	380204	0.999
5.30	-1.43	-480	372885	0.999
7.00	-1.71	-348	361934	0.999

7.5.2.6 Dynamic Viscosity of Diesel and Biodiesel Fuels

The dynamic viscosity of diesel fuel was obtained by dividing the measured data by the density of the diesel obtained using a capacitance type densitometer in this work. As the density of diesel and biodiesel fuel is less than unity, the dynamic viscosity is always higher than the data measured by the ViscoScope viscometer. Figure 7.97 shows the

dynamic viscosity of diesel fuel used in this study. The dynamic viscosity of diesel decreased from 2.60 mPa-s at 293 K to 0.26 mPa-s at 523 K at atmospheric pressure. At 3.50 MPa, the dynamic viscosity of diesel decreased from 2.79 mPa-s at 293 K to 0.27 mPa-s at 523 K. At 7.00 MPa, the dynamic viscosity of diesel decreased from 2.79 mPa-s at 293 K to 0.30 mPa-s at 523 K.

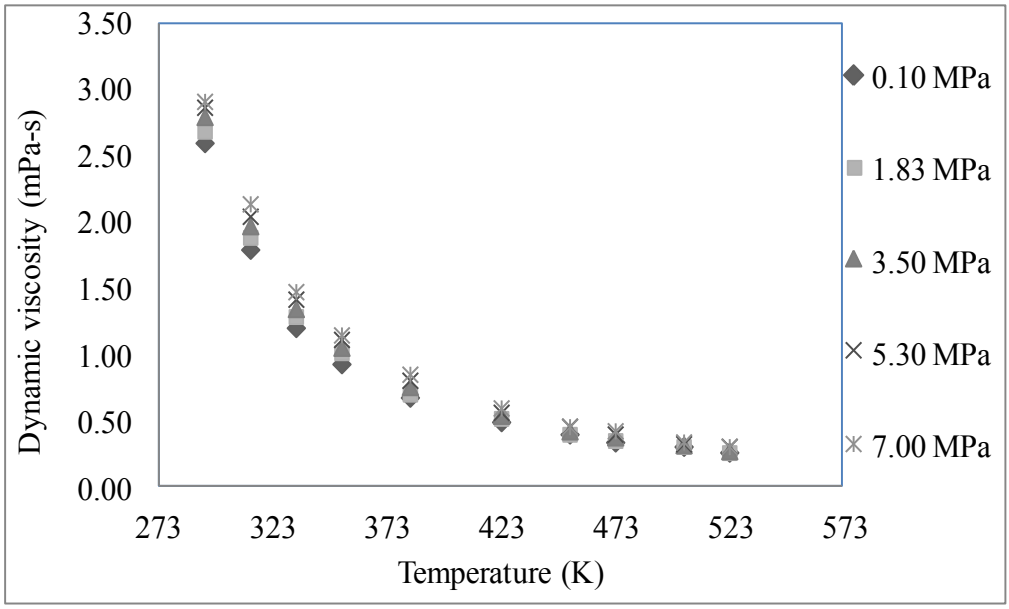

Figure 7.97 Dynamic viscosities of diesel for five pressures at different temperatures (mPa-s)

Figure 7.98 shows the dynamic viscosities of canola biodiesel B100 for five pressures at different temperatures. The dynamic viscosity of canola biodiesel B100 decreased from 6.24 mPa-s at 293 K to 0.35 mPa-s at 523 K at atmospheric pressure. The dynamic viscosity at 3.50 MPa decreased from 6.38 mPa-s at 293 K to 0.39 mPa-s at 523 K. Similarly, the dynamic viscosity at 7.00 MPa decreased from 6.57 mPa-s at 293 K to 0.40 mPa-s at 523 K.

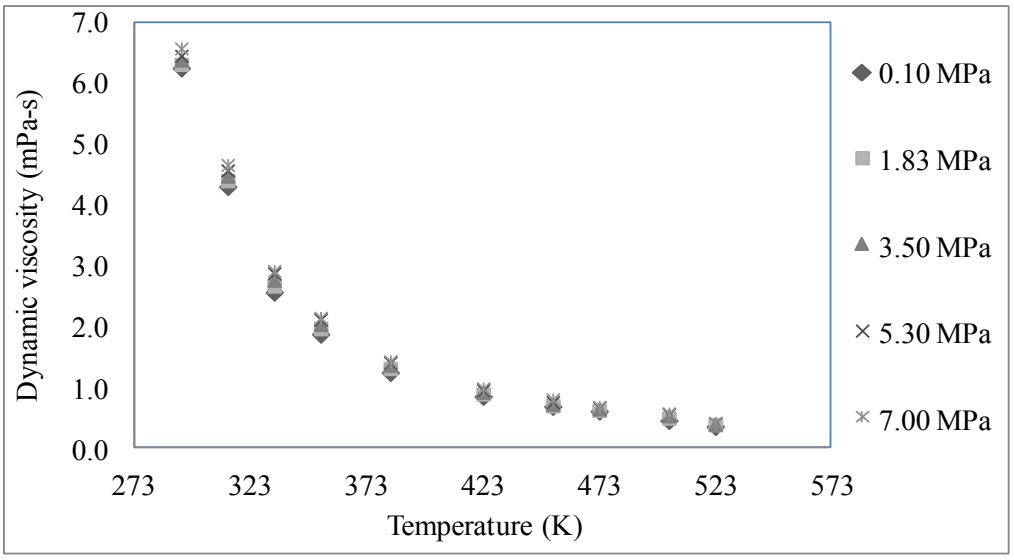

Figure 7.98 Dynamic viscosities of canola biodiesel B100 for five pressures at different temperatures (mPa-s)

Figure 7.99 represents the dynamic viscosities of jatropha biodiesel B100 for five pressures at different temperatures. The dynamic viscosity at 0.10 MPa decreased from 5.76 mPa-s at 296 K to 0.29 mPa-s at 523 K. The dynamic viscosity at 3.50 MPa decreased from 5.93 mPa-s at 296 K to 0.33 mP-s at 523 K. Similarly, the dynamic viscosity at 7.00 MPa decreased from 6.22 mPa-s at 296 K to 0.33 mPa-s at 523 K.

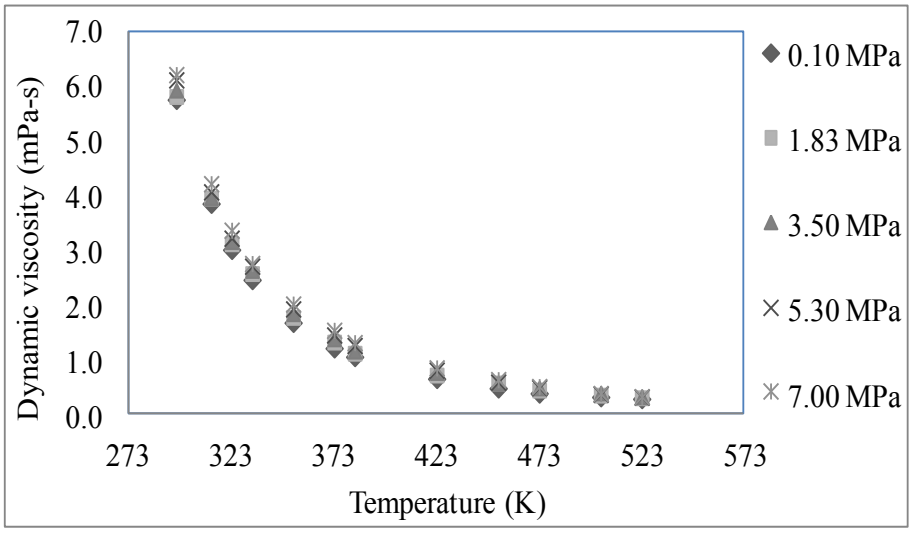

Figure 7.99 Dynamic viscosities of jatropha biodiesel B100 for five pressures at different temperatures (mPa-s)

The dynamic viscosities of soapnut biodiesel B100 for five pressures at different temperatures is presented in Figure 7.100. The dynamic viscosity at 0.10 MPa decreased from 6.83 mPa-s at 297 K to 0.35 mPa-s at 523 K. The dynamic viscosity at 3.50 MPa decreased from 6.88 mPa-s at 297 K to 0.36 mP-s at 523 K. Similarly, the dynamic viscosity at 7.00 MPa decreased from 7.48 mPa-s at 297 K to 0.38 mPa-s at 523 K.

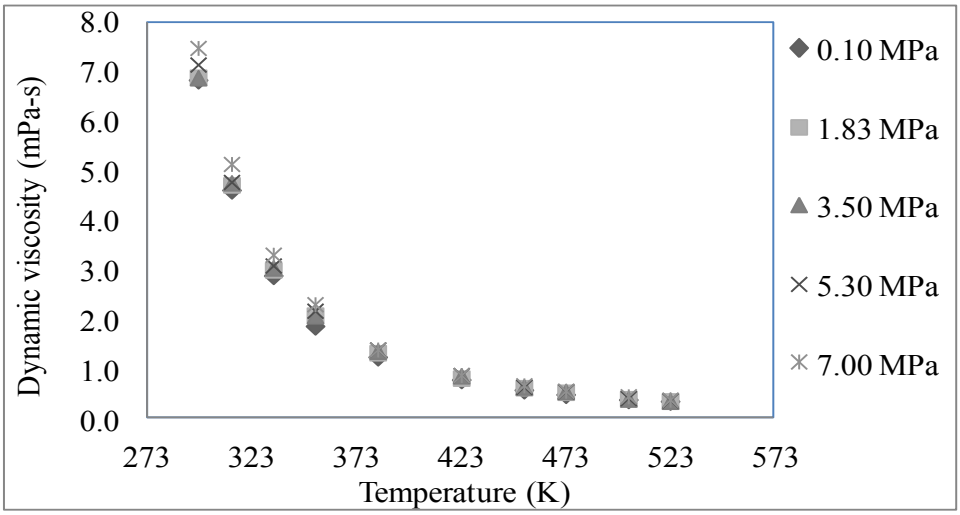

Figure 7.100 Dynamic viscosities of soapnut biodiesel B100 for five pressures at different temperatures (mPa-s)

7.5.2.7 Kinematic Viscosity, Temperature and Pressure Relationship

Equation 7.9 represents the kinematic viscosity relations at elevated temperature. Based on the regression data, the relationship was found to hold good for all five pressures up to 7.00 MPa and up to 523 K. In order to establish the direct relationship with pressure and equation 7.9, regression analysis was performed for kinematic viscosity with all five pressures and temperatures for which the viscosity was measured. Equation 7.10 below is the representation of kinematic viscosity of diesel as a function of temperature and pressure. The equation was tested for regression data for pressures up to 7.00 MPa and 523 K from room temperature for diesel and three biodiesel fuels.

$$\ln(\eta) = A + \frac{B}{T} + \frac{C}{T^2} + DP \qquad (7.10)$$

where T is the absolute temperature in K, P is the pressure in kPa, A is the equation constant, B and C are the temperature coefficients and D is the pressure coefficient.

Table 7.44 gives the summary of regression data obtained from viscosity, temperature and pressure for diesel, canola, jatropha and soapnut biodiesel. The R^2 values show a high correlation of the model equation 7.10 with the experimental data for different blends.

Table 7.44 Summary of regressions data from regression of viscosity, temperature and pressure

Fuel Type	Blend	A	B	C	D	R^2
Diesel fuel	B0	-4.26	1161	91167	0.000032	0.999
Canola biodiesel	B100	-2.31	434	239670	0.000002	0.995
	B80	-2.57	546	214332	0.000030	0.998
	B50	-3.74	1320	86994	0.000006	0.999
	B20	-3.20	984	84820	0.000018	0.996
Jatropha biodiesel	B100	-3.34	898	187493	0.000018	0.998
	B80	-4.65	1398	121335	0.000043	0.995
	B50	-0.99	-716	453745	0.000015	0.998
	B20	-2.42	361	210249	0.000021	0.984
Soapnut biodiesel	B100	-2.56	390	289422	0.000010	0.999
	B80	-2.49	416	271362	0.000003	0.998
	B50	-2.03	95	295925	0.000002	0.998
	B20	-1.34	-533	379301	0.000002	0.998

Figure 7.101 shows the plot of regressed kinematic viscosities of diesel fuel for temperatures between room temperature and 533 K and from atmospheric pressure and 7.00 MPa. Figures 7.102, 7.103 and 7.104 show the regressed viscosity canola, jatropha and soapnut biodiesel respectively. All the diesel and biodiesel blends follow similar trends as they all follow equation 7.10. However, it was observed from the regressed viscosity of canola biodiesel that the pressures have very little effect in viscosity compared to the effect of temperatures.

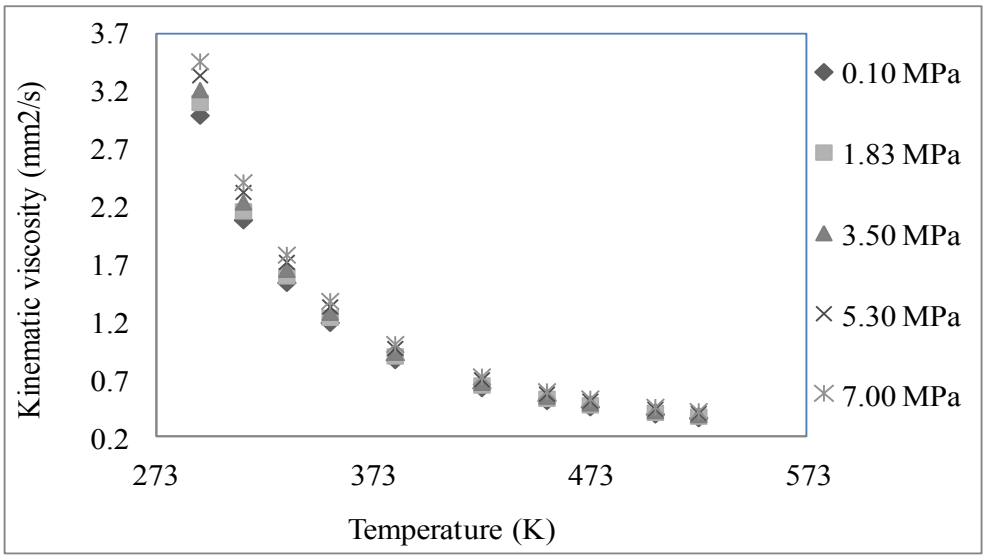

Figure 7.101 Regressed kinematic viscosities of diesel for five pressures at different temperatures (mm^2/s)

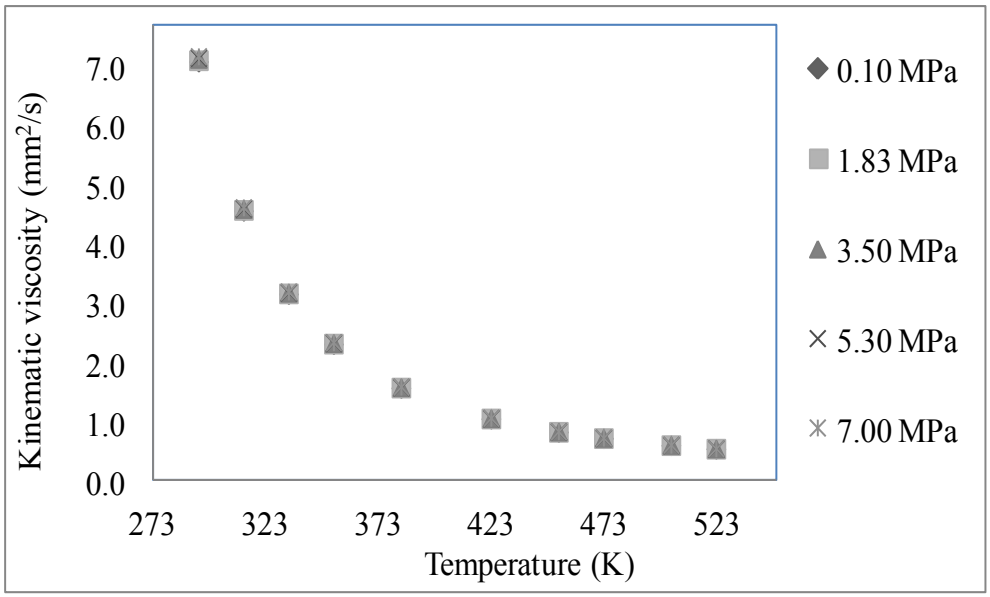

Figure 7.102 Regressed kinematic viscosities of canola biodiesel B100 for five pressures at different temperatures (mm^2/s)

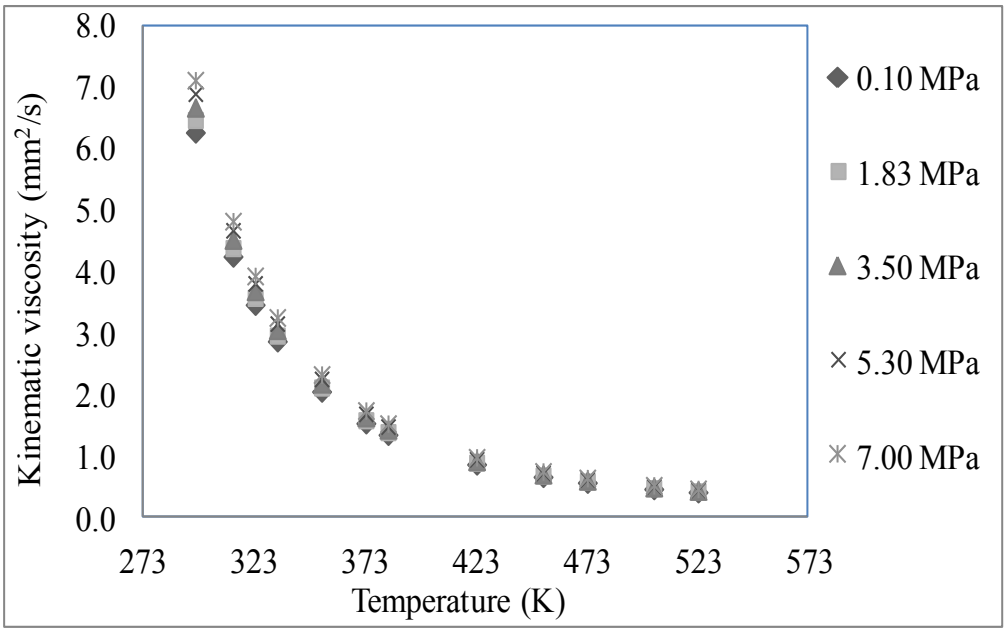

Figure 7.103 Regressed kinematic viscosities of jatropha biodiesel B100 for five pressures at different temperatures (mm^2/s)

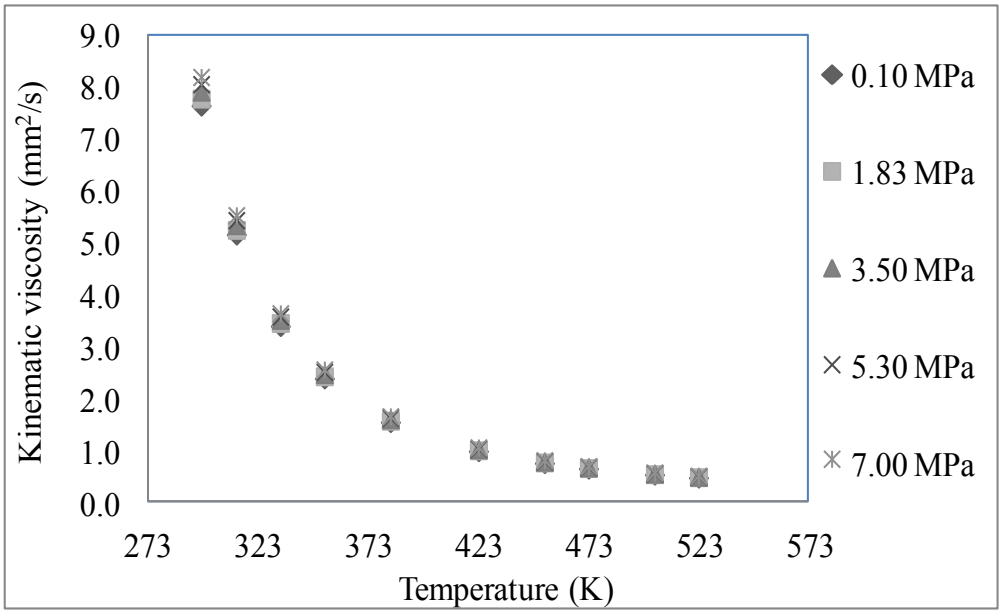

Figure 7.104 Regressed kinematic viscosities of soapnut biodiesel B100 for five pressures at different temperatures (mm^2/s)

7.6 SUMMARY OF CHAPTER 7

Section 7.1 in this Chapter includes a waste cooking oil survey within ring road of Kathmandu Valley in Nepal. The waste oil generation data were compiled according to restaurant type, type of oil used and end use of waste cooking oil. The restaurants (unspecialized) were found to be the highest contributor for waste cooking oil generation followed by hotels, fast food restaurants, lodges and guest houses and bakery and sweets. Section 7.2 includes the experimental results of biodiesel production using canola, waste cooking oil, jatropha and soapnut oil in the lab. The oils used in the test were analyzed for their fatty acid content using GC. The biodiesel conversion methods were chosen based on the free fatty acid content of the feedstock. The optimum catalyst and methanol content required for the transesterification was determined from several experimental tgrials. The biodiesel produced in the lab were characterized for their fuel characteristics such as flash point, pour point, water content, glycerin content etc. The biodiesel samples were tested in Iatroscan to determine the conversion rate and the efficiency of the transesterification process.

Section 7.3 includes the density measurement of three different biodiesel and diesel fuels at elevated temperature and pressure. The density was measured using capacitance type densitometer. The impact of temperature, pressure and depth of submergence on the dielectric constant were studied. The measured densities were regressed and a regression model was suggested based on the measured data. In most cases, the density showed linear relationship with temperatures as well as for pressures. Some of the trends were slightly non-linear as well. The Section 7.4 presents the surface tension of canola, jatropha, soapnut biodiesel and diesel fuels at elevated temperatures and pressures. The surface tension varied linearly with temperatures as well as with pressures.

Section 7.5 includes the measurement of viscosity of biodiesel and diesel fuels at elevated temperatures and pressures measured using a ViscoScope viscometer. The change of viscosity with temperature followed modified Andrade Equation. The change of viscosities with pressure was also measured for three biodiesel and diesel fuels.

The next chapter includes the discussion of experimental results.

CHAPTER 8 DISCUSSION OF EXPERIMENTAL RESULTS

8.1 SUSTAINABILITY EVALUATION OF ENERGY SYSTEMS IN NEPAL

Micro hydro projects and biodiesel fuel production were evaluated as sustainable energy systems in Nepal. The micro hydro projects were evaluated based on the real project data. The evaluation of jatropha biodiesel was based on theoretical analysis as there are no life cycle data available for jatropha biodiesel production in Nepal. The sustainability evaluation was carried out for generally accepted indicators such as environmental, social and economics. The sustainability analysis of micro hydro projects showed that micro hydro projects are sustainable at least locally. The biodiesel production from jatropha on the other hand has also been considered to be sustainable as any amount of biodiesel production would reduce import of oil from abroad, savings hard earned dollars. Biodiesel production locally would also reduce the environmental impact created from the processing and transportation of diesel from India. The production and use of biodiesel would have less environmental impacts compared to that of diesel. The biodiesel production would also create some economic and job opportunities enhancing the local economy. Hence, promotion of both micro hydro projects and biodiesel production would contribute towards sustainable energy development in Nepal.

8.2 POTENTIAL OF BIODIESEL PRODUCTION FROM WASTE COOKING OIL

The waste cooking oil survey showed that based on the generation current level of waste cooking oil, there is a very little feasibility for a biodiesel plant in the studied area. The diverse use of currently generated waste cooking oil and relatively small amount generated contributes to this conclusion. However, the research should be expanded to the neighboring towns to see if more oil can be collected for a plant to be feasible.

8.3 BIODIESEL FUEL PRODUCTION AND CHARACTERIZATION

8.3.1 Oil Content, Transesterification and Fatty Acid Analysis of Biodiesel Feedstocks

The oil content analysis from jatropha seeds collected from Nepal was found to be approximately 28%. Due to the unavailability of jatropha oil from Nepal at the time of testing, jatropha oil was imported from India for fuel characterization and fuel atomization tests. Kumar and Sharma (2008) reported that the kernels of jatropha yield 46–58% of oil by weight. Koh and Ghazi (2011) recently reported the variation of oil content in jatropha in the range of 50-60%.

The soapnut (s.mukorossi) seeds from Nepal were found to have 30% oil content by weight. Ucciani et al. (1994) reported that the oil content in S. trifoliatus which is very similar to S. mukorossi seed kernels was on average 51.8% of seed weight. Misra and Murthy (2011) in a report stated that the soapnut seed (s.mukorossi) they tested had approximately 23% oil content by weight. The oil content result for a particular seed varies as the specie varieties change, the climatic conditions change and extraction methodology used. Sims et al. (1993) reported that increased water led to decreased oil content in the case of canola seed. Also, an increased nitrogen content in canola farming decreased the oil content (Taylor et al., 1991). Hence, various factors including water, nitrogen content in the soil, and altitude may affect the oil content in particular plant seeds.

A single stage base catalyst transesterifiction was carried out to prepare biodiesel from canola oil. Lee et al. (2009) reported that the use of base catalyst requires less methanol and the reaction is faster. Industrial processes usually favor base catalysts compared to acid catalysts because they are less corrosive than acidic catalyst. In base catalyst transesterification, the first step produces an alkoxide ion (RO^-) through proton extraction from the alcohol by the base catalyst, and metallic elements of alkaline oxides react with triglycerides from the liquid phase (Di Serio et al., 2008). In this work, it was found that

approximately 20-25 minutes of reaction was sufficient to complete the conversion of oil into biodiesel esters.

Two stage process was employed for waste cooking oil, jatropha and soapnut oils because of their higher free fatty acid content. Waste cooking oil, jatropha and soapnut oil used in this experiment was found to have 6.5%, 14.5% and 17.5% free fatty acids respectively. Sulfuric acid was used for acid catalyst sesterification process. In all cases, sodium hydroxide was used in the base catalyst transesterification process. Tiwari et al. (2007) reported a pretreatment with acid catalyst was required for jatropha oil with 14% free fatty acid. H_2SO_4 was used for esterification in the first stage with methanol oil ratio 6:1. NaOH was used in the second stage, as a base catalyzed transesterification using approximately 1% NaOH by weight. The actual catalyst content was found by titration for each oil sample. Ramadhas et al.(2005) carried out tests with rubber seed oil with 17% free fatty acids and reported that if the free fatty acid of oil is greater than 2%, the biodiesel yield is significantly reduced. Hence to bring down the free fatty acid level to lower lever where yield is maximized, acid treatment is required. Canakci and Van Gerpan (1999; 2001) found that transesterification would not occur efficiently if FFA content in the oil were above 3%.

Fatty acid contents were analyzed in GC for the biodiesel derived from canola oil biodiesel. Biodiesel derived from canola oil contained 60.28% oleic acid followed by 20.02% linoleic acid, 8.73% linolenic acid, 4.77% palmitic acid, 1.97% stearic acid, 1.28% ecosenoic acid and rest the others. This is very similar to the fatty acid content for canola biodiesel reported by Lang et al. (2001).

Biodiesel derived from waste cooking oil from this work was found to have oleic acid (59.7%) followed by linoleic acid (19.31%), linolenic acid (6.82%), palmitic acid (5.18%), stearic acid (2.1%), ecosenoic acid (1.21%) and rest the others. This result differed significantly from the fatty acid content reported by Issariyakul et al., (2007). This was possibly due to the fact that all waste cooking oils usually come from a variety of feedstocks and are exposed to different cooking environment. Approximately 60% of

the fatty acids were found to be mono-unsaturated (C18:1) in the waste cooking oil biodiesel. Poly-unsaturated fatty acids were found to be approximately 26% (C18:2, C18:3). Only approximately 8% fatty acids were saturated. Palmitic acid and stearic acid were the major saturated fatty acids found in our waste cooking oil ethyl ester. Over 4% of the products were unidentified. The amount and type of fatty acid content in the biodiesel are the major factors that determine the viscosity of biodiesel. The qualitative and quantitative analysis of fatty acid content is comparable with the study reported by Issariyakul et al. (2007) for waste cooking oils. The amount of oleic acid content in biodiesel from waste cooking oil was also found comparable with the amount of oleic acid content in peanut oil (53-71%) as summarized by Allen (1998). Similarly, jatropha biodiesel was found to have 47.79% oleic acid, 32.27% linoleic acid, 13.37% palmitic acid, 5.43% stearic acid and 1.93% others. Palmitic and stearic acid were the major saturated fatty acids found in jatropha oil. The total unsaturated fatty acid content in jatropha oil was found to be approximately 80%. Gubitz et al. (1999) reported a similar fatty acid profile for jatropha oil.

Soapnut oil was found to have 52.64 % oleic acid, 23.85% eicosenic acid followed by 7.02% arachidic acid, 4.73% linoleic acid, 4.67% palmitic acid, 1.94% alpha or gamma-linolenic acid, 1.45% stearic acid, 1.09% erucic acid and the rest others. Soapnut biodiesel was found to contain approximately 15% of saturated fatty acids, 77% monounsaturated fatty acids, and rest polyunsaturated fatty acids totaling altogether approximately 85% unsaturated fatty acids. Misra and Murthy (2011) recently carried out fatty acid analysis of soapnut oil in India and reported to have 62.8 % oleic acid, 22.4% eicosenic acid, 4.6% linolenic acid, 4.4 % arachidic acid, 4% palmitic acid, 1.6% linolenic acid and 0.2% stearic acid. The oleic acid reported by them was approximately 10% higher than the result obtained in this work of which the sample was brought from Nepal. There could be various reasons for this difference including climatic effects as well as variety of soapnut seeds used to extract oil.

Compared to the biodiesel from other seed oil such as rapeseed oil, soybean oil and sunflower oil, some fatty acids in soapnut oil biodiesel were found to have a different

composition while some fatty acids were found similar (Figure 8.1). For example, the palmitic acid content of soapnut oil biodiesel (4.67%) was found comparable to that of rapeseed biodiesel (3.6%) and sunflower oil biodiesel (6.4%), while soybean oil biodiesel had a higher amount of palmitic acid (11%). Oleic acid (62.8 %) was found to be in highest quantity in soapnut oil biodiesel. Eicosenic acid was found in soapnut biodiesel at a significant amount (23.85%). Palmitoleic acid content was found in traces (0.37%) in soapnut oil biodiesel but did not exist in rapeseed, soybean and sunflower oil biodiesel. In summary, the fatty acid profile of the soapnut oil biodiesel differs to other fatty acid content of oils. As most of the other biodiesel feedstocks, soapnut oil also has high oleic acid content.

Table 8.1 FA content of soapnut biodiesel compared to rapeseed, soybean and sunflower oils

FA	**Structure**	**Amount (%)**			
		Soapnut	Rapeseed[a]	Soybean[a]	Sunflower[b]
Palmitic acid	16:00	4.67	3.6	11	6.4
Patmitoleic acid	16:01	0.37			
Stearic acid	18:00	1.45	1.5	4	4.5
Oleic acid	18:01	52.64	61.6	23.4	24.9
Linoleic acid	18:02	4.73	21.7	53.2	63.8
Alpha or gamma-linolenic acid	18:03	1.94	9.6	7.8	Traces
Arachidic acid	20:00	7.02	-	-	
Eicosenic /Gadoleic acid	20:01	23.85	1.4		
Behenic acid	22:00	1.45	-	-	
Erucic acid	22:01	1.09			
Lignoceric acid	24:00	0.47			
Others		0.32	0.2	traces	Traces
Total		100	100	100	100

*[a]Gunstone and Harwood, 2007; [b]Rashid et al., 2008. *Note: Carbon number with 'zero' double bonds are saturated fatty aids, with 'one' double bonds are monosaturated and with 'two' and 'three' double bonds are polyunsaturated FA.*

The biodiesel samples used in this work were repeatedly heated and cooled during the density, surface tension and viscosity measurement and hence it was of great interest to know whether the heating from 293 to 533 K would cause any significant changes in the fatty acid composition. The biodiesel samples of jatropha and soapnut used in the

experiment were analyzed in the GC. Tables 8.2 and 8.3 show the GC analysis of jatropha and soapnut before and after the exposure to heat between 293K to 533K. The fatty acid content was found to differ slightly before and after exposure to the heat. One of the reasons for such difference was that jatropha sample studied for fatty acid content at the beginning of this work was brought from Nepal and was tested to know the fatty acid content. The jatropha oil used to produce the biodiesel was brought from India. The small difference is an indication that the fatty acid content does not change much either in location or after exposure to heat up to 533 K. Moreover, Tate (2005) carried out tests for biodiesel methyl ester heating from 293K to 593K to see if the fatty acid content changes. The study indicated that there was no change in fatty acid composition of the biodiesel sample even though it was observed that the color of biodiesel became dark or red depending on feedstock type.

Table 8.2 Fatty acid composition of jatropha biodiesel before and after heating to 533K

FA type	Structure	FA Content Before Heating (%)	FA Content After Heating (%)
Lauric acid	12:00	0.31	0.06
Palmitic acid	16:00	13.38	14.32
Patmitoleic acid	16:01	0.88	0.84
Stearic acid	18:00	5.44	6.87
Oleic acid	18:01	45.79	44.47
Linoleic acid	18:02	32.27	32.42
Others		1.93	1.02
Total		100	100

Table 8.3 Fatty acid composition of soapnut biodiesel before and after heating to 523 K

FA	Structure	FA Content Before Heating (%)	FA Content After Heating (%)
Palmitic acid	16:00	4.67	4.39
Patmitoleic acid	16:01	0.37	0.37
Stearic acid	18:00	1.45	1.67
Oleic acid	18:01	52.64	55.22
Linoleic acid	18:02	4.73	6.25
Alpha or gamma-linolenic acid	18:03	1.94	1.1
Arachidic acid	20:00	7.02	6.83
Eicosenic acid	20:01	23.85	21.44
Behenic acid	22:00	1.45	1.22
Erucic acid	22:01	1.09	0.98
Lignoceric acid	24:00	0.47	0.32
Others		0.32	0.21
Total		100	100

8.3.2 Biodiesel Conversion Efficiency

The average overall conversion efficiency of 92.4% was achieved for canola oil ethyl ester during base catalyst reaction. The efficiency was estimated based on the Iatroscan analysis of the ester after the reaction was considered complete. The conversion might have been overstated because the samples after taking out from the reactor at fixed time intervals were not neutralized. Further reaction might have occurred after the sample was taken because of the fact that the sample still contains some catalyst and heat.

The waste cooking oil yield was found to be approximately 94%. Issariyakul et al. (2007) reported the ethyl ester conversion of waste cooking oil to be up to 97%. Leung and Gau (2006) reported that the conversion of waste cooking oil using sodium hydroxide catalysts was approximately 86%. Zheng et al. (2006) showed that methyl ester conversion of waste cooking oil in acid catalyzed transesterification could reach up to

99%. The variation in ester yield could be due to several reasons including the samples with different fatty acids, different reaction conditions, presence of some water and the alcohol.

The biodiesel yield for jatropha oil after 20 minutes of the base catalyst reaction was approximately 99%. This time does not include the time taken by acid catalyst esterification. For acid catalyst esterification, the time depends on the amount of free fatty acid content and the methanol to oil ratio used during esterification. Tiwari et al. (2007) reported that they achieved 99% conversion to methyl esters from jatropha oil using two stage transesterification. Similar two stage transesterification was employed for soapnut oil biodiesel. The soapnut oil transesterification resulted in approximately 98% conversion after 20 minutes of reaction. This oil was treated with H_2SO_4 before carrying out base catalyst reaction.

8.3.3 Fuel Characterization of Biodiesel Products

Biodiesel esters produced from canola, waste cooking oil, jatropha and soapnut were tested for their fuel characteristics to meet the recommended fuel quality standard. Table 8.4 summarizes the fuel characteristics test results compared with ASTM or EN standards.

Table 8.4 Fuel characterization for different biodiesel fuels

Test name	**ASTM Limit**	**Canola biodiesel**	**WCO biodiesel**	**Jatropha Bio diesel**	**Soapnut biodiesel**
Free Glycerine (%mass)	Max 0.020	0.038	0.022	0.006	0.004
Monoglycerides (mass %)	N/A	0.350	0.293	0.074	0.052
Diglycerides (mass %)	N/A	0.353	0.19	0.019	0.044
Triglycerides (mass %)	N/A	0.445	0.061	0.005	0.087
Total Glycerin (mass %)	Max 0.240	1.186	0.566	0.104	0.187
Flash Point, Closed Cup (K)	Min 403	449	437	433	381
Methanol Content (wt %)	Max 0.20			0.024	0.024
Phosphorous (ppm)	Max 10	5	2	2	0
Calcium+magnesium (ppm)	EN 1.0	1	1	Not measured	Not measured
Sodium and potassium (ppm)	EN 5	117	66	Not measured	Not measured
Water & sediment (vol %)	Max 0.050	0	0	0	0
Sulfur, by UV (ppm)	Max 15	1	2	6	7
TAN (mg KOH/g)	Max 0.80	0.3	0.29	0.15	0.18
Viscosity @ 313 K(mm^2/s)	1.9 - 6.0	5.36	5.03	4.20	5.04
Cloud Point (K)	N/A	273	272	275	278
Cetane Index	Min 47	61	61	58	64
API Gravity @ 288.6 K (°API)	N/A				31.5
Pour Point (K)	N/A	250	257		284

The test results from canola oil ethyl ester showed that the total and free glycerin content in the sample exceeded the ASTM allowable limit. The ASTM free and total glycerin allowable limits are 0.02 and 0.24 % by mass respectively whereas the experimental results were found to be 0.038 and 1.186 % by mass respectively. The sodium and potassium content from the test was found to be 117 against EN standards of 5 ppm.

Similarly, waste cooking oil biodiesel was also found to have exceeded the free and total glycerin and sodium and potassium content in the product. After careful review of the impurities from the results and related literatures, it was suspected that insufficient cleaning and washing could have contributed for impurities. While producing biodiesel from jatropha and soapnut, the washing was carried out by using warm water of approximately 333 K and the number of washes was also increased. Kemp (2006) and Issariyakul et al., (2007) recommended that hot water wash can help to reduce the total glycerin content and catalyst content of the biodiesel. In order to reduce the catalyst concentration, a few drops of acetic acid was also added until the pH was measured to be close to 7. The free and the total glycerin for jatropha biodiesel were 0.006 and 0.104 % and that for soapnut biodiesel were 0.040% and 0.187 % which were within the ASTM recommended limit.

To remove the glycerin impurity, commercial glycerin was poured from the top of the flask which helped to settle the glycerin to the bottom of the flash. Issariyakul et al. (2007) reported that the glycerin phase in the case of waste cooking oil was difficult to separate only by gravity and free and total glycerin was completely removed by adding the pure glycerin in the sample. With such measures, the biodiesel produced from jatropha and soapnut met all ASTM requirements of fuel quality standard in the Table 8.3.4. As an exception, the flash point of soapnut oil was less than the recommended values. In principle, if the flash point of the biodiesel does not meet the ASTM requirement, methanol content of the fuel should be tested. High methanol content in the fuel could lower the flash point significantly depending on the amount of methanol present in it. In this case, methanol content of the soapnut oil biodiesel was found to be within the limit recommended by ASTM and was concluded that the methanol was not the reason to lower the flash point. The flash points of all other fuels were found to be higher than the value suggested by ASTM. The ASTM allowable limit for water and sediment content is 0.05% by volume. In this work, the water content of all the biodiesel samples were found to be zero and no sediments were reported.

The total acid number (TAN) for canola, waste cooking oil, jatropha and soapnut biodiesel were 0.3, 0.29, 0.15 and 0.18 mgKOH/g respectively. The ASTM standard for acid value (acid number) for pure biodiesel is 0.8 mgKOH/g. Lang et al. (2001) reported that the acid value of ethyl ester of for linseed oil, canola oil, sunflower oil and rapeseed oil were 0.884, 0.869, 0.876 and 0.873 mgKOH/g respectively. This can further be improved by controlling the transesterification process, cleaning and drying. High acid values on the feedstock indicate unrefined or poorly refined product oil source due to poor process control, such as ethanol carry over. Fuel with a high acid number could also cause degradation of rubber parts in older engines resulting in filter clogging etc.

The viscosity of the canola, waste cooking oil, jatropha and soapnut biodiesel were found to be 5.36, 5.03, 4.20 and 5.04 mm^2/s at313 K. ASTM D445 recommends that the viscosity at 4313 K should be between 1.9-6.0 mm^2/s. The viscosities of all samples were within the ASTM recommended values. ASTM D4951 requires that the phosphorus content of the biodiesel fuel should not exceed 10 ppm. The phosphorus content of canola, waste cooking oil, jatropha and soapnut oil biodiesel were found to be 5, 2, 2, and 0 pm respectively.

The cloud point of ethyl ester produced from canola oil, waste cooking oil, jatropha and soapnut oil were 272, 272, 275 and 278 K respectively. Lang et al. (2001) reported the cloud point of ethyl esters of linseed oil, canola, sunflower and rapeseed oil were 271 K, 272 K, 271 K and 271 K respectively whereas the corresponding methyl esters had cloud point 273 K, 274 K, 274 K and 273 K respectively. The cloud point of ethyl esters were approximately 2 K lower than those of the corresponding methyl esters. This indicates that the ethyl esters marginally perform better in cold temperatures than the corresponding methyl esters. The pour point of canola, waste cooking oil and soapnut biodiesel was found to be 250 K, 257 K and 284K respectively. As reported by Lang et al. (2001), the pour point of ethyl esters of linseed oil, canola, sunflower and rapeseed oil were 267 K, 267 K, 268 K and 258 K respectively where the methyl esters of corresponding oils were reported to be 264 K, 264 K, 265 K and 256 K respectively. Lee et al. (1995) argued that the cloud point were affected by the presence of monoglycerides,

however, the pour points were not affected. Moreover, the cis double bond present in the erucic acid of rapeseed oil hampered the lowering of the pour point of esters.
The sulfur content of canola, waste cooking oil, jatropha and soapnut biodiesel were 1, 2, 6 and 7 ppm respectively. Biodiesel fuels contain significantly less sulfur than petroleum diesel fuels, which is one of the advantages of biodiesel over fossil fuels. The cetane index of biodiesel from canola, waste cooking oil, jatropha oil and soapnut oil are 61, 61, 58 and 64 respectively. For all the samples, the cetane index results exceeded the ASTM requirements. Hilber et al. (2006) reported the cetane number of methyl ester from rapeseed oil, soybean oil, palm oil, lard and beef tallow to be 58, 53, 65, 65 and 75 respectively.

8.4 DISCUSSION ON DENSITY RESULTS

There are limited number of studies carried out to determine the densities of biodiesel feedstocks at elevated temperature and pressures. Some studies were carried out at high pressure only and some studies were done for temperatures up to 373 K. Tat and Van Gerpen (2000) measured the specific gravity of biodiesel up to 373 K and developed a linear relationship in terms of temperature as, SG= a+bT, where SG is specific gravity, T is the temperature in ^{o}C and a and b are the constants depending on % of biodiesel concentration in the blend specific gravity is defined as the ratio of density of liquid or solid substance to the density of water at 277.15 K and 1 atmospheric pressure. They performed regression on their data and found a linear equation to predict the density of biodiesel as, $\rho=1077.82-662 \times T$. In the equation, ρ is the density in kg/m^3 and T is the temperature in K.

Tate (2005) carried out the density tests using capacitance type densitometer for canola, soybean and fish oil biodiesel up to 573 K and derived a relationship expressed in terms of depth of submergence of capacitance as a function of frequency and temperature. The variations in the depth of submergence of capacitor are proportional to the volume of liquid of which the density is to be determined and the density of liquid. The density was

determined from the regression of the experimental data. Tate et al. (2006) measured the density of canola, soybean and fish oil biodiesel between 273 and 573 K and found a relationship in a linear form after regression. The canola biodiesel density decreased from 851.44 kg/m^3 at 293 K to 537.23 kg/m^3 at 573 K. Similarly, the density of soy biodiesel and fish-oil biodiesel decreased from 834.16 and 841.46 kg/m^3 at 293 K to 519.10 kg/m^3 and 511.81 kg/m^3 respectively. Joshi (2007) carried out the tests to determine the density of canola biodiesel fuel up to 573 K and 6.9 MPa. The density of canola biodiesel decreased from 882.86 kg/m^3 at 293 K to 730.02 kg/m^3 at 573 K at atmospheric pressures. Similarly, at 6.9 MPa, canola biodiesel density decreased from 886.57 kg/m^3 at 293 K to 735.50 kg/m^3 at 573 K.

Alptekin and Canakci (2008) also carried out density tests of different biodiesel made of soybean oil, waste palm oil, sunflower oil, corn oil, canola oil, and cottonseed and suggested a first degree empirical equation relating the density of biodiesel blend with percentage of biodiesel used for the tests. The empirical equation they proposed for density was, $\rho = Ax + B$, where ρ is the density of biodiesel, A and B are the constants that vary with the type of biodiesel and x is the biodiesel fraction. Blagino et al. (2008) carried out density experiment for the biodiesel at temperatures between 273-373 K and found that the density data well fitted by a linear equation up to 373 K. They developed a regression equation from their experimental data with R^2 value of 0.999 as, $\rho = -0.673 \times T + 1084.23$, where ρ is the density in kg/m^3 and T is the temperature in K. Baroitian et al. (2008) carried out the density tests for biodiesel using Rackett equation modified by Spencer and Danner (1972), where ρ_R is the reference density, Z_{RA} is the Rackett compressibility factor, ϕ is calculated using the ratio of temperature and critical temperature. The density calculated using this equation was found to behave as a linear function.

Feitosa et al. (2010) studied the densities of coconut, colza and soybean biodiesels between 293.15 to 373.15 K at atmospheric pressure. They found that the densities of coconut biodiesel decreased from 870.9 kg/m^3 at 293.15 to 809.3 k/m^3 at 343.15 K. The densities of colza decreased from 884.6 kg/m^3 at 293.5 K to 824.8 k/m^3 at 343.15 K.

Similarly, the densities for soybean biodiesel decreased from 885.3 kg/m^3 at 293.15 to 827.2 kg/m^3 at 343.15 K. Nogueira et al. (2010) measured the density of cotton seed, soybean and babassu biodiesel between 293.15 to 373.15 K at atmospheric pressure. The density of cotton seed biodiesel decreased from 881.6 kg/m^3 at 293.15 K to 823.4 kg/m^3 at 373.15 K. The soybean oil density decreased from 885.6 kg/m^3 at 293.15 to 828.0 kg/m^3 at 373.15 K. Similarly, for babassu biodiesel, the density decreased from 876.2 kg/m^3 at 293.15 K to 814.6 kg/m^3 at 373.15. The density showed a linear trend with temperature.

Payri et al. (2011) carried out density measurement of some conventional diesel (reference fuel), rapeseed biodiesel and arctic fuel (fuel used in winter season in Spain) from 298 to 348 K and developed an empirical equation based on the measured data. The empirical equation was developed as a non-linear fit and is presented in the Table 8.3.5, where p_o is the initial pressure, T is the temperature in K, and ρ is the density, C_1, C_2, C_3, C_4 are the non-linear constants. The density of diesel, rapeseed biodiesel and arctic fuel at 313 K and atmospheric pressure were 825, 863, 812 kg/m^3 respectively.

Pratas et al. (2011) measured the densities of three biodiesel up to 45 MPa and 333.15 K. The densities were found to increase linearly with increase in pressure. The densities of rapeseed and palm biodiesel decreased from 885 kg/m^3 at 283.15 K to 848.2 kg/m^3 at 333.15 K at atmospheric pressure. The density on the other hand increased from 885 kg/m^3 to 907.4 kg/m^3 from 0.101 MPa to 45 MPa at 283.15 K. Similarly, the density of soybean biodiesel was found to decrease from 893.2 kg/m^3 at 283.15 K to 857.1 kg/m^3 at 333.15 K at atmospheric pressure. The density of soybean biodiesel increased from 893.6 kg/m^3 at 0.101 MPa to 916 kg/m^3 at at 45 MPa at 283.15 K. Ramírez-Verduzco et al. (2011) used mixtures of biodiesel and ultra low sulfur diesel to study the variation of density (ρ) as a function of percent volume (V) and temperature (T). The experimental measurements were carried out for six biodiesel blends at nine temperatures in the range of 293–373K. The densities increased because of the increase in the concentration of biodiesel in the blend, and both of them decrease as temperature increases.

Table 8.5 shows the summary of different studies done previously as well as the regression equation developed using the experimental data from this work.

Table 8.5 Regression equations from previous studies

Temperature	Regression Equation	References
Up to 373 K	Specific gravity (SG)= a+bT	Tat and Van Gerpen (1999)
	ρ = 1076 -650 T.	Tat and Van Gerpen (2000)
293- 573 K	P = mT + b	Tate et al. (2006)
273-373 K	ρ = -0.673 × T +1084.23	Blagino et al. (2008)
290-360 K	ρ = -0.69 T +1075	Tesfa et al. (2010)
290-360 K	ρ (diesel) = -0.657 T +1051	Tesfa et al. (2010)
293-373 K	$\rho = A_o + A_1 T$	Nogueira et al.(2010)
298-343 K	ρ (p, T)= ρ (p_o, T) + $\int_{p_o}^{p} \frac{dp}{(C_1+C_2p+C_3P^2+C_4p^3)2}$	Payri et al.(2011)
283-333 K	ρ (T, p=0.1 MPa)= $a_1+a_2T+a_3T^2$	Pratas et al. (2011)
293-373 K	$\rho = \alpha \cdot V + \beta \cdot T + \delta$	Ramírez-Verduzco et a. (2011)
293-523 K	ρ (Canola biodiesel) = 1076 + 0.00421 P - 0.650 T	This work
293-523 K	ρ (Jatropha biodiesel) = 1037 + 0.00488 P - 0.547 T	This work
293-523 K	ρ (Soapnut biodiesel) = 1071 + 0.00580 P - 0.653 T	This work
293-523 K	ρ (diesel) = 1036 + 0.00423 P - 0.643 T	This work

The densities of diesel, canola biodiesel, jatropha biodiesel and soapnut biodiesel were calculated using the capacitance measured by capacitance type densitometer as described in Figure 6.4 in Chapter 6. The capacitance was measured in terms of frequency. The density was calculated by measuring the capacitance of the biodiesel and diesel fuels. For all the temperatures and pressures, the average of three frequency readings were used to calculate the densities of all fuels tested. MINITAB was used for regression analysis of the calculated density. The model developed from regression of the calculated density data were used to predict the densities at elevated temperatures and pressures for all fuels

tested. The measured and regressed densities are in good agreement for the three biodiesel fuels and diesel.

The density of the three biodiesels and diesel fuel were also measured using hydrometer. Figure 8.1 shows the densities of three biodiesel fuels and diesel measured using hydrometer and capacitance type densitometer. The densities measured using hydrometer and capacitance type densitometer was found to differ each other by 1.24, 0.72, 0.38 and 0.03 % for canola, jatropha, soapnut biodiesel and diesel respectively.

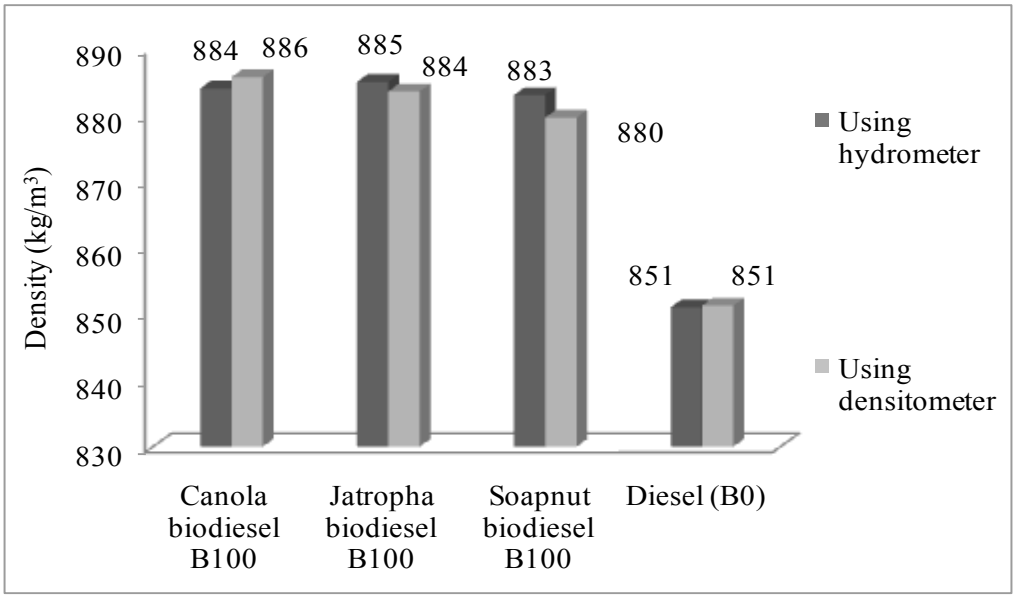

Figure 8.1 Density of three biodiesels and diesel measured using hydrometer and capacitance type densitometer

The results of the experiments for canola biodiesel were compared with previous studies. Figure 8.2 shows the canola biodiesel densities from previous studied as well as from this work. Tate (2005) carried out density experiment using capacitance type densitometer between 293 to 573 K and the densities were reported to vary from 851 kg/m^3 at 293 K and 537 kg/m^3 at 573 K. This result was found to have the lowest slope of all the other studies compared here. Joshi (2007) also measured density of canola biodiesel using capacitance type densitometer and reported that the densities for canola decreased from 883 kg/m^3 at 293 K to 730 kg/m^3 at 473 K at atmospheric pressure. In this work, canola

density was found to decrease from 886 kg/m^3 at 295 K to 722 kg/m^3 at 523 K at atmospheric pressure. Table 8.6 shows the regression coefficients of the densities from different studies presented in the Figure 8.2.

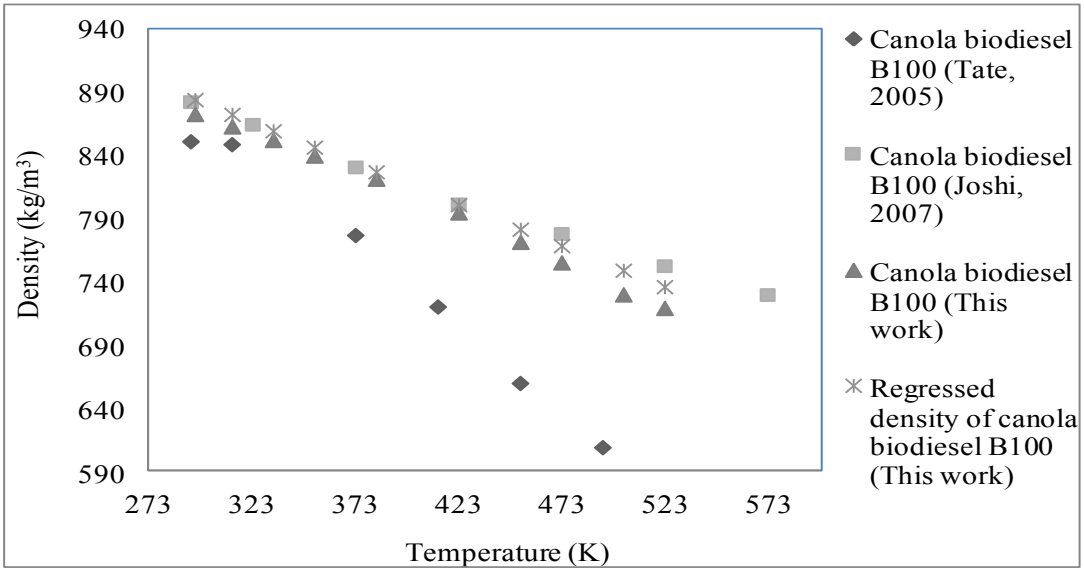

Figure 8.2 Densities of canola biodiesel B100 from this work compared with the results from Joshi (2007) and Tate (2005)

Table 8.6 Regression coefficients from different experiments for canola biodiesel B100

Fuel Type	**Slope (kg/m^3/K)**	**Intercept (kg/m^3/K)**	**R^2**
Canola biodiesel B100 (Tate, 2005)	-1.19	1211.5	0.993
Canola biodiesel B100 (Joshi, 2007)	-0.548	1039.2	0.995
Canola biodiesel B100 (This work)	-0.687	1080.8	0.996
Regressed Canola biodiesel B100 (This work)	-0.650	1076.3	1.000

There were no data available in the literature to compare the jatropha and soapnut biodiesel density results at elevated temperatures and pressures. However, the densities

showed similar values to those of canola, soybean and other biodiesel fuels. The variation in fatty acid compositions of the three biodiesel fuels used in these experiments did not show a significant variation in their densities. A regression model with temperature and pressure parameters was developed based on the measured density data. The measured density data were regressed for diesel and all three biodiesel fuels. The maximum relative errors for measured and regressed densities of diesel and canola, jatropha and soapnut biodiesel B100 were 2.64%, 1.88%, 2.95% and 2.38% respectively (Tables D.2, D.4, D.17 and D.29).

The densities of all three biodiesel fuel blends B80, B50 and B20 were predicted using the Kay's mixing rule and were compared with the measured densities. Kay's mixing rule works in agreement with less than 5% error with predicted data for canola, jatropha and soapnut biodiesel blends.

Some previous studies (Yuan et al., 2003; Rodrigues et al., 2006; Pratas et al. 2010) have reported that the densities of biodiesel are also affected by the fatty acid composition. This is confirmed in this work, where neither the fatty acid composition of the three biodiesel fuels nor the experimental density values obtained were significantly different.

8.5 SURFACE TENSION OF BIODIESEL FUELS

8.5.1 Surface Tensions of Canola Biodiesel

Surface tension of canola biodiesel B100 was measured. The canola biodiesel surface tension values were also compared with the results of previous studies. The surface tensions of liquids decrease with increasing temperatures and become zero when they reach the critical temperature (Vavruch, 1995). The experimental results of canola biodiesel surface tension values were found to have a linear relationship with temperature. Chunsheng and Chongli (2004) predicted the surface tension of 209 pure liquids. This method was independent of the density of liquid. The critical temperature and connectivity indices were used as an input to the model and the prediction was

carried out up to 400 K. The predicted model showed that the surface tension decreased linearly with temperature. The surface tension results from this work for canola oil biodiesel also decreased linearly with increased temperature. Yuan et al. (2003) predicted the surface tension of soybean oil biodiesel B100 and found the trend to be approximately linear. The surface tension of biodiesel was predicted from 280 K to critical temperature (760 K).

Figure 8.3 shows canola oil biodiesel B100 surface tension measured and obtained from regression in this work. The values were compared with the surface tension value measured by Joshi (2007) at atmospheric pressure.

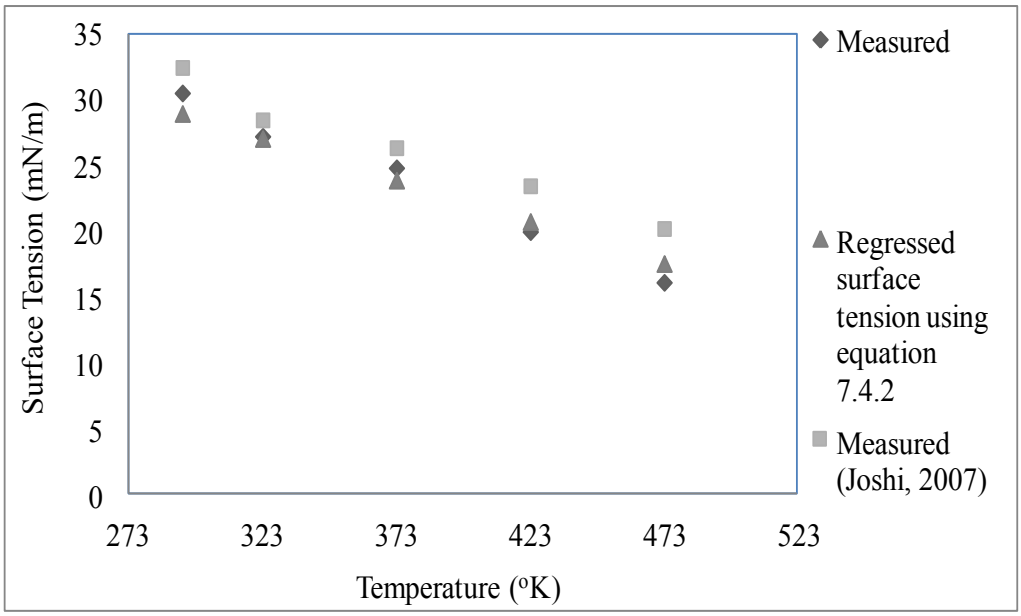

Figure 8.3 Comparison of measured surface tension for canola B100 at atmospheric pressure and predicted value using equation 7.8

The measured and regressed values of surface tension at room temperature were found to be 30.56 mN/m and 29.01 mN/m respectively while the value obtained by Joshi (2007) was 32.56 mN/m. Similarly, at elevated temperature (473 K), the measured and regressed surface tensions were 16.15 and 17.58 mN/m respectively, while the value obtained by Joshi (2007) was 20.25 mN/m. The R^2 value from regression of measured data for this work was found to be 0.990 while Joshi (2007) had an R^2 value of 0.982. There is a high correlation of the measured data in both the cases. Even though the same biodiesel source

was used, the difference between the two data could have occurred due to the different measurement systems. Joshi (2007) used pendant drop analysis using a CCD camera. This work used the Drop Shape Analysis equipment.

Figure 8.4 shows the measured and regressed surface tension for canola B100 at elevated pressure (7.00 MPa). The surface tension values were compared with the results of surface tension measured by Joshi (2007). The measured value from this work and Joshi (2007) differed by 3.84 mN/m at 293 K and 4.33 mN/m at 473 K respectively. The difference probably occurred due to the different methods of measurement as well as difference in density used as surface tension is dependent on the density of the liquid. The maximum absolute error was found to be 1.56 mN/m at 293 K at atmospheric pressure.

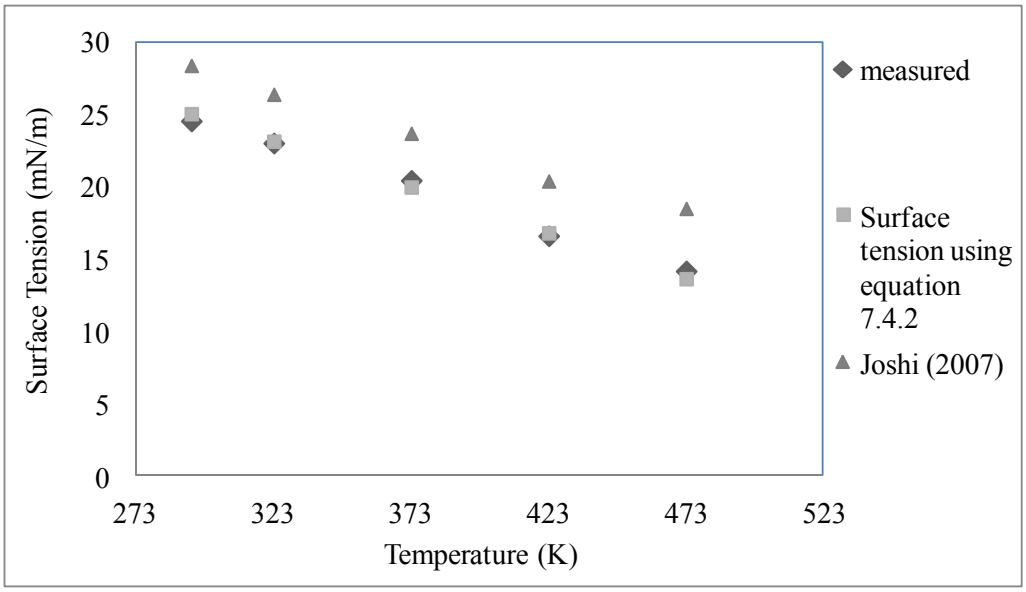

Figure 8.4 Comparison of measured and values of surface tension obtained using equation 7.7 for canola B100 at 7.00 MPa

Tate (2005) measured the surface tension of canola biodiesel using Axisymmetric Drop Shape Analysis and predicted the surface tension using the model employed by Yuan et al. (2003). At 273 K, the measured surface tension value was 28.19 mN/m and predicted surface tension was 22.18 mN/m with an absolute error of 6.00 mN/m in atmospheric pressure. The measured surface tension at 523 K was 11.07 mN/m, the predicted surface

tension was 9.97 mN/m with an absolute error of 1.10 mN/m. The differences found in all predicted values may have occurred due to difference in densities used in each model because the density of pure components were considered to be equal to the density of the mixture. Differences in measured values probably occurred due to the use of different camera and edge detection software.

Shu et al. (2008) calculated the surface tension of five biodiesel fuels including canola oil biodiesel using topological index method at 313 K. The calculated surface tension of canola, peanut, coconut, palm and soybean biodiesel were 28.49, 28.45, 26.23, 27.94, 28.33 mN/m. They compared their calculated surface tension results with Allen et al., (1999) and found that the relative errors were 2.19, 1.18, 0.46, 1.96, and 0.46 % respectively for canola, peanut, coconut, palm and soybean oil biodiesels. Similarly, the surface tension predicted using topological index methods for corn, safflower, sunflower, cottonseed and lard biodiesel were 28.37, 28.36, 28.37, 28.21 and 28.14 mN/m at 313 K respectively.

Ejim et al. (2007) predicted the surface tension of biodiesel from different biodiesel feedstocks. The predicted surface tension at 353 K for canola oil biodiesel B100 at atmospheric pressure was 27.21 (±6.5%) while the surface tension predicted from equation 7.7 from this work was 25.12 mN/m. The same study predicted the surface tension of biodiesel B100 for peanut, rapeseed, canola, coconut, palm, soybean and cottonseed as 26.93 (± 5.9%), 27.82 (± 5.8%), 24.01 (± 5.2%), 26.16 (± 6.0%), 27.15 (± 6.0%) and 26.81 (± 6.2%) respectively. Hence, the measured and regressed surface tensions of canola biodiesel from this work are well within the range reported in the previous studies.

8.5.2 Surface Tension of Jatropha and Soapnut Biodiesel

The surface tension trend for jatropha and soapnut biodiesel and their blends with diesel also showed the similar trends with that of canola biodiesel. Figure 8.5 shows the surface

tension of jatropha biodiesel (B100) and soapnut biodiesel (B100) compared to canola biodiesel B100 and diesel (B0) expressed as a function of temperature at atmospheric pressure. The surface tension of jatropha B100 and soapnut B100 were 30.10 mN/m and 29.50 mN/m at 293 K respectively at atmospheric pressure. At 473 K, the surface tensions for jatropha B100 and soapnut B100 were 17.82 mN/m 16.95 mN/m respectively. Diesel surface tension started at 25.84mN/m at 293 K and decreased to 15.84 mN/m at 473 K. It was found that the surface tensions of jatropha B100 and soapnut B100 had similar values at room temperature and atmospheric pressure.

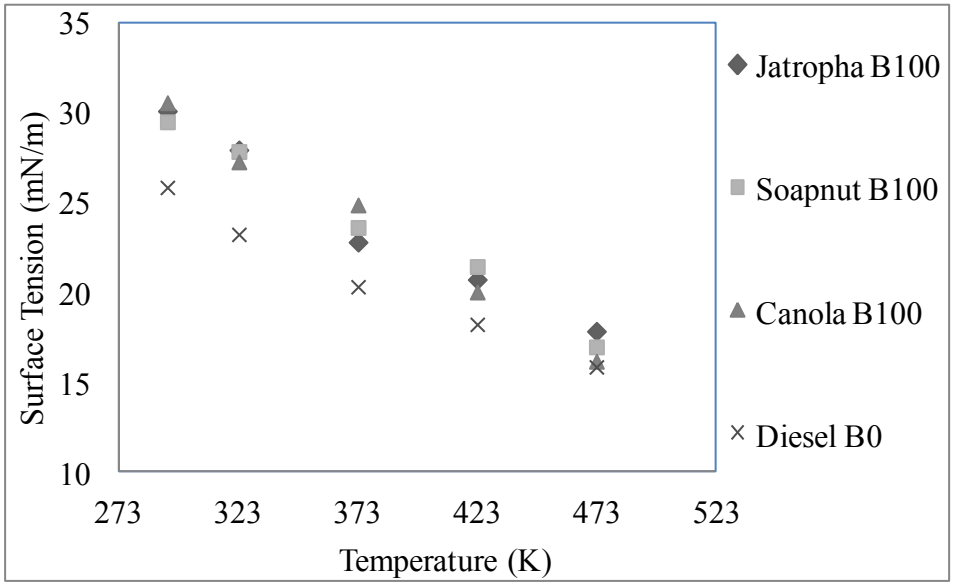

Figure 8.5 Comparison of surface tension results for canola, jatropha, soapnut and diesel fuels as a function of temperature at atmospheric pressure

Blangino at al. (2011) measured the surface tension of biodiesel fuels using standard ASTM D1331 with a Kruss K8 Interfacial Tensiometer with a De Nuoy ring between 293 K and 360 K. The surface tension measured between 293 K and at 360 K showed a linear trend with R^2 values of 0.908. Allen (1998) predicted the surface tension of various biodiesel fuels based on the fatty acid composition at 313 K. The predicted surface tension from Allen (1998) was used to compare the surface tension of jatropha and soapnut biodiesel at 313 K (Figure 8.6). The surface tension of jatropha and soapnut biodiesel at 313 K was also obtained from the regression of measured data. The

difference in the surface tension results may be due to various reasons. First, all the oil feedstock from which the biodiesel were obtained had different fatty acid compositions which may have affected the surface tension. Even in case of the same oil such as canola, the feedstock may have had different fatty acid components. Also, the density plays an important role in surface tension determination. Allen (1998) and Allen et al. (1999) applied their density model at one temperature using a density of 860 kg/m^3 for each saturate component, 870 kg/m^3 for mono-saturate, 880 kg/m^3 for each di-saturate and 890 kg/m^3 for each tri-saturate. The temperature dependency of density for biodiesel fuels was not considered.

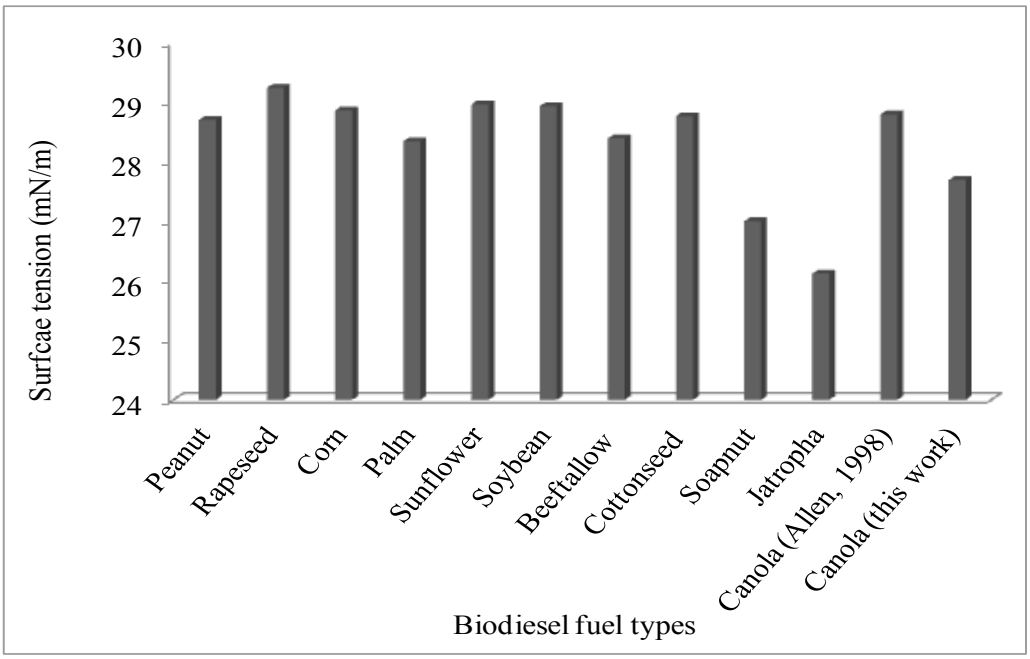

Figure 8.6 Predicted surface tension of different biodiesel fuels at 313 K at atmospheric pressure (combined with Allen, 1998)

The surface tension of jatropha and soapnut oil biodiesel at elevated temperature and pressure were not available in the literature. Soapnut oil was investigated for biodiesel for the first time. However, no data on atomization properties are available for soapnut. As all biodiesel must meet ASTM fuel quality standard, the jatropha and soapnut surface tension results were compared with biodiesel produced using other feedstock. Because the biodiesel, diesel blends were used for measurement, the surface tension of diesel was also measured and compared with data from previous studies. The surface tension of

jatropha and soapnut biodiesel also showed a linear trend as seen in canola and other biodiesel fuels. The surface tension results were found comparable with other biodiesel fuels available in the literature.

8.5.3 Surface Tension of Pure Diesel (B0)

Ahmed et al. (2006) predicted surface tension of diesel No. 2 to be 24.00 mN/m at 313 K. Similarly, Ali et al. (1995) reported the surface tension of diesel No. 2 at 313 K to be 22.5 mN/m. The differences in the surface tension results may have occurred due to different density of diesel used and different measurements techniques. Dechoz and Roze (2004) used the capillary waves generated on the liquid and a He–Ne laser beam reflected at the free surface of the diesel sample located in a pressured chamber and the surface tension is obtained in relation to the pressure for diesel fuel. The measured surface tension reduced from 28.6 mN/m at 293 K to 24.80 mN/m at 328 K. The results showed that the diesel surface tension decreased linearly. The pressure had very little effect in surface tension of diesel because the nitrogen has a very low and slow dissolution in diesel. The surface tension measurements of all liquids were carried out in a nitrogen environment.

In this work, the surface tension data for diesel was found to be reduced from 25.84 mN/m at 293 K to 15.84 mN/m at 448 K at atmospheric pressure. The surface tension decreased from 19.67 mN/m at 293 K to 13.73mN/m at 448 K at 7.00 MPa. The surface tension of diesel at 313 K from linear regression analysis was found to be 24.26 mN/m. The temperature had a greater effect on surface tension compared to pressure. Vavruch (1995) reported that after being heated up to 373 K and pressurized up to 10 MPa, the surface tension value remained constant.

8.6 DISCUSSION ON VISCOSITY OF DIESEL AND BIODIESEL FUELS

The kinematic and dynamic viscosities of diesel for different temperatures at atmospheric pressure are presented in Figure 8.7 below. The kinematic viscosities are higher than the dynamic viscosities. The kinematic viscosity is obtained by dividing the dynamic viscosity by the density as the density of diesel in kg/m^3 is less than unity. The kinematic viscosity of diesel was 3.05 mm^2/s at 296 K and was reduced to 0.26 mm^2/s at 523 K. The viscosity of diesel at 313 K was 2.14 mm^2/s. Alptekin and Canakci (2008) reported the viscosity of normal diesel at 288 K to be 2.71 mm^2/s. Nita et al. (2011) reported the kinematic viscosity of diesel at room temperature to be 3.54 mm^2/s. However, the density of diesel used by Nita et al. (2011) was 0.841 kg/m^3 while the density of the diesel used in this experiment was 0.851 kg/m^3. The difference could have occurred due to the difference in the type of diesel sample with different densities. Each diesel sample may vary in physical properties causing difference in viscosity.

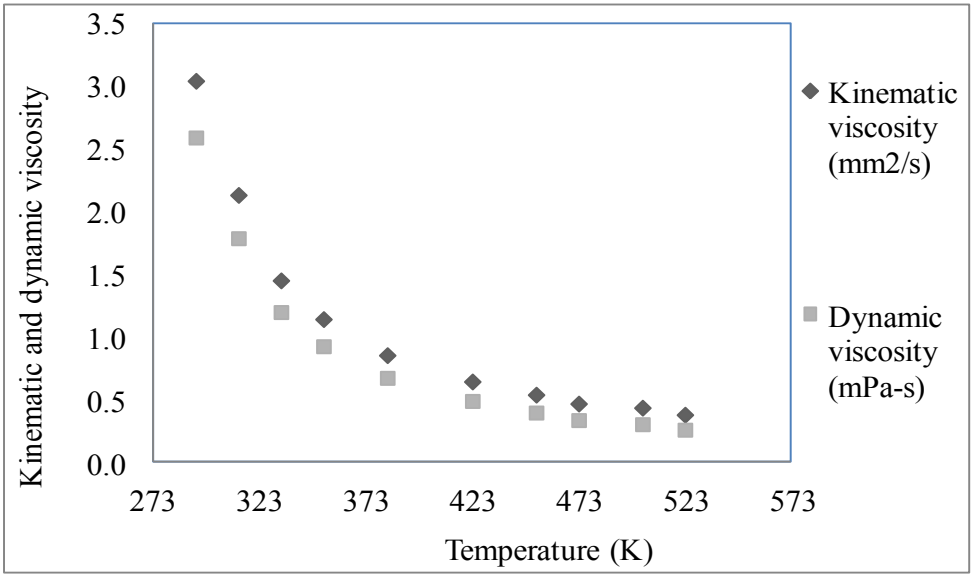

Figure 8.7 Kinematic and dynamic viscosity of diesel at different temperatures at atmospheric pressure

The viscosity of pure biodiesel is higher than the viscosity of diesel. Bhale et al. (2009) reported that the viscosity of biodiesel fuels can be up to 1.6 times the viscosity of diesel fuel. Figure 8.8 shows the dynamic viscosities of canola biodiesel at different temperatures at atmospheric pressure. The dynamic viscosities of canola biodiesel at different temperatures were compared with the dynamic viscosities measured by Tate (2005) and Tate et al. (2006). It was found that the dynamic viscosities in this work were found to be 6.24 mPa-s at 293 K and 4.29 mPa-s at 313 K, which were slightly higher - than the values reported by Tate (2005). The values reported by Tate for 293 K was 5.96 mPa-s and at 313 was 3.90 mPa-s. The dynamic viscosities in this work for temperatures 333, 353, 383, 423, 453, 473, 503 and 523 K were 2.56, 1.87, 1.24, 0.84, 0.68, 0.60, 0.45 and 0.35 mPa-s respectively. The values reported by Tate (2005) for temperatures 373, 413, 453, 493, 533 and 573 K were 1.63, 1.17, 0.84, 0.61, 0.51, and 0.47 mPa-s respectively. For all temperatures between 313 K and 523 K, the dynamic viscosities found in this work were lower than the values reported by Tate (2005). However, the values were fairly comparable with those values. The difference could have occurred due to the difference in density values used to calculate the dynamic viscosities. Some differences might have occurred due to different accuracies of the equipment used for

these tests. The modified Saybolt viscometer had a repeatability of 2%. The accuracy of the ViscoScope viscometer ±2%.

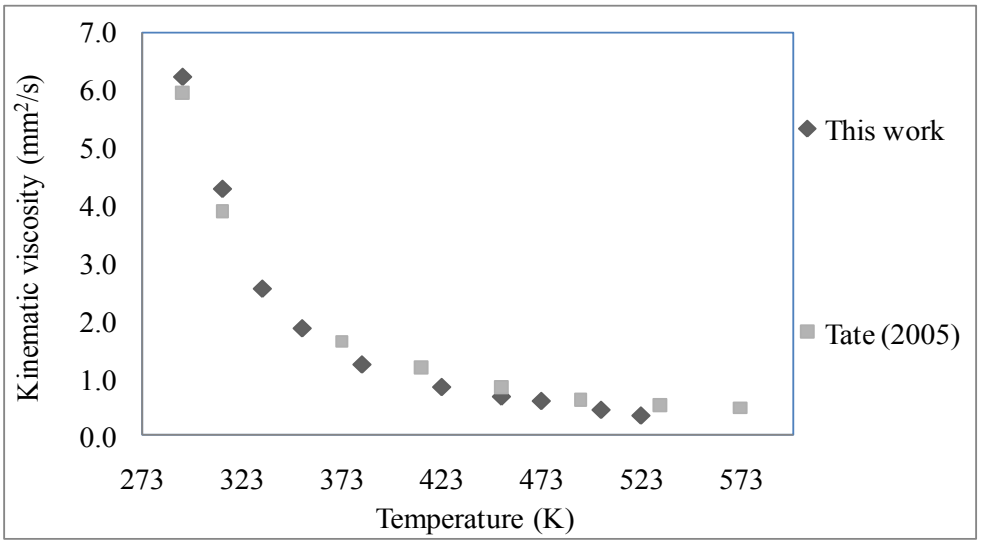

Figure 8.8 Dynamic viscosity of canola biodiesel from this work and reported Tate (2005) at different temperatures at atmospheric pressure

Figure 8.9 shows the kinematic viscosities of canola biodiesel B100 measured in this work and the kinematic viscosities reported by Tate (2005). The kinematic viscosities for canola biodiesel B100 reported by Tate (2005) decreased from 6.90 mm^2/s at 293 K to 0.90 mm^2/s at 573 K. The kinematic viscosities in this work decreased from 7.05 mm^2/s at 293 K to 0.48 mm^2/s at 523 K. As both the kinematic and dynamic viscosities were related to density, the kinematic viscosity also shows the similar behavior as in the case of dynamic viscosities.

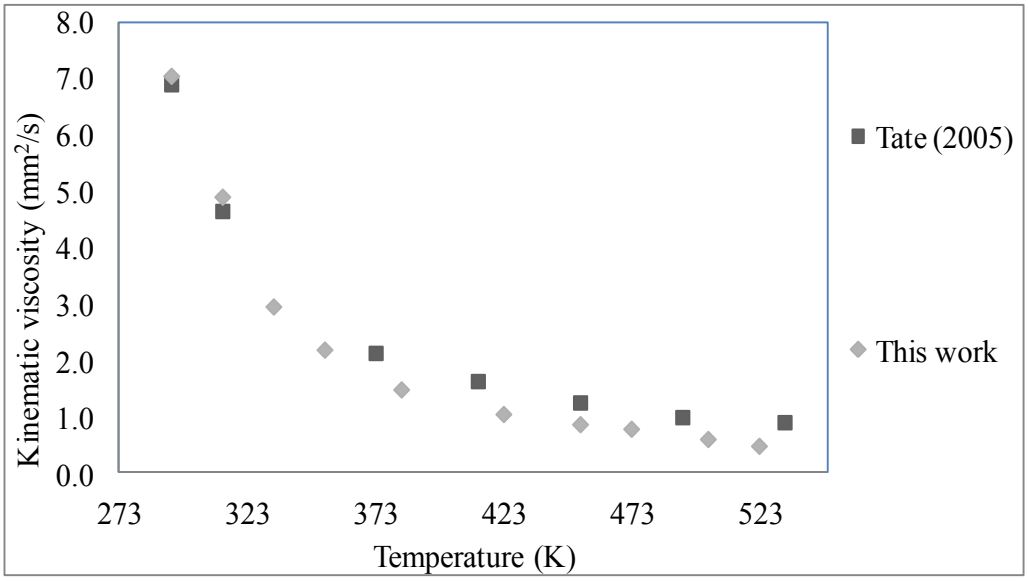

Figure 8.9 Kinematic viscosity of canola biodiesel from this work and reported by Tate (2005) at different temperatures at atmospheric pressure

Figure 8.10 shows the measured and regressed viscosities of canola biodiesel at atmospheric pressure from room temperature to 523 K. The R^2 values indicated a very good fit and the regressed and measured values are very close. The measured data were found to have high correlation with the model equation. The maximum error between the measured and predicted data was found to be 7.99 %.

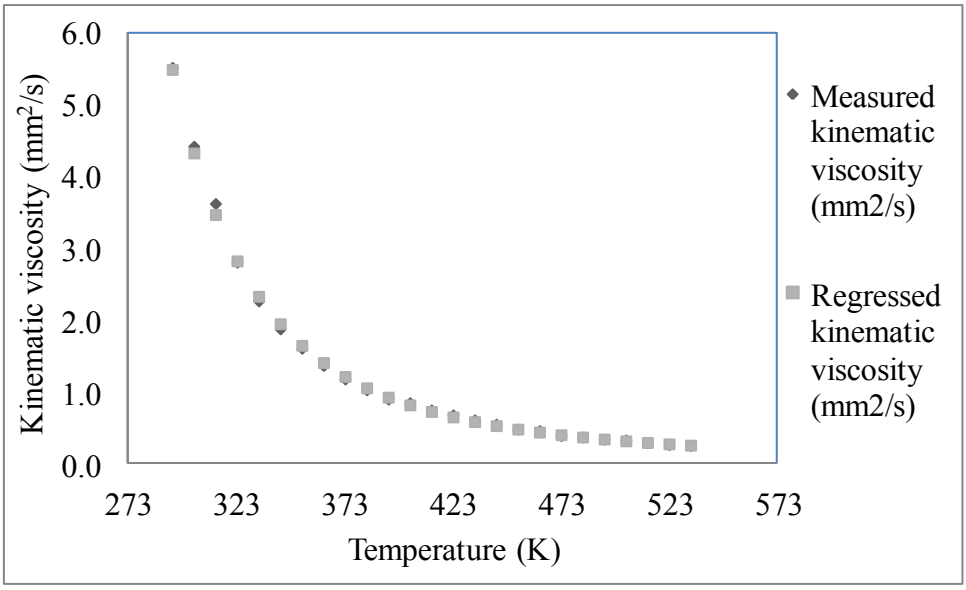

Figure 8.10 Measured and regressed kinematic viscosity of canola biodiesel B100 at atmospheric pressure

Yuan et al. (2003) calculated the dynamic viscosity data from the density and kinematic viscosity measured and predicted by Tat and Van Gerpen (1999) for commercially available biodiesel fuel using the ASTM standard method D445-88. Table 8.7 is the summary of dynamic viscosity data summarized by Yuan et al.(2003). The dynamic viscosities were calculated from the kinematic viscosities and densities measured by Tat and Van Gerpen (1999) from 273 k to 373 K. The relative error between the predicted and measured dynamic viscosities obtained using the measured density between 273 to 313 K ranged from 3.78% to 31.56 %. The measured and predicted dynamic viscosity of biodiesel from Tat and Van Gerpen (1999) study at 313 K were reported to be 3.89 mPa s and 5.07 mPa-s respectively. The relative error between the measured and predicted dynamic viscosity values at 313 K was 30.16%. The average relative error for dynamic viscosities between 273 to 323 K was 28.9 %. The relative error at 373 K was 3.78 %. The relative error decreased as the temperature increased. As the engine combustion modeling is usually performed in temperatures greater than 323 K (Yuan et al., 2003), these results were considered to be sufficiently accurate for atomization modeling.

Table 8.7 Predicted and measured dynamic viscosity of biodiesel (Tat and Van Gerpen, 1999)

Temperature (K)	Predicted dynamic viscosity (mPa s)	Measured dynamic viscosity (mPa s)	Absolute error (mPa-s)	Error (%)
273	14.98	12.07	2.91	24.14
283	11.1	8.61	2.49	29.91
293	8.4	6.4	2	31.27
303	6.47	4.92	1.55	31.56
313	5.07	3.89	1.17	30.16
323	4.03	3.16	0.87	27.41
333	3.25	2.63	0.62	23.66
343	2.65	2.23	0.43	19.19
353	2.19	1.92	0.27	14.24
363	1.83	1.68	0.15	9.01
373	1.54	1.49	0.06	3.78

The measured and regressed kinematic viscosities of canola biodiesel B100 in this work at 313 K were found to be 4.90 mm^2/s and 4.54 mm^2/s respectively. The error between the measured and regressed viscosity at 313 K was 7.99%, which represents the maximum error for canola B100 from room temperature to 473 K. The kinematic viscosity was also measured during ASTM fuel quality determination and the value observed at 313 K was 5.36 mm^2/s. This canola biodiesel sample tested for ASTM fuel quality was prepared in the Dalhousie University laboratory. The difference between the measured kinematic viscosity using the ViscoScope viscometer and the ASTM test was 8.5% using the canola biodiesel sample prepared in the laboratory. In order to compare the viscosity of canola biodiesel from ViscoScope viscometer and ASTM viscosity test, a sample of commercial canola biodiesel was also sent to the Bently Tribology Lab in the US. The viscosity of the commercial canola biodiesel measured in the US lab was 4.70 mm^2/s. The difference in values of kinematic viscosities using ViscoScope viscometer and the ASTM fuel quality test was 4.08%.

The measured and regressed kinematic viscosities of jatropha biodiesel B100 at 313 K were 4.43 and 4.35 mm^2/s respectively. The error between the measured and regressed viscosities was found to be 1.91%. The viscosity of the same jatropha biodiesel B100 sample was tested for ASTM fuel quality standard and was found to be 4.20 mm^2/s which differed by 5 % from the measured value. The dynamic viscosity of jatropha biodiesel B100 at 313 K was 3.86 mPa-s.

Similarly, the measured and regressed kinematic viscosities of soapnut biodiesel B100 were found to be 5.29 and 5.16 mm^2/s respectively. The error between the measured and the regressed viscosity was 2.46 %. The same sample of soapnut biodiesel tested for ASTM fuel quality standard by Bently Tribology lab was found to be 5.04 mm^2/s. The difference between these two values is 4.72 %.

Krisnangkura et al. (2006) predicted the kinematic viscosity of methyl ester from different biodiesel feedstocks at 313 K which is presented in Table 8.8. The kinematic viscosity obtained experimentally in this work at 313 K was found 1.45 mm^2/s higher than reported by Krisnangkura et al. (2006). They predicted the viscosities of the biodiesel using mass fraction of their components. Similarly, the dynamic viscosity obtained in this work was 0.231 mm^2/s higher than the dynamic viscosity reported by Krisnangkura et al. (2006). Krisnangkura et al. (2006) used the average density of 0.850 kg/m^3 to convert kinematic viscosities into dynamic viscosity for all biodiesel fuels. In this work, the density used to convert kinematic viscosity into dynamic viscosity was obtained experimentally. The density used for canola biodiesel at 313 K was 0.876 kg/m^3.

Table 8.8 Predicted viscosities of different biodiesels at 313 K (Krisnangkura et al., 2006)

	Biodiesel						
	Palm	Rapseed	Soybean	Coconut	Peanut	Canola	Canola (This work)
Kinematic viscosity (mm^2/s)	3.590	4.700	3.260	2.150	3.510	3.450	4.90
Dynamic viscosities (mPa-s)	4.224	5.529	3.835	4.059	2.529	4.059	4.29

Knothe and Steidley (2007) reported the kinematic viscosities of neat methyl ester at 293, 303 and 313 K were 6.43, 5.15 and was 4.15 mm^2/s respectively. Paton and Schaschke (2009) carried out viscosity tests using waste cooking oil biodiesel and biodiesel from vegetable oil using a falling-sinker type viscometer at 140 MPa, the pressure common at rail automotive diesel engines. The viscosity of waste cooking oil biodiesel at 293 K was 9.728 mPa s and vegetable oil was 7.557 mPa s for pressures between 0.1-140 MPa.

Yuan et al.(2009) measured and predicted the viscosity of canola biodiesel between 293 K and 373 K (Table 8.9). The difference between the measured and predicted viscosity values ranged from -7.11 to 3.04 %. The measured dynamic viscosity of canola biodiesel in this work has also been included in Table 8.9 for comparison with results from Yuan et al. (2009).

Table 8.9 Comparison of measured and predicted viscosities of biodiesel fuel from 293 K to 373 K (Yuan et al., 2009)

Viscosity (mPa s)	293 K	313 K	333 K	353 K	373 K
Canola biodiesel – measured	6.19	3.81	2.56	1.81	1.35
Canola biodiesel - predicted	5.75	3.56	2.44	1.80	1.39
Error (%)	-7.11	-6.55	-4.52	-0.08	3.04
Canola biodiesel (this work)	6.24	4.29	2.56	1.87	1.45

Shu et al. (2007) predicted the dynamic viscosity using mixture topological index which uses distance matrix and adjacent matrix of molecular structure. The topological index was estimated by the fatty acid composition of the respective biodiesel fuels at 313 K. They predicted the dynamic viscosities of biodiesel from corn oil, safflower oil, sunflower oil, cottonseed oil, butterfat and lard to be 3.507, 3.522, 3.526, 3.426, 2.930 and 3.410 mPa s respectively. The viscosities were predicted using a regression equation obtained with viscosities and the mean topological index of respective biodiesel fuels. The data were compared with predicted viscosities by Allen et al. (1999) and were found to differ by 1.3 %, 5.1 %, 4.0%, 1.0%. 11.4 % and 8.8 % respectively.

Figure 8.11 includes the kinematic viscosities of jatropha and soapnut biodiesel measured in this work. Achten et al.(2008) reported that the viscosity of jatropha biodiesel at 303 K ranged between 4.84 to 5.65 mm^2/s. Koh and Ghazi (2011) reported the kinematic viscosity of jatropha biodiesel B100 to be in the range of 2.35 to 2.47 mm^2/s at 313 K. The ASTM requirement for biodiesel to qualify as a transportation fuel should be within 1.9 to 6 mm^2/s. A large variation was found in the viscosities of jatropha biodiesel. This could be due to the processing technique, fuel quality and other physico-chemical properties of jatropha oil. The kinematic viscosities of soapnut biodiesel were slightly higher than the kinematic viscosities of jatropha biodiesel. No previous studies were available for soapnut biodiesel viscosities to compare at elevated temperatures and pressures. However, the viscosity data indicates a similar trend to that of canola, soybean and other biodiesel fuels reported in the literatures.

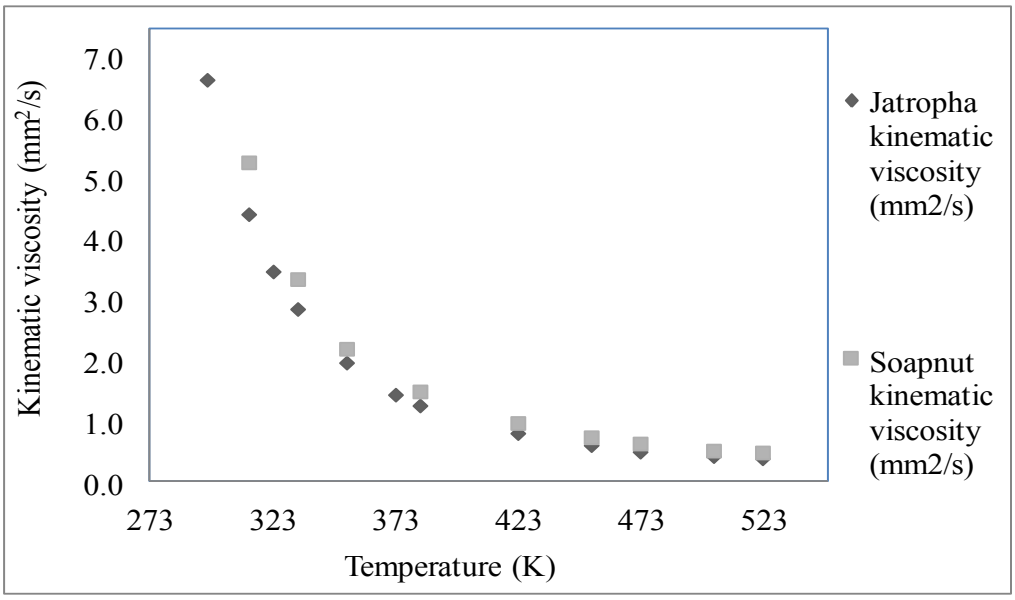

Figure 8.11 Kinematic viscosity of jatropha and soapnut biodiesel fuels at atmospheric pressure for different temperatures

Feitosa et al. (2010) carried out the viscosity test of mixture of coconut, colza and soybean oil biodiesel from 293.15 K to 373.15 K. The viscosities of coconut oil biodiesel at 293.15, 313.15, 333.15, 353.15 and 333.15 K were 3.84, 2.45, 1.72, 1.28 and 0.98 mPa s respectively. The viscosities of colza oil biodiesel at 293.15, 313.15, 333.15, 353.15 and 333.15 K were 7.42, 4.47, 2.99, 2.15 and 1.62 mPa s respectively. Similarly, the viscosities of soybean biodiesel at 293.15, 313.15, 333.15, 353.15 and 333.15 K were 6.44, 3.96, 2.69, 1.96 and 1.49 mPa s respectively. The dynamic viscosities of canola, jatropha and soapnut biodiesel in this work also showed a similar viscosity range.

Ramírez-Verduzco et al. (2011) predicted the viscosity of biodiesel from beef tallow, corn oil, cottonseed oil, soybean oil and sunflower oil from their compositions. The kinematic viscosities at 313 K for biodiesel from beef tallow, soybean oil, sunflower oil, corn oil and cottonseed oil were 4.29, 4.10, 4.05, 4.13 and 4.12 mm^2/s respectively. Ramírez-Verduzco et al. (2011) also measured the viscosities of biodiesel from beef tallow and soybean oil at 313 K were 4.36 and 4.07 mm^2/s respectively. Alptekin and Canakci (2009) reported the kinematic viscosities of biodiesel from soybean oil, sunflower oil, corn oil and cottonseed oil to be 3.97, 4.03, 4.18 and 4.06 mm^2/s

respectively. Tate et al. (2006) experimentally investigated the kinematic viscosity of soybean biodiesel and she reported it to be 3.99 mm^2/s at 313 K. The kinematic viscosities of canola, jatropha and soapnut biodiesel in this work were 4.90, 4.43 and 5.29 mm^2/s respectively. Moreover, all the biodiesel viscosities are within the range of ASTM requirement for biodiesel fuels.

Table 8.10 shows the summary of measured and regressed viscosities of canola biodiesel, jatropha biodiesel and soapnut biodiesel at atmospheric pressure from room temperature to 533 K from this work. The table also includes absolute errors for all three biodiesel fuels. The maximum absolute errors for canola, jatropha and soapnut oil biodiesel were found to be 0.36, 0.08 and 0.13 mm^2/s respectively (Table 8.10).

Table 8.10 Measured, regressed viscosities, absolute errors for canola, jatropha and soapnut biodiesel fuel

Fuel Type	Temperature (K)	Measured kinematic viscosity (mm^2/s)	Regressed kinematic viscosity (mm^2/s)	Absolute error (mm^2/s)
Canola biodiesel	293	7.05	7.08	0.03
	313	4.90	4.54	0.36
	333	2.95	3.13	0.18
	353	2.19	2.29	0.10
	383	1.48	1.55	0.07
	423	1.05	1.04	0.01
	453	0.86	0.81	0.05
	473	0.78	0.74	0.04
	503	0.60	0.59	0.01
	523	0.50	0.52	0.02
Jatropha biodiesel	296	6.65	6.69	0.04
	313	4.43	4.35	0.08
	323	3.48	3.48	0.01
	333	2.86	2.83	0.03
	353	1.98	1.98	0.00
	373	1.45	1.45	0.01
	383	1.27	1.27	0.00
	423	0.81	0.80	0.01
	453	0.61	0.61	0.00
	473	0.50	0.53	0.02
	503	0.43	0.43	0.00
	523	0.39	0.38	0.01
Soapnut biodiesel	297	7.77	7.85	0.09
	313	5.29	5.16	0.13
	333	3.36	3.33	0.03
	353	2.21	2.31	0.10
	383	1.50	1.49	0.01
	423	0.98	0.96	0.02
	453	0.74	0.74	0.00
	473	0.64	0.64	0.00
	503	0.52	0.54	0.01
	523	0.49	0.48	0.01

Allen (1998) and Allen et al. (1999) predicted the dynamic viscosity of 15 biodiesel fuels including canola oil biodiesel. The dynamic viscosity of canola biodiesel at 313 K was predicted to be 3.61 mPa s with lower and upper limit of 3.51 mPa s to 3.72 mPa s. The dynamic viscosity of canola biodiesel in this work was calculated to be 4.29 mPa-s. The dynamic viscosity predicted by Tate (2005) was 3.98 mPa s while the measured viscosity was reported as 3.90 mPa s. Figure 8.12 shows the predicted viscosities of 15-biodiesel fuels by Allen (1998) as well as the viscosities of canola, jatropha and soapnut oil biodiesel from this work. The viscosity of coconut oil was found to be the lowest of all while the rapeseed was found to have the highest viscosity of all. The dynamic viscosities of canola, jatropha and soapnut biodiesel were found comparable with the viscosities of other biodiesel fuels.

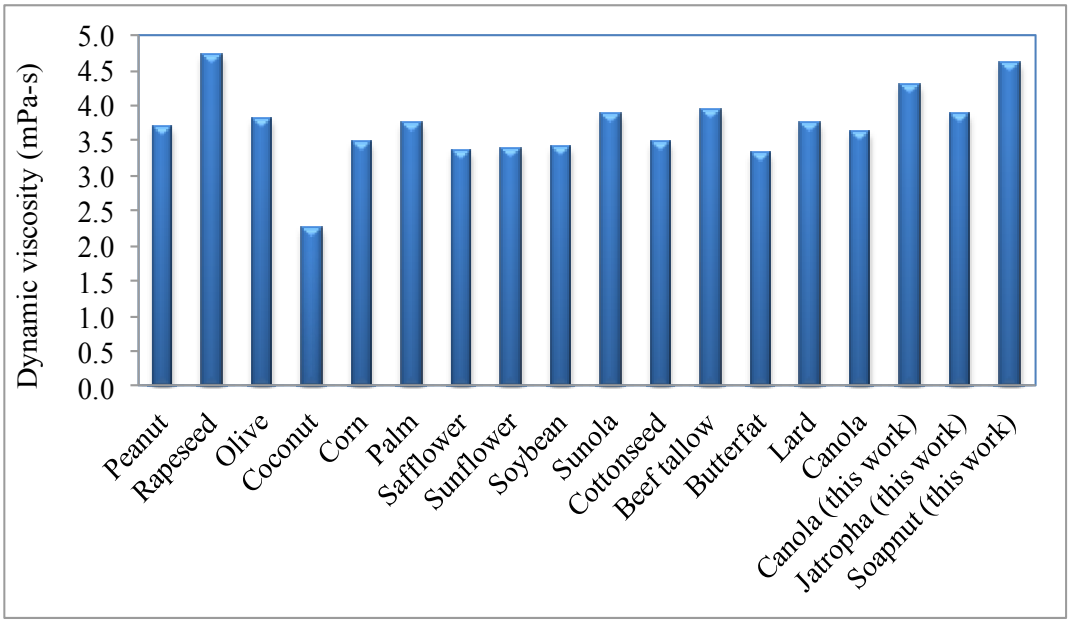

Figure 8.12 Dynamic viscosity predicted by Allen (1998) and dynamic viscosity from this work for different biodiesel fuels at 313 K

8.7 SUMMARY OF CHAPTER 8

This chapter includes the discussion of results from all analytical and experimental results. The experimental results obtained in this study has been compared with the data

from existing literature wherever possible. The density, surface tension and viscosity results for canola biodiesel and its blends at elevated temperatures and pressures were compared with the literature. However, the density, surface tension and viscosity results for jatropha and soapnut were not available for comparison. The results of these fuels were compared with other biodiesel fuels such as soybean, canola, peanut etc as each fuel has to meet ASTM fuel quality standards.

The next chapter includes the conclusions and recommendations of this thesis.

CHAPTER 9 CONCLUSIONS AND RECOMMENDATIONS

The potential of biofuel, especially the jatropha production in Nepal was analyzed. The analysis indicated that jatropha plantations could significantly contribute to the biodiesel production and reduce oil import. Some existing policy aspects of biodiesel promotion were also analyzed. Biodiesel production from jatropha oil was evaluated for its sustainability using five sustainability indicators. Canola, jatropha, soapnut and waste cooking oil biodiesel were characterized for their fuel properties. The atomization properties of canola, jatropha and soapnut biodiesel and their blends were also investigated from room temperature to 473 K for surface tension and up to 523 K for density and viscosity.

Based on the analytical study and experimental results, the following conclusions are drawn.

9.1 CONCLUSIONS

a. The existing biodiesel promotion policy is not sufficient enough to encourage entrepreneurs, community based organizations and non-governmental organization to be attracted into this area.

b. Provided that jatropha cultivation is promoted commercially in non-cultivated agricultural lands and other waste lands, biodiesel production can significantly reduce oil imports, saving Nepal's hard earned dollars.

c. The theoretical analysis of sustainability of jatropha biodiesel production in Nepal indicated that jatropha biodiesel could prove to be sustainable.

d. The waste cooking oil survey analysis indicated that the biodiesel production from waste cooking oil is not feasible due to the low quantity of waste cooking oil production and the competing use of waste oil for other purposes.

e. Soapnut oil was investigated for potential biodiesel feedstock for the first time and it was found that soapnut derived biodiesel meets all ASTM biodiesel specifications.

f. The density of all three biodiesel fuels studied show a linear relationship with temperature and pressure over the measured range. It was also found that densities increased linearly when the pressure was increased at constant temperature.

g. In the cases of canola biodiesel (B80) and jatropha biodiesel (B20) the density data showed a slightly non-linear trend as well. However, the R^2 values for both linear and non-linear analysis were very similar.

h. The density data for canola biodiesel obtained from capacitance type densitometer was comparable with the data from the literature over the measured range of temperatures and pressures. Density data for jatropha and soapnut were not available in the literature against which to compare the experimental data but they were well within the range of other biodiesel fuels and meet the ASTM fuel quality requirements.

i. The densities of all three biodiesel fuel blends B80, B50 and B20 were predicted using the Kay's mixing rule and were compared with the measured densities. Kay's mixing rule works in agreement with less than 5% error with measured data for canola, jatropha and soapnut biodiesel blends.

j. The surface tension results of all the three biodiesel fuels tested showed a linear relationship with temperature and pressure. The surface tension data for canola biodiesel obtained from the pendant droplet apparatus was comparable with the data from the literature over the measured range of temperatures and pressures. Surface tension data for jatropha and soapnut were not available in the literature against which to compare the experimental data but they were well within the range of surface tension of other biodiesel fuels, and meet the ASTM fuel quality requirements.

k. The surface tension of canola biodiesel B100 decreased linearly at an average rate of 0.063 mN/m/ K within the temperature range of 293-473 K at atmospheric pressure. Similarly, for jatropha biodiesel B100, B80 and B50, the surface tension decreased linearly at an average rate of 0.06 mN/m/ K. For B20 and diesel (B0), the surface tension decreased linearly at an average rate of 0.05 mN/m/ K. For soapnut biodiesel B100, B80, B50 and B20, the surface tension decreased linearly at average rate of 0.006, 0.06, 0.06 and 0.07 mN/m/ K at atmospheric pressure, showing that the surface tension of pure biodiesel is an order of magnitude less dependent on temperature than petro diesel.

l. It was found that the rate of decrease of surface tension was higher due to an increase in tempe[r]ature than that of pressure. Temperature has a higher impact on surface tension than pressure.

m. ViscoScope viscometer results showed that the kinematic viscosity values differed by a maximum of 7.34 % from the standard values when tested for distilled water from 293 to 363 K. Similar results were obtained when the tests were carried out from 363 K down to room temperature.

n. Viscosity –temperature relationship of all three biodiesel fuels tested for viscosity followed the Andrade equation modified by Tat and Van Gerpen (1999). The

modified Andrade equation was also applicable when the temperature and pressure were both applied simultaneously within the measured range of temperature and pressure.

o. The measured and regressed kinematic and dynamic viscosities for canola biodiesel in this work compare well with viscosities reported in the literature. Even though no viscosity data were available in the literature for jatropha and soapnut against which to compare them with the experimental data at elevated temperature and pressure, they all met the criteria for the ASTM fuel quality standard at 313 K and compared well with other biodiesel fuels.

9.2 RECOMMENDATIONS

a. As there are over 286 oil bearing plants are found in Nepal and 92 species produce seeds with oil content exceeding 30%, sal and other oil producing feedstocks should be investigated for fatty acid content, fuel and atomization characteristics.

b. Current sustainability analysis for jatropha biodiesel in Nepal is based on theoretical analysis only because no actual data on fertilizer requirement, fossil fuel input during life cycle, labor and other material cost are available. Once these data are available, a complete life cycle analysis with actual data should be carried out.

c. The impacts of jatropha plantations in non-cultivated agricultural land should be studied to determine if it creates any competition with potential agricultural lands.

d. A feasibility analysis for biodiesel production from soapnut should be carried out. Currently, soapnut grows wild in the natural forests and its plantation as a community forest should be evaluated. A sustainability analysis of biodiesel production from soapnut oil should be carried also out.

e. Biodiesel diesel blend regulations should be promulgated and the necessary policies for promoting biodiesel production should be in place to reduce the diesel import and reduce environmental impacts created by the use of diesel. A minimum of 10% blend requirement is essential to promote biodiesel development.

f. A further study needs to be done in order to assess the potential of waste cooking oil availability in major city centres across the country. The quality of waste cooking oil generation, its existing use compared to the proposed use for biodiesel production should also be evaluated.

g. An electronic copy of this thesis will be sent to the Alternative Energy Promotion Development Board, which is chaired by the Minister of Environment. Another copy will be sent to the Executive Director of Alternative Energy Promotion Centre (AEPC).

REFERENCES

Abdulagatov, I.M., Azizov, N.D., (2006). Densities and Apparent Molar Volumes Concentrated Aqueous LiCl Solutions at High Temperatures and High Pressures. *Chemical Geology* 230, 22–41.

Acharya, B.M. (2009). Soapnut: A Cash Crop Tree and Experience in Baitadi District. *Hamro Kalpabrikchay*, 223:1-10.

Achten, W.M.J., Verchot, L., Franken, Y.J., Mathijs, E., Singh, V.P., Aerts, R. and Muys, B.(2008). Jatropha Bio-Diesel Production and Use . *Biomass and Bioenergy,* 32(12):1063-1084.

Adamson, W.A., (1982). *Physical Chemistry of Surfaces.* 4th Edition. John Wiley and Sons, New York.

ADB, (1020). Asian Development Bank and Nepal Fact Sheet, 2010 published in December 31, 2010. http://www.adb.org/Documents/Fact_Sheets/NEP.pdf (Accessed on September 25, 2011).

ADB, (2007). Asian Development Bank, Nepal, Quarterly Economic Update, Vol IV, No 2, August, 2007.

Adhikari, N.P. and Wegstein, M. (2011). Financial Analysis o Jatropha Plantations in The Context Of Nepal. *Journal of the Institute of Engineering*, 18(1-2): 143 148.

AEPC, (2008). Solar Energy. http://www.aepcnepal.org/gen/se.php (Accessed on September 27, 2008).

AEPC, (2009). AEPC E-Newsletter, an Electronic Quarterly Publication of Alternative Energy Promotion Centre. Volume 11, June 2009. www:aepc.gov.np (accessed on July 28, 2010).

Ahmed, M.A, Ejim, C.E, Fleck, B.A. and Amirfazli, A. (2006). Effect of Biodiesel Fuel Properties and its Blends on Atomization. SAE World Congress, Detroit, Michigan, April 3-6, 2006.

Ale, B.B. and Bade Shrestha, S.O., (2008). Hydrogen Energy Potential of Nepal. *International Journal of Hydrogen Energy,* 33(15): 4030-4039.

Ali, Y. Hanna, M.A.,and Cuppett, S.L., (1995). Fuel Properties of Tallow and Soybean Oil Esters. Journal of the American Oil Chemists Society. 72 (12):1557-1564.

Al-Kahtani, H. (1991). Survey Quality of Used Frying Oils from Restaurants. *J Am Oil Chemist Soc,* 68 (11):857-862.

Allen C.A.W., Watts K.C. and Ackman R. (1999a). Predicting the Surface Tension of Biodiesel Fuels from Their Fatty Acid Ester Composition. *J Am Oil Chemist Soc,* 76(3):317–323.

Allen, C.A.W,, Watts, K.C., Ackman, R.G. and Pegg, M.J. (1999). Predicting the Viscosity of Biodiesel Fuels from Their Fatty Acid Ester Composition. *Fuel* 78:1319-1326.

Allen, C.A.W. (1998). Prediction of Biodiesel Fuel Atomization Characteristics Based on the Measured Properties. Ph.D. Thesis, Faculty of Engineering, Dalhousie University, pp 220.

Alptekin, E. and Canakci, M. (2008). Determination of the density and the Viscosities of Biodiesel– Diesel Fuel Blends. *Renewable Energy,* 33:2623– 2630.

Alptekin, E. and Canakci, M. (2009). Characterization of the Key Fuel Properties of Methyl-Ester Fuel Blends. *Fuel,* 88:75–80.

Amezaga, J. M., Von Maltitz, G. and Boyes, S., (Editors) (2010).Assessing the Sustainability of Bioenergy Projects in Developing Countries: A Framework for Policy Evaluation. Newcastle University, ISBN 978-9937-8219-1-9, 179 pp.

Arai, M., Tabata, M., Hiroyasu, H. and Shimizu, M. (1984). Disintegrating Process and Spray Characterization of the Fuel Jet Injected by a Diesel Nozzle, SAE, paper Number 840275.

Ashton, S. and Cassidy. P. (2007). *Energy Basics*. In: Hubbard, W.; L. Biles; C.Mayfield; S. Ashton (Eds.). 2007. Sustainable Forestry for Bioenergy and Bio based Products: Trainers Curriculum Notebook. Athens, GA: Southern Forest Research Partnership, Inc. Pages 189–192.

ASTM, (2009). ASTM Sets the Standard for Biodiesel, http://www.astm.org /SNEWS/JF2009/nelson_jf09.html (accessed on July 05, 2010)

Attanatho, L., Magmee, S. and Jenvanipanjakil, P. (2004). The Joint International Conference on 'Sustainable Energy and Environment', 1-3 December 2004, Huan Hin, Thailand.

Audonnet, F. and Padua, A.A.H.(2001). Simultaneous Measurement of Density an Viscosity of N-Pentane from 298 to 383K and up to 100 Using MPa a Vibrating Wire Instrument. *Fluid Phase Equilibria*, 181:147-161.

Ayres, R.U., Jeroen, C.J.M. van den Bergh and Gowdy, John Malcolm, (1998). Viewpoint: Weak versus Strong Sustainability. No 98-103/3, Tinbergen Institute Discussion Papers, Tinbergen Institute, pp 18.

Ayres, R.U., Van den Bergh, J.C.J.M., and Gowdy, J.M. (2001). Viewpoint: Weak Versus Strong Sustainability: Economics, Natural Sciences and Consilience. *EnvironmentalEthics,* 23 (2), 155-168.

Balat, M. (2011). Potential Alternative to Edible Oils for Biodiesel Production-a Review of Current work. *Energy Conversion and Management* (52):1479-1492.

Bamberger, J.A and Greenwood, M.S., (2004). Measuring Fluid and Slurry Density and Solids Concentration Non-Invasively. *Ultrasonics* 42: 563–567.

Banglore Mass Rail Corporation Ltd (BMRC) (2005). EIA of the Bangalore Mass Transit Scheme. http://www.bmrc.co.in/EIA.pdf (accessed on December 20, 2011).

Banskota, K. and Sharma, B., (1997). Impact of Alternative Energy Technology in Reducing Pressure on Forest Resources. Case studies from Ghandruk. Discussion Paper. Series No. MEI 97/5. ICIMOD. Kathmandu. Nepal.

Banskota, K. and Sharma, B., (1997a). Overview of Nepalese Energy Sector. Report Prepared for the International Center for Integrated Mountain Development (ICIMOD), Kathmandu, Center for Resource and Environmental Studies (CREST), Kathmandu:Project Report No 0297.

Bashforth, F. and Adams, J.C., (1883). *An Attempt to Test the Theory of Capillary Action by Comparing the Theoretical and Measured Forms of Drops of Fluid. Kessinger Publishing,* LLC, pp 148, ISBN-10: 0548623066.

Beale, J.C. and Reitz, R.D.(1999). Modeling Spray Atomization with the Kelvin Helmholtz/Rayleigh-Taylor Hybrid Model. *Atomization and Spray*, 9:623-650.

Bell, S. and Morse, S. (1999). *Measuring the Immeasurable*. the Theory and Use of Sustainability Indicators in Development. Earthscan: London, pp 192. ISBN 1 85383 498.

Benton, T.(1999). Sustainable Development and Accumulation of Capital:Reconciling Irreconcilable? In: Fairness and Futurity:Essays on Environmental Sustainability and Social Justice, Edited by A. Dobson. Oxford: Oxford University Press. pp. 199-229.

Bhale, P.V., Deshpande, N.V., Thombre, S.B. (2009). Improving the Low Temperature Properties of Biodiesel Fuel. Renewable Energy, 34(3):794-800.

Bhattarai, K.R. (2009). Jatropha Biodiesel. Makalu Publication, Kathmandu, Nepal, pp 148.

Biswas, P.K., Pohit, S. and Kumar, R. (2010). Biodiesel from Jatropha: Can India Meet 20% Blend Target?, *Energy Policy*, 38:1477-1484.

Blangino, E., Riveros, A.F. and Romano, S.D., (2008). Numerical Expressions for Viscosity, Surface Tension and Density of Biodiesel: Analysis and Experimental Validation. *Physics and Chemistry of Liquids*, 46 (5):527-547.

Bosswell, M.J, (2003). Plant Oils: Wealth, Health, Energy and Environment. In Proceeding of the International Conference of Renewable Energy Technology for Rural Development, Kathmandu, Nepal, Oct 12-14, 2003.

Boswell M. J. (1998): Exploration and Utilization of the Indigenous Renewable Oil Resources in Nepal: Jatropha Curcas a low Altitude Species, In Proceedings of International Conference on Role of Renewable Energy Technology for Rural Development, IOE, TU, Nepal, pp 98-106.

Broek, R.V.D and Lemmes, L., (1997). Rural Electrification in Tanzania. Constructive Sse of Project Appraisal. *Energy Policy* 25 (1) pp 43-54.

BSP, (2009). An Introduction of BSP-Nepal. http://www.bspnepal.org.np/about-us (accessed on July 24, 2010).

Budge, S. M.; Iverson, S. J.; Koopman, H. N. (2006). Studying Trophic Ecology in Marine Ecosystems Using Fatty Acids: A Primer on Analysis and Interpretation. Marine Mammal Science, 22, 759-801.

CADEC, (2003). Community Awareness Development Centre (CADEC), Micro-hydro Year Book of Nepal, June 2003.

Cai, X., Zhang,X. and Wang, D. (2011). Land Availability for Biofuel Production. *Environ. Sci. Technol.,* 45 (1): 334–339.

Camunas, M.J.P, Baylaucq, A., Boned, C. and Fernandez, J. (2001). High Pressure Measurements of Viscosity and Density of Two Polyethers and Two Dialkyl Carbonates. *International Journal of Thermophysics*, 22 (3): 749-768.

Canada Gazette (2010). Canada Gazette, volume 144, no. 15, Part I: Notices and ProposedRegulations,2010-04-10(http://www.gazette.gc.ca/rp pr/p1/2010/2010-04-10/html/reg1-eng.html#REF6) (accessed on June 26, 2010).

Canakci M, Van Gerpen, J. (1999). Biodiesel Production Via Acid Catalysis. *Trans. Am. Soc. Agric. Eng*. 42(5):1203–1210.

Canakci, M., Van Gerpen, J. (2001) Biodiesel production From Oils and Fats With High Free Fatty Acids. *Trans ASAE*, 44:1429–1436.

Carter, D., Darby, D., Halle, J., and Hunt, P. (2005). *How to Make Biodiesel*. Low Impact Living Initiative, Redfield Community, Winslow, Bucks, ISSN 0 9649171-0-3.
CBS (2011). Preliminary Result of National Population Census 2011, Published Central Bureau of Statistics, Nepal on September 27, 2011. http://census.gov.np (Accessed on September 28, 2011).
CDM-PDD (2011). Small-scale Voluntary Programme of Activities Design Document form:Solar Lighting in Rural Ethiopia VPoA, version -3. http://www.myclimate.org/fileadmin/images/ksp/kspinternational/741_solar_ethiopia/ Ethiopia_lighting-PoA-PDD.pdf (Accessed on April, 02, 2012).
Challen, B. and Baranescu, R. (1999) (eds). Diesel Engine Reference Book. 2nd (ed). Butterworth-Heinemann Ltd. Pp: 682.
Chhetri, A. B.; Islam, P., Mann, H. (2007). Zero-Waste Multiple Uses of Jatropha and Dandelion. *J. Nat. Sci. and Sust. Tech.* 1: 75-99.
Chhetri, A.B., Tango, M.S., Budge, S.M., Watts, K. C. and Islam, M.R. (2008a). Non Edible Plant Oils as New Sources for Biodiesel Production. *Int. J. Mol. Sci.,* 9(2): 169–180.
Chhetri, A.B., Watts, K. C. and Islam, M.R. (2008b). Waste Cooking Oil as an Alternate Feedstock for Biodiesel Production. *Energies* 2008, 1: 3-18.
Chunsheng, Y. and Chongli, Z. (2004). A New Model for Prediction of Surface Tension of Pure Fluids. *Chinese J. of Chem. Eng*. 12(1):85-91.
Claussen, M., Kubatzki, C., Brovkin, V., Ganopolski, A., Hoelzmann, P., Pachur, H.J., (1999).Simulation of an Abrupt Change in Saharan Vegetation at the End of the Mid-Holocene. *Geophys. Res. Letters*, 24 (14): 2037-2040.
Common, M. and C. Perrings, (1992). Towards an Ecological Economics of Sustainability. *Ecological Economics,* vol. 6: 7-34.
Coronado, M., W. Yuan, D. Wang and F.E. Dowell, (2009). Predicting the Concentration and Specific Gravity of Biodiesel-Diesel Blends Using Near- Infrared Spectroscopy. *Applied Eng. Agric.,* 25: 217-221.
Costanza, R., Cumberland, J., Daly H., Goodland R., Norgaard R. (1997). An *Introduction to Ecological Economics, International Society for Ecological Economics*, St. Lucie Press, Boca Raton, Florida. pp 275.
Couper, A. , Newton, R and Nunn, C., (1983). A Simple Derivation of Vonnegut's Equation for The Determination of Interfacial Tension by The Spinning Drop Technique. *Colloid Polymers Science*, 261:371-372.
Chalatlon, V., Roy, M.M., Dutta, A and Kumar, S., (2011). Jatropha: A multipurpose plant with considerable potential for the tropics. Journal of Petroleum Technology and Alternative Fuels, 2(5):76-85
Dahal, R.K., Bhattarai, K.D., Neupane, G. and Kafle, K.R, (2004). Wind Power Development in Kagbeni area, Mustang from View Point of Geological and Meteorological Concerns. Paper Presented in Fourth Nepal Geological Congress, April 9 to 11, 2004.
Daly, H. (1994). *Operationalising Sustainable Development by Investing in Natural Capital*.In A.M. Jansson, M. Hammer, C. Folke and R. Costanza (eds) Investing in Natural Capital: the Ecological Economics Approach to Sustainability.Washington DC: Island Press, pp. 22–37.
Daly, H. E. (1977). *Steady- State Economics*. San Francisco CA: W.H. Freeman.

Daly, H. E. (1999). *Ecological Economics and the Ecology of Economics*: Essays in Criticism, Cheltenham, UK and Northampton, MA, US: Edward Elgar.
Daly, H.E. and Cobb, J. (1989). For the Common Good: Redirecting The Economy Towards Community, the Environment and a Sustainable Future, Beacon Press, Boston, pp 554.
Dasgupta, P. (1982). *The Control of Resources.* Harvard University Press, Cambridge, MA, pp:240.
Dasgupta, P. and Maler, K-G. (1998). Decentralization Schemes, Cost-Benefit Analysis and Net National Product as A Measure of Social Well Being. STICERD / LSE Development Economics Discussion Paper DEDPS/12, Pp:1-38.
Dechoz, J and Roze, C. (2004). Surface Tension Measurement of Fuels and Alkanes at High Pressure Under Different Atmospheres. *Applied Surface Science*, 229:175-182.
Dee, N., J. Baker, N. Drobny, K. Duke, I. Whitman, and D. Fahringer. (1973). An Environmental Evaluation System for Water Resource Planning. *Water Resources Research*, 9 (3):523-535.
Del Rio, O.I., and Neumann, A.W., (1997). Axisymmetric Drop Shape Analysis: Computational Methods of Interfacial Properties from the Shape and Dimensions of Pendant and Sessile Drops. *Journal of Colloid and Interface Science*, 196: 136 147.
Dhakal, S. and Raut, A.K. (2010). Potential and Bottlenecks of the Carbon Market: The Case of A Developing Country, Nepal. *Energy Policy* 38:3781–3789.
Di Serio, M., Tesser, R., Pengmei, L. and Santacesaria, E (2008). Heterogeneous Catalysts for Biodiesel Production. *Energy and Fuels*, 22 (1):207-217.
Drelich, J., Fang, C. and White, C.L., (2002). Measurement of Interfacial Tension in Fluid-Fluid System. Encyclopedia of Surface and Colloid Science, 3152-3166.
Dindar, C. (2001). High-Pressure Viscosity and Density of Polymer Solutions at the Critical Polymer Concentration in Near Critical and Super Critical Fluids. M.Sc. Thesis, Virginia Polytechnic Institute and State University, USA, pp 141.
Drop Shape Analysis Manual (2006). DSA100 V1.9.
DSD, (2012). Division of Sustainable Development, United Nations. http://www.un.org/esa/dsd/index.shtml (accessed March 4, 2012).
Du Nouy, L.,(1919). A New Apparatus for Measuring Surface Tension. *The Journal General Physiology*, 521-524.
EIA (2010 A). International Energy Outlook 2010. World Energy Demand and Economic Outlook, http://www.eia.doe.gov/oiaf/ieo/world.html (Retrieved on 20 January 2011).
EIA (2010 B). International Energy Outlook 2010. Energy-Related Carbon Dioxide Emissions, http://www.eia.doe.gov/oiaf/ieo/emissions.html (Retrieved on 20 January 2011).
Erren, H.,1999. Density Measurement, CRC press, LLC.
Eastwood, A.R. (1979). The Viscous Properties of Liquids Under Extreme Conditions of Pressure. Symposium on Transport Properties of Fluids and Fluid Mixtures: Their Measurement, Estimation, Correlation and Use. Paper no.3.3

Ejim, C.E., Fleck, B.A. and Amirfazli, A. (2007). Analytical Study for Atomization of Biodiesels and Their Blends in a Typical Injector: Surface Tension and Viscosity Effects. *Fuel*, 86:1534–1544.

FAO, (2008). The State of Food and Agriculture, Part I: Biofuel: Prospects, Risks and Opportunities, Chapter 4, pp 138.

Flowers, A.E., (1914). Viscosity Measurement and a New Viscometer. Proceedings of the Annual Meeting, American Society for Testing Materials 14(2):565-616.

Fore, S.R., Porter, P. and Lazarus, W. (2011). Net Energy Balance of Small-Scale On Farm Biodiesel Production From Canola and Soybean. *Biomass and Bioenergy*, (35):2234-2244.

Freedman B., Pryde, E.H., Mounts, T.L. (1984). Variables Affecting the Yield of Fatty Ester From Transesterified Vegetable Oils. Journal of American Oil Chemists' Society, 61:1638–43.

Feitosa, F.X., Rodrigues, M. d. L., Veloso, C.B., Cavalcante, Jr., C.l L., Albuquerque, M.C.G.and de Sant Ana, H,B., (2010). Viscosities and Densities of Binary Mixtures of Coconut+Colza and Coconut +Soybean Biodiesel at Various Temperatures. *J. Chem. Eng. Data*, 55, 3909–3914.

Goodrum, J.W., Patel, V.C. and McClendon, R.W.(1996). Diesel Injector Carbonization by Three Alternative Fuels. *Trans ASAE*, 39(3): 817-821.

Gagnon, L. and Van de Vate, J.F. (1997). Greenhouse Gas Emissions from Hydropower: The State of Research In 1996. *Energy Policy,* 25 (1):7-13.

Gozalpour, F., Danesh, A., Todd, A.C. and Tohidi, B. (2001). Viscosity and Density Data of Two North Sea Gas Condensate Samples at Temperatures to 423 K and Pressures to 140 MPa. *Journal of Chemical Engineering Data*, 46:1305-1308.

Gozalpour, F., Danesh, A., Todd, A.C. and Tohidi, B. (2002). Viscosity and Density Data for a Six-Component Model Fluid at Temperatures to 423K and Pressures to 140 MPa. High Temperature- High Pressures, 34:483-486.

Grunberg, L. and Nissan, A.H., (1949). Mixture Law for Viscosity. Nature, 164:570-577.

Goodland, R. (1992). The Case That the World Has Reached Limits, More Precisely That Current Growth In The Global Economy Cannot Be Sustained. In: R. Goodland, Herman Daly, S.E. Serafy, B. von Droste: Environmentally Sustainable Economic Development: Building on Brundtland, UNESCO, Paris.

Goodland, Robert (1999): The Biophysical Basis of Environmental Sustainability. In:Van den Bergh, Jeroen C.J.M (ed). Handbook of Environmental and Resource Economics. UK and USA, pp 709-721.

Goldemberg, J. (1996). Energy, Environment and Development. Earthscan, London, UK, pp:11-37.

Goldemberg, J. (2003). Jobs Provided in The Energy Sector. Adapted from Grassi, G. (1996).

Gowdy, J.M. and C. McDaniel, 1999. The Physical Destruction of Nauru: An Example of Weak Sustainability. Land Economics, 75, May.

Gui, M.M., Lee, K.T. and Bhatia, S. (2008). Feasibility of Edible Oil vs Non-Edible Oil Vs.Waste Edible Oil As Biodiesel Feedstock. Energy (33):1646-1653.

GON (2008). Government of Nepal, Budget Speech 2008. http//www.mof.gov.np (Accessed on September 27, 2008).

GON (1989). Master Plan for the Forestry Sector Nepal. Ministry of Forests and Soil Conservation, His Majesty's Government, Nepal.
Gubitz, G.M., Mittlebach, M. and Trabi, M. (1999). Exploitation of Tropical Oil Seed Plant Jatropha Curcas L. *Bioresource Technology,* 67:73-82.
Gubitz, G.M., Mittelbach, M. and Trabi, M., (1999). Exploitation of The Tropical Oil Seed Plant Jatropha Curcas L. *Bioresource Technology* 67:73-82.
Gunstone, F.D. and Hardood, J.L., (2007). Occurance and Characterization of Oils and Fats. In : Gunstone,F.D. and Hardood, J.L., Dijkstra, A.J. (eds) The Lipid handbook. 3rd ed. CRC.Boca Raton. Pp 37-142, 2007.
Hoorfar, M. and Neumann, A.W., (2004). Axisymmetric Drop Shape Analysis (ASDA) for the Determination of Surface Tension and Contact Angle. *The Journal of Adhesion*, 80:727-743.
Hubbard, R.M. and Brown, G.G. (1943). Viscosity of n-Pentane. *Industrial and Engineering Chemistry,* 35(12):1276-1280.
Hong-Yi, L. and Guojie, L., (1995). A Generalized Equation of State for Liquid Density Calculation. *Fluid Phase Equilibria* 108:15-25.
Harkins, W.D. and Brown, F.F. (1919). The determination of Surface Tension and the Weight of Falling Drops:The Surface Tension of Water and Benzene By the Capillary Height Method. *Journal of American Chemical Society*, 41:499-525.
Hicks, J. (1946). Value and Capital, 2nd Edition, Oxford University Press, Oxford, UK, pp 340.
Hohmeyer, O., (1996). Social Costs of Climate Change—Strong Sustainability and Social Costs. In:Hohmeyer , O., Ottinger, R.L., Rennings, K. (Eds.), Social Costs and Sustainability-Valuation and Implementation in the Energy and Transport Sector. Springer, Berlin, pp. 61–83.
Haryana-online.com (2007). Ritha. http://www.haryana-online.com/Flora/ritha.htm (Accessed on October 14, 2007).
HAN (2008). Hotel Association of Nepal, Kathmandu. http://www.visitnepal.com/hotels/hotel_association_nepal.php (accessed on September, 15, 2010).
Hooda, N. and Rawat V.R.S.(2006). Role of Bio-Energy Plantations for Carbon-Dioxide Mitigation with Special Reference to India. Mitigation and Adaptation Strategies for Global Change 1:445–467.
Hiroyasu, H., Arai, M., and Tabata, M. (1989). Empirical Equations for Sauter Mean Diameter for a Diesel Spray. SAE Paper Number 890464.
Hiroyasu, H. (1991). Experimental and Theoretical Studies on the Structure of the Fuel Sprays in Diesel Engines. *ASME Fall Technical Conference,* ICE 31(1):3-15.
Hafer, R.F. and Laesecke, A. (2003). Extension of Torsional Crystal Viscometer To Measurements In The Time Domain. *Measurement Science and Technology*, 14 (5):663.
Hilber, T.; Mittelbach, M.; Schmidt, E. (2006) Animal Fats Perform Well in Biodiesel. Render , 16-18. http://www.rendermagazine.com/pages/pastarticles2006.html accessed on 30 Aug 2006).
Iqbal, M. (1991). Non-Timber Forest Products: Their Income-Generation Potential For Rural Women in North West Frontier Province (Pakistan). International Labour Organization and Government of NWFP, Peshawar.

Issariyakul, T., Kulkarni, M.G., Dalai, A.J. and Bakhshi, N., (2007). Production of Biodiesel From Fryer Grease Using Mixed Methanol/Ethanol System. *Fuel Processing Technology*, 88:429-436.

Issariyakul, T., Kulkarni, M.G., Meher, L.C., Dalai, A.K. and Bakhshi, N.N., (2007). Biodiesel Production From Mixtures of Canola Oil and Used Cooking *Oil.Chemical Engineering Journal,* 140(1-3): 77-85.

Janaun, J. and Ellis, N. (2010). Perspectives on Biodiesel as A Sustainable Fuel. Renewable and Sustainable *Energy Reviews*, 14:1312–1320.

Joshi, S.R., Bhandari, H., Paudel, J., Bhusal, M and Tandon, H. (2008). Village Development Committee Profile of Nepal. A Socio-Economic Development Database of Nepal, Intensive Study & Research Centre, Kathmandu, Nepal. Page 845, ISBN: 9937-2-0907-6.

Joshi, D.D., Maharjan, M., Johansen, M.V., Willingham, A.L. and Sharma, M., (2003) Improving Meat Inspection And Control In Resource-Poor Communities: The Nepal Example. *Acta Tropica* 87:119-127.

Johnston, M and Holloway, T., (2007). A Global Comparison of National Biodiesel Production Potentials. *Environmental Science and Technology*, 41 (23):7967 -7973.

Jackson, J.K. (1994). Manual of Afforestation In Nepal. Vol.2, Forest Research and Survey Centre, Ministry of Forest and Soil Conservation, Kathmandu, Nepal.

Joshi, R.M. (2007). Physical Properties of Biodiesel Fuels at Elevated Temperatures and Pressures. M.A.Sc thesis, Process Engineering and Applied Science, Dalhousie University, Halifax, NS, Canada. pp 195.

Joshi, R.M. and Pegg, M.J. (2007). Flow Properties of Biodiesel Fuel Blends at Low Temperature, *Fuel,* 86:143-151.

Karmacharya, J.L., (2004). Trans-Boarder Power Supply: Opportunities and Challenges For Power Trade Between Nepal And India, 19th World Energy Congress, Sydney, Australia September 5-9, 2004.

Kwok, D.Y., Cheung, L.K., Park, C.B. and Neumann, A.W., (1998). Study of the Surface Tensions of the Polymer Melts Using Axisymmetric Drop Shape Analysis. *Polymer Engineering and Science*, 35 (5): 757-764.

Kandill, M. (2005). The Development Of A Vibrating Wire Viscometer And A Microwave Cavity Resonator For The Measurement Of Viscosity, Dew Points, Density And Liquid Volume Fraction at High Temperature And Pressure. Ph.D. Thesis, University of Calgary, Calgary, pp 189.

Kilmeck, J., Kleinrahm, R. and Wagner, W., (1998). An Accurate Single-Sinker Densimeter and Measurements of ρ, r, T Relation of Argon and Nitrogen in the Temperature Range from 235 to 520 K at Pressures up to 30 MPa Using a New Accurate Sinker-Sinker Densimeter. Journal of Chemical Thermodynamics. 30 (12):1571-1588.

Kilmeck, J., Kleinrahm, R. and Wagner, W., (2001). Measurements of the ρ, r, T Relation of Methane and Carbon Dioxide in the Temperature Range 240 K to 520 K at Pressures up to 30 MPa Using a New Accurate Single-Sinker Densimeter. *Journal of Chemical Thermodynamics.* 33:251-267.

Kiran, E. and Sen, Y.L. (1991). High pressure Viscosity and Density of N-Alkanes. *International Journal of Thermodynamics*, 13(3):411-442.

Kunen, E. and Chalmers, J. (2010). Sustainable biofuel development policies, programs and practices in APEC economies. Asia Pacific Economic Cooperation, Project no EWG 19/2009, prepared by Winrock International, November 2010, pp:127.
Khatiwada, D. (2010). Assessing the Sustainability of Bioethanol Production In Nepal. Licentiate Thesis in Energy Technology, KTH School of Industrial Engineering and Management, Stockholm, Sweden, pp-79.
Khennas, S. and Barnett, A., 2000. Best Practices for Sustainable Development of Micro Hydropower in Developing Countries. Final Synthesis Report. DFID/ITDG, UK.www.itdg.org (Accessed: April 25, 2008)
Kumar, L.N.V., Dhavala, P., Goswami, A., and Maithel, S. (2006). Liquid biofuels in South Asia: Resources and Technologies. *Asian Biotechnology and Development Review*, 8(2):31-49.
Kivits, R., Charles, M.B. and Ryan, N. (2010). A Post-Carbon Aviation Future: Airports And The Transition To A Cleaner Aviation Sector. *Futures* 42:199–211.
Kulkarni, M.G. and Dalai, A.K.(2006). Waste Cooking Oils an Economical Source for Biodiesel: A Review. *Ind. Eng. Chem. Res.* 45:2901-2913.
Karthikeyan, K., and Mahalakshmi, N.V. (2007). Performance and Emission Characteristics of A Turpentine–Diesel Dual Fuel Engine. Energy 32:1202–1209.
Kommalapati, R.R., Valsaraj, K.T., Constant, W. D. and Roy, D. (1998). Soil Flushing Using Colloidal Gas Aphron Suspensions Generated From A Plant-Based Surfactant. *Journal of Hazardous Materials* 60: 73–87.
Knothe, G. (2004). The History of Vegetable Oil-Based Diesel Fuels. In: The Biodiesel Handbook. Knothe, G., Van Gerpen, J. and Krahl, J. (2004). AOCS Press, Champaign, Illinois.
Kim, T., Beckman, M.S., Farell, P.V. and Gandhi, J.B. (2002). Evaporating Spray Concentration Measurements from Small and Medium Bore Diesel Injectors. Society of Automotive Engineers, Paper Number 2002-01-0219.
Kim, H.J., Park, S.H., Suh, H.K. and Lee, C.S. (2009). Atomization and Evaporation Characteristics of Biodiesel Dimethyl Ether Compared to Diesel Fuel in a High-Press Injection System. *Energy and Fuels* 23, 1734–1742.
Knothe, G. and Steidley, Kevin, R. (2007). Kinematic Viscosity Of Biodiesel Components (Fatty Acid Alkyl Esters) And Related Compounds At Low Temperatures. *Fuel*, 86:2560–2567.
Krisnangkura, K., Yimsuwan, T. and Pairintra, R. (2006). An Empirical Approach In Predicting Biodiesel Viscosity at Various Temperatures. *Fuel*, 85:107–113.
Koh, M.Y. and Ghazi, T. I. M. (2011). A review of Biodiesel Production From Jatropha Curcas L. Oil. Renewable and Sustainable Energy Reviews 15:2240–2251.
Kumar, A. and Sharma, S., (2008). An Evaluation Of Multipurpose Crop for Industrial Uses A Review. *Ind. Crops. Prod*. 28:1–10.
Lele, S. M. (1991). Sustainable Development. A Critical Review. World Development 19 (6). pp 607-621.
Lozano, R. (2008): Envisioning Sustainability Three-Dimensionally. *Journal of Cleaner Production,* 16:1838–1846.
Lee C.S., Park S.W., (2002). An Experimental And Numerical Study On Fuel Atomization Characteristics Of High-Pressure Diesel Injection Sprays. *Fuel* 81, 2417 2423.

Lee, C.S, Park, S.W. and Kwon, S.I. (2005). An Experimental Study on The Atomization And Combustion Characteristics Of Biodiesel –Blended Fuels. *Energy and Fuels,* 19:2201-2208.

Lee, D.W., Park, Y.M., and Lee, K.-Y, (2009). Heterogeneous Base Catalysts for Transesterification in Biodiesel Synthesis. *Catal. Surv. Asia*:13:63–77.

Lee, I., Johnson, L.A., and Hammond, E.G. (1995). Use of Branched-Chain Esters to Reduce The Crystallization Temperature Of Biodiesel. *JAOCS,* 72 (10):1155 1160.

Lefebvre, H. (1989). *Atomization and Sprays.* New York: Hemisphere Publishing Corporation, 1989, pp: 421.

Leung, D.Y.C., Koo, B.C.P. and Guo, Y. (2006): Degradation of Biodiesel Under Different Storage Conditions. *Bioresource Technology* 97(2): 250-256

Li, Y-L, Wang, Y-H, Lu, S-X, (2010). Ignition of the Leaked Diesel On A Heated Horizontal Surface. *Fire Safety Journal* 45:58–68.

Lang, X., Dalai, A.K., Bakhsi, N.N., Reaney, M.J. and Hertz, P.B. (2001). Preparation and Characterization of Bio-Diesels from Various Bio-Oils. *Bioresource Technology,* 80:53-62.

Liptak, B.G., 2003. *Instrument Engineers' Handbook,* 4th Edition, Process Measurement and Analysis, Volume 1, pp 1920.

Lewis, H.W. (1953). Calibration Of The Rolling Ball Viscometer. *Analytical Chemistry*. 25(3):507-508.

Lord Rayleigh, O.M.(1916). On The Theory of The Capillary Tube. Proceedings of The Royal Society Of London, Series A, Containing Papers of A Mathematical And Physical Character, 92(637):184-195.

MOF (2007): Economic Survey, Fiscal Year 2006/07, Ministry of Finance, Nepal.

MOF, (2009). Economic Survey, 2008-2009. Ministry of Finance, Government of Nepal http://www.mof.gov.np/publication/budget/2010/pdf/chapter10.pdf (accessed on July 24, 2010).

MOF, (2010). Ministry of Finance, Economic Survey. Kathmandu; Nepal Rastra Bank.2010. Macroeconomic Situation. Kathmandu; Central Bureau of Statistics.http://www.adb.org/Documents/Economic_Updates/NEP/ co update-aug10.pdf

Matveev, V.A., Orlov, O.E., and Berg, V.I., (2005). Measurement of Viscosity Of A Liquid At High Pressures. Measurement Techniques, 48 (10) 1009-1013.

Meissner, H.P. and Michaels, A.S.(1949). Surface Tension of Pure Liquids and Liquid Mixtures. Industrial and Engineering Chemistry, 41(12): 2782-2787.

Mathieu, J. and Schweitzer, P., (2004). Measurement of Liquid Density by Ultrasound Backscattering Analysis. Measurement of Science and Technology. 15(8): 869-876

Munasinghe, M. (1992). Environmental Economics and Sustainable Development, Paper presented at the UN Earth Summit, Rio de Janeiro, Environment Paper No.3, World Bank, Wash. DC, USA. http://www.eoearth.org/article/Sustainable_ development_Triangle (accessed on October 10, 2011)

Mandava, S.S. (1994). Application Of A Natural Surfactant from Sapindus Emerginatus to in Situ Flushing Of Soils Contaminated With Hydrophobic Organic Compounds. M.S. Thesis in Civil and Environmental Engineering, Faculty of Louisiana State University and Agricultural and Mechanical College.

Maltsoglou, I. and Taniguchi, K. (2004). Poverty, Livestock and Household Typologies in Nepal, ESA Working Paper No. 04-15, FAO page 1-48, at http://www.fao.org/docrep/ 007/ae125e/ae125e00.htm, (accessed on June 26, 2010).

MOAC (Ministry of Agriculture and Cooperatives), Government of Nepal. (2008). Exports to overseas countries 2006/2007, Statistics,at<http://www.moac.gov.np/home/statistics.php>, (accessed on June 27, 2010)

Marimex (2010). ViscoSCope Viscometer Sensor Model VA-300 xx LT/ST/HT,Operator Manual.

Ma. F., Hanna, M.A.(1999). Biodiesel Production: A Review. Bioresource Technology 70:1– 15.

Misra, R.D. and Murthy, M.S. (2011).Performance, Emission and Combustion Evaluation of Soapnut Oil Diesel Blends in a Compression Ignition Engine. Fuel, 90:2514-2518.

NOC, (2007). Nepal Oil Corporation, Status of Import of Petroleum Products, Quarterly Review, April, 2007.

NOC, (2009). Nepal Oil Corporation, Status of Import of Petroleum Products, Quarterly Review, December, 2009.

NEA (2007). Nepal Electricity Authority Fiscal Year 2006-2007, a Year in Review, pp 62.http://www.nea.org.np//reports/annualReports/ePpFTGEarOanrep7.pdf (accessed on July 08, 2010).

NPC, (2003). Nepal Planning Commission, the Tenth Plan (2002–2007), Government of Nepal, Kathmandu.

Namarmi, A.M., Shrestha, J.N., Shrestha, N.P., Bajracharya, .T.R., Vaidya, B., Poudyal, K.N., Pokharel, M.D., Nainabasti, B., Shrestha, S. and Shakya, I., (2002). Energy country analysis Brief: Nepal, February, 2002.

Neupane, K. (2010). Restaurants and Bar Association of Nepal (REBAN). Personal Communication (January 2010).

Nayaju, R.P. and Lilleso, J.P.B. (2000). Nation-wide Climate Tables, Database at HGM Danida NARMSAP/TISC, Kathmandu, Nepal.

Nita, I., Geacai, S. and Iulian, O. (2011). Measurements and Correlations of Physic Chemical Properties To Composition of Pseudo-Binary Mixtures With Biodiesel. Renewable Energy (36): 3417-3423.

Nogueira, Jr., C.A., Feitosa, F.X., Fernandes, F. A. N., Santiago, R.S. and deSantAna, H.B.,(2010). Densities And Viscosities of Binary Mixtures Of Babassu Biodiesel Cotton Seedor Soybean Biodiesel At Different Temperatures. J. Chem. Eng.Data, 55:5305–5310.

Ou,X., Zhang, X. and Chang, S.(2010). Alternative Fuel Buses Currently in Use in China:Life Cycle Fossil Fuel Use, GHG Emissions and Policy Recommendations. *Energy Policy*, 38: 406-418.

Oli, P.P. (2001). Spatial Data for Land Use Planning in Nepal. International Conference on Spatial Information for Sustainable Development Nairobi, Kenya, 2–5 October 2001.

Omer, A. M. (2008). Energy, Environment and Sustainable Development. *Renewable and Sustainable Energy Reviews*, 12:2265–2300.

Olsen, C.S. (1997). A Qualitative Assessment of the Sustainability of Commercial Non-TimberForest Product Collection in Nepal. Forestry discussion paper 12, Royal Veterinary andAgricultural University, Copenhagen, 30 pp.

Peterson, C. and Reece, D. (1996). Emission Characterization of Ethyl and Methyl Esters of Rapeseed oil Compared with Low Sulfur Diesel Control Fuel in a Chassis Dynamometer Test of a Pickup Truck. *Trans ASAE*, 39(3): 805-816.

Peterson, C.L., Reece, D.L., Cruz, R., and Thompson, J. (1992). A Comparison of Methyl and Ethyl Esters of Vegetable Oils as Diesel Engine Substitutes. In: Liquid Fuels from Renewable Resources. Proceedings on Alternative Energy Conference. ASAE, St. Joseph, MI. pp 99-105.

Peterson, C.L., Kordus, R.A., Mora, J.P and Madsen, J.P.(1987). Fumigation with Propane and Transesterification Effects on Injector Coking with Vegetable Oil Fuels. *Trans ASAE,* 31(1): 28-35.

Pokharel, S.R.(2007). Kyoto Protocol and Nepal's Energy Sector. *Energy Policy* 35:2514-2525.

Pokharel, G.R. (2006). Promoting Sustainable Development by Creating Enterprises on Renewable Energy Technologies in Nepal: Case Studies Based on Micro Hydropower Project. Ph.D. thesis, University of Flensburg, Germany, pp 400.

Pokharel, G.R., Chhetri, A, B., Khan, M.I. and Islam, M.R., (2008). Decentralized Micro-hydro Energy Systems in Nepal: En Route to Sustainable Energy Development. *Energy Sources*. 3(2):144-154.

Pokharel, G.R. and Sharma, S. (2008). Biofuel: Potential and Prospects in Nepal as an Alternative to Fossil Fuels. *International Energy Journal*, 9: 78-88.

Pokharel, G.R., Chhetri, A, B., Devkota, S. and Shrestha, P., (2003). En Route to Strong Sustainability: Can Decentralized Community Owned Micro Hydro Energy systems in Nepal Realize the Paradigm? A case study of Thampalkot VDC in Sindhupalchowk District in Nepal. International Conference on Renewable Energy Technology for Rural Development. October 12-14, Kathmandu, Nepal, pp. 272-276.

Pandey, B., R., (2006). Financing biogas in Nepal Through CDM. Special Issue on First Birthday of Kyoto Protocol entry into force. Clean energy Nepal , Vol. 6, Number 13, 16 February 2006.

Passerone, A. and Ricci, E., 1998. High Temperature Tensiometry. Drops and Bubble in *Interfacial Research*, 475-524.

Prugh, T., Costanza, R., Cumberland, J.H., Dal, H.E., and Norgaard, R.B., (1999).Natural Capital and Human Economic Servival, 2nd Edition. pp 180.

Prugh, T., Costanza, R. and Daly, H.E. (2000). *The Local Politics of Global Sustainability,* Island Press, pp:196.

Pezzey J.C. V. and Toman, M.A. (2002). The Economics of Sustainability. Resources for Future. Discussion Paper 02-03, pp 1-36.

Phillip, J. (2010). The Advancement of A Mathematical Model of Sustainable Development. *Sustain.Sci.,* 5:217-142.
Pezzey, J. (1992). Sustainable Development Concepts:An Economic Analysis. World Bank Environment Paper No. 2 World Bank, Washington D.C. Report no 11425, pp 1-73.
Pearce, D., Turner R. K., O'Riordan T. (1994). Blueprint 3, Measuring Sustainable Development, Earthscan, U.K.
Pearce, D. W., Barbier, E., Markandya, A. 1990. Sustainable Development, Economics and Environment in the Third world, Edward Elgar, London, U.K.
Pearce, D. W. and G. Atkinson, 1995. Measuring Sustainable Development. In: D. W. Bromley (ed.). The Handbook of Environmental Economics. Blackwell, Oxford.
Plas, R., V. and De Graaff, A.B., (1988). A Comparison of Lamps for Domestic Lighting in Developing Countries. Household Energy Unit, Energy Sector Management and Assessment Division, Industry and Energy Department, the World Bank. Washington, DC, 20433.
Pleanjai, S. and Gheewala, S.H. (2009). Full Chain Energy Analysis of Biodiesel Production from Palm Oil in Thailand. *Applied Energy* (86):5209-5214.
Pradhan, A., Shrestha, D.S., Van Gerpen, J. and Duffeld, J. (2005). The Energy Balance of Soybean Oil Biodiesel Production:A Review Of Past Studies. *Am. Soc. Biol. Eng.*(51)185-194.
Parajuli, R. (2009). Fostering Jatropha Curcas for Reducing Fossil Fuel Dependency; A Study on Potentiality of Jatropha Curcas in Nepal, http://www.environmental-expert.com/resultEachArticle.aspx?cid=0&codi=72737&lr=1&word=Fostering+Jatropha+Curcas (Accessed on July, 2010).
Panhwar, F. (2005). Non-Traditional Seed Oils. DigitalVerlag, GmBH, Germany. http://www.chemlin.depublications/documents/non%20traditional%20oilseeds%20and%20oils.pdf (accessed on July 20, 2010).
Pariyar, D. (2006). Country Pasture/Forage Resource Profiles, Nepal. FAO, Grassland and Pasture Crops, at http://www.fao.org/ag/AGP/AGPC/doc/Counprof/Nepal.htm (accessed on June 25, 2010).
Pant, P.R. and Dongol, D. (2009). Kathmandu Valley profile-A Briefing Paper Presented in "Governance and Infrastructure Development Challenges in the Kathmandu Valley", Workshop Organized by Kathmandu Metropoliton City, 11-13 February, 2009.
Pramanik, K. (2003). Properties And Use Of Jatropha Curcas Oil And Diesel Fuel Blends In Compression Ignition Engine. *Renewable Energy* 28, 239–248.
Pratas, M.J, Oliveira, M.B., Pastoriza-Gallego, M.J., Queimada, A.J., Piñeiro, M.M, and Coutinho, J.A.P, (2011): High-Pressure Biodiesel Density: Experimental Measurements, Correlation and CPA Eos Modeling. Energy and Fuels. Accepted, DOI: 10.1021/ef200807m.
Pratas, M. J.; Freitas, S.; Oliveira, M. B.; Monteiro, S. C.; Lima, A. S.; Coutinho, J. A. P. (2010).Densities And Viscosities of Fatty Acid Methyl And Ethyl Esters. *J.Chem.Eng. Data*, 55: 3983–3990.
Paton, J.M. and Schaschke, C.J.(2009). Viscosity Measurement of Biodiesel at High Pressure with A Falling Sinker Viscometer. *Chemical Engineering Research and Design* 87: 1520–1526.

Payri, R., Salvador, F.J., Gimeno, J. and Bracho, G. (2011). The Effect of Temperature and Pressure on Thermodynamic Properties of Diesel and Biodiesel Fuels. *Fuel* 90:1172–1180.

Rajbhandari, K,D.,(1998). Technology of Renewable Energy: For the Sustainable Development, In Nepal. Publication of NESS - Technology - *A Journal of Engineering*, Vol. 7, May 1998.

Raza, H. (2005). *Co-operation Fuels Development,* The World Energy Book, World Energy Council, London, pp. 18–20.

Ranjit, M., (2005b). Geothermal Energy Update of Nepal, Proceedings World Geothermal Congress Antalya, Turkey, 24-29 April 2005, pp 10.

Ranjit, M. (2005a). Geothermal Energy Update of Nepal. Proceedings World Geothermal Congress 2005 Antalya, Turkey, 24-29 April 2005.

Rice, O.K., (1947). The Effect of Pressure on Surface Tension. *The Journal of Chemical Physics,* 15 (5): 333-335.

Rotenberg, Y., Boruvka, L., and Neumann, A.W., (1982). Determination of Surface Tension and Contact Angle from the Shapes of Axisymmetric Fluid Interfaces. Journal of Colloid and Interface Science, 93 (1): 169-183.

Reid, R.C., Prausnitz, J.M., and Poling, B.E., (1987). The Properties ff Gases And Liquids. McGraw-Hill, New York. pp 741.

Roy, D., Kommalapati, R.R., Mandava, S., Valsaraj, K.T. and Constant, W.D. (1997). Soil Washing Potential of A Natural Surfactant. *Environ. Sci. Technol.* 31 (3): 670–675.

Statistics Canada (2006). Canada's Population Clock. Statistics Canada, Demography Division Updated in October 27.

Radich, A. (2006). Biodiesel Performance, Costs And Use. US Energy Information Administration.http://www.eia.doe.gov/oiaf/analysispaper/biodiesel/index.html (accessed on September 15, 2010).

Ramesh, P and Murughan, M (2008). Edible Oil Consumption in India. AMEFT, 3: 8. http://www.ameft.com/picture/upload/file/08.pdf (accessed on September 15, 2010).

Ricart, L.M., Reltz, R.D., and Dec, J.E. (2002). Comparisons of Diesel Spray Liquid Penetration And Vapor Fuel Distribution With In-Cylinder Optical Measurements. Journal of Engineering For Gas Turbines And Power. Transactions of the ASME, 122:588-595.

Ramadhas A.S, Jayaraj S., Muraleedharan, C. (2005). Biodiesel Production from High FFA Rubber Seed Oil. *Fuel,* 84:335–340.

Rywotycki, R. (2002). The Effect of Fat Temperature on Heat Energy Consumption During Frying of Food. *Journal of Food Engineering* 54, 257-261.

Rodrigues, J., Cardoso, F., Lachter, E., Estevão, L., Lima, E. and Nascimento, R. J.(2006). Correlating Chemical Structure and Physical Properties of Vegetable Oil Esters. *J. Am. Oil Chem. Soc.* 83: 353-357.

Ramírez-Verduzco, L.F., Rodríguez-Rodríguez, J.E., Jaramillo-Jacob, A.D.L, (2012). Predicting Cetane Number, Kinematic Viscosity, Density and Higher Heating Value of Biodiesel From its Fatty Acid Methyl Ester Composition. *Fuel,* 91 (1):102-111.

Ramírez-Verduzco, L.F., García-Flores, B. E., Rodríguez-Rodríguez, J. E., and Jaramillo-Jacob, A.D.R, (2011). Prediction of the Density and Viscosity in Biodiesel Blends at Various Temperatures. *Fuel*, 90:1751–1761.

Rashid, U., Anwar, F., Moser, B.R. and Knothe, G. (2008). Moringa Oleifera oil: A Possible Source of Biodiesel. *Bioresource Technology*, 99:8175-8179.

Rotmans, J., Grosskurth, J., Van Asselt, M.and Loorbach, D. (2001). Sustainable development:From draft to implementation. Maastrich:ICIS.

Roberts, J. (2004). *Environmental Policy*, Routledge, London, pp 272.

Smalley, R.E. (2005). Future Global Energy Prosperity: The Terawatt Challenge. MRS Bulletin, Vol 30, June 2005. www.mrs.org/publications/bulletin (Retrieved on January 20, 2011).

Shrestha, J.N., Bajracharya, T.R., Shakya, S.R. and Giri, B.(2003). Renewable energy in Nepal—Progress at a glance from 1998 to 2003, in Proceedings of Renewable energy technology for rural development, Kathmandu, Nepal, pp. 1–10.

SWERA (2006), Solar and wind energy resource assessment in Nepal (SWERA), Final Report. Alternative Energy Promotion Centre Nepal, Government of Nepal, Ministry of Environment., Science and Technology, 89p.

Silveira, S. and Khatiwada, D.(2010). Ethanol Production and Fuel Substitution InNepal Opportunity to Promote Sustainable Development and Climate Change Mitigation. *Renewable and Sustainable Energy Reviews*, 14 (6):1644-1652.

Sonntag, H., 1982. Koloidy, PWN, Warszawa. Advances in Colloid Interface. 16:337.

Saran, S. (1999). Soil Dynamic and Machine Foundations. Galgotia Publication Pvt.Ltd. New Delhi, India, pp: 486

Spencer, C.F. and R.P. Danner, (1972). Improved Equation for Prediction of Saturated Liquid Density. *J. Chem. Eng.Data*, 17(2):236-241.

Sestak, J. and Ambros, F., (1973). On The Use of the Rolling-Ball Viscometer for the Measurement of Rheological Parameters of Power Law Fluids. *Rheol. Acta* 12:7076.

Segnestam, L. (2002). Indicators of Environment and Sustainable Development: Theories and Practical Experience. Environmental Economics Series, the World Bank Discussion Paper no 89, pp 1-66.

Schellnhuber, H-J. (1998) Part 1: Earth System Analysis—the Concept. In: Schellnhuber H-J, Wenzel V (Eds) Earth System Analysis: Integrating Science for Sustainable Development. Springer,Berlin, pp 3–195

Schellnhuber, H-J. (1999) 'Earth System' Analysis and the Second Copernican Revolution.Nature 402. (Millennium Supplement).

Schellnhuber, H-J., (2001) Earth System Analysis and Management. In: Ehlers E, Kraf (Eds) Understanding the Earth System: Compartments, Processes and Interactions. Springer, Berlin, pp 17–55

$(S\&T)^2$ consultants Inc. (2010). Life Cycle Analysis of Canola Biodiesel-Prepared for Canola Council of Canada. pp 46, http://www.canolacouncil.org/uploads/Canola%20Lifecycle % 20Analysis.pdf (accessed on April 02, 2012).

Sheehan, J., Camobreco, V., Duffield, J.Graboski, M. and Shapouri, H. (1998). An Overview of Biodiesel and Petroleum Diesel Life Cycles. National Renewable Energy Laboratory, US Department of Energy. NREL/TP-580-24772.http://www.nrel.gov/ vehiclesandfuels/npbf/pdfs/24772.pdf (Accessed on December 21, 2011).

Singh, N. (1980). A Study on Vegetable Oils, Oil Seed-Bearing Plants in Nepal. Research Centre, for Applied Science and Technology (RECAST), Tribhuwan Unibversity, Nepal, pp 28.

Shu, Q., Wang, J., Peng, B., Dezheng, Wang, G., (2008). Predicting Surface Tension of Biodiesel Fuels by a Mixture Topological Index Method At 313 K. *Fuel,* 87:3586-3590.

Shu,Q., Yang, B., Yang, J. and Qing, S.(2007). Predicting the Viscosity Of Biodiesel Fuels Based On The Mixture Topological Index Method. *Fuel*, 86: 1849–1854.

Sims, J.R., Solum, D.J. Wichman, D.M., Kushnak, G.D., Welty, L.W., Jackson, G.D., Stallknecht, G.F., Westcott, M.P. and Carlson, G.R. (1993). Canola Variety Yield Trials. *Montana Ag.Res*. 10(2): 15-20.

Spencer, C.F. and R.P. Danner, (1972). Improved Equation for Prediction of Saturated Liquid Density. *J. Chem. Eng.Data*, 17(2):236-241.

Tat, M.E. and Van Gerpen, J.H.(2002). Physical Properties and Composition Detection of Biodiesel-Diesel fuel Blends. An ASAE Meeting Presentation. Paper Number: 026084.

Tat, M.E. and Van Gerpen, J.H. (2003). Fuel Property Effects on Biodiesel. ASAE Paper Number: 036034.

Tat, M.E., Van Gerpen, J.H., Soylu, S., Canakci, M., Monyem, A. and Wormley, S. (2000). The Speed of Sound and Isentropic Bulk Modulus of Biodiesel at 21°C from Atmospheric Pressure to 35 MPa. *J. American Oil Chem. Soc*., 77(3): 285 289.

Tat, M.E., Van Gerpen, J.H. (2000). The Specific Gravity of Biodiesel and its Blends with Diesel Fuel. *J. American Oil Chem. Soc*., 77(2):115-119.

Tat, M. E., and Van Gerpen, J. H. (1999). The Kinematic Viscosity of Biodiesel and its Blends With Diesel Fuel. *J. American Oil Cem. Soc.* 76(12): 1511-1513.

Tohidi, B., Burgass, R.W., Danesh, A. and Todd, A.C.(2001). Viscosity and Density of Methane+Methylcylcohexane from (323 To 423) K and Pressure to 140 Mpa. *Journal of Chemical Engineering Data*, 46:385-390.

Tate, R.E., 2005. Measurement of Physical Properties of Biodiesel Fuels at Temperatures Up to 300oC.M.A.Sc thesis, Biological engineering, Dalhousie University, Canada.

The Kathmandu Post (2001). Nepal/UK Oil Seed Project, 2001. http://freespace.virgin.net/himal.proj/ theseshimal.htm; Project Background (Accessed on October 14, 2007).

The Associated Press (2011). KLM to Turn Used Cooking Oil into Aviation Biofuel. http://www.metronews.ca/london/world/article/897020--klm-to-turn-used-cooking-oil-into-aviation-biofuel (Retrieved on June 23, 2011).

Tate, R.E., Watts, K.C., Allen, C.A.W. and Wilkie, K.I. (2005). The Viscosities of Three Biodiesel Fuels at Temperatures Up to 300 oC. *Fuel*, 85: 1010-1015.

Tate, R.E. (2005). Measurement of physical properties of biodiesel fuels at temperatures up to 300 oC. M.A.Sc Thesis, Biological Engineering, Dalhousie University, Halifax, NS, Canada, pp 126.

Tesfa, B., Mishra, R., Gu, F. and Powles, N. (2010). Prediction Models for Density and Viscosity of Biodiesel and Their Effects on Fuel Supply System in CI Engines. *Renewable Energy,* 35:2752-2760.

Tate, R. E.; Watts, K. C.; Allen, C. A. W.; Wilkie, K. I.(2006). The densities of three biodiesel fuels at temperatures up to 300°C. *Fuel:*85, 1004–1009.

Taylor, A.J., Smith, C.J., and Wilson, I.B. (1991). Effect of Irrigation and Nitrogen Fertilizer on Yield, Oil Content, Nitrogen Accumulation and Water Use of Canola (Brassica napus L.). Nutrient Cycling in Agroecosystems, 29(3): 249-260.

Tiwari, A.K., Kumar, A., Raheman, H. (2007). Biodiesel Production from Jatropha (Jatropha Curcas) with High Free Fatty Acids: An Optimized Process. *Biomass & Bioenergy* 31, 569-575.

Talos (2003). The Road Towards A Socially Sustainable Society. Tilburg:Telos.

UNCTAD (2009). The Least Developed Countries Report 2009-The State And Development Governance. United Nations Conference on Trade and Development (UNCTAD). http://www.unctad.org/en/docs/ldc2009_en.pdf (accessed on January 23, 2011).

Upreti, B.N. and Shakya, A. (2010). Wind Energy Potential Assessment in Nepal. A Report Prepared for Alternative Energy Promotion Centre, Nepal http://www.wind.arch.t-kougei.ac.jp/APECWW/Report/2009/NEPAL.pdf (Assessed on September 8, 2010).

UNEP (2006). Energy Technology Fact Sheet: Small Scale Hydro: UNEP Division of Technology, Industry and Economics-Energy and OzonAction Unit. http://www.unep.fr/energy/information/publications/factsheets/pdf/hydro.PDF (Accessed on May 02, 2012).

United Nations, (1999). Indicators of Sustainable Development: Framework and Methodologies, New York.

U.S. Department of Energy, 2006. Biodiesel. Alternative Fuel Data Centre. http://www.eere.energy.gov/afdc/altfuel/biodiesel.html (accessed on December 19, 2011).

Ucciani, E., Mallet, J. F. and Zahra, J. P. (1994). Cyanolipids And Fatty Acids of Sapindus Trifoliatus L. (Sapindaceae) Seed Oil. Fat Science Technology, 96 (2): 69-71.

Viswanath, D.S., Gosh, T.K., Prasad, D.H.L., Dutt, N.V.K. and Rani, K.Y., (2006).Viscosity of Liquids: Theory, Estimation, Experiment, and Data. Springer, pp: 676.

Vantomme, P., Markkula, A. and Leslie, R.N. (2002). Non-Wood Forest Product in 15 Countries in Tropical Asia, An Overview. EC-FAO Partnership Program. Information and Analysis for Sustainable Forest Management: Linking National and International Efforts in South and Southeast Asia, pp 202.

Van Gerpen, J., Shanks, B., Pruszko, R., Clements, D., Tyson, K.S. and Knothe, G. (2004). Biodiesel Production Technology. National Renewable Energy Laboratory 1617 Cole Boulevard, Golden, Colorado.NREL/SR 51036244<www.nrel.gov>http://journeytoforever.org/biodieselyield2.html#biodstds (accessed on August 20, 2010)

Vavruch, I, (1995). On The Evaluation of the Surface Tension–Pressure Coefficient of Pure Liquids. J. Colloid Interface Sci. 169: 249–250.

WECS (1996). Energy Synopsis Report: Nepal 1994/95, Water and Energy Commission Secretariat, Ministry of Water Resources, Kathmandu, Nepal.

WECS, (2006): Energy Synopsis Report: Nepal 2006, Water and Energy Commission Secretariat, Ministry of Water Resources, Government of Nepal.

WECS, (2010). Energy Sector Synopsis Report, Nepal, July 2010. Water and Energy December 31, 2010. http://www.adb.org/Documents/Fact_Sheets/NEP.pdf (Accessed on September 25, 2011).

Wiegand, G. and Franck, E.U., (1994). Interfacial Tension Between Water and Non-Polar Fluids up to 473 K and 2800 bar. Berichte der Bunsen-Gesellschaft fur Physikalische Chemie. 98 (1):809-817.

Wagner, W., Brachthauser, K. Kleinrahm, R. and Losch, H.W. (1995). A New, Accurate Single-Sinker Densitometer for Temperatures from 233 K to 523 K at Pressures up to 30 MPa. International Journal of Thermophysics, 16(2): 399-411.

Wisniewski, R., Siegozynski, R.M. and Rostocki, A.J., (2005). High Pressure Research 25:(1):63-70.

Wazer, V., J.R., Lynons, J.W., Kim, K.Y., and Colwell, R.E., (1963). Viscosity and Flow Measurement: A Laboratory Handbook. Interscience Pub, N.Y., pp406.

Westwood, B. M. and Kabadi, V. N., (2003). A Novel Pycnometer for Density Measurements of Liquids at Elevated Temperatures. *Journal of Chemical Thermodynamics.* 35 (12):1965-1974.

WCED, (1987). Our Common Future. World Commission on Environment and Development (WCED), Oxford University Press, U.K.

World Bank (1996). Rural Energy and Development, Improving Energy Supplies for Two Billion People. Washington D.C.

Winrock International (2010). Sustainable Biofuel Development Policies, Programs and Practices in APEC Economies. Asis Pacific Economic Cooperation (APEC) Project Report (APEC#210-RE-01.20), pp 127.

Whitaker, M. and Heath, G. (2009). Life Cycle Assessment Of The Use of Jatropha Biodiesel in Indian Locomotives. Technical Report, National Renewable Energy Laboratory-NREL/TP-6A2-44428.www.nrel.gov/biomass/pdfs/44428.pdf (accessed on December 22, 2011).

Wang, Z., Calderon, M.M. and Lu, Y. (2011). Life Cycle Assessment of the Economic, Economical and Energy Performance of Jatropha Curcas L. Biodiesel in China. Biomass and Bioenergy, (35):2893-2902.

W.B. (2009). Community Development Carbon Fund Project Portfolio. Carbon Finance Unit, The World Bank. http://wbcarbonfinance.org/Router.cfm?Page= CDCF&FID=9709&ItemID =9709&ft=Projects (accessed on 14th May 2009).

Windholz, M. (1983). The Merck Index: An Encyclopedia of Chemicals, Drugs, and Biologicals, Merck, Rathway, NJ.

Yang, H-H., Chien, S-M., Lo, M-Y., Lan, J. C.-W., Lu, W-C., and Ku, Y-Y. (2007).Effects of Biodiesel on Emissions of Regulated Air Pollutants and Polycyclic Aromatic Hydrocarbons Under Engine Durability Testing. *Atmospheric Environment,* 41:7232–7240.

Yuan, W., Hansen, A.C. and Zhang, Q. (2003). Predicting the Physical Properties of Biodiesel for Comnbustion Modeling.American Society of Agricultural Engineers, 46(6): 1487-1493.

Yang, D.Y.; Tontiwachwuthikul, P. and Gu, Y.G. (2005). Interfacial Interactions Between Reservoir Brine and CO_2 at High Pressures and Elevated Temperatures. *Energy & Fuels*, 19:216-223.

Yuan, W., Hansen, A.C. and Zhang, Q. (2009). Predicting the Temperature Dependent Viscosity of Biodiesel Fuels. *Fuel,* 88:1120–1126

Zahnd, A., McKay, H. K. and Komp, R., (2006). Renewable Energy Village Power Systems for Remote and Impoverished Himalayan Villages in Nepal. Proceedings of the International Conference on Renewable Energy for Developing Countries 2006, pp 35.

Zahnd, A. and Kimber, H.K., (2009). Benefits from a Renewable Energy Village Electrification System. *Renewable Energy,* 34(2):362-368.

Zhou, Z., Jiang, H. and Qin, L. (2007). Life Cycle Sustainability Assessment of Fuels. *Fuel,* 86:256–263.

Zhang Y., Dube, M.A., McLean, D.D. (2003). Kates M. Biodiesel Production from Waste Cooking Oil. Process Design and Technological Assessment. *Bioresource Technology,* 89:1–16.

Zhu, Y. and Granick, S. (2001). Viscosity of Interfacial Water. *Phys. Rev. Lett.* 8 (9): 96-104.

Zheng, S.; Kates, M.; Dube, M.A.; McLean, D.D., (2006). Acid-Catalyzed Production of Biodiesel from Waste Frying Oil. *Biomass and Bioenergy*, 30, 267-272

APPENDIX A: REVIEW OF EXPERIMENTAL METHODS

A.1 DENSITY MEASUREMENT

Various methods of measuring fluid density have been reviewed and presented below with the purpose of determining the methods to be used in this thesis.

A. 1.1 Hydrometer

Hydrometers offer the simplest and economic method to measure the specific gravity of liquids based on Archimedes principle of buoyancy. The specific gravity is the ratio of density of the material to the density of water at specified temperature and is a dimensionless unit. Hydrometers are normally comprised of a calibrated float with a calibrated scale (graduated tube) that floats in the liquid of which the specific gravity is to be measured (Joshi, 2007). The specific gravity is measured by directly reading level of liquid corresponding to the mark in the hydrometer.

This method is suitable only for liquids at atmospheric pressure and room temperature. Kilmeck et al (1998) developed a hydrometer based on Archimedes principle but in a modified way. The buoyancy force exerted by the fluid of which specific gravity is to be measured on an immersed sinker is transferred through the wall of the measuring cell by a magnetic suspension which is coupled to an analytical balance. This method was capable in measuring specific gravities in the range of -40^{o}C to 250^{o}C and 0.2 MPa to 30 MPa. Kilmeck et al., (1998 and 2001) measured specific gravity to 0.02% accuracy. As the measurement taking process is too complex and time consuming, this method was not used for this work.

A. 1.2 High Temperature Pycnometer

Temperature dependent density of any liquid can be determined from either the change in volume of a known mass (also called dilatometry) or the change in mass in a known volume (also known as pycnometry). A pycnometer consists of a calibrated cup of known volume that has an overflow spout. In case the density is to be measured at elevated temperatures and pressures, the apparatus is constructed of steel and pressure fittings, and is heated in an oven. The stainless steel cell is connected to a small-bore tube with and expansion fittings that allows overflow due to thermal expansion (Westwood and Kabadi, 2003). The sample with desired temperature and pressure is heated in an oven. The remaining mass of sample is measured after it is depressurized and cooled. This is a very time consuming system to measure the density at high temperatures and pressures. It was shown that this method can be used to measure the density of some pure liquids and mixtures up to a temperature of 485 K and pressures up to 4.93 MPa (Westwood and Kabadi, 2003). In this work, we intended to measure the density 523 K and 7 MPa. High precision pycnometers are very expensive and hence this method was not chosen.

A.1.3 Measurement of Density by Ultrasound

Mathieu and Schweitzer (2004) proposed a new method of liquid density measurement based on resonant scattering theory (RST). The RST theory showed that the influence of liquid density on the backscattering ultrasound pressure is weak in absolute value but shows a strong relationship in relative value (Mathieu and Schweitzer, 2004). In this method, a comparison was made between the spectrum of the ultrasound pressure backscattered by a wire were compared for a liquid of known and unknown density (e.g. water). By comparing the spectra of curves for two liquids, a characteristic of the relative density of the test liquid with respect to the reference liquid density can be obtained. In this experiment, the measurement is carried out in four different stages with two different wires. One wire is used to calibrate the instrumental chain while another wire allows effective measurement of the spectrum and echo for each wire in each liquid is acquired

(in both test liquid and reference liquid). The density results found from this method were reported to be comparable with the theoretical values for different liquids.

Bamberger and Greenwood (2004) developed a highly sensitive, non-invasive, self-calibrating, on-line ultrasonic sensor to measure the speed of sound, density, and attenuation of ultrasound for a liquid flowing through a pipeline. It was concluded that this method can also be applied in vessels. The acoustic impedance is determined by multiplying the density and the speed of sound. In order to determine the acoustic impedance, multiple reflections within the stainless steel wall are used and the density of liquid is calculated from the relationship between impedance, density and speed of sound. This method was too complex and was not chosen for this work.

A .1.4 Buoyancy-Type Densitometer

This densitometer works on Archimedes Principle. A mass of known volume is attached to a fine wire and then suspended in the test liquid. The density of the liquid can be calculated from the known mass, volume and supporting weight of the material called sinker (buoy). Wagner et al.(1995) used a magnetic suspension to measure the density of the fluid at a wide range of temperatures of 233 to 523 K and up to a pressure of 30 MPa at an uncertainty of $\pm$ 0.02% to $\pm$ 0.03%. A special compact version of such a single-sinker densitometer can be used at temperatures from 80 to 523 K at pressures up to 100 MPa. This method can measure a density in the range of 10-2000 kg/m^3. The following relation is used to measure the density (ρ) of sinker

.

$$\rho = \frac{m_s - m^*_s}{V_s(T,p)} \qquad \text{(A.1)}$$

where ms is the "true" mass of the sinker (weighted in the evacuating cell), ms*is the "apparent" mass of the sinker (weighed in the fluid-filled measuring cell), and Vs(T, p) is the temperature- and pressure-dependent volume of the sinker. The value of Vs (T,p) is known from calibration with water at 293 K and 0.1 MPa (calibration uncertainty $\leq \pm$

0.003 %). It is claimed that this new single-sinker method compensates all side effects which drastically reduces the error when the Archimedes principle is used for density measurements in its classical application. Due to the lower temperature range and several complexities, this method was not chosen for this work.

A. 1.5 Radioactive Densitometer

The radioactive densitometer consists of a radioactive source beam through a pipe and a detection system to measure the amount of transmitted radiation. Theoretically, when gamma rays are passed through the fluid of which the density is to be determined, the rays are absorbed in proportion to the density of the test fluid. Due to an increase in the density of the fluid due to absorption of the radiation, the output current is reduced. To measure the density of fluid flowing smaller pipe, the Z-shape arrangement for flow (Figure A.1) is considered to have more accuracy. For the pipe flow of larger diameter, flow can be arranged as in Figure A. 2.

The size of a radiation source is expressed in millicuries (mCi). One millicurie is defined as 37 million disintegrations of the source material. For density application, the source size ranges from 5 to 10,000 mCi for cesium isotope. According to Liptak (2003), the amount of radiation exposure received by a source is expressed in Roentgen equivalent man (rem) units and expressed as follows.

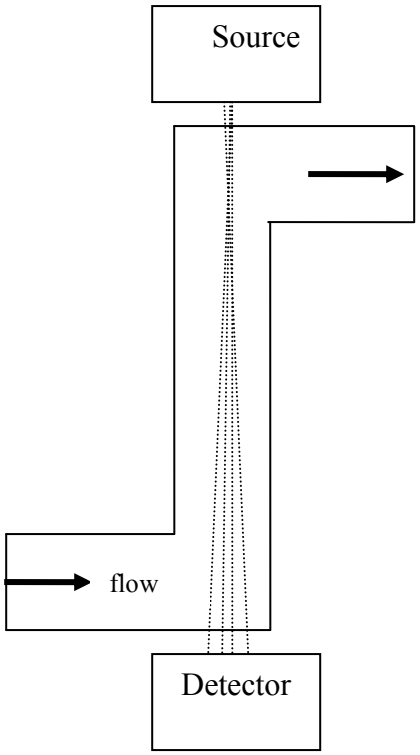

Figure A.1 For smaller pipe flow

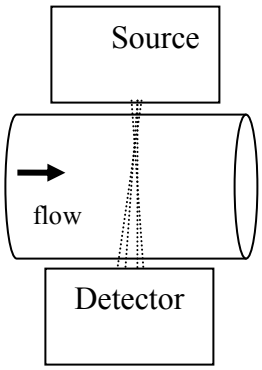

flow

Figure A.2 For larger pipe flow (Liptak, 2003)

$$D = 1000 \frac{KmCi}{d^2} \quad \text{(A.7)}$$

where, D is intensity (mr/hr), mCi is the size of source in millicuries, d is the distance to the sources in inches and K is constant (0.6 for cesium 137).

The radiation intensity exposure drops with the square of distance to the source of radiation. There are various limitations of measuring density from radiation densitometers such as the detector temperature should not rise above 333 K, effect due to the air entrainment, pipe wall deposit and source decay etc.

Eren (1999) developed a relationship to measure the density of liquid using the radioactivity of gamma (γ) rays. The γ rays are passed through the test liquid and are

received on the other side. The Intensity J of the γ rays after passing through a material of density (ρ) and thickness d is expressed as below.

$$J = Jo.\exp(n.\rho.d) \qquad (A.8)$$

where n is the mass absorption coefficient and Jo is initial intensity.

This system was not available and was not chosen to pursue in this work.

A.1.6 Vibrating Densitometers

Vibrating densitometers are based on the phenomenon that the natural frequency of oscillation varies with the mass of the oscillating body. Hence, the frequency of oscillation can be used to measure the density if mass varies with density. Eren (1999) reported that if the vibrating element is introduced in the test fluid, the frequency is directly proportional to the stiffness of the element and inversely proportional to the product of mass of the element and the test fluid. Eren (1999) showed that equation of the resonant frequency can be expressed as follows.

$$f = \sqrt{\left[\frac{K}{(M + k.\rho}\right]} \qquad (A.9)$$

where f is resonant frequency, k is the system constant, M is the transducer mass, K is the system stiffness, and ρ is the density of the fluid.

There are various types of vibrating element densitometers commercially available. In the vibrating tube densitometer, a tube of known mass is vibrated at its natural frequency. The test liquid flows through the tube and the change of frequency is proportional to the change in density of the test fluid. These densitometers can have either one tube or two tubes. The second type is called the vibrating cylinder densitometer. In this densitometer,

a thin walled cylinder is maintained at its frequency by using a magnetic drive on the side or outside of the cylinder. The cylinder wall thickness depends on the range of density to be measured. The third type of vibrating densitometers is called a tuning fork densitometer. A low mass electromechanical tuning fork is inserted in the liquid of which the density is to be measured and the frequency is measured to determine the density (Joshi, 2007). The vibrating densitometers are generally used inline process requiring large amount of samples and are expensive compared to other methods and was not chosen for this work.

A. 1.7 Oscillating Coriolis Densitometer

This densitometer can be used to measure the density of liquids, slurries, compressed gases and liquified gases. This can be used to measure the density of fluid up to 1160 Psig at 550 K (Liptak, 2003). This densitometer consists of a U-shaped tube that works on the same principle as that of vibrating element densitometer. This densitometer is very expensive and was not used for this work.

A.1.8 Balance-Flow Densitometer

In this method of density measurement, the test fluid continuously flows through a vessel. The vessel is automatically weighed by a spring balance system while the test liquid flows through it. Density can be directly calculated from the known volume and the measured weight.

Gozalpour et al. (2001) and Gozalpour et al. (2002) reported the density of methane and methylcyclohexane at temperatures ranging from 323 K C to 423 K and pressures up to 140 MPa. The test vessel consisted of the high pressure cells with the volume of 15.6 ml filled with mercury. The cells are emptied and filled with the test fluid and mercury is injected to the desired starting pressure. The cells are placed in an oven and heated to the desired temperature. The cells are removed from the oven and reweighed. The volume of test fluid is calculated from the volume of mercury injected, which can be estimated

from the mass and density of mercury. Tat and Van Gerpen (2002 and 2003) and Tat et al. (2000) measured the density of biodiesel using this method at temperatures ranging from 294 to 313 K and pressures up to 140 MPa. As it can only be used for lower temperature ranges, this method was not adapted for this work.

There are some other types of balance flow densitometers. In the Chain Balanced Float type densitometer, a self-centered, fixed volume plummet is fully submerged in the test liquid. The plummet consists of a metallic transformer which transmits a signal for any change in its position due to vibration. The plummet attains a stable condition under steady-state condition. Any change in variation in density is recorded by the coil. This method is not applicable at high temperatures.

Other methods such as Gas Specific Gravity Balance and Buoyancy Gas Balance methods are applicable only to measure the density of gases and hence not discussed here.

A.1.9 Capacitance Type Densitometer

Capacitance type densitometers are low cost instruments for measuring the density of liquid at elevated temperatures and pressures. This densitometer consists of small semi-cylindrical parallel plate capacitors made up of conducting materials. The principle of capacitance type densitometer is that the capacitance, C, of the capacitor plates varies with the change in area of the plates wetted with the oil, the dielectric constant of the fluid and the distance between the two plates. The capacitance is proportional to the dielectric constant, which is proportional to the density (Joshi, 2007). Hence, the capacitance, C can be expressed as

$$C = K\frac{A}{t} \tag{A.10}$$

where K is the effective dielectric constant of the fluid, A is the wetted area of the capacitor plate (i.e. the product of the perimeter of semicircular plate times its depth), t is the distance between the plates. If the distance between the two capacitor plates is kept constant and the space between the plates is filled by a non-conducting fluid such as oil, the change in dielectric constant and effective plate area varies with depth of submergence (d) (Joshi, 2007; Tate, 2005). The capacitance is directly proportional to the variation in submergence depth and dielectric constant as follows:

$$Co+\Delta C \propto (Ko+\Delta K)\,(do+\Delta d) \tag{A.11}$$

where, Ko is initial dielectric constant, ΔK is the change in dielectric constant due to change in temperature, pressure and fuel type, Δd is the change in depth of capacitor submergence.

Capacitance is also directly proportional to the frequency. Hence the equation can be expressed as below ($Co+\Delta C \approx Fo+\Delta F$);

$$Fo+\Delta F = Ko\ do + Ko\,\Delta d + \Delta K\ do + \Delta K\,\Delta d \qquad \text{(assuming that Fo = Ko do)}$$

$$\Delta d = \frac{\Delta F - \Delta K do}{Ko - \Delta K} \tag{A.12}$$

where ΔK is the change in dielectric constant due to temperature and pressure. This calibration constant is obtained for temperature variation at each measurement. In the case of the test under atmospheric pressure, ΔK is affected by temperature and depth of submergence. When both pressure and temperature are applied, ΔK is affected as a result of temperature and pressure as well as the depth of submergence. However, the calibration data were carried out at full submergence depth of the capacitor, keeping the depth of submergence constant. Hence, ΔKt is calculated using the following relationship.

$$\Delta \mathrm{Kt} = \frac{\Delta f}{\Delta t} \times \frac{\Delta t}{\mathrm{d}_{\mathrm{maximum}}} \tag{A.13}$$

where Δf is change in frequency due to temperature change Δt at constant pressure and $d_{maximum}$ is the total depth of submergence of capacitor in the liquid to be tested. In other words, $\frac{\Delta f}{\Delta t}$ is the slope of calibration with temperature at constant pressure.

When the liquid of which the density is to be found out is heated, the submergence of capacitor will increase due to expansion of the liquid. As the frequency is inversely proportional to the depth of submergence, the frequency will be reduced due to increase in submergence depth. However, when the liquid is heated at atmospheric pressure, the capacitance will increase due to the rise in temperature. The change in capacitance can be measured as frequency (kHz) and equated to a change in liquid level using equation (A.13). Because of the simplicity and lower cost and works under high temperature and pressure range, this method was used in this work.

A.2 VISCOSITY MEASUREMENTS

Viscosity is defined as the measure of internal resistance of the fluid to flow. Viscosity is of two types: dynamic and kinematic. The dynamic (absolute) viscosity is the ratio of shear stress to shear strain and is termed as η. The kinematic viscosity γ, is the ratio of dynamic viscosity μ, and density ρ.

The viscosity of fluids differs depending on whether the fluid is Newtonian or non-Newtonian. A Newtonian fluid shows a linear relation between shear stress and shear strain (Saran, 1999). In the case of non-Newtonian fluids, viscosity varies with the applied strain rate. Joshi and Pegg (2007) and Tate (2005) reported that viscosity of

biodiesel follows Newtonian behavior from temperatures below pour point and to temperatures up to 573 K.

The viscosity of Newtonian fluids decreases with increase in temperature according to the Arrhenius relationship.

$$\mu = A\, e^{-B/T} \qquad \text{(A.14)}$$

where T is absolute temperature, and A and B are fluid constants.

Eastwood (1979) presented the variation of viscosity with pressure to be linear and can be expressed as follows.

$$\ln(\mu) = A + Bp \qquad \text{(A.15)}$$

where p is absolute pressure and A and B are fluid constants. Barnes et al. (1989) reported that viscosity of fluids increased exponentially with pressure.

Matveev et al. (2005) expressed the relationship between viscosity, temperature and pressure as following.

$$\mu(\rho, T) = \mu_o . \exp(\alpha.p + \beta/T) \qquad \text{(A.16)}$$

where μ_o is viscosity of fluid at pressure p and temperature T (=T_o) and α, β are the fluid constants.

Measuring viscosity at high temperature and pressure is always a challenge due to the sealing of the component parts. To measure the viscosity of fluids at high temperatures, fall ball viscometers, rolling ball viscometers, Hoepplers viscometers, capillary viscometers, orifice viscometers, Saybolt viscometers, and vibrating type viscometers can be used.

A.2.1 Falling Ball Viscometer

Flowers (1914) first developed the concept of a falling ball viscometer. The falling ball viscometer consists of a tube with the fluid the viscosity of which needs to be determined, and the time taken for a ball to travel a known distance through the fluid is measured to determine the velocity of the ball (Flowers (1914). Falling ball viscometer was designed based on Stokes law. Stokes law is related to the resistance to the motion of a falling body exerted by the fluid. Wazer et al. (1963) presented the following relationship to calculate the viscosity of the falling ball in a test fluid.

$$\mu = \left(\frac{2}{9}\right)\left(\frac{r^2 g}{V}\right)\left(\rho_s - \rho_f\right) \tag{A.17}$$

where r is the radius of sphere, V is the velocity of the falling ball, ρ_s is the density of the falling ball, ρ_f is the density of the fluid being tested, g is the acceleration due to gravity, η which is also called the Stokes' viscosity. Velocity is calculated by the measured time taken from the ball to travel from one point to another known point. In this case, it is assumed that sphere moves with a very slow velocity in a Newtonian fluid of infinite extent. However, this assumption is ideal and cannot be achieved in actual viscometers. Corrections due to a finite Reynolds number, due to wall effects and due to end effects were reported in Wazer et al. (1963). After the corrections, equation (4) becomes:

$$\mu = (\rho_s - \rho_l) * t \tag{A.18}$$

where t is the time required for the ball to fall a known distance, K is the viscometer constant and determined by calibration with a fluid of known viscosity, t is the time taken by the ball to travel a known distance. This operates in lower temperature range and hence was not selected for this work.

A.2.2 Rolling Ball Viscometer

In the rolling ball viscometer, a sphere rolls down a cylindrical tube filled with a test fluid and inclined at a certain angle to the base to give a measure of viscosity of the fluid. However, Sestak and Ambros (1973) argued that the flow field induced by the rolling ball is more complex than the flow induced by falling ball. Hubbard and Brown (1943) studied the rolling ball system theoretically and experimentally, and derived the following relationship:

$$\mu = K^{'}\left(\rho_s - \rho_l\right)/v \qquad \text{(A.19)}$$

where K' is the instrument constant and is a function of temperature, v is the translational velocity.

In case of tilt angles, the viscosity of a fluid by using rolling ball viscometer can be calculated using the equation developed by Hubbard and Brown (1943):

$$\mu = \left(\frac{5\pi}{42}\right) g\ (\sin\theta) K \left(\frac{\rho_s - \rho_l}{V_t}\right) D\ (D+d) \qquad \text{(A.20)}$$

where D is the diameter of the tube and d is the diameter of the rolling ball and θ is the tilt angle with horizontal, Vt is terminal velocity, K is the calibration constant for the instrument. ρs and ρi are the densities of sphere and liquid. The calibration constant K can be estimated from Lewis (1953):

$$K = 0.333\ g\ \sin\theta\ d\ (D+d)\left[\left(\frac{D-d}{D}\right)\right]^{\frac{5}{2}}/l \qquad \text{(A.21)}$$

Even though this viscometer is capable of measuring viscosity at high temperature and pressure, some technical difficulties were encountered while measuring viscosities. Only

few observations were done by this equipment in this work and due to technical difficulties at higher temperatures, it was decided to use the torsional oscillating resonance viscometer.

A.2.3 Hoepplers Viscometer

This viscometer is also an inclined tube viscometer with precision bore, heat resistant, chemically inert 16 mm in diameter and 200 mm glass tube. The viscometer is mounted in a thermostatic jacket at an angle of 10^{o} inclined from the vertical. This instrument can be operated within the temperature range of 238 to 423 K. The reproducibility of the results from this instrument was reported to be 0.1 to 0.5%. The viscosity is calculated by using the following relations:

$$\mu = K\left(\rho_s - \rho_l\right)^* t \tag{A.22}$$

The temperature range it operates is lower than planned in this work and was not used.

A. 2.4 Capillary Viscometer

Capillary viscometers are the instruments used to measure the viscosity of Newtonian fluids. This is simple in operation, inexpensive, and requires little sample. The flow rate of liquid flowing through a capillary tube is measured recording the time to flow a known volume of liquid. Viscosity is calculated by the measure of flow rate, pressure and the dimensions of instrument where the liquid passes through. Viswanath et al. (2006) reported that various types of capillary viscometers have been designed such as Modified Ostwald viscometers, suspended-level viscometers and reserve-flow viscometers. The following Poiseuille's equation is used in case of capillary viscometers for Newtonian liquids.

$$\sigma = \eta \frac{dv}{dr} \tag{A.23}$$

where, η is the dynamic viscosity, σ is the shear stress, r is any distance from the center of the capillary tube occurring the flow and v is the velocity, and. Flow in viscometers can be found using;

$$Q = \frac{\pi \Delta p a^4}{8 \eta l} \tag{A.24}$$

where $\Delta p = \rho g h$, Q=V/t, a is the external diameter of the tube and h is the height of the liquid in capillary tube, p is hydrostatic pressure. Hence, the viscosity can be found using the relationship

$$\eta = \frac{\pi g h a^4}{8 l v} \rho t \tag{A.25}$$

Hence, viscosity in capillary viscometers can be found as;

$$\eta = K \tag{A.26}$$

K is the constant of a particular viscometer can be found for each instrument.

Various researchers have used capillary viscometers to measure the viscosity of oil and other chemicals. Abdulagatov and Azizov (2006) measured viscosity of calcium chloride and lithium sulphate solutions between the temperature range of 298 to 575 and pressures up to 60MPa. Wisnewski et al. (2005) used capillary viscometer to measure the viscosity of caster oil and methanol. Viscosity of methane and methylcyclohexane for temperatures from 323-423 K and pressures up to 140 MPa was measured by Tohidi et al. (2001). This system was not available to use in the lab.

A. 1.5 Orifice Viscometers

Orifice viscometers are used in oil industry. They consist of a reservoir, an orifice and a receiver. The length of the orifice is less than 10 times its diameter (Viswanath et al., 2006). A known volume of liquid is poured into a cup maintained at a constant temperature in a bath. The orifice valve is opened and the time taken to flow the known volume of liquid through the orifice is measured to calculate the viscosity of the liquid. The viscosity is calculated using an empirical expression which is specific to each instrument. The general form of relationship for the orifice viscometer is as follows.

$$\mu = \frac{\eta}{\rho} = kt - \frac{K}{t} \tag{A.27}$$

where t is the viscometer second, k and K are instrument constants.

A.2.6 Saybolt Viscometer

Saybolt viscometers are of two types: Saybolt universal viscometer and Saybolt furol viscometer. The Saybolt universal viscometer is generally used to determine the viscosity of lubricating oil while the Saybolt Furol viscometer is used to determine the viscosity of fuels oils (Viswanath et al., 2006). The Saybolt viscometer is one of the orifice type viscometers commonly used.

A.2.7 Modified Saybolt Viscometer

Tate (2005) modified the ASTM D 88 Saybolt viscometer design to operate from room temperature to the boiling point of the most volatile oil fraction. The orifice diameter was 1.016 mm was selected for the Modified Saybolt tip. A two-section chamber was designed to house the viscometer to facilitate the inert and heated environment. Each chamber contained independent components to make disassembling easier to clean after testing each sample. To raise the temperature of the fluid, two 250 W band heaters were attached to the reservoir and controlled by an external on-off temperature controller. The biodiesel samples were tested between 293 and 573 K temperatures at 20 K intervals.

A.2.8 Vibrating-Quartz Viscometers

A vibrating-quartz viscometer consists of a quartz cylinder deposited in four thin gold electrodes on the lateral surface. When a sinusoidal wave is applied to the electrodes, torsional vibration of the same frequency as the excitations wave is produced. The damping of the frequency due to the surrounding test fluid is measured by the change is the electrical impedance of the crystal for calculating the viscosity of the test fluid. The first torsionally vibrating-quartz viscometer was used by Santos and Castro for temperatures up to 373 K and pressures up to 200 MPa (Dindar, 2001). Collings and McLaughlin also used this method to measure viscosity up to 373 K and 686 MPa (Kiran and Sen, 1991). The temperature range was not sufficient for this work.

A.2.9 Vibrating Wire Viscometers

This method requires the density of fluids to be measured first for the accurate determination of the viscosity. A tungsten wire is set to transversal vibration and the damping in the vibration caused due to the surrounding test fluid is used to measure the viscosity. Audonnet and Padua (2001) introduced a method to simultaneously measure the density and viscosity of n-heptane from 298 to 383 K up to 100 MPa using the vibrating wire technique. This method was not used because the maximum temperature range of 383 K was not enough to suit the present study test requirement.

A.2.10 Magneto Viscometer

A magnetic viscometer operates on the principle of Stokes falling body. Such viscometer was used to measure the viscosity of fluid up to 343 K and 100 MPa. This viscometer consists of a brass cylinder filled with test fluid. The cylinder is closed with screw and the cell is placed in a heating block and rotated in the centre of magnetic field. The velocity and position of sphere can be found by placing two coils at known distance and

viscosity is calculated based on the velocity of the sphere. The equipment operates in lower temperature range and was not selected for this work.

A.2.11 Torsional Oscillating Resonance Viscometer

The torsional oscillating viscometer is a surface loading device that is used to measure the viscosity at the interface between the liquid and the solid surface. A constant amplitude was maintained at all times during the measurements. The viscosity of the fluid is the power required to achieve the constant amplitude. ViscoScope viscometer is designed based on this principle and is relatively cheap, easy to use with no moving parts. This device was used in this research work. A detailed description of this viscometer is provided in Chapter 6, Section 6.2.4.

A.3 SURFACE TENSION MEASUREMENTS

Surface tension is defined as the cohesive forces between liquid molecules. The molecules at the surface do not have other like molecules on all sides, as a result, they are attracted strongly to those directly associated with them on the surface (Viswanath et al., 2006). The polar liquid molecules in the bulk liquid arrange themselves so that the cohesive forces between the molecules are shared by the neighboring molecules which lead to zero net force. However, in the surface, the molecules lack equalizing force leading it to a non-zero net force. It is known that distilled water at 293.15 K has a surface tension of 72.8 mN/m. Surface tension can be measured with various techniques. They are generally classified in the following groups.

A.3.1 Wilhelmy Plate

In this method, a thin plate is used to measure the surface tension. A thin plate generally made up of roughened platinum-iridium alloy or platinum. Surface tension can be found out directly by dividing the force by perimeter of the plate. The following relationship can be used for this purpose.

$$\sigma = \frac{F}{[2(1+t)]\cos\theta} \tag{A.28}$$

where σ is the surface tension, l is the plate length, t is the thickness of the plate, F is the force vertically acting on the plate by the liquid meniscus, and θ is the contact angle measured for the liquid meniscus in contact with the surface.

To make this measurement more accurate, it should be made sure that the plate is completely wetted. This equipment operates in a lower temperature range and was not selected for this work.

A.3.2 Du Nouy Ring Method

This method is also called as maximum pull method. This consists of a ring made up of platinum or platinum iridium alloy with a perimeter of approximately 6 cm is pulled out from a liquid and air interface. The force required to detach the ring from the interface is measured by a microbalance. The surface tension is calculated from the following relationship (Du Nouy, 1919).

$$\sigma = \left(\frac{F}{p\cos\theta}\right) f \tag{A.29}$$

where 'f' is correction factor, θ is the angle (also known as wettability), p is the ideal surface tension calculated from (Wtot=Wring+$4\pi R\gamma$) and F is the total force required to pull the ring out from the interface.

The correction factor 'f' can be found from the following relationship:

$$\mathrm{f} = 0.725 + \left[\left(\frac{9.075\mathrm{E}10^{-4} F}{\pi^3 \Delta\rho g R^3}\right) - \left(\frac{1.679\gamma}{R}\right) + 0.04534 \right]^{0.5} \tag{A.30}$$

where R is radius of the ring, Δp is the change in density of the liquid, γ is surface tension of water at 293 K (72.94mJ/m^2) the density of fluid. This method can also be used for tests at high temperatures and high pressures in a specially equipped pressure cell, but was not used in this work due to unavailability.

A.3.3 Maximum Bubble Pressure Method

This method is used within a flowing system requiring a large volume of test fluid. The surface tension of the test fluid is obtained from the pressure difference inside and outside the bubble.. Adamson (1982) showed that the surface tension (σ) is measured using Young-Laplace equation as below.

$$\sigma = \frac{r}{2}(p_{\max} - \Delta\rho g h) \tag{A.31}$$

where Δp is the density difference between the two fluids, h is is the distance between the liquid surface and capillary tip and r is the radius of curvature which is given by Adamson (1992). The results are also affected by the type and position of capillary (Passerone and Ricci, 1998). This method is used in inline measurement with continuous measurements and was not used in this work.

A.3.4 Capillary Rise Method

The surface tension is directly proportional to the height of rise, h, of the liquid in the capillary relative to the liquid surface in the container (Joshi, 2007). In this method, a capillary of known inner radius (r) is immersed in the test fluid. The shape of the meniscus is spherical and the surface tension can be calculated from the following relationship (Lord Rayleigh, 1916).

$$\sigma = \frac{\Delta\rho.g.h.r}{2.\cos\theta} \tag{A.32}$$

$$\sigma = \frac{1}{2}.\Delta\rho.g.r.h\left[1 + \frac{r}{3h} - 0.1288\frac{r^2}{h^2} + 0.1312.\frac{r^3}{h^3}\right]$$

This method is considered to be one of the most accurate methods but its scope is limited in use as it is only used for measuring the surface tension of pure liquids.

A.3.5 Drop Volume or Weight Method

This is one of the simple techniques to measure the surface tension of a liquid. This method involves the measurement of the volume or the weight of a drop of falling from a capillary tube. The interfacial tension can be calculated from the weight W, volume V of the drop falling off the capillary tube with radius 'r' from the following relationship:

$$W = V\Delta\rho\, g = 2\pi\, r\, f\left(\frac{r}{\sqrt[3]{V}}\right) \qquad \text{(A.33)}$$

Harkins and Brown (1919) presented the values for correction factor 'f'. This measurement method is very sensitive to vibrations. This leads to complexities to measure weight at high temperatures and pressures. Hence, this method was not selected for this work.

A.3.6 Spinning Drop Method

This method is used to measure the surface tension of ultra low interfacial tensions. A device called spinning drop tensiometer is used for this purpose. This is based on the principle of the balance of centrifugal force and interfacial tension forces at mechanical equilibrium are usually used to measure the surface tension of the fluids which assumes the fluid drop to be a circular cylinder. In this method, a horizontal tube with sealed ends is filled with dense liquid. The test fluid is injected inside the tube. The tube is then spun about its horizontal axis at high speed. It is considered that at low rotational velocities ω, the test fluid drop is ellipsoidal in shape whereas in high rational velocities, the test fluid

takes the shape of the cylinder. The surface tension is calculated from the following relationship (Couper et al., 1983):

$$\sigma = \frac{1}{2} r^3 \Delta\rho\omega^2 \qquad \text{(A.34)}$$

where r is the radius of cylindrical droplet, Δρ is the density difference between the drop and the surrounding fluid.

The limitation of this method is that it is extremely difficult to construct a glass tube rotating at high speed at high temperatures and pressures and was not used for this work.

A.3.7 Gravity-Distorted Drop Method

The determination of surface tension using the drop shape technique has been of major interest recently. Bashforth and Adams (1883) derived an equation for the shape of the liquid droplet formed by the presence of gravity as follows:

$$\sigma\left(\frac{\sin\theta}{x} + \frac{1}{R_1}\right) = \frac{2\sigma}{b} + \Delta\rho g z \qquad \text{(A.35)}$$

where b is the radius of curvature at the origin and θ is the turning angle respectively, x and z are drop shape coordinates.

The Laplace equation of capillarity can also be used to describe the drop shape of the liquid:

$$\frac{\Delta P}{\sigma} = \left[\frac{1}{R_1} - \frac{1}{R_2}\right] \qquad \text{(A.36)}$$

where R1 and R2 are the principle radii of curvature at any point on the drop surface and ΔP is the pressure difference across the drop which can be calculated as $\Delta P = \Delta P_o + \Delta\rho hz$.

A.3.8 Sessile Drop Method

The pendent or sessile drop method has been extensively used for surface tension measurements. The surface tension in this method is determined by analyzing the profile of the drop sitting on a solid substrate. Sonntag (1982) developed the following relationship to determine the surface tension by using the sessile drop method:

$$\sigma = \frac{\Delta\rho g z_e^2}{2} \tag{A.37}$$

To effectively measure the surface tension using this method, the drop should have a contact angle larger than 90 degrees. The height from the top of the drop to its equator (z) should be measured. However, it is always difficult to locate the equator in a liquid surface and care should be taken in order to locate it (Drelich et al., 2002).

This method is fairly objective and the measurement yields data which are averaged over the wetted length giving more accurate results. The major disadvantage is that the drop size needs to be produced with a uniform cross section and the wetted length must be measured with precision.

A.3.9 Pendant Drop Method

This is one of the most popular methods of determining the surface tension of liquids in high temperature and pressures (Joshi, 2007). The test liquid is injected from a syringe to form a hanging droplet at the end of the needle. The shape of an axisymmetric pendant or sessile drop depends on the bond number (β) (Allan, 1998). The following relationship is used to calculate the surface tension by the pendant drop method (Figure A.3):

$$\sigma = \frac{\Delta\rho g b^2}{\beta} \tag{A.38}$$

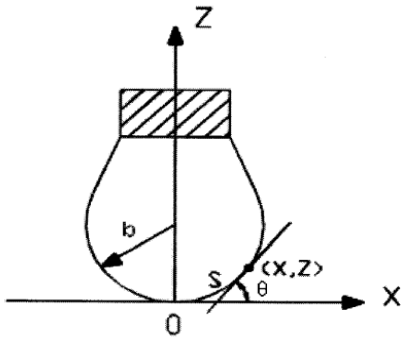

Figure A.3 Pendant drop profile (adapted from Joshi, 2007)

It is found that the drop is spherical if the bond number is zero. At large bond numbers, the droplet is significantly distorted. This method basically involves obtaining an image of the drop by a digital camera and compares the drop profile with the theoretical values obtained from equation 5.13. The axisymmetric drop shape analysis profile (ADSA-P) was developed by Rotenberg et al. (1982). The computational method for ADSA-P was developed by del Rio and Neumann (1997).

The advantages of this method is that it only requires a small amount of test fluid and can also be used for both liquid-liquid and liquid-vapor interfacial tensions. It can be used at high temperatures and pressures from elevated to vacuum conditions. This method is considered more attractive by many researchers due to its higher reliability, efficiency and minimal time required. The ADSA-P method was used to determine the surface tension of biodiesel fuels at temperatures up to 300^{o}C by Tate (2005) and Joshi (2007). Due to the above mentioned reasons, the pendant drop method was selected for the present work.

This method was also was used by many other researchers in the past (Wiegand and Franck, 1994; Kwok et al., 1998 and Hoorfar and Neumann, 2004). Using this method, in which a pressure is exerted by an inert gas on the liquid, a decrease in surface tension was found by Kundt in 1881 which was reported by Rice (1947) on diethyl ether and H_2 or CO_2. It was reported that the surface tension of diethyl ether decreased by 6.5mN/m,

when the pressure was increased from atmospheric to 2.8 MPa in CO_2. Equipment using the Drop Shape Analysis pendant drop principle was specially purchased and was used to measure the surface tension of biodiesel and diesel fuels.

APPENDIX B: SURVEY QUESTIONNAIRE FOR WASTE COOKING OIL USAGE IN NEPAL

1. Date: ……/……/…….. (DD/MM/YYYY)
2. Name of the business (hotel/restaurants):
3. Address of the Business:
4. Type/Nature of Business: Hotel ( ), Restaurant ( ) , Others :……
5. Purpose of oil use: frying meat products ( ), making sweets ( ), others ( )
6. Type/name of oil used
   ( ) Rapeseed
   ( ) Soybean oil
   ( ) Mustard oil
   ( ) …….
   ( ) …….
7. Average daily consumption of oil: ……..litres
8. Hours of oil usage in a day……hours
9. Working days in a week ……days
10. Number of days of operation in a year: ……..
11. Average temperature of cooking/frying ……^{o}C
12. Average time before oil replacement ---------- days
13. Is oil fully replaced or added?……
14. Total oil consumed in a year …….litres (from 7-10).
15. Disposal of waste cooking oil..
    i. thrown in waste bin ( )
    ii. used as animal feed ( )
    iii. used for soap making ( )
    iv. other use if any ……

Additional comment:……..

……

Note: The information in this questionnaire will not be used for any commercial purposes and only be used for research purposes.

APPENDIX C: FATTY ACID ANALYSIS OF BIODIESEL FUELS

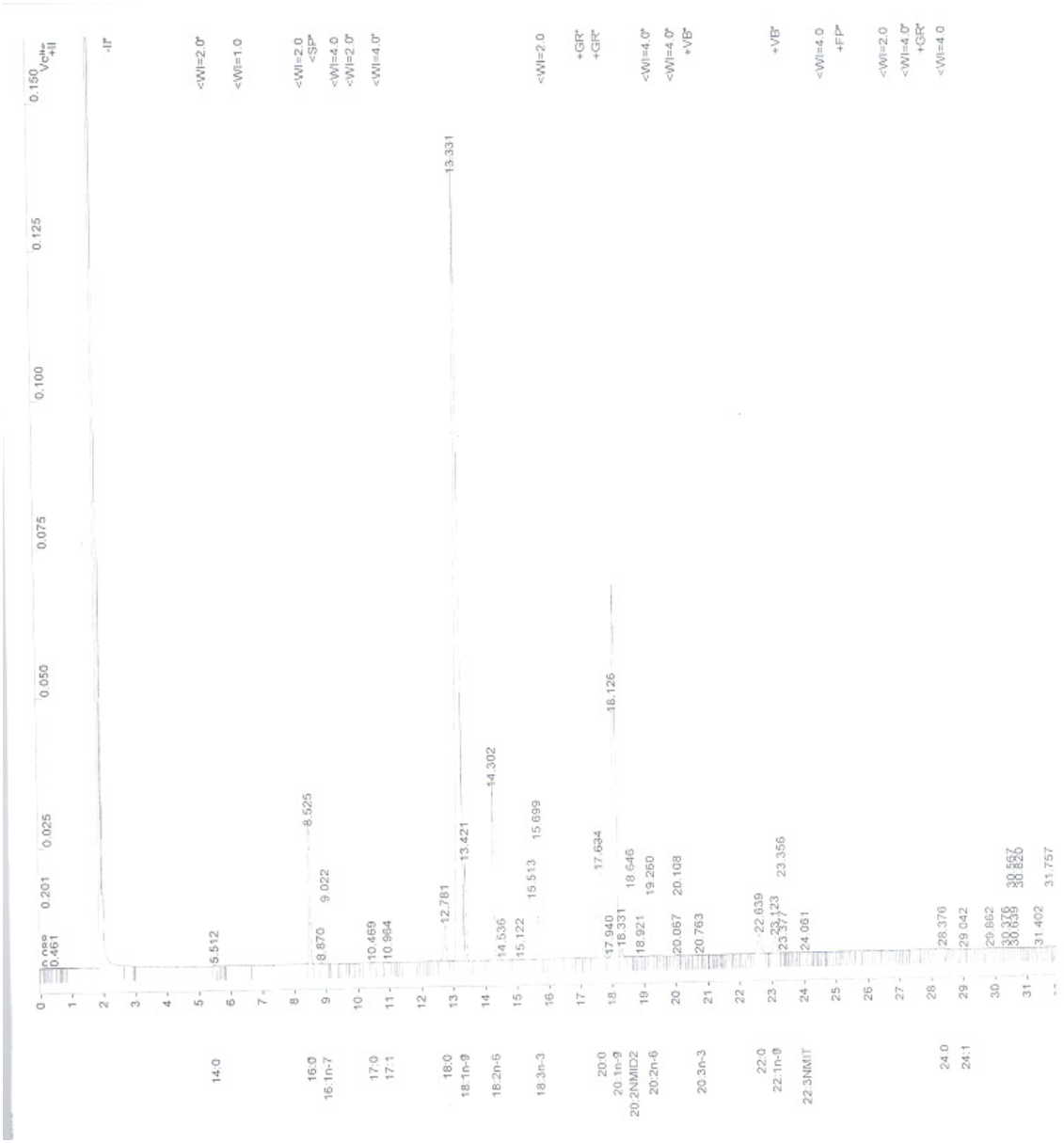

Figure C.1 Gas Chromatographic analysis of soapnut oil for its fatty acid determination

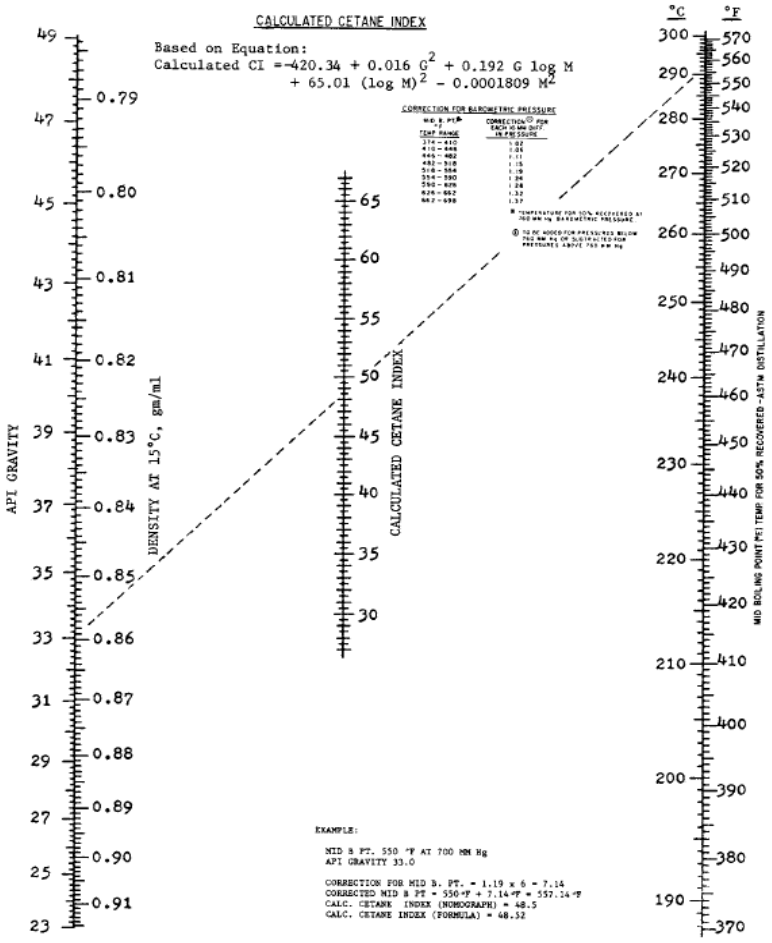

NOTE—The Calculated Cetane Index equation represents a useful tool for *estimating* cetane number. Due to inherent limitations in the equation's application, Index values may not be a valid substitute for ASTM cetane numbers as determined in a test engine.

FIG. 1 Nomograph for Calculated Cetane Index (ECS-1 Meter Basis—Test Method D 613)

Figure C.2 Nomograph for calculated cetane index

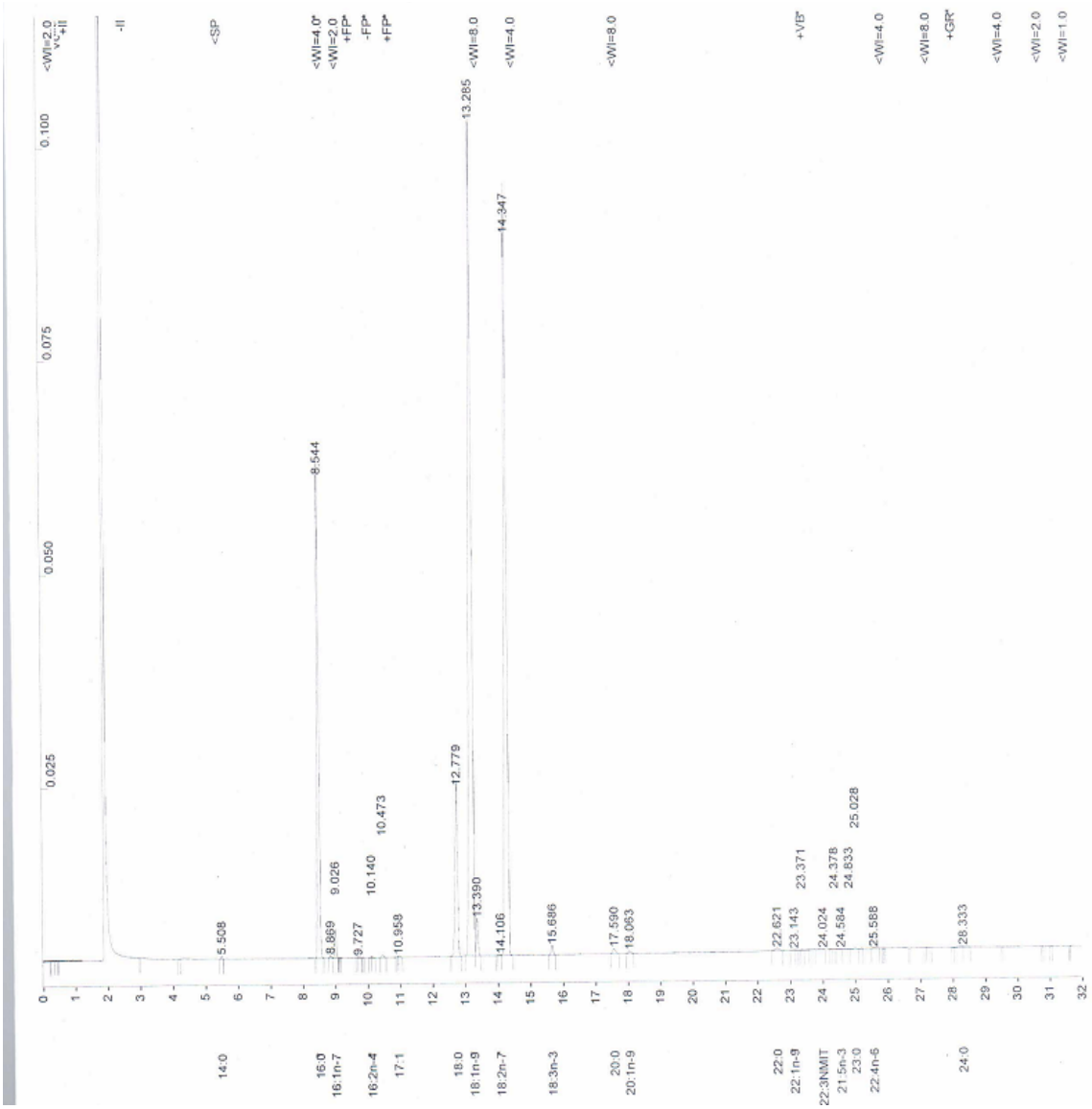

Figure C.3 Gas Chromatic analysis of jatropha biodiesel

APPENDIX D: DENSITY DATA

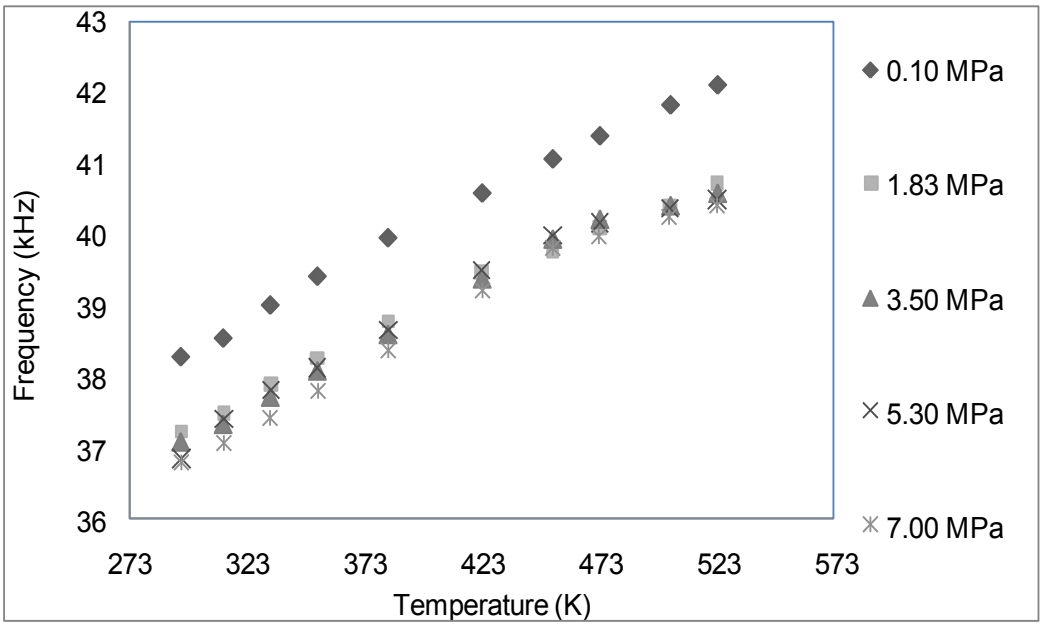

Figure D.1 Calibration data for canola B100 with variation in temperature and pressure in full submergence

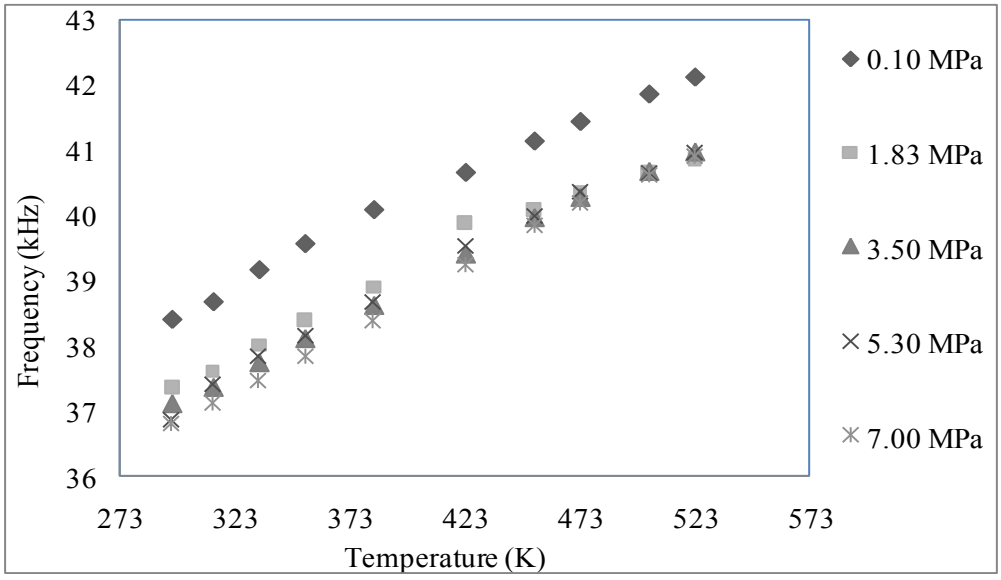

Figure D.2 Calibration data for canola B80 with variation in temperature and pressure in full submergence

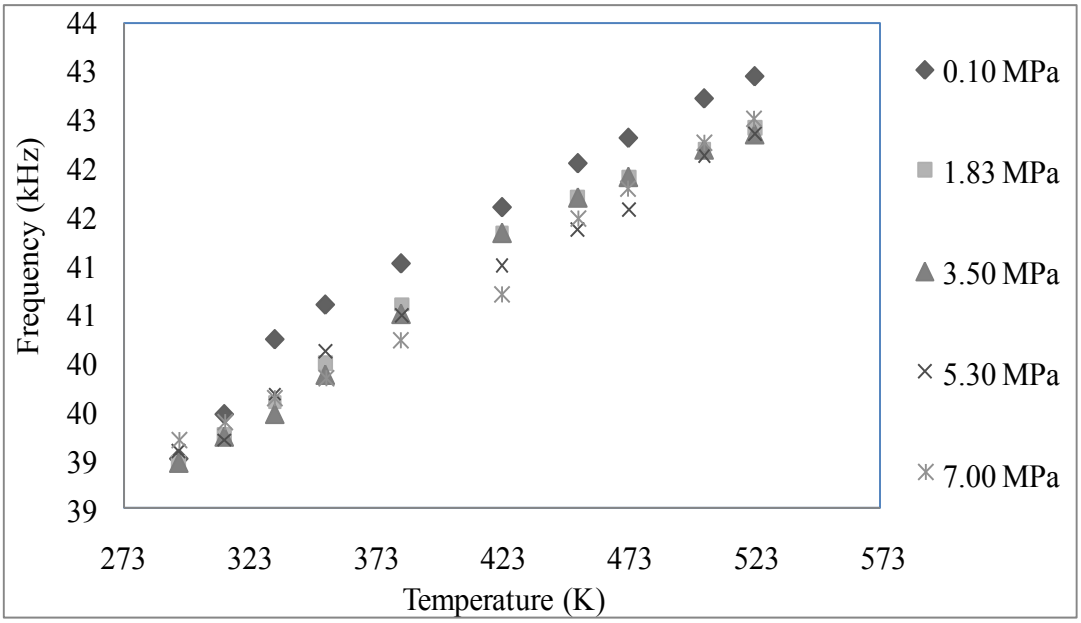

Figure D.3 Calibration data for canola B50 with temperature and pressure variation in full submergence

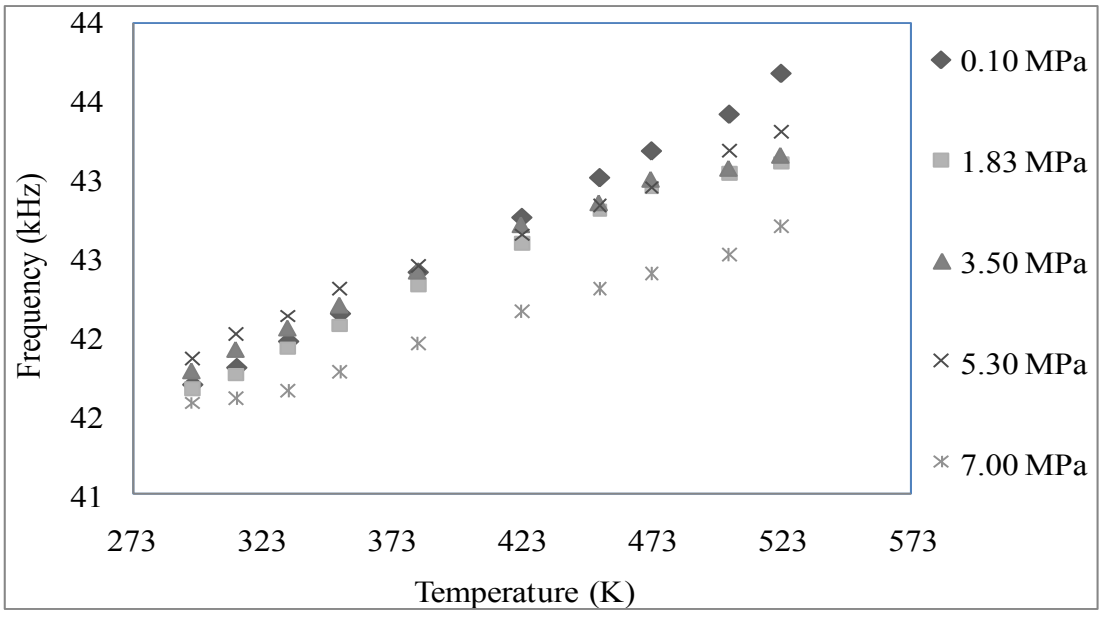

Figure D.4 Calibration data for canola B20 with temperature and pressure variation in full submergence

Table D.1 Regression analysis for diesel at different temperatures for five pressures

Regression Analysis: D versus P, T

The regression equation is

D = 1036 + 0.00423 P - 0.643 T

Predictor	Coef	SE Coef	T	P
Constant	1036.46	5.18	200.05	0.000
P	0.0042291	0.0003826	11.05	0.000
T	-0.64314	0.01212	-53.09	0.000

S = 6.60777 R-Sq = 98.4% R-Sq(adj) = 98.4%

Analysis of Variance

Source	DF	SS	MS	F	P
Regression	2	128382	64191	1470.16	0.000
Residual Error	47	2052	44		
Total	49	130434			

Source	DF	Seq SS
P	1	5335
T	1	123047

Unusual Observations

Obs	P	D	Fit	SE Fit	Residual	St Resid
8	101	716.927	732.587	1.812	-15.660	-2.46R
9	101	695.522	713.292	2.003	-17.770	-2.82R
10	101	682.342	700.430	2.155	-18.088	-2.90R

R denotes an observation with a large standardized residual.

Table D.2 Measured and regressed density and absolute and percent error for diesel for 0.10, 1.83 and 3.50 MPa

Absolute Temperature (K)	Absolute Pressure (MPa)	Measured density (kg/m^3)	Regressed density (kg/m^3)	Absolute error (kg/m^3)	Error (%)
296	0.1	851	846	5	0.59
313		838	835	3	0.36
333		826	823	3	0.36
353		810	810	0	0
383		788	790	2	0.25
423		758	765	7	0.92
453		734	745	11	1.5
473		717	733	16	2.23
503		696	713	17	2.44
523		682	700	18	2.64
296	1.83	857	854	3	0.35
313		845	843	2	0.24
333		833	830	3	0.36
353		821	817	4	0.49
383		803	798	5	0.62
423		777	772	5	0.64
453		761	753	8	1.05
473		749	740	9	1.2
503		729	721	8	1.1
523		714	708	6	0.84
296	3.5	863	861	2	0.23
313		853	850	3	0.35
333		842	837	5	0.59
353		828	824	4	0.48
383		810	805	5	0.62
423		783	779	4	0.51
453		765	760	5	0.65
473		751	747	4	0.53
503		732	728	4	0.55
523		718	715	3	0.42

Table D.3 Measured and regressed density and absolute and percent error for diesel for 5.30 and 7.00 MPa

Absolute Temperature (K)	Abslute Pressure (MPa)	Measured density (kg/m^3)	Regressed density (kg/m^3)	Absolute error (kg/m^3)	Error (%)
296	5.3	869	868	1	0.12
313		852	857	5	0.59
333		841	845	4	0.48
353		828	832	4	0.48
383		810	812	2	0.25
423		786	787	1	0.13
453		769	767	2	0.26
473		758	755	3	0.40
503		743	735	8	1.08
523		727	722	5	0.69
296	7	873	876	3	0.34
313		857	865	8	0.93
333		842	852	10	1.19
353		830	839	9	1.08
383		814	820	6	0.74
423		792	794	2	0.25
453		774	775	1	0.13
473		761	762	1	0.13
503		744	742	2	0.27
523		730	730	0	0.00

Table D.4 Regression analysis for canola biodiesel B100 at different temperatures for five pressures

Regression Analysis: Density versus P, T

The regression equation is

Density = 1076 + 0.00421 P - 0.650 T

Predictor	Coef	SE Coef	T	P
Constant	1075.90	5.02	214.34	0.000
P	0.0042141	0.0003714	11.35	0.000
T	-0.65007	0.01174	-55.38	0.000

S = 6.41400 R-Sq = 98.6% R-Sq(adj) = 98.5%

Analysis of Variance

Source	DF	SS	MS	F	P
Regression	2	131472	65736	1597.89	0.000
Residual Error	47	1934	41		
Total	49	133406			

Source	DF	Seq SS
P	1	5297
T	1	126175

Unusual Observations

Obs	P	Density	Fit	SE Fit	Residual	St Resid
10	101	721.700	736.245	2.091	-14.545	-2.40R
40	5301	743.828	758.158	1.777	-14.330	-2.33R
41	7001	898.556	913.537	2.035	-14.981	-2.46R

R denotes an observation with a large standardized residual.

Table D.5 Measured and regressed density and absolute and percent error for canola biodiesel B100 for 0.10 MPa, 1.83 and 3.50 MPa

Absolute Temperature (K)	Absolute Pressure (MPa)	Measured Density (kg/m^3)	Regressed Density (kg/m^3)	Absolute Error (kg/m^3)	Error (%)
295	0.1	886	884	2	0.23
313		876	873	3	0.34
333		865	860	5	0.58
353		852	847	5	0.59
383		834	827	7	0.84
423		807	801	6	0.74
453		783	782	1	0.13
473		766	769	3	0.39
503		741	749	8	1.08
523		722	736	14	1.94
295	1.83	887	892	5	0.56
313		877	880	3	0.34
333		865	867	2	0.23
353		854	854	0	0.00
383		837	835	2	0.24
423		814	809	5	0.61
453		796	789	7	0.88
473		782	776	6	0.77
503		760	757	3	0.39
523		741	744	3	0.40
295	3.5	891	899	8	0.90
313		884	887	3	0.34
333		874	874	0	0.00
353		863	861	2	0.23
383		847	842	5	0.59
423		821	816	5	0.61
453		799	796	3	0.38
473		784	783	1	0.13
503		762	764	2	0.26
523		746	751	5	0.67

Table D.6 Measured and regressed density and absolute and percent error for canola biodiesel B100 for 5.30 and 7.00 MPa

Absolute Temperature (K)	Absolute Pressure (MPa)	Measured Density (kg/m^3)	Regressed Density (kg/m^3)	Absolute Error (kg/m^3)	Error (%)
295	5.3	897	906	9	-1.00
313		890	895	5	-0.56
333		879	882	3	-0.34
353		868	869	1	-0.12
383		851	849	2	0.24
423		825	823	2	0.24
453		802	804	2	-0.25
473		786	791	5	-0.64
503		761	771	10	-1.31
523		744	758	14	-1.88
295	7	899	914	15	-1.67
313		897	902	5	-0.56
333		891	889	2	0.22
353		885	876	9	1.02
383		867	856	11	1.27
423		841	830	11	1.31
453		820	811	9	1.10
473		805	798	7	0.87
503		782	778	4	0.51
523		766	765	1	0.13

Table D.7 Regression analysis for canola biodiesel B80 for five pressures and between room temperatures and 523 K

Regression Analysis: Density versus P, T

```
The regression equation is
Density = 1087 + 0.00361 P - 0.680 T

Predictor       Coef    SE Coef       T      P
Constant     1086.89       5.36  202.81  0.000
P          0.0036076  0.0003965    9.10  0.000
T           -0.68040    0.01253  -54.29  0.000

S = 6.84791   R-Sq = 98.5%   R-Sq(adj) = 98.4%

Analysis of Variance

Source          DF      SS     MS        F      P
Regression       2  142107  71053  1515.20  0.000
Residual Error  47    2204     47
Total           49  144311

Source  DF  Seq SS
P        1    3882
T        1  138224

Unusual Observations
Obs    P  Density      Fit  SE Fit  Residual  St Resid
  9  101  728.581  744.915   2.075   -16.334     -2.50R
 10  101  704.187  731.307   2.233   -27.121     -4.19R

R denotes an observation with a large standardized residual.
```

Table D.8 Measured and regressed density and absolute and percent error for canola biodiesel B80 for 0.10 MPa, 1.83 and 3.50 MPa

Absolute Temperature (K)	Absolute Pressure (MPa)	Measured density (kg/m^3)	Regressed density (kg/m^3)	Absolute error (kg/m^3)	Error (%)
295	0.1	883	886	3	0.34
313		878	874	4	0.46
333		867	861	6	0.69
353		855	847	8	0.94
383		836	827	9	1.08
423		807	799	8	0.99
453		781	779	2	0.26
473		762	765	3	0.39
503		729	745	16	2.19
523		704	731	27	3.84
295	1.83	891	893	2	0.22
313		877	880	3	0.34
333		869	867	2	0.23
353		854	853	1	0.12
383		830	833	3	0.36
423		808	806	2	0.25
453		788	785	3	0.38
473		772	772	0	0.00
503		750	751	1	0.13
523		735	738	3	0.41
295	3.5	892	899	7	0.78
313		884	886	2	0.23
333		874	873	1	0.11
353		864	859	5	0.58
383		847	839	8	0.94
423		821	812	9	1.10
453		803	791	12	1.49
473		788	778	10	1.27
503		763	757	6	0.79
523		743	744	1	0.13

Table D.9 Measured and regressed density and absolute and percent error for canola biodiesel B80 for 5.30 and 7.00 MPa

Absolute Temperature (K)	Absolute Pressure (MPa)	Measured density (kg/m^3)	Regressed density (kg/m^3)	Absolute error (kg/m^3)	Error (%)
295	5.3	896	905	9	1.00
313		885	893	8	0.90
333		874	879	5	0.57
353		863	866	3	0.35
383		846	845	1	0.12
423		820	818	2	0.24
453		801	798	3	0.37
473		786	784	2	0.25
503		763	764	1	0.13
523		746	750	4	0.54
295	7	905	911	6	0.66
313		895	899	4	0.45
333		885	885	0	0.00
353		872	872	0	0.00
383		854	851	3	0.35
423		828	824	4	0.48
453		808	804	4	0.50
473		793	790	3	0.38
503		767	770	3	0.39
523		754	756	2	0.27

Table D.10 Regression analysis for canola biodiesel B50 for five pressures and between room temperatures and 523 K

Regression Analysis: Density versus P, T

The regression equation is

Density = 1044 + 0.00662 P - 0.595 T

Predictor	Coef	SE Coef	T	P
Constant	1041.91	4.54	229.65	0.000
P	0.0066226	0.0003357	19.73	0.000
T	-0.59543	0.01061	-56.12	0.000

S = 5.79726 R-Sq = 98.7% R-Sq(adj) = 98.6%

Analysis of Variance

Source	DF	SS	MS	F	P
Regression	2	118940	59470	1769.50	0.000
Residual Error	47	1580	34		
Total	49	120519			

Source	DF	Seq SS
P	1	13083
T	1	105857

Unusual Observations

Obs	P	Density	Fit	SE Fit	Residual	St Resid
10	101	716.076	731.083	1.890	-15.007	-2.74R

R denotes an observation with a large standardized residual.

Table D.11 Measured and regressed density and absolute and percent error of canola biodiesel B50 for 0.10 MPa, 1.83 and 3.50 MPa

Absolute Temperature (K)	Pressure (MPa)	Measured density (kg/m^3)	Regressed density (kg/m^3)	Absolute error (kg/m^3)	Error (%)
295	0.1	876	867	9	1.03
313		862	856	6	0.70
333		850	844	6	0.71
353		838	832	6	0.72
383		819	814	5	0.61
423		796	791	5	0.63
453		776	773	3	0.39
473		760	761	1	0.13
503		734	743	9	1.23
523		716	731	15	2.09
295	1.83	878	878	0	0.00
313		868	868	0	0.00
333		851	856	5	0.59
353		839	844	5	0.60
383		823	826	3	0.36
423		800	802	2	0.25
453		780	784	4	0.51
473		767	772	5	0.65
503		748	754	6	0.80
523		735	743	8	1.09
295	3.5	885	889	4	0.45
313		878	879	1	0.11
333		869	867	2	0.23
353		860	855	5	0.58
383		845	837	8	0.95
423		821	813	8	0.97
453		802	795	7	0.87
473		790	783	7	0.89
503		771	766	5	0.65
523		756	754	2	0.26

Table D.12 Measured and regressed density and absolute and percent error for canola biodiesel B50 for 5.30 and 7.00 MPa

Absolute Temperature (K)	Pressure (MPa)	Measured density (kg/m^3)	Regressed density (kg/m^3)	Absolute error (kg/m^3)	Error (%)
295	5.3	892	901	9	1.01
313		884	891	7	0.79
333		876	879	3	0.34
353		866	867	1	0.12
383		848	849	1	0.12
423		824	825	1	0.12
453		807	807	0	0.00
473		794	795	1	0.13
503		776	777	1	0.13
523		762	766	4	0.52
295	7	902	913	11	1.22
313		895	902	7	0.78
333		887	890	3	0.34
353		878	878	0	0.00
383		864	860	4	0.46
423		843	836	7	0.83
453		827	818	9	1.09
473		812	807	5	0.62
503		793	789	4	0.50
523		779	777	2	0.26

Table D.13 Regression analysis for canola biodiesel B20 for five pressures and between room temperatures and 523 K

Regression Analysis: Density versus P, T

The regression equation is

Density = 1007 + 0.00789 P - 0.555 T

Predictor	Coef	SE Coef	T	P
Constant	1006.69	7.57	133.01	0.000
P	0.0078924	0.0005599	14.10	0.000
T	-0.55539	0.01770	-31.38	0.000

S = 9.67058 R-Sq = 96.2% R-Sq(adj) = 96.0%

Analysis of Variance

Source	DF	SS	MS	F	P
Regression	2	110680	55340	591.75	0.000
Residual Error	47	4395	94		
Total	49	115076			

Source	DF	Seq SS
P	1	18580
T	1	92100

Unusual Observations

Obs	P	Density	Fit	SE Fit	Residual	St Resid
1	101	863.42	843.56	3.07	19.86	2.17R
9	101	708.48	728.04	2.93	-19.56	-2.12R
10	101	694.06	716.93	3.15	-22.87	-2.50R

R denotes an observation with a large standardized residual.

Table D.14 Measured and regressed density and absolute and percent error of canola biodiesel B20 for 0.10 MPa, 1.83 and 3.50 MPa

Absolute Temperature (K)	Pressure (MPa)	Measured density (kg/m^3)	Regressed density (kg/m^3)	Absolute error (kg/m^3)	Error (%)
295	0.1	863	844	19	2.20
313		851	834	17	2.00
333		836	822	14	1.67
353		820	811	9	1.10
383		796	795	1	0.13
423		767	772	5	0.65
453		743	756	13	1.75
473		729	745	16	2.19
503		708	728	20	2.82
523		694	717	23	3.31
295	1.83	866	857	9	1.04
313		854	847	7	0.82
333		843	836	7	0.83
353		830	825	5	0.60
383		815	808	7	0.86
423		791	786	5	0.63
453		773	769	4	0.52
473		759	758	1	0.13
503		746	742	4	0.54
523		732	731	1	0.14
295	3.5	868	870	2	0.23
313		856	860	4	0.47
333		845	849	4	0.47
353		836	838	2	0.24
383		823	822	1	0.12
423		794	799	5	0.63
453		781	783	2	0.26
473		771	772	1	0.13
503		754	755	1	0.13
523		744	744	0	0.00

Table D.15 Measured and regressed density and absolute and percent error for canola biodiesel B20 for 5.30 and 7.00 MPa

Absolute Temperature (K)	Absolute Pressure (MPa)	Measured density (kg/m^3)	Regressed density (kg/m^3)	Absolute error (kg/m^3)	Error (%)
295	5.3	870	885	15	1.72
313		862	875	13	1.51
333		854	863	9	1.05
353		844	852	8	0.95
383		831	836	5	0.60
423		811	814	3	0.37
453		796	797	1	0.13
473		785	786	1	0.13
503		770	769	1	0.13
523		763	758	5	0.66
295	7	887	898	11	1.24
313		879	888	9	1.02
333		870	877	7	0.80
353		862	866	4	0.46
383		850	849	1	0.12
423		836	827	9	1.08
453		819	810	9	1.10
473		811	799	12	1.48
503		798	782	16	2.01
523		789	771	18	2.28

Table D.16 Regression analysis for jatropha biodiesel B100 for five pressures and between room temperatures and 523 K

Regression Analysis: Density versus P, T

The regression equation is

Density = 1037 + 0.00488 P - 0.547 T

Predictor	Coef	SE Coef	T	P
Constant	1036.94	5.44	190.46	0.000
P	0.0048806	0.0003971	12.29	0.000
T	-0.54689	0.01306	-41.89	0.000

S = 7.51245 R-Sq = 97.1% R-Sq(adj) = 97.0%

Analysis of Variance

Source	DF	SS	MS	F	P
Regression	2	107552	53776	952.85	0.000
Residual Error	57	3217	56		
Total	59	110769			

Source	DF	Seq SS
P	1	8526
T	1	99026

Unusual Observations

Obs	P	Density	Fit	SE Fit	Residual	St Resid
11	101	745.941	762.267	2.185	-16.326	-2.27R
24	1831	745.043	759.772	2.041	-14.730	-2.04R
49	7001	894.148	909.149	2.125	-15.002	-2.08R

R denotes an observation with a large standardized residual.

Table D.17 Measured and regressed density and absolute and percent error for jatropha biodiesel B100 for 0.10 MPa, 1.83 and 3.50 MPa

Absolute temperature (K)	Absolute pressure (P)	Measured density (kg/m^3)	Regressed density (kg/m^3)	Absolute error (kg/m^3)	Error (%)
296	0.1	879	875	4	0.36
313		871	866	5	0.52
323		865	861	4	0.55
333		860	855	5	0.59
353		850	844	6	0.72
373		839	833	6	0.72
383		833	828	5	0.61
423		808	806	2	0.25
473		771	779	8	0.98
503		746	762	16	2.14
523		729	751	22	2.95
296	1.83	885	884	1	0.15
313		876	875	1	0.18
323		871	869	2	0.17
333		865	864	1	0.1
353		855	853	2	0.23
373		844	842	2	0.29
383		837	836	1	0.11
423		815	814	1	0.06
473		780	787	7	0.93
503		759	771	12	1.58
523		745	760	15	1.94
296	3.5	895	892	3	0.32
313		887	883	4	0.43
323		881	877	4	0.46
333		876	872	4	0.49
353		867	861	6	0.75
373		860	850	10	1.13
383		853	844	9	1.01
423		830	823	7	0.94
473		799	795	4	0.48
503		781	779	2	0.25
523		767	768	1	0.06

Table D.18 Measured and regressed density and absolute and percent error for jatropha biodiesel B100 for 5.30 and 7.00 MPa

Absolute temperature (K)	Absolute pressure (P)	Measured density (kg/m^3)	Regressed density (kg/m^3)	Absolute error (kg/m^3)	Error (%)
296	5.3	890	901	11	1.17
313		884	892	8	0.87
323		880	886	6	0.64
333		877	881	4	0.41
353		869	870	0	0.05
373		858	859	0	0.06
383		855	853	1	0.16
423		836	831	5	0.57
453		824	815	9	1.14
473		812	804	8	0.97
503		798	788	10	1.28
523		778	777	2	0.22
296	7	894	909	15	1.65
313		888	900	12	1.31
323		884	894	10	1.16
333		879	889	9	1.06
353		871	878	7	0.83
373		863	867	4	0.47
383		859	862	3	0.34
423		843	840	3	0.35
453		829	823	5	0.64
473		819	812	7	0.84
503		805	796	9	1.18
523		794	785	9	1.2

Table D.19 Regression analysis for jatropha biodiesel B80 for five pressures and between room temperature and 523 K

Regression Analysis: Density versus P, T

The regression equation is

Density = 1019 + 0.00462 P - 0.510 T

Predictor	Coef	SE Coef	T	P
Constant	1018.73	5.23	194.69	0.000
P	0.0046206	0.0003816	12.11	0.000
T	-0.51015	0.01255	-40.66	0.000

S = 7.22034 R-Sq = 96.9% R-Sq(adj) = 96.8%

Analysis of Variance

Source	DF	SS	MS	F	P
Regression	2	93810	46905	899.71	0.000
Residual Error	57	2972	52		
Total	59	96782			

Source	DF	Seq SS
P	1	7642
T	1	86168

Unusual Observations

Obs	P	Density	Fit	SE Fit	Residual	St Resid
11	101	744.877	762.514	2.100	-17.638	-2.55R
12	101	724.138	752.311	2.269	-28.173	-4.11R

R denotes an observation with a large standardized residual.

Table D.20 Measured and regressed density and absolute and percent error for jatropha biodiesel B80 for 0.10 MPa, 1.83 and 3.50 MPa

Absolute temperature (K)	Absolute pressure (P)	Measured density (kg/m^3)	Regressed density (kg/m^3)	Absolute error (kg/m^3)	Error (%)
296	0.1	873	868	5	0.57
313		862	859	3	0.35
323		856	854	2	0.23
333		850	849	1	0.12
353		838	839	1	0.12
373		825	829	4	0.48
383		817	824	7	0.86
423		798	803	5	0.63
473		765	778	13	1.70
503		745	763	18	2.42
523		724	752	28	3.87
296	1.83	879	877	2	0.23
313		872	868	4	0.46
323		868	862	6	0.69
333		864	857	7	0.81
353		855	846	9	1.05
373		847	836	11	1.30
383		843	830	13	1.54
423		822	809	13	1.58
473		791	782	9	1.14
503		772	766	6	0.78
523		753	755	2	0.27
296	3.5	882	885	3	0.34
313		876	876	0	0.00
323		869	871	2	0.23
333		865	866	1	0.12
353		856	855	1	0.12
373		848	844	4	0.47
383		844	839	5	0.59
423		827	817	10	1.21
473		802	791	11	1.37
503		784	775	9	1.15
523		771	764	7	0.91

Table D.21 Measured and regressed density and absolute and percent error for jatropha biodiesel B80 for 5.30 and 7.00 MPa

Absolute Temperature (K)	Absolute pressure (P)	Measured density (kg/m^3)	Regressed density (kg/m^3)	Absolute error (kg/m^3)	Error (%)
296	5.3	886	895	9	1.02
313		880	886	6	0.68
323		876	880	4	0.46
333		871	875	4	0.46
353		863	864	1	0.12
373		853	853	0	0.00
383		848	848	0	0.00
423		832	827	5	0.60
453		815	811	4	0.49
473		805	800	5	0.62
503		790	784	6	0.76
523		781	773	8	1.02
296	7	889	903	14	1.57
313		883	894	11	1.25
323		879	889	10	1.14
333		874	884	10	1.14
353		863	873	10	1.16
373		856	862	6	0.70
383		851	857	6	0.71
423		835	835	0	0.00
453		822	819	3	0.36
473		812	809	3	0.37
503		798	793	5	0.63
523		786	782	4	0.51

Table D.22 Regression analysis for jatropha biodiesel B50 for five pressures and between room temperatures and 523 K

Regression Analysis: Density versus P, T

The regression equation is
Density = 1039 + 0.00527 P - 0.589 T

Predictor	Coef	SE Coef	T	P
Constant	1039.32	3.62	286.81	0.000
P	0.0052715	0.0002643	19.95	0.000
T	-0.589479	0.008690	-67.84	0.000

S = 5.00018 R-Sq = 98.9% R-Sq(adj) = 98.8%

Analysis of Variance

Source	DF	SS	MS	F	P
Regression	2	124996	62498	2499.74	0.000
Residual Error	57	1425	25		
Total	59	126421			

Source	DF	Seq SS
P	1	9947
T	1	115049

Unusual Observations

Obs	P	Density	Fit	SE Fit	Residual	St Resid
11	101	731.149	743.256	1.454	-12.107	-2.53R
12	101	714.528	731.466	1.571	-16.938	-3.57R
60	7001	777.881	767.839	1.573	10.042	2.12R

R denotes an observation with a large standardized residual.

Table D.23 Measured and regressed density and absolute and percent error for jatropha biodiesel B50 for 0.10 MPa, 1.83 and 3.50 MPa

Absolute temperature (K)	Absolute pressure (P)	Measured density (kg/m^3)	Regressed density (kg/m^3)	Absolute error (kg/m^3)	Error (%)
296	0.1	870	865	5	0.57
313		860	855	5	0.58
323		854	849	5	0.59
333		847	843	4	0.47
353		835	832	3	0.36
373		824	820	4	0.49
383		817	814	3	0.37
423		794	790	4	0.50
473		758	761	3	0.40
503		731	743	12	1.64
523		715	731	16	2.24
296	1.83	873	874	1	0.11
313		866	864	2	0.23
323		861	858	3	0.35
333		855	853	2	0.23
353		845	841	4	0.47
373		835	829	6	0.72
383		827	823	4	0.48
423		801	800	1	0.12
473		769	770	1	0.13
503		751	752	1	0.13
523		732	741	9	1.23
296	3.5	878	883	5	0.57
313		870	873	3	0.34
323		865	867	2	0.23
333		861	861	0	0.00
353		850	850	0	0.00
373		839	838	1	0.12
383		833	832	1	0.12
423		812	808	4	0.49
473		783	779	4	0.51
503		764	761	3	0.39
523		746	749	3	0.40

Table D.24 Measured and regressed density and absolute and percent error for jatropha biodiesel B50 for 5.30 and 7.00 MPa

Absolute temperature (K)	Absolute pressure (P)	Measured density (kg/m^3)	Regressed density (kg/m^3)	Absolute error (kg/m^3)	Error (%)
296	5.3	885	893	8	0.90
313		877	883	6	0.68
323		871	877	6	0.69
333		866	871	5	0.58
353		857	859	2	0.23
373		846	847	1	0.12
383		839	841	2	0.24
423		817	818	1	0.12
453		801	800	1	0.12
473		787	788	1	0.13
503		769	771	2	0.26
523		755	759	4	0.53
296	7	894	902	8	0.89
313		886	892	6	0.68
323		882	886	4	0.45
333		877	880	3	0.34
353		870	868	2	0.23
373		860	856	4	0.47
383		854	850	4	0.47
423		831	827	4	0.48
453		813	809	4	0.49
473		802	797	5	0.62
503		789	780	9	1.14
523		778	768	10	1.29

Table D.25 Regression analysis for jatropha biodiesel B20 for five pressures and between room temperatures and 523 K

Regression Analysis: density versus P, T

The regression equation is
density = 1003 + 0.00489 P - 0.506 T

Predictor	Coef	SE Coef	T	P
Constant	1003.16	6.14	163.48	0.000
P	0.0048898	0.0004476	10.93	0.000
T	-0.50570	0.01472	-34.36	0.000

S = 8.46745 R-Sq = 95.8% R-Sq(adj) = 95.7%

Analysis of Variance

Source	DF	SS	MS	F	P
Regression	2	93229	46614	650.15	0.000
Residual Error	57	4087	72		
Total	59	97316			

Source	DF	Seq SS
P	1	8558
T	1	84671

Unusual Observations

Obs	P	density	Fit	SE Fit	Residual	St Resid
10	101	746.88	764.38	2.21	-17.50	-2.14R
11	101	727.98	749.21	2.46	-21.24	-2.62R
12	101	712.60	739.10	2.66	-26.50	-3.30R

R denotes an observation with a large standardized residual.

Table D.26 Measured and regressed density and absolute and percent error for jatropha biodiesel B20 for 0.10 MPa, 1.83 and 3.50 MPa

Absolute temperature (K)	Absolute pressure (MPa)	Measured density (kg/m^3)	Regressed density (kg/m^3)	Absolute error (kg/m^3)	Error (%)
296	0.1	858	854	4	0.47
313		848	845	3	0.35
323		843	840	3	0.36
333		838	835	3	0.36
353		828	825	3	0.36
373		819	815	4	0.49
383		812	810	2	0.25
423		778	790	12	1.54
453		761	774	13	1.71
473		747	764	17	2.28
503		728	749	21	2.88
523		713	739	26	3.65
296	1.83	864	862	2	0.23
313		859	854	5	0.58
323		856	849	7	0.82
333		851	844	7	0.82
353		843	834	9	1.07
373		834	823	11	1.32
383		829	818	11	1.33
423		809	798	11	1.36
453		791	783	8	1.01
473		776	773	3	0.39
503		746	758	12	1.61
523		742	748	6	0.81
296	3.5	868	871	3	0.35
313		862	862	0	0.00
323		858	857	1	0.12
333		853	852	1	0.12
353		846	842	4	0.47
373		838	832	6	0.72
383		833	827	6	0.72
423		816	806	10	1.23
453		801	791	10	1.25
473		790	781	9	1.14
503		772	766	6	0.78
523		759	756	3	0.40

Table D.27 Measured and regressed density and absolute and percent error for jatropha biodiesel B20 for 5.30 and 7.00 MPa

Absolute temperature (K)	Absolute pressure (MPa)	Measured density (kg/m^3)	Regressed density (kg/m^3)	Absolute error (kg/m^3)	Error (%)
296	5.3	870	879	9	1.03
313		863	871	8	0.93
323		860	866	6	0.70
333		856	861	5	0.58
353		847	850	3	0.35
373		839	840	1	0.12
383		835	835	0	0.00
423		819	815	4	0.49
453		804	800	4	0.50
473		794	790	4	0.50
503		779	775	4	0.51
523		770	765	5	0.65
296	7	873	888	15	1.72
313		867	879	12	1.38
323		864	874	10	1.16
333		861	869	8	0.93
353		853	859	6	0.70
373		844	849	5	0.59
383		841	844	3	0.36
423		826	823	3	0.36
453		811	808	3	0.37
473		802	798	4	0.50
503		788	783	5	0.63
523		780	773	7	0.90

Table D.28 Regression analysis for soapnut biodiesel B100 for five pressures and between room temperature and 523 K

Regression Analysis: Density versus P, T

The regression equation is

Density = 1071 + 0.00580 P - 0.653 T

Predictor	Coef	SE Coef	T	P
Constant	1071.04	4.88	219.28	0.000
P	0.0057979	0.0003601	16.10	0.000
T	-0.65300	0.01142	-57.16	0.000

S = 6.23083 R-Sq = 98.7% R-Sq(adj) = 98.6%

Analysis of Variance

Source	DF	SS	MS	F	P
Regression	2	136909	68454	1763.23	0.000
Residual Error	47	1825	39		
Total	49	138733			

Source	DF	Seq SS
P	1	10062
T	1	126847

Unusual Observations

Obs	P	Density	Fit	SE Fit	Residual	St Resid
10	101	712.987	730.007	2.030	-17.020	-2.89R
31	5301	893.316	908.386	1.654	-15.070	-2.51R

R denotes an observation with a large standardized residual.

Table D.29 Measured and regressed density and absolute and percent error for soapnut biodiesel B100 for 0.10, 1.83 and 3.50 MPa

Absolute temperature (K)	Absolute pressure (MPa)	Measured density (kg/m^3)	Regressed density (kg/m^3)	Absolute error (kg/m^3)	Error (%)
296	0.1	880	878	2	0.23
313		872	867	5	0.57
333		859	854	5	0.58
353		846	841	5	0.59
383		828	821	7	0.85
423		802	795	7	0.87
453		778	776	2	0.26
473		760	763	3	0.39
503		732	743	11	1.50
523		713	730	17	2.38
296	1.83	883	888	5	0.57
313		874	877	3	0.34
333		864	864	0	0.00
353		853	851	2	0.23
383		836	831	5	0.60
423		810	805	5	0.62
453		788	786	2	0.25
473		774	773	1	0.13
503		751	753	2	0.27
523		733	740	7	0.95
296	3.5	890	898	8	0.90
313		881	887	6	0.68
333		872	874	2	0.23
353		863	861	2	0.23
383		847	841	6	0.71
423		824	815	9	1.09
453		802	795	7	0.87
473		787	782	5	0.64
503		762	763	1	0.13
523		745	750	5	0.67

Table D.30 Measured and regressed density and absolute and percent error for soapnut biodiesel B100 for 5.30 and 7.00 MPa

Absolute temperature (K)	Absolute pressure (MPa)	Measured density (kg/m^3)	Regressed density (kg/m^3)	Absolute error (kg/m^3)	Error (%)
296	5.3	893	908	15	1.68
313		886	897	11	1.24
333		878	884	6	0.68
353		869	871	2	0.23
383		854	852	2	0.23
423		832	825	7	0.84
453		812	806	6	0.74
473		797	793	4	0.50
503		774	773	1	0.13
523		757	760	3	0.40
296	7	914	918	4	0.44
313		905	907	2	0.22
333		896	894	2	0.22
353		884	881	3	0.34
383		868	861	7	0.81
423		844	835	9	1.07
453		821	816	5	0.61
473		804	803	1	0.12
503		779	783	4	0.51
523		763	770	7	0.92

Table D.31 Regression analysis for soapnut biodiesel B80 for five pressures and between room temperatures and 523 K

Regression Analysis: Density versus P, T

The regression equation is

Density = 1033 + 0.00421 P - 0.539 T

Predictor	Coef	SE Coef	T	P
Constant	1033.34	3.48	296.94	0.000
P	0.0042086	0.0002538	16.58	0.000
T	-0.538601	0.008345	-64.54	0.000

S = 4.80176 R-Sq = 98.7% R-Sq(adj) = 98.7%

Analysis of Variance

Source	DF	SS	MS	F	P
Regression	2	102387	51193	2220.31	0.000
Residual Error	57	1314	23		
Total	59	103701			

Source	DF	Seq SS
P	1	6340
T	1	96047

Unusual Observations

Obs	P	Density	Fit	SE Fit	Residual	St Resid
12	101	736.404	751.994	1.509	-15.590	-3.42R
24	1831	748.775	759.275	1.304	-10.500	-2.27R
33	3501	814.383	804.005	0.783	10.378	2.19R

R denotes an observation with a large standardized residual.

Table D.32 Measured and regressed density and absolute and percent error for soapnut biodiesel B80 for 0.10 , 1.83 and 3.50 MPa

Absolute temperature (K)	Absolute pressure (MPa)	Measured density (kg/m^3)	Regressed density (kg/m^3)	Absolute error (kg/m^3)	Error (%)
296	0.1	876	874	2	0.23
313		863	865	2	0.23
323		858	860	2	0.23
333		853	854	1	0.12
353		845	844	1	0.12
373		837	833	4	0.48
383		833	827	6	0.72
423		814	806	8	0.98
453		795	790	5	0.63
473		780	779	1	0.13
503		755	763	8	1.06
523		736	752	16	2.17
296	1.83	884	882	2	0.23
313		876	872	4	0.46
323		867	867	0	0.00
333		859	862	3	0.35
353		849	851	2	0.24
373		840	840	0	0.00
383		834	835	1	0.12
423		812	813	1	0.12
453		796	797	1	0.13
473		784	786	2	0.26
503		762	770	8	1.05
523		749	759	10	1.34
296	3.5	885	889	4	0.45
313		878	879	1	0.11
323		873	874	1	0.11
333		868	869	1	0.12
353		860	858	2	0.23
373		852	847	5	0.59
383		847	842	5	0.59
423		829	820	9	1.09
453		814	804	10	1.23
473		805	793	12	1.49
503		780	777	3	0.38

Table D.33 Measured and regressed density and absolute and percent error for soapnut biodiesel B80 for 5.30 and 7.00 MPa

Absolute temperature (K)	Absolute pressure (MPa)	Measured density (kg/m^3)	Regressed density (kg/m^3)	Absolute error (kg/m^3)	Error (%)
296	5.3	892	896	4	0.45
313		885	887	2	0.23
323		881	882	1	0.11
333		877	876	1	0.11
353		861	865	4	0.46
373		855	855	0	0.00
383		849	849	0	0.00
423		830	828	2	0.24
453		814	812	2	0.25
473		802	801	1	0.12
503		781	785	4	0.51
523		769	774	5	0.65
296	7	897	903	6	0.67
313		890	894	4	0.45
323		884	889	5	0.57
333		880	883	3	0.34
353		871	873	2	0.23
373		863	862	1	0.12
383		858	856	2	0.23
423		837	835	2	0.24
453		824	819	5	0.61
473		812	808	4	0.49
503		794	792	2	0.25
523		780	781	1	0.13

Table D.34 Regression analysis for soapnut biodiesel B50 for five pressures and between room temperatures and 523 K

```
The regression equation is
Density = 1035 + 0.00661 P - 0.543 T


Predictor       Coef    SE Coef       T      P
Constant     1034.54       6.30  164.19  0.000
P          0.0066118  0.0004618   14.32  0.000
T           -0.54262    0.01510  -35.94  0.000


S = 8.68773   R-Sq = 96.3%   R-Sq(adj) = 96.2%


Analysis of Variance

Source          DF      SS     MS       F      P
Regression       2  112957  56479  748.29  0.000
Residual Error  57    4302     75
Total           59  117259


Source  DF  Seq SS
P        1   15472
T        1   97485


Unusual Observations

Obs    P  Density     Fit  SE Fit  Residual  St Resid
 12  101   724.33  751.34    2.74    -27.01     -3.28R

R denotes an observation with a large standardized
residual.
```

Table D.35 Measured and regressed density and absolute and percent error for soapnut B50 for 0.10 MPa, 1.83 and 3.50 MPa

Absolute temperature (K)	Absolute pressure (MPa)	Measured density (kg/m^3)	Regressed density (kg/m^3)	Absolute error (kg/m^3)	Error (%)
296	0.1	873	875	2	0.23
313		865	865	0	0.00
323		860	860	0	0.00
333		854	854	0	0.00
353		845	844	1	0.12
373		835	833	2	0.24
383		830	827	3	0.36
423		805	806	1	0.12
453		785	789	4	0.51
473		771	778	7	0.91
503		747	762	15	2.01
523		724	751	27	3.73
296	1.83	886	887	1	0.11
313		881	877	4	0.45
323		877	872	5	0.57
333		873	867	6	0.69
353		866	856	10	1.15
373		859	845	14	1.63
383		855	839	16	1.87
423		834	818	16	1.92
453		810	801	9	1.11
473		799	791	8	1.00
503		777	774	3	0.39
523		758	763	5	0.66
296	3.5	894	897	3	0.34
313		887	888	1	0.11
323		881	882	1	0.11
333		876	877	1	0.11
353		868	866	2	0.23
373		860	855	5	0.58
383		854	850	4	0.47
423		838	828	10	1.19
453		819	812	7	0.85
473		806	801	5	0.62
503		783	785	2	0.26
523		773	774	1	0.13

Table D.36 Measured and regressed density and absolute and percent error of soapnut biodiesel B50 for 5.30 and 7.00 MPa

Absolute temperature (K)	Absolute pressure (MPa)	Measured density (kg/m^3)	Regressed density (kg/m^3)	Absolute error (kg/m^3)	Error (%)
296	5.3	896	909	13	1.45
313		889	900	11	1.24
323		884	894	10	1.13
333		878	889	11	1.25
353		869	878	9	1.04
373		861	867	6	0.70
383		855	862	7	0.82
423		839	840	1	0.12
453		821	824	3	0.37
473		806	813	7	0.87
503		788	797	9	1.14
523		772	786	14	1.81
296	7	905	920	15	1.66
313		904	911	7	0.77
323		900	905	5	0.56
333		902	900	2	0.22
353		895	889	6	0.67
373		885	878	7	0.79
383		883	873	10	1.13
423		864	851	13	1.50
453		848	835	13	1.53
473		832	824	8	0.96
503		815	808	7	0.86
523		799	797	2	0.25

Table D.37 Regression analysis for soapnut biodiesel B20 for five pressures and between room temperatures and 523 K

Regression Analysis: Density versus P, T

The regression equation is
Density = 1056 + 0.00752 P - 0.631 T

Predictor	Coef	SE Coef	T	P
Constant	1056.47	3.48	303.26	0.000
P	0.0075248	0.0002573	29.25	0.000
T	-0.630800	0.008146	-77.44	0.000

S = 4.44299 R-Sq = 99.3% R-Sq(adj) = 99.3%

Analysis of Variance

Source	DF	SS	MS	F	P
Regression	2	135259	67630	3425.99	0.000
Residual Error	47	928	20		
Total	49	136187			

Source	DF	Seq SS
P	1	16889
T	1	118370

Unusual Observations

Obs	P	Density	Fit	SE Fit	Residual	St Resid
10	101	714.180	727.226	1.449	-13.046	-3.11R
50	7001	792.328	779.147	1.450	13.181	3.14R

R denotes an observation with a large standardized residual.

Table D.38 Measured and regressed density and absolute and percent error for soapnut biodiesel B20 for 0.10 MPa, 1.83 and 3.50 MPa

Absolute temperature (K)	Absolute pressure (MPa)	Measured density (kg/m^3)	Regressed density (kg/m^3)	Absolute error (kg/m^3)	Error (%)
296	0.1	871	870	1	0.11
313		861	860	1	0.12
333		849	847	2	0.24
353		839	834	5	0.60
383		822	816	6	0.73
423		794	790	4	0.50
453		774	771	3	0.39
473		757	759	2	0.26
503		740	740	0	0.00
523		714	727	13	1.82
296	1.83	883	883	0	0.00
313		875	873	2	0.23
333		865	860	5	0.58
353		854	847	7	0.82
383		833	829	4	0.48
423		804	803	1	0.12
453		786	784	2	0.25
473		768	772	4	0.52
503		749	753	4	0.53
523		740	740	0	0.00
296	3.5	891	896	5	0.56
313		882	885	3	0.34
333		870	873	3	0.34
353		859	860	1	0.12
383		841	841	0	0.00
423		815	816	1	0.12
453		797	797	0	0.00
473		781	784	3	0.38
503		766	765	1	0.13
523		755	753	2	0.26

Table D.39 Measured and regressed density and absolute and percent error for soapnut biodiesel B20 for 5.30 and 7.00MPa

Absolute temperature (K)	Absolute pressure (MPa)	Measured density (kg/m^3)	Regressed density (kg/m^3)	Absolute error (kg/m^3)	Error (%)
296	5.3	903	910	6	0.7
313		896	899	3	0.29
333		886	886	0	0.01
353		874	874	1	0.08
383		854	855	1	0.07
423		825	829	5	0.57
453		802	811	8	1.03
473		790	798	8	0.95
503		777	779	2	0.22
523		768	766	2	0.2
296	7	919	922	4	0.39
313		911	912	1	0.12
333		901	899	2	0.17
353		889	886	3	0.31
383		870	867	2	0.24
423		843	842	1	0.07
453		824	823	1	0.1
473		812	811	2	0.19
503		800	792	8	1.04
523		792	779	13	1.69

APPENDIX E: SURFACE TENSION DATA

Table E.1 Regression analysis of surface tension of diesel as function of temperature and pressure

Regression Analysis: σ versus T, P

The regression equation is

σ = 39.7 - 0.0519 T - 0.000545 P

Predictor	Coef	SE Coef	T	P
Constant	39.7438	0.7797	50.97	0.000
T	-0.051909	0.002019	-25.70	0.000
P	-0.00054484	0.00004824	-11.29	0.000

S = 0.589099 R-Sq = 97.3% R-Sq(adj) = 97.0%

Analysis of Variance

Source	DF	SS	MS	F	P
Regression	2	273.58	136.79	394.16	0.000
Residual Error	22	7.63	0.35		
Total	24	281.21			

Source	DF	Seq SS
T	1	229.30
P	1	44.27

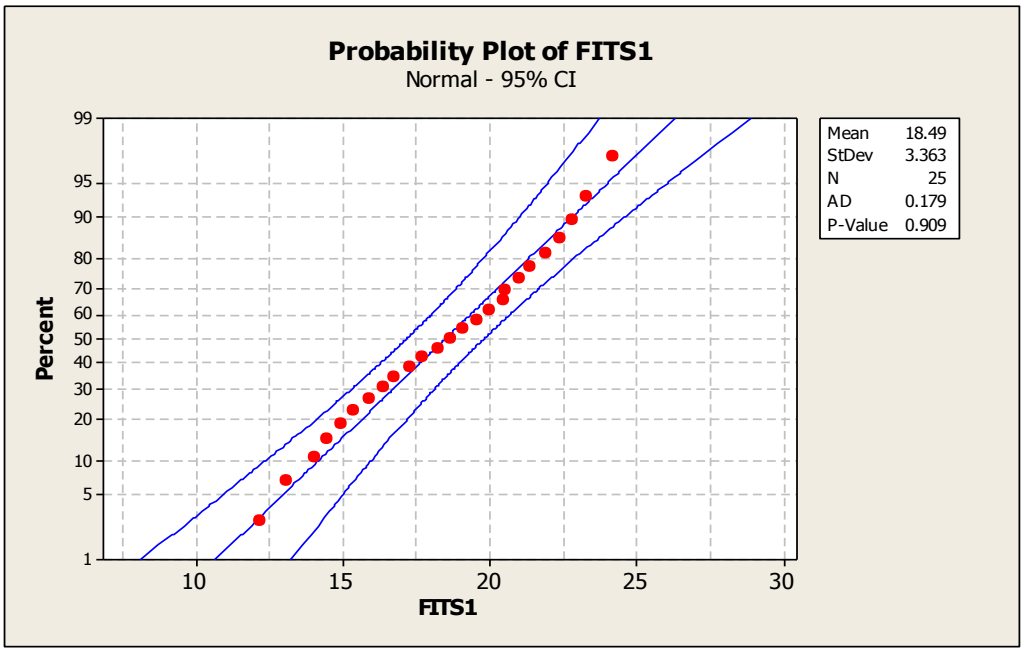

Figure E.1 Probability plot of regressed surface tension of diesel B0.

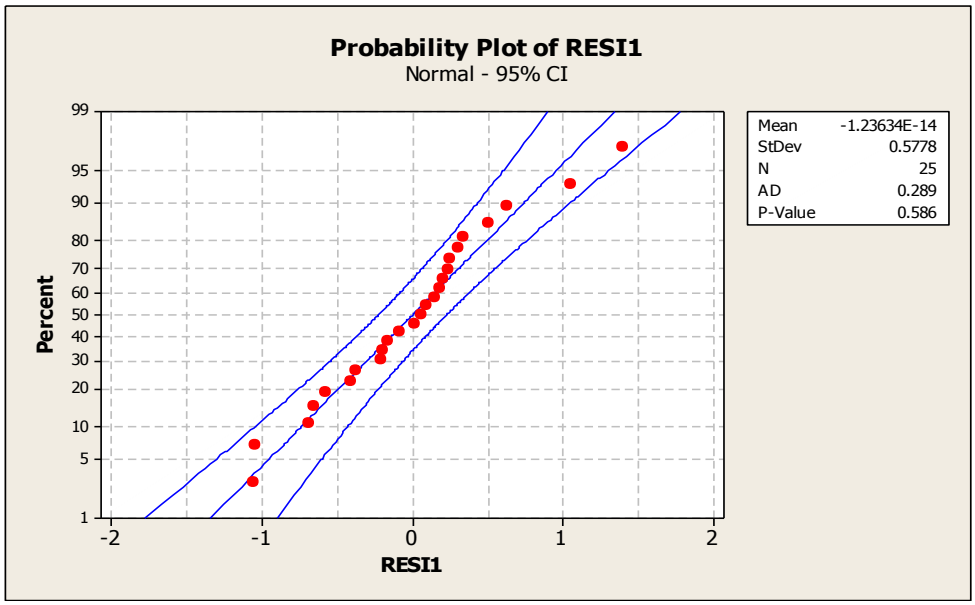

Figure E.2 Probability plot of residuals for surface tension of diesel fuel (B0)

Table E.2 Measured and regressed surface tension and absolute and percent error for diesel (B0)

Absolute Temperature (K)	Absolute Pressure (MPa)	Measured Surface Tension (mN/m)	Regressed Surface Tension (mN/m)	Absolute Error (mN/m)	Error (%)
293	0.10	25.84	24.47	1.37	5.30
323		23.22	22.91	0.31	1.33
373		20.31	20.32	0.01	0.06
423		18.21	17.72	0.48	2.65
448		15.84	16.43	0.59	3.72
293	1.83	23.73	23.53	0.20	0.84
323		21.58	21.97	0.39	1.82
373		19.21	19.38	0.17	0.88
423		16.15	16.78	0.63	3.89
448		14.46	15.48	1.02	7.05
293	3.50	22.73	22.62	0.11	0.48
323		21.22	21.06	0.16	0.75
373		18.32	18.47	0.14	0.79
423		15.81	15.87	0.06	0.38
448		14.40	14.57	0.17	1.21
293	5.30	20.95	21.64	0.69	3.28
323		19.71	20.08	0.37	1.86
373		17.81	17.49	0.32	1.80
423		15.36	14.89	0.47	3.04
448		13.87	13.59	0.27	1.97
293	7.00	19.67	20.71	1.04	5.29
323		19.37	19.16	0.21	1.10
373		16.63	16.56	0.07	0.39
423		14.21	13.96	0.25	1.76
448		13.73	12.67	1.07	7.76

Table E.3 Regression analysis of surface tension of canola biodiesel B100 as a function of temperature and pressure

Regression Analysis: σ versus P, T

The regression equation is

σ = 47.7 - 0.000549 P - 0.0638 T

Predictor	Coef	SE Coef	T	P
Constant	47.7400	0.8085	59.05	0.000
P	-0.00054915	0.00005481	-10.02	0.000
T	-0.063814	0.002050	-31.13	0.000

S = 0.669393 R-Sq = 98.0% R-Sq(adj) = 97.8%

Analysis of Variance

Source	DF	SS	MS	F	P
Regression	2	479.07	239.54	534.57	0.000
Residual Error	22	9.86	0.45		
Total	24	488.93			

Source	DF	Seq SS
P	1	44.98
T	1	434.09

Obs	P	σ	Fit	SE Fit	Residual	St Resid
1	101	30.518	28.978	0.289	1.540	2.55R

R denotes an observation with a large standardized residual.

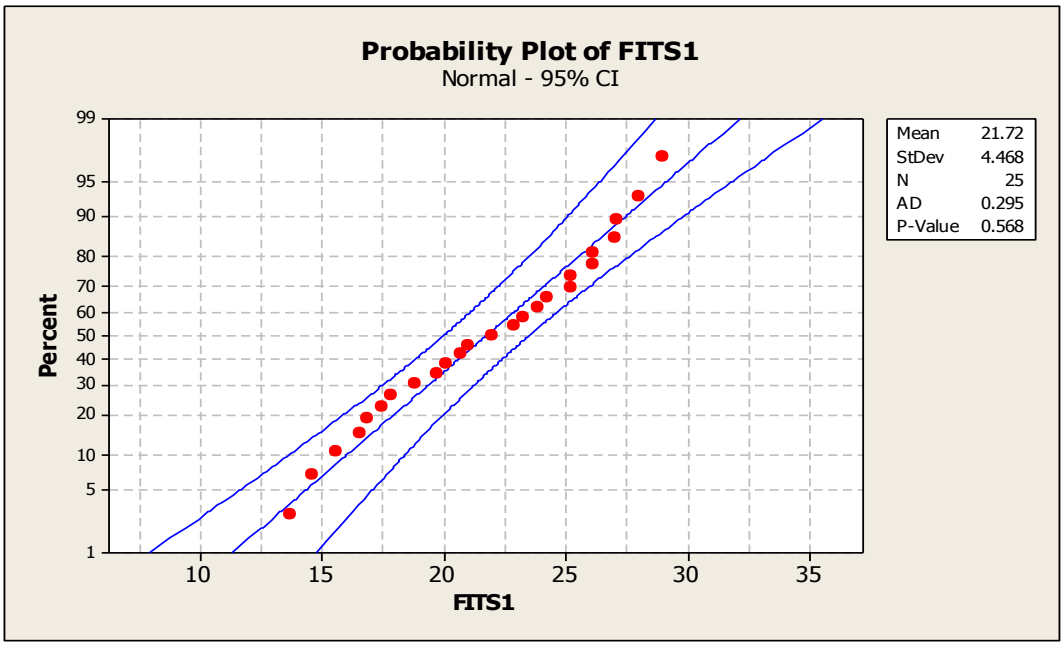

Figure E.3 Probability plot of regressed values of surface tension of canola biodiesel B100

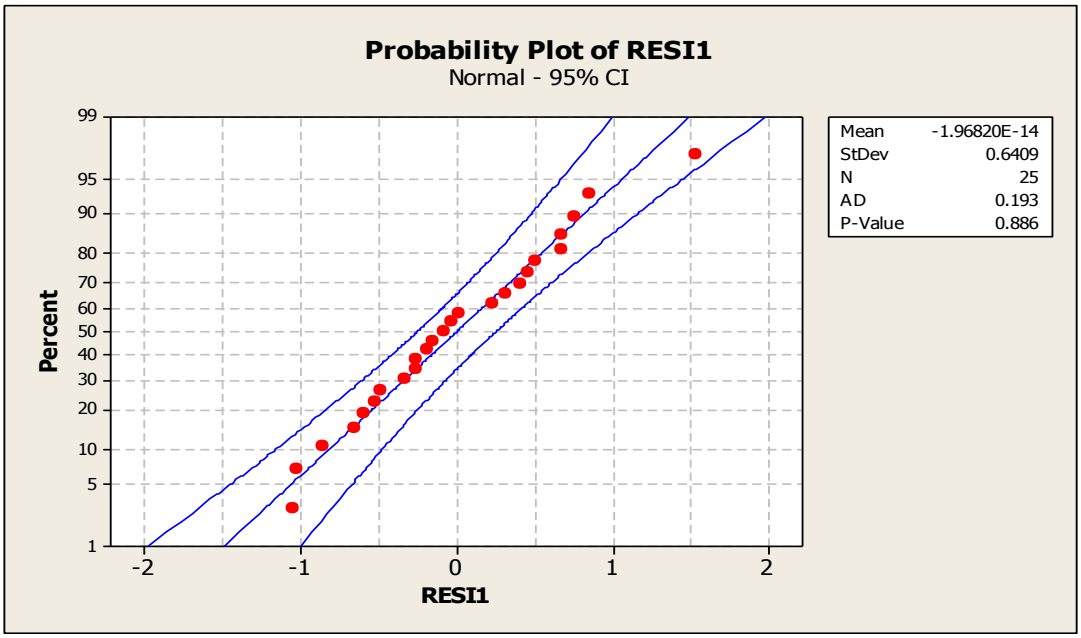

Figure E.4 Probability plot of residual values of surface tension of canola biodiesel B100

Table E.4 Measured and regressed surface tensions, absolute and percent error of canola biodiesel B100 for five temperatures and five pressures

Absolute Temperature (K)	Absolute Pressure (MPa)	Measured Surface Tension (mN/m)	Regressed Surface Tension (mN/m)	Absolute Error (mN/m)	Error (%)
293	0.10	30.52	28.96	1.56	5.12
323		26.98	27.04	0.06	0.22
373		23.69	23.85	0.16	0.68
423		20.03	20.66	0.63	3.14
473		16.47	17.47	1.00	6.07
293	1.83	28.00	28.05	0.05	0.18
323		26.14	26.14	0.00	0.00
373		23.60	22.95	0.65	2.77
423		19.58	19.75	0.17	0.89
473		16.29	16.56	0.27	1.68
293	3.50	26.07	27.12	1.05	4.05
323		25.70	25.21	0.50	1.93
373		22.68	22.02	0.66	2.91
423		18.33	18.83	0.50	2.71
473		16.09	15.64	0.45	2.82
293	5.30	25.26	26.12	0.86	3.39
323		24.52	24.21	0.32	1.29
373		21.78	21.02	0.76	3.50
423		17.30	17.83	0.52	3.03
473		15.49	14.64	0.85	5.52
293	7.00	24.59	25.18	0.58	2.37
323		22.94	23.26	0.32	1.40
373		20.31	20.07	0.24	1.20
423		16.63	16.88	0.25	1.50
473		14.12	13.69	0.43	3.04

Table E.5 Regression analysis of jatropha biodiesel B100 surface tension as a function of temperature and pressure

Regression Analysis: σ versus P, T

The regression equation is

σ = 41.9 - 0.000671 P - 0.0480 T

Predictor	Coef	SE Coef	T	P
Constant	41.910	1.483	28.26	0.000
P	-0.0006711	0.0001006	-6.67	0.000
T	-0.047954	0.003762	-12.75	0.000

S = 1.22844 R-Sq = 90.4% R-Sq(adj) = 89.5%

Analysis of Variance

Source	DF	SS	MS	F	P
Regression	2	312.30	156.15	103.48	0.000
Residual Error	22	33.20	1.51		
Total	24	345.50			

Source	DF	Seq SS
P	1	67.17
T	1	245.13

Unusual Observations

Obs	P	σ	Fit	SE Fit	Residual	St Resid
1	101	30.104	27.792	0.530	2.313	2.09R
21	7001	20.652	23.161	0.530	-2.509	-2.26R

R denotes an observation with a large standardized residual.

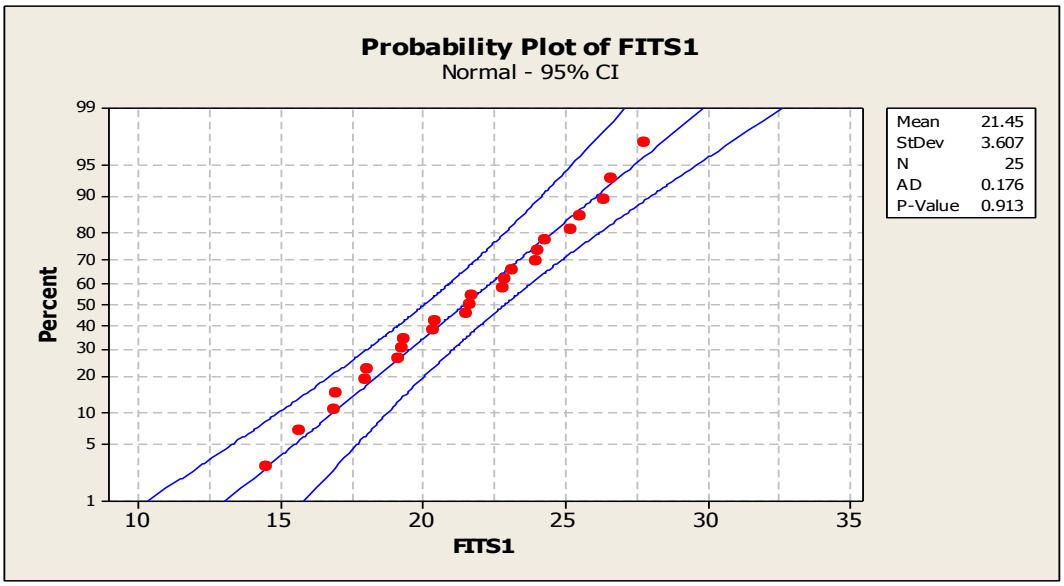

Figure E.5 Probability plot of regressed values of surface tension of jatropha biodiesel B100

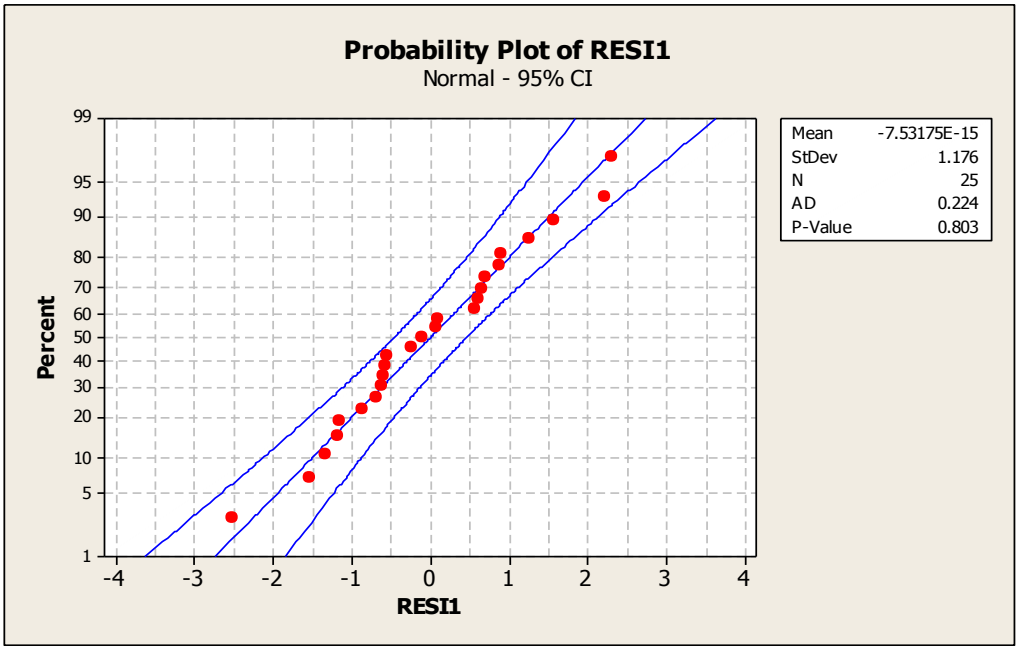

Figure E.6 Probability plot of residual values of surface tension of jatropha biodiesel B100

Table E.6 Measured and regressed surface tension and absolute and percent error of jatropha biodiesel B100 for five temperatures and five pressures

Absolute Temperature (K)	Absolute Pressure (MPa)	Measured Surface Tension (mN/m)	Regressed Surface Tension (mN/m)	Absolute Error (mN/m)	Error (%)
293	0.10	30.10	27.79	2.31	7.68
323		27.94	26.35	1.58	5.66
373		22.79	23.96	1.16	5.10
423		20.71	21.56	0.85	4.10
448		17.82	19.16	1.34	7.50
293	1.83	27.54	26.63	0.90	3.28
323		25.26	25.19	0.07	0.27
373		22.26	22.79	0.54	2.42
423		20.49	20.40	0.09	0.46
448		16.86	18.00	1.14	6.77
293	3.50	25.27	25.51	0.24	0.93
323		23.48	24.07	0.59	2.52
373		22.28	21.67	0.61	2.73
423		19.95	19.28	0.67	3.36
448		16.30	16.88	0.57	3.52
293	5.30	22.78	24.30	1.52	6.68
323		22.25	22.86	0.61	2.73
373		21.72	20.47	1.26	5.79
423		18.95	18.07	0.88	4.65
448		15.56	15.67	0.11	0.69
293	7.00	20.65	22.16	2.51	7.31
323		21.04	21.72	0.68	3.22
373		19.88	19.32	0.56	2.81
423		19.14	17.93	2.21	6.34
448		15.23	14.53	0.70	4.61

Table E.7 Regression analysis of jatropha biodiesel B80 surface tension as a function of temperature and pressure

Regression Analysis: σ versus P, T

The regression equation is

σ = 43.2 - 0.000420 P - 0.0533 T

Predictor	Coef	SE Coef	T	P
Constant	43.2445	0.9638	44.87	0.000
P	-0.00041984	0.00006537	-6.42	0.000
T	-0.053327	0.002445	-21.81	0.000

S = 0.798295 R-Sq = 95.9% R-Sq(adj) = 95.5%

Analysis of Variance

Source	DF	SS	MS	F	P
Regression	2	329.44	164.72	258.47	0.000
Residual Error	22	14.02	0.64		
Total	24	343.46			

Source	DF	Seq SS
P	1	26.29
T	1	303.15

Unusual Observations

Obs	P	σ	Fit	SE Fit	Residual	St Resid
16	5301	23.875	25.394	0.284	-1.520	-2.04R

R denotes an observation with a large standardized residual.

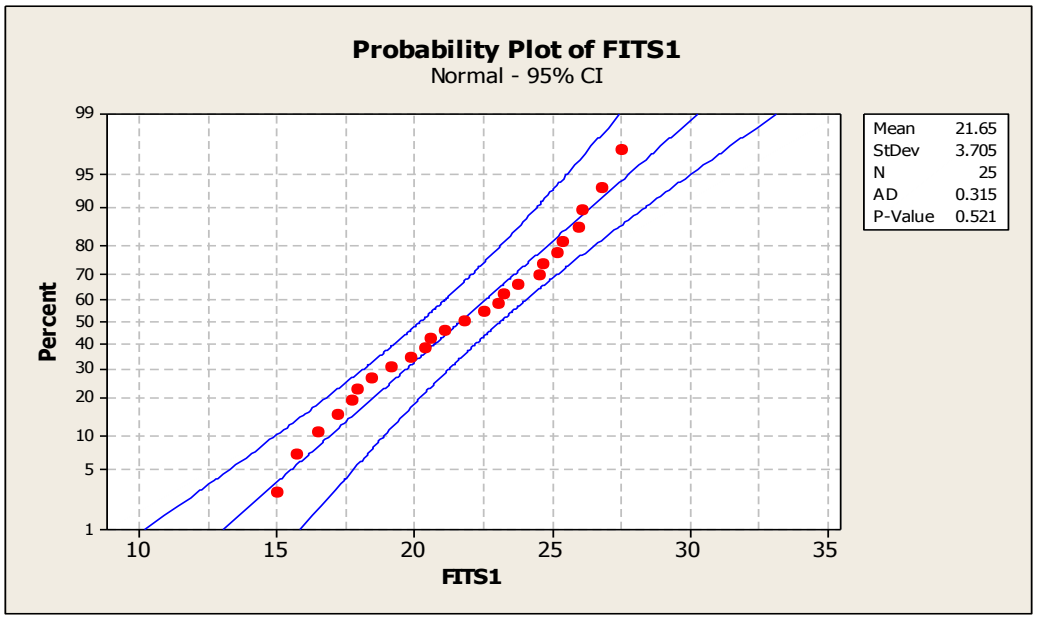

Figure E.7 Probability plot of regressed values of surface tension of jatropha biodiesel B80

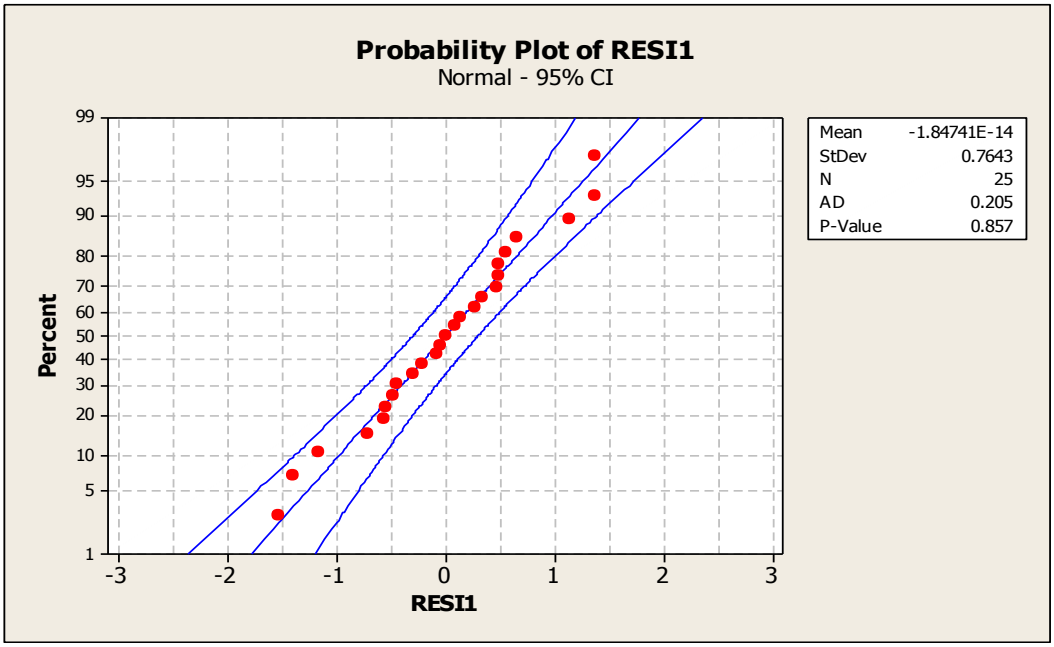

Figure E.8 Probability plot of residual values of surface tension of jatropha biodiesel B80

Table E.8 Measured and regressed surface tension and absolute and percent error of jatropha biodiesel B80 for five temperatures and five pressures

Absolute Temperature (K)	Absolute Pressure (MPa)	Measured Surface Tension (mN/m)	Regressed Surface Tension (mN/m)	Absolute Error (mN/m)	Error (%)
293	0.10	28.95	27.41	0.64	5.31
323		27.36	25.83	1.53	5.58
373		23.32	23.20	0.12	0.53
423		19.49	20.57	1.08	5.53
448		17.41	17.94	0.53	3.03
293	1.83	26.41	26.72	0.31	1.18
323		25.52	25.14	0.38	1.50
373		22.54	22.51	0.03	0.14
423		19.37	19.88	0.51	2.62
448		16.55	17.25	0.70	4.25
293	3.50	25.67	26.05	0.39	1.51
323		24.69	24.47	0.21	0.87
373		21.81	21.84	0.03	0.14
423		19.77	19.21	0.56	2.81
448		16.25	16.58	0.33	2.01
293	5.30	23.87	25.33	1.46	6.12
323		24.14	23.76	0.38	1.57
373		21.61	21.13	0.49	2.25
423		19.61	18.49	1.11	5.68
448		15.89	15.86	0.03	0.17
293	7.00	23.29	24.66	1.37	5.86
323		23.57	23.08	0.49	2.07
373		20.21	20.45	0.24	1.17
423		18.40	17.82	0.59	3.19
448		15.57	15.19	0.38	2.46

Table E.9 Regression analysis of jatropha biodiesel B50 surface tension as a function of temperature and pressure

Regression Analysis: σ versus T, P

The regression equation is

σ = 41.1 - 0.0493 T - 0.000685 P

Predictor	Coef	SE Coef	T	P
Constant	41.140	1.413	29.11	0.000
T	-0.049337	0.003586	-13.76	0.000
P	-0.00068525	0.00009586	-7.15	0.000

S = 1.17068 R-Sq = 91.6% R-Sq(adj) = 90.9%

Analysis of Variance

Source	DF	SS	MS	F	P
Regression	2	329.51	164.76	120.22	0.000
Residual Error	22	30.15	1.37		
Total	24	359.66			

Source	DF	Seq SS
T	1	259.48
P	1	70.03

Unusual Observations

Obs	T	σ	Fit	SE Fit	Residual	St Resid
21	293	18.461	21.887	0.505	-3.426	-3.24R

R denotes an observation with a large standardized residual.

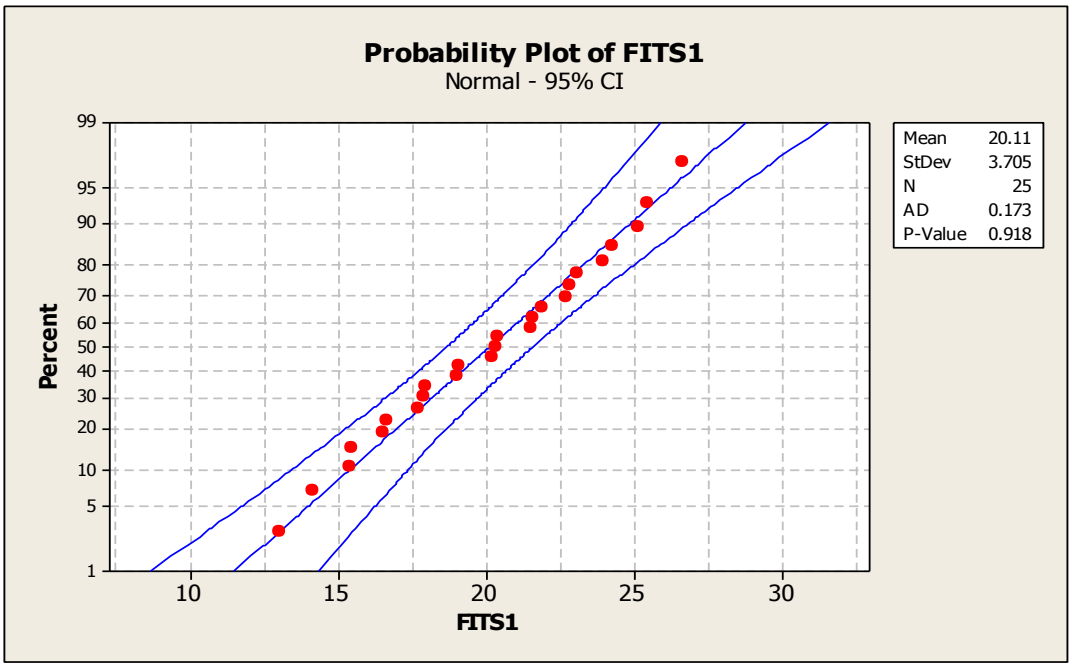

Figure E.9 Probability plot of regressed values of surface tension of jatropha biodieselB50

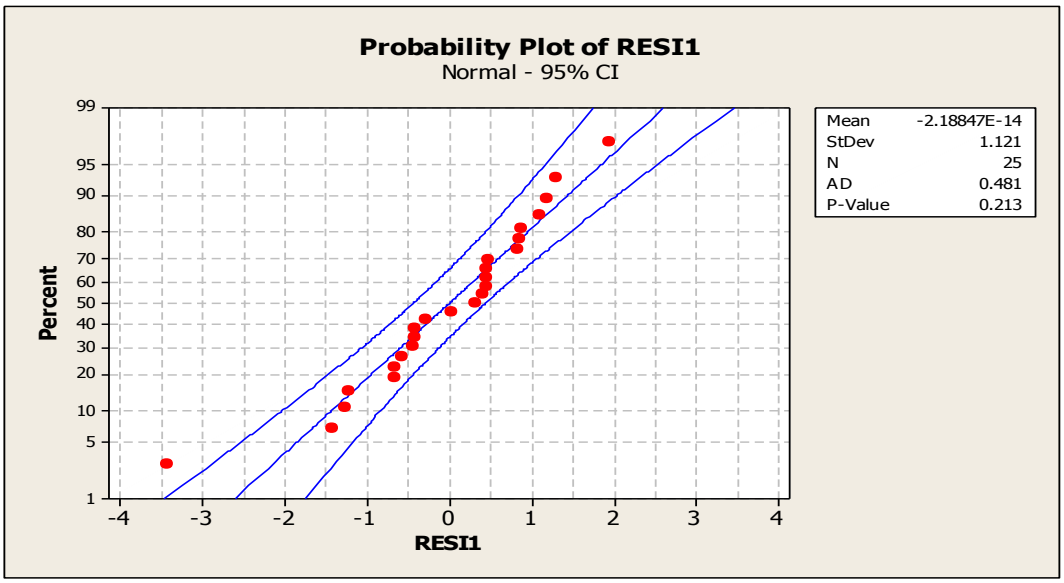

Figure E.10 Probability plot of residual values of surface tension of jatropha biodiesel B50

Table E.10 Measured and regressed surface tension and absolute and percent error of jatropha biodiesel B50 for five temperatures and five pressures

Absolute Temperature (K)	Absolute Pressure (MPa)	Measured Surface Tension (mN/m)	Regressed Surface Tension (mN/m)	Absolute Error (mN/m)	Error (%)
293	0.10	28.57	26.92	1.96	5.80
323		26.02	25.14	0.89	3.41
373		22.25	22.67	0.42	1.87
423		19.00	20.12	1.20	5.92
448		16.31	17.13	1.42	5.06
293	1.83	26.28	25.43	0.85	3.25
323		24.36	23.95	0.41	1.70
373		20.83	21.48	0.65	3.14
423		18.58	19.02	0.44	2.36
448		16.27	16.55	0.28	1.72
293	3.50	23.63	24.29	0.66	2.79
323		23.27	22.81	0.46	1.98
373		20.81	20.34	0.47	2.27
423		17.90	17.87	0.03	0.18
448		14.84	15.40	0.56	3.80
293	5.30	21.78	23.05	1.27	5.83
323		22.89	21.57	1.31	5.74
373		19.94	19.11	0.84	4.20
423		16.97	16.64	0.33	1.94
448		14.64	14.17	0.46	3.17
293	7.00	18.46	21.89	3.43	18.56
323		19.99	20.41	0.42	2.10
373		18.39	17.94	0.45	2.46
423		16.57	15.67	1.10	5.43
448		14.19	13.41	1.19	5.54

Table E.11 Regression analysis of jatropha biodiesel B20 surface tension as a function of temperature and pressure

Regression Analysis: σ versus P, T

The regression equation is

σ = 37.4 - 0.000820 P - 0.0411 T

Predictor	Coef	SE Coef	T	P
Constant	37.418	1.350	27.72	0.000
P	-0.00082011	0.00009154	-8.96	0.000
T	-0.041128	0.003424	-12.01	0.000

S = 1.11787 R-Sq = 91.1% R-Sq(adj) = 90.3%

Analysis of Variance

Source	DF	SS	MS	F	P
Regression	2	280.63	140.31	112.28	0.000
Residual Error	22	27.49	1.25		
Total	24	308.12			

Source	DF	Seq SS
P	1	100.31
T	1	180.32

Unusual Observations

Obs	P	σ	Fit	SE Fit	Residual	St Resid
21	7001	17.527	19.626	0.482	-2.099	-2.08R

R denotes an observation with a large standardized residual.

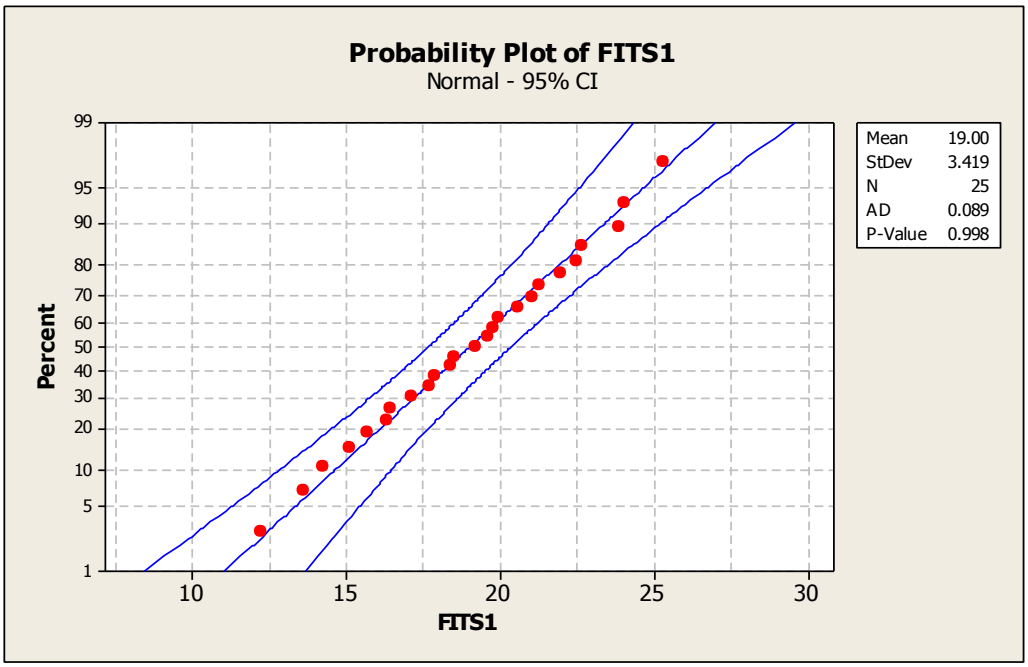

Figure E.11 Probability plot of regressed values of surface tension of jatropha biodiesel B20

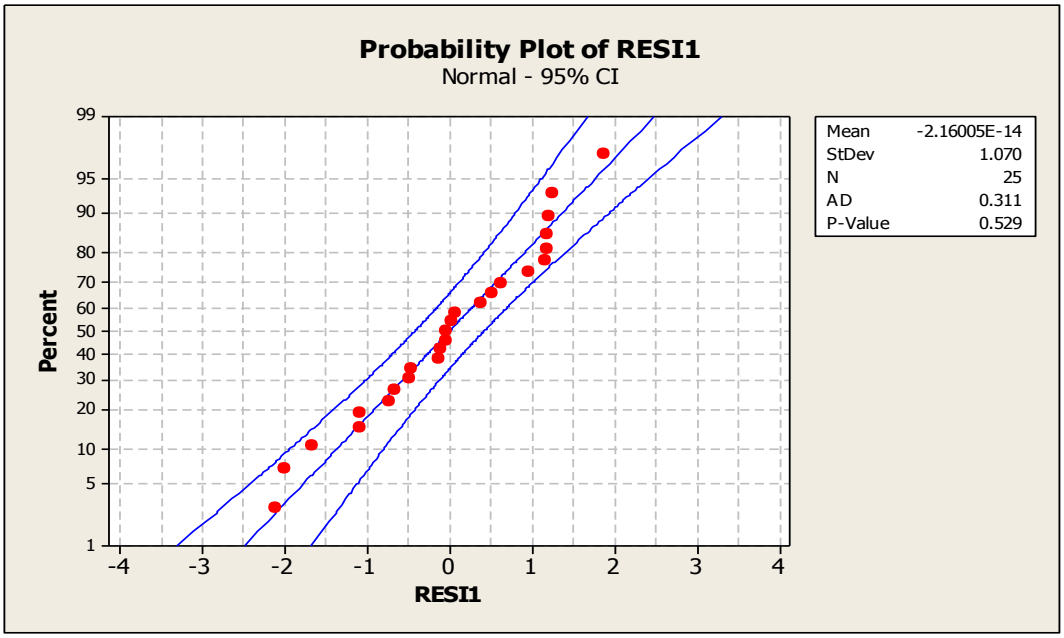

Figure E.12 Probability plot of residual values of surface tension of jatropha biodiesel B20

Table E.12 Measured and regressed surface tension and absolute and percent error for jatropha biodiesel B20 for five temperatures and five pressures

Absolute Temperature (K)	Absolute Pressure (MPa)	Measured Surface Tension (mN/m)	Regressed Surface Tension (mN/m)	Absolute Error (mN/m)	Error (%)
293	0.10	26.45	25.28	1.16	4.39
323		25.27	24.05	1.22	4.84
373		23.24	21.99	1.25	5.37
423		19.28	19.94	0.65	3.39
448		16.23	17.88	1.65	10.16
293	1.83	23.40	23.87	0.47	1.99
323		23.61	22.63	0.98	4.14
373		20.47	20.58	0.10	0.50
423		17.79	18.52	0.73	4.09
448		15.38	16.46	1.08	7.05
293	3.50	22.45	22.50	0.04	0.19
323		21.90	21.26	0.64	2.93
373		19.73	19.21	0.52	2.66
423		16.08	17.15	1.07	6.65
448		15.06	15.09	0.03	0.22
293	5.30	19.02	21.02	2.00	10.52
323		19.82	19.79	0.04	0.19
373		17.24	17.73	0.49	2.84
423		15.76	15.67	0.08	0.53
448		14.81	13.92	1.19	6.02
293	7.00	17.53	18.63	2.10	6.27
323		18.26	18.39	0.13	0.71
373		18.23	16.34	1.89	10.37
423		14.66	14.28	0.38	2.61
448		13.41	12.82	1.18	4.36

Table E.13 Regression analysis of soapnut biodiesel B100 surface tension as a function of temperature and pressure

Regression Analysis: σ versus P, T

The regression equation is

σ = 43.0 - 0.000670 P - 0.0508 T

Predictor	Coef	SE Coef	T	P
Constant	42.970	1.314	32.70	0.000
P	-0.00066965	0.00008912	-7.51	0.000
T	-0.050840	0.003334	-15.25	0.000

S = 1.08840 R-Sq = 92.9% R-Sq(adj) = 92.3%

Analysis of Variance

Source	DF	SS	MS	F	P
Regression	2	342.40	171.20	144.52	0.000
Residual Error	22	26.06	1.18		
Total	24	368.47			

Source	DF	Seq SS
P	1	66.88
T	1	275.52

Unusual Observations

Obs	P	σ	Fit	SE Fit	Residual	St Resid
22	7001	19.411	21.861	0.418	-2.450	-2.44R

R denotes an observation with a large standardized residual.

Table E.14 Regression analysis of soapnut biodiesel B80 surface tension as a function of temperature and pressure

Regression Analysis: σ versus P, T

The regression equation is

σ = 39.1 - 0.000650 P - 0.0426 T

Predictor	Coef	SE Coef	T	P
Constant	39.128	1.482	26.40	0.000
P	-0.0006501	0.0001005	-6.47	0.000
T	-0.042649	0.003760	-11.34	0.000

S = 1.22770 R-Sq = 88.6% R-Sq(adj) = 87.5%

Analysis of Variance

Source	DF	SS	MS	F	P
Regression	2	256.94	128.47	85.23	0.000
Residual Error	22	33.16	1.51		
Total	24	290.10			

Source	DF	Seq SS
P	1	63.04
T	1	193.90

Unusual Observations

Obs	P	σ	Fit	SE Fit	Residual	St Resid
1	101	29.043	26.566	0.529	2.476	2.24R

R denotes an observation with a large standardized residual.

Table E.15 Regression analysis of soapnut biodiesel B50 surface tension as a function of temperature and pressure.

Regression Analysis: ST versus P, T

The regression equation is

ST = 46.3 - 0.000476 P - 0.0609 T

Predictor	Coef	SE Coef	T	P
Constant	46.2503	0.5579	82.89	0.000
P	-0.00047621	0.00003784	-12.58	0.000
T	-0.060875	0.001415	-43.01	0.000

S = 0.462127 R-Sq = 98.9% R-Sq(adj) = 98.8%

Analysis of Variance

Source	DF	SS	MS	F	P
Regression	2	428.86	214.43	1004.06	0.000
Residual Error	22	4.70	0.21		
Total	24	433.55			

Source	DF	Seq SS
P	1	33.82
T	1	395.03

Unusual Observations

Obs	P	ST	Fit	SE Fit	Residual	St Resid
1	101	29.2607	28.3658	0.1992	0.8948	2.15R

R denotes an observation with a large standardized residual.

Table E.16 Regression analysis of soapnut biodiesel B20 surface tension as a function of temperature and pressure

Regression Analysis: ST versus P, T

The regression equation is

ST = 43.8 - 0.000621 P - 0.0570 T

Predictor	Coef	SE Coef	T	P
Constant	43.794	1.204	36.37	0.000
P	-0.00062077	0.00008168	-7.60	0.000
T	-0.057032	0.003055	-18.67	0.000

S = 0.997458 R-Sq = 94.9% R-Sq(adj) = 94.4%

Analysis of Variance

Source	DF	SS	MS	F	P
Regression	2	404.20	202.10	203.13	0.000
Residual Error	22	21.89	0.99		
Total	24	426.09			

Source	DF	Seq SS
P	1	57.47
T	1	346.73

Unusual Observations

Obs	P	ST	Fit	SE Fit	Residual	St Resid
5	101	14.312	16.755	0.453	-2.443	-2.75R

R denotes an observation with a large standardized residual.

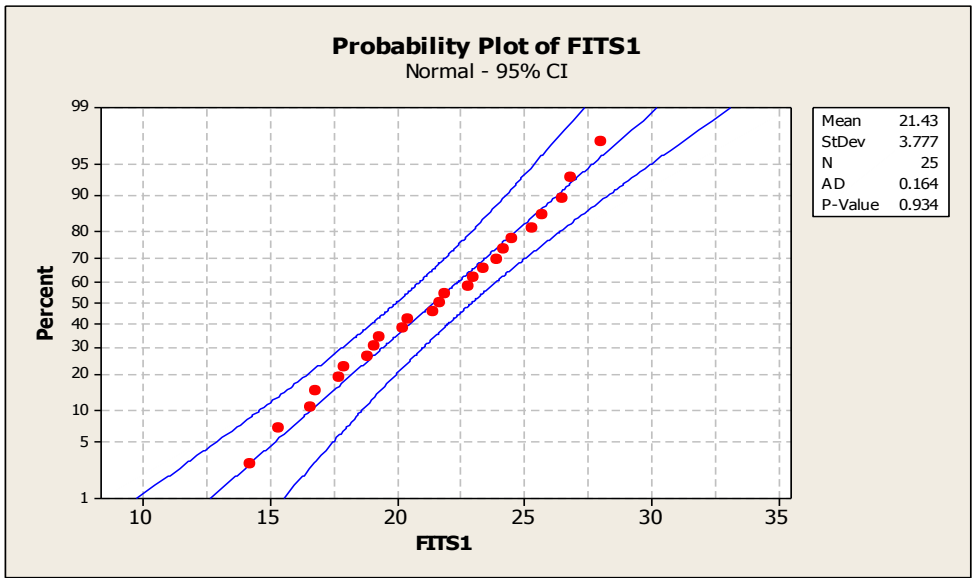

Figure E.13 Probability plot of regressed values of surface tension of soapnut biodiesel B100

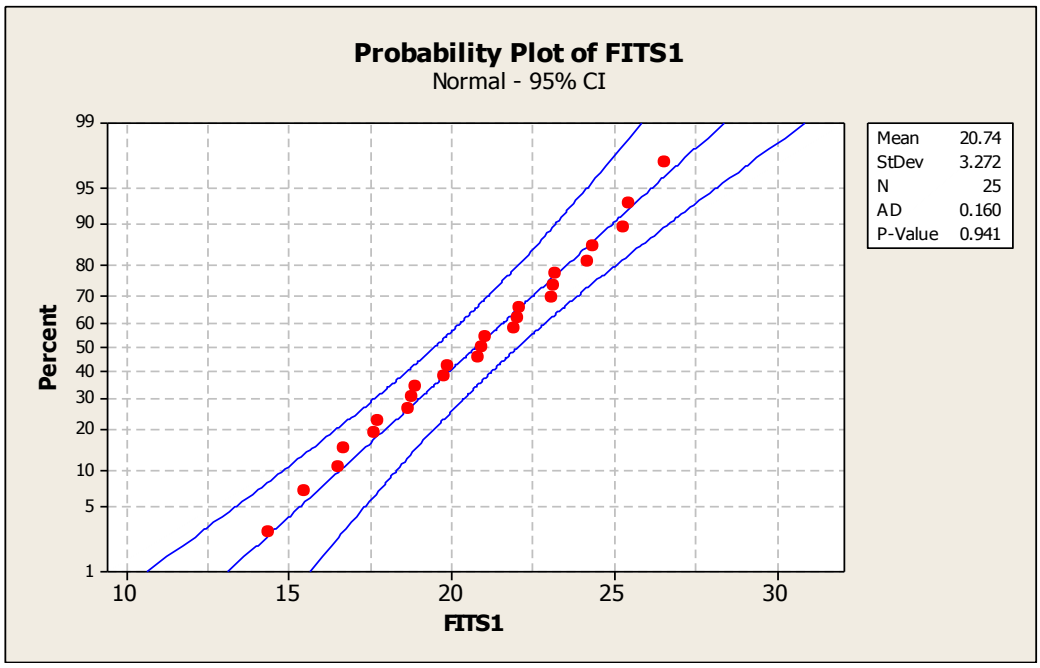

Figure E. 14 Probability plot of regressed values of surface tension of soapnut biodiesel B80

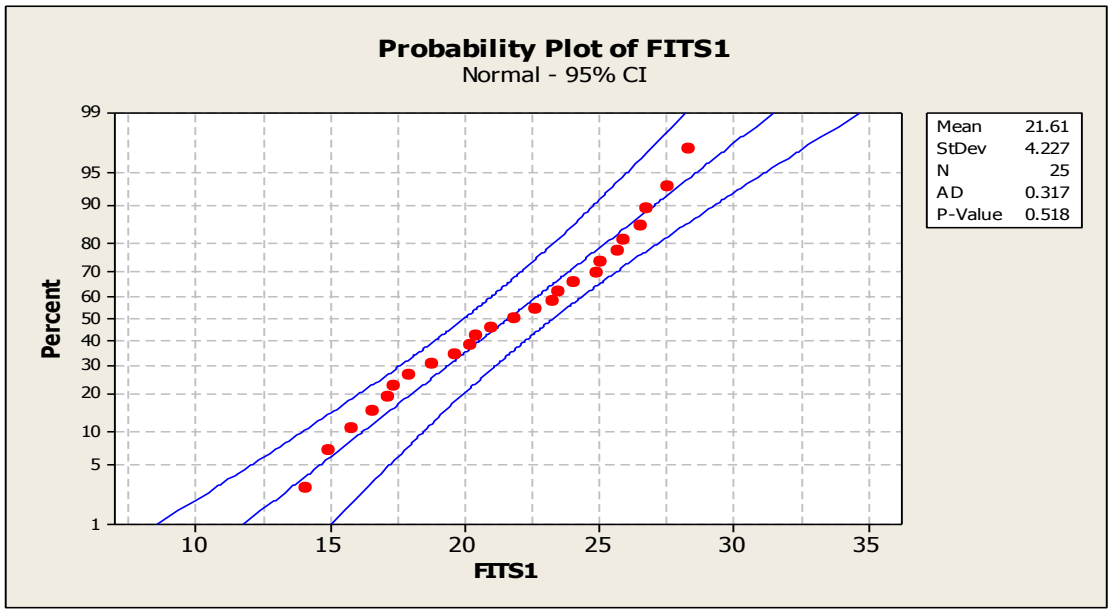

Figure E. 15 Probability plot of regressed values of surface tension of soapnut biodiesel B50

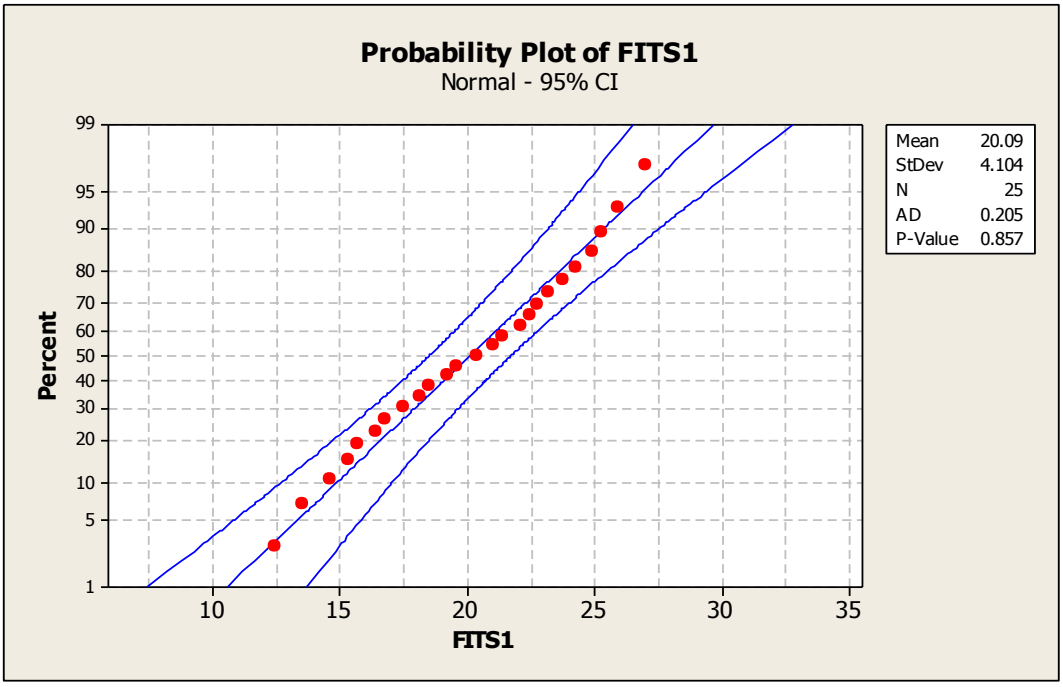

Figure E. 16 Probability plot of regressed values of surface tension of soapnut biodiesel B20

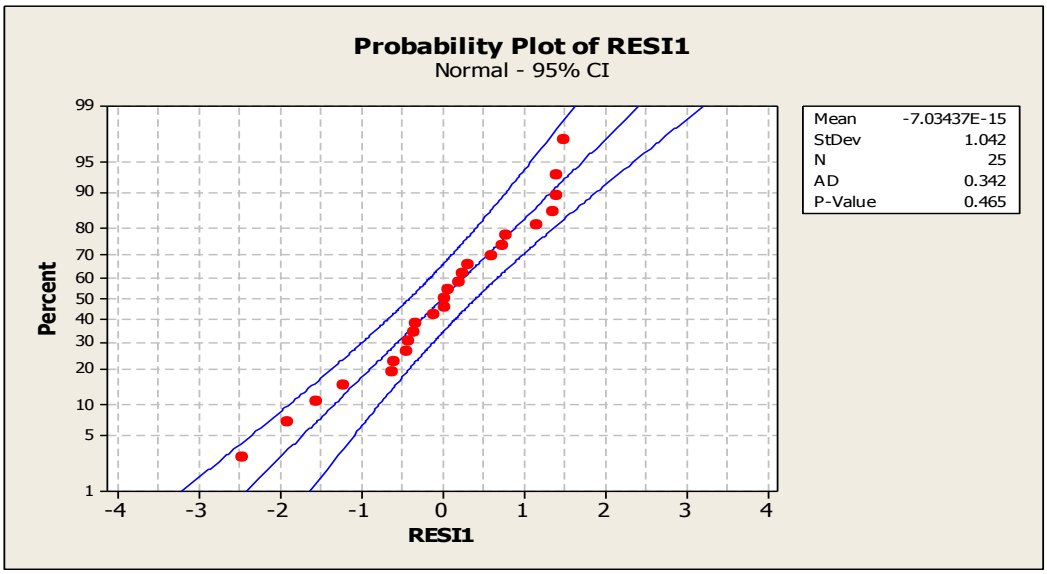

Figure E.17 Probability plot of residual values of surface tension of soapnut biodiesel B100

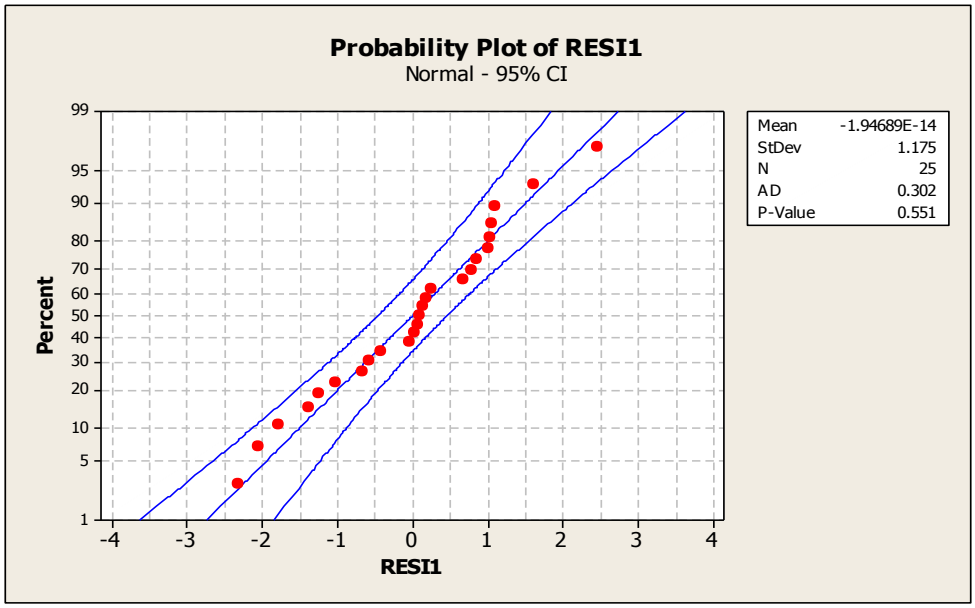

Figure E.18 Probability plot of residual values of surface tension of soapnut biodiesel B80

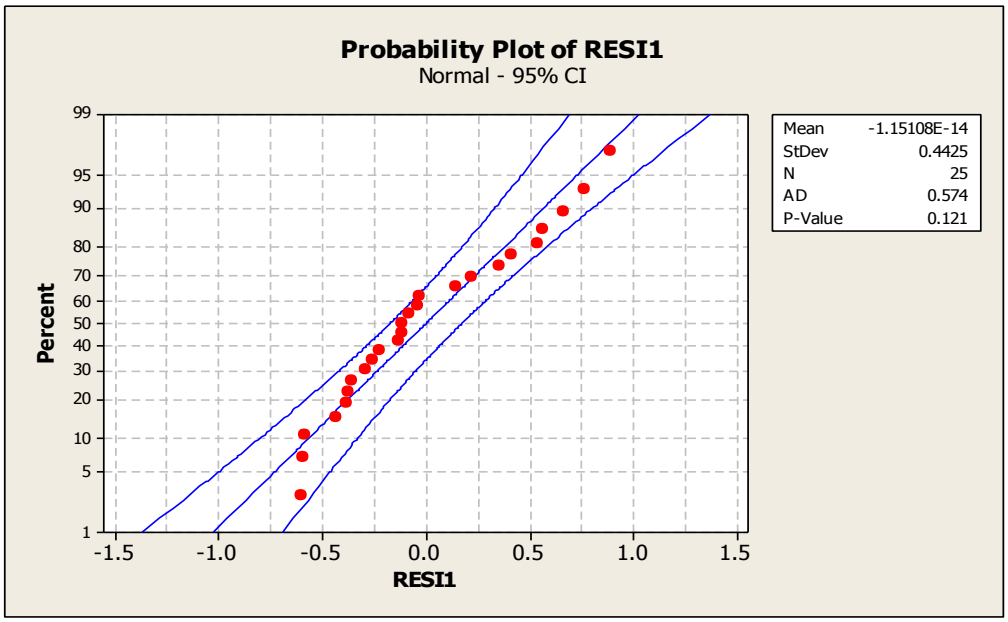

Figure E.19 Probability plot of residual values of surface tension of soapnut biodiesel B50

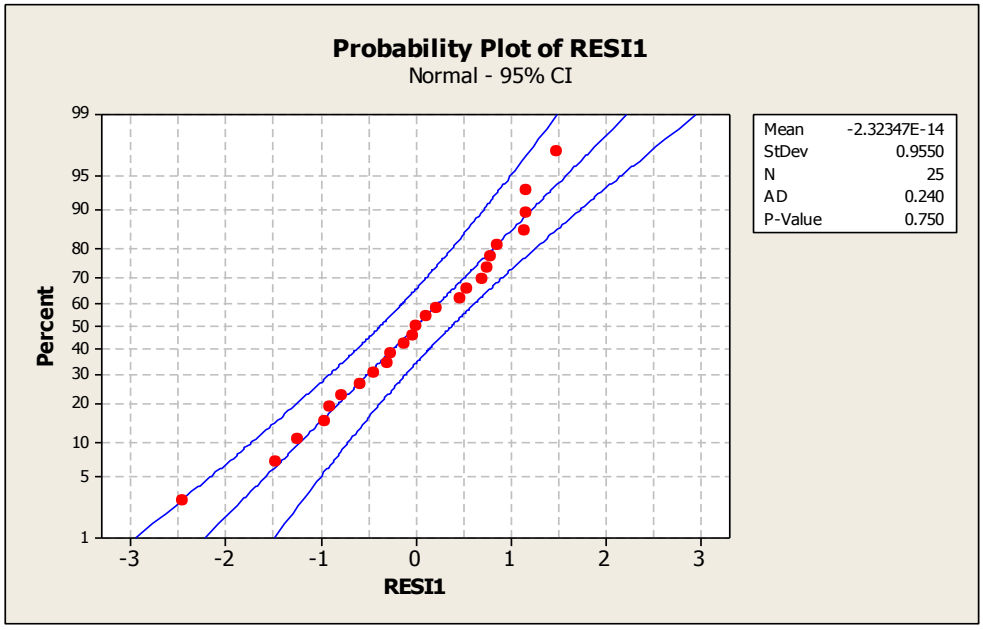

Figure E.20 Probability plot of residual values of surface tension of soapnut biodiesel B20

Table E.17 Measured and regressed surface tension and absolute and percent error of soapnut biodiesel B100 for five temperatures and five pressures

Absolute Temperature (K)	Absolute Pressure (MPa)	Measured Surface Tension (mN/m)	Regressed Surface Tension (mN/m)	Absolute Error (mN/m)	Error (%)
293	0.10	29.50	28.01	1.49	5.06
323		27.85	26.48	1.36	4.90
373		23.61	23.94	0.33	1.39
423		21.43	21.40	0.04	0.17
448		16.95	17.86	0.90	5.33
293	1.83	26.50	26.85	0.35	1.33
323		26.12	25.32	0.80	3.06
373		22.82	22.78	0.03	0.15
423		20.32	20.24	0.08	0.40
448		16.48	17.70	1.22	7.40
293	3.50	25.32	25.73	0.41	1.61
323		23.61	24.20	0.60	2.54
373		21.87	21.66	0.21	0.95
423		19.44	19.12	0.32	1.65
448		16.14	16.58	0.44	2.71
293	5.30	24.42	24.52	0.11	0.44
323		21.46	23.00	1.54	7.18
373		21.88	20.46	1.42	6.48
423		19.08	17.92	1.16	6.09
448		15.63	15.37	0.25	1.63
293	7.00	22.78	23.39	0.60	2.65
323		19.41	20.26	0.85	4.38
373		20.07	19.32	0.75	3.75
423		18.20	16.78	1.42	7.80
448		14.84	14.24	0.60	4.05

Table E.18 Measured and regressed surface tension and absolute and percent error of soapnut biodiesel B80 for five temperatures and five pressures

Absolute Temperature (K)	Absolute Pressure (MPa)	Measured Surface Tension (mN/m)	Regressed Surface Tension (mN/m)	Absolute Error (mN/m)	Error (%)
293	0.10	29.04	27.99	1.06	3.64
323		24.88	25.29	0.40	1.63
373		23.95	23.15	0.79	3.31
423		20.98	21.02	0.04	0.18
448		17.12	18.09	0.97	5.69
293	1.83	25.48	25.44	0.04	0.14
323		23.49	24.16	0.67	2.85
373		23.06	22.03	1.03	4.47
423		18.87	19.90	1.03	5.44
448		17.19	17.76	0.58	3.35
293	3.50	24.43	24.36	0.08	0.31
323		20.77	22.01	1.24	5.97
373		21.97	20.99	0.98	4.46
423		18.91	18.81	0.10	0.53
448		16.87	16.68	0.19	1.14
293	5.30	23.33	23.19	0.14	0.62
323		19.87	20.91	1.03	5.21
373		21.38	20.77	0.61	2.86
423		18.33	17.64	0.69	3.75
448		16.37	15.51	0.86	5.25
293	7.00	22.33	22.08	0.25	1.11
323		19.43	20.80	1.37	7.03
373		19.78	18.67	1.11	5.60
423		15.29	16.14	0.84	5.50
448		15.45	14.80	0.65	4.21

Table E.19 Measured and regressed surface tension and absolute and percent error of soapnut biodiesel B50 for five temperatures and five pressures

Absolute Temperature (K)	Absolute Pressure (MPa)	Measured Surface Tension (mN/m)	Regressed Surface Tension (mN/m)	Absolute Error (mN/m)	Error (%)
293	0.10	29.26	28.37	0.89	3.06
323		27.08	26.54	0.54	2.01
373		23.14	23.50	0.35	1.53
423		19.85	20.45	0.60	3.02
448		16.82	17.41	0.59	3.49
293	1.83	27.96	27.54	0.42	1.50
323		26.07	25.72	0.35	1.35
373		22.42	22.67	0.25	1.13
423		19.34	19.63	0.29	1.50
448		16.47	16.58	0.11	0.68
293	3.50	26.89	26.75	0.14	0.53
323		24.88	24.92	0.04	0.14
373		21.45	21.88	0.43	2.00
423		18.72	18.83	0.12	0.62
448		16.45	15.79	0.66	4.04
293	5.30	25.76	25.89	0.13	0.51
323		23.84	24.06	0.22	0.92
373		20.44	21.02	0.58	2.83
423		17.94	17.98	0.03	0.18
448		15.50	14.93	0.57	3.65
293	7.00	24.70	25.08	0.38	1.54
323		22.88	23.25	0.37	1.62
373		20.13	20.21	0.08	0.41
423		17.39	17.17	0.23	1.30
448		14.89	14.12	0.77	5.16

Table E.20 Measured and regressed surface tension and absolute and percent error of soapnut biodiesel B20 for five temperatures and five pressures

Absolute Temperature (K)	Absolute Pressure (MPa)	Measured Surface Tension (mN/m)	Regressed Surface Tension (mN/m)	Absolute Error (mN/m)	Error (%)
293	0.10	28.18	27.02	1.16	4.11
323		26.17	25.31	0.86	3.29
373		23.22	22.46	0.76	3.28
423		19.32	19.61	0.29	1.49
448		14.31	15.16	0.84	5.89
293	1.83	25.83	25.95	0.11	0.44
323		25.39	24.24	1.15	4.54
373		22.09	21.38	0.70	3.18
423		18.51	18.53	0.02	0.12
448		14.45	15.68	1.23	8.51
293	3.50	24.14	24.91	0.78	3.21
323		22.77	23.20	0.43	1.91
373		20.90	20.35	0.55	2.63
423		17.61	17.50	0.12	0.65
448		14.38	14.64	0.26	1.82
293	5.30	22.85	23.79	0.95	4.14
323		21.51	22.08	0.58	2.68
373		20.02	19.23	0.79	3.96
423		16.85	16.38	0.47	2.82
448		13.75	13.53	0.23	1.65
293	7.00	21.27	22.74	1.47	6.90
323		20.14	21.03	0.89	4.43
373		18.18	18.18	0.00	0.00
423		16.81	15.82	0.99	5.87
448		13.64	12.97	0.67	4.89

APPENDIX F: VISCOCITY DATA

Table F.1 Kinematic and dynamic viscosity and absolute and percent error of diesel for 0.10, 1.83 and 3.50 MPa at different temperatures

Absolute Temperature (K)	Absolute Pressure (MPa)	Dynamic viscosity (mPa-s)	Measured Kinematic viscosity (mm^2/s)	Regressed kinematic viscosity (mm^2/s)	Absolute error (mm^2/s)	Error (%)
293	0.1	2.6	3.05	3.04	0.01	0.33
313		1.79	2.14	2.07	0.07	3.27
333		1.2	1.45	1.51	0.06	4.14
353		0.93	1.14	1.17	0.02	1.75
383		0.67	0.85	0.85	0	0.00
423		0.49	0.64	0.63	0.02	3.13
453		0.4	0.54	0.53	0.01	1.85
473		0.33	0.47	0.48	0.01	2.13
503		0.3	0.43	0.42	0.01	2.33
523		0.26	0.38	0.39	0.01	2.63
293	1.83	2.68	3.13	3.14	0.01	0.32
313		1.88	2.23	2.17	0.06	2.69
333		1.28	1.54	1.59	0.05	3.25
353		1.01	1.23	1.23	0	0.00
383		0.7	0.87	0.89	0.02	2.30
423		0.51	0.66	0.64	0.03	4.55
453		0.39	0.52	0.52	0	0.00
473		0.35	0.46	0.47	0	0.00
503		0.3	0.41	0.4	0.01	2.44
523		0.26	0.36	0.37	0.01	2.78
293	3.5	2.79	3.24	3.23	0.01	0.31
313		1.97	2.31	2.25	0.06	2.60
333		1.34	1.6	1.66	0.06	3.75
353		1.05	1.27	1.28	0.01	0.79
383		0.75	0.93	0.93	0	0.00
423		0.54	0.69	0.67	0.02	2.90
453		0.42	0.55	0.55	0	0.00
473		0.37	0.5	0.49	0.01	2.00
503		0.31	0.43	0.42	0.01	2.33
523		0.27	0.37	0.39	0.01	2.70

Table F.2 Kinematic and dynamic viscosity and absolute and percent error of diesel for 5.30 and 7.00 MPa at different temperatures

Absolute Temperature (K)	Absolute Pressure (MPa)	Dynamic viscosity (mPa-s)	Measured Kinematic viscosity (mm^2/s)	Regressed kinematic viscosity (mm^2/s)	Absolute error (mm^2/s)	Error (%)
293	5.3	2.86	3.3	3.31	0.01	0.30
313		2.04	2.39	2.33	0.06	2.51
333		1.41	1.68	1.73	0.05	2.98
353		1.11	1.34	1.35	0.01	0.75
383		0.8	0.99	0.99	0	0.00
423		0.56	0.71	0.71	0	0.00
453		0.45	0.59	0.58	0.01	1.69
473		0.4	0.52	0.52	0	0.00
503		0.32	0.43	0.45	0.02	4.65
523		0.3	0.42	0.41	0.01	2.38
293	7	2.91	3.33	3.36	0.03	0.90
313		2.14	2.49	2.4	0.09	3.61
333		1.47	1.75	1.8	0.05	2.86
353		1.14	1.38	1.41	0.03	2.17
383		0.85	1.04	1.03	0.01	0.96
423		0.59	0.75	0.74	0.01	1.33
453		0.45	0.58	0.6	0.02	3.45
473		0.42	0.55	0.53	0.02	3.64
503		0.34	0.45	0.46	0.01	2.22
523		0.3	0.41	0.42	0.01	2.44

Table F.3 Regression data for kinematic viscosity of diesel at atmospheric pressure for different temperatures

Regression Analysis: ln(mu) versus 1/T, 1/T^2

The regression equation is

ln(mu) = - 1.50 - 305 1/T + 313899 1/T^2

Predictor	Coef	SE Coef	T	P
Constant	-1.4996	0.3449	-4.35	0.003
1/T	-305.0	269.5	-1.13	0.295
1/T^2	313899	51036	6.15	0.000

S = 0.0317610 R-Sq = 99.8% R-Sq(adj) = 99.8%

Analysis of Variance

Source	DF	SS	MS	F	P
Regression	2	4.5978	2.2989	2278.95	0.000
Residual Error	7	0.0071	0.0010		
Total	9	4.6049			

Source	DF	Seq SS
1/T	1	4.5597
1/T^2	1	0.0382

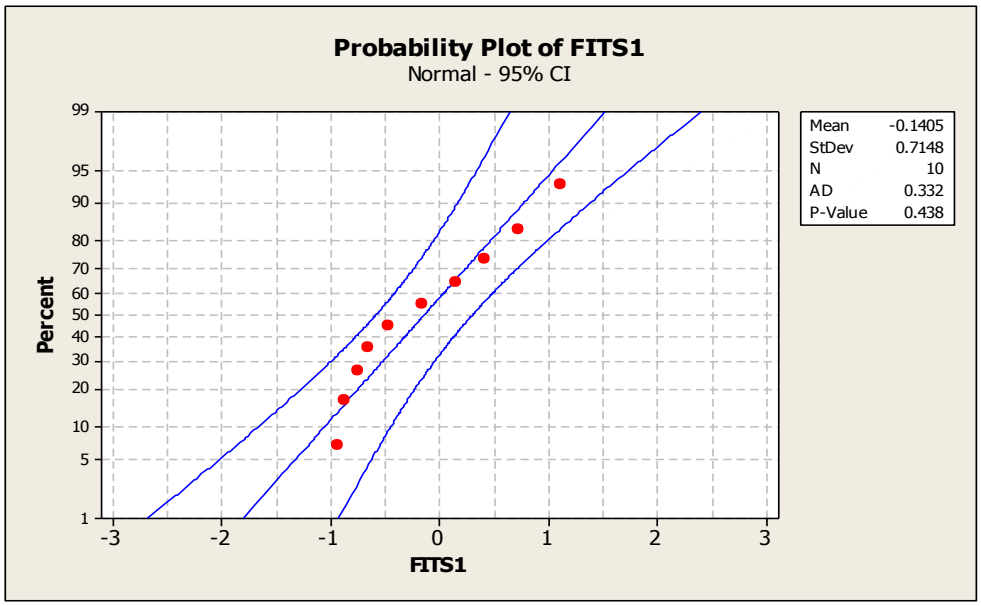

Figure F.1 Probability plot of regressed kinematic viscosity data of diesel fuel at atmospheric pressure.

Table F. 4 Regression data for kinematic viscosity of canola biodiesel B100 at 0.10 MPa for different temperatures

Regression Analysis: Ln(mu) versus 1/T, 1/T^2

The regression equation is

Ln(mu) = - 2.31 + 409 1/T + 246800 1/T^2

Predictor	Coef	SE Coef	T	P
Constant	-2.3101	0.8050	-2.87	0.024
1/T	409.0	629.1	0.65	0.536
1/T^2	246800	119118	2.07	0.077

S = 0.0741298 R-Sq = 99.5% R-Sq(adj) = 99.3%

Analysis of Variance

Source	DF	SS	MS	F	P
Regression	2	7.3484	3.6742	668.62	0.000
Residual Error	7	0.0385	0.0055		
Total	9	7.3869			

Source	DF	Seq SS
1/T	1	7.3248
1/T^2	1	0.0236

Table F. 5 Regression data for kinematic viscosity of canola biodiesel B100 at 1.83 MPa for different temperatures

Regression Analysis: ln(mu) versus 1/T, 1/T^2

The regression equation is

ln(mu) = - 2.31 + 450 1/T + 236660 1/T^2

Predictor	Coef	SE Coef	T	P
Constant	-2.3123	0.6275	-3.68	0.008
1/T	449.7	490.5	0.92	0.390
1/T^2	236660	92864	2.55	0.038

S = 0.0577913 R-Sq = 99.7% R-Sq(adj) = 99.6%

Analysis of Variance

Source	DF	SS	MS	F	P
Regression	2	7.2379	3.6189	1083.57	0.000
Residual Error	7	0.0234	0.0033		
Total	9	7.2613			

Source	DF	Seq SS
1/T	1	7.2162
1/T^2	1	0.0217

Unusual Observations

Obs	1/T	ln(mu)	Fit	SE Fit	Residual	St Resid
10	0.00191	-0.6747	-0.5879	0.0388	-0.0868	-2.03R

R denotes an observation with a large standardized error.

Table F. 6 Regression data for kinematic viscosity of canola biodiesel B100 at 3.50 MPa for different temperatures

Regression Analysis: ln(mu) versus 1/T, 1/T^2

The regression equation is

ln(mu) = - 2.26 + 454 1/T + 231432 1/T^2

Predictor	Coef	SE Coef	T	P
Constant	-2.2602	0.6939	-3.26	0.014
1/T	454.4	542.3	0.84	0.430
1/T^2	231432	102678	2.25	0.059

S = 0.0638986 R-Sq = 99.6% R-Sq(adj) = 99.5%

Analysis of Variance

Source	DF	SS	MS	F	P
Regression	2	7.0434	3.5217	862.52	0.000
Residual Error	7	0.0286	0.0041		
Total	9	7.0720			

Source	DF	Seq SS
1/T	1	7.0226
1/T^2	1	0.0207

Unusual Observations

Obs	1/T	ln(mu)	Fit	SE Fit	Residual	St Resid
10	0.00191	-0.6526	-0.5461	0.0429	-0.1065	-2.25R

R denotes an observation with a large standardized residual.

Table F. 7 Regression data for kinematic viscosity of canola biodiesel B100 at 5.30 MPa for different temperatures

Regression Analysis: ln(mu) versus 1/T, 1/T^2

The regression equation is

ln(mu) = - 2.25 + 490 1/T + 220519 1/T^2

Predictor	Coef	SE Coef	T	P
Constant	-2.2452	0.7019	-3.20	0.015
1/T	489.6	548.5	0.89	0.402
1/T^2	220519	103860	2.12	0.071

S = 0.0646343 R-Sq = 99.6% R-Sq(adj) = 99.5%

Analysis of Variance

Source	DF	SS	MS	F	P
Regression	2	6.8558	3.4279	820.55	0.000
Residual Error	7	0.0292	0.0042		
Total	9	6.8851			

Source	DF	Seq SS
1/T	1	6.8370
1/T^2	1	0.0188

Unusual Observations

Obs	1/T	ln(mu)	Fit	SE Fit	Residual	St Resid
10	0.00191	-0.6121	-0.5037	0.0434	-0.1084	-2.26R

R denotes an observation with a large standardized residual.

Table F. 8 Regression data for kinematic viscosity of canola biodiesel B100 at 7.00 MPa for different temperatures

Regression Analysis: ln(mu) versus 1/T, 1/T^2

The regression equation is

ln(mu) = - 2.35 + 562 1/T + 209140 1/T^2

Predictor	Coef	SE Coef	T	P
Constant	-2.3498	0.7932	-2.96	0.021
1/T	561.6	619.9	0.91	0.395
1/T^2	209140	117374	1.78	0.118

S = 0.0730442 R-Sq = 99.5% R-Sq(adj) = 99.3%

Analysis of Variance

Source	DF	SS	MS	F	P
Regression	2	6.9545	3.4772	651.72	0.000
Residual Error	7	0.0373	0.0053		
Total	9	6.9918			

Source	DF	Seq SS
1/T	1	6.9375
1/T^2	1	0.0169

Unusual Observations

Obs	1/T	ln(mu)	Fit	SE Fit	Residual	St Resid
10	0.00191	-0.6369	-0.5121	0.0491	-0.1248	-2.31R

R denotes an observation with a large standardized residual.

Table F.9 Measured and regressed kinematic viscosity, dynamic viscosity an absolute and percent error of canola B100 for 0.10, 1.83, and 3.50 MPa at different temperatures

Absolute Temperature (K)	Absolute Pressure (MPa)	Dynamic viscosity (mPa-s)	Measured Kinematic viscosity (mm^2/s)	Regressed kinematic viscosity (mm^2/s)	Absolute error (mm^2/s)	Error (%)
293	0.1	6.24	7.05	7.08	0.03	0.43
313		4.29	4.9	4.54	0.36	7.35
333		2.56	2.95	3.13	0.18	6.10
353		1.87	2.19	2.29	0.1	4.57
383		1.24	1.48	1.55	0.07	4.73
423		0.84	1.05	1.04	0.01	0.95
453		0.68	0.86	0.81	0.05	5.81
473		0.6	0.78	0.74	0.04	5.13
503		0.45	0.6	0.59	0.01	1.67
523		0.35	0.48	0.52	0.04	8.33
293	1.83	6.31	7.11	7.21	0.1	1.41
313		4.39	5.01	4.65	0.36	7.19
333		2.66	3.07	3.22	0.15	4.89
353		1.96	2.29	2.36	0.07	3.06
383		1.3	1.56	1.61	0.05	3.21
423		0.88	1.09	1.07	0.01	0.92
453		0.69	0.87	0.85	0.02	2.30
473		0.61	0.78	0.74	0.05	6.41
503		0.49	0.64	0.62	0.02	3.13
523		0.38	0.51	0.56	0.05	9.80
293	3.5	5.68	7.16	7.26	0.1	1.40
313		3.95	5.05	4.72	0.34	6.73
333		2.41	3.15	3.28	0.13	4.13
353		1.75	2.35	2.42	0.07	2.98
383		1.15	1.6	1.65	0.05	3.13
423		0.75	1.11	1.11	0	0.00
453		0.57	0.89	0.88	0.02	2.25
473		0.5	0.81	0.77	0.05	6.17
503		0.4	0.69	0.64	0.05	7.25
523		0.29	0.52	0.58	0.06	11.54

Table F.10 Measured and regressed kinematic viscosity, dynamic viscosity and absolute and percent error of canola B100 for 5.30 and 7.00 MPa at different temperatures

Absolute Temperature (K)	Absolute Pressure (MPa)	Dynamic viscosity (mPa-s)	Measured Kinematic viscosity (mm^2/s)	Regressed kinematic viscosity (mm^2/s)	Absolute error (mm^2/s)	Error (%)
293	5.3	6.45	7.19	7.32	0.13	1.81
313		4.56	5.13	4.79	0.33	6.43
333		2.87	3.26	3.36	0.1	3.07
353		2.11	2.43	2.48	0.06	2.47
383		1.4	1.64	1.71	0.06	3.66
423		0.95	1.15	1.15	0.01	0.87
453		0.75	0.93	0.91	0.02	2.15
473		0.66	0.84	0.8	0.04	4.76
503		0.55	0.73	0.67	0.06	8.22
523		0.4	0.54	0.6	0.06	11.11
293	7	6.57	7.31	1	6.31	86.32
313		4.65	5.19	1	4.19	80.73
333		2.91	3.26	1	2.26	69.33
353		2.14	2.41	1	1.41	58.51
383		1.42	1.64	1	0.64	39.02
423		0.98	1.16	1	0.16	13.79
453		0.79	0.97	1	0.03	3.09
473		0.67	0.83	1	0.17	20.48
503		0.56	0.72	1	0.28	38.89
523		0.4	0.53	1	0.47	88.68

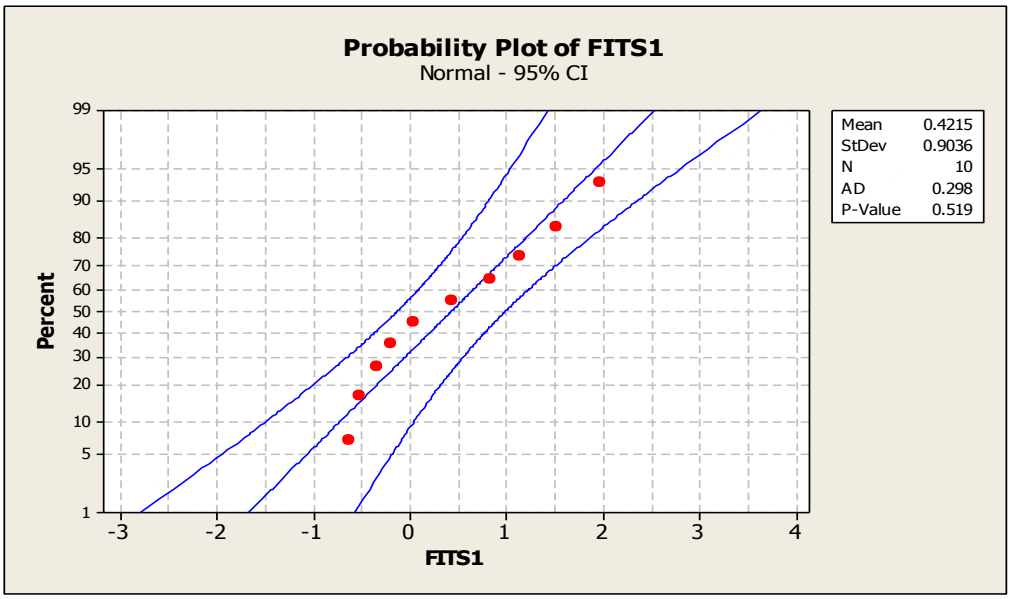

Figure F.2 Probability plot of regressed data for canola biodiesel B100 at atmospheric pressure for different temperatures

Table F. 11 Regression data for kinematic viscosity of canola biodiesel B100 at 0.10 MPa for different temperatures

Regression Analysis: ln(mu) versus 1/T, 1/T^2

The regression equation is

ln(mu) = - 2.10 + 135 1/T + 301833 1/T^2

Predictor	Coef	SE Coef	T	P
Constant	-2.0987	0.3183	-6.59	0.000
1/T	134.7	248.8	0.54	0.605
1/T^2	301833	47107	6.41	0.000

S = 0.0293159 R-Sq = 99.9% R-Sq(adj) = 99.9%

Analysis of Variance

Source	DF	SS	MS	F	P
Regression	2	7.4934	3.7467	4359.57	0.000
Residual Error	7	0.0060	0.0009		
Total	9	7.4994			

Source	DF	Seq SS
1/T	1	7.4581
1/T^2	1	0.0353

Table F. 12 Regression data for kinematic viscosity of canola biodiesel B100 at 1.83 MPa for different temperatures

Regression Analysis: ln(mu) versus 1/T, 1/T^2

The regression equation is
ln(mu) = - 2.22 + 263 1/T + 275037 1/T^2

Predictor	Coef	SE Coef	T	P
Constant	-2.2232	0.3729	-5.96	0.001
1/T	262.6	291.5	0.90	0.398
1/T^2	275037	55183	4.98	0.002

S = 0.0343419 R-Sq = 99.9% R-Sq(adj) = 99.9%

Analysis of Variance

Source	DF	SS	MS	F	P
Regression	2	7.3737	3.6869	3126.15	0.000
Residual Error	7	0.0083	0.0012		
Total	9	7.3820			

Source	DF	Seq SS
1/T	1	7.3444
1/T^2	1	0.0293

Table F. 13 Regression data for kinematic viscosity of canola biodiesel B100 at 3.50 MPa for different temperatures

Regression Analysis: ln(mu) versus 1/T, 1/T^2

The regression equation is
ln(mu) = - 2.20 + 395 1/T + 235108 1/T^2

Predictor	Coef	SE Coef	T	P
Constant	-2.1976	0.3009	-7.30	0.000
1/T	395.3	235.1	1.68	0.137
1/T^2	235108	44522	5.28	0.001

S = 0.0277068 R-Sq = 99.9% R-Sq(adj) = 99.9%

Analysis of Variance

Source	DF	SS	MS	F	P
Regression	2	6.7146	3.3573	4373.39	0.000
Residual Error	7	0.0054	0.0008		
Total	9	6.7200			

Source	DF	Seq SS
1/T	1	6.6932
1/T^2	1	0.0214

Unusual Observations

Obs	1/T	ln(mu)	Fit	SE Fit	Residual	St Resid
9	0.00199	-0.42776	-0.48329	0.01516	0.05553	2.39R

R denotes an observation with a large standardized residual.

Table F. 14. Regression data for kinematic viscosity of canola biodiesel B100 at 5.30 MPa for different temperatures

Regression Analysis: ln(mu) versus 1/T, 1/T^2

The regression equation is
ln(mu) = - 3.31 + 1242 1/T + 84292 1/T^2

Predictor	Coef	SE Coef	T	P
Constant	-3.3119	0.2082	-15.91	0.000
1/T	1242.3	162.7	7.64	0.000
1/T^2	84292	30803	2.74	0.029

S = 0.0191694 R-Sq = 100.0% R-Sq(adj) = 100.0%

Analysis of Variance

Source	DF	SS	MS	F	P
Regression	2	7.1350	3.5675	9708.45	0.000
Residual Error	7	0.0026	0.0004		
Total	9	7.1376			

Source	DF	Seq SS
1/T	1	7.1323
1/T^2	1	0.0028

Table F. 15 Regression data for kinematic viscosity of canola biodiesel B100 at 7.00 MPa for different temperatures

Regression Analysis: ln(mu) versus 1/T, 1/T^2

The regression equation is

ln(mu) = - 2.48 + 696 1/T + 175387 1/T^2

Predictor	Coef	SE Coef	T	P
Constant	-2.4793	0.3485	-7.12	0.000
1/T	696.2	272.3	2.56	0.038
1/T^2	175387	51564	3.40	0.011

S = 0.0320894 R-Sq = 99.9% R-Sq(adj) = 99.9%

Analysis of Variance

Source	DF	SS	MS	F	P
Regression	2	6.5940	3.2970	3201.81	0.000
Residual Error	7	0.0072	0.0010		
Total	9	6.6012			

Source	DF	Seq SS
1/T	1	6.5821
1/T^2	1	0.0119

Table F.16 Measured and regressed kinematic viscosity, dynamic viscosity and absolute and percent error of canola B80 for 0.10, 1.83, and 3.50 MPa at different temperatures

Absolute Temperature (K)	Absolute Pressure (MPa)	Dynamic viscosity (mPa-s)	Measured Kinematic viscosity (mm^2/s)	Regressed kinematic viscosity (mm^2/s)	Absolute error (mm^2/s)	Error (%)
293	0.1	5.53	6.26	6.51	0.25	3.99
313		3.77	4.29	4.09	0.2	4.66
333		2.46	2.84	2.79	0.05	1.76
353		1.71	2	2.02	0.02	1.00
383		1.15	1.37	1.36	0.01	0.73
423		0.72	0.89	0.91	0.02	2.25
453		0.55	0.7	0.72	0.01	1.43
473		0.47	0.62	0.63	0.01	1.61
503		0.38	0.53	0.53	0	0.00
523		0.35	0.49	0.48	0.01	2.04
293	1.83	5.6	6.29	6.51	0.22	3.50
313		3.81	4.34	4.14	0.21	4.84
333		2.51	2.89	2.84	0.05	1.73
353		1.74	2.04	2.07	0.02	0.98
383		1.13	1.37	1.4	0.03	2.19
423		0.76	0.94	0.94	0	0.00
453		0.56	0.71	0.74	0.03	4.23
473		0.52	0.67	0.64	0.03	4.48
503		0.41	0.55	0.54	0.01	1.82
523		0.35	0.48	0.49	0.01	2.08
293	3.5	5.87	6.58	6.6	0.01	0.15
313		3.81	4.32	4.32	0	0.00
333		2.65	3.04	3.03	0.01	0.33
353		1.93	2.24	2.24	0	0.00
383		1.31	1.55	1.55	0	0.00
423		0.88	1.07	1.05	0.02	1.87
453		0.65	0.81	0.83	0.03	3.70
473		0.57	0.72	0.73	0.01	1.39
503		0.5	0.65	0.62	0.04	6.15
523		0.4	0.54	0.56	0.02	3.70

Table F.17 Measured and regressed kinematic viscosity, dynamic viscosity and absolute and percent error of canola B80 for 0.10, 1.83, and 3.50 MPa at different temperatures

Absolute Temperature (K)	Absolute Pressure (MPa)	Dynamic viscosity (mPa-s)	Measured Kinematic viscosity (mm^2/s)	Regressed kinematic viscosity (mm^2/s)	Absolute error (mm^2/s)	Error (%)
293	5.3	6.15	6.87	6.73	0.14	2.04
313		3.95	4.47	4.55	0.08	1.79
333		2.83	3.24	3.24	0	0.00
353		2.03	2.35	2.42	0.07	2.98
383		1.42	1.68	1.66	0.02	1.19
423		0.91	1.11	1.1	0.01	0.90
453		0.69	0.86	0.85	0.01	1.16
473		0.59	0.74	0.73	0.01	1.35
503		0.46	0.6	0.6	0	0.00
523		0.39	0.52	0.53	0.01	1.92
293	7	6.27	6.93	6.93	0	0.00
313		4.22	4.72	4.63	0.09	1.91
333		2.8	3.17	3.29	0.12	3.79
353		2.12	2.43	2.46	0.03	1.23
383		1.52	1.78	1.7	0.08	4.49
423		0.98	1.18	1.16	0.02	1.69
453		0.71	0.87	0.92	0.05	5.75
473		0.63	0.8	0.8	0	0.00
503		0.51	0.66	0.67	0.01	1.52
523		0.46	0.62	0.6	0.02	3.23

Table F.18 Regression data for kinematic viscosity of canola biodiesel B50 at 0.10 MPa for different temperatures.

Regression Analysis: ln(mu) versus 1/T, 1/T^2

The regression equation is

ln(mu) = - 3.22 + 884 1/T + 160956 1/T^2

Predictor	Coef	SE Coef	T	P
Constant	-3.2245	0.2277	-14.16	0.000
1/T	884.4	178.0	4.97	0.002
1/T^2	160956	33698	4.78	0.002

S = 0.0209711 R-Sq = 100.0% R-Sq(adj) = 99.9%

Analysis of Variance

Source	DF	SS	MS	F	P
Regression	2	7.5354	3.7677	8567.15	0.000
Residual Error	7	0.0031	0.0004		
Total	9	7.5385			

Source	DF	Seq SS
1/T	1	7.5254
1/T^2	1	0.0100

Table F.19 Measured and regressed kinematic viscosity, dynamic viscosity and absolute and percent error of canola B50 for 0.10, 1.83, and 3.50 MPa at different temperatures

Absolute Temperature (K)	Absolute Pressure (MPa)	Dynamic viscosity (mPa-s)	Measured Kinematic viscosity (mm^2/s)	Regressed kinematic viscosity (mm^2/s)	Absolute error (mm^2/s)	Error (%)
293	0.1	4.6	5.26	5.29	0.03	0.57
313		3.03	3.51	3.46	0.05	1.42
333		2	2.35	2.41	0.06	2.55
353		1.5	1.79	1.77	0.03	1.68
383		1	1.22	1.2	0.03	2.46
423		0.63	0.79	0.79	0	0.00
453		0.46	0.6	0.61	0.02	3.33
473		0.39	0.52	0.53	0.01	1.92
503		0.33	0.45	0.44	0.01	2.22
523		0.28	0.39	0.39	0	0.00
293	1.83	4.66	5.3	5.38	0.08	1.51
313		3.15	3.63	3.56	0.07	1.93
333		2.1	2.47	2.49	0.02	0.81
353		1.57	1.87	1.83	0.05	2.67
383		1.01	1.23	1.23	0.01	0.81
423		0.64	0.8	0.8	0.01	1.25
453		0.47	0.61	0.62	0.01	1.64
473		0.4	0.53	0.53	0	0.00
503		0.32	0.43	0.43	0	0.00
523		0.29	0.39	0.38	0.01	2.56
293	3.5	4.69	5.3	5.42	0.13	2.45
313		3.25	3.7	3.64	0.06	1.62
333		2.28	2.62	2.57	0.06	2.29
353		1.64	1.91	1.88	0.02	1.05
383		1.07	1.26	1.26	0	0.00
423		0.65	0.79	0.81	0.02	2.53
453		0.49	0.61	0.61	0.01	1.64
473		0.41	0.51	0.52	0.01	1.96
503		0.32	0.42	0.41	0.01	2.38
523		0.28	0.37	0.36	0	0.00

Table F.20 Measured and regressed kinematic viscosity, dynamic viscosity and absolute and percent error of canola B50 for 5.30 and 7.00 MPa at different temperatures

Absolute Temperature (K)	Absolute Pressure (MPa)	Dynamic viscosity (mPa-s)	Measured Kinematic viscosity (mm^2/s)	Regressed kinematic viscosity (mm^2/s)	Absolute error (mm^2/s)	Error (%)
293	5.3	4.91	5.51	5.42	0.09	1.63
313		3.39	3.84	3.64	0.2	5.21
333		2.31	2.63	2.57	0.06	2.28
353		1.6	1.85	1.88	0.03	1.62
383		1.05	1.24	1.26	0.02	1.61
423		0.67	0.81	0.81	0	0.00
453		0.51	0.63	0.61	0.02	3.17
473		0.42	0.52	0.52	0	0.00
503		0.34	0.43	0.41	0.02	4.65
523		0.29	0.38	0.36	0.02	5.26
293	7	4.97	5.51	5.59	0.08	1.45
313		3.36	3.76	3.73	0.03	0.80
333		2.39	2.7	2.62	0.08	2.96
353		1.67	1.9	1.92	0.02	1.05
383		1.1	1.27	1.29	0.02	1.57
423		0.7	0.83	0.83	0	0.00
453		0.52	0.63	0.63	0	0.00
473		0.43	0.53	0.53	0	0.00
503		0.34	0.43	0.43	0	0.00
523		0.3	0.38	0.38	0	0.00

Table F.21 Regression data for kinematic viscosity of canola biodiesel B20 at 0.10 MPa for different temperatures

Regression Analysis: ln(mu) versus 1/T, 1/T^2

The regression equation is

ln(mu) = - 3.56 + 1224 1/T + 47311 1/T^2

Predictor	Coef	SE Coef	T	P
Constant	-3.5570	0.5572	-6.38	0.000
1/T	1223.9	435.5	2.81	0.026
1/T^2	47311	82448	0.57	0.584

S = 0.0513091 R-Sq = 99.7% R-Sq(adj) = 99.6%

Analysis of Variance

Source	DF	SS	MS	F	P
Regression	2	5.4438	2.7219	1033.91	0.000
Residual Error	7	0.0184	0.0026		
Total	9	5.4622			

Source	DF	Seq SS
1/T	1	5.4429
1/T^2	1	0.0009

Unusual Observations

Obs	1/T	ln(mu)	Fit	SE Fit	Residual	St Resid
6	0.00236	-0.2916	-0.4003	0.0231	0.1087	2.37R

R denotes an observation with a large standardized residual.

Table F.22 Measured and regressed kinematic viscosity, dynamic viscosity and absolute and percent error of canola B20 for 0.10, 1.83, and 3.50 MPa at different temperatures

Absolute Temperature (K)	Absolute Pressure (MPa)	Dynamic viscosity (mPa-s)	Measured Kinematic viscosity (mm^2/s)	Regressed kinematic viscosity (mm^2/s)	Absolute error (mm^2/s)	Error (%)
293	0.1	2.78	3.22	3.22	0	0.00
313		2.02	2.38	2.3	0.08	3.36
333		1.42	1.7	1.72	0.02	1.18
353		1.04	1.26	1.33	0.07	5.56
383		0.74	0.93	0.96	0.03	3.23
423		0.57	0.75	0.67	0.08	10.67
453		0.39	0.53	0.53	0	0.00
473		0.34	0.47	0.47	0	0.00
503		0.27	0.38	0.39	0.01	2.63
523		0.24	0.35	0.35	0	0.00
293	1.83	2.82	3.26	3.32	0.06	1.84
313		2.09	2.44	2.35	0.09	3.69
333		1.47	1.74	1.74	0	0.00
353		1.07	1.29	1.34	0.05	3.88
383		0.79	0.96	0.96	0	0.00
423		0.54	0.69	0.67	0.02	2.90
453		0.41	0.54	0.53	0.01	1.85
473		0.34	0.45	0.47	0.02	4.44
503		0.29	0.4	0.39	0.01	2.50
523		0.26	0.35	0.35	0	0.00
293	3.5	2.89	3.33	3.37	0.04	1.20
313		2.16	2.52	2.45	0.07	2.78
333		1.55	1.84	1.85	0.01	0.54
353		1.17	1.4	1.44	0.04	2.86
383		0.86	1.05	1.05	0	0.00
423		0.58	0.73	0.73	0	0.00
453		0.46	0.59	0.58	0.01	1.69
473		0.4	0.52	0.51	0.01	1.92
503		0.32	0.42	0.43	0.01	2.38
523		0.28	0.38	0.38	0	0.00

Table F.23 Measured and regressed kinematic viscosity, dynamic viscosity and absolute and percent error of canola B20 for 5.30 and 7.00 MPa at different temperatures

Absolute Temperature (K)	Absolute Pressure (MPa)	Dynamic viscosity (mPa-s)	Measured Kinematic viscosity (mm^2/s)	Regressed kinematic viscosity (mm^2/s)	Absolute error (mm^2/s)	Error (%)
297	5.3	2.98	3.3	3.25	0.05	1.52
313		2.05	2.29	2.31	0.02	0.87
333		1.42	1.6	1.63	0.03	1.88
353		1.08	1.23	1.22	0.01	0.81
383		0.73	0.85	0.87	0.02	2.35
423		0.52	0.63	0.62	0.01	1.59
453		0.42	0.53	0.51	0.02	3.77
473		0.35	0.45	0.46	0.01	2.22
503		0.31	0.4	0.4	0	0.00
523		0.29	0.37	0.37	0	0.00
297	7	3.12	3.4	3.38	0.02	0.59
313		2.19	2.4	2.39	0.01	0.42
333		1.47	1.63	1.66	0.03	1.84
353		1.09	1.23	1.23	0	0.00
383		0.74	0.85	0.86	0.01	1.18
423		0.52	0.62	0.6	0.02	3.23
453		0.41	0.5	0.49	0.01	2.00
473		0.34	0.42	0.44	0.01	2.38
503		0.3	0.38	0.38	0	0.00
523		0.28	0.35	0.35	0	0.00

Table F. 24 Regression data for kinematic viscosity of jatropha biodiesel B100 at 0.10 MPa for different temperatures.

Regression Analysis: ln(mu) versus 1/T, 1/T^2

The regression equation is

ln(mu) = - 2.67 + 300 1/T + 311982 1/T^2

Predictor	Coef	SE Coef	T	P
Constant	-2.6698	0.2079	-12.84	0.000
1/T	300.1	162.8	1.84	0.098
1/T^2	311982	31016	10.06	0.000

S = 0.0197727 R-Sq = 100.0% R-Sq(adj) = 100.0%

Analysis of Variance

Source	DF	SS	MS	F	P
Regression	2	10.1854	5.0927	13026.15	0.000
Residual Error	9	0.0035	0.0004		
Total	11	10.1889			

Source	DF	Seq SS
1/T	1	10.1459
1/T^2	1	0.0396

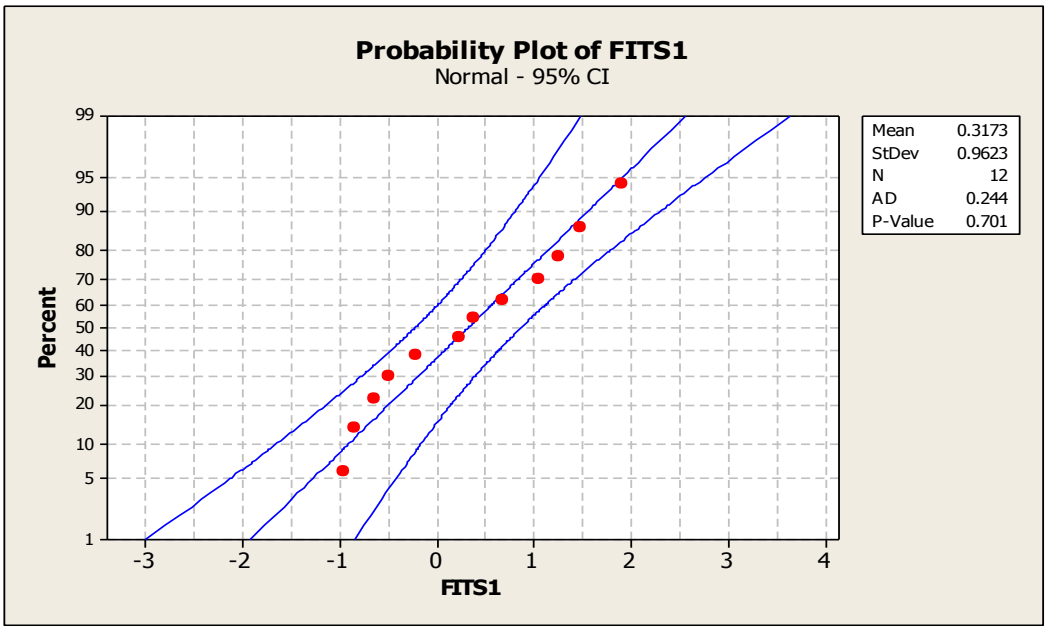

Figure F. 3 Probability plot of regressed kinematic viscosity data for jatropha B100 at 0.10 MPa for different temperatures

Table F.25 Measured and regressed kinematic viscosity, dynamic viscosity and absolute and percent error of jatropha B100 for 0.10, 1.83, and 3.50 MPa at different temperatures

Absolute Temperature (K)	Absolute Pressure (MPa)	Dynamic viscosity (mPa-s)	Measured kinematic viscosity (mm^2/s)	Regressed kinematic viscosity (mm^2/s)	Absolute error (mm^2/s)	Error (%)
296	0.10	5.82	6.55	6.69	0.14	2.14
313		3.96	4.43	4.35	0.08	1.81
323		3.12	3.48	3.48	0	0.00
333		2.58	2.86	2.83	0.03	1.05
353		1.78	1.98	1.98	0	0.00
373		1.33	1.45	1.45	0	0.00
383		1.12	1.27	1.27	0	0.00
423		0.72	0.81	0.80	0.01	1.23
453		0.58	0.61	0.61	0	0.00
473		0.45	0.50	0.53	0.03	6.00
503		0.36	0.43	0.43	0	0.00
523		0.31	0.39	0.38	0.01	2.56
296	1.83	5.82	6.57	6.60	0.03	0.46
313		3.96	4.52	4.43	0.09	1.99
323		3.12	3.59	3.60	0.01	0.28
333		2.58	2.98	2.97	0.01	0.34
353		1.78	2.08	2.11	0.03	1.44
373		1.33	1.57	1.58	0.01	0.64
383		1.12	1.34	1.38	0.04	2.99
423		0.72	0.89	0.89	0	0.00
453		0.58	0.73	0.68	0.05	6.85
473		0.45	0.58	0.58	0	0.00
503		0.36	0.47	0.47	0	0.00
523		0.31	0.41	0.42	0.01	2.44
296	3.50	5.93	6.63	6.60	0.03	0.45
313		3.97	4.48	4.45	0.03	0.67
323		3.17	3.59	3.62	0.03	0.84
333		2.64	3.01	3.00	0.01	0.33
353		1.84	2.13	2.14	0.01	0.47
373		1.38	1.61	1.60	0.01	0.62
383		1.16	1.36	1.41	0.05	3.68
423		0.77	0.93	0.91	0.02	2.15
453		0.58	0.71	0.70	0.01	1.41
473		0.49	0.61	0.60	0.01	1.64
503		0.40	0.51	0.50	0.01	1.96
523		0.33	0.42	0.44	0.02	4.76

Table F.26 Measured and regressed kinematic viscosity, dynamic viscosity and absolute and percent error of jatropha B100 for 5.30 and 7.00 MPa at different temperatures

Absolute Temperature (K)	Absolute Pressure (MPa)	Dynamic viscosity (mPa-s)	Measured Kinematic viscosity (mm^2/s)	Regressed kinematic viscosity (mm^2/s)	Absolute error (mm^2/s)	Error (%)
296	5.3	6.12	6.88	6.67	0.21	3.05
313		4.07	4.61	4.6	0.01	0.22
323		3.23	3.66	3.78	0.12	3.28
333		2.71	3.09	3.15	0.06	1.94
353		1.93	2.22	2.26	0.04	1.80
373		1.46	1.7	1.69	0.01	0.59
383		1.26	1.48	1.48	0	0.00
423		0.81	0.97	0.94	0.03	3.09
453		0.59	0.72	0.71	0.01	1.39
473		0.49	0.61	0.6	0.01	1.64
503		0.37	0.47	0.48	0.01	2.13
523		0.32	0.41	0.42	0.01	2.44
296	7	6.22	6.95	6.72	0.23	3.31
313		4.22	4.76	4.72	0.04	0.84
323		3.37	3.81	3.9	0.09	2.36
333		2.76	3.14	3.27	0.13	4.14
353		2.02	2.32	2.36	0.04	1.72
373		1.54	1.79	1.77	0.02	1.12
383		1.32	1.53	1.56	0.03	1.96
423		0.85	1.01	0.98	0.03	2.97
453		0.64	0.77	0.73	0.04	5.19
473		0.51	0.63	0.62	0.01	1.59
503		0.38	0.48	0.49	0.01	2.08
523		0.33	0.41	0.43	0.02	4.88

Table F. 27 Measured and regressed kinematic viscosity, dynamic viscosity and absolute and percent error of jatropha B80 for 5.30 and 7.00 MPa at different temperatures

Absolute Temperature (K)	Absolute Pressure (MPa)	Dynamic viscosity (mPa-s)	Measured Kinematic viscosity (mm^2/s)	Regressed kinematic viscosity (mm^2/s)	Absolute error (mm^2/s)	Error (%)
297	0.1	5.75	6.59	6.63	0.04	0.61
313		3.71	4.36	4.42	0.06	1.38
333		2.38	2.88	2.86	0.02	0.69
353		1.63	2.02	1.98	0.04	1.98
373		1.15	1.47	1.44	0.03	2.04
383		0.96	1.26	1.25	0.01	0.79
423		0.54	0.74	0.77	0.03	4.05
453		0.39	0.56	0.57	0.01	1.79
473		0.32	0.47	0.48	0.01	2.13
503		0.25	0.4	0.39	0.01	2.50
523		0.21	0.34	0.34	0	0.00
297	1.83	5.83	6.59	6.64	0.05	0.76
313		3.86	4.43	4.44	0.01	0.23
333		2.48	2.9	2.9	0	0.00
353		1.75	2.09	2.03	0.06	2.87
373		1.24	1.51	1.5	0.01	0.66
383		1.09	1.34	1.31	0.03	2.24
423		0.61	0.78	0.84	0.06	7.69
453		0.47	0.63	0.65	0.02	3.17
473		0.41	0.58	0.56	0.02	3.45
503		0.32	0.47	0.46	0.01	2.13
523		0.26	0.41	0.41	0	0.00
297	3.5	5.96	6.69	6.66	0.03	0.45
313		3.94	4.49	4.52	0.03	0.67
333		2.53	2.96	2.99	0.03	1.01
353		1.8	2.14	2.12	0.02	0.93
373		1.36	1.65	1.58	0.07	4.24
383		1.1	1.35	1.39	0.04	2.96
423		0.68	0.86	0.9	0.04	4.65
453		0.53	0.7	0.69	0.01	1.43
473		0.45	0.61	0.6	0.01	1.64
503		0.36	0.5	0.5	0	0.00
523		0.3	0.44	0.44	0	0.00

Table F.28 Measured and regressed kinematic viscosity, dynamic viscosity and absolute and percent error of jatropha B80 for 5.30 and 7.00 MPa at different temperatures

Absolute Temperature (K)	Absolute Pressure (MPa)	Dynamic viscosity (mPa-s)	Measured Kinematic viscosity (mm^2/s)	Regressed kinematic viscosity (mm^2/s)	Absolute error (mm^2/s)	Error (%)
297	5.3	6.09	6.77	6.59	0.18	2.66
313		3.98	4.48	4.53	0.05	1.12
333		2.56	2.94	3.04	0.1	3.40
353		1.79	2.1	2.17	0.07	3.33
373		1.42	1.7	1.63	0.07	4.12
383		1.18	1.43	1.43	0	0.00
423		0.73	0.92	0.93	0.01	1.09
453		0.56	0.74	0.72	0.02	2.70
473		0.47	0.63	0.62	0.01	1.59
503		0.38	0.53	0.52	0.01	1.89
523		0.31	0.44	0.46	0.02	4.55
297	7	6.33	6.98	6.92	0.06	0.86
313		4.22	4.72	4.74	0.02	0.42
333		2.8	3.19	3.17	0.02	0.63
353		1.86	2.17	2.27	0.1	4.61
373		1.5	1.79	1.71	0.08	4.47
383		1.23	1.48	1.5	0.02	1.35
423		0.77	0.96	0.99	0.03	3.13
453		0.61	0.78	0.77	0.01	1.28
473		0.52	0.68	0.67	0.01	1.47
503		0.41	0.57	0.56	0.01	1.75
523		0.34	0.49	0.5	0.01	2.04

Table F. 29 Measured and regressed kinematic viscosity, dynamic viscosity and absolute and percent error of jatropha B50 for 5.30 and 7.00 MPa at different temperatures

Absolute Temperature (K)	Absolute Pressure (MPa)	Dynamic viscosity (mPa-s)	Measured Kinematic viscosity (mm^2/s)	Regressed kinematic viscosity (mm^2/s)	Absolute error (mm^2/s)	Error (%)
297	0.1	5.01	5.77	5.83	0.06	1.04
313		3.27	3.79	3.87	0.08	2.11
323		2.69	3.15	3.1	0.05	1.59
333		2.24	2.65	2.54	0.11	4.15
353		1.53	1.83	1.81	0.02	1.09
373		1.1	1.34	1.38	0.04	2.99
403		0.78	0.96	1	0.04	4.17
423		0.67	0.84	0.84	0	0.00
453		0.54	0.7	0.69	0.01	1.43
473		0.48	0.63	0.62	0.01	1.59
503		0.41	0.56	0.54	0.02	3.57
523		0.35	0.49	0.51	0.02	4.08
297	1.83	5.13	5.87	5.99	0.12	2.04
313		3.57	4.12	3.99	0.13	3.16
323		2.75	3.2	3.2	0	0.00
333		2.28	2.66	2.63	0.03	1.13
353		1.6	1.89	1.88	0.01	0.53
373		1.15	1.38	1.43	0.05	3.62
403		0.8	0.97	1.03	0.06	6.19
423		0.7	0.87	0.87	0	0.00
453		0.59	0.75	0.71	0.04	5.33
473		0.51	0.66	0.63	0.03	4.55
503		0.43	0.57	0.55	0.02	3.51
523		0.36	0.49	0.52	0.03	6.12
297	3.5	5.2	5.92	6.03	0.11	1.86
313		3.66	4.21	4.08	0.13	3.09
323		2.86	3.3	3.3	0	0.00
333		2.35	2.72	2.72	0	0.00
353		1.64	1.93	1.95	0.02	1.04
373		1.25	1.49	1.49	0	0.00
403		0.86	1.04	1.07	0.03	2.88
423		0.73	0.9	0.9	0	0.00
453		0.59	0.74	0.72	0.02	2.70
473		0.51	0.65	0.64	0.01	1.54
503		0.43	0.57	0.56	0.01	1.75
523		0.37	0.5	0.51	0.01	2.00

Table F.30 Measured and regressed kinematic viscosity, dynamic viscosity and absolute and percent error of jatropha B50 for 5.30 and 7.00 MPa at different temperatures

Absolute Temperature (K)	Absolute Pressure (MPa)	Dynamic viscosity (mPa-s)	Measured Kinematic viscosity (mm^2/s)	Regressed kinematic viscosity (mm^2/s)	Absolute error (mm^2/s)	Error (%)
297	5.30	5.28	5.96	5.95	0.01	0.23
313		3.59	4.09	4.09	0.00	0.02
323		2.93	3.36	3.34	0.02	0.61
333		2.41	2.79	2.77	0.01	0.40
353		1.70	1.99	2.01	0.03	1.36
373		1.31	1.55	1.54	0.01	0.35
403		0.91	1.08	1.12	0.04	3.73
423		0.76	0.93	0.94	0.01	1.36
453		0.64	0.80	0.76	0.04	4.65
473		0.55	0.69	0.67	0.02	2.92
503		0.45	0.59	0.58	0.01	1.86
523		0.38	0.51	0.53	0.03	4.98
297	7.00	5.47	6.12	6.01	0.11	1.85
313		3.77	4.26	4.19	0.07	1.55
323		2.86	3.24	3.44	0.20	6.07
333		2.59	2.95	2.87	0.08	2.68
353		1.81	2.08	2.09	0.02	0.87
373		1.37	1.60	1.61	0.01	0.53
403		0.96	1.12	1.16	0.03	3.10
423		0.81	0.97	0.97	0.00	0.09
453		0.65	0.80	0.77	0.03	3.58
473		0.57	0.71	0.68	0.03	4.54
503		0.47	0.59	0.58	0.01	2.26
523		0.39	0.50	0.53	0.03	6.70

Table F. 31 Measured and regressed kinematic viscosity, dynamic viscosity and absolute and percent error of jatropha B20 for 0.10, 1.83, 3.50 MPa at different temperatures

Absolute Temperature (K)	Absolute Pressure (MPa)	Dynamic viscosity (mPa-s)	Measured Kinematic viscosity (mm^2/s)	Regressed kinematic viscosity (mm^2/s)	Absolute error (mm^2/s)	Error (%)
296	0.1	3	3.49	3.52	0.03	0.86
313		2.1	2.47	2.43	0.05	2.02
323		1.74	2.07	2.01	0.06	2.90
333		1.38	1.65	1.7	0.04	2.42
353		1.04	1.25	1.27	0.01	0.80
373		0.81	0.99	1	0.01	1.01
383		0.7	0.86	0.9	0.03	3.49
423		0.51	0.66	0.64	0.02	3.03
453		0.42	0.55	0.54	0.02	3.64
473		0.37	0.5	0.48	0.02	4.00
503		0.3	0.42	0.43	0.01	2.38
523		0.28	0.39	0.4	0.01	2.56
296	1.83	3.07	3.55	3.44	0.1	2.82
313		2.12	2.47	2.47	0	0.00
323		1.79	2.09	2.08	0.01	0.48
333		1.46	1.71	1.77	0.06	3.51
353		1.08	1.28	1.35	0.06	4.69
373		0.84	1.01	1.07	0.06	5.94
403		0.76	0.92	0.8	0.12	13.04
423		0.54	0.67	0.68	0.01	1.49
453		0.44	0.56	0.56	0	0.00
473		0.39	0.5	0.5	0	0.00
503		0.32	0.43	0.43	0	0.00
523		0.28	0.38	0.39	0.01	2.63
296	3.5	3.14	3.62	3.5	0.12	3.31
313		2.22	2.57	2.56	0.02	0.78
323		1.86	2.17	2.17	0	0.00
333		1.51	1.77	1.87	0.1	5.65
353		1.16	1.37	1.43	0.06	4.38
373		0.91	1.08	1.14	0.05	4.63
403		0.8	0.97	0.85	0.11	11.34
423		0.59	0.72	0.72	0	0.00
453		0.47	0.59	0.59	0	0.00
473		0.42	0.53	0.52	0.01	1.89
503		0.34	0.44	0.45	0.01	2.27
523		0.3	0.4	0.41	0.01	2.50

Table F.32 Measured and regressed kinematic viscosity, dynamic viscosity and absolute and percent error of jatropha B20 for 5.30 and 7.00 MPa at different temperatures

Absolute Temperature (K)	Absolute Pressure (MPa)	Dynamic viscosity (mPa-s)	Measured Kinematic viscosity (mm^2/s)	Regressed kinematic viscosity (mm^2/s)	Absolute error (mm^2/s)	Error (%)
296	5.3	3.18	3.66	3.55	0.11	3.01
313		2.32	2.68	2.65	0.03	1.12
323		1.97	2.29	2.27	0.02	0.87
333		1.6	1.87	1.97	0.1	5.35
353		1.22	1.43	1.52	0.08	5.59
373		0.97	1.15	1.21	0.06	5.22
403		0.86	1.03	0.9	0.13	12.62
423		0.62	0.76	0.77	0.01	1.32
453		0.5	0.62	0.61	0	0.00
473		0.44	0.55	0.54	0.01	1.82
503		0.35	0.44	0.46	0.01	2.27
523		0.31	0.4	0.41	0.01	2.50
296	7	3.24	3.71	3.56	0.16	4.31
313		2.31	2.66	2.68	0.02	0.75
323		2.01	2.33	2.3	0.03	1.29
333		1.63	1.89	2	0.11	5.82
353		1.25	1.47	1.55	0.08	5.44
373		1.01	1.19	1.24	0.05	4.20
403		0.89	1.06	0.94	0.12	11.32
423		0.64	0.78	0.79	0.02	2.56
453		0.53	0.65	0.64	0.01	1.54
473		0.47	0.59	0.56	0.03	5.08
503		0.37	0.47	0.48	0.01	2.13
523		0.32	0.41	0.43	0.02	4.88

Table F.33 Measured and regressed kinematic viscosity, dynamic viscosity and absolute and percent error of soapnut biodiesel B100 for 0.10, 1.83, 3.50 MPa at different temperatures

Absolute Temperature (K)	Absolute Pressure (MPa)	Dynamic viscosity (mPa-s)	Measured Kinematic viscosity (mm^2/s)	Regressed kinematic viscosity (mm^2/s)	Absolute error (mm^2/s)	Error (%)
297	0.1	6.83	7.77	7.85	0.08	1.03
313		4.61	5.29	5.16	0.13	2.46
333		2.89	3.36	3.33	0.03	0.89
353		1.87	2.21	2.31	0.1	4.52
383		1.24	1.5	1.49	0.01	0.67
423		0.79	0.98	0.96	0.02	2.04
453		0.58	0.74	0.74	0	0.00
473		0.49	0.64	0.64	0	0.00
503		0.38	0.52	0.54	0.01	1.92
523		0.35	0.49	0.48	0.01	2.04
297	1.83	6.89	7.8	7.83	0.04	0.51
313		4.71	5.39	5.3	0.09	1.67
333		3	3.47	3.5	0.03	0.86
353		2.09	2.45	2.46	0.02	0.82
383		1.33	1.59	1.6	0.01	0.63
423		0.81	1.01	1.02	0.01	0.99
453		0.62	0.79	0.78	0.01	1.27
473		0.53	0.68	0.67	0.02	2.94
503		0.4	0.53	0.54	0.01	1.89
523		0.35	0.48	0.48	0	0.00
297	3.5	6.88	7.72	7.7	0.03	0.39
313		4.76	5.4	5.28	0.11	2.04
333		3.04	3.48	3.52	0.04	1.15
353		2.07	2.4	2.49	0.09	3.75
383		1.36	1.6	1.62	0.02	1.25
423		0.86	1.05	1.03	0.02	1.90
453		0.64	0.79	0.78	0.01	1.27
473		0.55	0.69	0.66	0.03	4.35
503		0.39	0.52	0.54	0.02	3.85
523		0.35	0.47	0.48	0.01	2.13

Table F.34 Measured and regressed kinematic viscosity, dynamic viscosity and absolute and percent error of soapnut biodiesel B100 for 5.30 and 7.00 MPa at different temperatures

Absolute Temperature (K)	Absolute Pressure (MPa)	Dynamic viscosity (mPa-s)	Measured Kinematic viscosity (mm^2/s)	Regressed kinematic viscosity (mm^2/s)	Absolute error (mm^2/s)	Error (%)
297	5.3	7.14	7.99	7.91	0.08	1.00
313		4.77	5.39	5.39	0	0.00
333		3.09	3.52	3.57	0.05	1.42
353		2.17	2.5	2.52	0.02	0.80
383		1.39	1.63	1.63	0	0.00
423		0.88	1.05	1.04	0.01	0.95
453		0.64	0.79	0.79	0	0.00
473		0.55	0.69	0.67	0.02	2.90
503		0.41	0.53	0.55	0.02	3.77
523		0.37	0.49	0.49	0	0.00
297	7	7.48	8.18	8.31	0.13	1.59
313		5.14	5.67	5.59	0.08	1.41
333		3.31	3.69	3.66	0.03	0.81
353		2.31	2.61	2.56	0.05	1.92
383		1.39	1.6	1.66	0.06	3.75
423		0.88	1.04	1.05	0.01	0.96
453		0.67	0.82	0.81	0.01	1.22
473		0.56	0.7	0.69	0.01	1.43
503		0.45	0.58	0.57	0.01	1.72
523		0.38	0.5	0.51	0.01	2.00

Table F.35 Measured and regressed kinematic viscosity, dynamic viscosity and absolute and percent error of soapnut biodiesel B80 for 0.10, 1.83, 3.50 MPa at different temperatures

Absolute Temperature (K)	Absolute Pressure (MPa)	Dynamic viscosity (mPa-s)	Measured Kinematic viscosity (mm^2/s)	Regressed kinematic viscosity (mm^2/s)	Absolute error (mm^2/s)	Error (%)
297	0.1	6.05	6.91	7.25	0.34	4.92
313		4.35	5.04	4.93	0.11	2.18
323		3.59	4.18	3.98	0.2	4.78
333		2.81	3.3	3.28	0.02	0.61
353		1.99	2.35	2.33	0.02	0.85
373		1.42	1.7	1.74	0.04	2.35
383		1.26	1.51	1.53	0.02	1.32
423		0.81	1	1	0	0.00
453		0.64	0.81	0.78	0.03	3.70
473		0.47	0.61	0.67	0.06	9.84
503		0.44	0.58	0.56	0.02	3.45
523		0.38	0.52	0.5	0.02	3.85
297	1.83	6.08	6.87	7.09	0.22	3.20
313		4.31	4.92	4.89	0.03	0.61
323		3.59	4.14	3.97	0.17	4.11
333		2.84	3.31	3.29	0.02	0.60
353		2.01	2.37	2.35	0.02	0.84
373		1.45	1.73	1.77	0.04	2.31
383		1.29	1.55	1.55	0	0.00
423		0.83	1.02	1.01	0.01	0.98
453		0.63	0.8	0.78	0.02	2.50
473		0.48	0.62	0.68	0.06	9.68
503		0.45	0.59	0.56	0.03	5.08
523		0.38	0.51	0.5	0.01	1.96
297	3.5	6.15	6.95	7.16	0.21	3.02
313		4.33	4.93	4.9	0.03	0.61
323		3.6	4.12	3.97	0.15	3.64
333		2.86	3.29	3.28	0.01	0.30
353		2.02	2.35	2.33	0.02	0.85
373		1.47	1.72	1.74	0.02	1.16
383		1.3	1.53	1.53	0	0.00
423		0.83	1	0.99	0.01	1.00
453		0.61	0.75	0.76	0.01	1.33
473		0.48	0.6	0.66	0.06	10.00
503		0.45	0.57	0.54	0.03	5.26
523		0.38	0.49	0.49	0	0.00

Table F.36 Measured and regressed kinematic viscosity, dynamic viscosity and absolute and percent error of soapnut biodiesel B80 for 5.30 and 7.00 MPa at different temperatures

Absolute Temperature (K)	Absolute Pressure (MPa)	Dynamic viscosity (mPa-s)	Measured Kinematic viscosity (mm^2/s)	Regressed kinematic viscosity (mm^2/s)	Absolute error (mm^2/s)	Error (%)
297	5.3	6.14	6.89	7.11	0.22	3.19
313		4.33	4.89	4.88	0.01	0.20
323		3.6	4.08	3.96	0.12	2.94
333		2.86	3.27	3.27	0	0.00
353		2.06	2.39	2.33	0.06	2.51
373		1.5	1.75	1.74	0.01	0.57
383		1.32	1.55	1.53	0.02	1.29
423		0.8	0.96	0.99	0.03	3.13
453		0.63	0.77	0.76	0	0.00
473		0.49	0.61	0.66	0.05	8.20
503		0.44	0.56	0.54	0.01	1.79
523		0.39	0.51	0.49	0.02	3.92
297	7	6.31	7.03	7.19	0.16	2.28
313		4.37	4.92	4.94	0.03	0.61
323		3.69	4.17	4.01	0.16	3.84
333		2.91	3.31	3.31	0	0.00
353		2.05	2.36	2.35	0.01	0.42
373		1.51	1.75	1.75	0.01	0.57
383		1.33	1.55	1.53	0.02	1.29
423		0.8	0.96	0.98	0.02	2.08
453		0.62	0.75	0.75	0	0.00
473		0.51	0.62	0.64	0.02	3.23
503		0.42	0.52	0.52	0	0.00
523		0.37	0.48	0.46	0.01	2.08

Table F. 37 Measured and regressed kinematic viscosity, dynamic viscosity and absolute and percent error of soapnut biodiesel B50 for 0.10, 1.83, 3.50 MPa at different temperatures

Absolute Temperature (K)	Absolute Pressure (MPa)	Dynamic viscosity (mPa-s)	Measured Kinematic viscosity (mm^2/s)	Regressed kinematic viscosity (mm^2/s)	Absolute error (mm^2/s)	Error (%)
297	0.1	4.54	5.2	5.19	0.01	0.19
313		3.13	3.62	3.61	0.01	0.28
323		2.56	2.97	2.96	0.01	0.34
333		2.13	2.49	2.48	0.02	0.80
353		1.53	1.81	1.81	0.01	0.55
373		1.15	1.38	1.4	0.02	1.45
383		1.01	1.22	1.25	0.03	2.46
423		0.71	0.88	0.86	0.02	2.27
453		0.56	0.71	0.7	0.01	1.41
473		0.49	0.64	0.62	0.02	3.13
503		0.4	0.54	0.54	0	0.00
523		0.35	0.48	0.5	0.01	2.08
297	1.83	4.59	5.18	5.19	0.01	0.19
313		3.19	3.62	3.6	0.03	0.83
323		2.62	2.99	2.94	0.05	1.67
333		2.13	2.44	2.45	0.01	0.41
353		1.52	1.76	1.79	0.03	1.70
373		1.15	1.34	1.38	0.03	2.24
383		1.04	1.22	1.23	0.01	0.82
423		0.71	0.85	0.84	0.01	1.18
453		0.57	0.7	0.68	0.02	2.86
473		0.49	0.61	0.6	0.01	1.64
503		0.41	0.53	0.52	0.01	1.89
523		0.35	0.46	0.48	0.02	4.35
297	3.5	4.62	5.17	5.17	0	0.00
313		3.23	3.64	3.63	0.01	0.27
323		2.69	3.05	2.99	0.07	2.30
333		2.16	2.47	2.5	0.04	1.62
353		1.58	1.82	1.83	0.01	0.55
373		1.2	1.39	1.41	0.01	0.72
383		1.05	1.23	1.25	0.02	1.63
423		0.72	0.85	0.85	0	0.00
453		0.56	0.69	0.68	0.01	1.45
473		0.5	0.62	0.6	0.02	3.23
503		0.41	0.52	0.51	0.01	1.92
523		0.34	0.44	0.46	0.02	4.55

Table F. 38 Measured and regressed kinematic viscosity, dynamic viscosity and absolute and percent error of soapnut biodiesel B50 for 5.30 and 7.00 MPa at different temperatures

Absolute Temperature (K)	Absolute Pressure (MPa)	Dynamic viscosity (mPa-s)	Measured Kinematic viscosity (mm^2/s)	Regressed kinematic viscosity (mm^2/s)	Absolute error (mm^2/s)	Error (%)
297	5.3	4.7	5.25	5.17	0.08	1.52
313		3.26	3.67	3.63	0.04	1.09
323		2.79	3.16	2.99	0.17	5.38
333		2.32	2.64	2.5	0.14	5.30
353		1.67	1.92	1.83	0.09	4.69
373		1.25	1.46	1.41	0.05	3.42
383		1.12	1.31	1.25	0.06	4.58
423		0.75	0.9	0.85	0.04	4.44
453		0.58	0.71	0.68	0.03	4.23
473		0.51	0.63	0.6	0.03	4.76
503		0.41	0.52	0.51	0.01	1.92
523		0.34	0.44	0.46	0.02	4.55
297	7	4.74	5.24	5.2	0.04	0.76
313		3.3	3.65	3.72	0.07	1.92
323		2.84	3.16	3.09	0.07	2.22
333		2.36	2.62	2.6	0.02	0.76
353		1.69	1.89	1.91	0.02	1.06
373		1.29	1.46	1.47	0.01	0.68
383		1.12	1.27	1.3	0.03	2.36
423		0.76	0.88	0.87	0.01	1.14
453		0.59	0.7	0.68	0.01	1.43
473		0.5	0.61	0.59	0.01	1.64
503		0.4	0.5	0.49	0	0.00
523		0.34	0.43	0.44	0.01	2.33

Table F. 39 Measured and regressed kinematic viscosity, dynamic viscosity and absolute and percent errors of soapnut biodiesel B20 for 0.10, 1.83, 3.50 MPa at different temperatures.

Absolute Temperature (K)	Absolute Pressure (MPa)	Dynamic viscosity (mPa-s)	Measured Kinematic viscosity (mm^2/s)	Regressed kinematic viscosity (mm^2/s)	Absolute error (mm^2/s)	Error (%)
297	0.1	2.7	3.1	3.06	0.04	1.29
313		1.92	2.23	2.21	0.02	0.90
333		1.31	1.54	1.57	0.03	1.95
353		0.98	1.16	1.19	0.03	2.59
383		0.71	0.86	0.86	0	0.00
423		0.5	0.63	0.62	0.01	1.59
453		0.41	0.53	0.52	0.01	1.89
473		0.37	0.49	0.47	0.02	4.08
503		0.3	0.4	0.42	0.02	5.00
523		0.28	0.39	0.39	0	0.00
297	1.83	2.75	3.12	3.07	0.04	1.28
313		1.95	2.23	2.21	0.03	1.35
333		1.32	1.52	1.57	0.05	3.29
353		1	1.17	1.19	0.02	1.71
383		0.71	0.85	0.86	0.01	1.18
423		0.51	0.63	0.62	0.01	1.59
453		0.42	0.53	0.52	0.01	1.89
473		0.38	0.49	0.47	0.02	4.08
503		0.31	0.41	0.42	0.01	2.44
523		0.28	0.38	0.39	0.01	2.63
297	3.5	2.83	3.17	3.14	0.04	1.26
313		1.99	2.26	2.24	0.02	0.88
333		1.35	1.55	1.58	0.04	2.58
353		1	1.16	1.19	0.03	2.59
383		0.71	0.85	0.85	0	0.00
423		0.5	0.62	0.61	0.01	1.61
453		0.41	0.52	0.5	0.02	3.85
473		0.36	0.46	0.45	0	0.00
503		0.3	0.39	0.4	0.01	2.56
523		0.28	0.37	0.37	0	0.00

Table F. 40 Measured and regressed kinematic viscosity, dynamic viscosity and absolute and percent error of soapnut biodiesel B20 for 5.30 and 7.00 MPa at different temperatures.

Absolute Temperature (K)	Absolute Pressure (MPa)	Dynamic viscosity (mPa-s)	Measured Kinematic viscosity (mm^2/s)	Regressed kinematic viscosity (mm^2/s)	Absolute error (mm^2/s)	Error (%)
297	5.3	2.98	3.3	3.25	0.05	1.52
313		2.05	2.29	2.31	0.02	0.87
333		1.42	1.6	1.63	0.03	1.88
353		1.08	1.23	1.22	0.01	0.81
383		0.73	0.85	0.87	0.02	2.35
423		0.52	0.63	0.62	0.01	1.59
453		0.42	0.53	0.51	0.02	3.77
473		0.35	0.45	0.46	0.01	2.22
503		0.31	0.4	0.4	0	0.00
523		0.29	0.37	0.37	0	0.00
297	7	3.12	3.4	3.38	0.02	0.59
313		2.19	2.4	2.39	0.01	0.42
333		1.47	1.63	1.66	0.03	1.84
353		1.09	1.23	1.23	0	0.00
383		0.74	0.85	0.86	0.01	1.18
423		0.52	0.62	0.6	0.02	3.23
453		0.41	0.5	0.49	0.01	2.00
473		0.34	0.42	0.44	0.01	2.38
503		0.3	0.38	0.38	0	0.00
523		0.28	0.35	0.35	0	0.00